NUCLEAR PHYSICS AT GANIL A COMPILATION 1994-1995

M. Bex, J. Galin, S. Geswend

GANIL

a COMPILATION

NUCLEAR PHYSICS

AT

GANIL

A COMPILATION

1994 - 1995

Editors : Monique BEX, Joël GALIN
Typing and layout of the manuscript : S. GESWEND

September 1996

FOREWORD

This compilation, without beeing exhaustive, gives an overview of the scientific activities performed at GANIL during the years 1994-1995. Once again, it should be stressed that it is not a traditional progress report as it reflects only the research programme in nuclear physics through the contributions of physicists from various laboratories who have been performing experiments at the GANIL national facility.

During that period, the main addition to the facility has been the installation of the SISSI device which made possible the production and delivery of radioactive beams in all experimental area with an increased intensity. Despite the required improvement of the reliability of the system, the operation of SISSI has led to achieve successfull original experiments. The present period is also extremely promising for the future of the laboratory. The SPIRAL radioactive beam facility is under construction. This major upgrade of the GANIL facility is scheduled to be commissioned by the end of 1998. This should make the GANIL laboratory a major european center dedicated to radioactive beams.

On the physics side, a large number of exciting results have been obtained both in collision dynamics and in nuclear structure studies.

Major results on reaction dynamics studies were obtained from the full analysis of experiments performed at GANIL with the NAUTILUS multidetector system, with ORION and with TAPS. They clearly contribute to a much better knowledge of the timescales involved during the collision and on the mechanisms for energy dissipation.

The first data from INDRA have now been analyzed and demonstrate the quality and the high efficiency of this 4π detector. The first two campaigns have tackled all the various aspects of reaction dynamics. Let us mention the exciting results on the vaporization and the controversial problem of the caloric curve.

The number of experiments dealing with nuclear structure studies, mainly performed with the LISE and SPEG spectrometers, has been constantly increasing during that period. In particular, those concerning nuclei far from stability have led to many new results. Among them are the production of ^{100}Sn as well as the first measurement of its mass, the observation of many new isomeric states and the emerging programme on isomeric beams.

Among the first experiments performed with SISSI, one may stress elastic scattering and charge exchange studies with light neutron-rich beams.

Many other interesting results are presented in this compilation, including the theoretical work performed by on-site physicists, they demonstrate the richness of the research programme presently ongoing at GANIL.

We are much indebted to all the authors for the quality of their contributions.

Daniel GUERREAU
Director

Jérôme FOUAN
Deputy Director

CONTENTS

I. COMPILATION

A - NUCLEAR STRUCTURE

A1 - NUCLEAR SPECTROSCOPY

A2 - EXOTIC NUCLEI AND DECAY MODES

B - NUCLEAR REACTION

B1 - PERIPHERAL COLLISIONS - PROJECTILE-LIKE FRAGMENTS

B2 - DISSIPATIVE COLLISIONS

B3 - FLOW AND RELATED PHENOMENA

B4 - MULTIFRAGMENT EMISSION

B5 - MESONS AND PHOTONS

C - MISCELLANEOUS

A - NUCLEAR STRUCTURE

A1 - NUCLEAR SPECTROSCOPY

Elastic scattering of light neutron rich exotic beams on a proton target

M.D. Cortina-Gil[1], P. Roussel-Chomaz[1], N. Alamanos[2], J. Barrette[3], W. Mittig[1], F. Auger[2], Y. Blumenfeld[4], J.M. Casandjian[1], M. Chartier[1], V. Fekou-Youmbi[2], B. Fernandez[2], N. Frascaria[4], A. Gillibert[2], H.Laurent[4], A.Lépine-Szily[1,5], N.A. Orr[6], V. Pascalon[4], J.A. Scarpaci[4], J.L. Sida[2], T. Suomijärvi[4]

1) GANIL (DSM/CEA,IN2P3/CNRS), BP 5027, 14021 Caen Cedex, France
2) CEA/DSM/DAPNIA/SPhN Saclay, 91191 Gif-sur-Yvette Cedex, France
3) Foster Radiation Lab., Mc Gill University, Montreal, Canada H3A 2B1
4) IPN, IN2P3/CNRS, 91406 Orsay Cedex, France
5) IFUSP,DFN, C.P. 20516, 01498, Sao Paulo, S.P., Brasil
6) LPC-ISMRA, Blvd du Maréchal Juin, 14050 Caen, France

Abstract: The elastic scattering of ^{6}He, ^{10,11}Be secondary beams on a $(CH_2)_3$ target has been measured. A microscopic optical potential was used to reproduce the proton-nucleus elastic scattering data.

1 Introduction

The nucleon-nucleus and nucleus-nucleus elastic scattering has gained a new interest with the availability of unstable nuclear beams[1-6], especially in the case of halo nuclei where this type of study is expected to provide information on the nuclear densities of dripline nuclei and on the components of interactions which depend on the isospin.

We have started an experimental programme at GANIL for the study of elastic scattering induced by light unstable nuclei. These experiments benefit from the high resolution magnetic spectrometer SPEG and from the high quality secondary beams that are provided by the double superconducting solenoid SISSI.

2 Experimental procedure

The secondary beams were produced by fragmentation of a 75 MeV/nucleon primary ^{13}C beam, delivered by the GANIL accelerator, on a 1155 mg/cm^2 carbon production target, located between the two superconducting solenoids of the SISSI device [7,8]. The position of SISSI at the exit of the second cyclotron and at the entrance of the beam analysing α–

spectrometer allows for an improved collection of the produced secondary beams and for a better transmission to the different experimental areas. The total momentum acceptance of the system SISSI+α-spectrometer was of the order of 0.6% and the angular acceptance was about 100 mr in the horizontal and vertical planes. This results in roughly one order of magnitude increase in beam intensity with respect to an ion-optical system without the SISSI device.

In this work, the magnetic rigidity of the alpha spectrometer was set at 2.82 T.m. At this rigidity, the total intensity of the secondary beams was of the order of 10^7 pps in the acceptance of the system for a primary intensity of $2x10^{12}$ pps. The intensity for the neutron-rich nuclei ^{6}He and ^{11}Be was of the order of a few percent of the total intensity, whereas the intensity for the nuclei closer to the stability valley such as ^{7}Li and ^{10}Be was around 1/5 of the total intensity.

The elastic scattering was studied using the energy loss spectrometer SPEG [9]. The reaction target was a 100μm thick polypropylene foil, $(CH_2)_3$. All the scattered particles were unambiguously identified in the focal plane of the spectrometer with an ionisation chamber and a plastic scintillator. The momentum and scattering angle were measured with two position sensitive drift chambers [10] placed 70 cm apart and located near the focal plane of the spectrometer. The elastic scattering of the secondary beams was measured on ^{1}H and ^{12}C in the range θ_{lab}=0.7°-6.0°. The energy resolution which could be achieved in this experiment with secondary beams was of the order of 10^{-3} whereas the angular resolution was of the order of 0.3°.

3 Proton-nucleus elastic scattering

The experimental angular distributions for the elastic scattering of the ^{6}He, ^{7}Li, ^{10}Be and ^{11}Be on the protons contained in the polypropylene target are presented in Fig. (1). We have analysed these data by using the nucleon-nucleus optical model potential calculated by Jeukenne *et al.* (JLM) [11]. The JLM central potential has been extensively studied by S.Mellema *et al.* [12] and J.S. Petler *et al.* [13]. It has been particularly successful in describing elastic neutron and proton scattering from stable nuclei, provided the imaginary potential is adjusted downward by a normalisation factor of the order of $\lambda_W \approx 0.8$.

The solid curves on Fig. (1) present the results obtained with the JLM potential with the "standard" normalisation factors for the real part (λ_V= 1.0) the imaginary part (λ_W = 0.8). The density distributions have been calculated within a Hartree Fock model with shell model occupation probabilities[14]. The agreement obtained in the case of the stable ^{7}Li secondary beam is excellent with the standard normalisation factors. However the calculated angular distribution overpredict the data for the neutron-rich nuclei. For these nuclei, the normalisation

factors λ_v or λ_w were allowed to vary in order to obtain a best fit of the data, based on χ^2 minimisation (dashed and dotted lines on Fig. (1)). The optimum values are plotted on Fig.(2) for the four beams used in the present data, and also for the ^{9}Li and ^{11}Li data of Ref. [4], and the ^{8}He data of Ref. [1]

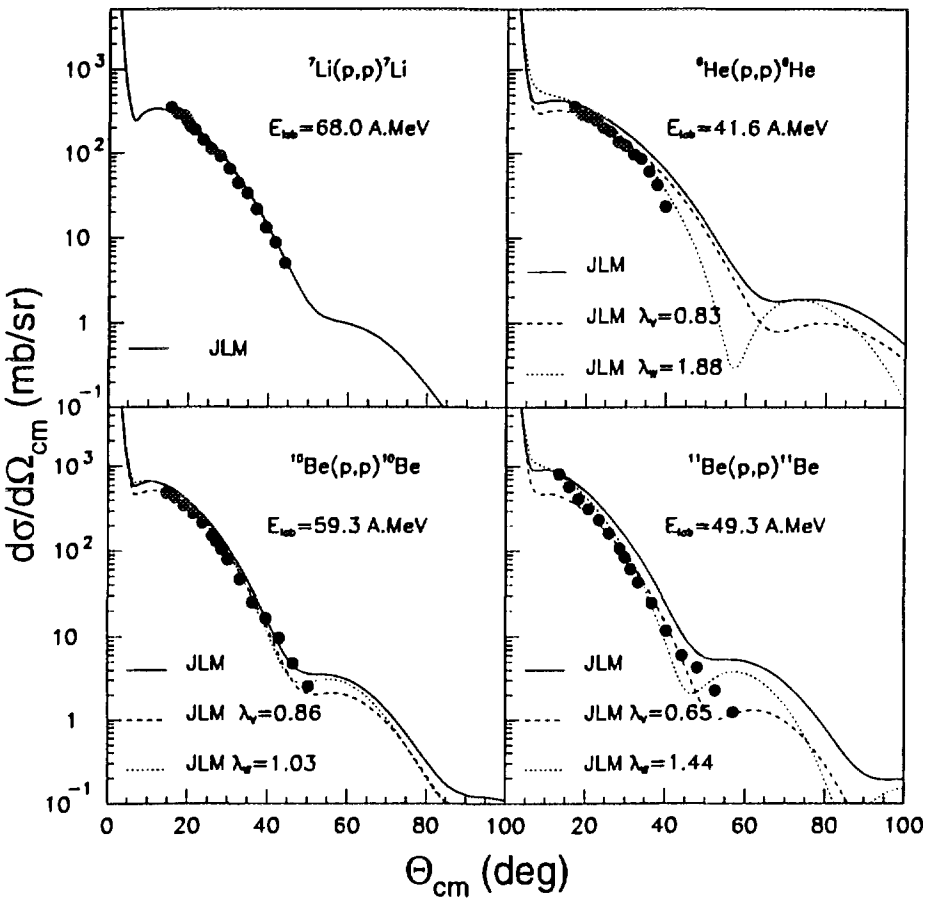

Fig. (1): Elastic scattering angular distributions measured for ^{6}He, ^{7}Li, ^{10,11}Be on proton

The normalisation factors obtained in the case of ^{7}Li and ^{9}Li are the same as those found in previous studies with stable nuclei, whereas all other cases require a decrease of the real potential and an increase of the imaginary potential. This is exactly what can be expected from a dynamic polarisation potential representation of the break-up effects [15].

4 Conclusions

We have shown that the combined use of SISSI and SPEG offers new opportunities for measuring elastic scattering cross sections of neutron-rich nuclei to high accuracy.

The elastic scattering of the secondary beams on the proton target studied in the present work has been analysed with the JLM microscopic optical model potential. In order to reproduce the data for the neutron rich nuclei, the real or imaginary potential have to be renormalised, in order to take into account the break-up processes which become important for these loosely bound nuclei.

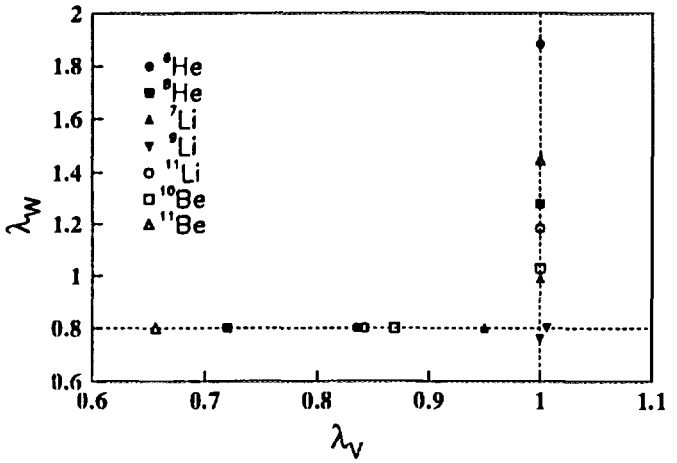

Fig. 2: Normalisation factors applied to the real (λ_V) and imaginary part (λ_W) of the JLM potential to best fit the data

References

[1] A.A. Korsheninnikov et al., Phys. Lett. B 316 (1993) 38

[2] J.J. Kolata et al., Phys. Rev. Lett. 69 (1992) 2631

[3] M. Lewitowicz et al., Nucl. Phys. A 562 (1993) 301

[4] C.B. Moon et al., Phys. Lett. B 268 (1992) 39

[5] M. Zahar et al., Phys. Rev. C 49 (1994) 1540

[6] I. Pecina et al., Phys. Rev C 52 (1995) 191

[7] W. Mittig, Nucl. Physics News 1 (1990) 30

[8] A. Joubert et al., 1991 Particle Accelerator Conference IEEE Vol 1 (1991) 594

[9] L. Bianchi et al., NIM A 276 (1989) 509

[10] A.C.C. Villari et al., NIM B 281 (1989) 240

[11] J.P. Jeukenne, A. Lejeune and C. Mahaux, Phys. Rev. C16 (1977) 80

[12] S. Mellema et al, Phys. Rev. C 28 (1983) 2267

[13] J. S. Petler et al., Phys. Rev. C32 (1985) 673

[14] H. Sagawa, Phys. Lett. B 286 (1992) 7

[15] J.S. Al-Khalili, Nucl. Phys. A 581 (1995) 315

Refractive Scattering and Reactions in the $^{16}O + ^{16}O$ System[1]

G. Bartnitzky[1], A. Blazevic[2], H.G. Bohlen[2], J.M. Casandjian[3], M. Chartier[3], H. Clement[1], B. Gebauer[2], A. Gillibert[4], Th. Kirchner[2], Dao T. Khoa[2], A. Lepine-Szily[3], W. Mittig[3], W. von Oertzen[2], A.N. Ostrowski[2], P. Roussel-Chomaz[3], J. Siegler[1], M. Wilpert[2], Th. Wilpert[2]

[1]Physikalisches Institut der Universität Tübingen, D-72076 Tübingen, Germany
[2]Hahn-Meitner-Institut, Glienicker Str. 100, D-14109 Berlin, Germany
[3]GANIL, Bd. Henri Becquerel, BP 507, F-14021 Caen Cedex, France
[4]CEN Saclay, F-91191 Gif-sur-Yvette Cedex, France

have been extracted

Abstract: *The elastic scattering cross sections as well as one neutron stripping for ^{16}O ions on ^{16}O has been measured with high accuracy over large angular ranges at incident energies from 250 to 704 MeV. From these data which sample both diffractive and refractive scattering processes, ~~we extract~~ the underlying scattering potentials using model-unrestricted analysis methods. The extracted potentials fit very well into the systematics found in light-ion scattering. ~~The real potential is also obtained from microscopically calculated folding potentials with a density-dependence of the underlying effective nucleon-nucleon interaction. The best result obtained is a weak density dependence, which yields a 'soft' equation of state for cold nuclear matter.~~*

Recently the question of the effective scattering potentials in heavy-ion (HI) reactions has found renewed interest, since its solution may supply important information on the underlying effective nucleon-nucleon (NN) interaction at high nuclear densities, which in turn determines the equation of state for cold nuclear matter. The latter is of great interest also in astrophysics for a deeper understanding of, e.g., neutron stars and super novae phenomena.

In the early studies of HI scattering often very shallow HI potentials have been favoured as suggested by the analyses of scattering data in the forward angle, diffractive, regime only [1]. However, the first HI data extending up to the refractive nuclear rainbow region unambiguously demonstrated [2] that realistic HI potentials have to be deep — as expected from the double-folding concept as well as from the systematics found in light-ion (LI) scattering. Another approach based on a model-unrestricted analysis has shown there [3,4] that the potentials underlying the scattering process may be extracted very reliably from the data — as long as those are measured with high precision from the Coulomb rainbow region at very forward angles all the way down to the nuclear rainbow region at backward angles. As a result the extracted potentials for p-, d-, ^{3}He- and α-scattering are found to be well defined over the whole radial region. The extracted depths of the real

[1] supported by a grant from the HMI Az. 120/531, the DFG (Graduiertenkolleg, Mu 705/3) and the European Community under contract n° CHGE-CT94-0056 (Human Capital and Mobility, Access to the GANIL large scale facility)

central potentials approximately scale with the number of nucleons in the projectile and can be very well described by double-folding calculations, if the density dependence of the underlying effective NN-interaction is assumed to be weak.

In order to clarify the situation with the HI scattering potentials we persued a program to accurately measure ^{16}O $+^{16}O$ scattering from very forward up to maximum feasible scattering angles covering both diffraction and refraction scattering phenomena. The closed shell nucleus has been selected to keep collective excitations leading to strong coupled channel effects in the elastic channel at a minimum. The projectile energies of $T_{lab} = 250 - 704$ MeV (i.e. kinetic energies per projectile nucleon: $T_{lab}/A = 16 - 44$ MeV) have been chosen to optimize the condition for observing nuclear rainbow phenomena.

The measurements on the ^{16}O + ^{16}O system at $T_{lab} = 250, 350$ and 480 MeV, published already in part in ref [2,5], have been carried out at HMI using the Q3D magnetic spectrograph. Additional recoil detection providing kinematical coincidences for background suppression has been performed in particular at backward angles, where the measured scattering cross sections reach the nb/sr-level. The scattering data for ^{16}O + ^{16}O at $E_{lab} = 704$ MeV have been obtained at GANIL using the high-resolution SPEG magnetic spectrometer. In all these measurements special attention has been paid to the calibration of the scattering angles and of the absolute cross section. The absolute scattering angles have been determined by the evaluation of kinematical shifts observed in the line spectra. The absolute cross section normalization has been obtained by overlapping forward angle measurements on $^{6}Li_2$ O, ^{40}Ca O, $^{51}V_2$ O_3 and ^{51}V targets, where the ^{16}O + ^{16}O measurements on the oxide targets can be related to each other and to the ^{16}O + ^{51}V measurements on the Vanadium target. The latter scattering has been measured up to very forward angles, where the cross section gets equal to the Coulomb cross section and effects from the strong interaction are negligible — allowing thus a reliable absolute normalization of the cross section as well as a further check of the scattering angle calibration. For a conservative estimate of the random uncertainties inherent in these measurements we have set the uncertainties of the data points to twice their values from pure count rate statistics. Details of these measurements are given in ref. [6].

The results of the measurements for the elastic scattering at all mentioned energies are shown in fig. 1, where they are plotted in dependence of the asymptotic momentum transfer $q = 2k \sin \frac{\Theta}{2}$. In this representation the diffraction pattern should be approximately independent of the projectile energy as is the case for pure Fraunhofer diffraction. Fig. 1 shows that the data in the diffractive region nicely support these expectations. The signature of refractive scattering is seen to develop steadily with increasing bombarding energy: focusing effect and shadow region are getting more pronounced and the refractive (rainbow) maximum (at position $q_N \sim 1/\sqrt{E}$, see ref. [7]) is moving towards smaller momentum transfers as the incident energy increases.

In fig. 2 we show the result of cross sections in mb/sr for the elastic, inelastic and reaction channels. Note that the cross sections have been measured over 9 orders of magnitude. The refractive (rainbow) bump is also well observed in the inelastic as well as in the transfer channel at $\Theta_{CM} \approx 20$ to 25°.

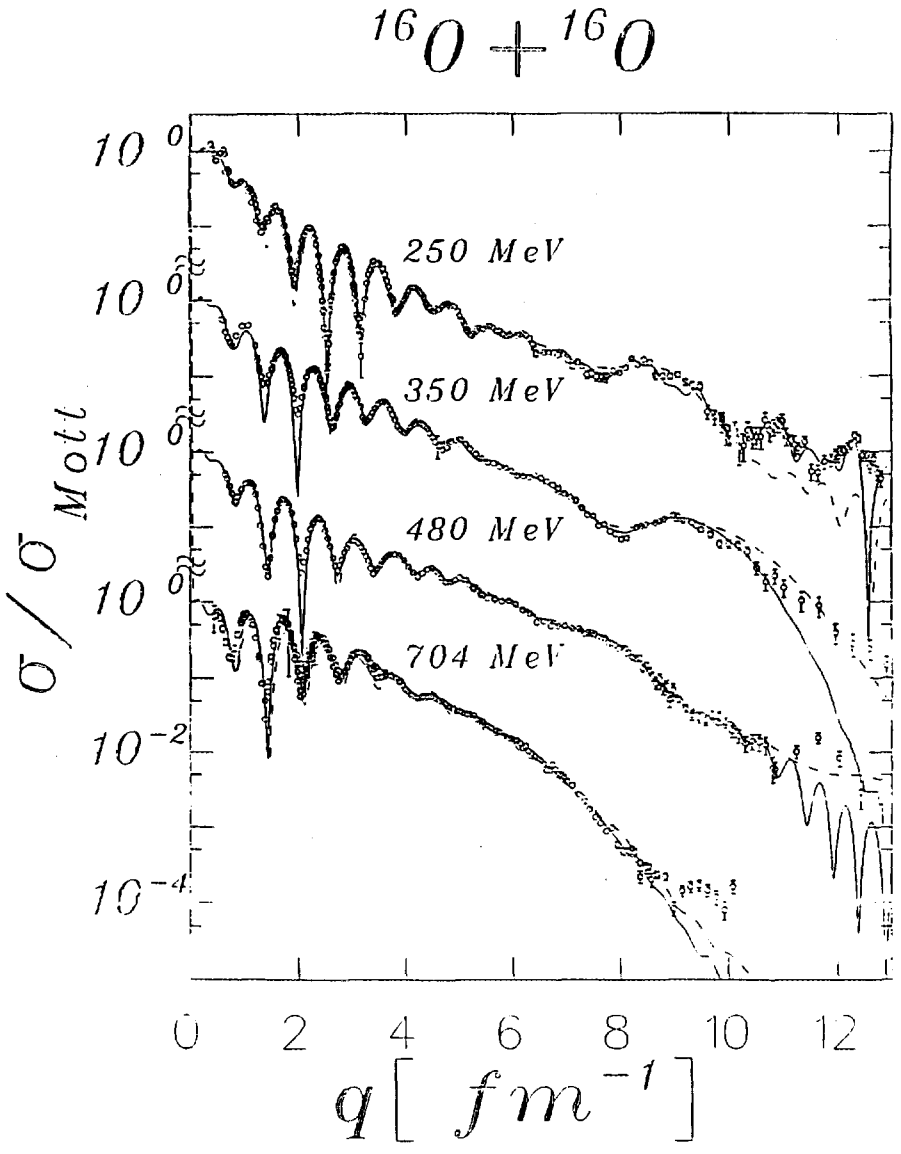

Fig. 1. *Elastic scattering cross sections, normalized to the Mott cross section, in dependence of the asymptotic momentum transfer q for* $^{16}O + ^{16}O$ *at* $T_{lab} = 250, 350, 480$ *and 704 MeV. The solid curves show the model-unrestricted LG-fits, whereas the dotted lines represent the* WS^2*-fits.*

The analysis of the data has been carried out in two different ways, at first in the conventional manner of using Woods-Saxon type form factors and secondly in the framework of model-unrestricted methods. Since in the folding concept the convolution of two Fermi distributions with a short ranged force leads to a potential form of "Woods-Saxon-Squared" type (WS^2), we used such form factors for the conventional Optical Model analysis. For the imaginary potential in addition we introduced a derivative WS^2 form to account for surface absorption phenomena. The result of these 9-parameter fits is shown in fig. 1 by the dashed lines with a chi square per degree of freedom, χ^2/F, being in the range 2 – 6. We note that we observe no longer a family problem [8,9,10] regarding potential depth-radius correlations as soon as we require a quantitative description of the data both in the diffractive and in the refractive scattering regions. In particular, the simultaneously mea-

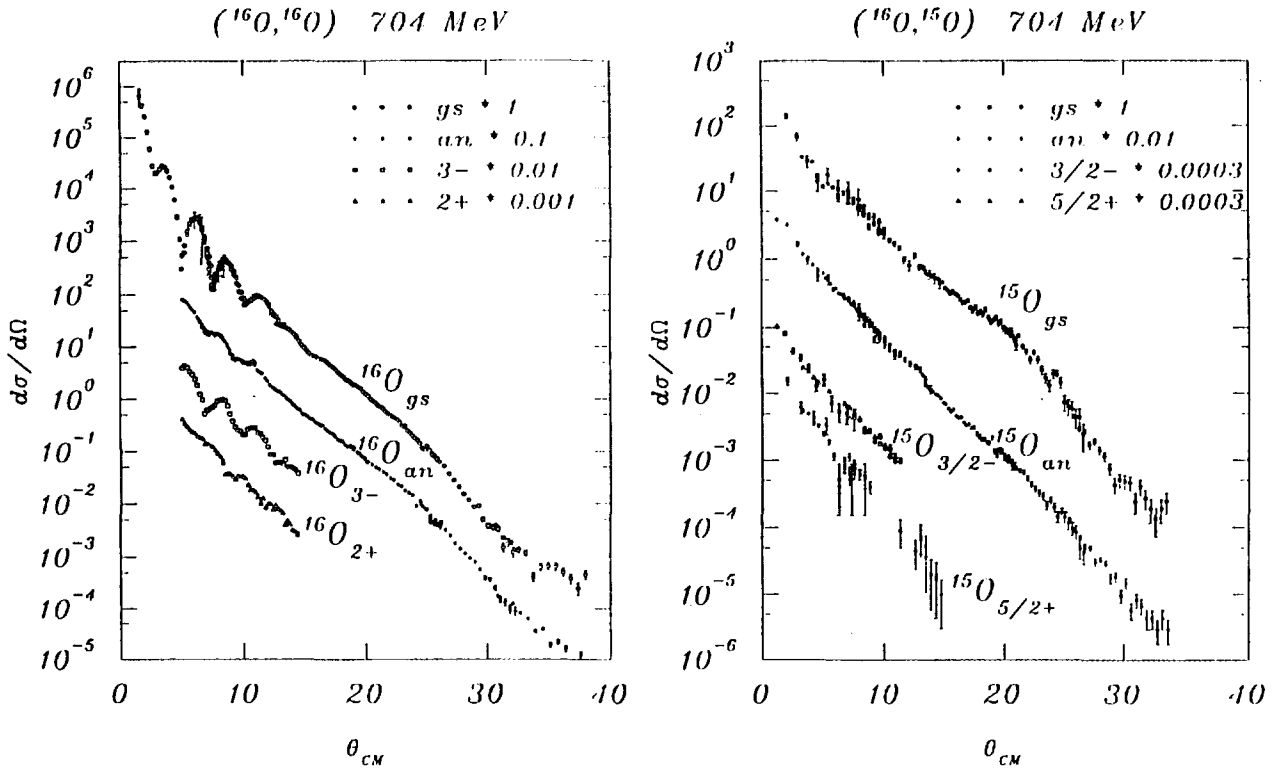

Fig. 2. *Experimental results for:*
a) elastic and inelastic scattering of $^{16}O + {}^{16}O$ *at* $E_{lab} = 704$ *MeV.*
b) the one neutron stripping channel ^{16}O $(^{16}O,^{15}O)$ ^{17}O. *Note the refractive (rainbow) bumbs in the region of* $\Theta_{CM} \approx 20$ *to* $25°$.

sured data for inelastic scattering and single-nucleon transfer require the correct potential family for a consistent description.

For the model-unrestricted analysis we expand real and imaginary potential parts into a series of Fourier-Bessel (FB) functions $j_0(q_n r)$ or Laguerre-Gaussian (LG) functions, the eigenfunctions of the 3-dimensional harmonic oscillator:

$$\begin{aligned} \text{FB:} \quad & U(r) = U_0(r) + \sum_{n=1}^{N} a_n j_0(q_n r); \qquad q_n = \frac{n\pi}{R_c}; \qquad r \le R_c \\ \text{LG:} \quad & U(r) \quad = U_0(r) + \sum_{\nu=1}^{N} b_\nu e^{-x^2} L_\nu^{1/2}(2x^2); \qquad x = r/b \end{aligned} \tag{1}$$

$U_0(r)$ is a conveniently chosen starting potential, e.g., the result of WS or WS^2 analyses. Of course, the final result of the model-unrestricted analyses must not depend on the particular starting potential. This has been verified in all our cases. R_c denotes a conveniently chosen cutoff radius, beyond which the FB expansion is set to zero. Further details are given in ref.[11]. The extracted model-unrestricted potentials are shown in fig. 3 together with their symmetric uncertainties (hatched areas) derived from the χ^2 error matrix in the usual way. The results of the conventional WS^2 type analyses are displayed by the dotted

lines. Both types of analyses give compatible results within the uncertainties derived in the LG analyses.

The volume integrals per nucleon pair and rms-radii of the real and imaginary potentials as obtained in the analyses of the scattering data at 250, 350, 480 and 704 MeV vary from 330 MeV fm^3 at 250 MeV to 275 MeV fm^3 at 704 MeV. Their energy dependence turns out to be quite small. The volume integrals of the imaginary potential per nucleon pair, J_I, are in the region of 100 – 140 MeV fm^3, i.e., within uncertainties compatible with values obtained in analyses of LI scattering [3,4].

These results from the model-unrestricted analyses show good agreement also with recent folding model analyses [5] on partially the same data basis. In these analyses real folding

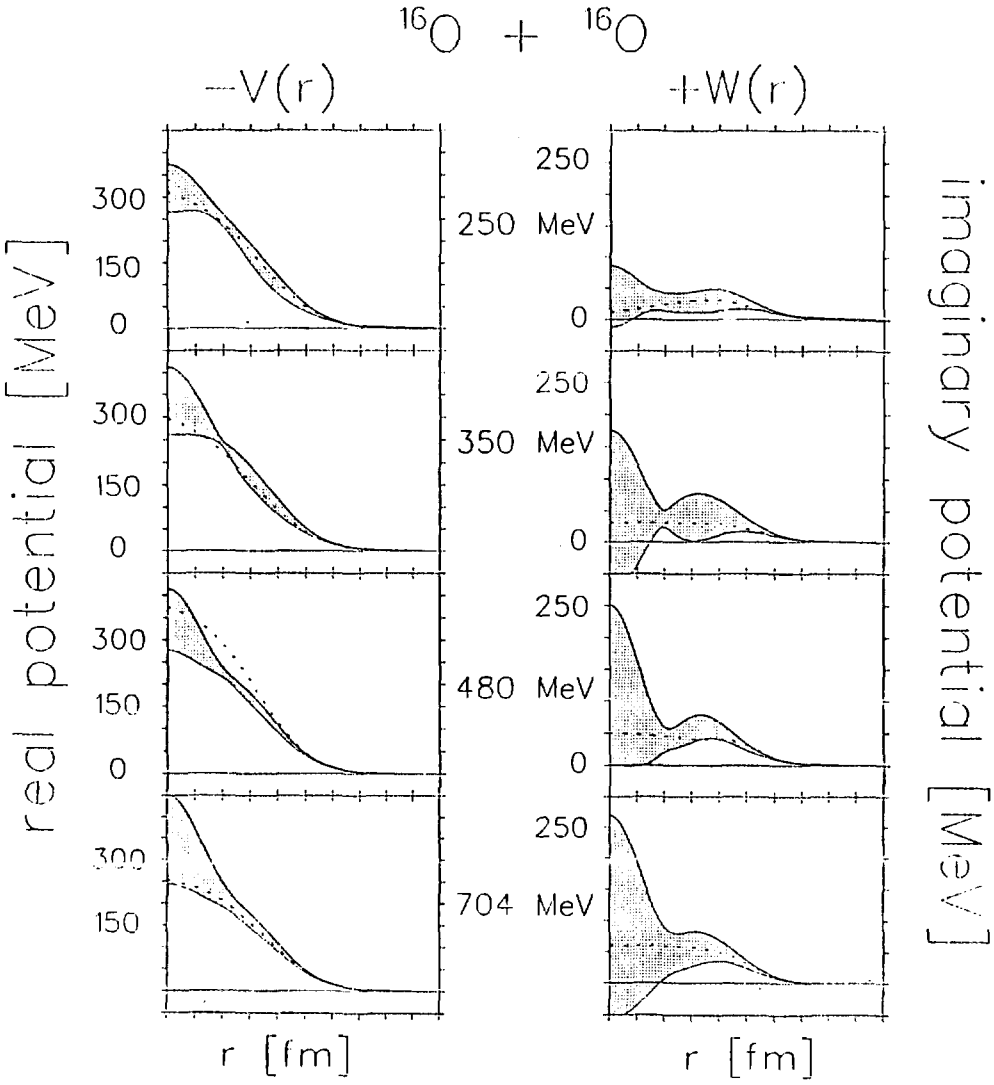

Fig. 3. *Real and imaginary potentials for the system ^{16}O + ^{16}O as extracted from the analyses of the scattering data. The solid lines show the model-unrestricted LG-results together with their uncertainties (hatched areas), whereas the dotted lines give the WS^2-results.*

potentials have been generated based on the M3Y representation [12] of the G-matrix elements of the Paris and the Reid-Elliot NN-interactions. The overall normalization of the real folding potential and the density dependence of the NN-interaction had been adjusted phenomenologically to fit the data and to reproduce the saturation properties of cold nuclear matter in a Hartree-Fock calculation. As a result it was found that the HI scattering data are compatible with folding potentials only, if the density dependence of the underlying effective NN interaction is weak in agreement with the findings in LI-scattering [4,5,13]. The model-unrestricted analyses of this work corroborate this statement.

We gratefully acknowledge valuable discussions with H. Müther and G. Staudt. We are gratefull to P. Maier-Komor for supplying us with Li_2O targets.

References

[1] for a survey see, e.g., G.R. Satchler: Direct Nuclear Reactions, Clarendon Press, Oxford 1983

[2] E. Stiliaris et al., Phys. Lett. **B223** (1989) 291
H.G. Bohlen et al., Z. Phys. **A346** (1993) 189

[3] M. Ermer et al., Phys. Lett. **B224** (1989) 40

[4] N. Heberle et al., Phys. Lett. **B250** (1990) 15

[5] Dao T. Khoa et al., Phys. Rev. Lett. **74** (1995) 34

[6] G. Bartnitzky, Ph.D. thesis, University of Tübingen, 1995;
A. Blazevic, diploma thesis, University of Tübingen, 1994
J. Siegler, diploma thesis, University of Tübingen, 1995

[7] J. Knoll and R. Schaeffer, Phys. Rep. **31** (1977) 159

[8] Y. Kondo, F. Michel, R. Reidemeister, Phys. Lett. **B242** (1990) 340

[9] M.E. Brandan and G.R. Satchler, Phys. Lett **B256** (1991) 311
M.E. Brandan, K.W. McVoy and G.R. Satchler, Phys. Lett. **B281** (1992) 185

[10] Y. Sugiyama et al., Phys. Lett. **B312** (1993) 35

[11] G. Bartnitzky et al., Phys. Lett. **B365** (1996) 23

[12] N. Anantaraman, H. Toki and G.F. Bertsch, Nucl. Phys. **A398** (1983) 269;
G.F. Bertsch et al., Nucl. Phys. **A284** (1977) 399

[13] Dao T. Khoa and W. von Oertzen, Phys. Lett. **B342** (1995) 6

Preliminary Results from E244: Spectroscopy of Very Proton-rich Nitrogen Isotopes

A. N. Ostrowski, A. Lépine-Szily*, A. Blasevic**, H.-G. Bohlen**, C. Borcea, V. Guimaraes*, R. Kalpakchieva***, R. Lichtenthäler Filho*, M. MacCormick, W. von Oertzen**, J. .M. Oliveira*, Y. E. Penionzhkevich***, N. A. Orr****, P. Roussel-Chomaz, T. Stolla**, J. S. Winfield****

*GANIL, Caen, France; * USPIF, São Paulo, Brazil **Hahn-Meitner-Institute, Berlin, Germany; ***JINR Dubna, Russia; ****LPC Caen, France;*

~~We have used ^{14}N-induced~~ Multi nucleon transfer reactions have been ~~performed~~ investigated at E_{lab}=426MeV on Carbon- and Boron-targets for the spectroscopy of the very proton-rich Nitrogen isotopes ^{11}N and ^{10}N, which are the mirror nuclei of ^{11}Be and ^{10}Li, respectively. The experiments have taken place at the energy-loss spectrometer of GANIL, SPEG. The spectra gained are presented.

We performed the ^{12}C(^{14}N,^{15}C)^{11}N reaction (Q_o = -31.92MeV) for the spectroscopy of ^{11}N, since it offers, ab initio, the most favourable conditions taking target impurity problems and accessible luminosities into account. The same reaction was used in the spectroscopy of ^{57}Cu performed by Stiliaris et al.[1]. As ^{15}C has two particle stable states, the spectrum is a superposition of the recoil's spectrum with both states. However, from the ^{57}Cu-spectroscopy we know, that the $5/2^+$ excited state of ^{15}C at 0.74MeV excitation energy is much more strongly populated than its ground state.

With the used beam/target combination, several two-body reactions with similar Q-value were strongly populated and their observation was a convenient means to confirm and improve our momentum resolution. The upper figure present our spectrum of the ^{12}C(^{14}N,^{14}C)^{12}N reaction (Q_o=-17.49MeV). Here, the ground state and two excited states of ^{12}N at 1.075MeV and 4.14MeV, respectively, are clearly to be seen. From the ground state spectrum we could deduce our resolution to be 400keV and the precision found was 40keV. A further analysis of this spectrum asked for a deconvolution of the first excited state into two states at 0.96MeV and 1.19MeV excitation energy. In addition, two states at 3.13MeV and 3.56MeV contribute significantly to the spectrum as well as a background coming from highly excited ^{15}N-nuclei that decayed in flight into ^{14}C and a proton.

In the lower figure we present a partial spectrum of the ^{15}C ejectiles, corresponding to the ^{12}C(^{14}N,^{15}C)^{11}N reaction, obtained with a 0.5mg/cm^2 carbon target and accumulating data during 10 hours. This spectrum does not show the whole statistics we accumulated during the experiment for this reaction, since we are still analyzing data. Gaussian peaks were adjusted to the peaks superimposed on a background originating in highly excited ^{16}N-nuclei that decayed in flight into ^{15}C and a proton. Two broad peaks dominate the spectrum. Using the fact, that only the excited state in ^{15}C is strongly populated, they have been deconvoluted into two states each by using the known energies and widths parameters measured by Benenson et al.[2] (E_x=2.24MeV) and Guimaraes et al.[3] (E_x=3.57MeV and 4.29MeV, respectively). In addition, a week indication of a resonance at E_x=1.92MeV is found, which is the ground state value that has been deduced from the

mirror nucleus ^{11}Be and was adopted in the Audi and Wapstra tables. We acknowledge support from the European Community under contract n° CHGE-CT94-0056 (Human Capital and Mobility, Access to the GANIL large scale facility)

[1] E. Stiliaris et al., Z. Phys. A330, 227 (1988)
[2] W. Benenson et al., Phys. Rev. C9, 2130 (1974)
[3] V. Guimaraes et al. private communication

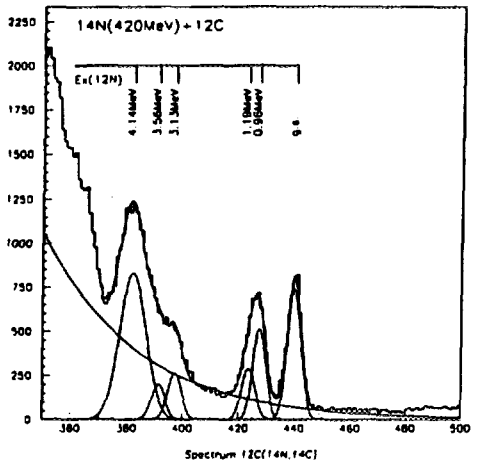

$^{12}C(^{14}N,^{14}C)^{12}N$

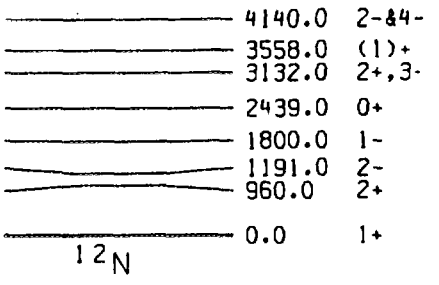

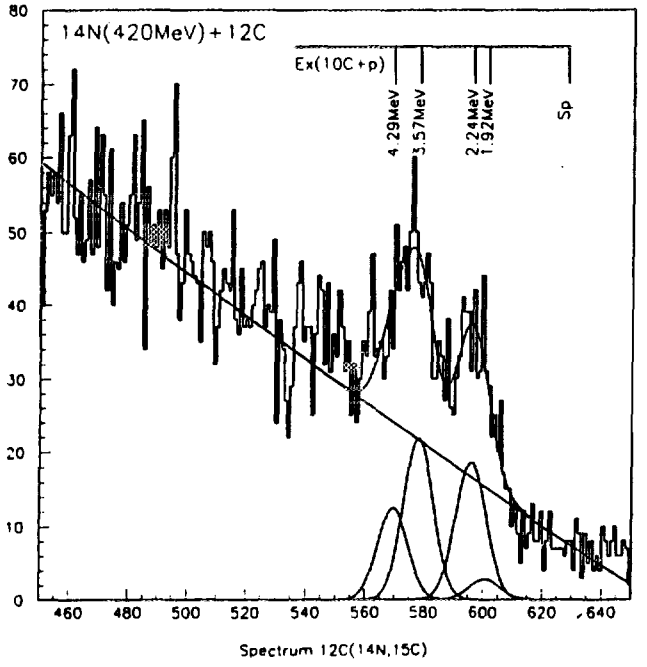

$^{12}C(^{14}N,^{15}C)^{11}N$

Charge exchange reaction induced by ^{6}He

M.D. Cortina-Gil[1], P. Roussel-Chomaz[1], N. Alamanos[2], J. Barrette[3], W. Mittig[1], F. Auger[2], Y. Blumenfeld[4], J.M. Casandjian[1], M. Chartier[1], V. Fekou-Youmbi[2], B. Fernandez[2], N. Frascaria[4], A. Gillibert[2], H.Laurent[4], A.Lépine-Szily[1,5], N.A. Orr[6],V. Pascalon[4], J.A. Scarpaci[4], J.L. Sida[2], T. Suomijärvi[4]

1) GANIL (DSM/CEA,IN2P3/CNRS), BP 5027, 14021 Caen Cedex, France
2) CEA/DSM/DAPNIA/SPhN Saclay, 91191 Gif-sur-Yvette Cedex, France
3) Foster Radiation Lab., Mc Gill University, Montreal, Canada H3A 2B1
4) IPN, IN2P3/CNRS, 91406 Orsay Cedex, France
5) IFUSP,DFN, C.P. 20516, 01498, Sao Paulo, S.P., Brasil
6) LPC-ISMRA, Blvd du Maréchal Juin, 14050 Caen, France

Abstract: The charge exchange reaction p(^{6}He,^{6}Li)n has been measured. No clear signature of a halo structure was found in the present data, due to the lack of large angle measurement.

1 Introduction

The (p,n) charge exchange reaction has been a privileged tool to explore nuclear structure and nuclear interactions. This reaction is highly selective since only isobaric analog states (IAS) and Gamow-Teller (GT) resonances are strongly populated. The transition to the IAS is a $\Delta T=1$, $\Delta S=0$ non spin flip Fermi transition (F), whereas the excitation of GT resonances proceeds via a $\Delta T=1$, $\Delta S=1$ spin flip transition, induced respectively by the V_{τ} and $V_{\sigma\tau}$ components of the nucleon-nucleon interaction. In particular, these studies provide information on the spectroscopic strength of the states involved in these reactions, on the fraction of the sum rule exhausted by these transitions, and on the interactions V_{τ} and $V_{\sigma\tau}$ [1].

Both the ground state of ^{6}He and its isobaric analog state in ^{6}Li are expected to behave like halo states [2-5], therefore two reasons motivated us for the study of the p(^{6}He,^{6}Li)n reaction: one is the possibility to get information on the interactions V_{τ} and $V_{\sigma\tau}$ in a low density region, the other is the sensitivity of the transition leading to the IAS with respect to the differences between the neutron and proton density distributions, as this was shown for example for a series of Sn isotopes [6]. Taking into account the significant effect observed for very small differences of radii in the Sn case, we would expect very strong effects in the case of the halo nuclei considered here.

2 Charge exchange reaction: p(^{6}He,^{6}Li)n

The experimental method has been described in another contribution to this compilation.

The charge exchange reaction cross section can be compared to β decay strength. This comparison for Fermi and GT transitions provides an essentially model independent means to

extract the V_τ and $V_{\sigma\tau}$ interactions or more precisely their volume integral. A detailed review of this aspect can be found in ref. [1].

We have studied in the case of the present data for the p(^{6}He,^{6}Li)n reaction if we could extract a signature of the presence of a halo structure in $^6He_{g.s.}$ and its IAS in ^{6}Li, from the ratio of the cross sections for the Fermi and GT transitions. Indeed, the ratio R defined by the relation

$$R^2=\widehat{\sigma_{GT}}/\widehat{\sigma_F} \qquad (2)$$

where σ is a unit cross section depending on the incident energy and the target mass, is closely related to the ratio of the volume integral J_τ and $J_{\sigma\tau}$ of the interactions V_τ and $V_{\sigma\tau}$. It can be expressed as:

$$R=\left|\frac{J_{\sigma\tau}}{J_\tau}\right|\left(\frac{N_{\sigma\tau}}{N_\tau}\right)^{1/2}\approx\left|\frac{J_{\sigma\tau}}{J_\tau}\right| \qquad (3)$$

where N_τ and $N_{\sigma\tau}$ are distortion factors defined by the ratio of the plane wave to distorted wave amplitudes. At the present energy, the ratio $N_{\sigma\tau}/N_\tau$ is close to 1.

As shown is ref. [1], R can be determined experimentally and it is related to the 0° cross sections by the relation:

$$R^2=\frac{\sigma_{GT}(0°)(N-Z)}{\sigma_F(0°)B(GT)} \qquad (4)$$

A compilation of the ratio R obtained using equation (4) for N=Z+2 nuclei is shown on Fig. (1). The data corresponding to ^{7}Li, ^{14}C, ^{18}O, ^{26}Mg(p,n) reactions are from ref [7-10],

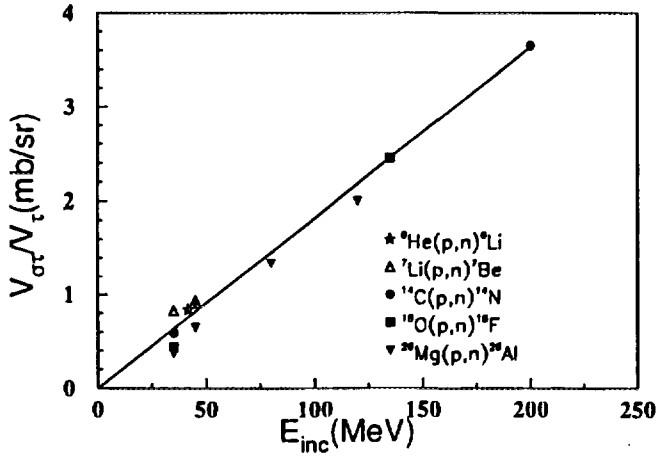

Fig. (1): Compilation of the reduced transition strength ratio R of GT and Fermi charge exchange transitions in light nuclei as a function of the incident energy of the proton.

and the calculation used the B(GT) values from Taddeucci et al [1]. The linear energy dependence of R is a well established behaviour observed for many stable nuclei [1] and has

been attributed to the energy dependence of the V_τ potential. Brown, Speth and Wambach [11] have shown, using a meson exchange model, that this energy dependence arises essentially from a two pion exchange contribution to the V_τ potential.

The ratio R was also computed for the transitions measured in the present experiment, by applying equation (4). The value of B(GT) which is necessary to compute R was obtained from β decay lifetime measurements and is given in ref. [1] for the inverse β decay transition ^{6}Li--->^{6}He.

It is known that the volume integral of the spin-isospin term $J_{\sigma\tau}$ measured for ^{6}Li(n,p)^{6}He ground state (GT) transition is in good agreement with the values obtained for other systems [12], as well as with the theoretical predictions of Nakayama and Love [13]. The ratio R, or $\left|\frac{J_{\sigma\tau}}{J_\tau}\right|$ measured in the present experiment is in agreement with the systematic behaviour established for T=1 nuclei. This means that the isospin term J_τ also shows no deviation from the values obtained for stable nuclei. Therefore we conclude that, from the ratio of the cross sections at 0°, we can not see any difference between a transition connecting two halo states, or one halo state and a standard one, and finally two standard states[14].

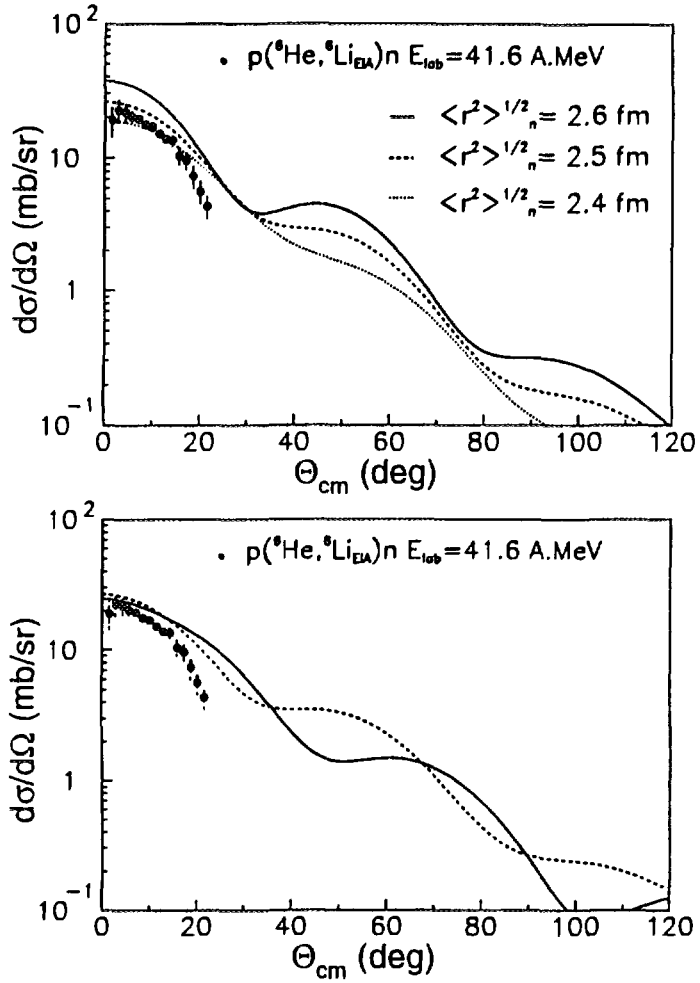

Fig(2): Top, Influence of the r.m.s. radius of the density distribution on the charge exchange density distribution. Bottom, Influence of the shape of the density distribution (see text)

The upper part of Figure (2) presents the angular distribution measured for the Fermi transition connecting the ^{6}He ground state and its isobaric analog state compared to the predictions obtained by using the JLM optical potential for the entrance and exit channel, and by estimating the transition potential with the Lane equations [15]. The different curves correspond to different values of the r.m.s. radius for the ^{6}He density distribution, which was assumed for these calculations of gaussian shape.

The rather large differences observed between the different curves show that the angular distribution is very sensitive on the complete angular range to the value of the r.m.s. radius of the density distribution. However differences in the detailed shape of the densities manifest themselves only at large angles. The lower part of Figure (2) compares the angular distributions obtained for different density distributions of ^{6}He and ^{6}Li having the same r.m.s. radius but different shape in the tail: the dashed line corresponds to gaussian shape, whereas the solid line corresponds to the density distributions calculated by Arai et al.[5]. The calculated angular distributions differ significantly only above Θ_{cm}=40°, whereas the present data do not extend above Θ_{cm}=20°. Therefore it would be extremely interesting to obtain new data at larger angles.

3 Conclusions

From the analysis of the (p,n) charge exchange reaction at 0° connecting the ^{6}He ground state and the ^{6}Li ground state or the IAS at 3.56 MeV, we conclude that the presence or absence of a halo structure does not influence the transition strength in a (p,n) reaction. The influence of the halo seems to manifest itself only in the backward part of the angular distributions of the charge exchange reaction.

References

[1] T.N. Taddeucci et al., Nuclear Physics A 469 (1987) 125

[2] I. Tanihata et al., Phys. Rev. Lett. 55 (1985) 2676

[3] M.V. Zhukov et al., Nucl.Phys. A 533 (1991) 428

[4] K. Varga, Y. Suzuki,and Y. Ohbayashi, Phys.Rev. C 50 (1994) 189

[5] K. Arai,Y. Suzuki, and K. Varga, Phys. Rev. C 51 (1995) 2488

[6] S.D. Schery et al., Phys. Rev C 14 (1976) 1800

[7] S. M. Austin et al, Phys. Rev. Lett. 44 (1980) 972

[8] T.N. Taddeucci and R.R. Doering, Phys. Rev. C 29 (1984) 764
W.P. Alford et al, Phys. Lett. B 179 (1986) 20
M. Kabasawa et al, Phys. Rev. C 45 (1992) 1220

[9] B.D. Anderson et al, Phys. Rev.C 27 (1983) 1387
M. Oura et al, Nucl. Phys. A 586 (1995) 20

[10] W.A. Sterrenburg et al, Phys. Lett. B 91 (1980) 337

[11] G.E. Brown, J. Speth, and J. Wambach, Phys. Rev. Lett. 46 (1981) 1057

[12] D.S.Sorensen et al, Phys. Rev. C 45 (1992) R500

[13] K. Nakayama and W.G. Love, Phys. Rev. C 38 (1988) 51

[14] M.D. Cortina-Gil et al, Phys.Lett. B371 (1996) 14

[15] A.M. Lane, Nucl. Phys. 35 (1962) 676

Search for Double Gamow-Teller Strength by Heavy-Ion Double Charge Exchange

J. Blomgren[1], K. Lindh[2], N. Anantaraman[3], Sam M. Austin[3], G.P.A. Berg[4], B.A. Brown[3], J.-M. Casandjian[5], M. Chartier[5], M.D. Cortina-Gil[5], S. Fortier[6], M. Hellström[3], J.R. Jongman[6], J.H. Kelley[3], A. Lepine-Szily[7], I. Lhenry[6], M. Mac Cormick[5], W. Mittig[5], J. Nilsson[1], N. Olsson[1], N.A. Orr[8], E. Ramakrishnan[3], P. Roussel-Chomaz[5], B.M. Sherrill[3], P.-E. Tegnér[2], J.S. Winfield[3], J.A. Winger[3]

1) Department of Neutron Research, Uppsala University, Uppsala, Sweden
2) Department of Physics, Stockholm University, Stockholm, Sweden
3) NSCL, Michigan State University, East Lansing, MI 48824, USA
4) Indiana University Cyclotron Facility, Bloomington, IN 47408, USA
5) Grand Accélérateur National d'Ions Lourds, Caen, France
6) Institut de Physique Nucléaire, Orsay, France
7) IFUSP, DFN, Sao Paulo, Brazil
8) Laboratoire de Physique Corpusculaire, IN2P3 - CNRS, Caen, France

Abstract →

Among two-phonon giant resonances, the double Gamow-Teller resonance (DGTR) is of special interest, not only for the understanding of nuclear phenomena, but also because of links to particle and astroparticle physics via the connection to the double beta decay and its implications for the neutrino mass, lepton number conservation and the missing dark matter of the universe.

Heavy-ion double charge exchange has been suggested as a probe for DGT strength. Studies at NSCL-MSU and GANIL of the (^{6}Li,^{6}He) and (^{12}C,^{12}N) reactions at 35 and 70 MeV/nucleon, respectively, show that heavy ion reactions can be used to extract (single) Gamow-Teller strength [1]. However, the double charge-exchange (DCX) reaction rates are expected to be small. A way of increasing them is to use a projectile and an ejectile which belong to the same $SU(4)$ multiplet in S and T. This is in practice fulfilled only when the projectile and ejectile are located symmetrically around $N = Z$.

The only giant resonance for which both the one- and two-phonon cross sections have been measured with similar reactions is the IVDR, which has been studied by the ($\pi^{\pm}$,π^0) (one-phonon) [2] and the (π^+,π^-) (two-phonon) [3] reactions. Using a B(GT) calibration from single charge exchange, the shell model calculation below, and a simple model for the DCX cross section in terms of the SCX cross sections by Bertsch [4] yields a cross section of 24 μb/sr.

Bertulani [5] has developed an eikonal approximation model for heavy-ion charge exchange reactions, in which he predicted that the cross sections for DGT excitation in heavy-ion reactions should be - at most - in the μb/sr region. It was pointed out that there is a suppression mechanism of heavy-meson exchange in heavy-ion reactions. Instead of a large contribution from ρ mesons in the reaction mechanism - which is the case for reactions induced by pions and nucleons - the larger interaction distance in heavy-ion reactions favour pion exchange. This

results in a much weaker charge-exchange, and hence much smaller cross sections. Thus, these two predictions differ by several orders of magnitude.

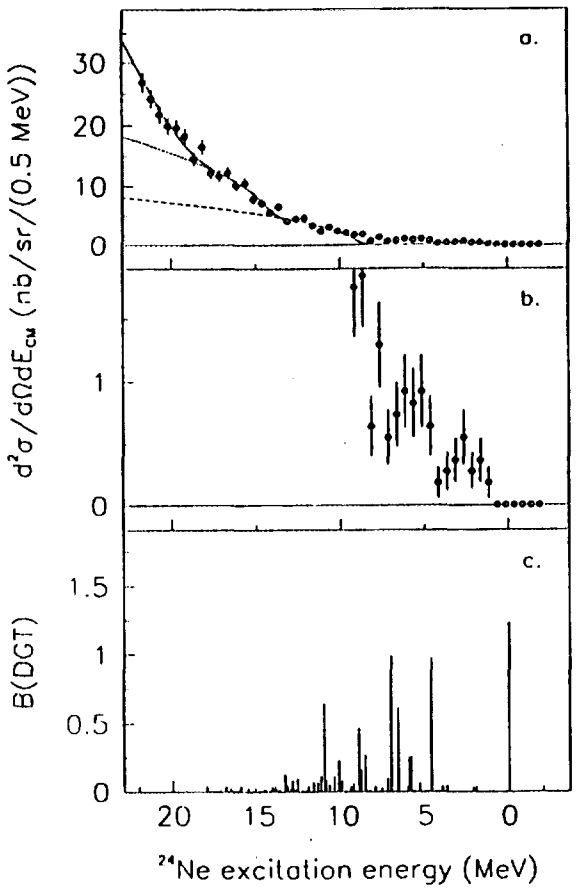

Figure 1: The differential cross section for the ^{24}Mg(^{18}O,^{18}Ne)^{24}Ne reaction at 76 · A MeV, for the entire solid angle covered. Panel a) shows a fit of a sum (solid) of the phase-space distributions for one-neutron(dashed), two-neutron (dotted) and one-proton breakup(solid). Panel b) shows the ground-state region with an expanded vertical scale. In panel c), our DGT strength calculation calculation is displayed. See the text for details.

Theoretical calculations by B. A. Brown indicate that significant concentration of DGT strength in ^{24}Ne should be found in the ground state and an excited state at 4.7 MeV, with the remaining strength spread broadly at higher energies.

~~Guided by this, we have carried out a search for~~ Double Gamow-Teller excitations, ~~employing~~ the ^{24}Mg(^{18}O,^{18}Ne)^{24}Ne reaction at 100 and 76 MeV/nucleon ~~at NSCL-MSU and GANIL, respectively~~ [6]. The first attempt was made at NSCL-MSU, where an upper limit of the cross sections to low-lying states in the 100 nb/sr region was established. The meagre statistics prompted a second experiment at GANIL, where substantially more intense beams can be delivered, although at a slightly lower energy. The results presented here are from the GANIL run only.

are searched for, using

In the experiment, $^{18}O^{8+}$ ions of $76 \cdot A$ MeV, with an intensity of 100-200 enA, were extracted from the GANIL accelerator system. The momentum analysis of the ejectiles was performed with the energy-loss spectrometer SPEG, covering an angular range from $-1°$ to $+3°$. A self-supporting ^{24}Mg target, 3.5 mg/cm^2 thick, and with an isotopic purity of 99 %, was mounted in the scattering chamber. The energy resolution of 1.0 MeV was dominated by the target energy loss difference for ^{18}O and ^{18}Ne.

The data for the entire solid angle acceptance are displayed in figs. 1a and b. No pronounced peaks are present in the spectrum. In b, which displays the ground-state region, there might be structures at excitation energies of 2.8 and 6.2 MeV in ^{24}Ne. These structures do not correspond to any known states in ^{24}Ne. The statistical uncertainty prevents any far-reaching conclusions. One feature to note, however, is that the low-energy excitation intervals display rather flat angular distributions. This does not support a double Gamow-Teller origin of these excitations, at least not as two consecutive $L = 0$ transitions, which can be expected to be more forward-peaked.

From the data, we can deduce that in the 0–1°(C.M.) interval, the average differential cross section to states which are unambiguous excitations in ^{24}Ne, i.e., which lie below the neutron breakup threshold (E_x = 8.9 MeV), is 20.1 ± 2.9 nb/sr. The error quoted is statistical. The systematic error is estimated to be about 30 %.

The present results provide evidence for a strong suppression of double Gamow-Teller excitations. Thereby, they are qualitatively compatible with the Bertulani model. However, we can only deduce an upper limit of the cross section, and it cannot be excluded that the DGT excitation is even weaker. This result seems to preclude the use of heavy ions at intermediate energies for probing double Gamow-Teller strength.

1) N. Anantaraman, J.S. Winfield, Sam M. Austin, J.A. Carr, C. Djalali, A. Gillibert, W. Mittig, J.A. Nolen, Jr., Zhan Wen Long, Phys. Rev. **C44** (1991) 398.

2) A. Erell, J. Alster, J. Lichtenstadt, M.A. Moinester, J.D. Bowman, M.D. Cooper, F. Irom, H.S. Matis, E. Piasetzky, U. Sennhauser, Phys. Rev. **C34** (1986) 1822

3) S. Mordechai and C. Fred Moore, Nature **352** (1991) 393.

4) G. Bertsch, private communication.

5) C. Bertulani, Nucl. Phys. **A554** (1993) 493.

6) J. Blomgren, K. Lindh, N. Anantaraman, Sam M. Austin, G.P.A. Berg, B.A. Brown, J.-M. Casandjian, M. Chartier, M.D. Cortina-Gil, S. Fortier, M. Hellström, J.R. Jongman, J.H. Kelley, A. Lepine-Szily, I. Lhenry, M. Mac Cormick, W. Mittig, J. Nilsson, N. Olsson, N.A. Orr, E. Ramakrishnan, P. Roussel-Chomaz, B. Sherrill, P.-E. Tegnér, J.S. Winfield, J.A. Winger, Phys. Lett. **B362** (1995) 34.

NUCLEAR SPIN ALIGNMENT AND QUADRUPOLE MOMENT OF LIGHT PROJECTILE FRAGMENTS STUDIED WITH THE LEVEL MIXING RESONANCE (LMR) METHOD.

G.Neyens[+], N.Coulier[*], S.Ternier[*], K.Vyvey, R.Coussement and D.Balabanski[#]
Katholieke Universiteit Leuven, Instituut voor Kern- en Stralingsfysica,
Celestijnenlaan 200D, B-3001 Leuven, Belgium

J.M.Casandjian, M.Chartier, D.Cortina-Gil, M.Lewitowicz, W.Mittig, A.N.Ostrowski and P.Roussel-Chomaz
Grand Accélérateur National d'Ions Lourds, BP 5027, F-14021 Caen Cedex, France

N.Alamanos
Dapnia/SPhN, Batiment 703, Orme des Merisiers, C.E. Saclay
F-91191 Gif-sur-Yvette Cedex, France

~~We have determined~~ The spin alignment of ^{12}B and ^{18}N projectiles produced in intermediate energy projectile fragmentation reactions ~~and mass separated with the GANIL mass spectrometers SPEG and LISE3~~. The spin alignment was derived from the resonant change of the β-anisotropy as a function of an externally applied magnetic field. The amplitude of the measured resonance is proportional to the initial alignment of the projectile fragments, while the position of the resonance is proportional to their quadrupole moment. This measuring technique, called the "Level Mixing Resonance" method, thus allows to extract information on the reaction mechanism as well as on the nuclear structure of the projectile fragments.

Introduction

Recent experiments on intermediate and high energy projectile fragmentation reactions have shown that the spins of the projectile fragments emitted in the forward direction are aligned when a cut in the longitudinal momentum distribution is selected [1,2]. Alignment of the projectile fragments allows us to study the magnetic and quadrupole moment of these exotic nuclei, which are of current interest in many theoretical and experimental investigations [3-6]. These light nuclei decay by emission of β^- or β^+ particles, which allow to measure the polarization of the nuclear ensemble. If we are starting from an aligned ensemble produced in a fragmentation reaction, an interaction that transforms the alignment into polarization is needed to allow a β-asymmetry measurement. The Level Mixing Resonance method allows this transfer of alignment into polarization. The great advantage of such measuring technique is that the fragments emitted in the forward direction can be selected, giving the highest yield, and β-detection can be used, which is much more efficient than γ-detection. This should make the study of nuclear moments of weakly produced nuclei possible, which is highly interesting near the neutron and proton drip-lines.

Experimental procedure.

A detailed description of the Level Mixing Resonance method is given in reference 7. Modifications to the theory for measurements at a fragment mass analyzer are described in reference 8. Two interactions play a crucial role in a LMR-experiment : a quadrupole interaction between the static quadrupole moment of the nucleus and the electric field gradient induced by the host lattice and a magnetic interaction between the nuclear magnetic moment and an externally applied static magnetic field. In the experiments described here, a Mg single crystal (hcp-lattice, 348 mg/cm^2) was used to stop the secondary beam of interest. To slow down the secondary beam and to stop heavy contaminants, an Al-degrader was placed in front of the crystal but well shielded from the detectors. The crystal was oriented such that its c-axis makes a well defined angle $\beta = 6(1)°$ with respect to the magnetic field axis. The β-anisotropy was measured in two plastic scintillators placed at 0° (N_u) and 180° (N_d) with respect to B. To correct the measured anisotropy for experimental asymmetries and beam intensity fluctuations, we calculated the normalized ratio $R = \left(\frac{N_u}{N_d}\right) / \left(\frac{N_u}{N_d}\right)_{B=0}$. For pure Gamov-Teller β^- decay, the function $F = \frac{1-R}{1+R}$ equals the polarization P of the β-particles. In general, the function F is related to the theoretical angular distribution as $\frac{1-R}{1+R} = \frac{W(180)-W(0)}{W(180)+W(0)}$. For an initially aligned ensemble of nuclear spins and detection of allowed β-decay this expression can be written as

$$F = -A_1 B_1^0(\nu_Q, \omega_B, \tau, I) = -A_1 B_2^0(t=0) G_{12}(\nu_Q, \omega_B, \tau, I).$$

A_1 is the asymmetry parameter of the $\beta^\pm$ - decay, $B_1^0(\nu_Q, \omega_Q, \tau, I)$ is related to the measured polarization, $B_2^0(t=0)$ is the initial orientation tensor related to the alignment of the secondary beam and G_{12} is related to the Level Mixing interaction causing a change of alignment into polarization [8]. This perturbation factor can be calculated numerically by diagonalizing the interaction Hamiltonian. It also contains all information on the experimental situation (such as use of Wien filter, dipole fields between point of production and point of measurement, ...). It has a resonant behavior as a function of the magnetic field strength.

Results

Four experiments have been performed with two different primary beams. An overview is given in the table below. The first experiment was with a parasitic beam and was performed in 1 hour of actual beam time. In two experiments projectiles were selected in the wing of the longitudinal momentum distribution, because previous measurements by Asahi et al [1] reported a larger alignment in this situation.

Nr	Primary beam	Target	Second. beam	momentum	count rate
1	^{13}C, 75 MeV/u	^{12}C (35 mg/cm^2)	^{12}B at SPEG	center	2000 c/s
2	^{22}Ne, 60 MeV/u	^{9}Be (185.5 mg/cm^2)	^{12}B at LISE3	right wing	600 c/s
3	"	"	^{18}N at LISE3	right wing	250 c/s
4	"	"	^{18}N at LISE3	center	50 c/s

The measured LMR-curves are given in figure 1. The data are fitted with the theoretical curve described in [8]. The parameters in the fit procedure are the asymmetry parameter, the initial orientation parameter, the quadrupole frequency, the magnetic moment and the nuclear spin. For ^{12}B all parameters are known ($I^{\pi} = 1^{+}$, $t_{1/2}$ = 20.4 ms, μ =1.003 n.m., ν_Q = 46.5(5) kHz) [9,10], except the initial orientation, while for ^{18}N ($I^{\pi} = 1^{-}$, $t_{1/2}$ = 630 ms) the quadrupole frequency and the magnetic moment, as well as the asymmetry parameter are unknown. We used a calculated value A_1 = 0.19(3) to extract the initial alignment from the fitted amplitude. The position of the resonance is sensitive to the ratio ν_Q/μ and the data have been fitted using a value $\mu(\pi p_{1/2}^{-1} \nu d_{3/2})$ = 0.46 n.m. The results of the fits are on the pictures. We can conclude that the alignment of the secondary beam is largest in the center of the momentum distribution, in contrast to the result of Asahi [1]. In Ref. [2] a similar result was found but for a higher-energy reaction. Remark that even if 10 nucleons have to be removed from the projectile (^{22}Ne → ^{12}B), we still have some small alignment. As for the quadrupole moment of ^{18}N, we can not draw any firm conclusions yet. The large frequency indeed indicates a large Q-moment for ^{18}N, but we have to complete these data with measurements of the magnetic moment of ^{18}N as well as the electric field gradient of N(Mg) at liquid He temperature to extract its value from the experimental data.

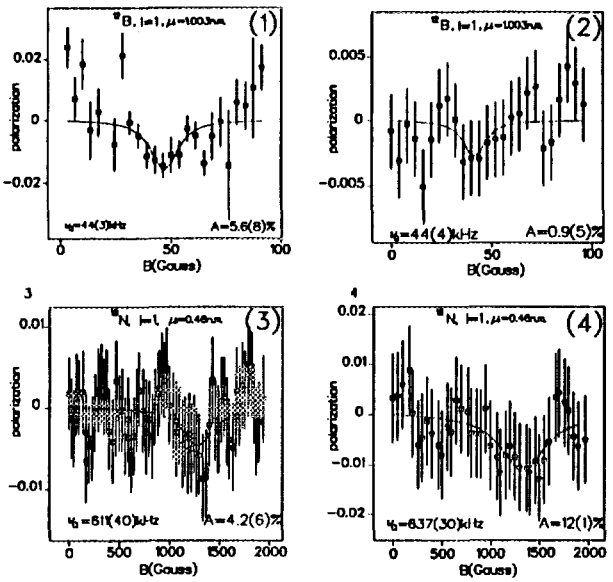

Figure 1 : Results of the 4 LMR-measurements performed on projectile fragments. The numbers on the figures refer to the experiment number in table.

(*,+) N.C. and S.T. are gratefull for the financial support by the I.W.T. and G.N. is a post-doctoral researcher of the Belgian National Science Foundation (N.F.W.O.)

(#) On leave from the University of Sofia, Bulgaria

References

[1] K. Asahi et al., Phys. Rev. C 43 (1991) 456
[2] W.-D. Schmidt-Ott et al., Z. Phys. A350 (1994) 215
[3] S.K. Patra, Nucl. Phys. A559 (1992) 73
[4] H. Horiuchi et al., Z. Phys. A349 (1994) 279
[5] T. Otsuka et al., Phys. Rev. Lett. 70 (1993) 1385
[6] M. Keim et al., Hyp. Int. 97/98 (1995) 543
[7] R. Coussement et al., Hyp. Int. 23 (1985) 273
[8] G. Neyens et al., Nucl. Inst. and Methods A340 (1994) 555
[9] P. Raghavan, At. Dat. & Nucl. Dat. Tab. 42 (1989) 189
[10] R. Vianden, Hyp. Int. 35 (1987) 1079

DECAY OF GIANT RESONANCES AND MULTIPHONON STATES.

J.A.Scarpaci, D.Beaumel, Y.Blumenfeld, N.Frascaria, J.P.Garron
H.Laurent, J.H.Le Faou, I.Lhenry, V.Pascalon-Rozier, J.C.Roynette, T.Suomijärvi
Institut de Physique Nucléaire
91406 Orsay Cedex, France

and

P.Roussel-Chomaz, Ph.Chomaz
GANIL, BP 5027, 14021 Caen Cedex, France

and

A.Van der Woude
Kernfysisch Versneller Institut, 9747 AA Groningen, The Netherlands

1. Introduction

Giant resonances (GR) are the most important collective modes of the nucleus. They have been studied for more than 40 years, however an important piece of the puzzle was missing. Indeed, if a GR is understood as the first oscillator quantum, higher quanta are expected, the multiphonons: a GR built on top of other GRs[1]. One powerful method to get a clear evidence of their excitation is to compare their particle decay to the GR decay.

2. Decay of GRs and multiphonon states

As it is well known, particle decay of GRs can occur through various processes [2], mainly the direct decay into hole states of the (A-1) residual nucleus with an escape width $\Gamma^{\uparrow}$, and the statistical decay leading to the spreading width, $\Gamma^{\downarrow}$. Statistical decay depends only on the excitation energy and angular momentum of the state. Direct decay, on the other hand, can yield information on the microscopic nature of a resonance. This is of utmost importance to sign the excitation of multiphonon states. If one admits the harmonic approximation, all phonons of a multiphonon state will decay independently, each phonon exhibiting the same fingerprints as the decay of the one-phonon GR.

2.1. Experimental method

~~We have studied~~ The decay of GRs and high lying states in ^{40}Ca[3], ^{48}Ca[4] and ^{94}Zr excited through inelastic scattering of ^{40}Ca, ^{20}Ne and ^{36}Ar respectively at about 50 MeV per nucleon. Recent data on ^{58}Ni and ^{62}Ni are currently under analysis.

The excitation energy E^* is obtained from the energy loss of the projectile measured by a spectrometer. At GANIL, the SPEG spectrometer associated with its

standard detection system is used[5]. An unambiguous identification of scattered projectiles is achieved. The energy resolution is 800 keV in the case of the Ca beam and about 400 KeV for the Ne beam. The angular resolution is around 0.2°.

To detect the light particles emitted, 30 CsI elements of the multi-detector array PACHA[6] were placed around the target in the reaction chamber for the proton decay (^{40}Ca). The total solid angle covered is about 3% of 4π. The proton energy resolution was about 2%. In the case of ^{48}Ca and ^{94}Zr which decay preferentially by neutron emission, EDEN, a time of flight neutron multidetector composed of 40 NE213 liquid scintillators[7] was used. The modules were located outside of the reaction chamber at 1.75 m from the target and at backward angles with respect to the beam. They covered a solid angle of about 3% of 4π.

To extract the direct decay pattern of the GR and of the excitation energy region where the multiphonon GRs are expected, the missing energy spectra must be constructed for these two regions: $E_{miss} = E^* - E_p^{CM} - E_{Tr}$, where E^* is the initial excitation energy in the target, E_p^{CM} the particle energy in the center of mass of the recoiling target, and E_{Tr} the recoil energy of the target remnant.

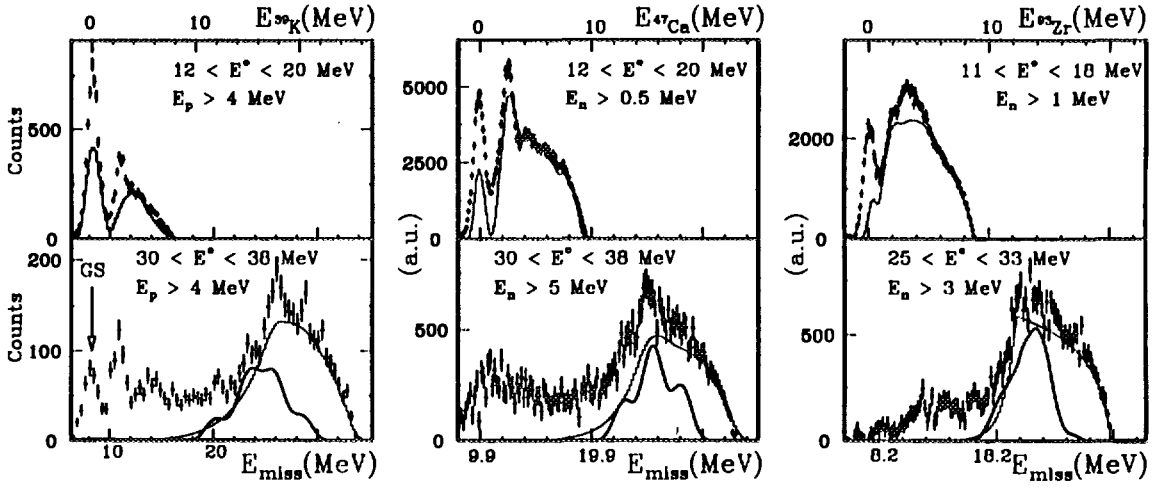

Figure 1: *Missing energy spectra for the GR region and the two-phonon state region in ^{40}Ca (left), ^{48}Ca (middle) and ^{94}Zr (right).*

2.2. Missing Energy Spectra

Missing energy spectra are shown in figure 1 for the three reactions. For the top figures, a gate was set on the GR region and a non negligible yield to the ground state (GS) and the first excited state of the daughter nuclei is not reproduced by the statistical calculation performed with CASCADE[8] (thin line) and can be ascribed to the direct decay of the GQR. On the bottom figures the gate on the excitation energy was set on the region where the double phonon state is expected. Peaks are clearly seen superimposed on the statistical decay bump. Such peaks can only occur

if the decay proceeds through specific states in the A-1 nucleus. Simulations of the contribution of the direct decay of the double phonon are shown as thick lines and reproduce the observed peaks, giving clear evidence for the presence of the double phonon states in these regions.

At higher excitation energy one expects the presence of the three-phonon state which should bring more information on the harmonicity of nuclear vibrations. The direct decay method presented here should allow its observation, but a larger solid angle coverage for the particle detection is required to measure all the decaying particles in coincidence.

3. Conclusion

The double phonon excitation built with the GQR has been observed in several nuclei, through their proton decay or their neutron decay. The direct decay method presented here is a powerfull tool to sign the presence of multiphonon states and could be applied to higher order phonons provided that all decay particles be detected. The use of the multidetector INDRA coupled to the SPEG spectrometer would perfectly suit the purpose.

4. References

1. Ph.Chomaz and N.Frascaria, Physics Reports, Vol 252 Feb 1995
2. A. van der Woude, Prog. Part. Nucl. Phys., **18** (1987) 217
3. J.A.Scarpaci et al., Phys. Rev. Lett., **71** (1993) 3766
4. H.Laurent et al., Nouvelles du GANIL, Jan 1995
5. L. Bianchi et al. Nucl. Inst. Meth., **A276** (1989) 509
6. J.A. Scarpaci, PhD Thesis, Orsay (1990), report IPNO-T-90-04 (Orsay)
7. H. Laurent et al. Nucl. Inst. Meth., **A326** (1993) 517
8. F.Pühlhofer, Nucl. Phys., **A280** (1977) 267
9. Y.Blumenfeld, Nucl. Phys. **A599** (1996) 289c

EVIDENCE FOR ELASTIC ^{16}O BREAKUP INTO THE α-^{12}C CONTINUUM

V. Tatischeff[1], P. Aguer[1], G. Bogaert[1], A. Coc[1], D. Disdier[2], J. Kiener[1], L. Kraus[4], A. Lefebvre[1], I. Linck[2], W. Mittig[3], T. Motobayashi[4], F. Oliveira-Santos[1], P. Roussel-Chomaz[3], C. Stephan[5], J.P. Thibaud[1]

1) C.S.N.S.M., IN2P3-CNRS, 91405 Orsay Campus, France
2) C.R.N., IN2P3-CNRS, Univ. Louis Pasteur, B.P.20, 67037 Strasbourg, France
3) GANIL, IN2P3-CNRS, IRF-CEA, BP 5027, 14021 Caen Cedex, France
4) Department of Physics, Rikkyo Univ., 3 Nishi-Ikebukuro, Toshima, Tokyo, 171, Japan
5) I.P.N., IN2P3-CNRS, B.P.1, 91406 Orsay, France

Introduction

The radiative capture reaction $^{12}C(\alpha,\gamma)^{16}O$ is one of the most important thermonuclear reactions in non-explosive astrophysical sites. Its thermonuclear reaction yield determines directly the ratio of carbon and oxygen abundances at the end of helium burning and indirectly the abundances of all elements between carbon and iron, which are produced in later hydrostatic burning stages like carbon-, oxygen- and silicon burning [1]. In spite of its importance in nuclear astrophysics, the cross section of this reaction is still very uncertain in the stellar energy domain ($E_{cm} \approx 300$ keV for helium-burning, $T \approx 2\times10^8$ K). The reason lies in the extremely small cross section at astrophysical energies and the superposition of E1 and E2 capture. Two recent experiments on the β-delayed α-decay of ^{16}N [2] [3], however succeeded to extract the E1-part with good precision, although there is some discussion about the reliability of the interpretation [4].

We aimed to measure this radiative capture cross section by the method of breakup of a ^{16}O beam at 95 MeV/A, which is particularly sensitive to the E2 part [5]. The elastic breakup of ^{16}O into ^{12}C and α induced by Coulomb interaction with the electric field of a heavy nucleus may be regarded as the time reversed radiative capture reaction. Then the center-of-mass energy spectrum between the carbon and α fragment after breakup is related by known relations to the energy dependence of the radiative capture cross section [6]. The advantage of the breakup reaction is its usually larger cross section compared to the capture reaction, due to the great number of virtual photons produced during the collision of a fast projectile with a high-Z target.

Experiment

A first experiment of the break-up of 95 MeV/A ^{16}O projectiles has been performed in July 1994 at GANIL with the magnetic spectrograph SPEG and we obtained good evidence for elastic breakup into the α-^{12}C continuum with center-of-mass energies between the fragments ranging from 0.9 to 1.8 MeV. In the experiment, the ^{16}O beam (intensity of $\approx$ 20 nA) has been sent onto a 3.2 mg/cm^2 thick ^{208}Pb target. The two fragments entering the angular acceptance of the spectrograph, set to a reaction angle of 3°, were detected in coincidence in the focal plane. Four especially modified drift chambers for coincidence detection were used for the complete reconstruction of the fragment trajectories in the spectrograph. They were followed by two 3.5 mm thick plastic scintillators, providing particle identification and the fragment time correlation. Undesired elastically scattered particles were stopped in a copper block situated in the middle of the focal plane in front of the first drift chamber. This limited the single count rates in the detectors to about 15000 s^{-1}. The beam current was integrated in a shielded Faraday cup located at the entrance of the spectrograph.

A crucial point for the interpretation of breakup events is the angular correlation of the fragments after breakup [7]. Therefore, extensive ion-optical calibrations of the spectrograph were undertaken to achieve a precise determination of the diffusion angles and energies of the fragments. This resulted in a center-of-mass energy resolution better than 100 keV between the fragments at E_{cm} = 1 MeV

and better than 30° angular resolution for the c.m. breakup angle. A total of 80000 α-α and 15500 α-^{12}C coincidences were accumulated in a coincidence run of about 16 hours with 20 nA of beam current and a solid angle of the spectrograph of 44 mrad × 65 mrad.

Data processing and results

The sum energy spectrum of α-^{12}C coincidences is shown in figure 1. Two prominent features are seen: a relatively broad bump between 1450 MeV and 1510 MeV, and a pronounced peak at 1515 MeV. The peak at 1515 MeV has been unambiguously identified as the excitation of ^{16}O to the 12.53 MeV (plus few events from the 12.97 MeV level) 2^- level with subsequent decay into α and the ^{12}C fragment in its first excited state at 4.44 MeV without target excitation. The broad bump contains excitation to both 2^- levels of ^{16}O at 12.53 MeV and 12.97 MeV with additional excitation of the ^{208}Pb target. The relative energy spectrum of events in the 1515 MeV peak exhibits a peak at 926 keV, which is in excellent agreement with the tabulated value for the decay of that level (930 keV), as well as the extracted c.m. angular distribution of the fragments after decay, which agrees well with the theoretical prediction. Another verification of the absolute energy and angular calibration is the decay energy of the 12.97 MeV level, measured to be 1384 keV (tabulated 1370 keV) and the experimentally measured peak at 92 keV in the c.m. relative energy spectrum for α-α due to the ground state ^{8}Be decay (tabulated value 90 keV).

The astrophysically interesting direct breakup into the ground states of the two fragments lies 4.44 MeV above the prominent peak at 1519.2 MeV, indicated by the arrow in fig. 1. After subtraction of uncorrelated accidental coincidences, approximately 30 counts are found for that reaction path. The c.m. relative energy spectrum is shown in fig. 2. A net accumulation of events in the background substracted spectrum (fig. 2b) can be seen between $\approx$ 900 keV and $\approx$ 1800 keV.

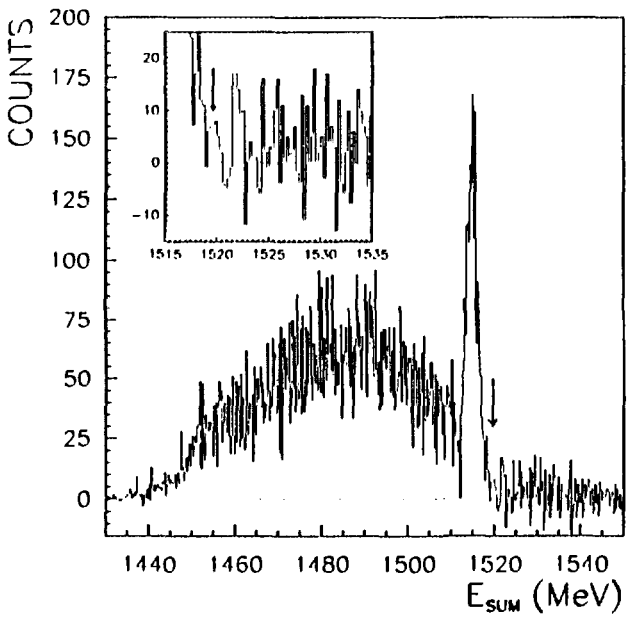

Figure 1 : Sum energy spectrum of α-^{12}C coincidences. The background due to accidential coincidences from subsequent beam bursts has been substracted. The arrow indicates the position of elastic breakup with both fragments in its ground state. A zoom of the interesting energy region is shown in the insert.

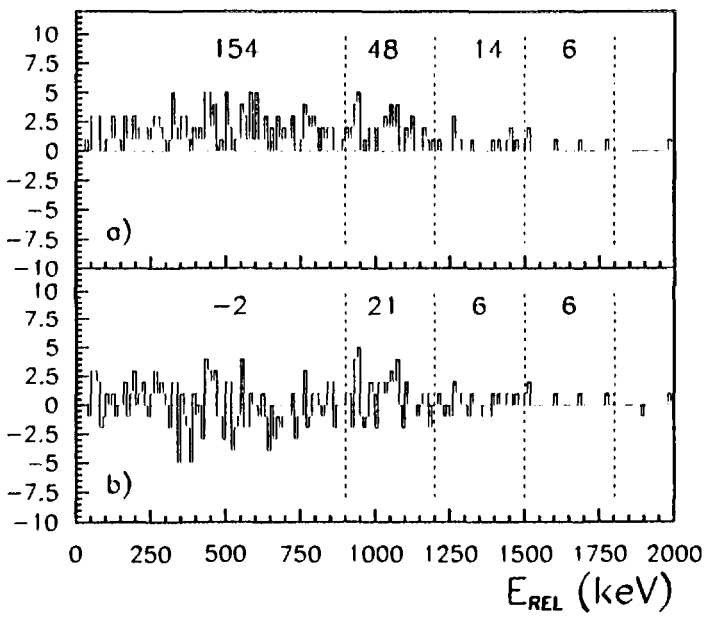

Figure 2 : Relative energy spectrum of events from the marked peak in the sum energy spectrum with an energy window of 1519.2±0.8 MeV.
a:without background substraction
b:with background substraction.
The numbers above the spectra quote the integrated counts for the different energy regions.

Above and below these energies, the net counting rate is compatible with zero, in agreement with estimated breakup cross sections and the energy acceptance of the spectrograph. For sum energies above 1520 MeV, all events are located below 1 MeV in the relative energy spectrum; that background may be due to breakup of elastically scattered particles in the copper block. We defined four regions in the relative energy spectrum (see fig.2). The extracted differential cross sections for the three energy ranges 900-1200 keV, 1200-1500 keV and 1500 keV-1800 keV have been determined with the help of a detailed simulation of the experiment for the determination of the coincidence detection efficiency. The cross sections are respectively $249\pm103_{stat.}{}^{+101}_{-69}{}_{syst.}$ μb/srMeV, $214\pm168_{stat.}\pm78_{syst.}$ μb/srMeV and $808\pm323_{stat.}\pm177_{syst.}$ μb/srMeV. Assuming E2 excitation into the continuum [5], the measured cross sections are related to the B(E2)-values, which can be transformed into the capture cross section. For the determination of the B(E2)-values, the measured cross sections were compared to coupled-channel calculations with the optical potential parameter set of [8]. Our thus determined E2 capture cross sections are compared in fig. 3 with a compilation of available experimental data from direct measurements.

These results give evidence that the direct breakup into the α-^{12}C continuum has been observed for the first time in ^{16}O breakup. It has also been shown, that fragment angular distributions can be extracted from such measurements, which supply additional information on the reaction mechanism, as shown in [7]. This may allow in future experiments with increased statistics to reach lower relative energies with reliable cross sections for the longstanding problem of the $^{12}C(\alpha,\gamma)^{16}O$ thermonuclear reaction rate.

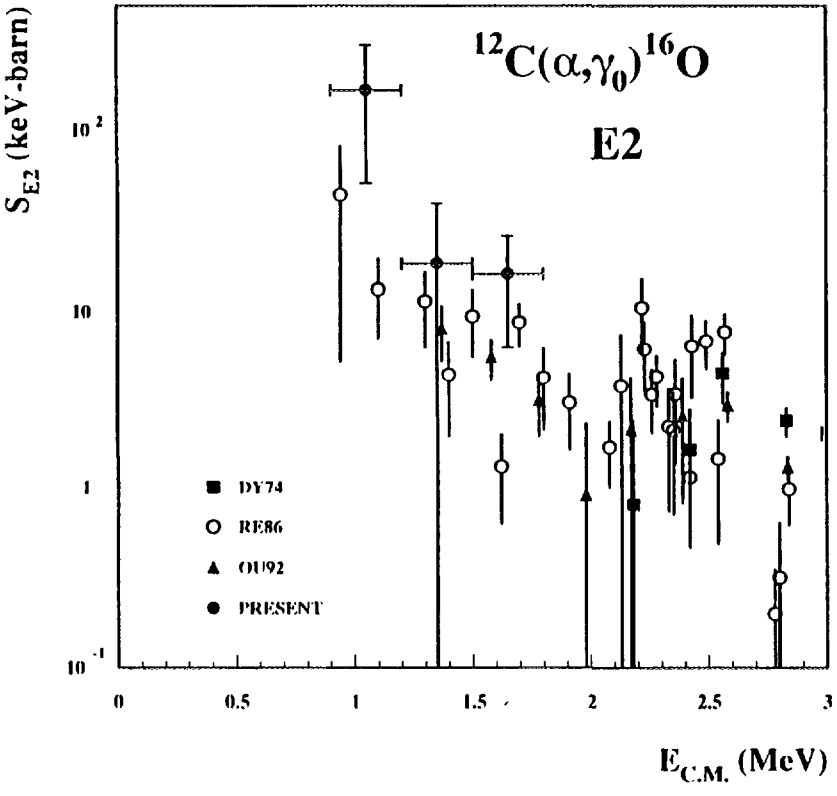

Figure 3 : Compilation of available data for the astrophysical S-factor S^{E2} of the $^{12}C(\alpha,\gamma)^{16}O$ reaction. The data were taken from DY74[9] RE86[10] OU92[11].

References

[1] T.A. Weaver and S.E. Woosley, Phys. Rep. 227(1993)65

[2] Z. Zhao et al., Phys. Rev. Lett. 70(1993)2066

[3] L. Buchmann et al., Phys. Rev. Lett. 70(1993)726

[4] F.C. Barker, Phys. Rev. C50(1994)2244

[5] T.D. Shoppa and S.E. Koonin, Phys. Rev. C46(1992)382

[6] G. Baur, C.A. Bertulani and H. Rebel, Nuclear Physics A458(1986)188

[7] V. Tatischeff et al., Phys. Rev. C51(1995)2789

[8] P. Roussel-Chomaz et al., Nuclear Pysics A477(1988)345

[9] P. Dyer and C.A. Barnes, Nuclear Physics A233(1974)221

[10] A. Redder et al., Nuclear Physica A462(1987)385

[11] J.M.L. Ouellet et al., Phys. Rev. Lett. 69(1992)1896

Dimers Based on the $\alpha + \alpha$ Potential

and

Chain States of Carbon Isotopes, ^{12}C to ^{16}C

W. von Oertzen

Hahn Meitner Institut, Berlin and Fachbereich Physik, Freie Universität Berlin
D-14109 Berlin, Glienicker Straße 100

PACS: 21.10; 21.60 Gx

Abstract :

Using the well established binding energies of one and two valence neutrons in the two-center $\alpha + \alpha$ system (forming the states ^{9}Be and $^{10}Be^{*m}$) the structure of nuclear dimers and their rotational bands with more than 2 nucleons are discussed using published transfer reaction data for Be and Boron isotopes. Based on the 0_2^+ state in ^{12}C which is supposed to be an 3α particle chain at an excitation energy of 7.65 MeV and using the binding energy of these neutrons in ^{9}Be and $^{10}Be^{*}$, chain states in the system $^{12}C^{*}$ + x neutrons are constructed. The energy position of the lowest chain states are estimated and ways for their population in reactions on ^{9}Be and using radioactive beams are proposed. ~~It is expected that these states are metastable and could have appreciable branches for γ-decay. Some extrapolations to longer chain states in neutron rich light isotopes are made~~.

Submitted to Zeitschrift für Physik A

Width and Strength of the Hot Giant Dipole Resonance: the Role of the Life Time of the compound nucleus and the Transition from Order to Chaos.

Ph. Chomaz[a]

[a] GANIL, BP 5027, 14021 Caen Cedex

One of the most surprising discoveries of the past decade is that hot compound nuclei which were thought of as very chaotic systems [1] may exhibit regular collective motions [3]. In particular, looking at the γ decay spectrum one observes a bump at high energies which is due to the excitation of the Giant Dipole Resonance (GDR) in the compound nucleus. It was shown that this collective state is very "robust" and that it remains nearly unaffected by the increase of excitation energy. It was even proposed that the presence of collective states can be a signature of the existence of a compound nucleus and that the disappearing of the GDR can be interpreted as a signal of the liquid-gas phase transition in nuclei [4]. However, the behavior of the GDR for temperature around 5 MeV is still a matter of controversy.

In particular it has been recently proposed based on the possible existence of pre-equilibrium effects in the γ-ray emission from a hot system [10]. Indeed, if the evaporation time becomes larger than the spreading width of the GDR one might expect that during the time the resonance gets equilibrated the compound nucleus will have cooled down by particle emission. However, we have recently discussed that this idea cannot apply to reactions for which an explicit dipole moment (or strong fluctuation) is present in the entrance channel [13] and so new experimental results looking at the effects of the N/Z entrance channel assymmetry are called for [13].

Since the observed photons are coming from transitions between two states of the compound nucleus which have finite life times, the total width of the photo-absorption peak must contain their individual widths. Since these widths are rapidly increasing with the temperature of the system they will induce a strong brosdening of the GDR photo-absorption peak which may partly explain the rapid suppression of the GDR photons at high excitation energy.

In order to make this point clear it can be useful to discuss the difference between the spreading width and the life time of the compound nucleus. A resonance can be understood as a coherent excitation of particle-hole configuration on a hot nucleus. This is obviously not an eigen state of the compound nucleus therefore it acts as a doorway state and, as the time goes on, it couples with more complicated configurations. Eventually, it will reach a compound nucleus state which is a mixture of many particle-many hole excitations. This "decay" must be understood as the beating of the various compound nucleus states composing the resonance because of their spreading in frequency.

This is not really associated with a life time. In particular for a finite number of compound nucleus states one might observe a Poincare recurrence time where the system

is coming back to the initial configuration. Moreover, a life time implies an exponential decrease of the initial population of excited states, consequently it is always associated with a Lorentzian shape of the strength function which is nothing but a Fourier transform of the time evolution. Conversely the shape of the spreading width is not constrained at all.

The only real life time is the one due to the decay of the compound nucleus states through evaporation of particles. This decay induces an exponential decrease of the amplitude associated with each compound nucleus level and a broadening of the corresponding peak in the strength.function.

Since gamma-rays are transitions between two levels of the compound nucleus the broadening will correspond to the sum of the initial and final width. If we now replace the width of the initial and final states by the average evaporation width of the compound nucleus, Γ_{ev}, and if we approximate the shape of the GDR by a gaussien centered at the energy E_{GDR} with a finite width Γ[1] we can demonstrate that the position of the photoabsorption peak is not affected but the width becomes [2]:

$$\Gamma_{GDR} = \sqrt{\Gamma^2 + (2\Gamma_{ev})^2} \tag{1}$$

This result demonstrates that the width of any structure in the photo-absorption spectrum is bigger than $2\Gamma_{ev}$ in perfect agreement with the Heisenberg uncertainty principle. This yields to the conclusion that

$$\Gamma_{GDR} \geq 2\Gamma_{ev} \tag{2}$$

At low excitation energy the life time of the compound nucleus is so long that the influence of this width can be neglected. However at high temperature this life time becomes so small that the induced widths will eventually dominate over the spreading width of the resonance. The life time of a compound nucleus at such temperature is not really known experimentally. However, as far as no anomalous diffusion is appearing at high excitation energy, this life time can be inferred from statistical calculations. Typical results of such calculations are shown in Fig 1 for a ^{120}Sn nucleus. The life time of the compound nucleus rapidly decreases so that Γ_{ev} reaches 10 MeV between 300 and 600 MeV excitation energy depending upon the various level density parameter used in the calculation of the life time. Therefore, the total width of the resonance will show a rapid increase irrespectively of the actual calculations of the spreading width of the resonance. This fact is simply illustrated in Fig. 1 assuming a constant spreading width of 4.4 MeV for the GDR. On the various curves one can see that the width induced by the finite life time of the compound nucleus states dominates above 300 to 500 MeV excitation energy.

This calculation must only be considered as qualitative because of the uncertainties on the estimation of the width of the compound nucleus states. In particular, one may worry about the fact that the introduction of new decay channels such as the emission of intermediate mass fragment will reduce further the life time of the compound nucleus.

[1]This width represents not only the spreading width but is supposed to be an effective width which includes all the other sources of broadening (deformation, shape fluctuations, ...). These processes being statistical it is normal to assume that the strength function is akin to a normal distribution.

[2]If the various components of the folding product are rather akin to normal distributions than to Lorentzian, the total width becomes the square root of the quadratic sum of the various widths[19]

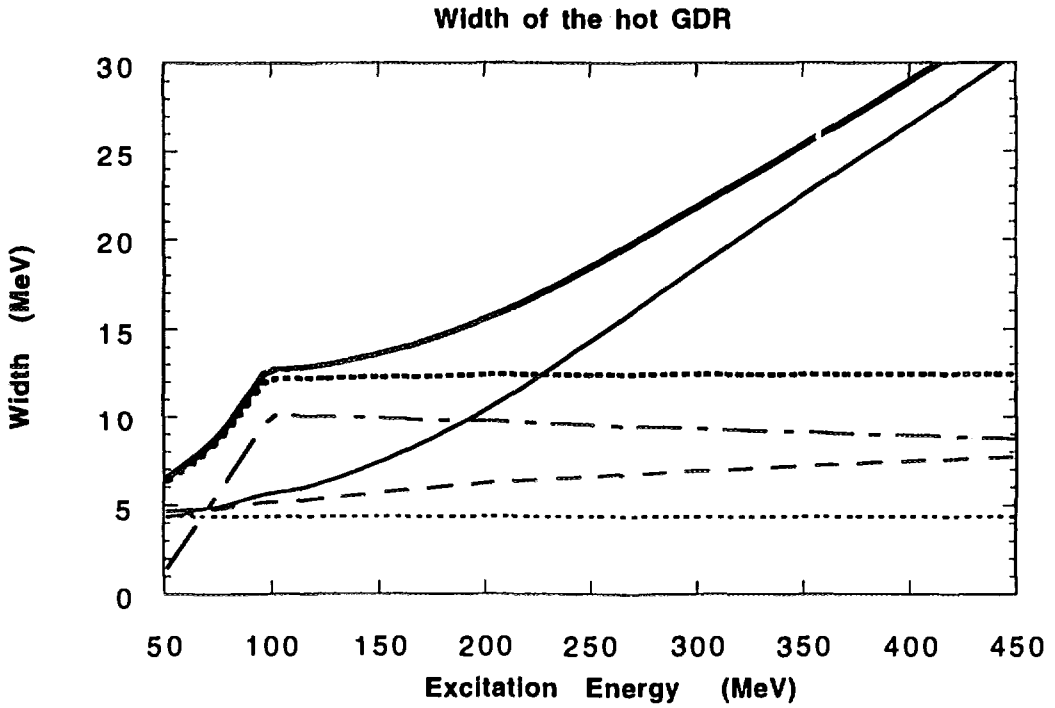

Figure 1. Evolution of the various Widths as a function of the excitation energy of the Sn nucleus, the thick lines represent the width of the GDR, the thin lines the width of the compound nucleus. The solid lines are associated with a level density parameter $a = A/12$, the dash lines with $a = A/10$ and the dash-dotted lines with $a = A/8$.

However this effect will increase the width of the compound nucleus states and so the increase of the GDR width will be faster but the overall picture will not be changed.

The second explanation of the quenching of the GDR strength is related to the fact that each individual particle emission induces a strong fluctuation of the dipole moment of the nucleus. Indeed, if a neutron is emitted the dipole moment will fluctuate with an amplitude

$$\Delta D \approx R/N \approx 0.2fm \tag{3}$$

where R is the nucleus radius and N its number of neutrons. This value is of the same order of magnitude than the amplitude of one dipole phonon ($\Delta D_1 \approx 4/\sqrt{AmE_{GDR}} \approx 0.2fm$). Therefore the evaporation of one particle is giving strong kicks to the collective vibration. This classical picture is confirmed by the experimental observation of the particle decay of the GDR. Therefore, the description of the dipole collective variable is akin to the problem of a brownian motion in an harmonic potential. If the time between two evaporations is long in comparison with the period of the vibration, the system will present harmonic dipole oscillation and therefore will be able to emit γ-rays at the dipole frequency. Conversely, when the time between two particle emissions becomes much shorter than the time the system needs to complete one oscillation, the dynamics become stochastic. In such a case the motion is no more characterized by the GDR frequency and the observed γ-spectrum will be flat.

One can conclude that when the time between two particle emissions becomes comparable to the period of the harmonic oscillation, the transition between the order and the

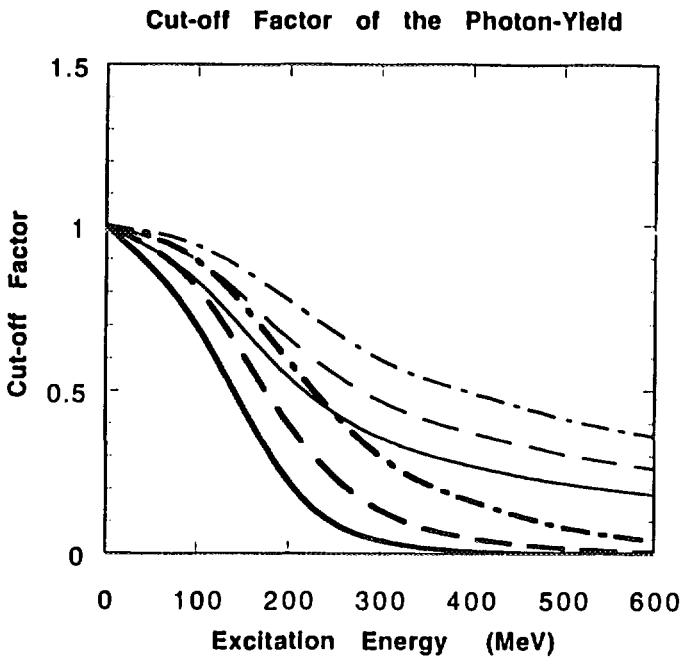

Figure 2. Evolution of the suppression factor as a function of the excitation energy of the Sn nucleus, the thick lines are computed from Eq. (7), the thin lines represent the cut-off factor proposed in ref [10]. The solid lines are associated with a level density parameter $a = A/12$, the dash lines with $a = A/10$ and the dash-dotted lines with $a = A/8$.

chaos is reached and the collective vibration is suppressed (see Fig. 2).

From this simple argument a quenching factor can be deduced and compared with the existing suppression factors. This factor can be easily estimated by computing the number of systems which were able to perform at least one vibration:

$$S(E) = \exp\left(\frac{-2\pi\Gamma_{ev}}{E_{GDR}}\right) \tag{4}$$

This factor is represented on Fig. 2 and compared with the cut-off factor used in fitting the data. One can see that the two are rather similar and so the factor (4) may be a good alternative in order to explain the observed suppression of the γ emitted in heavy ion reactions. Indeed, we demonstrated in reference [13] that the cut-off factor proposed by Bortignon et al was not applicable in the case of reaction with asymmetric N/Z ratio between the target and the projectile. In particular, it is clear that as soon as the incomplete fusion regime is reached this factor which is due to pre-equilibrium effects is not present because of the strong entrance channel fluctuations. However, the suppression seems to be present in the experimental data and can be explained by this transition between regular and stochastic motion.

In this paper we have discussed the fact that the total width of the γ-ray spectrum of the GDR transitions must contain twice the width of the compound nucleus levels. This implies that one must expect a rapid increase of the width of the GDR. This increase contributes to the observed saturation of the photon multiplicity.

Finally, we proposed a new suppression factor due to the lost of collectivity induced by

is proposed.

the fast particle emission. This factor is important when the time between two particle emissions (the life time of the compound nucleus) is shorter than the vibration period. This cut-off factor can be a good alternative to the one proposed by Bortignon et al [10] which has been demonstrated to be not applicable in asymmetric N/Z reactions and in incomplete fusion regime where the saturation is observed[13] .

These two effects related to the short life time of the Hot compound Nucleus are important and must be considered in the study of the GDR γ-rays. They may provide a physical interpretation of the observed increase of the GDR width and of the saturation of the photon yield.

Acknowledgements We want to thank P.F. Bortignon for helpful suggestions during the elaboration of the project. Useful discussions with R. Alba, Y. Blumenfeld, M. Di Toro, .E. Migneco, P. Piattelli, M. Ploszajczak A. Smerzi, T. Suomijärvi and the MEDEA collaboration are acknowledged. We want also mention the special role played by P. Fox in the maturation of this work.

REFERENCES

1. A. Bohr and B. R. Mottelson, "Single Particle Motion", Eds. Benjamin, (1969)
2. A. Bohr and B. R. Mottelson, "Nuclear Structure", Eds. Benjamin, (1975)
3. K.A. Snover, Ann. Rev. Nucl. Part. Sci. **36** (1986) 545
   J.J. Gaardhoje, Nucl. Phys. **A488** (1988) 261c
4. Ph. Chomaz and D. Vautherin, private communication (1987), and Experimental Proposal 142 at GANIL.
5. A. Bracco et al, Phys. Rev. Let. **62** (1989) 2080
6. J.J. Gaardhoje, Phys. Rev. Let. **59** (1987) 1409
7. K. Yoshida, Phys. Let. **B245** (1990) 7
8. E. Sureaud, C. Gregoire and B. Tamain; Prog. Nucl. Part. Sci. **23**(1989)278
9. F. Saint-Laurent; Phys. Lett. **B202**(1988)190
10. P.F. Bortignon, A. Bracco, D. Brink and R.A. Broglia, Phys. Rev. Lett. **67**(1991)3360
11. M. Goldhaber and E. Teller, Phys. Rev. **74** (1948) 1046
12. A.Smerzi, A.Bonasera and M.Di Toro, Phys.Rev.**C44**(1991)1713
13. Ph.Chomaz, invited talk, Colloque Franco-Japonais St.Malo, Oct.1992 and Preprint GANIL 92-27
    Ph.Chomaz et al, Preprint GANIL 93-02 and Nucl. Phys. **A** in press.
14. D. Vautherin and N. Vinh Mau, Nucl. Phys. **A422** (1984) 140
15. See many contributions to this conference and the included references.
16. A.A. Abrikosov, L.P. Gorkov and I.E. Dzyaloshiinski, Methods of Quantum fields theory in statistical physics (Prentice- Hall Cliffs. 1963)
17. A.L. Fetter and J.D. Walecka, Quantum theory of many-particle systems (McGraw-Hill, New York, 1971).
18. P. Ring, L.M. Robledo, J.L. Egido and M. Faber, Nucl. Phys. **A419** (1984) 261
19. Ph. Chomaz and N.V. Giai. Phys. Lett. **B 282** (1992) 13

Role of anharmonicities and non-linearities in heavy ion collisions. A microscopic approach.

Abstract →

E.G. Lanza,[1] M.V. Andrés,[2] F. Catara,[1] Ph. Chomaz,[3] and C. Volpe,[3]

[1] Dipartimento di Fisica Universitá di Catania and INFN, Sezione di Catania, I-95129 Catania, Italy
[2] Departamento de Física Atómica, Molecular y Nuclear, Universidad de Sevilla, Apdo 1065, 41080 Sevilla, Spain
[3] GANIL, B.P. 5027, F-14021 Caen Cedex, France
LNS, Viale Andrea Doria
Catania, Italy

States that can be interpreted as the first quanta of collective vibrations are a general property of quantum mesoscopic systems which can be found in various fields of physics. In nuclear physics, such vibrational states of the nucleus have been known for many years [1]. These one-phonon states are present both in the low-lying excitation spectra of nuclei and at higher energies. The latter are the Giant Resonances (GR). The existence of two-phonon states, i.e. states which can be described as double excitations of elementary modes, has also been predicted since the early days of the collective model [1]. Such states have been observed long time ago in the low-lying spectra. More recently, two-phonon states built with giant resonances have been populated in heavy ion inelastic scattering [2], in double charge exchange ($\pi^{\pm}, \pi^{\mp}$) reactions [3] and in Coulomb excitation at high energy [4, 5, 6]. For a review, see ref. [7].

The microscopic theory suited for the description of collective vibrational states is the Random Phase Approximation (RPA). Two-phonon states and their mixing among themselves and with one-phonon states can be generated by using boson mapping techniques and by taking into account terms of the residual interaction which do not enter at the RPA level [8, 9]. In this way one has an RPA based approach to treat anharmonicities.

In a nucleus-nucleus collision, the mutual excitation of the two partners is described as due to the action of the mean field of each nucleus on the other one, i.e. by a one body operator. Assuming that it induces small deformations of the density, only the particle-hole (ph) terms of the external mean field are usually taken into account. This amounts to consider as elementary processes only those corresponding to the creation or annihilation of one phonon. In this approximation, the external field is linear in the creation and annihilation operators of phonons. When the particle-particle (pp) and

hole-hole (hh) terms of the external field are also included, the direct excitation from the ground state to two-phonon states as well as the transition between one-phonon states become possible. These terms can be expressed as quadratic in the creation and annihilation operators of phonons and so correspond to non-linear terms in the excitation operator.

In the "standard" approach, based on the independent multiphonon picture, the effects coming from both anharmonicities and non-linearities are neglected (see for instance ref.[10]). Recent experimental data on Coulomb excitation at relativistic energies have raised some questions on the adequacy of that picture. Indeed, in the excitation of ^{136}Xe on ^{208}Pb, the experimental cross section to the double GDR (DGDR) has been found to be 2 to 4 times larger than the theoretical one [4]. Recently, new experimental results [6] on the excitation of several nuclei have shown that the disagreement ranges from about 10% to 60%, being about 30% in the case of ^{208}Pb. In a previous paper [11], by using a one-dimensional oscillator model to mimick nuclear states, we have shown that the effects of anharmonicities and non-linearities can lead to an important enhancement of the cross section in the energy range around twice that of the GDR. In this model neither spin nor parity were taken into account. Besides, only one type of phonons was considered.

We have done Calculations for the ^{208}Pb+^{208}Pb system at 641 and 1000 MeV per nucleon for which experimental data exist [6]. We have also studied the Coulomb excitation of ^{40}Ca in the reaction ^{208}Pb+^{40}Ca at 1000 MeV/A although there are no experimental data for this case. In both cases we consider as elementary modes all natural-parity RPA phonons whose multipolarity is lower than 4 and whose contribution to the associated energy weighted sum rule (EWSR) is larger than 5%. Then, we have built the residual interaction in the one and two-phonon space and we have diagonalized the hamiltonian in this subspace in order to define the mixed states $|\phi_\alpha>$. By solving the time dependent Schrödinger equation in this subspace we get the probability amplitudes for each of the $|\phi_\alpha>$ states from which we calculate the cross section. We will describe in detail the results for the ^{208}Pb+^{208}Pb system at 641 MeV/A, the results at 1000 Mev/A being essentially the same except for the absolute values of the cross section which are higher in the latter case.

The one phonon basis is calculated in the self-consistent RPA with SGII Skyrme interaction [12]. Although we are using an explicit neutron proton representation the isospin results to be a rather good quantum number as far as collective states are concerned. We have selected all the states which exhaust at least 5% of the appropriate EWSR and, for a particular spin and parity (and isospin). We have considered the various components of the isoscalar monopole resonance (GMR), the components of the isovector dipole resonance (GDR), the low-lying 2^+ state and the quadrupole resonances, both isoscalar (ISGQR) and isovector (IVGQR), and finally the collective low-lying (3^-) and high-lying ($HEOR$) isoscalar octupole states.

We have then constructed The residual interaction between the one- and two-phonon states and also among the two-phonon states. The two-phonon states are coupled to a total angular momentum and parity. In the case of the 1^- states, while the coupling between one- and two-phonon states is of the order of 1/2 MeV up to 1 MeV, the coupling between two phonon states is, in average, about one order of magnitude smaller.

Then for each spin and parity the total matrix has been diagonalised in order to get the states $|\Phi_\alpha>$. Since these states are always dominated by one component we have

decided to label them by the name of this dominant component. The anharmonicities predicted by our microscopic calculations are small, the typical shifts in energy (ΔE) being a few hundred keV. Each multiplet appears to be splitted with a characteristic spreading equal to the global shift. The mixing coefficients are in average also small, around 0.05 and at maximum around 0.2.

The various states have now two paths to be excited in one step, either through the W^{10} direct excitation of their one-phonon component or via the W^{20} interaction exciting directly their two-phonon part. Now, depending on the respective sign of the mixing coefficients, these two contributions may interfere constructively or destructively.

In addition to these direct transitions from the ground-state, the term W^{11} of the external field may induce transitions between excited states. These new excitation routes may modify the distribution of the excitation probabilities associated with different states.

Let us now put all these ingredients together in order to compute the excitation probabilities and cross sections. All the natural parity states with angular momentum less or equal to 3 have been included in the calculations while for the non natural parity states we have included only the 1^+ and the 2^- ones. By solving the coupled equations we get the probability amplitude for each $|\phi_\alpha>$ state, from which we calculate the cross section by integrating over the various impact parameters associated with Coulomb inelastic excitations. The b_{min} has been chosen according to the systematics of ref [13]. We will describe in detail the results for the ^{208}Pb+^{208}Pb system at 641 MeV/A and we will first focus our discussion on the excitation of dipole states.

Table 1 presents the Coulomb inelastic cross-sections for different states at several degrees of approximation. For example One can see that the 1^- state resulting from the coupling of the low-lying 3^- and 2^+ is almost not excited in the harmonic and linear picture. Indeed, at this level of approximation, the most direct way to excite this state requires one E3 and one E2 transitions which are not favourable. In this case the W^{11} term does not help much because either we reach the state by one E1 plus two E2 transitions or by one E3 plus two E1 if in the first step we excite the 3^- state. In any case, at least one of the involved transitions is of high multipolarity. Conversely, the direct transitions due to the W^{20} terms increases the cross section by a huge factor, bigger than 500. Indeed, this term is now a dipole transition which is strongly favoured. The importance of W^{20} will decrease as the excitation energy of the state increases. For instance, the enhancement factor 500 reduces to about 50 for the dipole states $|2^+ \otimes HEOR>$ or $|ISGQR \otimes HEOR>$ whose energies are around 30 MeV.

When the mixing of one- and two-phonons states is taken into account this state can be also populated by W^{10} through its small GDR component. In fact, although the mixing coefficient with the GDR component is small, this component gives a considerable contribution due to the fact that it is a one step dipole excitation. Moreover, the energy of the state (about 9 MeV) is lower than the one of the GDR state. All together the effect of the anharmonicities on the inelastic cross section is a factor about 100 times bigger with respect to our reference calculation.

Finally, when all these different contributions are taken into account this dipole two-phonon state built from low-lying 3^- and 2^+ is receiving 30 mb cross section, while in the harmonic and linear limit it was just 0.03 mb. In this case the effects of non-linearities and anharmonicities interfere constructively but this is not a general property.

Table 1. Coulomb inelastic target excitation cross sections (in mb) for the ^{208}Pb+^{208}Pb system at 641 MeV/A and for the mixed states which are identified by their dominant component (first column) and their angular momenta and parity (second column). In the third column is shown the reference result corresponding to a harmonic and linear calculation. In the fourth column the additional inclusion of only the W^{11} non-linear term is allowed. Similarly, in the fifth column the only difference with the reference calculation is due to the addition of only the W^{20} non-linear term. In the sixth column the results of an anharmonic and linear calculation are presented. The last column correspond to results of the anharmonic and non-linear approach.

States	J^π	harm. & lin.	W^{11}	W^{20}	anharm.	anharm. & non-lin.
$2^+ \otimes 3^-$	1^-	0.03	0.04	16.21	2.60	29.53
$ISGQR \otimes 3^-$	1^-	0.05	0.07	17.22	3.63	5.18
$22 < E < 28$ (MeV)	1^-	3.55	5.95	5.07	6.42	12.18
$2^+ \otimes GDR_1$	1^-	1.24	2.07	0.99	7.64	9.83
$ISGQR$	2^+	298.91	332.56	300.09	278.35	314.18

So far, we have discussed the influence on some particular states. In order to get a global view on the effects of both non-linearities and anharmonicities we must compute the complete inelastic cross section. Therefore, we have summed up all the contributions coming from the various states. We have observed that the single GDR region is not much affected by the anharmonicities and non-linearities while the cross-section in the DGDR region is increased by 10% when the anharmonicities and non-linearities are taken into account. We would like to point out that this increase is mainly due to the excitation of two-phonon states whose energies are in the DGDR region and whose population has been possible only because of the presence of the anharmonicities and the non-linear terms W^{11} and W^{20} in the external field. The low lying part of the spectrum is also affected and in particular, as we discussed before, a new dipole strength is visible in the 9 MeV region.

In table 2 we show a comparison between our theoretical results and the experimental cross-section for the GDR and the DGDR energy region. The agreement for the GDR seems satisfactory. The theoretical yield associated with the DGDR states explains about 60% of the experimental cross section. However, this disagreement between the experimental cross section in the DGDR region and our theoretical estimate is reduced to 18% $\pm$ 10% by the inclusion of all the different multiphonon states considered in our calculation and lying above the IVGQR.

In conclusion, both the introduction of different two-phonon states and the inclusion of anharmonicities and non-linearities are bringing the theoretical prediction rather close to the experimental observation for the Coulomb excitation of Pb nuclei in the DGDR region.

This work has been partially supported by the spanish DGICyT under contract PB92-0663, by the Spanish-Italian agreement between the DGICyT and the INFN and by the Spanish-French agreement between the DGICyT and the IN2P3.

Table 2. Comparison between our theoretical results and the experimental cross sections (in barn) reported in ref. [6] for the Pb + Pb reaction at 641 MeV per nucleon. The theoretical results (first line) correspond to the sum of all GDR (first column) and all DGDR (second column) cross-section. The third column contains the cross section associated with all the states above the IVGQR (E > 22 MeV). The theoretical cross sections are obtained from the non-linear and anharmonic calculation while the numbers in parenthesis refer to the linear and harmonic limit. The experimental results are reported in the second line. The first number corresponds to the extracted GDR cross section while the second number comes from a gaussian fit of the high energy cross section after subtraction of the GDR and GQR single-phonon strength.

	GDR	DGDR	DGDR energy region
σ_{th}	3.13 (3.14)	0.21 (0.22)	0.31 (0.28)
σ_{exp}	3.28 ± 0.05	0.38 ± 0.04	

REFERENCES

1. A. Bohr and B.R. Mottelson, Nuclear Structure, vol. II, (W.A. Benjamin, N.Y., 1975)
2. N. Frascaria, Nucl. Phys. A 282 (1988) 245c
3. S. Mordechai et al., Phys.Rev.Lett. 60(1988)408
4. R. Schmidt et al., Phys. Rev. Lett. 70 (1993) 1767
5. J. Ritman et al, Phys. Rev. Lett. 70 (1993) 533
6. J. Stroth et al, in the Proceedings of the "Groningen Conference on Giant Resonances", June 28-July 1, 1995, Nucl. Phys. A 599 (1996)307c; K. Boretzky et al., GSI preprint-96-27 to be published on Physics Letters B.
7. Ph. Chomaz and N. Frascaria, Phys. Rep. 252 (1995) 5
8. F. Catara, Ph. Chomaz and N. Van Giai, Phys. Lett. B 233 (1989) 6
9. D. Beaumel and Ph. Chomaz, Ann. Phys. (N.Y.) **213** (1992) 405.
10. C. A. Bertulani, L. F. Canto, M. S. Hussein and A. F. R. de Toledo Piza, Phys. Rev. C 53 (1996) 334
11. C. Volpe, F. Catara, Ph. Chomaz, M. V. Andrés and E. G. Lanza, Nucl. Phys. A 589 (1995) 521; Nucl. Phycs. A 599 (1996) 347c.
12. N. V. Giai, Suppl. Prog. Theor. Phys. 74-75 (1983) 330; N. V. Giai and H. Sagawa, Phys. Lett. B106 (1981) 379.
13. C. Benesh, B. Cook and J. Vary, Phys. Rev. C40 (1989) 1198.

A2 - EXOTIC NUCLEI AND DECAY MODES

A Test of Wigner's Spin-Isospin Symmetry from Double Binding Energy Differences

P. Van Isacker[a], D.D. Warner[b], and D.S. Brenner[c]

[a] *Grand Accélérateur National d'Ions Lourds, BP 5027, F-14021 Caen Cedex, France*
[b] *CCLRC Daresbury Laboratory, Daresbury, Warrington WA4 4AD, UK*
[c] *Clark University, Worcester, MA 01610, USA*

In the supermultiplet model of nuclei it is assumed that nuclear forces are independent of isospin as well as spin [1, 2, 3]. Nuclear states can then be characterized by the quantum numbers of the spin-isospin or SU(4) symmetry, giving rise to simple predictions concerning nuclear β-decay rates and masses. The former arise because the Fermi as well as Gamow-Teller operators are generators of SU(4) and as such β transitions can only occur between states belonging to the same supermultiplet; predictions of nuclear binding energies are obtained in a lowest-order approximation from the permutational symmetry of the *orbital* part of the many-body wavefunction which determines the degree of spatial overlap between the nucleons. Since the original work by Wigner [1] and Hund [2] it has become clear that SU(4) symmetry is badly broken in the majority of nuclei because of the increasing importance with mass of the spin-orbit term in the nuclear mean-field potential. Nevertheless, it remains a useful *ansatz* for studying global properties of *p*- and *sd*-shell nuclei from a simple perspective. Moreover, as will be shown in this Letter, it may have a particular and renewed relevance in the study of the heavier $N \simeq Z$ nuclei from ^{56}Ni to ^{100}Sn, a declared experimental goal of many of the current proposals for new facilities based on accelerated radioactive beams [4].

The most conclusive test of SU(4) symmetry is through a comparison with realistic shell-model calculations which can be readily performed for nuclei up to ^{40}Ca. The goodness of SU(4) symmetry in the ground state is then obtained by taking the overlap between the shell-model wavefunction and the favored SU(4) representation. This approach is followed, for example, for *sd*- and *pf*-shell nuclei by Vogel and Ormand [5]. The overall conclusion of such studies is that in nuclei heavier than ^{16}O significant departures from SU(4) symmetry occur.

To obtain a test of the goodness of SU(4) symmetry directly from masses is more difficult. Franzini and Radicati [6] suggested the use of a ratio $R(T_z)$ of ground-state energy differences involving four isobaric nuclei with different isospin projections T_z and showed that the values agree rather well with the SU(4) predictions for nuclei with masses up to $A \approx 110$. However, it was demonstrated subsequently [7] that this ratio $R(T_z)$ is not very sensitive to SU(4) symmetry mixing.

In [8] it is pointed out that a sensitive test of SU(4) symmetry can be made by using double binding energy differences which also provide information concerning the strength of the neutron-proton (np) interaction which is known to play a pivotal role in the structure of nuclei [9]. Recently, the quantity

$$\delta V_{\rm np}(N,Z) \equiv \tfrac{1}{4}\Big([B(N,Z) - B(N-2,Z)] - [B(N,Z-2) - B(N-2,Z-2)]\Big), \quad (1)$$

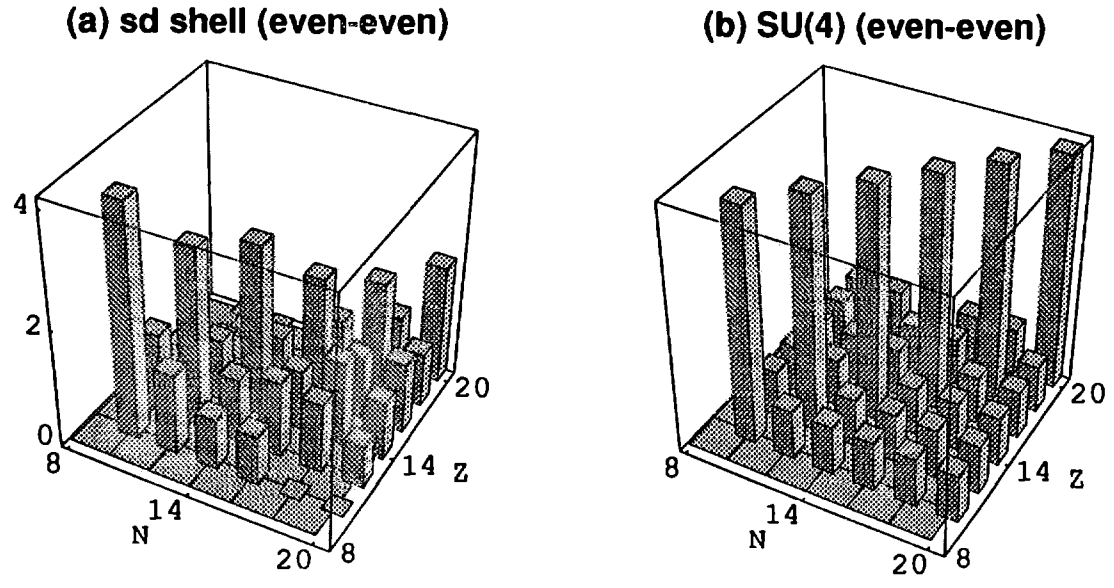

Figure 1: Barchart representation of double binding energy differences (a) as observed in even-even sd-shell nuclei and (b) as predicted by Wigner SU(4). The data are taken from [11]; an empty square indicates that data are lacking. The x and y coordinates of the centre of a cuboid define N and Z and its height z defines $-\delta V_{\rm np}(N,Z)$.

where $B(N,Z)$ is the (negative) binding energy of an even-even nucleus with N neutrons and Z protons, was used by Brenner *et al.* [10] to extract the empirical interaction strength of the last neutron with the last proton. A notable outcome of this analysis was the occurrence of particularly large interaction strengths for $N = Z$ nuclei. Although this feature is consistent with both schematic and realistic shell-model calculations [10], a simple interpretation of this result is still lacking. We have shown that the $N = Z$ enhancements of $|\delta V_{\rm np}|$ are an unavoidable consequence of Wigner's SU(4) symmetry and that the degree of the enhancement provides a sensitive test of the quality of the symmetry itself.

A representative sample of the data is shown in Fig. 1(a) which gives $-\delta V_{\rm np}(N,Z)$ (where known) for the *sd* shell.

While for $N \neq Z$ the np interaction strength is roughly constant and of the order of -1 MeV, the dramatic enhancement of $|\delta V_{\rm np}|$ occuring for $N = Z$ is clearly evident. This prominent feature can be understood from the simple perspective of Wigner's supermultiplet theory. Wigner's scheme in a harmonic-oscillator shell with degeneracy $\omega = \sum(2l+1)$ implies the classification

$$\mathrm{U}(4\omega) \supset \left(\mathrm{U}_{\rm orb}(\omega) \supset \cdots \supset \mathrm{O}_{\rm orb}(3)\right) \otimes \left(\mathrm{U}_{ST}(4) \supset \mathrm{SU}_{ST}(4) \supset \mathrm{SU}_S(2) \otimes \mathrm{SU}_T(2)\right). \quad (2)$$

The dots refer to an appropriate labelling scheme for the orbital part of the fermion wavefunction, such as Elliott's SU(3) scheme [12]. The total M-fermion wavefunction transforms antisymmetrically under $\mathrm{U}(4\omega)$ and is decomposed into an orbital part, behaving as $[M_1, M_2, M_3, M_4]$ under $\mathrm{U}_{\rm orb}(\omega)$, and a spin-isospin part. To ensure overall antisymmetry the latter by necessity transforms under $\mathrm{U}_{ST}(4)$ as the conjugate represen-

tation $[\widetilde{M}_1, \widetilde{M}_2, \widetilde{M}_3, \widetilde{M}_4]$ (i.e., rows and columns of the Young tableau interchanged) and determines the supermultiplet $SU_{ST}(4)$ representation $(\lambda\mu\nu)$ ($\lambda = \widetilde{M}_1 - \widetilde{M}_2$, $\mu = \widetilde{M}_2 - \widetilde{M}_3$, and $\nu = \widetilde{M}_3 - \widetilde{M}_4$). From the $SU_{ST}(4) \supset SU_S(2) \otimes SU_T(2)$ reduction the possible values of S and T follow.

The short-range character of the residual nuclear interaction favors maximal spatial overlap between the fermions which is achieved in the most symmetric $U_{orb}(\omega)$ representation. Antisymmetry of the overall wave function then requires the least symmetric $U_{ST}(4)$ representation or, equivalently, the one where the eigenvalue of the quadratic Casimir operator of $SU_{ST}(4)$,

$$g(\lambda\mu\nu) = 3\lambda(\lambda+4) + 3\nu(\nu+4) + 4\mu(\mu+4) + 4\mu(\lambda+\nu) + 2\lambda\nu, \tag{3}$$

is minimal.

For even-even nuclei the favored SU(4) representation is (0T0), where T is the isospin of the ground state. In lowest order (i.e., assuming unbroken SU(4) symmetry and neglecting orbital contributions) the binding energy is then $a + bg(0T0)$ with b positive. The coefficients a and b depend smoothly on mass number [6]. Assuming constant coefficients for the four nuclei in (1), a simple expression is found for δV_{np} that depends on b only. (In fact, the analysis presented below remains valid if a and b depend *linearly* on mass number.) The result is

$$\delta V_{np}(N,Z)/b = \begin{cases} \frac{1}{4}[g(000) - g(010) - g(010) + g(000)] = -10, & N = Z \\ \frac{1}{4}[g(0T0) - g(0,T-1,0) - g(0,T+1,0) + g(0T0)] = -2, & N \neq Z \end{cases} . \tag{4}$$

Wigner's supermultiplet theory in its *simplest* form (i.e., without symmetry breaking—dynamical or otherwise—in spin and/or isospin) therefore predicts $|\delta V_{np}|$ to be five times bigger for $N = Z$ than for $N \neq Z$. This result is displayed in Fig. 1(b).

Odd-mass nuclei can be treated in an identical way and give rise to similar conclusions [8].

References

1. E. P. Wigner, Phys. Rev. **51**, 106 (1937).
2. F. Hund, Z. Phys. **105**, 202 (1937).
3. I. Talmi, *Simple Models of Complex Nuclei. The Shell Model and Interacting Boson Model*, (Harwood, 1993), chapter 29.
4. D. D. Warner, Inst. Phys. Conf. Ser. **133**, 51 (1993).
5. P. Vogel and W. E. Ormand, Phys. Rev. C **47**, 623 (1993).
6. P. Franzini and L. A. Radicati, Phys. Lett. **6**, 322 (1963).
7. M. Chakraborty, V. K. B. Kota, and J. C. Parikh, Phys. Rev. Lett. **45**, 1073 (1980).
8. P. Van Isacker, D.D. Warner, and D.S. Brenner, Phys. Rev. Lett. **74**, 4607 (1995).
9. I. Talmi, Rev. Mod. Phys. **34**, 704 (1962).
10. D. S. Brenner, C. Wesselborg, R. F. Casten, D. D. Warner, and J.-Y. Zhang, Phys. Lett. B **243**, 1 (1990).
11. G. Audi and A. H. Wapstra, Nucl. Phys. A **565**, 1 (1993).
12. J. P. Elliott, Proc. Roy. Soc. A **245**, 128 (1958); 562 (1958).

Algebraic Description of the Scissors Mode in the Presence of a Neutron Skin

D.D. Warner[a] and P. Van Isacker[b]

[a] *CCLRC Daresbury Laboratory, Daresbury, Warrington WA4 4AD, UK*
[b] *Grand Accélérateur National d'Ions Lourds, BP 5027, F-14021 Caen Cedex, France*

In recent years, experiments with radioactive beams from projectile fragmentation facilities have revealed [1] the presence of a neutron halo in several of the lightest nuclei on the neutron drip line. This is now understood as a tunneling effect where the last one or two neutrons are in low angular momentum orbits very near the top of the well so that their wave functions have a very extended distribution which is manifest empirically in an anomalously large matter radius. There is, however, a distinctly different phenomenon which is predicted in some Hartree-Fock calculations [2, 3] to occur in heavier nuclei in which an excess of several neutrons builds up so that the neutron density actually extends out significantly further than that of the protons, resulting in a mantle of dominantly neutron matter.

The presence of this neutron "skin" may affect collective modes of nuclear excitation which involve the out-of-phase motion of neutrons against protons, such as the giant dipole resonance (GDR) [4] and the scissors mode [5], the first involving a lateral displacement of neutrons relative to protons and the second an angular displacement. There is also then the possibility of a "soft" dipole mode [6] in which the core nucleons move against the more weakly bound skin neutrons. Recently, the effect of an increasing skin thickness on the energy of these three modes was investigated [7] with a simple approach based on classical density oscillations, in which the change in the potential energy in each case was estimated from the density overlaps as a function of displacement. Not surprisingly, the effect on the first two modes was found to be minimal, while the soft dipole mode drops rapidly in energy, relative to the GDR.

~~We have investigated [8] further~~ The behaviour of the scissors mode in the presence of a neutron skin by extending the algebraic approach of the interacting boson model (IBM) [9] which has previously proved particularly ~~enlightening in characterising~~ the normal scissors mode [~~10, 11~~]. It ~~will be~~ shown that, as in the dipole case, the existence of a "soft" scissors mode may also be postulated.

In the following protons are denoted with π and neutrons with ν. The incorporation of both neutrons and protons in the IBM involves the algebra of the product $U_\pi(6) \otimes U_\nu(6)$. The starting point for the quadrupole modes of a nucleus with an additional neutron skin might therefore be taken as a triple product involving an additional algebra $U_{\nu_s}(6)$ with the remaining core neutrons being described by $U_{\nu_c}(6)$. The dynamical algebra of the system is then

$$\begin{array}{ccccc} U_\pi(6) & \otimes & U_{\nu_c}(6) & \otimes & U_{\nu_s}(6) \\ \downarrow & & \downarrow & & \downarrow \\ [N_\pi] & & [N_{\nu_c}] & & [N_{\nu_s}] \end{array} , \qquad (1)$$

where each U(6) algebra is characterised by a number of bosons N_i that are coupled symmetrically to $[N_i]$.

The fact that the skin neutrons are assumed to be weakly coupled to the core neutrons and protons, which are strongly coupled to each other, is represented in the reduction of (1) by coupling the corresponding U(6) algebra of the neutron skin *after* those describing the core nucleons. The reduction thus proceeds as

$$U_\pi(6) \otimes U_{\nu_c}(6) \otimes U_{\nu_s}(6) \supset U_{\pi\nu_c}(6) \otimes U_{\nu_s}(6) \supset U_{\pi\nu_c\nu_s}(6) \supset \cdots, \tag{2}$$

where the dots represent the usual reductions of U(6) in IBM [9].

It is the coupled nature of the algebra $U_{\pi\nu}(6)$ in IBM-2 that permits states with mixed symmetry [12], the lowest of which in deformed nuclei represent the normal scissors mode. In the reduction (2), $U_{\pi\nu_c}(6)$ is characterised by irreducible representations $[N_c - f, f]$ where N_c is the number of nucleon pairs in the core, $N_c = N_\pi + N_{\nu_c}$. The lowest states are then contained in the representation $[N_c, 0]$, which denotes the totally symmetric coupling. The lowest states of mixed symmetry are in the next representation, $[N_c - 1, 1]$. The triple-sum algebra $U_{\pi\nu_c\nu_s}(6)$ is characterised by up to three rows, with the lowest couplings arising from $[N_c, 0] \times [N_{\nu_s}]$ being $[N, 0, 0]$ and $[N - 1, 1, 0]$, N denoting the total number of bosons. Hence the first non-symmetric representation resulting from the triple-sum algebra describes *symmetric* coupling of the core nucleons and *non-symmetric* coupling of the skin neutrons. However, the non-symmetric representation $[N - 1, 1, 0]$ of $U_{\pi\nu_c\nu_s}(6)$ may also arise from the product $[N_c - 1, 1] \times [N_{\nu_s}]$. In this case, it is the core nucleons which are coupled non-symmetrically. The result is that there are now *two* scissors modes, one representing out-of-phase motion between the neutrons and protons in the core and the other denoting an angular oscillation between the core and the skin where, in this case, as in the soft dipole mode, the core protons carry the core neutrons with them.

The characteristic excitation of these angular oscillation modes is via magnetic dipole transitions. In even-even nuclei the existence of 1^+ scissors states excited in (e, e') or (γ, γ') is by now well established. The IBM-2 prediction for the M1 strength towards the 1^+ state corresponding to $|S\alpha\rangle$ in the above is

$$B(\mathrm{M1}; 0^+_\mathrm{G} \rightarrow 1^+_\mathrm{S}) = \frac{3}{4\pi}(g_\pi - g_\nu)^2 f(N) N_\pi N_\nu, \tag{3}$$

where g_π and g_ν are the boson g factors. The function $f(N)$ is known analytically in the three limits of the IBM. Equation (3) is valid for a scissors state in which all the protons oscillate against all neutrons. It also gives the sum rule for magnetic dipole strength.

A similar expression can be derived for the dipole strength to the soft-scissors state of limit a by considering the separate contributions to the M1 operator from the core and the skin neutrons,

$$\hat{T}(\mathrm{M1}) = g_\pi \hat{L}_\pi + g_\nu \hat{L}_\nu = g_\pi \hat{L}_\pi + g_\nu \hat{L}_{\nu_c} + g_\nu \hat{L}_{\nu_s}, \tag{4}$$

and this yields

$$B(\mathrm{M1}; 0^+_\mathrm{G} \rightarrow 1^+_\mathrm{SS}) = \frac{3}{4\pi}(g_\pi - g_\nu)^2 f(N) \frac{N_\pi^2 N_{\nu_s}}{N_\pi + N_{\nu_c}}. \tag{5}$$

In summary, the algebraic approach can be extended to describe a three-component system, as arises in the presence of a neutron skin in very neutron rich nuclei. The relative

coupling strengths between the components can be represented by the choice of coupling scheme and the method reveals the possibility of a soft-scissors mode in which the skin neutrons undergo angular oscillations against the remaining nucleons. The analogy with the soft dipole mode is clear and the probability of finding an empirical realisation of either depends critically on the extent to which the neutron skin develops in heavier nuclei as the neutron drip line is approached. If the extent of the skin is at least comparable to the range of the neutron-proton interaction, the notion of a partial decoupling of it from the core becomes valid and the soft modes may manifest themselves, albeit in a possibly fragmented form. The corollary is, of course, that evidence for such modes could serve as an empirical signature of the development of a neutron skin.

References

1. I. Tanihata *et al.*, Phys. Rev. Lett. **55**, 2676 (1985); Phys. Lett. **B206**, 592 (1988).
2. N. Fukunishi, T. Otsuka, and I. Tanihata, Phys. Rev. C **48**, 1648 (1993).
3. J. Dobaczewski, W. Nazarewicz, and T.R. Werner, Z. Phys. A **354**, 27 (1996).
4. M. Goldhaber and E. Teller, Phys. Rev. **74**, 1046 (1948).
5. N. Lo Iudice and F. Palumbo, Phys. Rev. Lett. **41**, 1532 (1978).
6. P.G. Hansen and B. Jonson, Europhys. Lett. **4**, 409 (1987).
7. P. Van Isacker, M.A. Nagarajan, and D.D. Warner, Phys. Rev. C **45**, R13 (1992).
8. D.D. Warner and P. Van Isacker, submitted.
9. F. Iachello and A. Arima, *The Interacting Boson Model* (Cambridge University Press, Cambridge, 1987).
10. F. Iachello, Phys. Rev. Lett. **53**, 1427 (1984).
11. D. Bohle *et al.*, Phys. Lett. B **137**, 27 (1984).
12. P. Van Isacker *et al.*, Ann. Phys. **171**, 253 (1986).

Supersymmetric Multiphonon Structure

Ka-Hae Kim[a], Takaharu Otsuka[a], A. Gelberg[b], P. von Brentano[b], and P. Van Isacker[c]

[a]Department of Physics, University of Tokyo, Hongo, Tokyo 113, Japan
[b]Institut für Kernphysik der Universität zu Köln, 50937 Köln, Germany
[c]Grand Accélérateur National d'Ions Lourds, BP 5027, F-14021 Caen Cedex, France

Multiphonon structures have recently received a renewed interest in nuclear physics [1]. In the context of the Interacting Boson Model (IBM) [2] it has been shown recently that the O(6) limit [3] possesses a multiphonon structure [4, 5]. The O(6) limit has a γ-unstable deformed ground state, upon which the multiphonon states are created by the quadrupole operator with proper symmetrization giving rise to the excitation energies represented in terms of phonon quanta and a two-phonon anharmonicity.

In [8] it is shown that multiphonon structures can also be defined for mixed systems of bosons and fermions, and the procedure is demonstrated with the example of the U(6|4) supersymmetry of the Interacting Boson-Fermion Model (IBFM) [6, 7]. In a supersymmetry both even-even and odd-A nuclei with zero, one, two or more fermions can be described by the same Hamiltonian. The resultant eigenstates are members of an appropriate supersymmetric multiplet (supermultiplet). Each supermultiplet is characterized by the same number $\mathcal{M} = N_B + N_F$ where N_B and N_F are the boson and fermion numbers respectively, and includes in general certain states of different nuclei. The limits of U(6|4) include the boson O(6) limit when no fermion is present and for which the multiphonon structure was demonstrated in [4]. When the bosons have O(6) symmetry and a single fermion occupies an orbit with $j = \frac{3}{2}$, the spinor symmetry Spin(6) of U(6|4) arises; this description has been used for several odd-even nuclei, for instance ^{197}Au in which case the fermion is identified with the odd proton. The Spin(6) subalgebra of U(6|4) contains only generators which separately conserve N_B and N_F. In [8] the multiphonon structure of the U(6|4) spectrum of systems with $N_F = 0$, 1 and 2 is demonstrated. In fact, it is shown that the idea of a multiphonon structure is valid for all limits of U(6|4) (ie., $0, 1, 2, \ldots$ fermions). The central purpose of this result is thus to extend the significance of multiphonon structures as a basic excitation mode, covering the entire supersymmetric multiplet of U(6|4)$_X$ is shown.

References

1. E.g., J. Kern, E. Garrett, J. Jolie and H. Lehmann, Nucl. Phys. **A593**, 21 (1995).
2. F. Iachello and A. Arima, *The Interacting Boson Model*, (Cambridge University Press, Cambridge, 1987).
3. A. Arima and F. Iachello, Ann. Phys. (NY) **123**, 468 (1979).
4. T. Otsuka and K.-H. Kim, Phys. Rev. **C50**, R1768 (1994).
5. G. Siems *et al.*, Phys. Lett. **B320**, 1 (1994).
6. F. Iachello and S. Kuyucak, Ann. Phys. **136**, 19 (1981).
7. F. Iachello and P. Van Isacker, *The Interacting Boson-Fermion Model*, (Cambridge University Press, Cambridge, 1991).
8. K.-H. Kim, T. Otsuka, A. Gelberg, P. von Brentano, and P. Van Isacker, Phys. Rev. Lett. **76**, 3514 (1996).

STUDY OF THE NEUTRON-RICH NUCLEI NEAR THE NEUTRON CLOSURE N=20 IN THE REACTION WITH A ^{36}S BEAM AT 78 AMeV

O.Tarasov [1], R.Allatt [2], J.C.Angélique [3], R.Anne [4], C.Borcea [5], Z.Dlouhy [6], C.Donzaud [7], S.Grévy [7], D.Guillemaud-Mueller [7], M.Lewitowicz [4], S.Lukyanov [1], A.C.Mueller [7], Yu.Oganessian [1], N.A.Orr [3], A.N.Ostrowski [4], R.D.Page [2], Yu.Penionzhkevich [1], F.Pougheon [7], A.Reed [2], M.G.Saint-Laurent [4], W.Schwab [7], E.Sokol [1], O.Sorlin [7], W.Trinder [4], J.S.Winfield [3]

[1] FLNR, JINR, 141980 Dubna, Russia
[2] University of Liverpool, UK
[3] LPC, Caen, France
[4] GANIL, BP 5027, 14021 Caen, France
[5] IAP, Bucharest, Romania
[6] NPI, Rez, Czech Republic
[7] IPN, Orsay, France

FR9700870

1. MOTIVATION

The study of the stability and of the properties of extremely neutron-rich nuclei of light elements is considered as an important and actual research subject in nuclear physics. The interest in this field has been stimulated by the of intriguing phenomena of the nuclei near the drip-line, such as "skin" or halo structure. Thus the synthesis and investigation of the properties of the extremely neutron rich isotopes of the lightest elements is of considerable interest both for locating the neutron drip-line and for testing various theories describing exotic nuclei.

One problem is the optimal nuclear reaction to reach neutron drip-line. In the sense of the highest rates of exotic nuclei as a nuclear reaction fragments, a fragmentation reactions at energies above 30 MeV/A is one of the most effective method. Moreover, as it was shown in [1] the highest rates for neutron rich products have been observed in the case of fragmentation of neutron-rich primary beam. The merits of using of ^{48}Ca-beam have been shown in this experiment while 20 new neutron rich nuclei had been synthesized for the first time. It was stressed that some of new neutron rich isotopes were produced with neutron number larger that for the projectile. The pick-up of some neutrons from target to fragments could be responsible for production of fragments with Neutron number larger then 28.

~~The goal of the present paper is the search~~ Stability of nuclei with neutron closure N=20 (mainly, ^{28}O) and ~~study of~~ β-delayed neutron decay of ~~the~~ nuclei in the region of N=20 neutron closure. As it will be shown later to produce extremely neutron rich nuclei, the fragmentation of an intense beam of the very neutron-rich ^{36}S has been chosen as a method for increasing the rates of exotic species.

Indeed, one of the interesting question in this mass region is stability of neutron-rich isotopes of oxygen. As it has been shown the heaviest experimentally known oxygen isotope was ^{24}O and ^{26}O was found to be unbound [1]. Most of theoretical models predict ^{26}O to be bound and ^{28}O unbound even of the last one is a double magic nucleus. The last attempt [2] to synthesize of ^{26}O (by reacting a 92MeV/A ^{40}Ar) have confirmed the nuclear unstability of neutron-rich oxygen isotope.

The other interesting aspect for this range of nuclei is deformation phenomenon observed close to N=20 in the Ne-Al region. The compact spherical shapes predicted to appear close to magic numbers may be replaced by some other deformed equilibrium configurations. It was shown [3] that , for instance, for ^{30}Na (one neutron hole with respect to the N=20 shell closure) the nuclear potential has one minimum at β=0 and other at β=0.35. As the neutron number increases the main equilibrium configuration for the Na isotopes will become the deformed one at β=0.4. The deformation in this region of the neutron closure could also result in the appearance of isomeric states for extremely neutron-rich oxygen, neon and sodium isotopes. Such effects may influence the decay properties of these nuclei (half-live, neutron emission probability) and as already observed in the some cases, masses and mean square radii. The present experiment is the first attempt to reach ^{28}O.

2. EXPERIMENTAL PROCEDURE

The search for nuclei near drip line which are expected to have a very low production yields was carried out at GANIL. For this search the spectrometer LISE [4] has been chosen where projectile-like fragments were collected at 0 degree by two dipole system. This attempt to synthesize ^{28}O nucleus have been performed using fragmentation of a ^{36}S(78.1 MeV/A) beam. In this new experiment, the production yield of the neutron-rich isotopes near the drip-line with N=20 have been increased by using the exotic ^{36}S primary beam at the highest energy and intensity. Another advantage was obtained by the use of an increased magnetic rigidity (up to 4.3 Tm) available after the upgrading of the first dipole of the LISE spectrometer.

As a result, the expected production yield of the neutron-rich isotopes in the region Z=8÷10 has been increased by using an exotic ^{36}S primary beam instead of the fragmentation of ^{48}Ca by factor 50 [1].

2.1. Experimental set-up

The detector system mounted in a vacuum chamber at the end of LISE, consisted of a four-stage semiconductor telescope. Two planar 500 μm Si detectors were followed by two 4.2 mm Si(Li) residual energy detectors. Time of flight of the fragments was measured with respect to the

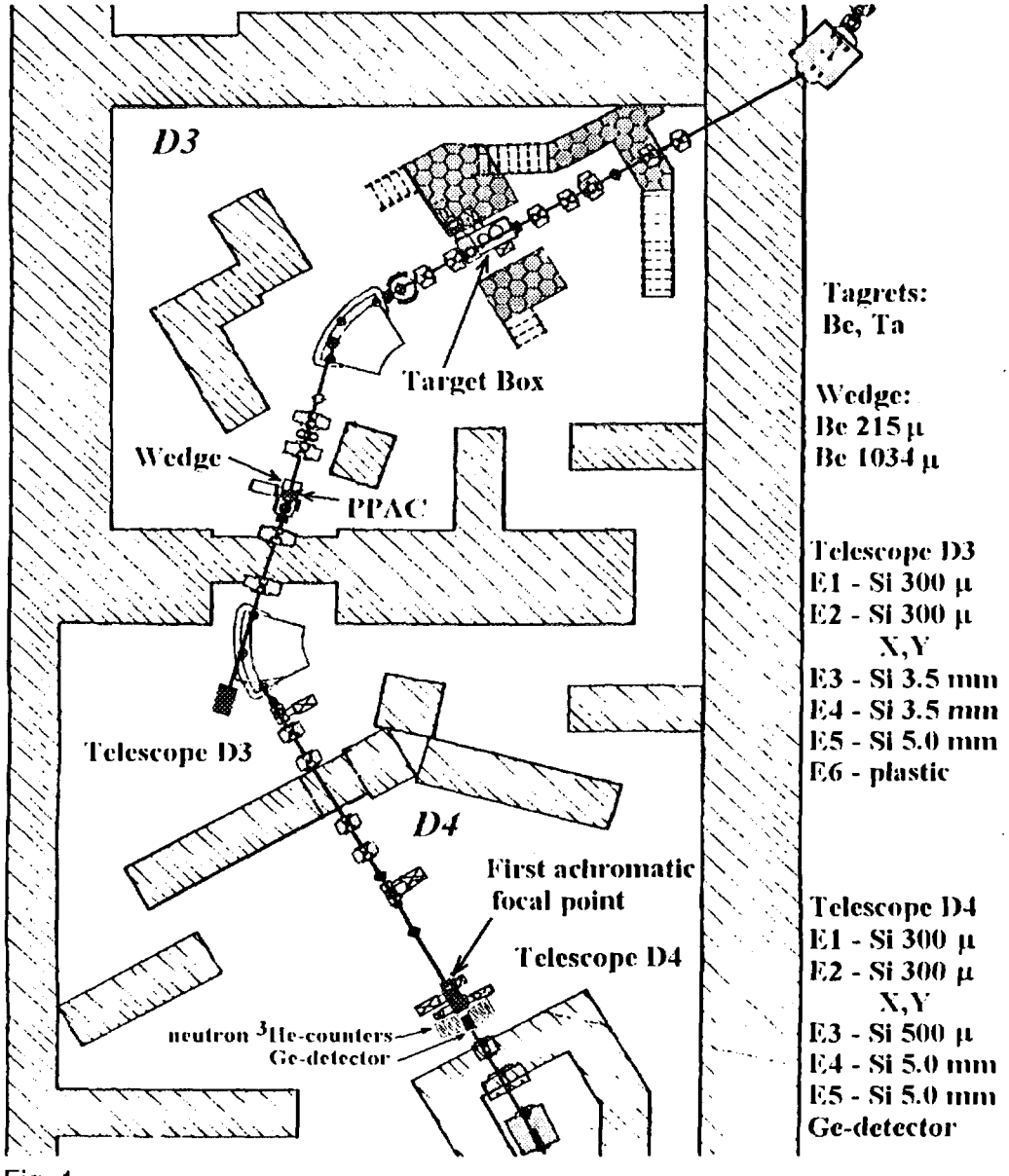

Fig. 1

radio frequency signal from the Cyclotron.

The lay-out of the detector system and spectrometer is given on the Fig. 1. The fragments were identified in a way: two first detectors allowed two independent Z determination, the mass was obtained from the total energy and the time of flight, or from the magnetic rigidity and the time of flight. The thickness of telescope was chosen so that fragments in the region of oxygen and neon could be stopped in the third detector Si(Li). A position sensitive Si detector was placed before the main telescope for spatial analysis of the secondary beam.

The signals from thick Si(Li) detectors were splitted into two signals: one for residual energy measurements and another for β-particle detection after decay of stopped ion. The data acquisition was triggered by third detector as well as by β-particle detectors. Each event was written on a tape with time of arriving.

The impantation detectors were surrounded by ^{3}He neutron counters and a 70% HPGe detector surrounding the final silicon telescope for the measuring of βn and βγ coincidences from the decay and a search of μ-second isomeric reach, for instance for $^{32}Al^{m}$ isomeric state.

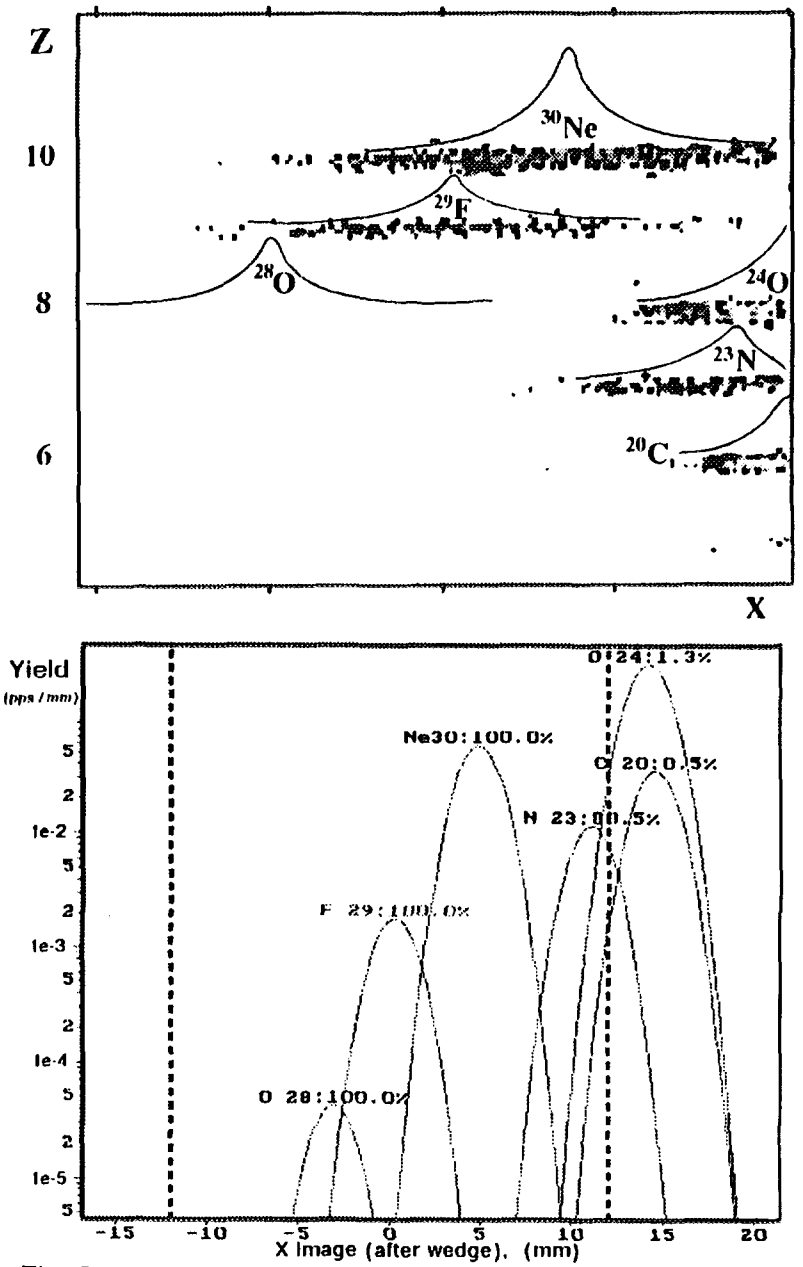

Fig. 2

2.2. Beam line optimization

To optimize the setting of the LISE spectrometer the momentum distributions of all isotopes in the region of N=20 were carefully measured. The beam line tuning was controlled by the position-sensitive Si-detector. The spectrometer was set to center the ^{28}O in the Si-telescope. For this purpose the position-sensitive detector was inserted before the telescope. On the bi-dimensional spectrum (Fig. 2) of the horizontal coordinate versus Z-value is given. A horizontal projection of this spectra is in a good agreement with computer simulation [5] of horizontal images in the focal point (one-dimensional spectra on this figure).

An optimization of the targets (Be, C, Ni, Ta) and measurements of momentum distribution of all fragments with N=20 have been undertaken for the best setting of the LISE spectrometer for ^{28}O. It was found that Ta target had produced the highest rates of the neutron-rich nuclei in agreement with earlier results.

3. EXPERIMENTAL DATA

3.1. Study of the stability of ^{28}O

An example of measured Z versus A/Q matrix coincidence is given in the Fig 3. A solid line is drawing through nuclei with N=20. This spectrum was obtained in the 53-hours measurement with an average beam intensity of 800 enA. The heaviest known isotope of ^{29}F is clearly visible. Finally we accumulated 519 events of ^{29}F nuclide. No events corresponding to ^{26}O and ^{28}O are seen.

The Fig. 4 shows the experimentally measured yields of light exotic nuclei with N=20 versus their Z-values. According to the estimation given by the modified formula of Summerer et al. [6] (solid curve) one could expect about 11 events corresponding to ^{28}O. The vertical arrow gives the counting rate for the observation of one event. The preliminary results of this investigation point to the particle instability of ^{28}O isotope as well as for ^{26}O. An upper limit for the cross section of the oxygen isotopes and some information about the stability and properties of nuclei near the closed shells N=20 ($^{27,29}F$, $^{24,26,28}O$, ^{30}Ne) could be also extracted from the data.

Thus the present experiment gives first evidence for the particle unstability of ^{28}O.

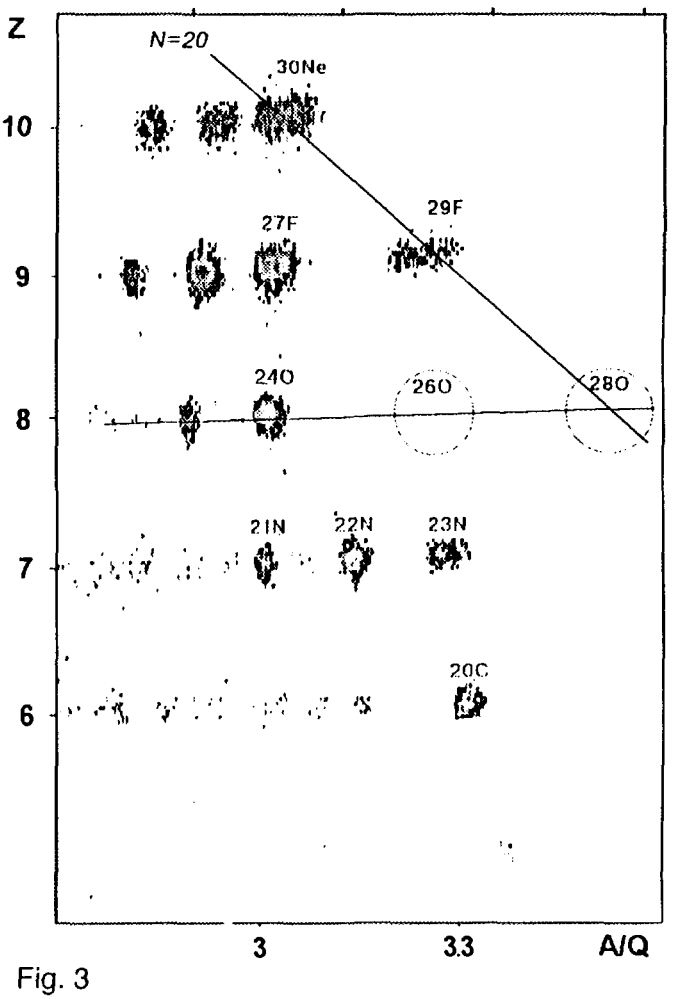

Fig. 3

3.2. β-delayed neutron decay of nuclei near neutron closure N=20

Our experiment also gives an opportunity to study the β-delayed neutron emission from neutron-rich nuclei with magic neutron number N=20, such as ^{29}F, ^{30}Ne and ^{31}Na. The first measurement of $T_{1/2}$ values for $^{27,29}F$, ^{30}Ne are presented. Additionally, the case of ^{8}He, ^{12}Be, ^{14}B and other nuclei, with neutron shell N=20, $^{28,29}Ne$, $^{30,31}Na$ are re-examined. For instance, the experimental curves of half-live measurement for ^{30}Ne and ^{31}Na are shown in the figure. The further data analysis and comparisons of presented data with various theories such as the gross theory [7] or QRPA [8] are in progress. The result of $^{32}Al^{m}$ isomeric state study is given elsewhere [11].

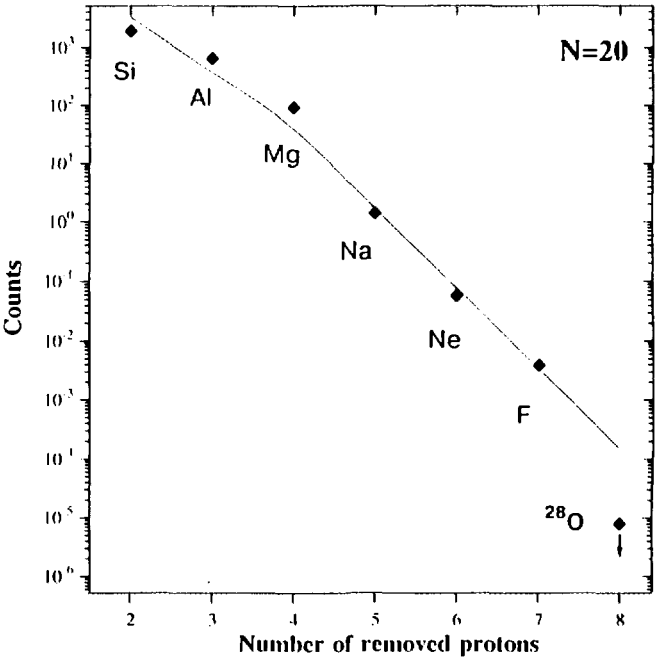

Fig. 4

Table

A, Z	This work		Reference	
	$T_{1/2}$	$\Delta T_{1/2}$	$T_{1/2}$	$\Delta T_{1/2}$
^{27}F	5.26	0.15	-	
^{29}F	2.41	0.33	-	
^{28}Ne	21.	3.	17[9]	4
^{29}Ne	15.	2.	200[9]	100
^{30}Ne	7.2	0.6	-	
^{30}Na	47.9	4.4	50[10]	3
^{31}Na	17.7	0.9	17[10]	0.4

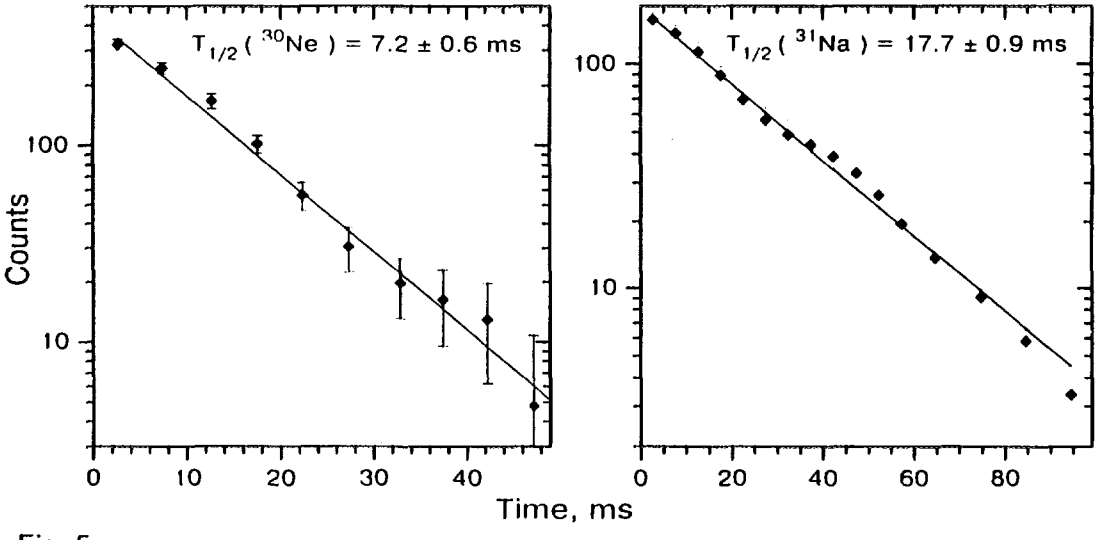

Fig. 5

References

[1] D.Guillemaud-Mueller, Yu.Penionzhkevich et.al., Physical Review **C41**[3](1990)

[2] M. Hellstrom M. Fauerbach et.al., In Proc.of Intern. Conf. on Exotic Nuclei and Atomic Masses, Arles, France, June 19-23, 1995.

[3] Lutostansky Yu. et.al., In Proc. of the 5th Int. Conf. on Nucl. Far from Stab., Canada, 1987

[4] R.Anne, D.Bazin, A.C.Mueller, J.C.Jacmart, M.Langevin, NIM **A257**(1987)215-232

[5] D.Bazin, to be published

[6] K.Sümmerer, W.Brüchle, D.J.Morrissey, M.Schädel, B.Szweryn, Y.Weifan, Physical Review **C42**[6](1990)2546-2561

[7] T.Tachibana et al., Report of Sci.and Eng.Res.Lab., Waseda University, No.88-4, 20 Dec., 1988, ISSN 0285-4333.

[8] A.C.Mueller et al., Nuclear Physics **A513**(1990)1

[9] O.Tengblad, M.J.G.Borge et al., Z.Phyz. **A342**(1992)303-307

[10] D.Guillemaud-Mueller, C.Detraz, M.Langevin, F.Naulin, M.De Saint-Simon, C.Thibault, F.Touchard, M.Epherre, Nuclear Physics **A426**(1984)37-76

[11] M.Robinson, P.Halse, W.Trinder, R.Anne, C.Borcea, M.Lewitowicz, S.Lukyanov, M.Mirea, Yu.Oganessian, N.A.Orr, Yu.Penionzhkevich, M.G.Saint-Laurent, O.Tarasov, Physical Review **C53**[4](1996)1465-1468

^{78}Kr fragmentation

New isotopes and β-delayed protons

B. Blank, S. Andriamonje, S. Czajkowski, F. Davi, R. Del Moral, J.P. Dufour, A. Fleury, A. Musquère, M.S. Pravikoff (CEN Bordeaux-Gradignan), R. Grzywacz, Z. Janas, M. Pfützner (Univ. Warsaw), A. Grewe, A. Heinz, A. Junghans (TH Darmstadt), M. Lewitowicz (GANIL Caen), J.-E. Sauvestre (CE Bruyères-le-Châtel), C. Donzaud (IPN Orsay)

As the path of the rp process is very close to the proton drip line, the knowledge of the limits of stability is of particular interest and determines most key points of the rp-process path such as waiting points and the ending point. Nuclei like ^{65}As, ^{69}Br, and ^{73}Rb have been considered as key nuclei for the rp-process path. If these nuclei were sufficiently bound so that their decay is dominated by β decay, the rp process could pass through them by proton capture and proceed to higher masses.

In addition to the astrophysical interest of new isotopes, this region of the chart of nuclei offers unstable nuclei having a high β-decay Q-value so that they decay by β-delayed particle emission. The measurement of the spectrum of emitted protons allows to test level-density formulae and to determine the difference (Q_{EC} - S_p) between the β-decay Q-value and the proton separation energy. The shape of the proton spectra and the absolute proton branching ratio may give some insight in the question about the deformation of these nuclei. On the other hand, β-delayed protons are a useful tool to determine β-decay half-lives.

In an experiment performed at the SISSI/LISE facility, we searched for new proton-rich isotopes [X] by means of projectile fragmentation of a primary ^{78}Kr beam at 73 MeV/nucleon and measured for the first time β-delayed protons from ^{67}Se, ^{71}Kr, and ^{75}Sr [X].

The fragments have been identified by a TOF-ΔE-E analysis. This identification was checked by measuring the γ decay of the known isomers ^{69,71}Se with four germanium detectors surrounding the silicon-detector telescope. The measurement of γ rays from isomer decays allowed us to measure for the first time the spectrum of the isomer ^{66}As [3]. The resulting ΔE-TOF plot purified by conditions on the low-resolution TOF as well as on the energy loss in a silicon detector behind the ΔE counter is shown in Fig. 1a. The energy loss signal has been corrected for the velocity dependence of the energy loss in order to yield the nuclear charge Z. Figs. 1b,c,d show the results of the projection for the rows with isospin projections T_z = -1/2, T_z = -1, and T_z = -3/2, respectively.

The new isotopes are indicated by the arrows. We find clear evidence for ^{60}Ga, ^{64}As, ^{69,70}Kr, and ^{74}Sr. On the other hand, we have no counts which can be attributed to ^{69}Br (arrow in Fig. 1b), whereas other nuclei with the same isospin projection T_z are observed with more than 1000 counts.

The isotope ^{69}Br is expected to be proton unbound by almost all commonly used mass predictions [4]. The present results demonstrate that ^{69}Br is proton-unbound by at least 450 keV to yield a barrier-penetration half-life of less than 100 ns. In the case of ^{60}Ga, the mass models differ in predicting its stability. However, all mass models predicit proton separation energies laying inside a band of $\pm$ 260 keV around S_p=0. Therefore, ^{60}Ga is expected to decay mainly by β decay. The nucleus ^{64}As is predicted to be unbound by about 100-400 keV according to commonly used mass models [4]. The observation of ^{64}As in our experiment and the comparison of the counting rate to neighboring nuclei excludes half-lives much shorter than about 1 μs. From different barrier-penetration calculations, we conclude that ^{64}As is unbound by less than about 400 keV or bound. The even-Z new isotopes ^{69,70}Kr and ^{74}Sr are predicted by all mass models to be stable against

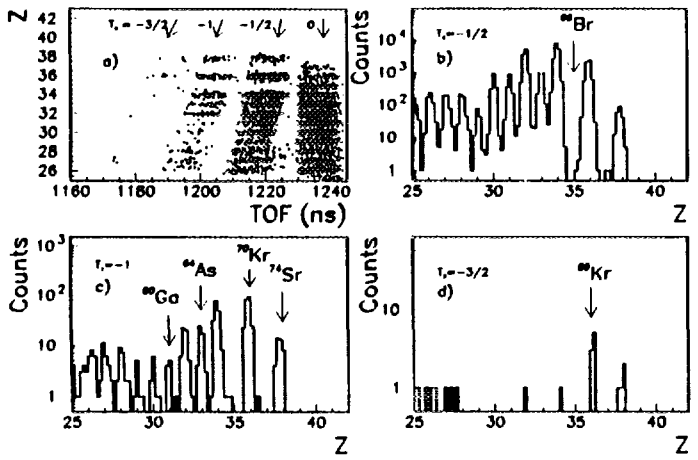

Figure 1: Two-dimensional plot of the nuclear charge Z versus the time of flight between the target and the silicon detector (a). The rows of almost constant TOF represent rows of constant isospin projection T_z. Parts b-d give the projections of the different isospin-projection rows on the nuclear charge for T_z = -1/2 (b), for T_z = -1 (c), and for T_z = -3/2 (d). The arrows indicate the new isotopes [c),d)] as well as the expected position of ^{69}Br [b)].

particle emission from their ground state.

The upper limit deduced from our data for the half-life of ^{69}Br shows that this nucleus is proton unbound. This finding together with the observation of ^{60}Ga and ^{64}As changes our understanding of the astrophysical rp-process in this region, ^{68}Se being now the ending point for rapid proton capture in the model of Ref. [5] due to its long half-life compared to the time scale of the rp process. The presence of ^{60}Ga and ^{64}As could open new branches for the rp process around these nuclei. However, it has to be shown that ^{60}Ga and ^{64}As are stable enough, i.e. that their decay is dominated by β decay.

In order to study the decay properties of proton-rich isotopes, nuclei of interest were stopped in the center of a silicon telescope. The range of the fragments was adjusted by using wheels with different thicknesses of aluminum. After the implantation of isotopes of interest, the primary beam was switched-off for 150 ms. During this interval, β decay of a given isotope could be observed under low-background conditions and time-correlated with the implantation event. Fig. 2 shows the energy spectra and time distributions of β-delayed particles measured for ^{67}Se, ^{71}Kr and ^{75}Sr.

On the basis of the fraction of the number of implanted nuclei as counted in the TOF-ΔE-E analysis and of the number of observed protons the branching ratios for proton emission has been deduced to be P_p = (6.5±3.3)% for ^{75}Sr, P_p = (5.2±0.6)% for ^{71}Kr, and P_p = (0.5±0.1)% for ^{67}Se. The factor of ten between the branching ratios for ^{75}Sr and ^{71}Kr on the one hand and of ^{67}Se on the other hand is most likely due to nuclear-structure effects like deformation. A similar effect has been observed by Hardy et al. [6] for the T_z=1/2 nuclei ^{69}Se, ^{73}Kr, and ^{77}Sr.

In order to calculate the energy spectra of β-delayed protons, we used a statistical model [7]. In the calculations, we assumed a constant β-strength function and (Q_{ec}-S_p) values of 7.84 MeV, 8.55 MeV, and 8.23 MeV for ^{67}Se, ^{71}Kr, and ^{75}Sr, respectively [8]. The spin of the decaying nuclei was assumed to be $I^\pi = 5/2^-$ and only transitions to the ground state of the final nucleus were considered. The probability of a proton emission from a given state, expressed in terms of angular-momentum dependent transmission coefficients through the Coulomb barrier and level densities, was calculated using different sets of spherical optical-model parameters and the level-density formula of Gilbert and Cameron [9]. The dashed lines in Figs. 2a-c show the predicted shapes of the proton spectra. The calculated curves were normalized to get the best agreement with the measured spectra.

Figs. 2d-f show the time distributions of protons emitted after β decay of ^{67}Se, ^{71}Kr, and ^{75}Sr,

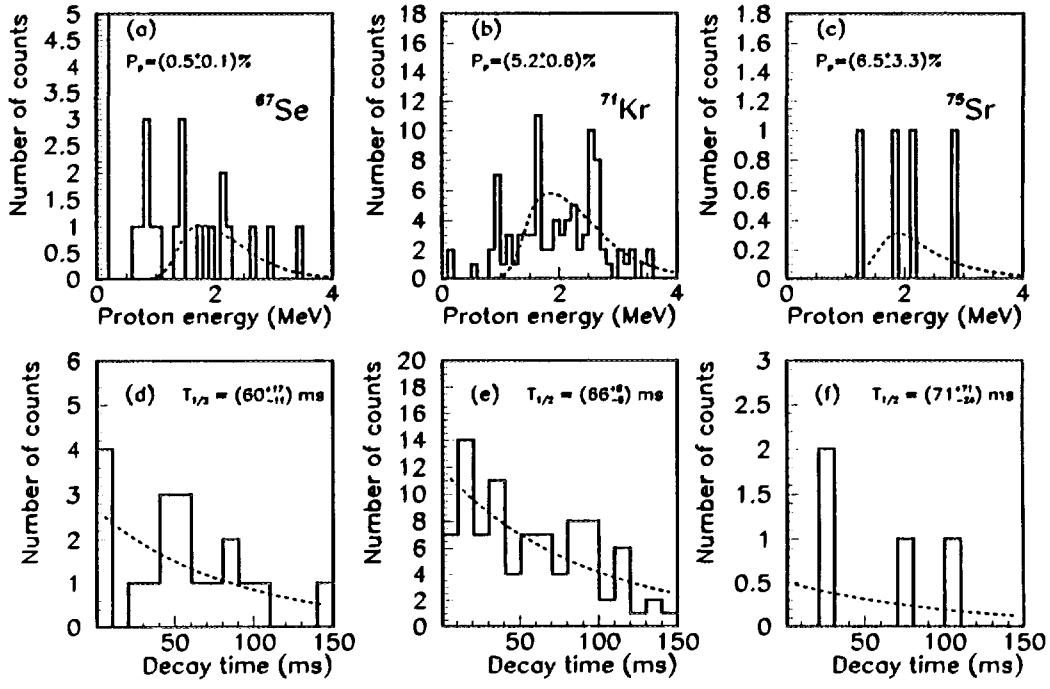

Figure 2: Upper panel: Energy spectra of particles emitted in the β decay of ^{67}Se (a), ^{71}Kr (b), and ^{75}Sr (c). The events with energy lower than 500 keV correspond to the detection of β particles, signals with energies higher than 500 keV are due to the registration of protons. The dashed line shows the results of statistical-model calculations (see text for details). Lower panel: Time distributions of protons emitted after β decay of the studied nuclei. The dashed line represents a maximum likelihood fit to the data using a single decay component.

respectively. To select protons, only signals with energies higher than 500 keV were accumulated in these spectra. The half-lives of the nuclei studied were deduced by fitting a single-component decay curve (dashed line in Figs. 2 d-f) to the measured time distribution. The half-lives of $T_{1/2} = (60^{+17}_{-11})$ms, (64^{+8}_{-5})ms, and (71^{+71}_{-24})ms for ^{67}Se, ^{71}Kr, and ^{75}Sr, respectively, were obtained.

References

[1] B. Blank et al., Phys. Rev. Lett 74, 4611 (1995)

[2] B. Blank et al., Phys. Lett. B364, 8 (1995)

[3] R. Grzywacz et al., this report

[4] 1986-1987 Atomic Mass Predictions, At. Data Nucl. Data Tables 39, 185 (1988)

[5] A.E. Champagne et al., Rev. Nucl. Part. Sci. 42, 39 (1992)

[6] J.C. Hardy et al., Phys. Lett. 63B, 27 (1976)

[7] D. Schardt, private communication

[8] G. Audi et al., Nucl. Phys. A565, 1 (1993)

[9] A. Gilbert et al., Can. J. Phys. 43, 1446 (1965)

Spectroscopy of ^{22}Al, and ^{22,23,24}Si

S. Czajkowski, B. Blank, F. Boué, S. Andriamonje, R. Del Moral, J.P. Dufour, A. Fleury, P. Pourre, M.S. Pravikoff (CEN Bordeaux-Gradignan), E. Hanelt (TH Darmstadt), K.-H. Schmidt (GSI Darmstadt), N.A. Orr (LPC Caen)

The fact that the sd shell is very well studied from a shell-model point of vue [1] makes nuclei in this region very attractive for detailed studies. A detailed comparison between model predictions and experimental results is possible. In the case of ^{22}Al, e.g. a yet unobserved decay mode via $\beta\alpha$ emission is predicted. ^{22,23}Si are possible candidates for β2p and β3p emission as well as for the yet unobserved βpα decay. ^{24}Si is a βp emitter with only one known transition [2]. Nevertheless, from mirror symmetry as well as from shell-model calculations one expects a variety of transitions.

In an experiment performed at the LISE3 facility, ~~we produced~~ ^{22}Al and ^{22,23,24}Si as projectile fragments from a ^{36}Ar primary beam at 95 MeV/u ~~and implanted them in a~~ detector telescope consisting of silicon detectors and a micro-strip gas counter (MSGC) [3]. The spectra obtained are presented.

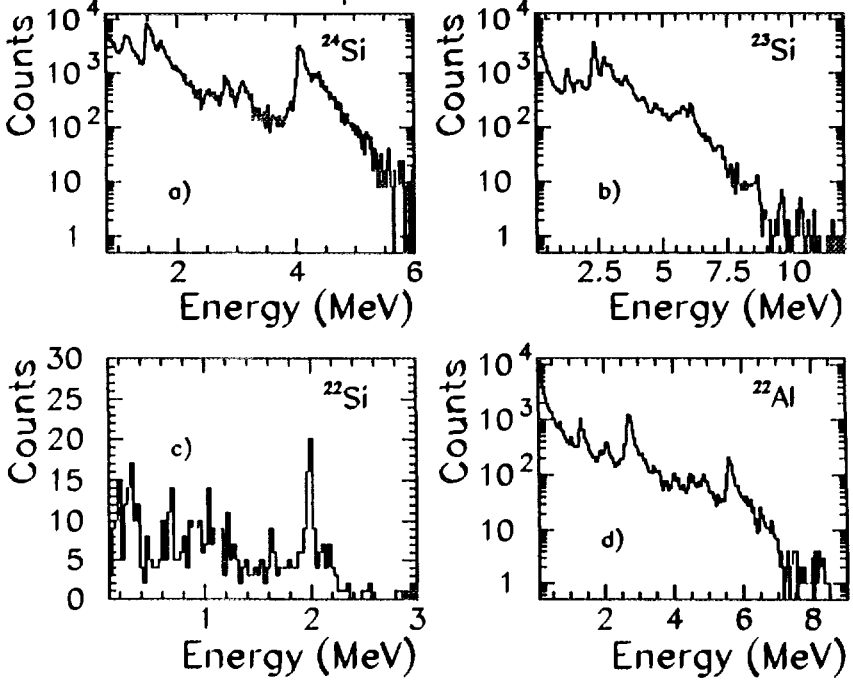

have been produced

Figure 1: β-delayed charge-particle spectra obtained after implantation of ^{24}Si (a) and ^{23}Si (b) in the silicon detector, of ^{22}Si in the MSGC (c), and of ^{22}Al (d) in the silicon detector.

Fig. 1 shows the resulting spectra taken with the silicon detector (a,b,d) and the micro-strip gas counter (c). We identify a variety of charged-particle peaks. For ^{24}Si, almost all

peaks can be attributed to transitions between known levels in the intermediate and final nucleus. Such an attribution is eased by the fact that several levels in the daughter nucleus are already known due to other measurements. This allows a detailed comparison with shell-model calculations [4]. This is done by means of the experimentally determined decay scheme which is confronted to the shell-model predictions in Fig. 3a. The experimental half-life is (140±3)ms.

For ^{23}Si, the mass excess of the IAS in ^{23}Al is calculated to be Δm = 18.74 MeV which corresponds to an excitation energy of 11.97 MeV. The decay of this level by proton emission to the ground state in ^{22}Mg releases a total energy of 11.85 MeV. In our spectra, we observe a weak proton group at 11.62 MeV which is due to this decay. The peak at 10.41 MeV belongs to the decay of the IAS to the first excited state. This allows us to determine the mass excess of ^{23}Si by means of the IMME. We find Δm = 23.42 MeV. Its half-life is (40.7±0.4)ms.

The charged-particle groups at 5.86 MeV and at 6.18 MeV belong to the decay of the IAS by β-delayed two-proton emission to the first excited state and the ground state of ^{21}Na. After the identification of this decay mode for ^{22}Al, ^{26}P, ^{35}Ca, ^{31}Ar, ^{27}S, ^{39}Ti, and for ^{43}Cr, ^{23}Si is the lightest β2p emitter of the T_z = -5/2 series.

The other peaks in spectrum b) of Fig. 1 are due to βp decays of excited levels in ^{23}Al fed by allowed Gamow-Teller transitions. In part, they can be attributed to decays between levels in ^{23}Al and in ^{22}Mg. In Fig. 3b, the experimental decay scheme is compared to predictions by the shell model [4]. Besides one allowed β transition not predicted as important but observed in the experiment, a very nice agreement is obtained.

In the ^{22}Si case, we have proton groups at (1.63±0.05) MeV, at (1.99±0.05) MeV, at (2.10±0.05) MeV, and at (2.17±0.05) MeV. The experimental branching ratios are (6±2)%, (20±2)%, (4±2)%, and (2±1)%, respectively. These proton groups can be attributed to transitions between ^{22}Al and ^{21}Mg. The half-life of ^{22}Si is (28±3)ms. A comparison to shell-model results shows that, as in the mirror decay of ^{22}O, one level at low excitation energy is much stronger fed than predicted by the model.

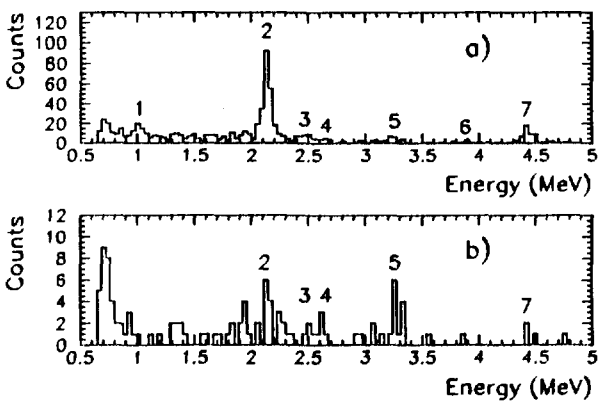

Figure 2: β-delayed α spectrum obtained after drift-time analysis in the MSGC (a). Peaks labeled 1-4 and 6,7 are identified as belonging to ^{20}Na. The peak at 3.25 MeV (5) originates from the decay of ^{22}Al. An additional condition on a ^{22}Al implantation in the MSGC (b) suppresses almost all ^{20}Na activity.

Besides βp emission from ^{22}Al as shown in Fig. 1d from the silicon detector, the feature of the MSGC to be able to distinguish protons from α particles [3] allowed us to search

for the predicted decay of the IAS via α emission. The α spectrum is shown in Fig. 2. Almost all activity in this spectrum is due to the decay of ^{20}Na, a contaminant in our measurement. However, the peak at 3.25 MeV belongs to the decay of ^{22}Al. First of all, this is the expected energy for a transition from the IAS in ^{22}Mg to the first excited state in ^{18}Ne. Secondly, for a possible transition in ^{20}Na the branching ratio is a factor of 500 too high as compared to the main peaks in ^{20}Na. Thirdly, the half-life of the activity is in agreement with the one of ^{22}Al ($T_{1/2}$ = (59±3)ms) and disagree with the one of ^{20}Na. We therefore attribute this activity to the decay of ^{22}Al.

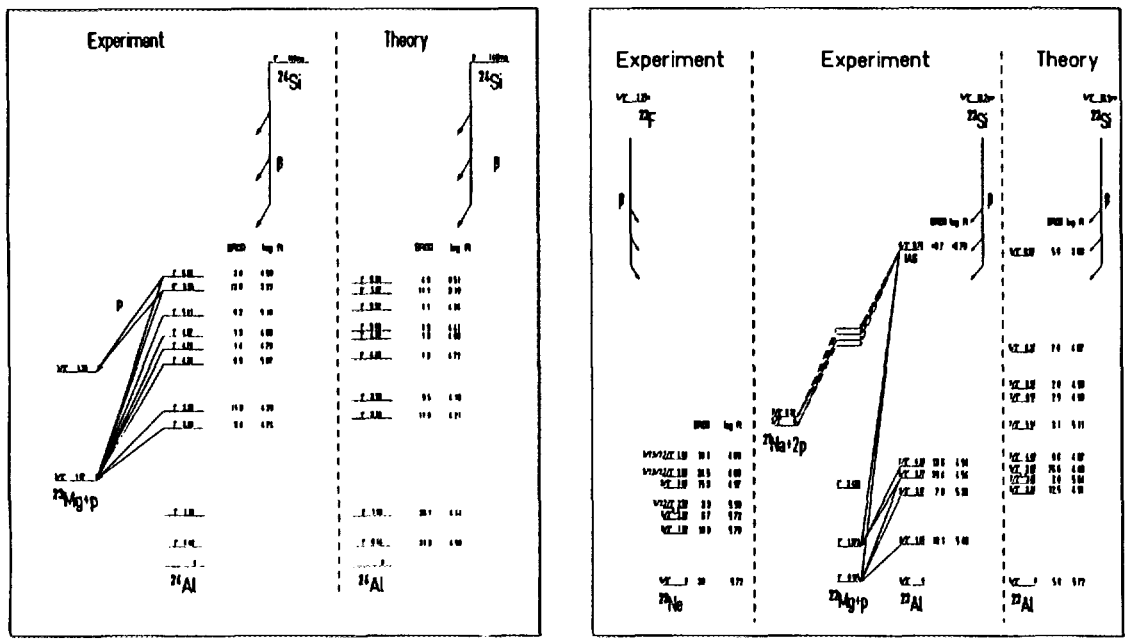

Figure 3: Comparison of the experimentally determined partial decay schemes for ^{24}Si and ^{23}Si to predictions of the shell model.

References

[1] B.A. Brown et al., At. Data Nucl. Data Tables 33, 347 (1985)

[2] Äystö et al., Phys. Rev. C23, 879 (1981)

[3] B. Blank et al., Nucl. Instr. Meth. A330, 83 (1993)

[4] B.A. Brown, private communication

IDENTIFICATION OF ^{100}Sn AND OTHER PROTON DRIP-LINE NUCLEI IN THE REACTION ^{112}Sn + ^{nat}Ni AT 63 MeV/nucleon

M. Lewitowicz[a], R. Anne[a], G. Auger[a], D. Bazin[a], C. Borcea [b], V. Borrel[c], J.M. Corre[a], T. Dörfler[d], A. Fomichov[e], R. Grzywacz[f], D. Guillemaud-Mueller[c], R. Hue[a], M. Huyse[g], Z. Janas[h],*, H. Keller[h], S. Lukyanov[e], A.C. Mueller[c], Yu. Penionzhkevich[e], M.Pfützner[f], F. Pougheon[c], K. Rykaczewski[f], M.G. Saint-Laurent[a], K. Schmidt[h], W.D. Schmidt-Ott[d], O. Sorlin[c], J. Szerypo[g],*, O. Tarasov [e], J. Wauters[g], J. Żylicz[f]

[a] *GANIL, BP 5027,14021 Caen Cedex, France*
[b] *IAP, Bucharest-Magurele P.O.Box MG6, Roumania*
[c] *IPN, 91406, Orsay Cedex, France*
[d] *University of Göttingen, D-3400, Göttingen, Germany*
[e] *FLNR, JINR 141980 Dubna, Moscow region, Russia*
[f] *IFD, Warsaw University, 00681 Warsaw, Poland*
[g] *IKS KU, B-3001, Leuven, Belgium*
[h] *GSI, Postfach 110552, D-64220, Darmstadt, Germany*

Abstract

The doubly-magic nucleus ^{100}Sn and six new neutron-deficient nuclei in the A~100 region were identified in the reaction ^{112}Sn + ^{nat}Ni at 63MeV/nucleon. The experiment was carried out using the high acceptance device SISSI and the Alpha and LISE3 spectrometers at GANIL. The identification of the reaction products (A, Z and Q) was made using the measurements of time-of-flight, energy-loss and kinetic energy.

Studies of N=Z and neighbouring nuclei, especially in the region of a double shell closure, are important for testing and further development of nuclear models [1, 2]. In particular, these studies provide information about the interaction between protons and neutrons occupying the same shell-model orbits.

While N=Z nuclides of low mass are mostly stable, the heavier ones lie away from the line of beta stability. In the case of ^{100}Sn, the deficit of neutrons with respect to the mean atomic mass of the stable tin isotopes is about 18 and it is expected [3] to be the heaviest N=Z nuclear system stable against ground-state proton decay. This stability is related to the doubly-magic character of ^{100}Sn. It may be noted that for heavier N=Z nuclei the condition of double shell closure is not sufficient to ensure stability: ^{164}Pb presumably lies well beyond the proton drip line. Mapping the proton-drip line in the neighbourhood of ^{100}Sn may also

*On leave of absence from IFD, Warsaw University, 00681 Warsaw, Poland

be of great importance in an astrophysical context as the properties of the proton-rich nuclei dictate the pathway of the rapid proton capture process in hot and dense stellar environments [4].

Beta decay in the ^{100}Sn region can be described in a very simple shell-model picture. It is strongly dominated by one channel, the $\pi g_{9/2} \rightarrow \nu g_{7/2}$ Gamow-Teller (GT) transition, and thus the observation of fast beta decays can lead to the unambiguous identification of the parent and daughter nuclear states. A meaningful verification of model predictions can be performed as, due to the high Q_{EC} values, the beta decay strength can be determined over a large energy range [5]. This had been a motivation for a series of experiments using on-line mass separators at GSI Darmstadt, LLN IKS Leuven and CERN/ISOLDE Geneva [1].

The nuclei ^{100}In ($T_{1/2} = 5 \pm 1$ s) and ^{101}Sn are the closest ones to ^{100}Sn discovered so far using a fusion-evaporation reaction (^{58}Ni (5 MeV/nucleon) + ^{50}Cr) and the on-line mass-separation technique [6, 7]. These nuclei were identified via the measurement of beta-delayed protons, a decay mode which becomes energetically possible in this region due to the high Q_{EC}. However, any attempt to produce and identify in the same way ^{100}Sn is most probably hopeless. Indeed, for ^{101}Sn approximately one proton was observed per hour, for a proton branching ratio that is predicted to be larger than 10 %. The production rate and the proton branching ratio in the case of ^{100}Sn are expected to be at least one and several orders of magnitude lower respectively. Obviously other production methods and identification techniques have to be used to reach and study ^{100}Sn [8].

Recently, in April 1994, ^{100}Sn was independently identified in two experiments employing a projectile-fragment separator technique. Here we report on the work performed at GANIL using a 63MeV/nucleon ^{112}Sn beam [9, 10]. The experiment carried out at GSI with a 1.1 GeV/nucleon ^{124}Xe beam is described in ref.[11].

To produce and identify ^{100}Sn at GANIL a fragmentation-like reaction was employed in conjunction with the SISSI device [15] and the magnetic spectrometers Alpha [16] and LISE3 [17] which provided for the collection, separation and in-flight identification of the different reaction products. In order to enhance the production of neutron-deficient isotopes a beam of the lightest, stable tin isotope,^{112}Sn, and a natural Ni target (68.3 % ^{58}Ni) were used. In an earlier experiment [9], we had already observed the neutron deficient tin isotopes down to ^{101}Sn, including the previously unknown ^{102}Sn. In addition, new isotopes of rhodium (^{92}Rh, ^{93}Rh) and palladium (^{93}Pd) were clearly observed and evidence for the production of even lighter isotopes of these elements, such as ^{91}Rh, ^{90}Rh, ^{89}Rh and ^{92}Pd, was also obtained (identification of these neutron-deficient rhodium and palladium isotopes has been recently reported by a group working at MSU [18]). The present experiment, performed with a substantially enhanced experimental arrangement provided a confirmation of these results and the discovery of several new nuclides, ^{100}Sn,^{103}Sb,^{104}Sb,^{98}In, ^{91}Pd,^{89}Rh and ^{87}Ru [12, 13].

The experimental set-up used for the identification of ^{100}Sn and neighbouring nuclei is shown in figure 1. The production target was located between the two superconducting solenoids of SISSI. Thus, in comparison with the previous experiment [9] the angular acceptance for the reaction products was increased by an order of magnitude and the flight-path (118m in the present experiment) increased by almost a factor of 3. The momentum analysis was

performed using the Alpha spectrometer ($B\rho$=1.876 Tm) with an acceptance Δp/p=0.29 %. To reduce the rate of the light, fully stripped fragments arriving at the final focus of LISE3 with A/Z≈2, a thin mylar foil (1.5μm) was placed at the intermediate focal plane (see figure 1). The function of this foil was to change the charge state distributions of the heavy fragments without modifying their velocities. For example, $^{100}Sn^{+48}$ was converted into a mixture of $^{100}Sn^{+49}$, $^{100}Sn^{+48}$ and $^{100}Sn^{+47}$ (the charge state Q=+48 was the most strongly populated after the target and stripping foil for the tin isotopes). Light fragments, however, remained fully stripped. Consequently, by employing an acceptance range in the second section of LISE3 from 1.013×$B\rho$ to 1.063×$B\rho$, the transmission of fully stripped ions was strongly suppressed and that of the nuclei in the region of interest was favoured. The number of unwanted particles was further reduced using the velocity filter located at the end of LISE3.

Fragments arriving at the final focus of LISE3 were stopped in a telescope consisting of four silicon detectors: E1 (300μm),E2 (300μm), E3 (300μm) and E4 (500μm). Since ions in the mass region of interest were stopped in the E2 detector, the E1 detector provided information on the energy-loss (ΔE), while the E1 and E2 detectors combined served to determine the total kinetic energy (TKE). The E3 and E4 detectors were used in veto mode to reject events corresponding to lighter ions. The time-of-flight (TOF) was measured using a start signal provided by the first Si detector (E1) and a stop signal derived from the radio-frequency of the second cyclotron.

The Ge detector array surrounding the implantation telescope used in the first experiment with the ^{112}Sn beam was replaced by a segmented BGO ring [19]. An increase in efficiency (from 6.4% to 50% for the 511 keV photopeak) was preferred to the good resolution. The priority of the gamma-detection was the recording of annihilation radiation (the 511-511 keV pairs in opposite segments) in correlation with heavy-ions, in order to obtain half-life information on the exotic nuclei. However, even with the poor resolution of the BGO ring, nine known decays of the short-lived isomeric states (from ^{43m}Sc to ^{96m}Pd) were clearly observed [14]. This confirmed unambiguously the standard ΔE-TKE-TOF isotope identification procedure, which was based on the calibrations with ^{112}Sn charge states.

The Ni target (144 mg/cm^2) was mounted such that the angle with respect to the beam axis could be changed from 0° to 45°. Angles between 36° and 45° were used to allow the transmission of ^{112}Sn ions with Q=+46 to +50 to the Si detector telescope in order to provide calibrations for the energy-loss, total kinetic energy and time-of-flight measurements. It should be noted that the magnetic rigidity of the beam line from the production target to the stripping foil remained fixed during the whole experiment at 1.876 Tm. This corresponded to the maximum calculated production rate for $^{100}Sn^{+48}$ ions.

The transmission of the beam line from the exit of the Alpha spectrometer to the final focus of LISE3 was measured using movable 300 μm Si detectors located at the exit of the Alpha spectometer, at the entrance to and at the intermediate focal plane of LISE3 and using the Si detector telescope. A transmission of nearly 100 % was found.

The resolution (FWHM) of the TOF measurement was about 1 ns, while the TOF ranged from 1.4 to 1.5 μs. The atomic number of the fragments (Z) was calculated using the ΔE measured with the E1 detector and absolute Z identification was obtained from the charge

states of ^{112}Sn primary beam [20, 9]. Another unambiguous assignment of Z was obtained from the direct identification of the light ions in the ΔE versus TOF spectrum.
From the measured TKE and TOF [20, 9] for a group of events, selected on the basis of the Z and A/Q (figure 2) it is possible to calculate the masses of the individual ions . The resulting mass distributions for ^{104}Sn^{+50}, ^{102}Sn^{+49}, ^{100}Sn^{+48} and ^{105}Sn^{+50}, ^{103}Sn^{+49}, ^{101}Sn^{+48} are given in figures 2*c* and *d* respectively. Eleven events corresponding to ^{100}Sn^{+48} were observed over a period of 44 hours with a primary beam intensity of ~2.4 pnA. The relative yields of the different isotopes of tin shown in figure 2 do not reflect the corresponding production cross-sections as they are affected by the distribution of the products over the different charge states as well as the different transmission efficiencies. The events attributed to the same fragment but produced in the different charge states Q at the target have been summed up. For even-mass nuclei the charge states corresponding to A-2Q=4 (e.g. ^{100}Sn^{+48}) and A-2Q=6 (e.g. ^{100}Sn^{+47}) have been taken into account, while for odd-masses A-2Q=3 (e.g. ^{101}Sn^{+49}) and A-2Q=5 (e.g. ^{101}Sn^{+48}) were included. The distributions of even- and odd-mass nuclei are presented in the separate pictures of Fig. 2 - as they were observed at the two-dimensional Z versus A/Q plot, see [12]. In these mass-spectra the respective neighbouring nuclei (with ΔA=2) are clearly separated. In addition to the eleven events of ^{100}Sn^{+48} reported in [12], thirteen more events have been assigned to the ^{100}Sn^{+47} ions, giving a total of 24 events of ^{100}Sn identified in this experiment.
The obtained data allow for the identification of six other new nuclei, namely ^{103}Sb, ^{104}Sb, ^{98}In, ^{91}Pd, ^{89}Rh and ^{87}Ru, which are clearly isolated from neighbouring heavier isotopes in the measured spectra given in Fig. 3.
The number of events observed may be used to obtain a lower limit for the production cross-section by taking into account the estimated transmission efficiency (~5 %) and the charge state distribution measured for the ^{112}Sn beam after the Ni target. For ^{100}Sn this leads to $\sigma \geq 120$ pb.
For the first time nuclei near and at the proton drip-line in the region of the doubly-magic nucleus ^{100}Sn have been produced with relatively high rates — about 5 per day for ^{100}Sn. This result confirms that medium energy fragmentation-like reactions combined with projectile-fragment separation techniques presently offer the most efficient method for the production of very neutron-deficient nuclei up to A≈100.

References

[1] K. Rykaczewski, Proc. of 6th Int. Conf. on Nuclei far from Stability and 9th Int. Conf. on Atomic Masses and Fundamental Constants, Bernkastel-Kues 1992, R. Neugarth, A. Wöhr (eds), IOP Conf. Ser. **132** (1993) 517

[2] A. Johnson et al., Nucl. Phys. A557 (1993) 401c

[3] P.E. Haustein (ed.), At. Data Nucl. Data Tables **39** (1988) 185

[4] R.K. Wallace and S.E. Woosley, Astrophys.J.Suppl. **45** (1981) 389

[5] B.A. Brown and K. Rykaczewski, Phys.Rev. C **50**, R2270

[6] J. Szerypo et al., Nucl. Phys. **A584** (1995) 221

[7] E. Roeckl, GSI-Nachrichten 09-93 (1993) 3

[8] R. Anne et al, "Towards the study of Gamow-Teller beta decay of ^{100}Sn", proposal to the GANIL Comite d'Experiences, June 1993, Ganil Report 93 06, p.70

[9] M. Lewitowicz et al., Nouvelles du Ganil **48** (1993) 7

[10] M. Lewitowicz et al., Nouvelles du Ganil **50** (1994) 3

[11] R. Schneider et al., Z.Phys.A **348** (1994) 241

[12] M. Lewitowicz et al., Phys. Lett. **B332** (1994) 20

[13] K. Rykaczewski et al., Phys. Rev. C **52** (1995) R2310

[14] R. Grzywacz et al., Phys. Lett. **B355** (1995) 439

[15] A.Joubert et al., Proc. of the Second Conf. of the IEEE Particle Accelerator, San Francisco, May 1991, p.594 and SISSI, Nuclear Physics News, Vol.1, N° 2, 1990, p.30

[16] R. Rebmeister et al., Report CRN/PN 1983-16, 1983

[17] R. Anne and A.C.Mueller, Nucl. Instr. and Meth. B70 (1992) 276

[18] M. Hencheck et al., Phys. Rev. C **50** (1994) 2219

[19] H. Keller et al., Z.Phys.A **340** (1991) 363

[20] D. Bazin et al., Nucl. Phys. **A515** (1990) 349

Figure Captions

1 Schematic diagram of the experimental facilities at GANIL used to produce and identify ^{100}Sn.

2 Identification of the reaction products: *a)* atomic number (Z) versus mass-to-charge ratio (A/Q); *b)* region of plot *a)* with two groups of tin isotopes indicated for which mass (A) distributions have been calculated as shown in panels *c)* and *d)*. The charge states indicated correspond to those before the stripping foli (see text).

3 Mass distributions separated into odd-A and even-A quasi-fragmentation products observed in the experiment with the ^{112}Sn beam at 63 MeV/nucleon: (a) for Z from 52 to 48, (b) for Z from 47 to 44. Nuclei identified for the first time in this study are indicated by solid arrows, while the events assigned to ^{100}Sn and ^{106}Te (discussed in the text) are marked by dashed arrows. The number of counts corresponds to the 2.4×10^{15} incident particles on the ^{nat}Ni (144 mg/cm^2) target.

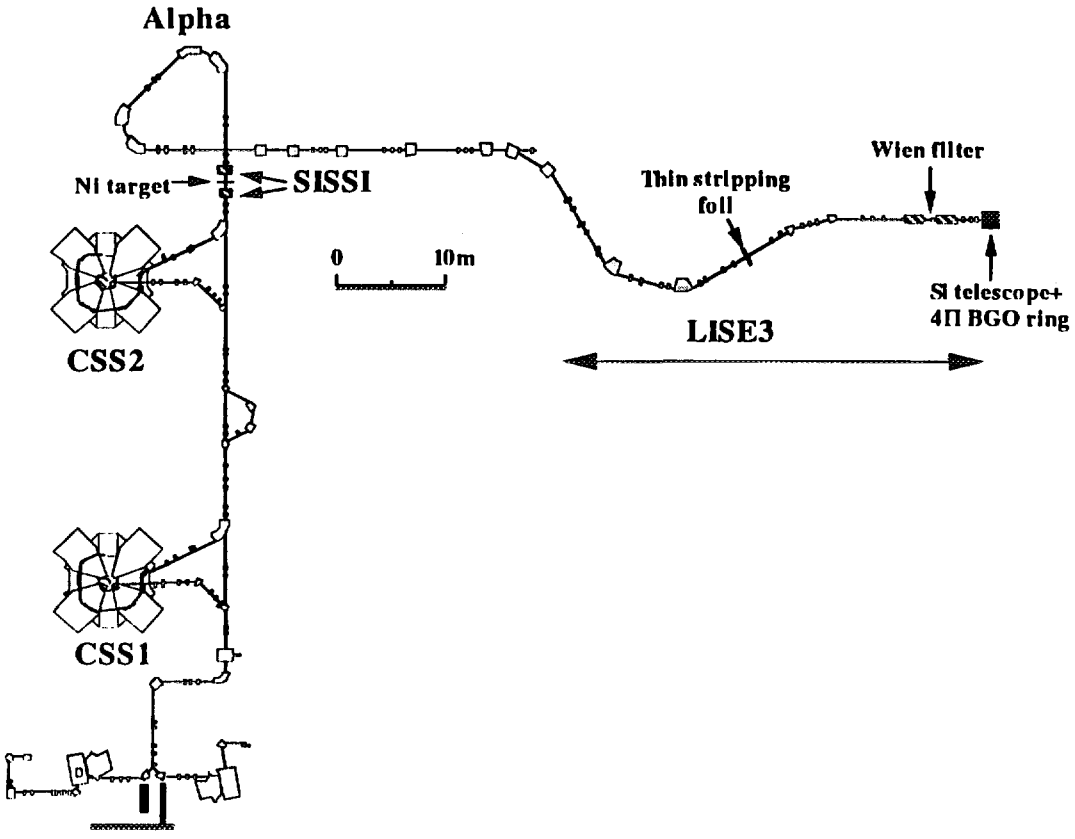
Alpha
Ni target
SISSI
0
10m
Thin stripping foil
Wien filter
Si telescope+ 4Π BGO ring
LISE3
CSS2
CSS1

Fig. 1

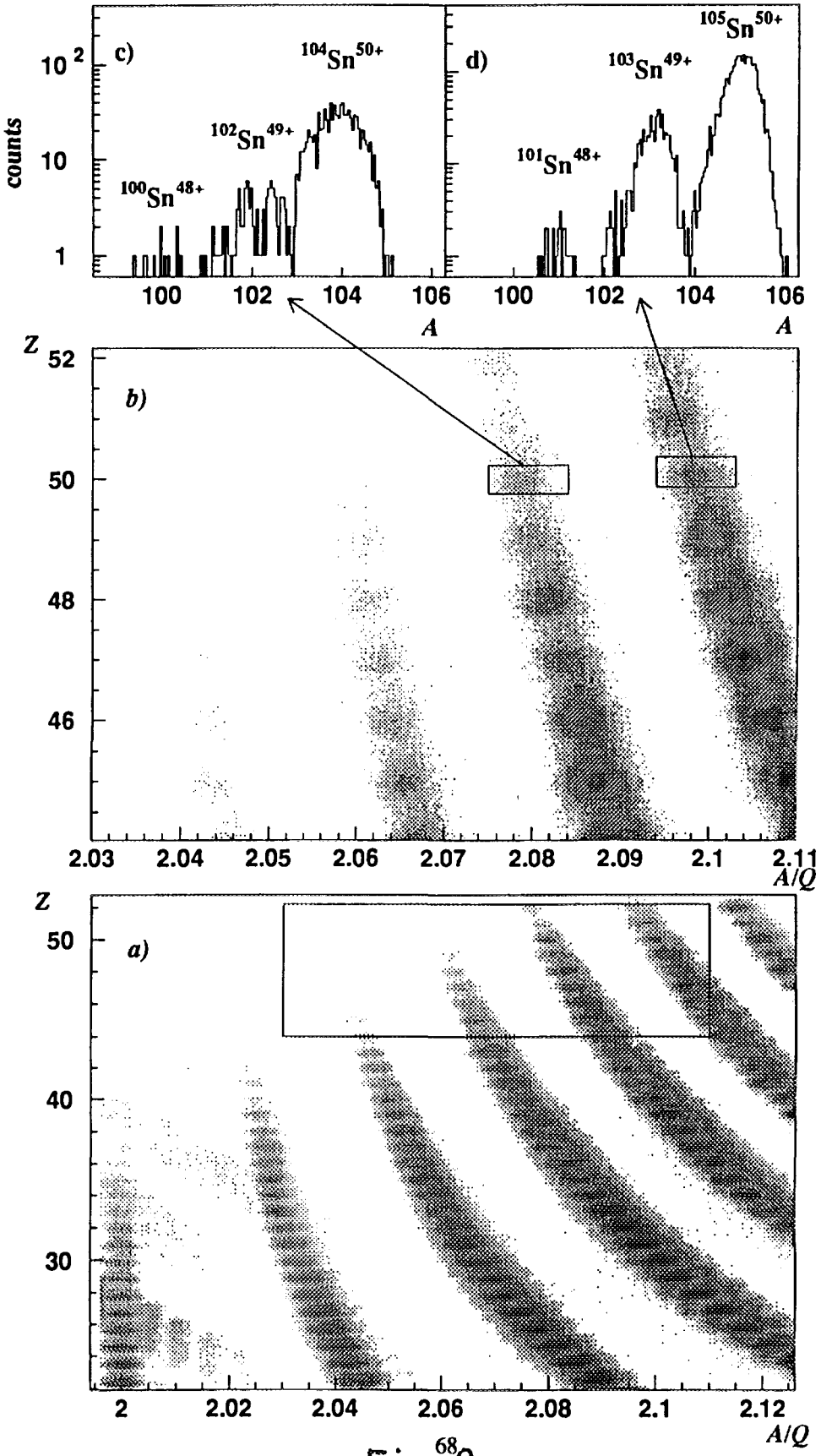
c)
d)
counts
$^{100}Sn^{48+}$
$^{102}Sn^{49+}$
$^{104}Sn^{50+}$
$^{101}Sn^{48+}$
$^{103}Sn^{49+}$
$^{105}Sn^{50+}$
A
b)
Z
A/Q
a)

Fig. 2

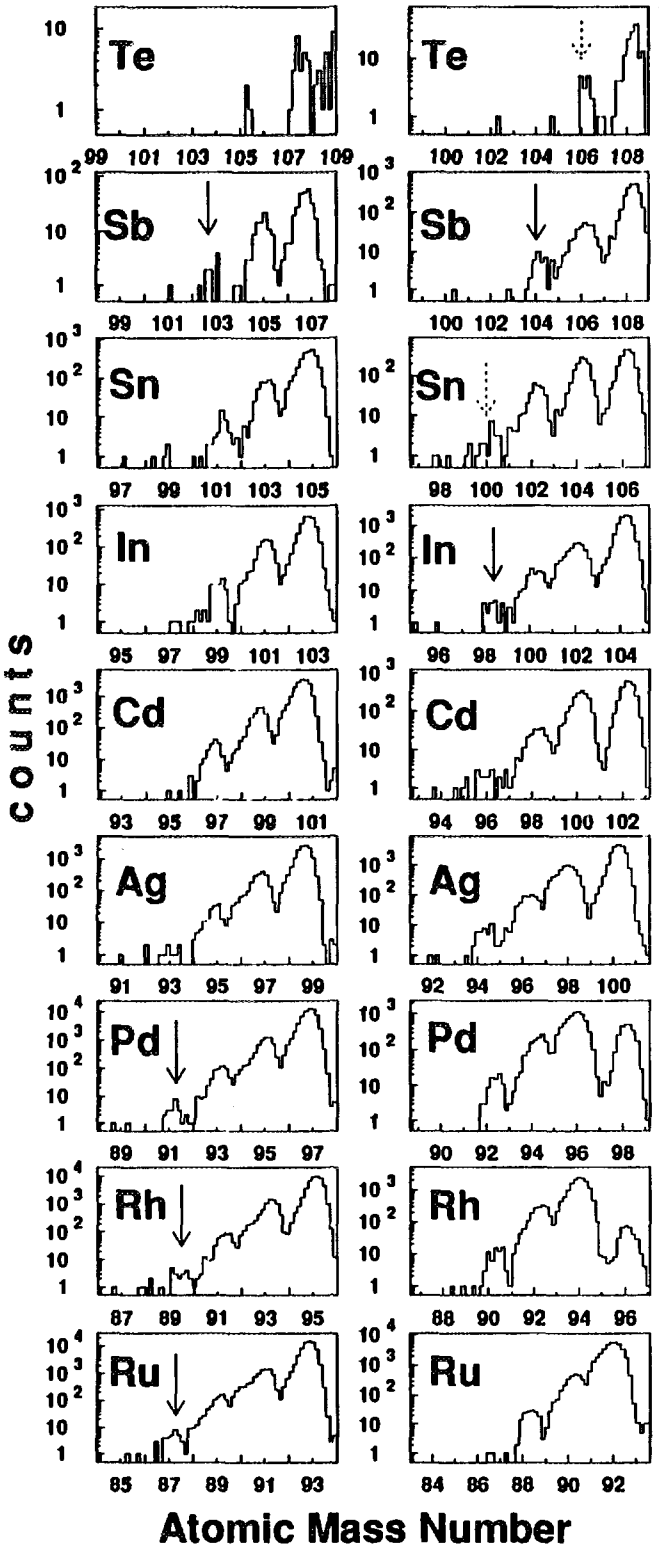
Te
Te
Sb
Sb
Sn
Sn
In
In
Cd
Cd
Ag
Ag
Pd
Pd
Rh
Rh
Ru
Ru
counts
Atomic Mass Number

Fig. 3

Mass Measurement of ^{100}Sn using the CSS2 cyclotron

M. Chartier[1], G. Auger[1], W. Mittig[1], A. Lépine–Szily[2], L.K. Fifield[3], J.M. Casandjian[1], M. Chabert[1], J. Fermé[1], A. Gillibert[4], M. Lewitowicz[1], M. Mac Cormick[1], M.H. Moscatello[1], O.H. Odland[5], N.A. Orr[6], G. Politi[7], C. Spitaels[1], A.C.C. Villari[1]

1. *GANIL, Bld Henri Becquerel, BP 5027, 14021 Caen Cedex, Franc*
2. *IFUSP-Universidade de São Paulo, C.P.66318, 05389-970 São Paulo, Brasil*
3. *Dep. of Nuclear Physics, RSPhySE, Australian National University, ACT 0200, Australia*
4. *CEA/DSM/DAPNIA/SPhN, CEN Saclay, 91191 Gif-sur-Yvette, France*
5. *Universitetet i Bergen, Fysisk Institutt, Allégaten 55, 5007 Bergen, Norway*
6. *LPC-ISMRA, Bld du Maréchal Juin, 14050 Caen Cedex, France*
7. *Universitá di Catania, Dip. di Fisica, Corso Italia 57, 95125 Catania, Italy*

FR9700874

1 Introduction

The doubly-magic nucleus ^{100}Sn was recently produced and identified in two independent experiments employing the projectile-fragments separator technique : at GSI with a 1.1 GeV/nucleon ^{124}Xe beam [1] and at GANIL using a 63 MeV/nucleon ^{112}Sn beam [2]. This nucleus is the subject of many searches since longtime, due to its N = Z character at the double shell closure, providing information on the interaction between protons and neutrons occupying the same high lying shell-model orbits and shell-closure near the proton drip-line. It is also the heaviest N = Z doubly-magic nucleus, stable against ground state proton decay, since ^{164}Pb is expected to lie far beyond the proton drip line. One of the fundamental quantities providing information on nuclear binding and structure of ^{100}Sn is its mass. The mass resolution achieved using the direct time-of-flight techniques developed mainly with the high precision magnetic spectrometers SPEG at GANIL and TOFI at Los Alamos is limited by the length of the fly path (less than 100 m) to $\sim 3 \times 10^{-4}$. This resolution is insufficient to measure the mass of ^{100}Sn with available countrates. Given the much increased path length when the ions follow a spiral path, we have proposed and tested the use of the second cyclotron of GANIL (CSS2) as a high precision spectrometer. The mass resolution obtained with the simultaneous acceleration of m/q = 3 light ions (^6He, ^9Li) was shown [3] to be 10^{-6}.

We have performed an experiment aimed at measuring with this good resolution the masses of radioactive ions of A = 100, produced via the fusion- evaporation reaction ^{50}Cr+^{58}Ni. ^{100}Ag^{22+}, ^{100}Cd^{22+}, ^{100}In^{22+} and ^{100}Sn^{22+} ions were accelerated simultaneously since their relative mass differences are less than 3×10^{-4}. Using the mass of ^{100}Ag as a reference, the masses of ^{100}Cd, ^{100}In and ^{100}Sn could be determined with a precision of 2×10^{-6}, 3×10^{-6} and 10^{-5} respectively.

is described.

2 Experimental method

The method consists in substituting the existing stripper located between the two cyclotrons by a production target, where the secondary nuclei are produced to be then injected and accelerated in CSS2. In the fundamental cyclotron equation, the mean magnetic induction B, the radio-frequency applied to the cavities f ($\omega = 2\pi f$), the harmonic h (number of radio-frequency periods/turn) are related to the mass-charge ratio m/q , the orbital radius ρ and the

velocity v by :

$$\frac{B}{\omega/h} = \gamma\frac{m}{q} = \frac{B\rho}{v} \tag{1}$$

where γ is the relativistic factor. Considering that the radio-frequency of the three GANIL cyclotrons (C0, CSS1 and CSS2) is the same, and given the harmonic of CSS1 ($h_1 = 5$), and the ratio between the injection radius of CSS2 and the ejection radius of CSS1 ($\rho_2/\rho_1 = 2/5$), the ratio between the extraction velocity of CSS1, v_1, and the injection velocity in CSS2, v_2, is given by :

$$\frac{v_2}{v_1} = \frac{2}{h_2} \tag{2}$$

where h_2 is the CSS2 harmonic. The secondary ions must then be degraded to an appropriate velocity to allow their injection in the cyclotron. As harmonics are integer numbers, the ratio $v_2/v_1 = 2/3$, $1/2$, $2/5$, etc, constitute a set of permitted solutions. Two ions injected into CSS2 with slightly different masses m and $m + \delta m$ (let call m our reference mass) will have different time-of-flights during their acceleration inside CSS2, the heavier mass will arrive δt later. The cyclotron transmission for the simultaneous acceleration of different ions is between $10^{-2} - 10^{-4}$, strongly dependent on target homogeneity and the specific reaction considered. To first order:

$$\frac{\delta t}{t} = \frac{\delta m}{m} \tag{3}$$

which consists in a calibration procedure : the unknown mass $m + \delta m$ can be determined from the well known reference mass m if the number of turns N_T or the total time-of-flight t are known. If they are not known, the calibration can still be achieved if we have more than one reference mass simultaneously accelerated with the unknown masses, or can be obtained by variation of the magnetic field [3] and/or frequency.

3 Acceleration of A = 100 secondary ions

The fusion-evaporation reaction using a ^{50}Cr beam accelerated by the first GANIL cyclotron (CSS1) and incident on a ^{58}Ni target located between the two cyclotrons was used to produce the radioactive nuclei of A = 100. This reaction is known to be very favorable to produce nuclei around ^{100}Sn [4]. The optimal energy for the production of ^{100}Sn with this reaction, E = 255 MeV, estimated with the Monte-Carlo codes PACE and HIVAP, and the ratio $v_2/v_1 = 2/5$ determine the incident energy (5.3 MeV/nucleon) and the target thickness (1.3 mg/cm^2) to be used. The tuning of CSS2 was done with the primary beam $^{50}Cr^{11+}$ degraded to 2/5 of its initial velocity in a 22 mg/cm^2 Ta target. After final corrections for the isochronism and tuning of the injection and initial phase, the individual orbits are perfectly separated and the phase is constant with the radius [5].

Both Ni and Ta targets, located between the two cyclotrons, were rotated and cooled to dissipate the heat and allow the use of an intense beam (i = 300-500 nAe). To conserve the same settings in the transport line and in the CSS2, the A = 100 secondary ions were selected in the 22^+ charge state. The accelerated ions were detected and identified inside the cyclotron using a Silicon detector telescope (ΔE 30μm, E_{xy} 300μm) mounted on a radial probe which can be moved from the injection radius 1.25 m up to the extraction radius 3.0 m, and with a radial dead zone of 2 mm, much less than the distance between the orbits (14 mm). The time-of-flight (phase) of the detected ions was measured relative to the radiofrequency HF signal of the CSS2 cyclotron. Figure 1 shows a schematic diagram of the experimental set-up.

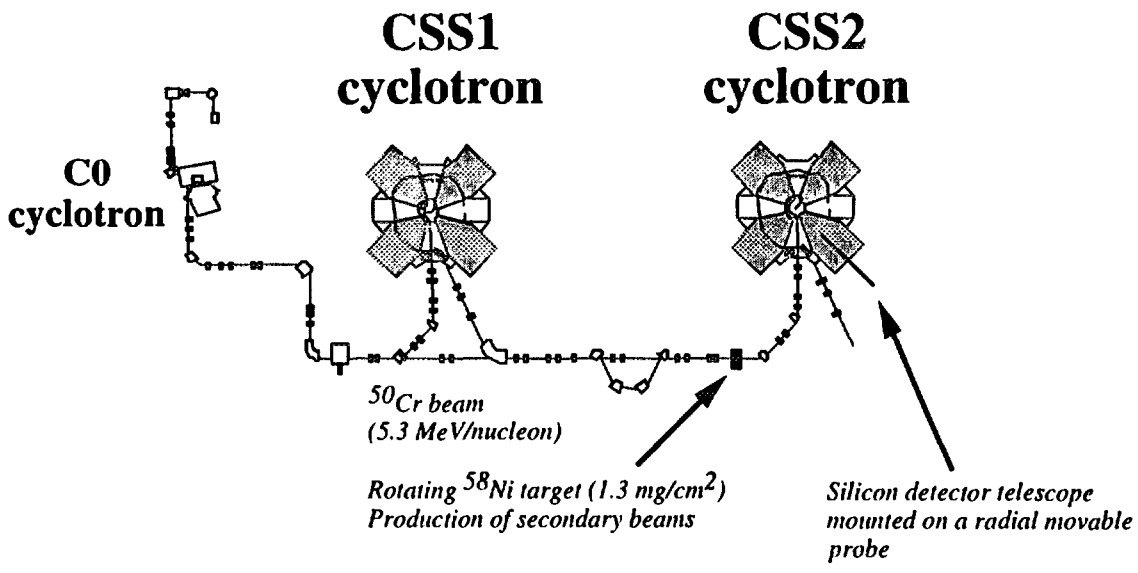

Figure 1: *Schematic diagram of the experimental set-up.*

3 Results

After the tuning procedure was completed, the magnetic field was increased by $\delta B/B = 4.7 \times 10^{-4}$ which equals the estimated fractional difference in the mass/charge ratio between $^{50}Cr^{11+}$ and $^{100}Sn^{22+}$ [6]. Hence, at this new field, $^{100}Sn^{22+}$ ions would have been accelerated with the same phase and isochronism curve as achieved for $^{50}Cr^{11+}$ at the end of the tuning process. However, with increasing radius, the phase of $^{100}In^{22+}$, $^{100}Cd^{22+}$, $^{100}Ag^{22+}$ ions moves further and further ahead of the isochronous phase. A simulation calculating the trajectories of the ions throughout the cyclotron to the detector can help us to understand the "Energy - Phase" spectra and identify the different nuclei. Moreover in order to separate genuine ^{100}Sn events from background, a particle identification parameter, proportional to the atomic number Z, was derived from a linear combination of the signals from the two detectors of the silicon detector telescope. Figure 2 shows the "Energy - Phase" spectra for events falling within the gates set on the identification parameter for In and Sn, and their projections on to the phase axis. There is an excess of 10-12 events in the Sn spectra around -10° which have correct phase, total energy and identification parameter value simultaneously, and these are attributed to $^{100}Sn^{22+}$ ions.

Finally, from the phases of the different isobars with respect to ^{100}Ag, we can determine their mass excesses :

$$M.E.(^{100}Cd) = -74.180 \pm 0.200(syst.)MeV$$

$$M.E.(^{100}In) = -64.650 \pm 0.300(syst.) \pm 0.100(stat.)MeV$$

$$M.E.(^{100}Sn) = -57.770 \pm 0.300(syst.) \pm 0.900(stat.)MeV$$

These masses are to be compared with the experimental values presented in the Audi-Wapstra mass table [6] for ^{100}Cd (-74.310 ± 0.100 MeV) [7] and also for ^{100}In (-64.130 ± 0.380 MeV) which was obtained from the combination of an indirect measurement [8] and our previous direct measurement using the CSS2 cyclotron technique [9]. The mass of ^{100}Sn (-56.860 ± 0.430 MeV) given in the Audi-Wapstra mass table [6] is an estimate based on extrapolating systematic trends. Our mass of ^{100}Cd is in good agreement with the existing measurement, which gives good confidence in the new results for ^{100}In and ^{100}Sn.

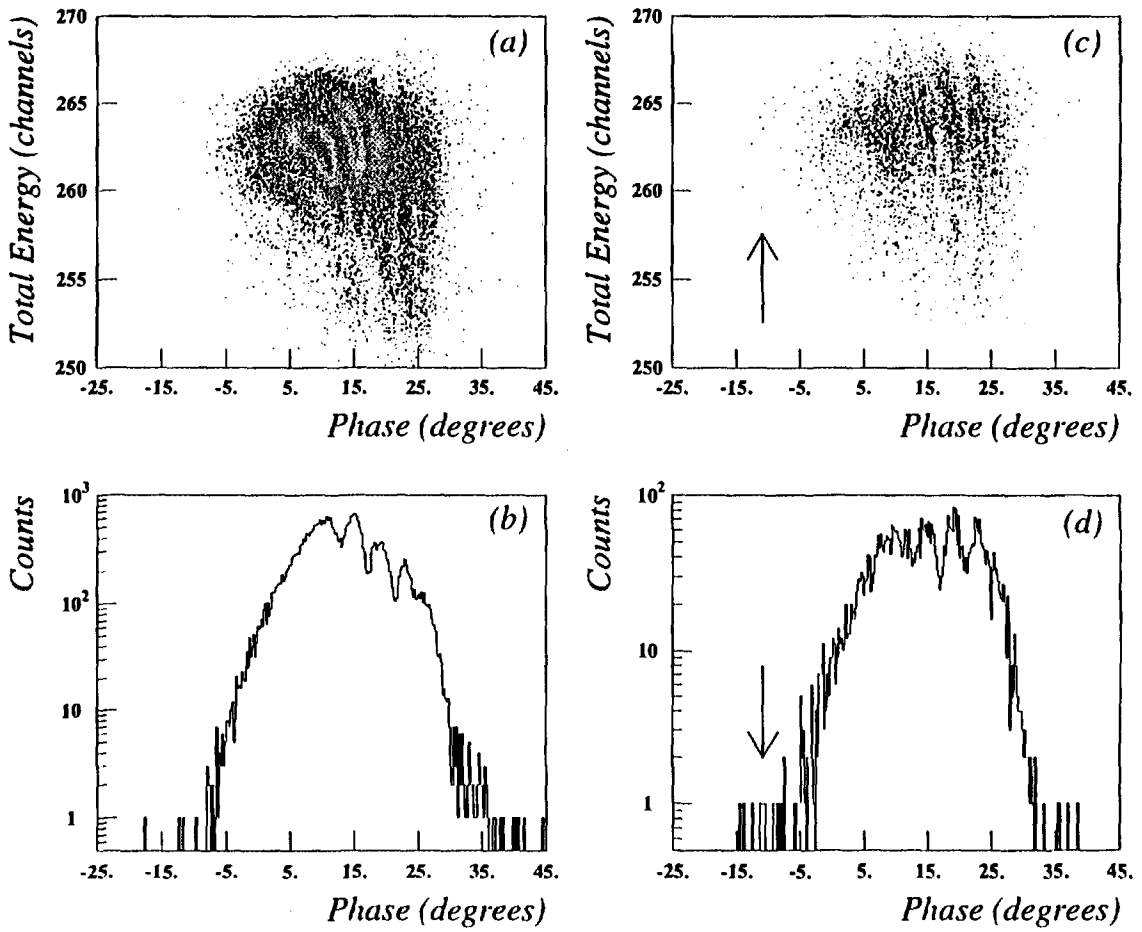

Figure 2: *"Energy - Phase" spectra and their projections on to the phase axis, both gated by the identification parameter for In [(a),(b)] and Sn [(c),(d)] respectively. The arrows indicate the location of* $^{100}Sn^{22+}$ *counts.*

	Present Work		Stat. Model	Stat. Model	Stat. Model
	(c/h/nAe)	(mb)	PACE (mb)	HIVAP (mb) [4, 11]	CASCADE (mb)
^{100}Ag	~ 40	3.9 [10]	30	38	38
^{100}Cd	~ 10	~ 1	16	7	3.2
^{100}In	~ 0.01	~ 0.001	0.02	0.014	0.027
^{100}Sn	$\sim 4 \times 10^{-4}$	$\sim 4 \times 10^{-5}$	-	0.0003	-

Table 1: *Experimental cross-sections of the present work normalized to the value of Schubart et al [10] for ^{100}Ag, and compared to statistical model calculations.*

We compared our experimental count rates to statistical model calculations. As noted above, the absolute transmission of the CSS2 is difficult to determine. However, if we suppose that the transmission of the four $A = 100$ isobars is approximately the same, we can obtain relative cross-sections. To our knowledge, only one value has been measured [10] for ^{100}Ag, which is 3.9 mb. This value is one order of magnitude lower than estimations from statistical model calculations. If we normalize our count rates to this experimental value [10] for ^{100}Ag, we obtain the cross-sections of Table 1, all of which are an order of magnitude lower than the statistical model predictions. Note that the small 40 nb cross-section for ^{100}Sn is nonetheless three orders of magnitude larger than the ones in fragmentation reactions [1, 2].

5 Conclusion

We have shown that the method of using the CSS2 cyclotron as a high precision spectrometer works well also for heavy $A = 100$ secondary ions. ^{100}Sn has been observed as the product of a fusion-evaporation reaction for the first time. The masses of not only ^{100}Sn, but also ^{100}In and ^{100}Cd were determined using ^{100}Ag as a reference. The known mass excess of ^{100}Cd has been confirmed within 2×10^{-6} and we measured for the first time the masses of ^{100}In and ^{100}Sn with a precision of 3×10^{-6} and 10^{-5} respectivly. A preliminary production cross-section of 40 nb has been determined for the fusion-evaporation reaction ^{50}Cr + ^{58}Ni $\longrightarrow$ ^{100}Sn at 255 MeV.

References

[1] R. Schneider et al, Z.Phys. **A348**, 241 (1994).

[2] M. Lewitowicz et al, Phys.Lett. **B332**, 20 (1994).

[3] G. Auger et al, Nucl.Instr.Meth. **A350**, 235 (1994).

[4] E. Roeckl, private communication (1994).

[5] G. Auger et al, Nouvelles du GANIL **54**, 7 (1995).

[6] G. Audi and A.H. Wapstra, Nucl.Phys. **A595**, 409 (1995).

[7] K. Rykaczewski et al, Z.Phys. **A332**, 275 (1989).

[8] J. Szerypo et al, Nucl.Phys. **A584**, 221 (1995).

[9] A. Lépine-Szily et al, ENAM 95 Conference, Arles, France, June 19-23 (1995).

[10] R. Schubart et al, Z.Phys. **A352**, 373 (1995).

[11] K. Rykaczewski, private communication (1995).

Observation of the μs-isomeric states in the nuclei produced in the ^{112}Sn + ^{nat}Ni reaction

R. Grzywacz[a,b], R. Anne[b], G. Auger[b], C. Borcea [c], J.M. Corre[b], T. Dörfler[e], A. Fomichov[f], S. Grevy[d], D. Guillemaud-Mueller[d], M. Huyse[g], Z. Janas[h], H. Keller[h], M. Lewitowicz[b], S. Lukyanov[f,b], A.C. Mueller[d], N. Orr[b], A. Ostrowski[b], Yu. Penionzhkevich[f], A. Piechaczek[g], F. Pougheon[d], K. Rykaczewski[a,b,i], M.G. Saint-Laurent[b], W.D. Schmidt-Ott[e], O. Sorlin[d], J. Szerypo[a], O. Tarasov [f,b], J. Wauters[g], J. Żylicz[a]

[a] *IFD, Warsaw University, Pl-00681 Warsaw, Hoża 69, Poland*
[b] *GANIL, BP 5027,14021 Caen Cedex, France*
[c] *IAP, Bucharest-Magurele P.O.Box MG6, Roumania*
[d] *IPN, 91406, Orsay Cedex, France*
[e] *University of Göttingen, D-37073, Göttingen, Germany*
[f] *FLNR, JINR 141980 Dubna, Moscow region, Russia*
[g] *IKS KU Leuven, B-3001, Leuven, Belgium*
[h] *GSI, Postfach 110552, D-64220, Darmstadt, Germany*
[i] *CERN, CH-1211 Geneve 23, Switzerland*

Fragmentation of a neutron-deficient ^{112}Sn beam at the intermediate energies by a ^{nat}Ni target studied by means of the magnetic spectrometers Alpha and LISE3 at GANIL has been proven as a method allowing to produce and identify very exotic nuclei in the ^{100}Sn region [2, 3]. It was also found that the fragments can be observed in their excited μs-isomeric states due to the reasonably high isomeric ratio (typically about 30 to 50%), characterizing such reactions [1]. The time correlation in the μs range between the implantation of the identified fragments into the Si-stack detector and the gamma-radiation following the isomer decay allowed to record the respective gamma-spectra in the practically background-free conditions. Therefore even very limited intensity of gamma signals can be used for the identification and study of new isomeric decays, see e.g. ^{66m}As case [4]. The evidence for new isomeric states in T_z=1 nuclei near doubly-magic ^{100}Sn, namely ^{94}Pd ($T_{1/2}$=0.6±0.1μs), ^{96}Ag ($T_{1/2}$=0.7±0.2μs), ^{98}Cd($T_{1/2}$ ≈0.2μs) and ^{102}Sn($T_{1/2}$ ≈0.3μs), has been obtained [5]. In addition, the correlation between detected ions and following gamma decay of the μs isomeric state provides for unambiguos identification of the nuclei implanted at the final focus of projectile fragment separators, see fig.1.

With respect to the future experiments with isomeric beams it is important to notice that in specific cases (where the isomer is decaying via strongly converted transition) the intensity losses due to the decay in-flight are substantially reduced. The increase of the isomeric half-life is caused by the absence of the electrons in the produced fragments.

Fragmentation of neutron-rich projectiles together with the present technique should allow for a search in regions of the nuclear chart which are not or only weakly populated in fission or fusion-evaporation reactions (e.g. very n-rich Sc to Co isotopes).

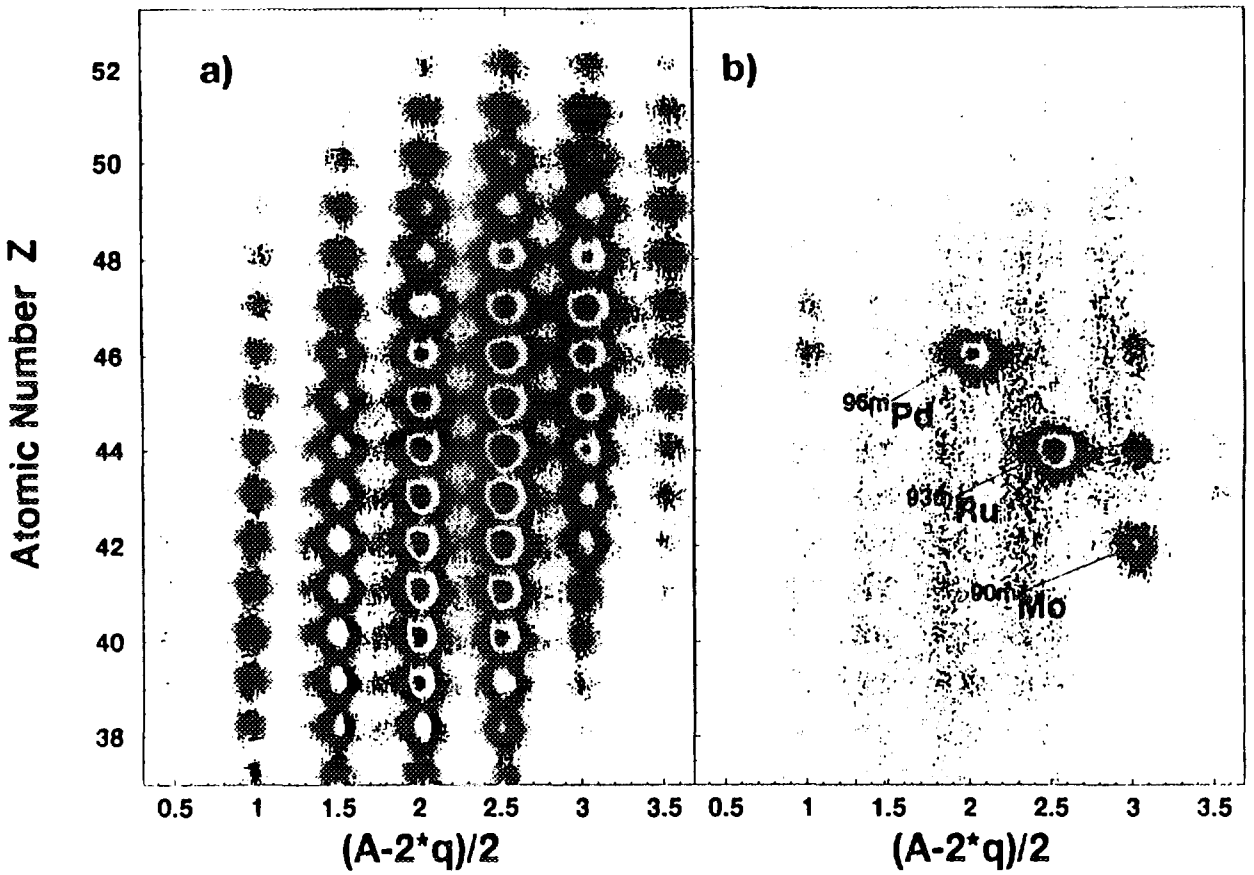

Figure 1: Identification plots a) all observed nuclei b) nuclei correlated with gamma radiation occuring within μs range after implantation signal.

References

[1] R. Grzywacz et al., Phys. Lett. **B355** (1995) 439

[2] M. Lewitowicz et al., Phys. Lett. **B332** (1994) 20

[3] K. Rykaczewski et al., Phys. Rev. **C52** (1995) R2310

[4] R. Grzywacz et al., this report

[5] R. Grzywacz et al., Proc. ENAM 95 Conference, 1995, Arles, France, p.561

Isomeric states in ^{66}As

R. Grzywacz, Z. Janas, M. Pfützner, M. Karny (Univ. Warsaw), B. Blank, S. Andriamonje, S. Czajkowski, F. Davi, R. Del Moral, J.P. Dufour, A. Fleury, A. Musquère, M.S. Pravikoff (CEN Bordeaux-Gradignan), M. Lewitowicz (GANIL Caen), J.-E. Sauvestre (CE Bruyères-le-Châtel), C. Donzaud (IPN Orsay)

New type of the experiments performed at LISE spectrometer is related to the search for the isomers with a microsecond lifetime. An experimental method sensitive to such isomers has been applied for the first time in the series of experiments [1, 2, 3, 4] with ^{112}Sn 63AMeV beam, resulting in the detection of over forty known isomers. The principle of this experimental technique is based on the time correlation between the detected gamma radiation and implantation of identified fragment, as described in [1].

Among other results, the signature for the decay of new ^{66m}As state has been observed in the experiment with the ^{112}Sn beam. The low resolution of BGO gamma detectors and low production rate of this particular nucleus excluded more precise measurement of the isomeric decay properties. The latter have been measured in the similar experiment, but with much better rate of ^{66}As ions achieved by using neutron deficient ^{78}Kr beam. Although main objective of the latter experiment was to serch for new proton-rich isotopes [5] and the spectroscopy of beta delayed protons [6], the isomeric decays have been also investigated. There was a setup of five high efficiency germanium detectors mounted around the implantation silicon stack detectors allowing to study the properties of isomeric decays. In addition, the important role of gamma-detection setup was the independent confirmation of the identification of the implanted nuclei by using known isomeric decays of ^{69m,71m}Se.

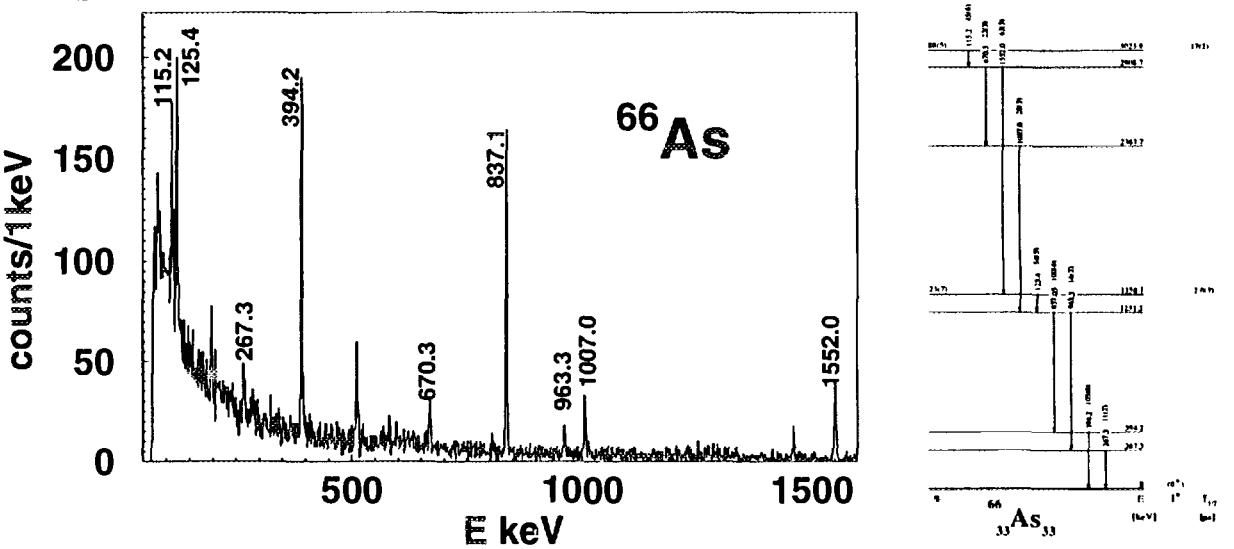

Figure 1: Energy spectrum of gamma radiation obtained in correlation with implanted ^{66}As fragments. The preliminary decay scheme deduced from measiured γ-energies and intensities as well as from γ-γ coincidence relations is also given. The intensities are normalized to the 393 keV transition. The relative population of the isomers is indicated.

is presented.

As for the most of the counting time the spectrometers ALPHA/LISE were optimized for the transmission of N=Z and more exotic nuclei around Z=32, the ^{66}As was one of the most frequently implanted fragments [5] (about 173000 ions). This allowed for the spectroscopy of isomeric states in ^{66}As, including gamma-gamma coincidences and the analysis of time periods between heavy-ion and gamma events resulting in the half-life determination. The measured energy spectrum for the gamma radiation correlated with ^{66}As implanted ions in the range of 50 μs is presented in the fig 1. The preliminary decay scheme, deduced from the analysis of the gamma spectra, is also given there. Two isomeric states were found in the ^{66m}As nucleus: at E*=3024 keV excitation energy having $T_{1/2}$ of 17(2)μs, and at E*=1357 keV having $T_{1/2}$ of 2.0(3)μs. Both isomeric states are populated directly in the reaction, however the deexcitation of the upper one populates low-lying isomer. The isomeric ratio for the production of the 3024 keV isomer (i.e. number of ions in this isomeric state vs total number of implanted ^{66}As ions) was 21$\pm$3%. The study of ^{66m}As demonstrates that the heavy ion - gamma correlation method applied to the fragmentation products is an efficient spectroscopy tool providing the information on the excited levels in nuclei at the limits of the nuclear stability.

References

[1] R. Grzywacz et al., Phys. Lett. B355 (1995) 439

[2] K. Rykaczewski et al., Phys. Rev. C52 (1995) 52

[3] M. Lewitowicz et al., Phys. Lett. B332 (1994) 20

[4] R. Grzywacz et al., Proc. ENAM 95, Arles, in print

[5] B. Blank et al., Phys. Rev. Lett 74, 4611 (1995)

[6] B. Blank et al., Phys. Lett. B364, 8 (1995)

Production of an Isomeric Beam and Total Reaction Cross Section Measurement

Ethvignot T., Lestrade D., Delbourgo-Salvador P., Méot V., Sauvestre J.E., Szmigiel M., Bonnereau B.
CEA/Bruyères-le-Châtel, DPTA/SPN, B.P.12, 91680 Bruyères-le-Châtel, FRANCE
Lefevre A., Lewitowicz M., St Laurent M.G.
GANIL, BP 5027, 14021 Caen Cedex, FRANCE
Mueller A. C., Sorlin O.
Institut de Physique Nucleaire, B.P. 1, 91406 Orsay Cedex, FRANCE
Marie F.
CEA/Saclay, DAPNIA/SPhN, 91190 Gif sur Yvette, FRANCE

1 Motivations

The production of energetic secondary beams of excited long lived nuclei (isomers) at GANIL is mainly motivated by the growing interest to extend our knowledge on nuclear structure and on the mechanisms of excitation as well as deexcitation of isomeric levels.

Furthermore, energy storage or GRASER (gamma LASER) could be direct applications in the future of these studies on isomers.

In a first step, as for exotic proton or neutron-rich exotic beams, isomeric beams are a powerful mean for testing classical nuclear models. Indeed, isomeric states have different properties like angular momentum (spin isomers) or deformation (fission isomers...), as they are excited states with different particule-hole configurations than that of the ground state.

In this paper, we present recent results on the production of isomeric beams at GANIL and report on a first experiment of the measurement of the total reaction cross section induced by a nucleus in an isomeric state.

2 Production of a $^{42}Sc^{m}$ Isomeric Beam with LISE3

Projectile fragmentation has been extensively used to produce secondary exotic beams at GANIL. Binary nuclear reactions, e.g. transfer, are an other possibility. In this case, reverse kinematics is used to obtain a focussed beam, the opening angle of the ejectile being mainly determined by the kinematics. In addition, we take advantage of selection rules of transfer reactions to populate preferentially the isomeric state.

During the period 1992-1995, we have tested both methods using the LISE3 spectrometer for the selection of a secondary $^{42}Sc^{m}$ beam. We were interested in measuring the isomeric purity of the secondary beam (number of isomers over total number of ^{42}Sc) as well as the intensity and the isotopic purity of the secondary beam.

In a first experiment, we have established that a pure isomeric beam could be produced at GANIL [1]. A ^{40}Ca primary beam at 30 MeV/A bombarded a ^{nat}C target (5 mg/cm^2 thick). A secondary $^{42}Sc^{m}$ ($J^{\pi} = 7^{+}$, E_x=617 keV) beam was separated with LISE3. It reached about 100 pps for a 5 nAp ^{40}Ca primary beam intensity. 30% of residual ^{40}Ca which has the same A over Z ratio contaminated the isomeric beam.

Isomeric purity was determined by measuring the γ-ray activity of ^{42}Sc identified and implanted in a solid state telescope, using a HPGe detector. The obtained value of 98% $\pm$ 5% is consistent with EFR-DWBA calculation predictions [2].

In order to increase the isomeric beam intensity, the production of $^{42}Sc^{m}$ by fragmentation has been investigated in a second experiment. For that purpose, a primary beam of ^{50}Cr which has a close N over Z ratio and a heavier mass than ^{42}Sc was accelerated at GANIL for the first time. Three different production targets (Be, C, Ni) were bombarded. The yields obtained are higher than for the transfer experiment (around 1000 pps). However, the isomeric purity is lower around 28% and is not affected -to first order- by the target nature. As for other measurements done elsewhere [3], theoritical models still fail to reproduce these results. A paper will be submitted shortly.

3 Total Reaction Cross-Section Measurements

The measurement of the total nuclear reaction cross section (σ_r) induced by a secondary isomeric beam has been performed recently. In a semi-geometrical framework, one can easily conceive that σ_r is sensitive to a significant difference of shape or radius between the isomeric and the ground state. Indeed excited and ground states exhibit different orbital wave functions. This experiment aimed at measuring the difference on σ_r induced by ^{42}Sc beams with various isomeric purities.

In this experiment, transfer reactions have been used to produce a $^{42}Sc^{m}$ beam via neutron-proton pick up from a ^{40}Ca primary beam at 30 MeV/A. Three systems have been studied : $^{4}He(^{40}Ca,^{42}Sc)d$,$^{3}He(^{40}Ca,^{42}Sc)p$,$^{12}C(^{40}Ca,^{42}Sc)^{10}B$ in order to measure the different isomeric purities. For the ^{12}C and ^{4}He targets, the direct transfer to the ground state is forbidden and it has been shown experimentally [1] that the population of the isomeric state is favored. For the ^{3}He target, the selection rules allow both ground and isomeric states to be populated.

Isomeric purities were measured with the same method than previously and results are shown in Table 1.

Production target	F(%)	I (pps)
^{4}He	63±5	≈300
^{3}He	55±5	≈ 300
^{12}C	84±5	≈ 300

Table 1 : Isomeric purity (F) and yield (I) for the different reactions.

The isomeric purities obtained are unexpectedly close to deduce fine differences in σ_r. This also shows that other channels are open. Indeed, these channels are kinematically allowed by the large spectrometer energy acceptance, especially for the helium targets. As a matter of fact, with an uncertainty of 10% on the total cross section measurement with the three mixed beams, only a ratio $R = \sigma_r^m/\sigma_r^{g.s}$ of 2 or more could be significantly deduced with the isomeric purity obtained.

For this reason, neighboring nuclei like ^{41}Ca and ^{38}Ar are used to validate the experimental method by the absolute value of the total cross section measured in the three experiments. They happen to induce similar total cross section values than the ^{42}Sc ground state. By comparison with these nuclei, one can increase the sensitivity of the R ratio, e.g. R=1.2 for a 10% uncertainty on the experimental results.

For this purpose, tuning of the LISE3 spectrometer was quite different than in the first experiment in order to allow those neighboring nuclei to be transported at the end of the beam line. This could also explain the difference of isomeric purity obtained with the carbon target compared to the first experiment based on the optimisation of the isomeric purity by transfer reaction. This confirms the sensitivity of the isomeric ratio to the different parameters of LISE3 that act in a different way as cuts in the excitation energy spectrum of the primary excited ^{42}Sc produced [6].

For the measurement of the total reaction cross section , the method of the associated γ-rays previously used at GANIL and SARA [4] [5] has been chosen. The experimental set up placed at the end of LISE3 and displayed on Figure 1 is the following:

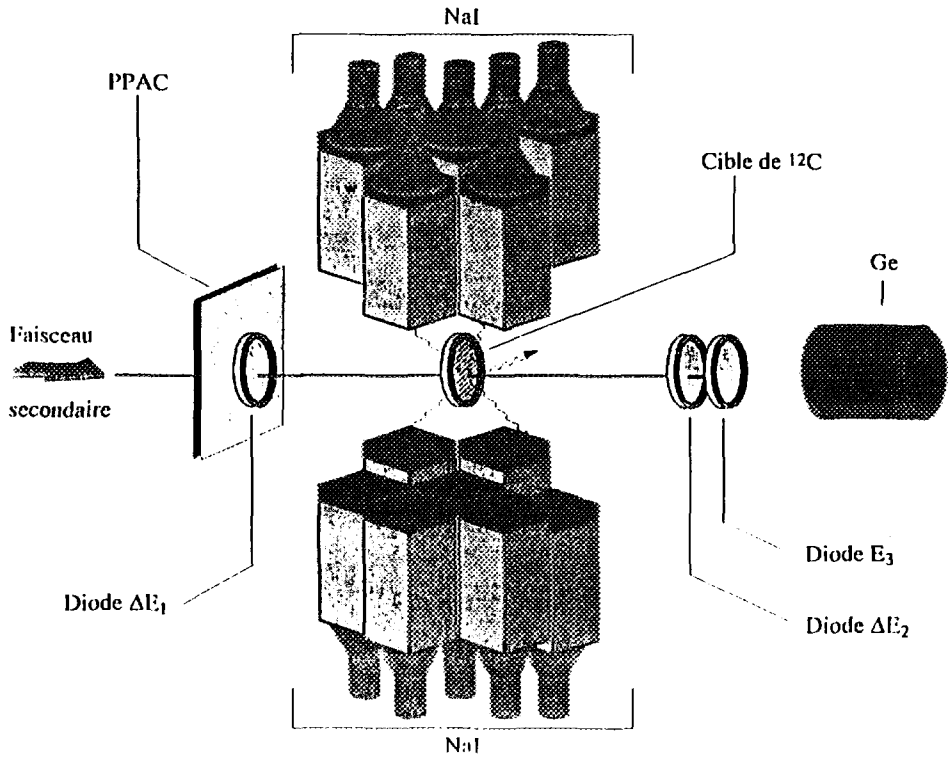

Figure 1: Experimental set up

The γ detector consists of 14 individual NaI counters arranged in a 4π geometry around the interaction target which is ^{12}C (11.45 mg/cm ^{2} thick). The efficiency of this set up is very high because of multiplicity and high intrinsic efficiency. Detectors are also very sensitive to the room γ background so they are surrounded by a lead shielding. A 50μm Si detector (ΔE1) used for identification of the incoming particles is placed 53 cm upstream the interaction target and a Parallel Plate Avalanche Counter (PPAC) gives also x,y position for each incident particle. A ΔE-E telescope and a HPGe detector used for identification of the isomers as in previous experiments is placed 39 cm after the interaction target. Coincidences between ΔE1 and the 4πNaI detector sign nuclear reactions to determine σ_r.

The experimental results are still under analysis. They will be published in a near future. Nevertheless, the very preliminary results seem to show that there is no significant enhancement of the value of the total reaction cross section on the isomeric state with respect to the $^{42}Sc^{gs}$ and the neighboring nuclei. We also see that the results are compatible with the Kox empirical formulae [7].

References

[1] J.L.Uzureau *et al*, 1994, Phys. Lett. **B331**, 280

[2] Mermaz M. *private communication*

[3] Young M. *et al*, 1993, Phys. Lett. **B311**, 22

[4] M.G. St Laurent *et al*, 1989, Z. Phys.**A332**, 457

[5] Liatard E., 1989, Thèse d'état, Université de Grenoble, ISN89-121

[6] W.D. Schmidt-Ott *et al*, 1994, Z. Phys. **A350**, 215

[7] Kox S. *et al*, 1987, Phys. Rev. **C35**, 1678

B - NUCLEAR REACTIONS

B1 - PERIPHERAL COLLISIONS PROJECTILE-LIKE FRAGMENTS

Fission fragment Z distributions for coulomb fission and nuclear fission are presented.

Coulomb fission of 24 AMeV ^{238}U in the field of a ^{197}Au nucleus*

E.Piasecki[1], L.Pienkowski[2, 5], M.Muchorowska[3], A.Tucholski[4], T.Czosnyka[2], A.Chbihi[5], E.Crema[6], W.Czarnacki[4], J.Galin[5], B.Gatty[7], D.Guerreau[5], J.Iwanicki[2], D.Jacquet[7], U.Jahnke[8], J.Jastrzebski[2], M.Kisielinski[4], A.Kordyasz[1], M.Lewitowicz[5], M.Morjean[5], J.Pouthas[5]

1) Institute of Experimental Physics, Warsaw University, Hoza 69, 00-681 Warsaw, Poland
2) Heavy Ion Laboratory, Warsaw University, Banacha 4, 02-097 Warsaw, Poland
3) Warsaw University of Agriculture, Rakowiecka 26-30, Warsaw, Poland
4) Soltan Institute for Nuclear Studies, 05-400 Swierk, Poland
5) GANIL, IN2P3-CNRS, DSM-CEA, BP5027, 14021 Caen-cedex, France
6) Instituto de Fisica, Universidad de Sao Paulo, Sao Paulo, Brazil
7) Institut de Physique Nucléaire, BP1, 91406 Orsay-cedex, France
8) Hahn Meitner Institut, Glienicker Strasse 100, 14109 Berlin, Germany

The context

Coulomb fission (CF) is a fission induced by the time-varying field of another nucleus passing by, outside the range of the strong nuclear force. The interest of such a process lies in the direct coupling of the electromagnetic field to collective degrees of freedom, which can result in a time scale much faster than in fission induced by the nuclear interaction. Experimental data about this phenomenon are rather scarce. The main difficulty in investigating this process stems from the presence of nuclear fission (NF) which can be easily confused with electromagnetic induced fission. Experiments have been mainly carried out either at sub-barrier energies[1] or, in contrast, at relativistic energies[2]. At sub-barrier energies and provided the beam energy is lowered enough (<85% the barrier) Coulomb fission is strongly dominant and nuclear fission comparatively small (negligible). At relativistic energies and due to the strong excitation of the Giant Resonance modes, CF represents a large fraction of the total fission cross section when induced by very heavy partner nuclei. At 24 MeV/nucleon -this experiment- looking for CF is a challenge since the expected cross sections are two to three orders of magnitude smaller than those for NF.

How is it possible to distinguish CF from NF at 24 AMeV?

The underlying idea is similar to the one exploited at sub-barrier energies. By keeping the closest distance of approach between the interacting nuclei sufficiently large to prohibit nuclear interaction, CF can be isolated. This is naturally fulfilled when choosing the beam energy to be much smaller than the barrier. The same can be done much above the barrier by selecting the closest distances of approach to be larger than the one usually referred to as a safe distance. The experiment thus requires an event by event determination of the closest distance of approach by utilizing a related observable: the scattering angle of the fissioning nucleus .

The experiment thus consists in a precise characterization of the correlated fission fragments enabling one to reconstruct the kinematical characteristics of the fissioning nucleus[3]. Due to the inverse kinematics, the fragments are emitted in a rather narrow forward cone and are detected by means of an annular telescope centered on the beam. The fragments are identified in Z from their ΔE^*E and their emission angles obtained thanks to the strip structure of the detectors (radial and annular strips respectively).

In addition each event is characterized by the neutron multiplicity as measured with ORION, a high efficiency, 4π, Gd loaded, liquid scintillator detector. The neutron multiplicity appears quite necessary in so far as it allows the distinction between Coulomb (rather cold events) and nuclear events, most of the latter corresponding to rather hot events.

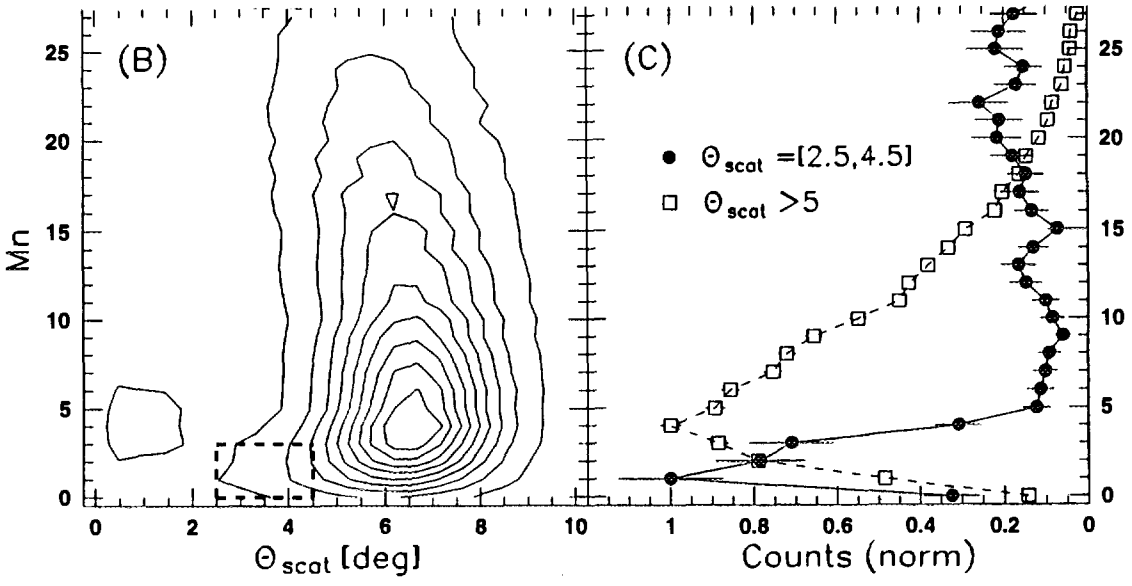

Fig.1: (B) Contour distribution of the fission events leading to a total atomic number of the two fragments equal to 92 (the region of interest for CF is delineated). The pattern of the neutron multiplicity distributions are shown in (C) in two angular domains of the fissioning nucleus where CF and NF are expected to be strongly dominant. .

The data are shown in Fig.1 after a selection of Z1+Z2=92, the sum of the atomic numbers of the two fission fragments. The selected CF events are characterized by Θ_{scat}=2.5 to 4.5 degrees. The lower angular limits is set to reject nuclear reactions on light contaminants. The upper one corresponds to a closest distance of approach of 25fm to be compared to 16fm for the two touching nuclei. The 9fm gap is sufficient to make the probability of fission after nuclear interaction very weak. This is best shown on the neutron multiplicity distributions (Fig.1C) for expected CF ($2.5<\Theta_{scat}<4.5$) and NF ($\Theta_{scat}>4.5$). The two distributions are markedly different in their pattern. The narrow peak observed for the former distribution is expected if the fissioning nucleus is only weakly excited. The rather flat distribution observed for Mn>4 is due to NF events which appear at such small angles because of our limited angular resolution. They can be easily rejected by requiring a Mn<4 condition for CF.

Fragment Z distributions: a comparison between nuclear-, Coulomb- and photo-fission data

As it is well known, the Z distribution of fission fragments brings interesting information on the characteristics of fissioning nuclei and in particular on their excitation energy . This is well shown on the present NF data when they are displayed as a function of the measured neutron multiplicity which is a function of excitation energy (Fig.2). The general pattern of the distribution evolves and this is best seen following also the peak-over-valley (symmetric splitting) ratio. At low Mn, there is a pretty good matchingbetween these data and the photo-fission data of ref[4]. A detailed comparison between Coulomb- and photo-fission data is more delicate because of the low statistics for the former process, however the overall distributions for both processes are evolving in a very similar way with increasing excitation energy (or neutron multiplicity).

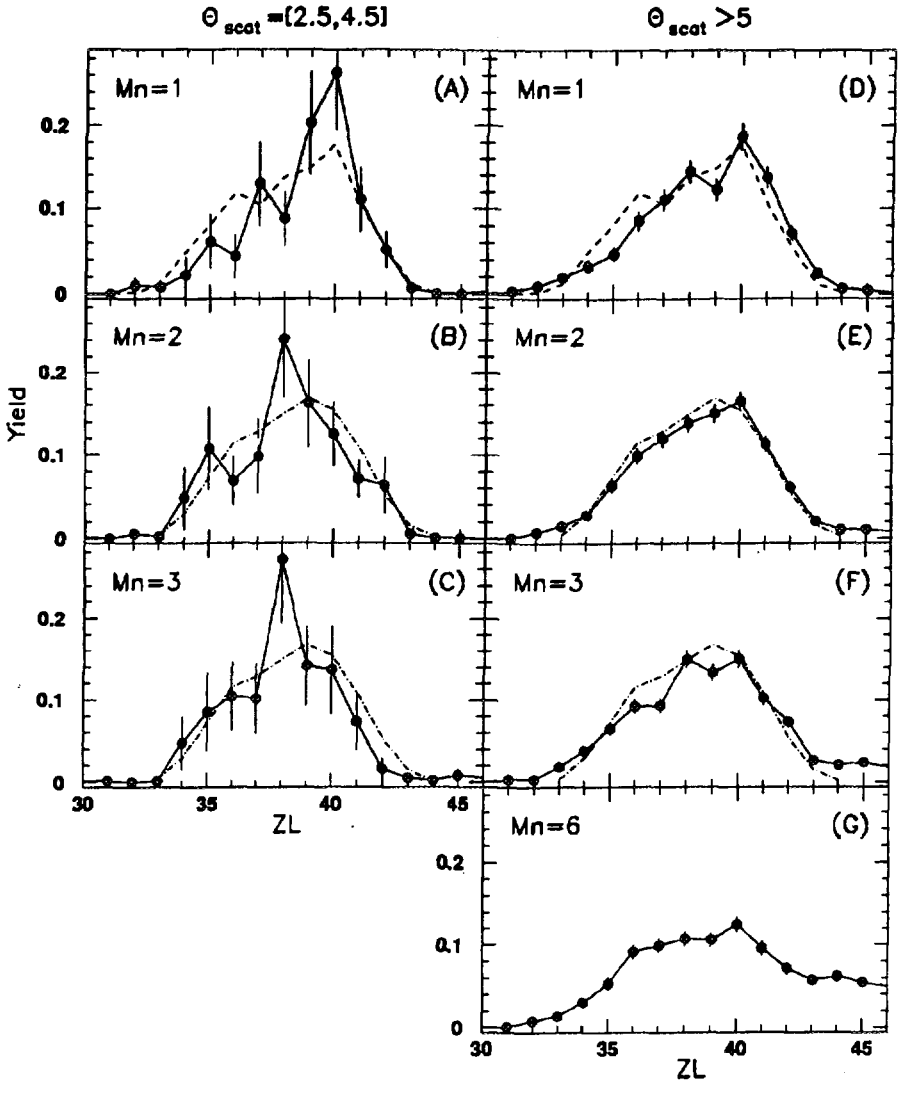

Fig.2: The fission fragment Z distributions (black dots and solid lines) for CF (left hand panels) and NF (right hand panels) are compared with photofission data[4] at different excitation energies (<E*> <8.4 MeV: dashed lines and <E*>=9.7 MeV dotted-dashed line). The data from ref[4] have been folded by our detector Z resolution in order to make the comparison meaningful.

References:

* A more detailed account of this work is in press at Phys. Lett. B
1) G.Himmele et al, Nucl. Phys. A391 (1982) 191
2) S.Polikanov et al, Z. Phys. A350 (1994) 221
3) E.Piasecki et al, Phys. Lett. B351 (1995) 412
4) S.Pommé et al, Nucl. Phys. A560 (1993) 689 and ibid A572 (1994) 237

PARTICLE EMISSION IN HEAVY ION INELASTIC SCATTERING.

J.A.Scarpaci, D.Beaumel, Y.Blumenfeld, N.Frascaria, J.P.Garron
H.Laurent, J.H.Le Faou, I.Lhenry, V.Pascalon-Rozier, J.C.Roynette, T.Suomijärvi
Institut de Physique Nucléaire
91406 Orsay Cedex, France

and

P.Roussel-Chomaz, Ph.Chomaz
GANIL, BP 5027, 14021 Caen Cedex, France

and

A.van der Woude
Kernfysisch Versneller Institut, 9747 AA Groningen, The Netherlands

1. Introduction

Inelastic scattering of heavy ions on different targets has been measured at GANIL in order to study target excitations and more specifically the giant resonances and their multiple excitations, the multiphonons.

However, the target excitation is not the only contribution to the inelastic channel. Other mechanisms giving rise to an ejectile identical to the projectile have a sizeable cross section. The pick-up break-up mechanism, where a nucleon is picked up by the projectile and emitted before the ejectile is detected, has been shown to contribute for 30% of the cross section between 40 and 80 MeV excitation energy in the ^{40}Ca + ^{40}Ca reaction[1] at 50 MeV/A. It gives rise to protons emitted in a forward cone of 30^o opening angle, around the ejectile.

A new contribution, giving rise to fast nucleons emitted in a narrow angular range on the same side of the beam as the ejectile, has been observed in all the following heavy ion reactions at intermediate energies: ^{208}Pb(^{17}O,^{17}O+n) at 84 MeV/A [2], ^{40}Ca(^{40}Ca,^{40}Ca+p), ^{48}Ca(^{20}Ne,^{20}Ne+n) [3] and ^{58}Ni(^{40}Ar,^{40}Ar+p) around 50 MeV/A. A large feeding of the GS and the first excited states of the daughter nuclei is observed, even for high apparent excitation energies.

2. Experimental observation

In all these experiments, the scattered projectile is detected in the SPEG spectrometer in coincidence with protons or neutrons detected in the PACHA and EDEN multidetectors respectively. Our new mechanism was first observed in the missing energy spectra defined as the excitation energy minus the particle energy. Even for high excitation energy regions a large contribution is observed leading to the ground state and the first excited states of the daughter nucleus, whereas statistical calculations do not predict any yield to these low lying states.

Figure 1 shows a missing energy spectrum obtained in the ^{40}Ca(^{40}Ca,^{40}Ca+p)

reaction for an apparent excitation energy between 40 and 55 MeV and for two groups of detectors, one at backward angles in the laboratory frame and the other in the forward direction, on the same side of the beam as the ejectile. While for the two spectra we observe a large bump around 30 MeV that corresponds to the decay

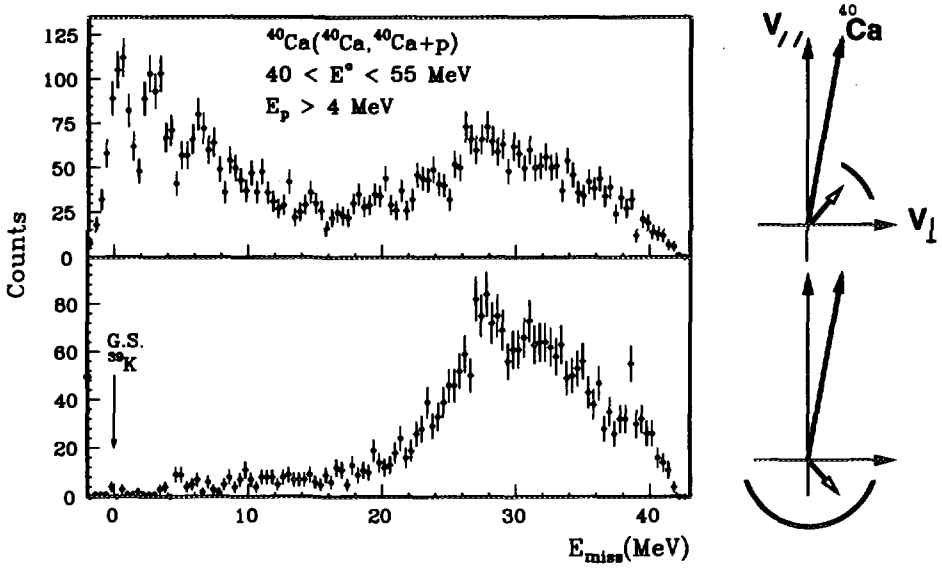

Figure 1: *Missing energy spectra in coincidence with protons detected in the forward direction and in the backward direction.*

of the target, only at forward angles (top figure) we see an important contribution populating the GS and the first excited states of the daughter nucleus, ^{39}K. The angular distribution of these protons is centered at +40 degrees (on the same side of the beam as the ejectile) which is not consistent with a target decay expected to be symmetrical around the direction of the recoil.

3. Contribution to the inelastic spectrum

The comparison of inelastic spectra in coincidence with forward and backward emitted protons allows us to extract the contribution of this mechanism to the inclusive inelastic spectrum. This is shown in figure 2 where we can see on the left column the inelastic spectra in coincidence with forward emitted protons (2.a) and with backward emitted protons (2.c). Figure 2.e is the result of the subtraction of 2.c from 2.a. The extracted contribution is peaked at 30 MeV and extends up to 60 MeV. On the right column, the same spectra are displayed with the condition that the missing energy be less than 8 MeV. The subtracted spectra (2.e and 2.f) look very similar, and have the same number of counts, which indicates that all the contribution of this new mechanism is concentrated at missing energies below 8 MeV. A tentative normalization gives a total contribution for the mechanism of 25% of the

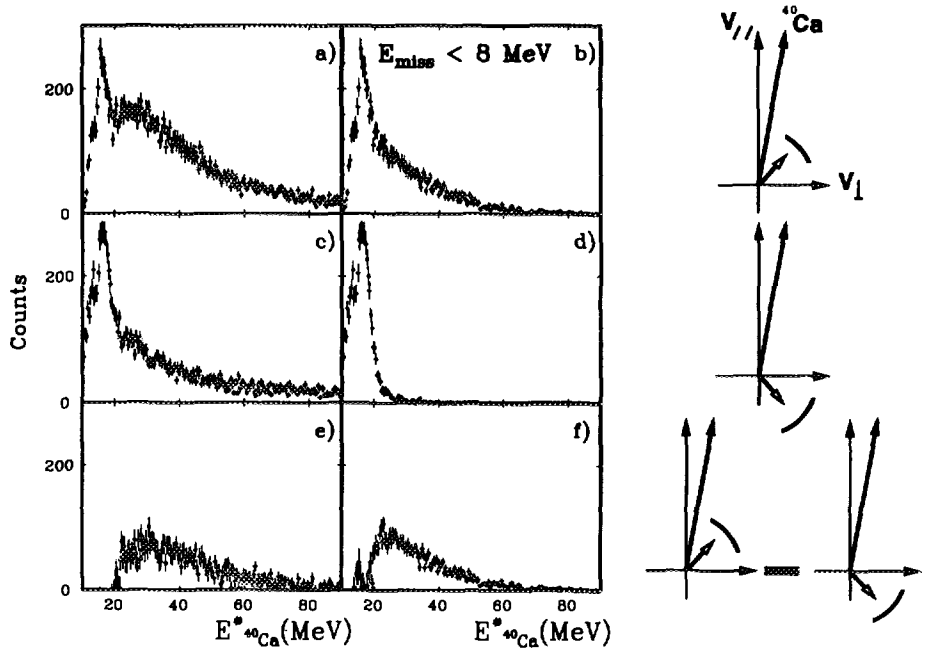

Figure 2: *Inelastic spectra in coincidence with forward (2.a, 2.b) and backward emitted protons (2.c, 2.d). Figure 2.e and 2.f are the result of subtractions.*

inclusive inelastic cross section.

4. Out of plane angular correlation

In the ^{58}Ni(^{40}Ar,^{40}Ar+p) reaction, we could extract information on the azimuthal angular correlation between the protons and the ejectile. By choosing an out-of-plane proton detector at ϕ_{lab}=-30°, we plotted in figure 3 the azimuthal angle distribution of the ejectile. Figures 3.a and 3.b correspond to the coincidence with protons emitted on the same side of the beam as the ejectile while figure 3.c and 3.d correspond to angles on the opposite side, where protons arising from the scattering on the hydrogen contaminant of the target are expected. On the left column, we gated on protons with a kinetic energy less than 10 MeV, corresponding mainly to protons coming from the decay of the target. Indeed, the flat azimuthal angular distributions of the ejectile (figures 3.a and 3.c) indicate no azimuthal angle correlation with the protons, which is expected for inelastic scattering followed by a decay of the target. The cuts observed at -30 and +30 degrees only reflect the acceptance of the spectrometer. On the right column are shown the same spectra, but gated on protons of energies higher than 10 MeV and missing energies less than 8 MeV. The corresponding distributions are now asymmetric. For the scattering on the hydrogen (figure 3.d) the asymmetry simply reflects the conservation of momentum. However, the asymmetry shown in figure 3.b is very interesting. It indicates that the proton goes in the same overall direction as the ejectile. This is depicted in the right hand drawings in the $V_\perp$ versus V_{vert} plane

where the proton is the circle and the ejectile the full dot.

This last information leads us to the conclusion that the proton is pulled by the projectile for a short while, thus the name given to this new mode, the "Towing Mode". Contrarily to the pick-up break-up process, the proton does not stick to the projectile long enough to be fully boosted to the projectile velocity. A possible interpretation could be a transfer to a very unbound level followed by a quasi instantaneous emission. A tentative estimate of the life time of the level reached, assuming that the nucleon trajectory around the projectile is less than a fourth of a revolution, gives less than 10^{-22} second. This could account for the angular correlation that shows the proton around $+40°$ while the projectile is emitted at $+2°$. Further experiments will allow us to bring new information such as the dependance of this phenomenon on the reaction studied and its connection to the pick-up break-up process.

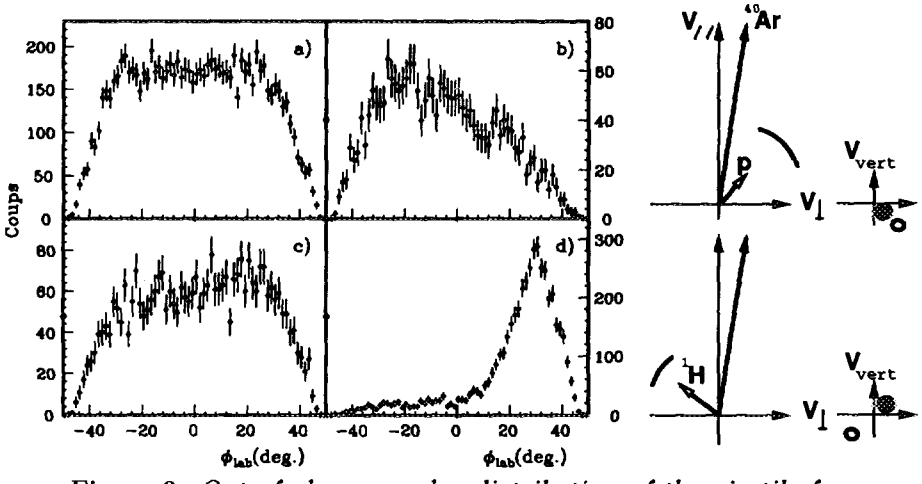

Figure 3: *Out-of-plane angular distribution of the ejectile for* $1.14 \leq \theta_{lab} \leq 1.43$ *degrees, in coincidence with protons detected at* ϕ = -30 ° *(see text).*

5. Conclusion

The measurement of light particles in coincidence with scattered ions has revealed some of the hidden complexity of inelastic heavy ion reactions. In addition to the excitation of giant resonances and multiphonons, two other mechanisms feed the inelastic channel at high excitation energies. Both the well known pick-up break-up process and the newly discovered "towing mode" account for 30% of the observed cross section at excitation energies from 30 MeV up to 80 MeV.

6. References

1. J.A.Scarpaci et al., Phys. Lett., **B258** (1991) 279
2. A.M.van den Berg et al., Nucl. Phys., **A578** (1994) 238
3. H.Laurent et al., Nouvelles du GANIL, Jan 1995

Excitation Energy and Angular Momentum Transfers in the $^{84}Kr+^{238}U$ Reactions at 35 A.MeV

M. Josset, M. Morjean, J. Galin, X. Ledoux, A.Lepine-Szily, B. Lott, A. Péghaire, B. Quednau
GANIL, B.P. 5027, 14021 Caen Cedex, France

P. Eudes, P. Lautridou, C. Lebrun, A. Rahmani
SUBATECH, 2 rue de la Houssinière, 44072 Nantes Cedex 03, France

D. Jacquet, S. Proschitzki
IPN, B.P. 1, 91406 Orsay Cedex, France

J. Quebert
CENBG, le Haut Vigneau, 33170 Gradignan, France

U. Jahnke
HMI, Glienicker Str. 100, D-14109 Berlin, Germany

It is now well established that, in nuclear reactions induced by heavy ion projectiles in the Fermi energy domain, large amounts of energy are dissipated and that large fractions of these latter are found as thermal energies in the nuclei resulting from these interactions. Despite many experimental efforts, the reaction mechanisms responsible for the energy dissipations are not yet quite well understood. For heavy systems, the very dominant reaction mechanism gives rise to a temporary di-nuclear system that separates into two heavy fragments, a projectile-like fragment and a target-like fragment [1,2]. Deep-inelastic models, as those developed for projectile velocities slightly above the coulomb barrier, reproduce in a quite satisfactory way the correlation between the deflection angle of the di-nuclear system and the damping of the total kinetic energy [2,3], assuming that dissipation takes place by nucleon exchanges through a window opened between the reaction partners before their separation [4]. Nevertheless, attempts [5] undertaken to take into account in a more realistic way some of the specific aspects associated with the reactions induced by projectiles in the Fermi energy domain could not preserve the good agreement between the experimental data and the revisited models.

Very interesting pieces of information can be gained on the involved reaction mechanisms from the correlation between the excitation energy and the angular momentum transferred into intrinsic spin of the nuclei resulting from the interaction. Applying a low bombarding energy picture, such as the one of reference [4], large amounts of spin are transferred to the projectile-like and target-like fragments as intrinsic spin. On the other hand, recent experimental results [6] indicate that, in the Kr+Au system at 150 A.MeV, the amount of spin of the target-like fragment is rather small. Very few experiments have been devoted to the spin determination in the energy range of several tenths of A.MeV[7-10]. Most of them have inferred rather low spin values, but these values are averaged over the impact parameters for all reactions leading either to a binary fission of one of the nuclei resulting from the interaction or to alpha particle emission. Two experiments [8,10] have tentatively determined the

correlation between spin and excitation energy, but the first one [8] was restricted to rather peripheral collisions involving small energy dissipation amounts and, in the second experiment [10], the excitation energy was determined using a quite unrealistic massive transfer hypothesis that overestimates by very large amounts the excitation energies.

In the present experiment, the angular momentum transfers were investigated in the 84Kr+238U system at 35 A.MeV as a function of the thermal part of the excitation energy. The intrinsic spin values of the target-like fragment (TLF) was inferred from the width of the out of the reaction plane angular distributions of fission fragments. The reaction plane was determined by the beam axis and the direction of the projectile-like fragment (PLF). The excitation energy was determined by the measurement of the neutron multiplicity associated with the detection of a fission event. Due to the high fissility of the uranium-like nuclei, the angular momentum transfers have been inferred in a very large range of the TLF excitation energy, from less than 10 MeV up to about 600 MeV.

The PLFs were identified in a single measurement between 3° and 7.2° by a large area telescope constituted of two silicon strip detectors (150µm and 500 µm in depth) covering an azimuth range of 84.5°. It has been checked that the reaction plane was safely determined even at very small detection angles of the PLF. A second setting of this telescope allowed to measure the PLF characteristics between 7.7° and 26°. The neutron multiplicity was measured by Orion, a high efficiency 4π detector. The fission events of the TLF were selected by a coincidence between two parallel plate avalanche counters providing us with the time of flight and the energy loss of both fission fragments. An accurate discrimination between fission fragments, intermediate mass fragments and heavy residues has then been performed using the correlation between the time of flight and the energy loss in the detectors.

The average binary aspect of the reaction is evidenced in Fig. 1 that presents, for all PLFs detected with Z larger than 20, the correlation between the deflection angle and the energy per atomic number unit (E/Z). The reactions induced on the carbon backing of the uranium target has been subtracted from this plot. It is quite reminiscent of a usual Wilczynski plot [11], as observed at lower incident velocities of the projectile: a di-nuclear system is formed that rotates from the grazing angle towards smaller angles until a separation occurs due to the repulsive effect of the coulomb and centrifugal forces. Due to the angular threshold at 3°, it is not possible from this figure to determine wether the events detected at low E/Z and at deflection angles much larger than the grazing angle arise from a di-nuclear system that has lived long enough to reach negative deflection angles before its scission or wether, for these highly excited PLFs, the angular spreading due to evaporation is responsible for the large detection angles. Whatever the origin of these events detected backward the grazing angle is, the average behavior of the experimental data shown in Fig.1 is in very good agreement with the solid curve that presents the average correlation predicted by the deep-inelastic model of J. Randrup [4]. Furthermore, this model, coupled with the evaporation code GEMINI [12], reproduces the measured yield for each element between Z=36 and Z=18 within a factor of 2.

In order to infer from the angular distributions of the fission fragments the spin of a fissioning nucleus, the characteristics of this nucleus at the saddle point need to be known: its mass, its temperature and its effective moment of inertia. Unfortunately, the time t_S for a nucleus to reach its saddle point is poorly known: few experimental works have allowed to measure, with very large uncertainties, the time for a nucleus to go from its equilibrium shape to the scission shape, but theoretical estimations on t_S are uncertain. In the present work, the initial TLF spins have been inferred from the angular distribution widths using 3 different hypotheses on t_S: i) ts = 10-23s, i.e. the nucleus at the saddle point is the initial TLF before any deexcitation; ii) t_S = 10-21s, i.e. for the highest excitation energies considered, the initial TLF has cooled down on the way

towards saddle and corrections have been performed following the same evaporation code PACE [13] for temperature and spin during these 10-21s; iii) t_S = 10-19s, i.e. the nucleus at the saddle point is almost cold and corrections have been performed

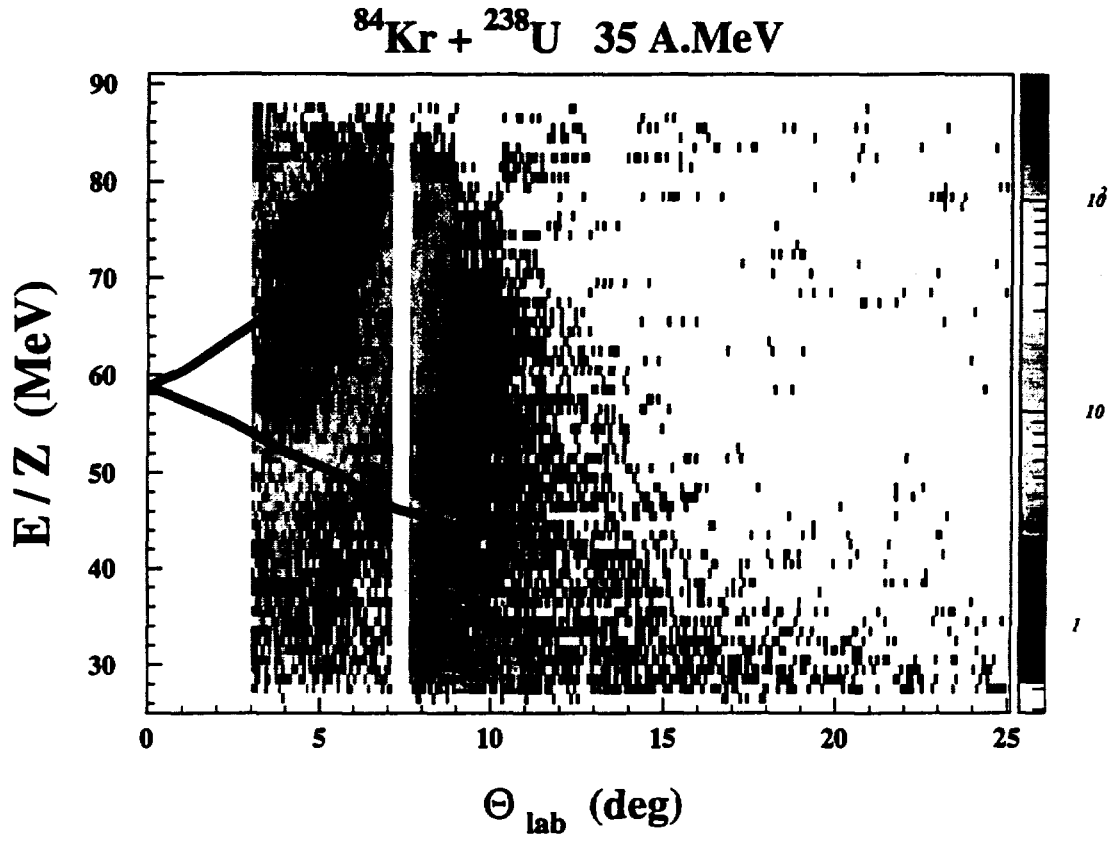

Fig. 1: Correlation between the deflection angle and the energy per atomic number unit for projectile-like fragments detected with an atomic number Z > 19.

according to the predictions of the code PACE. The effective moment of inertia have been calculated from the liquid drop model assuming no angular momentum in the fissioning nucleus. Large values of spin could increase this effective moment of inertia by an amount that could reach 30 per cent [14], but the final spins depend only on the square root of this quantity.

The TLF spin values inferred from the out of the reaction plane distributions are presented in Fig. 2 as a function of the TLF excitation energy. These values are the average values on the results of the 3 considered hypotheses on t_S. These hypotheses lead, due to compensation effects, to very similar initial spin values and the uncertainties due to t_S are shown as error bars in Fig. 2. In order to determine the TLF excitation energy from the total measured neutron multiplicity, a sharing of the excitation energy between the PLF and TLF was assumed according to the prediction of a Monte Carlo simulation for the nucleon exchanges during the interaction in the framework of the Randrup model [4]. The effect of the actual sharing is rather sensitive for TLF excitation energies lower than 100 MeV, but it becomes negligible at higher excitation energies. From Fig. 2, a continuous increase of the TLF spin is observed with the excitation energy up to about 400 MeV, then a saturation is observed. The

maximum spin value reaches about $60\hbar$, to be compared with the $180\hbar$ predicted by the Randrup model for the aligned part of this spin at an excitation energy of 600 MeV.

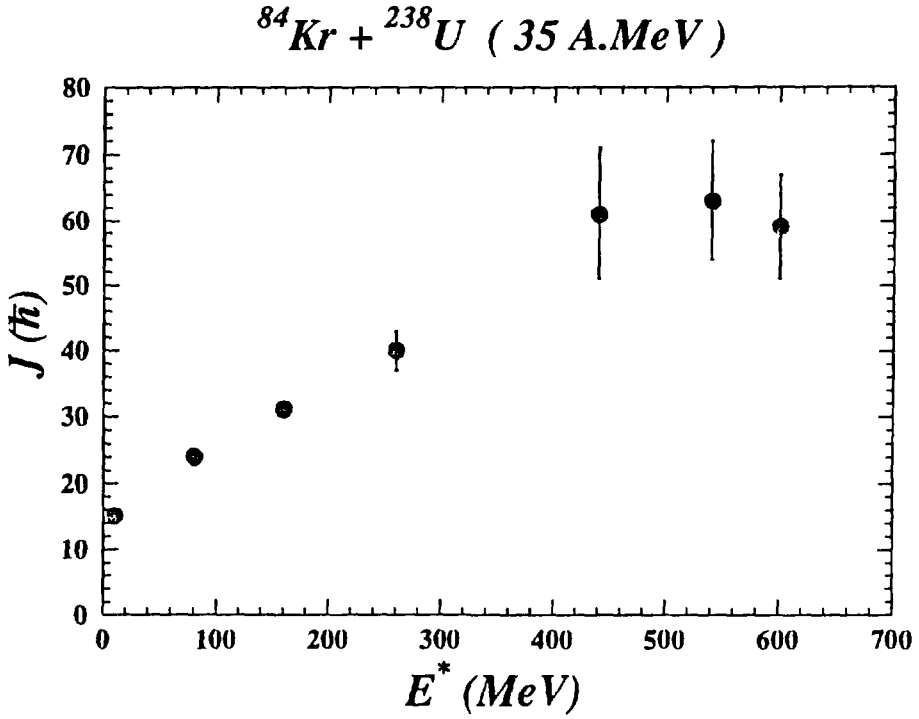

Fig. 2: Spin of the target-like fragment as a function of its excitation energy

The disagreement concerning the spin values between the Randrup model predictions and the experimental data can partly arise from the basic hypotheses of the model that are not well suited to this bombarding energy, as previously stressed, but it seems anyway difficult to reconcile, for binary reactions, very large thermal energies with rather small spin values. Large dealignment effects could explain the low measured values, but simulations do not support this hypothesis. Alternatively, for the highest angular momenta transferred, the lifetimes of the nuclei resulting from the interactions could become so short that they would no more undergo fission: it must be stressed that, within the experimental uncertainties, the spin values inferred in the present paper are close to the maximum spin predicted by the rotating liquid drop model [15] for nuclei in this mass range. In this spin domain, the limit of validity of the statistical theories applied in the present analysis could be reached.

References

[1] J.F. Lecolley et al., Phys. Lett. B325 (1994) 317

[2] E. Piasecki et al., Phys. Rev. Lett. 66 (1991) 671

[3] S.P. Baldwin et al., Phys. Rev. Lett. 74 (1995) 8

[4] J. Randrup, Nucl. Phys. A383 (1982) 468

[5] L. Tassan-Got et al., Nucl. Phys. A524 (1991) 121

[6] B. Quednau et al., accepted for publication in Nucl. Phys. A

[7] T. Ethvignot et al., Phys. Rev. C47 (1991) R2035

[8] S. Bresson, Ph.D. Thesis, Caen (1993), unpublished
[9] K. Ieki et al., Nucl. Part. Phys. 18 (1992) 401
[10] J. Colin et al., Nucl. Phys. A593 (1995) 48
[11] J. Wilczynski, Phys. Lett. B47 (1973) 484
[12] R.J. Charity et al., Nucl.Phys. A483 (1988) 371
[13] A. Gavron, Phys. Rev. C21 (1980) 230
[14] L.C. Vaz et al., Phys. Rep. 97 (1983) 1
[15] S. Cohen et al., Ann. Phys. 82 (1974) 557

Decay patterns of Target-like and Projectile-like Nuclei in $^{84}Kr+^{197}Au$, ^{nat}U Reactions at E/A=150 MeV*

B.M.Quednau[a,1], E.Crema[c], J.Galin[a], B.Gebauer[b], D.Hilscher[b], D.Jacquet[d], U.Jahnke[b], X.Ledoux[a], A.Lepine-Szily[a,c], S.Leray[f], B.Lott[a], M.Morjean[a], A.Péghaire[a], L.Pienkowski[f,2], S.Proschitski[d], G.Röschert[b], H.Rossner[b], R.H.Siemssen[e], C.Stéphan[d]

[a] GANIL (IN2P3-CNRS,DSM-CEA), BP 5025, F-14021 Caen Cedex
[b] Hahn-Meitner-Institut, Glienicker Str. 100, D-14109 Berlin
[c] IF-USP, DFN CP66318, 05389-970 Sao-Paulo, S.P., Brazil
[d] IPN Orsay, BP 1, F-91406 Orsay Cedex
[e] KVI, NL-9747 AA Groningen
[f] LN SATURNE (IN2P3-CNRS,DSM-CEA), F-91191 Gif-sur-Yvette Cedex
[1] supported in part by a "Human Capital Mobility" fellowship of the Commission of European Communities
[2] permanent address:Heavy Ion Lab. Warsaw Un., 02-097 Warsaw, ul.Banacha 4, Poland

Abstract:

The reactions $^{84}Kr+^{197}Au$ and $^{84}Kr+^{nat}U$ were studied at E/A=150 MeV employing the large-volume neutron multiplicity filter ORION at SATURNE. The observed correlations between the atomic number of projectile-like nuclei and neutron multiplicity indicate large excitation energies in the primary projectile- and target-like fragments. Angular correlations between the fission fragments of the U-like nucleus and the projectile-like fragments show a memory of the reaction plane, however no indications of spin effects are found.

The aim and context of this experiment

This experiment is part of an extensive programme which aims at investigating simultaneously the dissipation of translational energy into heat and the transfer of orbital angular momentum into intrinsic spin of the interacting nuclei in an extended energy domain. Data have been obtained for such a system at barrier energies[1)] and more recently at GANIL at E/A=35 MeV[2)]. It was thus interesting to complement the data at much higher energies where the dissipation mechanism is expected to be quite different. For this purpose the experiment was carried out at the National facility SATURNE where Kr could be accelerated at energies exceeding those available at GANIL. The Kr projectile is massive enough for the interaction with the target nucleus to be followed over a broad range of impact parameters through some leftover from the projectile. Two massive target nuclei were chosen: a highly fissionable one to study fission, very sensitive to spin effects, and a complementary target -Au- to get rid of the backing/impurities of any U target.

The experimental set-up (Fig.1)

The large efficiency, $4m^3$ scintillator detector ORION, was utilized in order to measure on an event-by-event basis the number of emitted neutrons and thus get a relevant information about the violence of the collision or associated dissipated energy. Due to the sectorization of the detector, spatial information could also be provided. The projectile-like nuclei, all with velocities close to that of the beam, were identified in Z and localized in Θ and Φ by means of a pair of annular strip Si-detector (annular and radial strips) mounted as a telescope with the beam passing through its central hole. As for the fission fragments, they were detected in coincidence by their energy loss and relative time of flight and located using two standard PPAC detectors set vis à vis and parallel to the beam direction. The fission events are thus characterized by a large set of observables: the

total and differential neutron multiplicity, the atomic number and the polar and azimuthal angles Θ and Φ of the projectile-like nucleus, the Θ and Φ of the two fission fragments issued from the target nucleus making possible kinematical reconstruction of the fissioning nucleus.

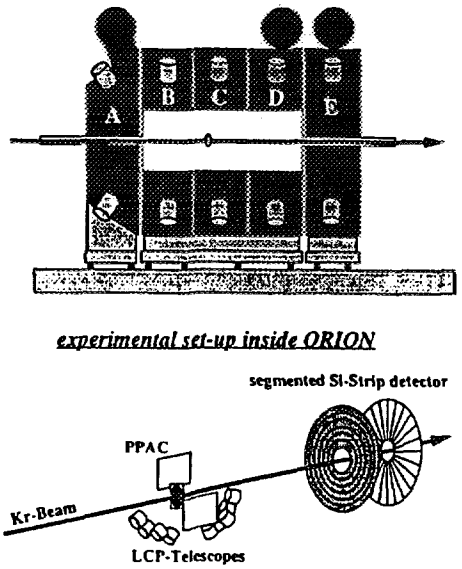

Fig.1. Schematic view of the experimental set-up

In addition to the previous detectors a set of nine silicon telescopes was aimed at the detection of light charged particles from 15 to 150 degrees.

Energy dissipation

The most sensitive data in order to infer the energy deposition are shown in Fig.2 where the measured average neutron multiplicity (filled squares) are given for the five sectors of ORION and the whole detector as a function of the Z of the outgoing projectile-like nucleus. These data have been checked against a two-step model including an Intra Nuclear Cascade step (described by the ISABEL computer code)[3] followed by the GEMINI[4] evaporation code for three contributing sources (the Pre-Equilibrium Particles, the Target-Like Nucleus and Projectile-Like Nucleus). Care is taken to include in these results the production of secondary neutrons generated by the primary reaction products in all materials of the reaction chamber, scintillator tank, shieldings and walls of the cave by employing the CERN-developed code GEANT/FLUKA[5]. Finally the neutron detection efficiency of ORION is taken into account to fold the calculated data and make them directly comparable with the measured ones.

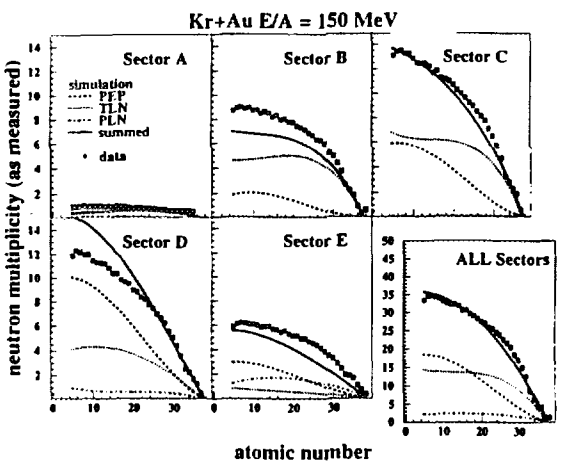

Fig.2. Comparison between the simulations and the experimental data (see text).

Such calculations lead to a general large over-estimate of the neutron multiplicity values and a factor of 0.4 has to be applied on the excitation energies generated by ISABEL in order to mach the measured neutron multiplicities. The overall agreement can then be considered as satisfactory. The detailed contribution of Projectile-like (PLN), Target-like Nuclei (TLN) and the Pre-Equilibrium Particles (PEP) to the total neutron multiplicity is shown in Fig.2. It has also been checked that the multiplicity of evaporated like charged particles from the TLN (inferred from the backward data) is in reasonable agreement with those deduced with the reduced excitation energies.

Mean E*/A of 1.1, 2.1, 3.2 and 5 MeV are thus deduced for TLN in coincidence with final PLN of Z=30, 25, 20 and 15 respectively, showing the efficient heating of nuclei following rather peripheral collisions of 150 MeV/A Kr with U. This confirms, at least qualitatively, the findings of previous high-energy experiments[6]. Clearly the interacting nuclei do not act as mere spectators at high bombarding energy.

Fission for probing the spin effects

With the U target, fission was observed for 47% of the total reaction cross section which makes this decay process a significant probe for the primary nucleus-nucleus interaction. The fission probability has been studied as a function of average Z of the outgoing PLN and associated neutron multiplicity. It shows a maximum close to 1 for PLN with Z=34 to 23 (associated measured neutron multiplicities from 10 to 30, respectively). For higher Z values of the PLN, fission becomes more and more unlikely but still represents a 20% probability for PLN with Z=15.

The coincidence events between the PLN and the two fission fragments of the TLN show that, despite the small scattering angle values at which most of the PLN are detected (close to the grazing angle of 0.9 degrees), a kinematical effect is preserved on the average between the PLN and the reconstructed TLN. As a consequence the plane containing the beam axis and the PLN velocity vector can be considered as the reaction plane and the fission process can be used to search for spin effects.

Whatever the violence of the collision -selected by the neutron multiplicity- no alignment or a weak alignment of the spin with the plane perpendicular to the fission plane has been observed as already noticed elsewhere[7]. This can be taken as an indication that the mechanism of generating spin and excitation energy in residual nuclei at such bombarding energies must be quite different from, e.g. binary dissipative collisions prevailing at lower bombarding energies.

Summary

For the first time, neutron multiplicity measurements were used for studying collisions between heavy nuclei at relativistic bombarding energies. Average secondary Z's of PLN and alpha-particle multiplicities were described qualitatively as a function of neutron multiplicity assuming an Intra Nuclear Cascade followed by evaporation, provided the predicted excitation energies are reduced by a factor 0.4. Large thermal energies (up to E*/A=5 MeV) are deposited in the TLN. Fission is observed up to high excitation energies in the Kr+U interaction. No indication of spin effects on the angular distribution of fission fragments was found in contrast with what is observed at smaller bombarding energy.

References

* A detailed account of the present data can be found in Nucl. Phys. (in press)
1) D.v.Harrach et al., Phys.Rev.42 (1979) 1728
2) M.Josset et al., this volume
3) Y.Yariv and Z.Fraenkel, Phys. Rev. C20 (1979) 2227, C24 (1981)488
4) R.J.Charity et al., Nucl. Phys. A483 (1988)371
5) CERN application software Group GEANT, CERN long Writeup W5013, 1993
6) C.Stéphan et al. , Phys. Lett. B262 (1991)6
7) W.Trautmann and the ALADIN collaboration, GSI-Nachrichten 07-93

A study of the projectile break-up mechanism at intermediate energies by means of the multidetector ARGOS

G. Lanzanò, E. De Filippo, M. Geraci, A. Pagano
S. Aiello, A. Cunsolo, R.Fonte, A. Foti, M. L. Sperduto
Istituto Naz. Fisica Nucleare and Dipartimento di Fisica
Corso Italia 57, 95129 Catania, Italy
C. Volant, J.L. Charvet, R. Dayras, R. Legrain
DAPNIA/SPhN, CEN-Saclay, 91191 Gif-sur-Yvette Cedex, France

May 20, 1996

Abstract

The reaction mechanism underlying the 44 MeV/u ^{40}Ar projectile break-up process has been studied on different targets, by measuring the coincidences between light particles or intermediate mass fragments detected in a large angular range, and projectile fragments or light charged particles, detected in the forward wall of the multidetector ARGOS. While the experimental data relative to projectile-like fragments (PLF) with charge close to the one of the projectile can be interpreted in the framework of a three source analysis, the anomalous light fragment production with $Z \leq 10$ rather suggests "fission" as one of the possible decay mode of the highly excited projectile or PLF. It is also observed that a great amount of the forward detected light charged particles are correlated, and due to the break-up or decay of light excited ions.

1 Introduction

As known, already from the first inclusive experiments at Ganil, it was clear that, while fusion processes were almost disappeared, on the contrary the projectile fragmentation played an important role, being a substantial fraction of the reaction cross-section [1]. As a first question physicists asked themselves on the possible scenario of the reaction. It was astonishing to observe how the participant-spectator model and the Goldhaber approach, typical of relativistic energies, accounted for many of the observed features [1, 2, 3]. More refined exclusive experiments [4, 5] were not able to distinguish between a three body participant-spectator model and a two-body collision, reminescent of a fast deep inelastic process.

Apart the reaction scenario, we would like to mention, amongst the others, two topics, connected to the reaction mechanism at these intermediate energies, and that are worth to be deepened. One is the problem of the pre-equilibrium processes, that are known to increase with the incident energy and that our group has already investigated [6]. In particular it would be extremely important to find an experimental signature for them, and their evolution with energy. The other one concerns the PLF "crumbling" after a violent collision with a target nucleus. It is known that the fission barrier depends on the excitation energy, so that also a relatively light nucleus, if enough excited, can fission, given that its fission barrier is lowered. Some recent data for the reaction $^{35}Cl(8MeV/u) + ^{12}C$ have been interpreted in this sense [7]. If the outgoing PLF is enough excited, we do not exclude this process also at intermediate energies, where it can compete with particle evaporation. In this sense an anomalous rise observed in the inclusive light-PLF production cross-section [1, 2] could suggest such an interpretation.

We think that an enrichment of the experimental phenomenology by more precise and/or selective measurements could help in clarifying the above mentioned subjects. At this aim we have undertaken a series of experiments with the multidetector ARGOS at different beam energies and using a variety of targets, ranging from Carbon to Thorium. In the following we shall report on preliminary data from the first E230 experiment carried out at Ganil in July 1994 by using a 44 MeV/n ^{40}Ar beam bombarding a selfsupporting Al target. The ARGOS multidetector and the E230 experimental layout is described elsewhere in this Compilation [8]

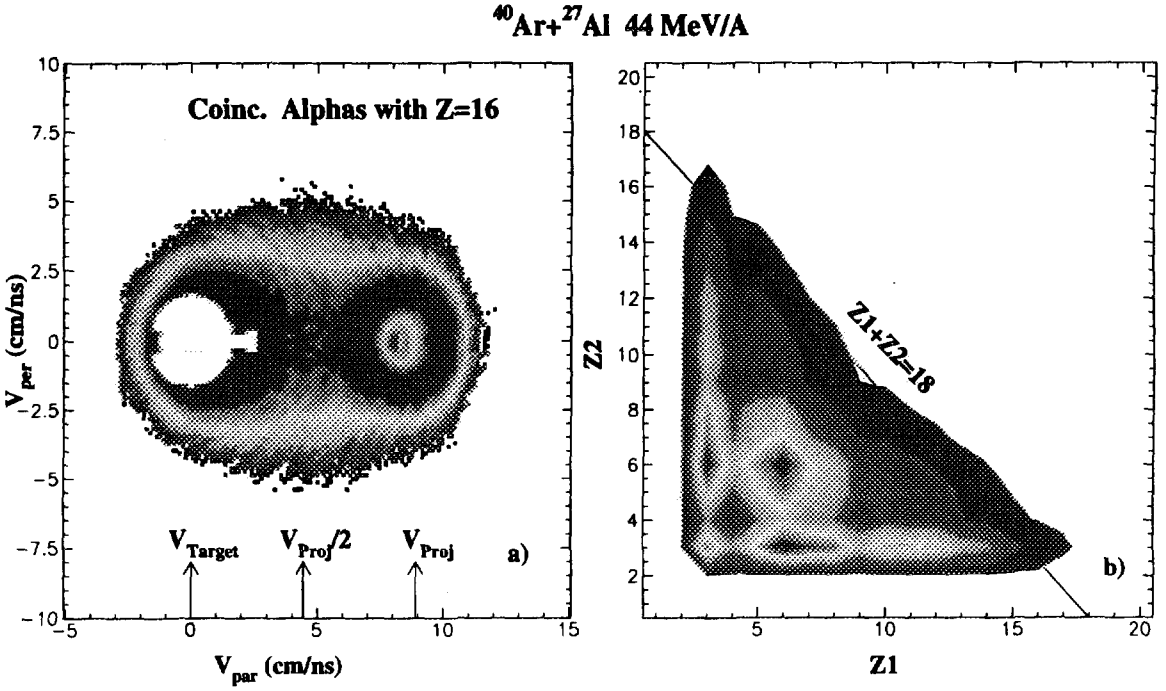

Figure 1: a) Lorentz invariant cross-section for α particles in coincidence with Z=16 PLF detected in the forward wall; b) Charge-charge correlation in the forward wall for Z1,Z2$\geq$3.

2 Preliminary results and Conclusion

Fig.1a shows a typical bidimensional plot of the invariant cross-section, for α-particles in coincidence with Z=16 PLF detected in the forward wall. Two sources are clearly visible, whose velocities are very close respectively to the initial velocities of the projectile and the target. However some particles with velocity intermediate between these two are also present in the plot, suggesting the occurrence of dynamically emitted particles from the overlap zone of the two interacting nuclei, that can be thought as a third source of particles. In effects for PLF of charge $\geq$ 10 all the particle energy spectra can be consistently interpreted in the frame of three equilibrated sources as predicted by an abrasion-ablation model. By means of a fit procedure we obtain typical temperature values of about 3 MeV for the PLF and TLF sources, but a much higher temperature, about 12 MeV, for the intermediate source. As a typical example Fig.2 shows the proton velocity spectra in coincidence with Z=16 in the forward wall, at all the investigated angles, from 1.5° to 172 °. The results of the fit (partial source components and total) are also shown. The backwards and forward emission from an equilibrated high velocity source, clearly visible in the spectra at very forward angles, are well reproduced. A similar and in general better accord is obtained for other different couples of particle and coincident PLF.

For Z<10 the probability of finding two coincident light ions in the forward wall with velocity close to the one of the projectile is increasing, as shown in Fig.1b, where the charge of a fragment is reported as a function of the other one. A maximum is observed for Z=6. A possible explanation, as said in the introduction, could reside in the statistical decay of a highly excited projectile or PLF, that then decays by fission or other multifragmentation modes. We remind that fission of compound systems as light as ^{47}V has already been observed at bombarding energies as low as 8 MeV/n [7]. At these intermediate energies and for some less peripheral collisions, the highly excited projectile or PLF could fission in two excited fragments, that then can again decay. The resulting scenario is that of a "crumbling" projectile or PLF, decaying with a multisequential mechanism, as described by Richert et al. [9]. The abundance of light fragments and especially α-particles in the forward wall and the fact that they are well correlated [8], are in favour of this mechanism.

In conclusion, by means of the multidetector ARGOS we have investigated the "fate" of a 44 MeV/n ^{40}Ar light projectile after collision with an ^{27}Al target. For PLF with charge close to the one of the

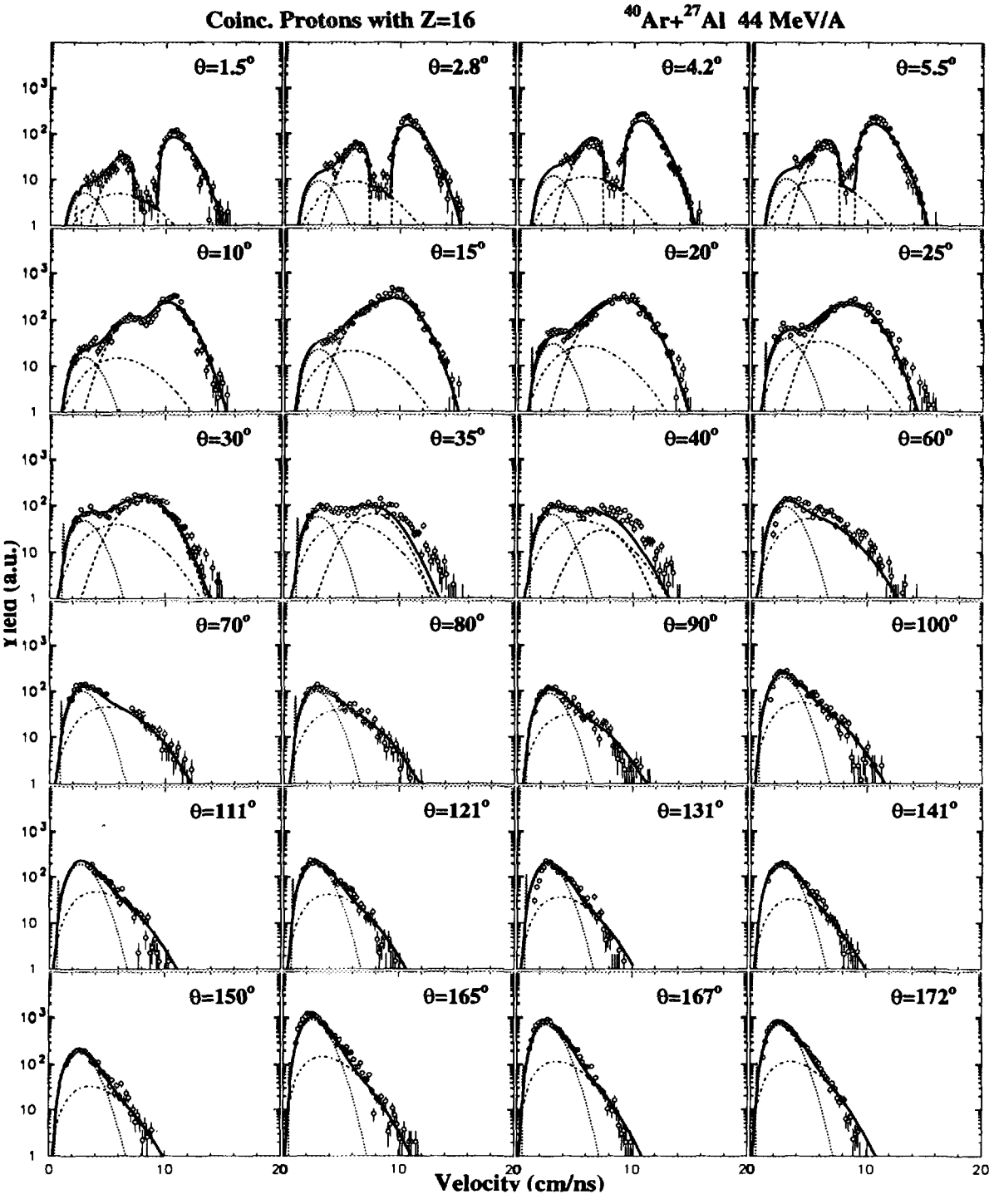

Figure 2: Proton velocity spectra (non normalized) from $\theta = 1.5°$ to $\theta = 172°$. The lines are the result of a three equilibrated sources fit procedure; TLF: dotted line, PLF: dashed lines, Intermediate source: dot-dashed line; Total: thick line. The beam velocity is 8.9 cm/ns.

projectile, two sources are clearly visible, and the velocity spectra can be succesfully interpreted in the framework of a participant spectator mechanism, with a fire-ball source simulating rather particles dynamically emitted from the overlapping nuclear matter. Lighter PLF are in general accompanied by an increase of their multiplicity, indicating that for higher excitation energies, the projectile can fission in two or more (excited) light fragments. Precise interferometric measurements of the relative momenta for alpha-particles and other light particles, suggest that they originate mainly from a multisequential decay mechanism.

References

[1] R. Dayras et al. Nucl. Phys. **A460**, 299 (1986).

[2] V. Borrel et al. Z. für Phys. **A314**, 191, (1983)

[3] A.S. Goldhaber Phys. Lett. **B53**, 306, (1974)

[4] R. Dayras et al. Phys. Rev. Lett. **62**, 1017 (1989).

[5] J.C. Steckmeyer et al. Nucl. Phys. **A500**, 372, (1989).

[6] J.E. Sauvestre et al. Phys. Lett. **B335**, 300, (1994).

[7] C. Beck et al., *Phys. Rev.* **C54** (1996) in press

[8] G. Lanzanò et al., Contr. to this Compilation

[9] J. Richert et al. Nucl. Phys. **A466**, 132, (1987).

B2 - DISSIPATIVE COLLISIONS

Anomalous diffusion in chaotic scattering of heavy ions

Tomasz Srokowski[†] and Marek Ploszajczak

[†] *Institute of Nuclear Physics, PL - 31-342 Kraków, Poland*

A65 1.

Close collisions of heavy ions, in which nuclei experience a considerable overlap of their density distributions, may lead either to the formation of a compound nucleus or to the deeply inelastic dissipative processes in which the system breaks apart before the compound nucleus is formed, i.e. before a complete statistical equilibrium is achieved. In this latter case, there exist 'collective' degrees of freedom which relax very slowly as compared to the relaxation of single particle degrees of freedom or to the contact time of colliding heavy ions. This process is associated with the mass transfer, kinetic energy loss and angular momentum dissipation. The phenomenological description of slowly relaxing , collective degrees of freedom employs the transport equations or the Langevin equations[1] . With respect to the collective variables, the dissipative collisions are similar to the induced fission in the highly excited nucleus and, indeed, the Langevin approach has been applied for the description of this process for a long time. Irreversibility of dissipative processes is related to the memory loss, quantitatively described by various time-dependent correlation functions. Analyzing those functions is important because they determine essentially the transport properties, in particular the diffusion coefficients.

Recently, the velocity autocorrelation function has been determined in the classical molecular dynamics with the realistic nuclear potential[2] and the slowly decaying algebraic velocity and force correlations have been demonstrated for peripheral collisions of nuclei. The decay of both velocity autocorrelation function (VACF) and force autocorrelation function (FACF) seems to be universal ($\sim t^{-\gamma}$ with $\gamma = 1$) and originates from the long free paths between collisions, similarly as in the strongly chaotic (ergodic) periodic Lorentz gas (PLG) with open horizon. This means also that the decay of the force (velocity) correlations is independent of both the details of the potential, in particular its short range features, and the fermionic/bosonic nature of the particles involved[3] , as was demonstrated on the example of fermionic diffusion in superlattices[5] . [1] Recently, we have shown how such slowly decaying correlations can be incorporated in the Langevin approach which is a usual framework for the description of the dissipative reactions and/or the induced fission of hot nucleus. The

[1]These results are relevant for modelling transport properties of fermions in e.g. Boltzmann-Langevin formalism if in medium two-particle cross-section is small with respect to the size of the topological hole due to the antisymmetrization. In this limiting case, two-particle collisions in the collision integral of the Boltzmann-Langevin equation would generate, even for large densities, the anomalously enhanced diffusion process with $D \sim t^{\alpha}$ ($\alpha \simeq 0.6$) and not the normal diffusion as it is usually assumed. The consequences of this finding for transport properties in realistic situations of nuclear heavy-ion collisions or metallic cluster collisions should be further studied.

Time dependent correlation functions of heavy ion collisions are investigated.

main problem is the generation of the properly correlated noise which drives a Brownian particle in each microscopic realization of its trajectory.

In the earlier exploratory studies[4] , we have designed the generator of such a stochastic force applying the velocity series of a point particle in the two-dimensional PLG as a generating process of the deterministic, chaotic random process. In case of the open horizon, the velocity autocorrelation function of the particle in the PLG is proportional to $1/t$ and identifying the time series $\{\mathbf{u}(t_0), \mathbf{u}(t_1)...\}$ with the time-series $\{\mathbf{F}(t_0), \mathbf{F}(t_1)...\}$ of the stochastic force $(\mathbf{F}(t) \sim \mathbf{u}(t))$, one obtains the non-Markovian generator of the stochastic force acting on the Brownian particle. This generator has desired correlation properties but its practical implementation may be cumbersome. More recently, we have studied Markovian generators of the stochastic force which are based on the Kangaroo process (KP)[6] . In particular, we have proposed a special, multidimensional generalization of the KP, conserving the norm and having the covariance $\tilde{\Gamma}(t) \sim t^{-1}$ as the PLG process for the open horizon case. We have found also that the path length distribution, which is $P(s) \sim s^{-3}$ for the non-Markovian PLG case independently of the dimensionality, equals $P(s) \sim s^{-2}$ in the generalized KP, also independently of the dimensionality of the problem. This difference is however not essential for the properties of the Brownian particles. In particular, both the survival probability for the Brownian particle to remain inside of the potential as well as the asymptotic energy distribution of particles are qualitatively the same and can be made almost identical by an appropriate change of the geometry of the PLG, i.e. by changing the radii R of the circular scatterers. These result remain unchanged if one allows variations of $|\mathbf{m}|$ (or $|\mathbf{u}|$ in the case of the PLG) of the stochastic process. The advantage of the Markovian generator lies in its flexibility to describe physical situations with a different degree of isotropy in the distribution of the long free path. One should also stress that both for the Markovian and non-Markovian generators, the long free paths are responsible for the appearance of the algebraic covariance of the process. is presented ~~has been found~~

For particles escaping from the attractive potential, either with or without external barrier, ~~we have found~~ an entangled relation between the FACF of the stochastic force, on one side, and both the survival probability and the asymptotic energy distribution of particles, on the other side. For fast (exponentially) decaying FACF, the survival probability decays exponentially and the asymptotic energy distribution of particles is always Maxwellian. For the FACF decaying as $\tilde{C}(t) \sim 1/t$, the situation is more involved. For a shallow potential , the asymptotic energy distribution of escaping particles exhibits a pronounced peak corresponding to pre-randomized particles which are associated with long trajectories in the adjoined billiard with the open horizon and leave the potential without any collision with particles of the molecular environment. With increasing depth (size) of the potential, this peak is shifted gradually to lower energies and finally it disappears. The peak for pre-randomized particles is superimposed on top of the Gaussian distribution. The Gaussian shape of the energy distribution is connected with the randomized particles. They can stay inside the potential well for a long time, never reaching the equilibration state. Decreasing magnitude of the fluctuating force leads, first of all, to the disappearance of the 'pre-randomized peak' and, moreover, the smooth part changes its shape gradually from the Gaussian distribution to the Maxwellian one. In the survival probability distribution one sees a similar tendency accompanying the decrease of the magnitude of the Langevin force. In the case of a strong force, the survival probability approaches the asymptotic $\sim 1/t$ dependence in a short time. With decreasing magnitude of the Langevin force, the exponential modifications of this de-

FACF = force autocorrelation function

pendence show up for short and intermediate times and the algebraic $1/t$-tail is seen only asymptotically. The passage time from exponential to algebraic regime of the decay law moves gradually towards higher values with decreasing magnitude of the stochastic force.

The simple laws relating the FACF to the properties of both the decay probability of the system $p(t)$ and the asymptotic energy distribution $P(E)$ are challenging. For peripheral collisions of particle aggregates such as heavy nuclei, the diffusion is anomalously enhanced and the diffusion coefficient grows from $D(t_0) = 0$ logarithmically in time. Hence, depending on the duration time of the process, the time-averaged diffusion constant may exhibit considerably different values. From this stand point , the long-lived orbiting dinuclear complexes, found in medium-heavy ion reactions, are particularly attractive for theoretical studies. On the one hand, classical molecular dyuamics and Langevin studies of this work predict characteristic dependencies for $N(t)$ and $P(E)$, associated with the anomalous diffusion. On the other hand, small number of open decay channels, which one expects in these configurations, yields by independent quantal arguments the algebraically decaying survival probability $N(t)$. The correspondence between these two formulations, if any, remains an intriguing open question.

Similarly, in the induced fission one would expect different time-averaged diffusion coefficients and, hence, different dissipations for low and high fissility systems which are characterized by substantially different path length from saddle to scission. The existing data on prescission neutron multiplicities and fission fragment kinetic energy are clearly incompatible with hydrodynamical two-body viscosity and hence with the fast decay of the temporal correlations. A much better description is obtained using the one-body/long-path type dissipation[7] . This is an indication that the dissipation mechanism for strongly elongated shapes, proposed in the present work, could be the correct one. Much systematic work has still to be done to address appropriately this challenging open problem.

References

[1] W. Nörenberg and H. A. Weidenmüller, "Introduction to the Theory of Heavy-Ion Collisions", *Lecture Notes in Physics*, Vol. 51, Springer Verlag, Berlin, Heidelberg, New York, 1980.

[2] T. Srokowski and M. Płoszajczak, *Phys. Rev. Lett.* **75** (1995), 209.

[3] S. Drożdż, J. Okołowicz, M. Płoszajczak, E. Caurier and T. Srokowski, Preprint GANIL P 95 04; ibid. Preprint GANIL 96 09.

[4] M. Płoszajczak and T. Srokowski, Preprint GANIL P 95 25, Annals of Physics (in print).

[5] S. Drożdż, J. Okołowicz, M. Płoszajczak and T. Srokowski, Preprint GANIL P 96 15.

[6] A. Brissaud and U. Frisch, *J. Quant. Spectrosc. Radiat. Transfer* **11** (1971), 1767.

[7] T. Wada, Y. Abe and N. Carjan, *Phys. Rev. Lett.* **70** (1993), 3538.

VERY EXCITED NUCLEI PRODUCED IN THE 60 MeV/A Ar+Au REACTION AND LEADING TO RESIDUES

F.R. Lecolley[1], G. Bizard[1], J. Colin[1],G. Costa[2], D. Durand[1], Y. El Masri[3], A Genoux-Lubain[1], G. Guillaume[2], F. Gulminelli[1], F. Hanappe[4], B. Heusch[2], A. Huck[2], C. Le Brun[1], J.F. Lecolley[1], F. Lefebvres[1], M. Louvel[1], J.Péter[1], R. Regimbart[1], G. Rudolf[2], J.C. Steckmeyer[1], L. Stuttgé[2], B. Tamain[1], I. Tilquin[3]

1) LPC Caen, ISMRA, 6 Boulevard Maréchal Juin, 14050 CAEN CEDEX (France)

2) CRN Strasbourg, BP 20 CR, 67037 STRASBOURG CEDEX (France)

3) Université Catholique de Louvain La Neuve, 2 Chemin du Cyclotron, LOUVAIN LA NEUVE, B1348 (Belgium)

4) Université Libre de Bruxelles (Belgium)

The limits of existence of excited nuclei are not yet precisely known, as a function of their mass, their temperature, their spin, and a better determination of these limits is the common goal of many experimental researches. One easy way to produce excited nuclei is to use heavy ion collisions. The purpose of the experiment described here was to detect the hottest nuclei produced in the 60 MeV/A Ar+Au reaction and leading to residues. Have been detected.

The final residues were detected in forward direction in a solid state detector. The total deposited energy and the time of flight were measured. A dedicated low energy experiment was made with the same detector to measure the pulse height defect (PHD) which can affect substancially the energy measurement for slow heavy nuclei. Once the PHD is known, the energy can be corrected and the mass of the residue can be determined. Not all the detected heavy nuclei are residues : some of them are fission fragments and have to be eliminated. For the identification of fission a parallel plate detector was disposed at backward angles in order to intercept the partner of an eventual fission fragment detected in the forward direction.

The neutrons emitted in coincidence with the residue were detected by the DEMON neutron detector. DEMON is an arrangement of 96 counters, each of them being essentially a container filled with liquid scintillator and coupled to a photomultiplier. The neutron/gamma ray discrimination is achieved using a standard pulse shape analysis method. The neutron energy is obtained from a time of flight measurement. Low energy charged particles are absorbed in lead absorbers (5 mm thick) placed in front of the liquid scintillator. High energy charged particles emitted at forward angles are rejected by thin plastic scintillators acting as anti-coincidences.

The residues were sorted in classes of events following their velocity which is qualitatively related to their initial excitation energy (the larger the velocity, the larger the excitation energy).

For each class of events, the initial excitation energy has been determined can be quantitatively determined in two independent ways :

i - from the energy distribution of the neutrons, which reflects the temperature of the emitter. Special care was taken to eliminate the pre-equilibrium neutrons : only these neutrons emitted backward in the residue center of mass were used to determine the temperature. The temperature obtained this way is an apparent temperature reflecting the continuously varying excitation energy of the residue along its de-excitation chain : a simulation shows that corrections as large as 60% have to be applied to these apparent temperatures to obtain the initial ones which are those we are interested in

ii - from the neutron multiplicity. Due to the low overall efficiency of DEMON, we have no access to the event by event neutron multiplicity. However, the mean neutron multiplicity may be statistically reconstructed. It can be related to the excitation energy of the emitter, via a statistical decay code.

The good coherence between these two independent determinations of the excitation energy in our experiment is attested by the figure 1 where the experimental correlation between initial temperature and neutron multiplicity is compared to the predictions of a simulation. This gives confidence into the validity of our temperature determination.

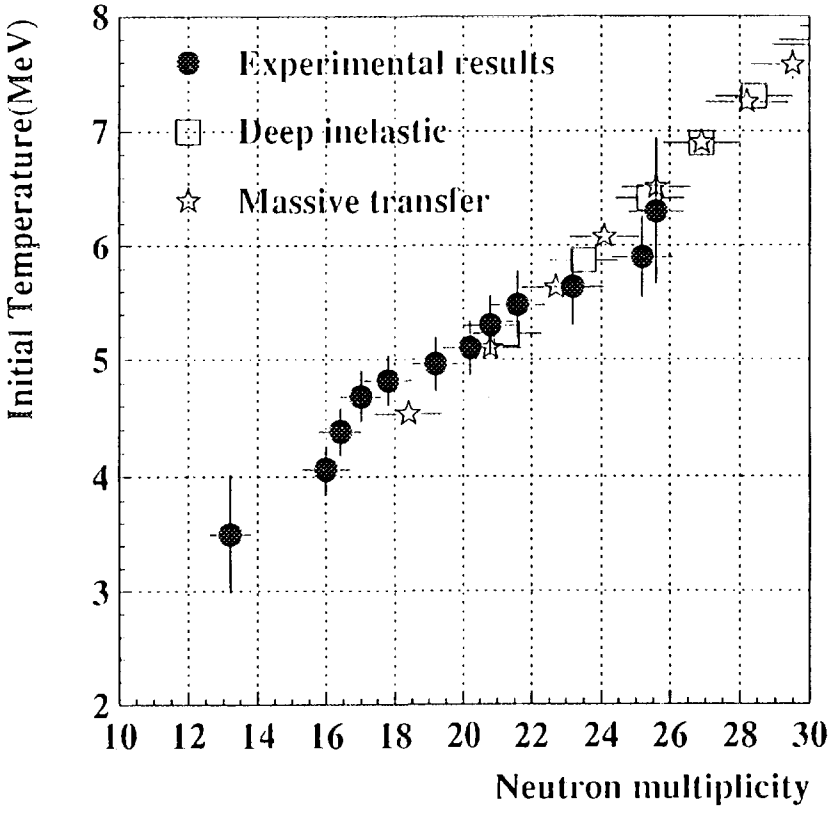

Figure 1

The production mechanism of the residues can be understood using a microscopic calculation (BNV) coupled to a statistical decay code : the temperature/velocity correlation of the primary excited nuclei is well reproduced (fig. 2) and the experimental cross section (50 mb for the production of nuclei hotter than 6 MeV leading to residues) is in good agreement with the theoretical expectation (≈ 60 mb).

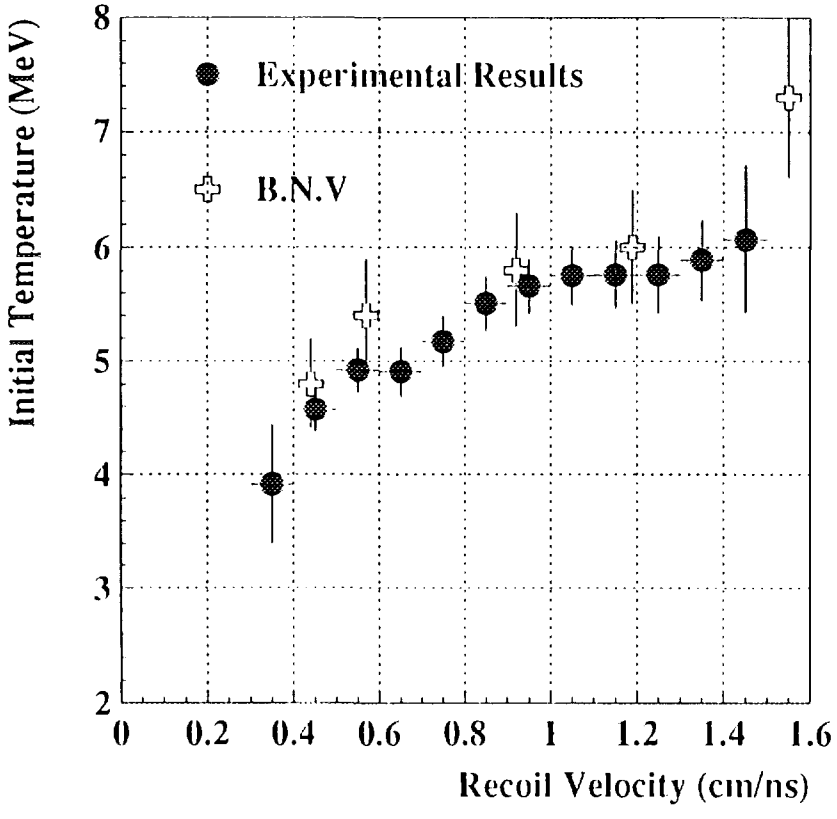

Figure 2

DOMINANCE OF BINARY DISSIPATIVE REACTIONS IN NEARLY SYMMETRIC NUCLEUS-NUCLEUS COLLISIONS ABOVE 35 MEV/U

A. KERAMBRUN[a)], J.C. ANGÉLIQUE[a)], G. AUGER[b)], G. BIZARD[a)], R. BROU[a)], A. BUTA[a-6)], C. CABOT[b-3)], Y. CASSAGNOU[c)], E. CREMA[b-4)], D. CUSSOL[a)], Y. EL MASRI[f)], P. EUDES[e)], M. GONIN[d-5)], K. HAGEL[d)], Z.Y. HE[a-1)], S.C. JEONG[a 2)], C. LE BRUN[e)], R. LEGRAIN[c)], A. PEGHAIRE[b)], J. PÉTER[a)], R. REGIMBART[a)], E. ROSATO[g)], F. SAINT-LAURENT[b)], J.C. STECKMEYER[a)], B. TAMAIN[a)], E. VIENT[a)], R.WADA[d)]

a) Laboratoire de Physique Corpusculaire, ISMRA, IN2P3-CNRS, 14050 Caen , FRANCE
b) GANIL, 14021 Caen, FRANCE
c) DAPNIA/SPhN, CEN Saclay, 91191 Gif-sur-Yvette, FRANCE
d) Cyclotron Institute, Texas A & M University, College Station, Texas 77843, USA
e) Laboratoire de Physique Nucléaire, Institut de Physique, 44072 Nantes , FRANCE
f) F.N.R.S. and Université Catholique de Louvain, Institut de Physique Nucléaire, 1348 Louvain-la-Neuve, BELGIUM
g) Dipartimento di Scienze Fisiche and I.N.F.N., Universita di Napoli, 80125 Napoli, ITALY

One of the first questions which arise is related to the number of nuclei (or nucleon systems) which are formed after the first step of the nucleus-nucleus encounter. At energies 20 to 100 MeV/u, incomplete fusion or massive transfer mechanisms were invoked to explain the observed distributions of products, especially for heavy residues. for the nearly symmetric systems, ^{36}Ar on ^{27}Al from 55 to 95 MeV/u, and ^{64}Zn on ^{nat}Ti, from 35 to 79 MeV/u, charged products were detected in a nearly 4π geometry using two complementary multidetector systems,MUR and TONNEAU. The events were sorted as a function of the violence of the collision with the total transverse momentum $P_\perp$. Lorentz invariant cross section maps [illegible] plotted for different products ([illegible]) show three sources for Z = 1 and 2 particles : quasi-projectile, quasi-target and a third source, located at mid-rapidity. For heavier fragments, the mid-rapidity contribution vanishes.

Fusion events ?

For nearly symmetric systems, it is not possible to disentangle complete fusion events from incomplete fusion events after mid-rapidity emission. In both cases, the source of particle emission seems to be unique and its rapidity is close to Y_{cm}. Data obtained at 55 and 86 MeV/u are presented in fig. 1. Several methods were tried to select possible fusion events.The best selectivity has been obtained with the ratio of the total transverse energy to the total c.m. longitudinal energy $E_\perp / E_{//}$. For two sources located away from Ycm, this ratio is small. It is close to 2, on the average, in the limit of an isotropically decaying source located at Ycm. We have taken a less stringent requirement, i.e. $E_\perp / E_{//} > 1.5$. One then obtains the lower row at each energy in fig. 1 where the quasi-projectile and quasi-target sources are strongly reduced, especially at the lower incident energies ; most events in the lower rows are issued from a different mechanism than the main portion in the upper rows. Their cross section amounts to less than 5% of the reaction cross section at 50 MeV/u and vanishes above.

Characteristics of the quasi-projectile

Since all products from the quasi-projectile are well above the detection threshold and their charges are well identified, we can determine the velocity, mass (or charge) and excitation energy of the primary excited quasi-projectile nucleus left after pre-equilibrium emission. The source velocity vector was reconstructed for each event from the momentum vectors of its products with $Z \geq 2$. In order to quantify the relative motion

damping seen in fig. 1, the velocity (or kinetic energy per nucleon) and deflection angle of the quasi-projectile source can be plotted in the center-of-mass. The distribution obtained with all well characterized events is shown in fig. 10 at 55 MeV/u. The grazing angle is ~1° and one observes a large range of energy damping and deflection angle. Very few events have a kinetic energy close to full damping of the relative motion. A more quantitative view is shown in the right panel, where the mean kinetic energy and mean deflection angle are plotted for each b_{exp} bin. The quasi-projectile mass can be reconstructed by adding up the masses of the detected products and taking into account the geometrical efficiency. Pre-equilibrium particles contribute to the mass. As in ref. [12], the best way of minimizing this contribution is to take for each event the products emitted in the forward hemisphere in the rest frame of the quasi-projectile and multiply their contributions by 2 in order to get the emission over 4 π.

This method leads to large fluctuations event-by-event, but the mean value in each b_{exp} bin is correct. The mean mass of this q-p remains below the projectile mass at all impact parameters, in agreement with the binary character of the collision : fig. 3.

A comparison to a Landau-Vlasov code is also shown in figure 15 . The mid-rapidity source is observed to be stronger than in the experiment. The solid triangles show the mass of the fast source when it separates from the target-like source, after a time of around 70-90 fm/c, depending on b. At 6 fm, it is equal to the experimentally reconstructed mass but it is lower at 2 fm.

In figure 4 is schematized the evolution of reaction mechanims with energy for central collisions below ~5% of σ_R (b_{exp}<1.5 fm). The solid line represents the proportion of the available energy transformed from relative motion into other degrees of freedom (Total Kinetic Energy Loss TKEL, dissipated energy). The short dashed line is the part given as excitation energy to the mono or di-nuclear system. In the most violent collisions, at low energies, fusion occurs.When deep inelastic collisions replace fusion, the relative motion is fully damped, and their total excitation energy is close to the available energy. When the beam energy increase, fully damped events are issued from smaller impact parameters, i.e. their cross section decreases. At the beam energies studied here, fully damped events are rare, thus the dissipated energy and the excitation energy are lower fractions of the available energy. Note that the plotted values are mean values in the 70 mb bin of most violent events. It contains very violent events with a larger damping of the relative motion and larger values of the dissipated energy and excitation energy. At high beam energies, the quasi-projectile and quasi-target have a low excitation energy per nucleon and a small mass and the name of spectators is justified.

The dotted line shows the part of available energy carried by emission from the interaction zone. Around the Fermi energy, pre-equilibrium emission sets in and becomes more important with the beam energy. At several hundreds of MeV/u, the participants carry most of the dissipated energy.

In conclusion, binary collision dynamics dominates above 35 MeV/u in the nearly symmetric systems $^{36}Ar+^{27}Al$ (or $^{40}Ar+^{27}Al$) and $^{64}Zr+^{nat}Ti$. This dominance is observed for all degrees of dissipation. Fusion is observed in central collisions with a cross section not exceeding a few percents of the reaction cross section. The transition from dominating fusion to dominating dissipative binary collisions occurs at incident energies around the Fermi energy for nearly symmetric light and medium-mass systems.

Publications :

- A. Kerambrun et al, Report LPCCaen 94-14, unpublished (1994)
- J. Péter et al, Nucl. Phys. A 593 (1995) 95-123

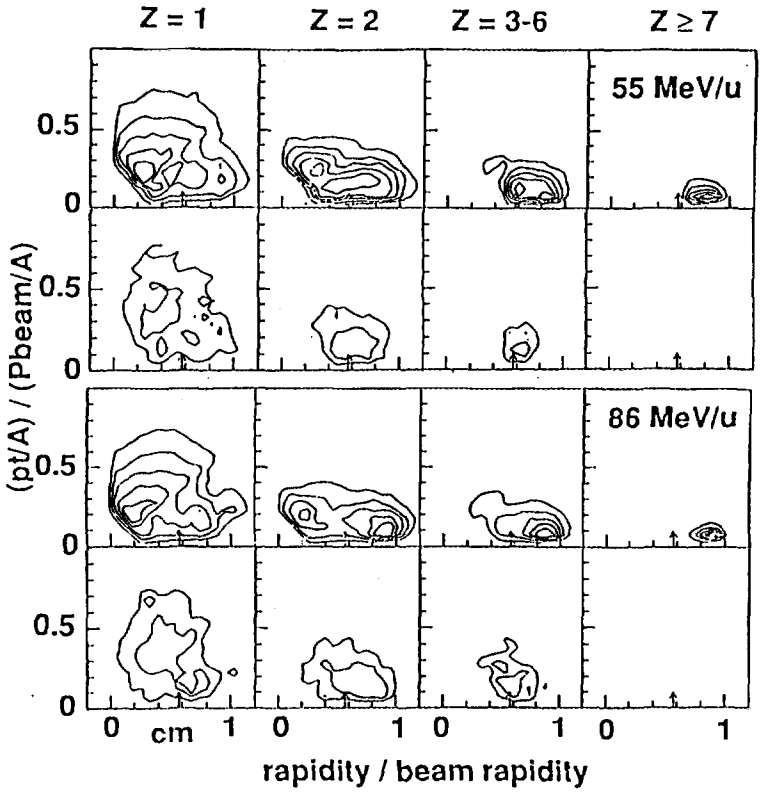

Figure 1 : Contour plots for Z=1, 2, 3-6 and ≥ 7 at 55 (top) and 86 MeV/u (bottom). At each energy, the upper row contains all events with an estimated impact parameter ≤ 1 fm, the lower row contains the events of the upper row which have a large $E_{\perp}/E_{//}$ ratio, i.e. possible fusion events. The abscissa is the laboratory rapidity normalized to the projectile rapidity and the ordinate is the transverse momentum per nucleon relative to the projectile momentum per nucleon.

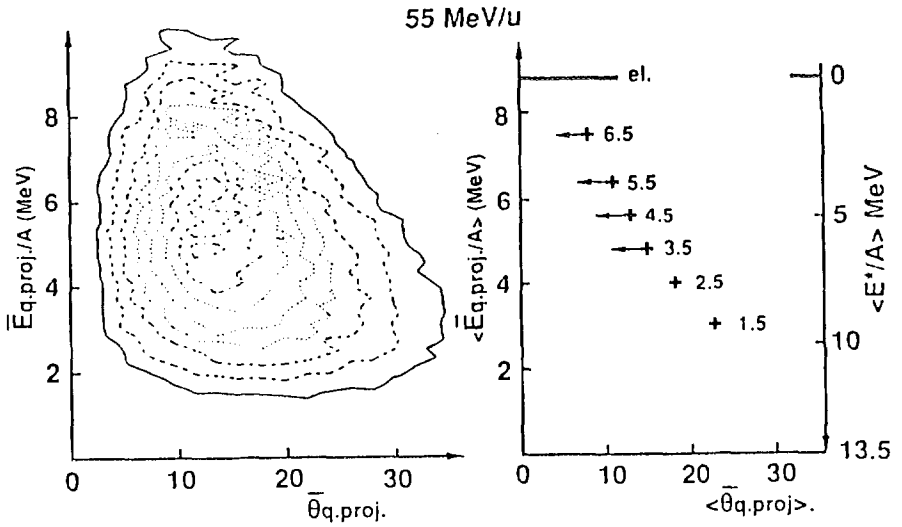

Figure 2 : Left panel : contour plots of the c.m. kinetic energy per nucleon of the reconstructed quasi projectile versus its c.m. deflection angle at 55 MeV/u. Right panel : mean values of the same bservables per b_{exp} bin. The label 1.5 means : b_{exp} = 0 to 1.5 fm, 2.5 means from 1.5 to 2.5 fm, and so on. The right-hand vertical scale is the corresponding dissipated energy per nucleon.

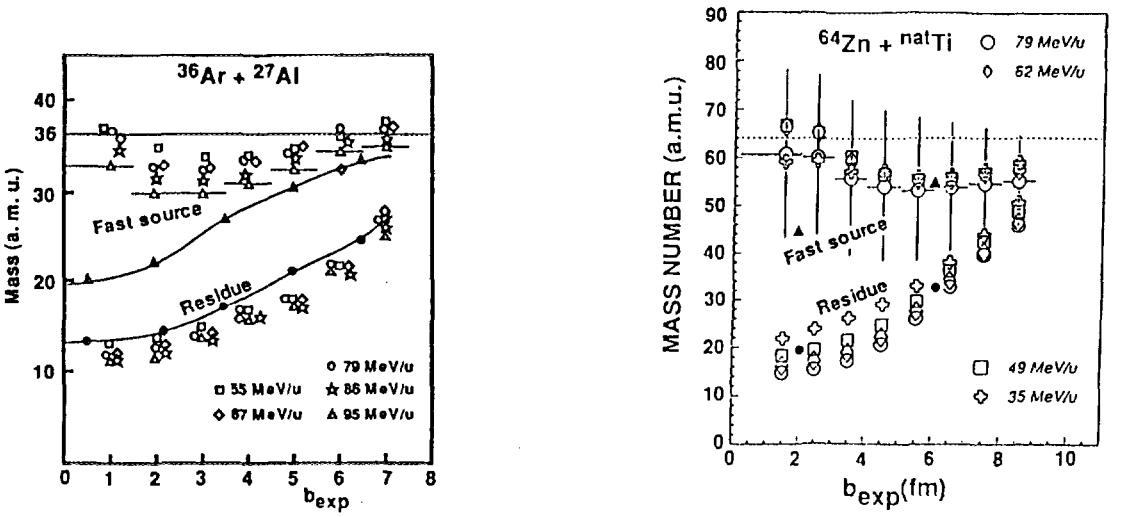

Figure 3 : Experimental data and Landau-Vlasov calculations for $^{36}Ar+^{27}Al$ (top) and $^{64}Zn+Ti$ (bottom) systems as a function of the impact parameter. The experimental data are shown by open symbols. In each figure, the lower points show the average residual mass of the fast source, the upper points show the average reconstructed mass of the fast source (projectile "spectator"). The reconstructed mass includes some pre-equilibrium contribution, especially in central collisions. The horizontal bars show the estimated impact parameter bins. The vertical bars in Zn+Ti show the variances of the distributions. Landau-Vlasov calculations results at 65 MeV/u for Ar+Al and 62 MeV/u for Zn+Ti are shown by closed symbols. Points : average residual mass of the fast source ; triangles : average mass of the fast source at the moment of separation, i.e. minimum mass of source.

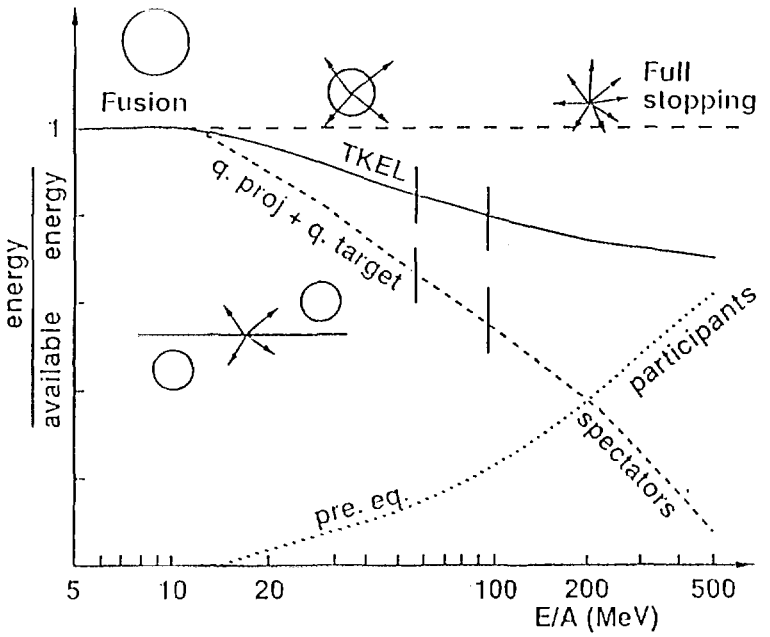

Figure 4 : Schematic picture of the evolution of reaction mechanisms with incident energy. Long dashed line : single source events (fusion or full stoping). Other lines : central collisions (<4% σ_R). Solid line : Total Kinetic Energy Loss TKEL (dissipated energy). Dotted line : total energy of particles emitted from the interaction zone (pre-equilibrium particles, or participants). Short dashed line : excitation energy of the quasi-projectile + quasi-target, or spectators).

Hot expanding source in 50 AMeV Xe+Sn central reactions

N. Marie[1], R. Laforest[2], R. Bougault[2], J.P Wieleczko[1], D. Durand[2], Ch.O Bacri[3], J.F Lecolley[2], G. Auger[1], J. Benlliure[1], E. Bisquer[5], B. Borderie[3], R. Brou[2], J.L Charvet[4], A. Chbihi[1], J. Colin[2], D. Cussol[2], R. Dayras[4], E. De Filipo[4], A. Demeyer[5], D. Doré[3], P. Ecomard[1], P. Eudes[6], D. Gourio[6], D. Guinet[5], P. Lautesse[5], J.L Laville[6], L. Lebreton[5], A. Le Fèvre[1], T. Lefort[2], R. Legrain[4], O. Lopez[2], M. Louvel[2], J. Lukasik[3], V. Métivier[6], L. Nalpas[4], A Ouatizerga[3], M. Parlog[3], J. Péter[2], E. Plagnol[3], A. Rahmani[6], T. Reposeur[6], M.F Rivet[3], E. Rosato[2], F. Saint-Laurent[1], S. Salou[1], M. Squalli[3], J.C Stekmeyer[2], B. Tamain[2], L. Tassan-Got[3], E. Vient[2], C. Volant[4]

[1] *GANIL (DSM-CEA/IN2P3), B.P.5027, F-14021 Caen cédex, France*
[2] *LPC Caen (IN2P3-CNRS/ISMRA et Université), F-14050 Caen cédex, France*
[3] *IPN Orsay (IN2P3-CNRS), F-91406 Orsay cédex, France*
[4] *CEA DAPNIA-SPhN, CE Saclay, F-691191 Gif sur Yvette, France*
[5] *IPN Lyon (IN2P3-CNRS/Université), F-69622 Villeurbanne cédex, France*
[6] *SUBATECH (IN2P3-CNRS/Université), F-44072 Nantes cédex 03, France*

1 Motivations

The predominant decay mode of highly excited nuclei is the disassembly into several intermediate size fragments (1). The understanding of this process, referred as nuclear multifragmentation, has triggered a blooming of theoretical works which differ upon the degrees of freedom involved (1,2), but the physics which drives the phenomenon is not yet delineated. In this context, the study of the multifragmentation phenomenon in very central nucleus-nucleus collisions is of particular interest since compressed matter is expected to be created early in the collision. Therefore, such investigation might reveal whether compression induces a specific pattern for multifragmentation and help to disentangle true dynamical mechanisms from phase-space effects. A good experimental signature of a compression-expansion cycle developped during the collision could be the kinetic energy of the emitted fragments (3-15). In this contribution we present evidence for a radial collective motion of the fragments emitted during the multifragmentation of a single source formed in central collisions of the quasi symmetric Xe+Sn system at 50 AMeV. This contribution is a part of an article submitted to Physics Letters B (16).

2 Experiment

The experiment was performed using a ^{129}Xe beam with an intensity of 5.10^7 pps and 50 AMeV incident energy delivered by the GANIL facility. This beam impinged on a 350µg/cm^2 thick self-supporting ^{nat}Sn target. Charged products were detected with the INDRA detector which covers the laboratory angles from 2° to 176° with a geometric acceptance of 90% of 4π. Charged particles were identified in atomic number with a resolution better than one unit up to Z=60; isotopic separation for Z≤4 was achieved up to about 200 AMeV. Absolute energy calibrations are estimated to be accurate to within 5%. Identification thresholds evolve from 0.7 AMeV to 1.7 AMeV when atomic number increases from 1 to around 60.

3 Selection of single source events in central reactions

A first selection is performed by imposing for each event two criteria: (i) the sum of the total charge exceeds 80% of the combined charged system (charge conservation); (ii) the sum of products of the charge by the parallel-velocity exceeds 80 % of the projectile linear momentum restricted to its charge (pseudo linear momentum conservation). Events satisfying both conditions represent about 6% of the reaction cross-section and correspond to the most dissipative collisions. On this sample we have performed an event by event shape analysis based on the 3-dimensional kinetic energy tensor (17,18,19) calculated in

the center of mass frame of the reaction. In order to minimize possible secondary emission and preequilibrium perturbation, only fragments with Z≥3 were included for the calculation of the tensor. In the following, we have chosen as the centrality selector the value of the angle θ_{flow} between the beam axis and the eigenvector associated to the largest eigenvalue extracted from the diagonalization of the tensor.
The overall properties of events selected with small θ_{flow} are typical of those of a mechanism where the colliding system retains a strong memory of the entrance channel. On the contrary, several clues suggest that a selection of events with $\theta_{flow} \geq 60°$ allows to isolate unique source events formed at small impact parameters (16):

i) the velocity distribution of the fragment is bell shaped and centered at the velocity of the center of mass which indicates that a high part of the initial relative kinetic energy is transformed into others degrees of freedom;

ii) the correlation function of relative azimuthal angle between alpha pairs emitted between $4.5° \leq \theta_{lab} \leq 110°$ is isotropic which is a strong indication of collisions at small impact parameter (20);

iii) over the covered angular domain the shape of the kinetic energy spectra of the detected fragments is the same, thus the fragments are emitted isotropically;

iv) for light charge particles (Z≤2), the $d\sigma/d\cos\theta_{cm}$ distribution is flat from 60° to 120°. This reflects an isotropic emission from a source moving at the center of mass velocity. However, deviations from isotropic emission are clearly observed for the light charge particles (lcp) emitted at forward and backward directions. This additional component reflects presumably some memory of the entrance channel dynamics.

To estimate the size of the isotropic source we take into account all fragments and twice the number of lcp emitted in the range 60°-120°. The measured isotropic component exhausts 90% of the total detected charges. The isotropic source represents 79% of the combined system, and simulations have shown that the missing charged products should preferentially be associated to the anisotropic component of the lcp. All these features supports the conclusion that events selected by means of largest values of θ_{flow} are strongly dominated by a mechanism where most of the available charge comes from a single source formed in very central collisions. The measured cross section of those events (for $\cos\theta_{flow} \geq 0.5$) is about 6mb. Therefore its represents 12mb and an estimation of the detector efficiency gives a correcting factor of about 2 to 3.
It is remarkable that a substantial part of the isotropic source is observed as fragments. The sum of the charge of all fragments is about 51, and over a mean multiplicity of 7 fragments, the mean size of the largest three fragments is 15, 10 and 8. These features are definitively in the regime of multifragmentation. Last, by means of the calorimetry method (21) applied on all detected fragments and twice the lcp associated to the isotropic source, we have estimated that the stored excitation energy is about 12 AMeV. This very high excitation energy rises the question is the stored energy purely thermal or is collective motion present?

4 Analysis of the kinetic energy of the fragments

We have addressed the nature of the excitation energy stored in the system by means of the analysis of the kinetic energy distributions of the fragments. In Fig. 1a we report, for collisions with $\theta_{flow} \geq 60°$ the Z dependence of the mean values of the center of .mass (c.m) kinetic energy spectra $\langle E_{cm} \rangle$, of all fragments with Z≥3 (filled circles). The mean kinetic energy increases steadily from about 60 MeV for Lithium up to a maximum value of about 110 MeV for Aluminium and then stays roughly constant. Indeed, integrating over the restricted domain 60°-120° (open circles) does not affect this behaviour. Thus, the overall trend, visible in Fig. 1a, stays remarkably stable regardless of the changes in the conditions chosen for the analysis. To investigate to what extent the trend for $\langle E_{cm} \rangle$ reflects the role of the largest fragment in each event we have built separate spectra for them (Fig. 1b) and for other fragments (Fig. 1c). Whereas the trend for the largest fragment does not depend on its own selection, the mean kinetic energy $\langle E_{cm} \rangle$ increases with Z for the other fragments. it is worth noting that for any given size, the mean kinetic energy is significantly smaller when the fragment is the largest in the event. Due to the high quality

of the experimental apparatus and its thorough calibration, this is the first time one sees clearly the details of the kinetic properties of the fragments.
For a quantitative interpretation of the experimental results we have performed calculations with a phenomenological model (SIMON) of simultaneous disassembly (22). In this model, the initial source is sampled to give a fixed number of prefragments whose size are randomly chosen and distributed in space by imposing a configuration as compact as possible. The initial momenta of the prefragments take into account the Coulomb and thermal motions and an eventual expansion effect mimicked with an initial selfsimilar velocity. The calculations, presented here, correspond to a desintegration of a 12 AMeV excited Gold nucleus and the initial partition have been determined to reasonably reproduce the experimental multiplicity and elemental distributions as well as the mean size of the largest three fragments.
First we compared the measured $<E_{cm}>$ to the prediction of the model assuming a pure thermal scenario (black area in Fig. 1a). This clearly fails to explain the kinematical observables. The calculated mean energy values are systematically too low and are roughly independant of the fragment charges, at variance with the data (Fig. 1a). Furthermore, the shape of the energy spectra distribution is not reproduced as it is shown for Z=8 in Fig. 1d. These disagreements illustrates the need for an additional motion to be superimposed onto a thermal plus Coulomb scenario. Indeed a clear improvement is observed when part of the total excitation energy is stored into a collective radial mode (<Er>). Best agreement are obtained when <Er> accounts for 2 AMeV and are presented in Fig. 1. (grey area). For $Z \leq 13$ the $<E_{cm}>$ and its Z dependence are remarkably reproduced (Fig. 1a) as well as the shape of the energy distribution (Fig. 1d for Oxygen). However, the calculated $<E_{cm}>$ continuously increases for $Z \geq 13$ in contradiction with the experimental saturation. As we know from the above experimental event by event analysis that the largest fragment dominates the mean energy profile for the highest Z, we have applied the unfolding procedure to the simulated events (Fig. 1b and 1c). The calculation is now consistent with the data regardless of the charge when the largest fragment in each event is excluded (Fig. 1c). This results suggests a better sensitivity to the collective motion when one concentrates on fragments excluding the largest one, and the simulation with 1 AMeV (3 AMeV) under- (over-) estimates the experimental value by 25%. On the other hand, the average kinetic energy of the largest fragments are overpredicted (Fig. 1b). This is presumably due to a badly handled determination of the location of the largest fragment in the simulated breaking configuration. Conversely, these details on the kinetic properties of the fragments may provide valuable information on the distribution of matter in the multifragmenting system. Finaly we have checked that the value of <Er> holds remarkably against changes of the initial characteristics of the source (size and excitation energy) giving reasonable agreement for elemental and multiplicity experimental distributions.

The extracted mean collective energy corresponds to about 17% of the total available kinetic energy of the Xe+Sn system at 50 AMeV. This fraction is of a same order of magnitude that compressional energy predicted by various transport model for this reaction (23,24). However, further investigations are needed to demonstrate that this extracted mean colletive energy is directly connected to the early compression phase of the collision or partly due to a thermal radial flow. Morever, a quantitative analysis of all features of the observed multifragmenting source has to be done to study the possible role of the expansion in the decay properties.

References

(1) See,for instance, L.G. Moretto and G.J Wozniak, Ann. Rev. Nucl. Part. Sci. (1993) 379.
(2) D.H.E Gross, Rep. Prog. Phys. 59 (1990) 605.
(3) H.W Barz et al., Nucl. Phys. A531 (1991) 453.
(4) R.T. de Souza et al.,Phys. Lett. B300 (1993) 29.
(5) W. Bauer et al., Phys. Rev. C47 (1993) R1838.
(6) R. Bougault et al, XXXII Int. Winter Meeting on Nuclear Physics (Bormio 1994).
(7) S.C Jeong et al., Phys. Rev. Lett. 72 (1994) 3468.
(8) W.C. Hsi et al., Phys. Rev. Lett. 73 (1994) 3367.
(9) D. Heuer et al., Phys. Rev. C50 (1994) 1943.
(10) F. Schussler et al., Nucl. Phys. A584 (1995) 704.
(11) G. Poggi et al., Nucl. Phys. A586 (1995) 755.
(12) M.A Lisa et al., Phys. Rev. Lett. 75 (1995) 2662.
(13) R. Kotte et al., Phys. Rev. C51 (1995) 2686.
(14) S.C. Jeong et al,to be published in Nucl. Phys. A.
(15) J.C. Steckmeyer et al., Phys. Rev. Lett. 76 (1996) 4895.
(16) N. Marie et al, submitted to Phys. Lett. B.
(17) J. Cugnon, D. L'Hote, Nucl. Phys. A397 (1983) 519.
(18) J.F Lecolley et al., Phys. Lett. B325 (1994) 317.
(19) M. D'Agostino et al., Phys. Lett. B368 (1996) 259.
(20) L. Phair et al., Nucl. Phys. A564 (1993) 453.
(21) D. Cussol et al., Nucl. Phys. A541 (1993) 298.
(22) O. Lopez et al., Phys. Lett. B315 (1993) 34.
(23) D.R Bowman et al., Phys. Rev. C46 (1992) 1834
(24) V. Metivier, Thèse de Doctorat, LPCC T 9501.

Fig. 1. Kinetic energy characteristics of the fragments for very central events ($\theta_{flow} \geq 60°$) in the c.m. The experimental data are shown by filled circles ($0° \leq \theta_{CM} \leq 180°$) and open circles ($60° \leq \theta_{CM} \leq 120°$). a) Average kinetic energy of the fragments as a function of their Z. b) Average kinetic energies of the largest fragment in each event. c) Average kinetic energy of the fragments but the largest. d) Center of mass oxygen energy spectrum. The results of a phenomenological multifragmentation model (see text) with and without expansion are presented in grey and black respectively.

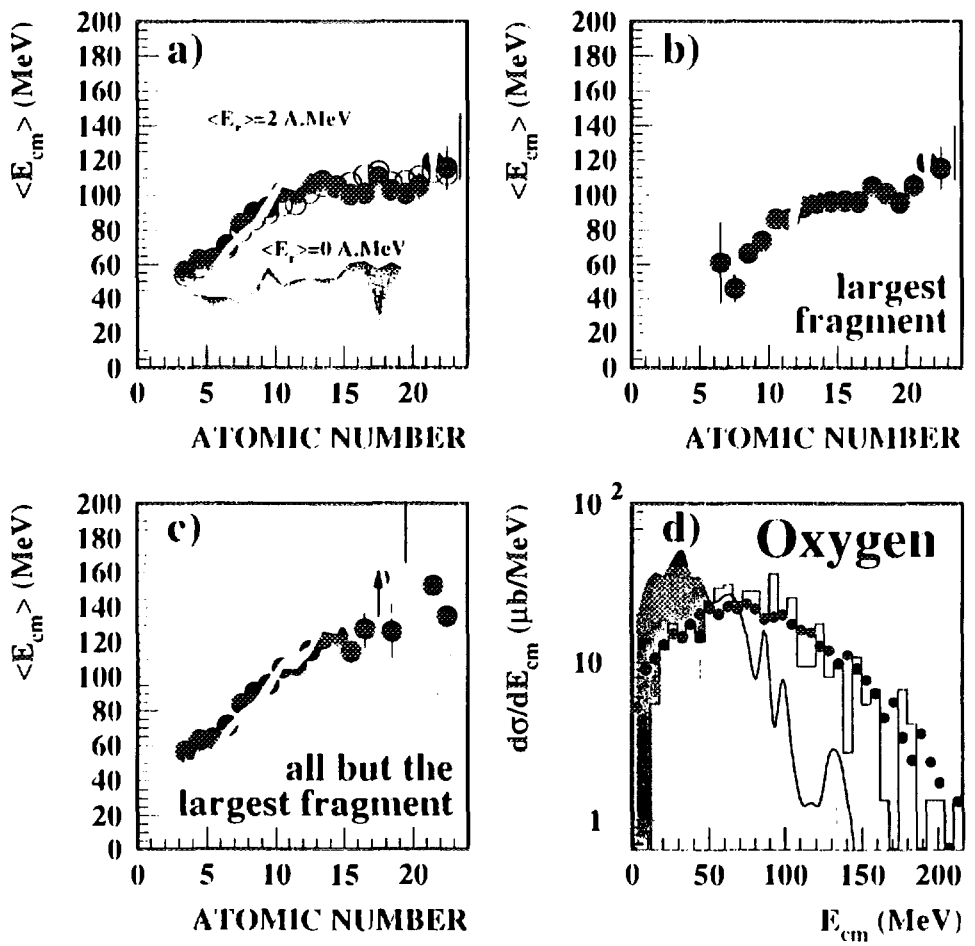

REACTION MECHANISMS IN SYMMETRICAL NUCLEUS-NUCLEUS COLLISIONS

V. Métivier[6], J. Benlliure[1], B. Tamain[2], O. Lopez[2], G. Auger[1], Ch. O. Bacri[3], E. Bisquer[5], B. Borderie[3], R. Bougault[2], R. Brou[2], J.L. Charvet[4], A. Chbihi[1], J. Colin[2], D. Cussol[2], R. Dayras[4], D. Durand[2], E. De Filippo[4], A. Demeyer[5], D. Doré[3], P. Ecomard[1], P. Eudes[6], D. Gourio[6], D. Guinet[5], R. Laforest[2], P. Lautesse[5], J.L. Laville[6], L. Lebreton[5], J.F. Lecolley[2], A. Le Fèvre[1], T. Lefort[2], R. Legrain[4], M. Louvel[2], J. Lukasik[3], N. Marie[1], L. Nalpas[4], A. Ouatizerga[3], M. Parlog[3], J. Péter[2], E. Plagnol[3], A. Rahmani[6], T. Reposeur[6], M.F. Rivet[3], E. Rosato[2], F. Saint-Laurent[1], S. Salou[1], M. Squalli[3], J.C. Steckmeyer[2], L. Tassan-Got[3], E. Vient[2], C. Volant[4], J.P. Wieloczko[1]

[1] GANIL (DSM-CEA/IN2P3), BP 5027, F-14021 Caen Cédex, France

[2] LPC Caen (IN2P3-CNRS/ISMRA et Université), F-14050 Caen Cédex, France

[3] IPN Orsay (IN2P3-CNRS), F-91406 Orsay Cédex, France

[4] CEA DAPNIA-SPhN, CE Saclay, F-69191 Gif-Sur-Yvette, France

[5] IPN Lyon (IN2P3-CNRS/Université), F-69622 Villeurbanne Cédex

[6] SUBATECH (IN2P3-CNRS/Université), F-44072 Nantes Cédex 03, France

Reaction mechanisms have been studied for symmetrical systems Ar+KCl and Xe+Sn with INDRA from 32 (~~resp. 25~~) to 74 (~~resp. 50~~) MeV/u. The large angular coverage and efficiency are very useful to look at the event topology. The first main result ~~which has been obtained~~ is the strong dominance of binary processes. Only a very small fraction of the cross section (< 100 mb) corresponds to fusion collisions whatever the bombarding energy is. All peripheral and most central ones lead to two sources behaviour[2]. As for lower bombarding energies, it is possible to get Wilczynski plots exhibiting generally an incomplete dissipation of the initial available energy (figure 1). However, a first difference with the low incident energy behaviour lies in the fact that the projectile-like (PLS) and target-like (TLS) sources have suffered a severe decay with particle and fragment emission ; the PLS and TLS remnants can hence be very distant from the initial fragments and a proper analysis needs a reconstruction of the initial TLS and PLS from the detected products. A second difference with the low incident energy regime concerns the PLS and TLS decays. It is impossible to resolve clearly in time the initial dissipative process from the decay step and some fragments are dynamically emitted. This feature can be recognized in figure 2 in which the invariant cross section for alpha particle emission is plotted as a function of the parallel and perpendicular velocity components. The best way of recognizing the binary character of the collision is to

construct such plots in a reference frame where the center of mass of the reaction is at rest and the parallel axis chosen as the main axis of the momentum tensor for each event. Such a treatment has been achieved in figure 2 for semi-peripheral events. One recognizes the binary nature of the collision but one notes too an additionnal contribution between both sources. It corresponds to a dynamical emission which can be either a neck-emission during the slowing-down process, or a PLS or TLS decay before complete decoupling between both partners.

It has been possible to estimate the proportion of mass corresponding to this dynamical emission. Up to about 20% of the total mass of the system[3]. Mainly alpha particles and IMF are involved : more than half of IMF can be dynamically emitted. A more complete analysis has been performed for events involving fission of the PLS or TLS. For the Xe+Sn system at 50 MeV/u, it has been possible to establish that the angular distribution of the fission fragments emitted from the PLS (resp TLS) source is peaked in the TLS (resp PLS) direction. Moreover, for asymmetric fission, the lighter fragment is emitted preferentially in this direction. This means that this fission phenomena has been dynamically initiated. Such a result is connected with viscosity properties of nuclear matter.

Another aspect of this reaction mechanism analysis is dealing with the measurement of the energy deposit. Values exceeding 10 MeV/u have been obtained for both Ar+KCl and Xe+Sn system in agreement with earlier data obtained with Nautilus[4]. It has been established that energy deposits expressed in MeV/u are similar in Ar+KCl and Xe+Sn which means that the underlying mechanisms do not depend significantly on the involved total masses .

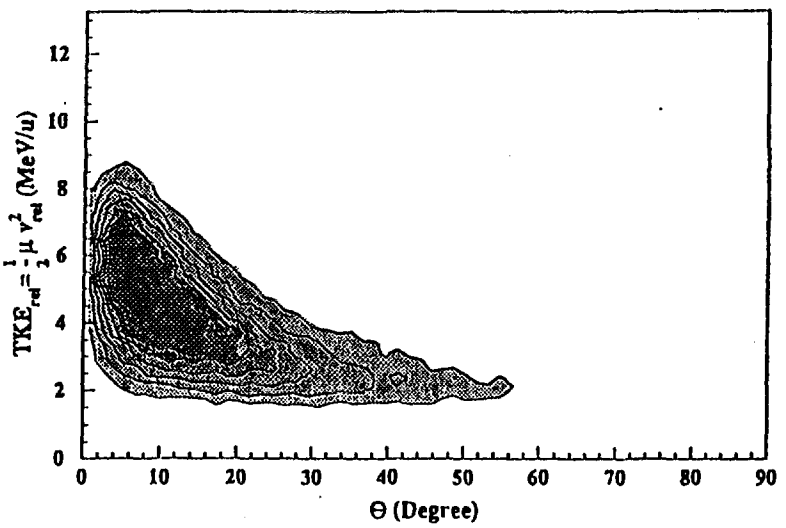

Figure 1

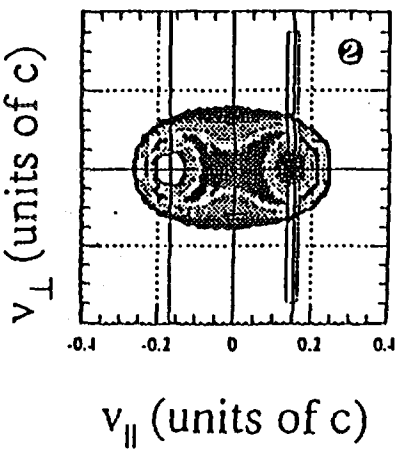

Figure 2

References

1) Metivier et al, Proceedings of the XXIIIrd Intern Winter Meeting on Nuclear Physics, Bormio, 1995

2) V. Métivier, Thesis, Caen 1995

3) Indra collaboration, Nouvelles du GANIL N° 56, 1995

4) J. Peter et al, Nucl. Phys. A593 (1995) 95

J.C. Steckmeyer et al, submitted to Phys. Rev. Lett.

Neck Formation and Decay in Pb + Au Collisions at 29 MeV/u

J.F. Lecolley[a], L. Stuttgé[b], M. Aboufirassi[a], B. Bilwes[b], R. Bougault[a], R. Brou[a], F. Cosmo[b], J. Colin[a], D. Durand[a], J. Galin[c], A. Genoux-Lubain[a], D. Guerreau[c], D. Horn[a-e], D. Jacquet[d], J.L. Laville[a], F. Lefebvres[a], C. Le Brun[a], O. Lopez[a], M. Louvel[a], M. Mahi[a], C. Meslin[a], M. Morjean[c], A. Péghaire[c], G. Rudolf[b], F. Scheibling[b], J.C. Steckmeyer[a], B. Tamain[a], S. Tomasevic[b].

a) Laboratoire de Physique Corpusculaire, ISMRa and Universite de Caen
b) Centre de Recherches Nucléaires, IN2P3-CNRS, Université Louis Pasteur
c) GANIL, IN2P3-CNRS-DSM-CEA
d) Institut de Physique Nucléaire
e) AECL Research, Chalk River Laboratories

Three fragment production has been studied in peripheral ^{208}Pb + ^{197}Au collisions at 29 MeV/u. The data suggests the formation and subsequent decay of necklike structures producing a small fragment emitted at mid-rapidity in between the two partners of a deep inelastic scattering. Data and trajectory calculations suggest also the existence of a competing process in which the neck is absorbed by one of the reactants, this latter decaying further by binary fission.

Peripheral reactions between heavy nuclei at moderate incident energies (less than 20 MeV/u) are dominated by deep inelastic scattering: a process in which a large amount of the kinetic energy is transformed into heat but in which the identity (mass and charge) of the two incoming partners remain approximately conserved. By contrast, nuclear collisions in the relativistic regime are known to be mostly governed by geometrical concepts. This leads to the formation of the so-called participant zone (also named "fireball") formed in the region corresponding to the geometrical overlap of the two nuclei. The situation is more complicated around and slighly above the Fermi energy: in the present work, we show the formation of necklike structures in peripheral collisions between two heavy nuclei.

We consider triple coincidences among fragments emitted in Pb+Au colllisions at 29 MeV/u studied with the Nautilus multi-detectors at the Ganil facility. We have been able to distinguish two classes of events: the first one (class I, left part of fig.1) in which a small fragment labelled 1 ($Z_1 < 20$) has been emitted and another class (class II, right part of the fig.) in which for most cases alll fragments have charge larger than 10. The three relative velocity distributions calculated bertween fragments taken two by two for events of class I are displayed in Fig. 1 up-

left. The distributions of the pairs (1, 2) and (1, 3) are both centered close to a value of 3.5 cm/ns. This value is in agreement with the Viola systematics and suggests a process schematically depicted in Fig 1-bottom-left. Two large fragments with masses close to those of the projectile and target move away after the collision with a large relative velocity leaving behind them a small fragment emitted at rest in the center-of-mass frame. Such a picture suggests the formation of a neck in between the two interacting nuclei and its subsequent decay due to Rayleigh instabilities: the neck is stretched and elongated as the two nuclei fly apart, then the density drops down and the ratio of the surface over the volume increases strongly leading to neck rupture.

Events of class II corresponds to 90 % of the 3-body events. For those events, a break-up of the pair (1, 2) is observed with a relative velocity peaked at 2.4 cm/ns. This is in agreement with the expectation value for the symmetric splitting of a nucleus with mass number around 200. Therefore, it can be concluded that these events result from a deep inelastic scattering followed by symmetric binary fission of one of the two partners as depicted in Fig. 1-bottom-right.

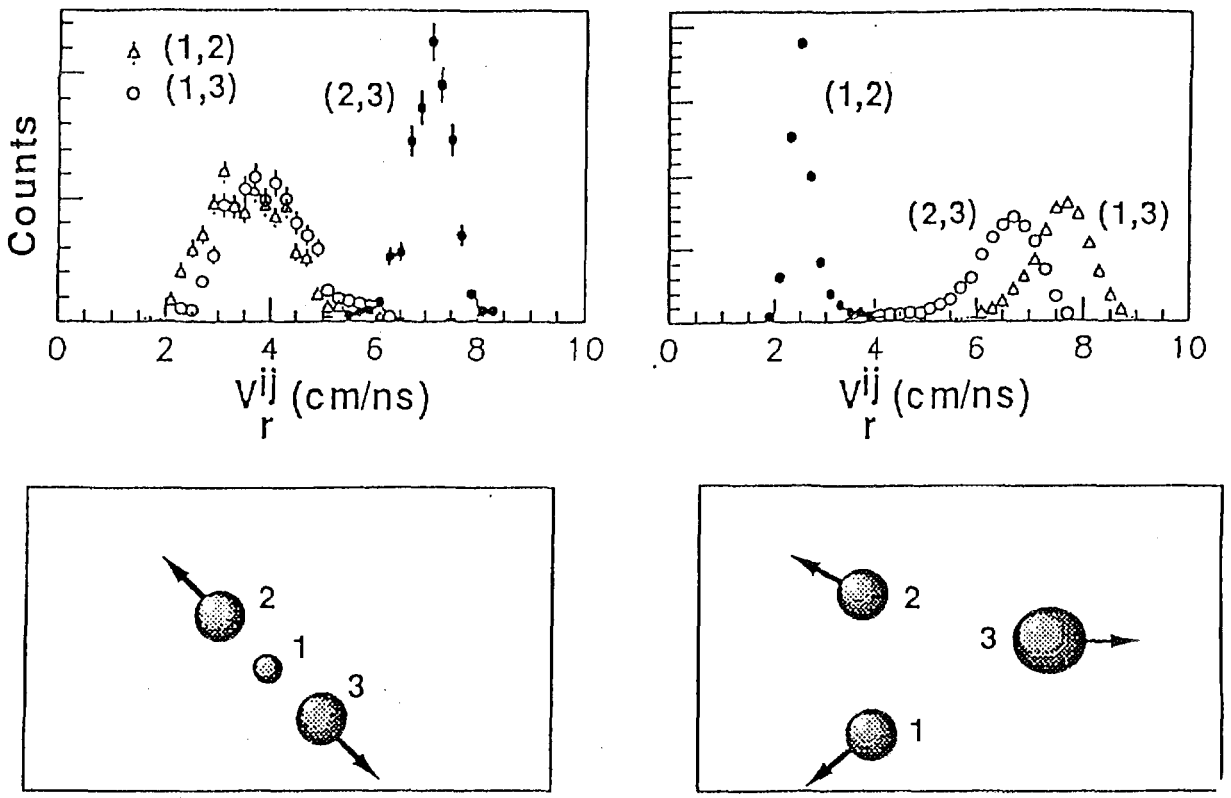

J. F. Lecolley et al Phys. Letters B354 (1995) 202

SURVEYING THE NUCLEAR CALORIC CURVE.

Ma Y.-G. , A. Siwek , J. Péter , D. Durand , F. Gulminelli , J.C. Steckmeyer , B. Tamain , E. Vient , G. Auger , Ch.O. Bacri , J. Benlliure , E. Bisquer , B. Borderie , R. Bougault , R. Brou , J.L. Charvet , A. Chbihi , J. Colin , D. Cussol , R. Dayras , E. De Filippo , A. Demeyer , D. Doré , P. Ecomard , P. Eudes , D. Gourio , D. Guinet , R. Laforest , P. Lautesse , J.L. Laville , L. Lebreton , J.F. Lecolley , A. Le Fèvre , T. Lefort , R. Legrain , O. Lopez, M. Louvel, J. Lukasik, N. Marie, V. Métivier, L. Nalpas, A. Ouatizerga, M. Parlog, E. Plagnol, A. Rahmani, T. Reposeur, M.F. Rivet, E. Rosato, F. Saint-Laurent, M. Squalli, L. Tassan-Got, C. Volant, J.P. Wieleczko

LPC Caen (IN2P3-CNRS/ISMRA et Université) - CEA DAPNIA-SPhN, CE Saclay - GANIL (DSM-CEA/IN2P3-CNRS) - IPN Orsay (IN2P3-CNRS) - IPN Lyon (IN2P3-CNRS/Université) - SUBATECH (IN2P3-CNRS/Université)

The dependence of nuclear temperature upon excitation energy has been experimentally studied, with increasing values of excitation energy over the years. The study of projectile "spectators" in reactions at several hundreds of MeV/u allowed to reach high excitation energies [1] . In this Aladin experiment, the temperature was obtained via double ratios of two isotope pairs [2] . The relation between this isotope temperature Tr^0 and E^*/A signaled a phase transition, with the nuclear gas regime dominating above $E^*/A = 10$ MeV.

We have undertaken a study of the relation between isotope temperatures and excitation energy up to 25 MeV per nucleon. The drawbacks relative to the Aladin experiment are a poorer separation between the sources of particles and a smaller mass of the decaying nucleus. The advantages are : i) this mass does not vary with excitation energy, ii) temperatures were obtained from several pairs of isotopes, and iii) kinetic temperatures were also obtained.

The system was $^{36}Ar + ^{58}Ni$ at 52,74 and 95 MeV/u. The kinetic energies of all charged products were measured with the 4π detector array INDRA. The selection of well characterized events, the impact parameter sorting, the reconstruction of the excited quasi-projectile, the determination of its charge and mass, and the determination of its excitation energy via calorimetry were made as in previous studies [3].

Determining a temperature value makes sense only if thermal equilibrium was attained in the source. Experimentally one can check that the angular distributions of various products are isotropic in the source frame. All QP products exhibit angular distributions in the QP frame which are nearly flat below 90°.

Temperatures were calculated for several pairs of isotopes differing by one neutron which have large values of the binding energy differences and no low energy levels. The relationship between the temperature and the yields Y of the isotopes was given in [2] :

$$Tr^0 = B/\ln(a.\frac{(Y_{light}/Y_{heavy})n)}{(Y_{light}/Y_{heavy})d)}) \quad (1)$$

where n (d) stands for the pair of isotopes with the smallest (largest) binding energy difference, and appears at the numerator (denominator) on the right side. B is the difference of binding energy differences. The greater the value of B, the better the accuracy of Tr, especially at high temperature.

In fig. 1 are shown the temperature values obtained at 95 MeV/u with various isotope pairs listed in the figure caption. The double ratio of isotones d^3He-$^6He^7Li$ was

also studied , but the very small number of ^{6}He did not allow to get significant results.

When B is not large ($\approx$ 5 MeV), i.e. p,d-^{6}Li,^{7}Li and ^{7}Li,^{8}Li-^{6}Li,^{7}Li, the curves increase very slowly with E^*/A and saturate at low Tr^0 values. Such ratios cannot be used. When the isotopes having the largest binding energy difference, $^3He - \alpha$, are involved (at the denominator) larger B values are obtained (13 to 18 MeV) and Tr^0 increase more with E^*/A. The curves obtained with isotopes $p - d$ and $d - t$ at the numerator , do not overreach $Tr^0 = 6$ MeV and do not show any increase of slope at high excitation energies. A different behavior is observed for the apparent temperature $T^0_{^6Li^7Li-^3He\alpha}$, which was the one used in the Aladin experiment[1] . It increases rapidly with E^*/A up to 3-4 MeV, then the slope becomes weaker, but no plateau is observed, at variance with Aladin . The T_r^0 values seem to be close to those shown in [1] , but in the present work the value of B is taken according to [2] whereas in Aladin it was increased by 20%. Thus our values are about 30% higher. Above E*/A=10 MeV, the temperature overcomes 6 MeV and the slope increases slightly, much less than in [1].

A difficult correction is to take into account the decay via particle emission of fragments emitted by the initial nucleus. This reduces the yields of the decaying fragments and increases the yields of daughter fragments : side-feeding. The large differences between the Tr^0 values obtained for the pairs Li-He, pd-He and dt-He are likely due to side feeding. Then the apparent temperatures in fig. 1a cannot be used directly. Initial temperatures must be obtained via calculations including the population of all excited states contributing to the reduction or the feeding of the isotopes of interest.

[1] J. Pochodzalla et al.,*Phys. Rev. Lett.*75 (1995) 1040.

[2] S. Albergo et al, *Nuovo Cimento* A89 (1985) 1.

[3] A. Kerambrun et al., Report LPC Caen 94-14 (1994), unpublished.
J.C. Steckmeyer et al. - V. Métivier et al., Proc. XXXIIIrd Int. Winter Meeting on Nuc. Phys., Bormio (Italy), January 1995, ed. by I. Iori.
J. Péter et al., *Nucl. Phys.* A593 (1995) 95.

Fig 1: Measured apparent temperatures versus excitation energy per nucleon.

a : Isotope temperatures. Solid symbols : average excitation energy obtained in bins of events sorted according to the violence of the collision. Open symbols : no such sorting, excitation energy obtained event by event.
Solid squares and open circles : isotope pairs ^{6}Li,^{7}Li - ^{3}He,α.
Light stars : d,t-^{3}He,α.
Solid triangles and open squares : p,d - ^{3}He,α.
Thick stars : ^{7}Li,^{8}Li - ^{6}Li,^{7}Li.
Solid and open triangles : p,d - ^{6}Li,^{7}Li.

b : Slope parameters from deuteron kinetic energy spectra at incident energies 52 (stars), 74 (crosses) and 95 MeV/u (circles).
For orientation, the Fermi gas correlation is shown with A/12 (thick line) and A/8 (dashed line) in a and with A/10 in b.
For clarity, error bars show statistical uncertainties only.

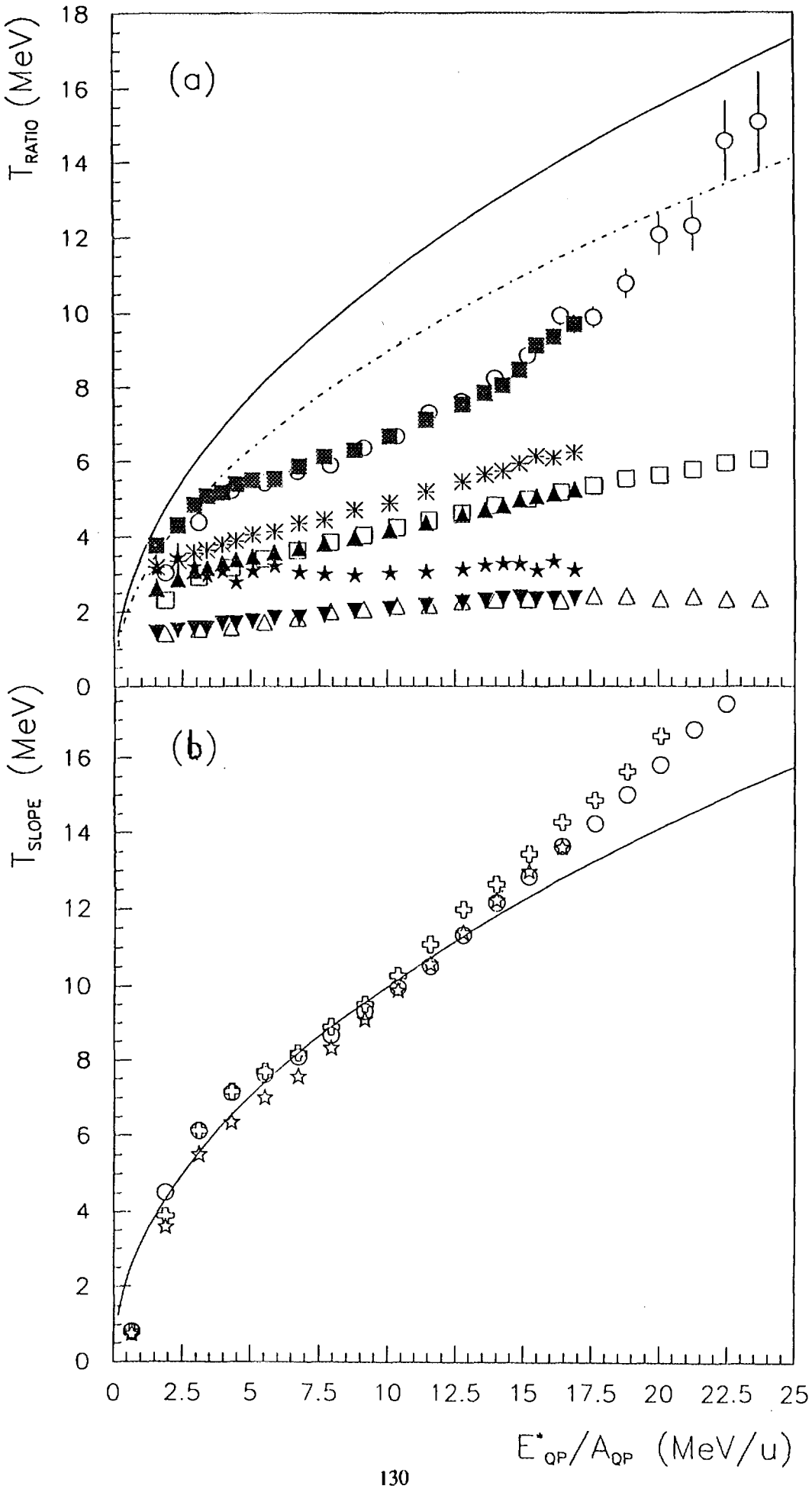
(a)
(b)
T_{RATIO} (MeV)
T_{SLOPE} (MeV)
E^*_{QP}/A_{QP} (MeV/u)
0
2
4
6
8
10
12
14
16
18
2.5
5
7.5
10
12.5
15
17.5
20
22.5
25

SEARCH FOR PHASE TRANSITION IN NUCLEAR MATTER FOR TEMPERATURES UP TO 7 MEV

M. Morjean[1], C. Lebrun[2], D. Ardouin[2], A. Chbihi[1], H. Dabrowski[2], B. Erazmus[2], P. Eudes[2], J. Galin[1], D. Guerreau[1], F. Guilbault[2], C. Ghisalberti[2], D. Jacquet[3], P. Lautridou[4], R. Lednicky[2], A. Péghaire[1], Y. Périer[1], J. Pluta[2], J. Quebert[4], A. Rahmani[2], T. Reposeur[2], L. Sezac[2], R.H. Siemssen[1,5]

1- GANIL, B.P. 5027, 14021 Caen Cedex, France
2- SUBATECH, 2 rue de la Houssinière, 44072 Nantes Cedex 03, France
3- IPN, B.P. 1, 91406 Orsay Cedex, France
4- CENBG, le Haut Vigneau, 33170 Gradignan, France
5- KVI, Zernikelaan 25, 9747 AA Groningen, The Netherlands

The $^{208}Pb + ^{197}Au$ system is investigated in order to search for phase transformation in the nuclear matter. + p.133

An experimental evidence for a phase transition in nuclear matter at high excitation energy can be the pattern of the correlation between the temperature and the thermal excitation energy of a nucleus. In a recent paper [1], such a caloric curve was built from a compilation of various experimental data, exhibiting a plateau at a constant temperature T=5 MeV for energies between 2.5 and 10 MeV per nucleon. This plateau was considered in this paper as a signature of a transition from a liquid phase towards a gaseous phase.

At the same time, the temperature range in which such a transition is evidenced in [1] was investigated in an experiment performed at GANIL on the very heavy and almost symmetric system $^{208}Pb + ^{197}Au$ at 29 A.MeV [2] and the data of this experiment lead to a different conclusion: there is no evidence for a phase transition in nuclear matter for temperatures up to 7 MeV.

The $^{208}Pb + ^{197}Au$ system at 29 A.MeV has been extensively studied at Ganil and the underlying reaction mechanisms well understood [3,4,5,6,7]. In the present experiment, a very sensitive selection on the violence of the collision was achieved by means of the energy deposited in the 4π neutron detector ORION operated as a calorimeter. The temperature of the projectile-like nuclei was determined from the slope of the alpha-particle energy spectra in an angular range dominated, for alpha-particle emission, by a pure evaporation process. For very heavy nuclei such as the primary projectile-like fragments formed in these collisions, collective effects such as rotation or expansion cannot modify in a significant way the slope of the spectra. The

temperature was deduced from four independent moving source fits at four different detection angles between 5.5° and 20°, leading to four values in agreement with each other within ± 0.5 MeV. This very good consistency confirms that mainly evaporated alpha-particles were selected in this angular domain, as also suggested by the pattern of the two-dimensional invariant scatter plots. For the most violent collisions selected in ref [2], the apparent temperature reaches 6.9 MeV. Despite the fact that this temperature is much higher than the limit given in ref [1] for the pure vapor phase of the nuclei (5 MeV), the hot nuclei do not end up as nucleons or light clusters, but they give rise to either many intermediate mass fragments with $Z > 6$ [3], or binary fission fragments, or even heavy evaporation residues [4].

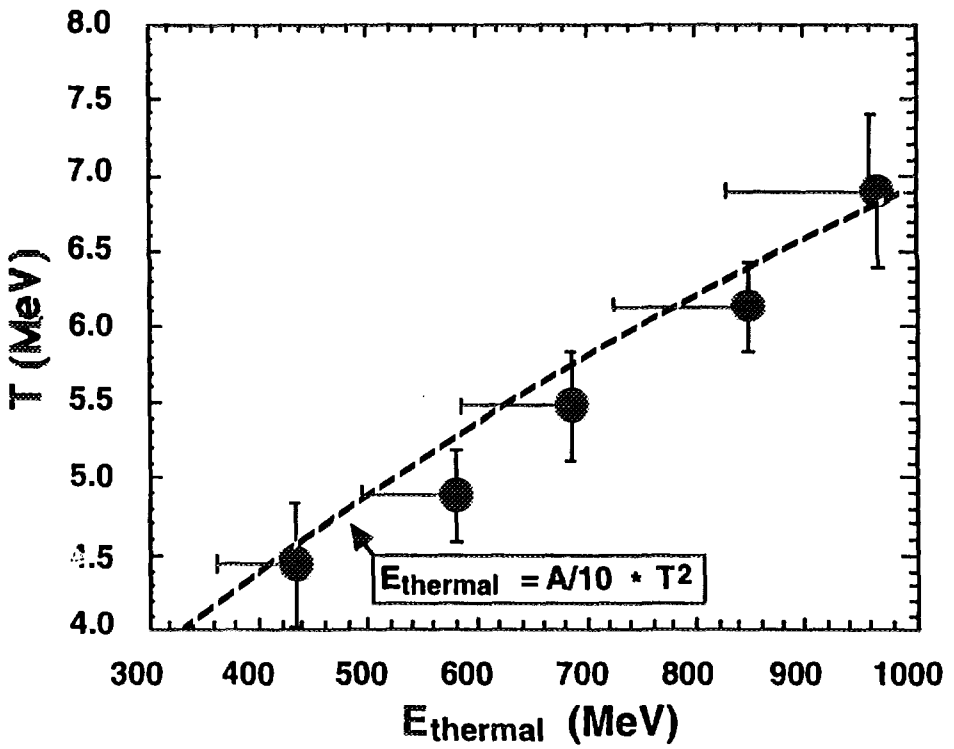

Fig.1: Correlation between thermal excitation energy and temperature

The amounts of energy dissipated during the reactions have been inferred from an energy balance assuming, as shown in ref [5], binary kinematics. The excitation energy of the projectile-like fragment was then deduced, taking advantage of the almost symmetric system considered that do not allow, on the average, a mass transfer between the reaction partners. The correlation between the excitation energy and the apparent temperature is shown in Fig. 1. An estimation of the errors on the excitation energies due to preequilibrium emissions has been performed from the data of [6] and [7]. The experimental correlation is in very good agreement with the solid curve showing the

prediction of the Fermi gas model with a level density parameter a =A/10. Applying corrections deduced from a classical evaporation code to infer from the apparent temperatures the initial temperatures leads to level density parameters depending on the temperature, as expected and in rather good agreement with the prediction of Shlomo and Natowitz [8].

In summary, no evidence can be found in our data for a phase transition in nuclear matter for temperatures up to 7 MeV. A possible explanation for the different behaviour of the caloric curve of ref [1] could be found in the way the temperature has been extracted, considering the yields of different He and Li isotopes.

References:

[1] J. Pochodzalla et al., Phys. Rev. Lett. 75 (1995) 1040
[2] M. Morjean et al., Nucl. Phys. A591 (1995) 371
[3] E. Piasecki et al., Phys. Rev. Lett. 66 (1991) 671
[4] R. Bougault et al., Nucl. Phys. A587 (1995) 499
[5] J.F. Lecolley et al., Phys. Lett. B325 (1994) 317
[6] B.M. Quednau et al., Phys. Lett. B309 (1993) 10
[7] S. Bresson, Thèse université de Caen, 1993
[8] S. Schlomo and J.B. Natowitz, Phys. Rev. C44 (1991) 2878

Light-particle correlations in $^{129}Xe + ^{48}Ti$ at 45 MeV/u

D. Nouais[a], L. Martin[a], B. Erazmus[a], J. Pluta[a], D. Ardouin[a], P. Eudes[a], F. Guilbault[a], P. Lautridou[a], C. Lebrun[a], R. Ledniczky[a*], A. Rahmani[a], T. Reposeur[a], D. Roy[a], L. Sezac[a], M. Lewitowicz[b], W. Mittig[b], P. Roussel-Chomaz[b], N. Carjan[c], P. Aguer[d], W. Burzynski[e], W. Peryt[e], H. Dabrowski[f], P. Stefanski[f]

[a] *Laboratoire SUBATECH, Université de Nantes / Ecole des Mines de Nantes / IN$_2$P$_3$/CNRS, 4 rue A. Kastler, 44070 Nantes Cedex 03, France*

[b] *Laboratoire GANIL, BP 5027, 14021 Caen Cedex, France*

[c] *Centre d'Etudes Nucléaires de Bordeaux-Gradignan, 33175 Gradignan Cedex, France*

[d] *Centre de Spectroscopie Nucléaire et de Spectroscopie de Masse, 91405 Orsay, France*

[e] *Warsaw University of Technology, ul. Koszykowa 75, 00-662 Warsaw, Poland*

[f] *Institute of Nuclear Physics, Kraków, Poland*

I. INTRODUCTION

(2) Numerous experiments as been performed in order to extract space-time characteristics of emitting sources produced in heavy ion collisions, using the intensity interferometry technique. The quantum statistics effects and the final state (Coulomb and nuclear) interactions between particles induce correlations as strong as their relative distance is small. The correlation function in relative momentum q (momentum of one particle in the rest frame of the pair), defined as the ratio of measured distribution of correlated pairs over an uncorrelated background constructed by mixing particles from different events, is a suitable quantity to reveal such correlations and thus to extract the size and the lifetime of a source. However, due to experimental limitations, the correlation function presents usually a threshold in relative momentum (5-10 MeV/c) whereas theoretical models predict a strong sensitivity below 10 MeV/c. In particular, in the case of large difference of emission time between two particles, correlations are restricted to the low relative momentum region. An original experiment has been performed at GANIL, using the (1) SPEG spectrometer, in order to measure precisely pairs of protons at very small relative momentum.

(4) The experiment and the results are described.

II. EXPERIMENTAL DETAILS

The SPEG spectrometer is not an apparatus dedicated to this kind of experiment, so its detection setup has been adapted to be able to measure light charged particles in coïncidence.

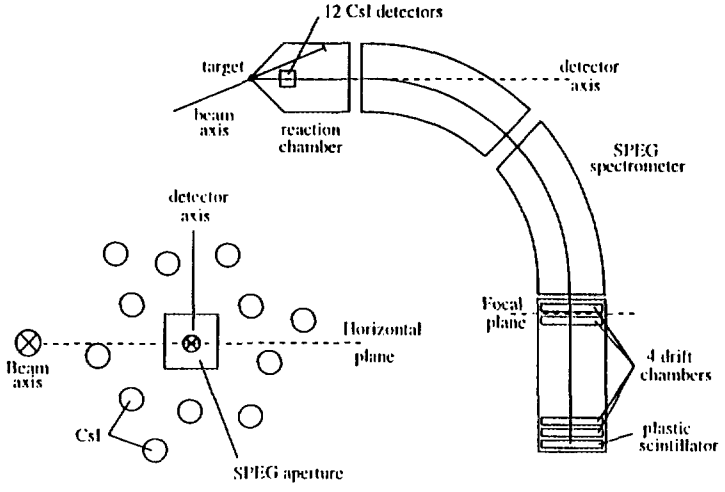

FIG. 1. Experimental setup

*Permanent address: Institute of Physics, Na Slovance 2, 18040 Prague 8, Czech Republic

(3) The reaction $^{129}Xe + ^{48}Ti$ has been investigated.

It was composed of 4 drift chambers to reconstruct the trajectory of two particles, in association with a plastic scintillator for their identification. Due to the small angular aperture and acceptance in momentum of the SPEG, the range covered extended from 1 to 10 MeV/c in relative momentum. Moreover, this system has been optimized for proton detection, and did not measure with the same efficiency heavier particles and especially unlike particle pairs. Thus, to complete the measurement, a set of 12 CsI(Tl) scintillators was installed in the reaction chamber, surrounding the SPEG aperture (fig 1). This setup has been placed at an average angle of 25 degrees with respect to the beam axis to measure backward emission from a projectile-like nucleus, produced in the reverse kinematic reaction $^{129}Xe + ^{48}Ti$ at 45 MeV/nucleon.

III. RESULTS

The analysis of the data measured in the SPEG spectrometer is described in details in reference [1]. The experimental two-proton correlation function constructed for the first time at very small relative momentum is presented in the figure 2. It can be fairly well reproduced using the new quantum approach describing particle correlations [2,4], which takes into account the quantum statistics effects and the final state interactions between particles as well as the emitter Coulomb field influence. The full three-body theoretical calculations, corrected for the experimental acceptance and resolution, predict a very large lifetime of the source (1500 fm/c).

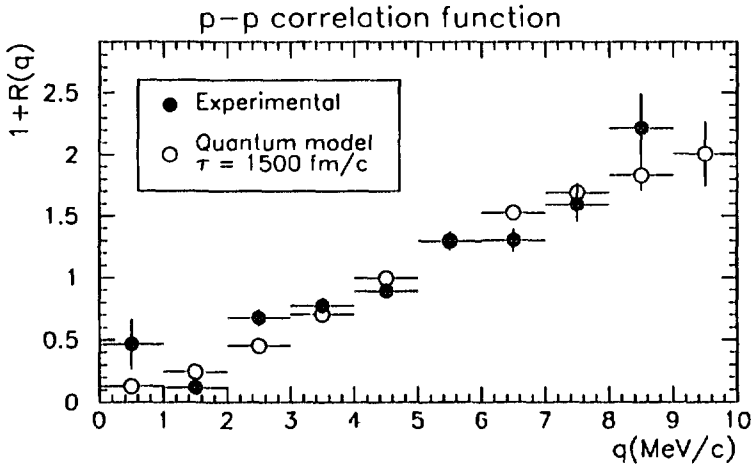

FIG. 2. Experimental two-proton correlation function measured in SPEG compared to the prediction of the three-body quantum model for a source lifetime $\tau = 1500 fm/c$

Moreover, we have estimated a velocity of the source equal to 90% of the beam velocity by selecting pairs on the relative orientation between their total velocity and their relative momentum [5].

Single spectra measured in the CsI detectors confirm the prediction of an emitting source with a mean velocity of 90% of the beam velocity and a temperature of 4 MeV. From the data measured in the detectors, we have constructed the correlation function of all possible two-particle systems involving p, d, t and α particles. Some of them are represented in figure 3.

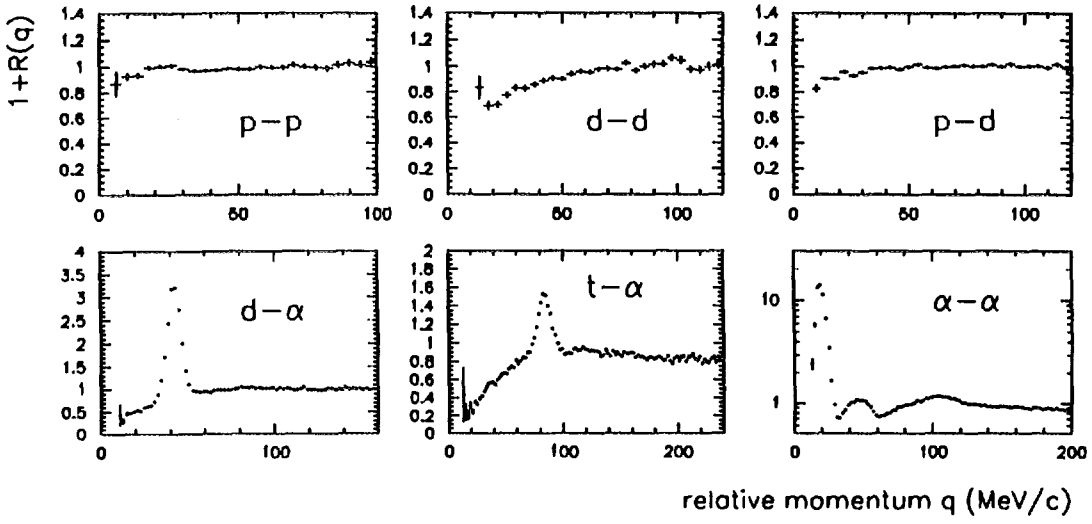

FIG. 3. Some experimental correlation functions constructed with data from the CsI detectors

Mean difference in emission times $\tau_{pp} = 400 fm/c$, $\tau_{dd} = 400 fm/c$ and $\tau_{pd} = 800 fm/c$ between respectively two protons, two deuterons and proton-deuteron has been estimated by comparing the experimental correlation functions for these pairs to the predictions of the quantum model. In the case of identical particles and exponential decay law, this mean interval is equal to the lifetime of the source for this particle.

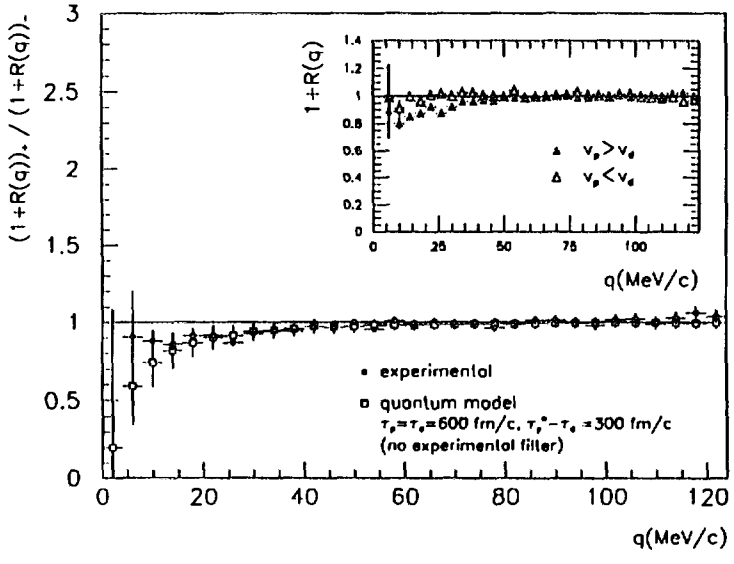

FIG. 4. Comparison of experimental and theoretical ratios of p-d correlation functions $(1 + R(q))_+$ and $(1 + R(q))_-$

One can observe that the value of τ_{pd} seams to be not compatible with the lifetimes for protons τ_{pp} and deuterons τ_{dd}. This leads to assume that a delay exists between the time distribution of protons and deuterons. It has been demonstrated in the reference [3,4] that it is possible to analyze the sequence of emission for unlike particles. The sensitivity of the correlation function to the order of emission is reflected on the relative orientation between their total velocity $\vec{v}$ and their relative momentum $\vec{q}$. Thus, we have constructed the two correlation functions $(1 + R(q))_+$ and $(1 + R(q))_-$ by selecting pairs according to the sign of the scalar product $\vec{q}.\vec{v}$. The result is presented in figure 4. The fact that the correlation function $(1 + R(q))_+$ presents a stronger anti-correlation than $(1 + R(q))_-$ is an indication that the deuterons are emitted, in average, earlier than protons.

A theoretical calculation performed with the quantum model with the same source lifetimes for protons and deuterons $\tau_p = \tau_d = 600 fm/c$, and a shift of the origin of the distribution of protons equal to $\delta t_0 = 300 fm/c$, is superimposed to the experimental data. Thee experimental ratio of the two correlation functions is quite well reproduced, (the difference at small relative momentum is due to the fact that the acceptance and resolution of the detectors have not been applied to the theoretical calculation). This estimation demonstrates that a quantitative analysis of the evolution in time of the source can be performed.

IV. CONCLUSION

In the very small relative momenta region, the correlation function is strongly sensitive to the long range Coulomb interaction, even for emitting source characterized by a very long lifetime.

The two-proton correlation function has been constructed for the first time in the range of very small relative momentum from the data measured in an original experiment. A very long lifetime has been extracted for the source produced in the reaction $^{129}Xe + ^{48}Ti$ at 45 MeV/u. Indeed, the quite flat p-p correlation function measured in CsI detectors, which exhibits a threshold of 5 MeV/c in relative momentum, does not constrained sufficiently the theoretical model to estimate accurately the value of τ.

Moreover, we have investigated a new possibility to analyze the emission sequence of particles of different types, which reveals that deuterons are emitted earlier than protons in average. This conclusion is consistent with the one obtained in an other experiment [6]. The coalescence scenario i.e. the deuteron production in the final state interactions between proton and neutron can qualitatively explain this observation. To quantitatively go beyond this result, and in particular to understand the mechanism of deuteron formation, it would be necessary to measure protons, neutrons and deuterons in the same experiment [7].

Usually, one uses a simple static description of the source of particles. However, the correlation function is very sensitive to the shape of the emitting source and to the correlations between the space-time coordinates of the emission points and the momenta of particles. A study is currently underway in collaboration with J. Aichelin and collaborators, to extract the latter information from the microscopic transport code QMD. Through this analysis, we aim to acquire more precise informations about the dynamic evolution of the source.

---

[1] L. Martin, Thèse de Doctorat, Université de Nantes (1993)

[2] R. Lednicky *et al*, Rapport interne SUBATECH 94-19
submitted to Nucl. Phys. A

[3] R. Lednicky *et al*, Phys. Lett. B373 (1996) 30

[4] D. Nouais *et al*, This compilation

[5] L. Martin *et al*, Nucl. Phys. A583 (1995) 407

[6] C. Ghisalberti, Thèse de Doctorat, Université de Nantes (1994)
C. Ghisalberti *et al*, Proc. of thee XXXI International Winter Meeting on Nuclear Physics, Bormio, Italy (1993) 293

[7] J.Pluta *et al* "Nuclear interferometry for two-neutrons systems"
Letter of Intent to the Committee of Experiments at GANIL

Formation and decay of Hot Nuclei in 2 GeV proton- and ^{3}He-induced reactions on Ag, Au, Bi and U targets*

X.Ledoux[a], H.G.Bohlen[b], J.Cugnon[c], H.Fuchs[b], J.Galin[a], B.Gatty[d], B.Gebauer[b], D.Guerreau[a], D.Hilscher[b], D.Jacquet[d], U.Jahnke[b], M.Josset[a], X.Ledoux[a], S.Leray[e], B.Lott[a], M.Morjean[a], A.Péghaire[a], L.Pienkowski[e], G.Röschert[b], H.Rossner[b], R.H.Siemssen[a,f], C.Stéphan[d]

[a] IN2P3-CNRS and DSM-CEA GANIL, BP 5027 14021 Caen Cedex
[b] Hahn Meitner Institut, Glienicker Str. 100 14109 Berlin
[c] University of Liège B-400 Sart-Tilman Liège 1
[d] IPN Orsay BP 1 91406 Orsay Cedex
[e] IN2P3-CNRS and DSM-CEA SATURNE, Saclay 91191 Gif/Yvette Cedex
[f] Permanent address: KVI, Zernikelaan 25, 9747 AA Groningen

The aim and context of this experiment

Using heavy projectiles of intermediate energies (several tens of MeV/A) and, more recently, of high energies (several hundreds of MeV/A) is generally considered as the most efficient approach for heating up nuclei. However this procedure suffers a number of drawbacks. First, the interacting nuclei get also collective excitation (compressional, rotational and deformation energies). The coupling of all these degrees of freedom makes the study of the heat effect *alone* extremely difficult. In some cases it can even be completely masked by the collective excitations. Second, it takes a rather long time (more than 100 fm/c) for the nuclei to achieve thermal equilibrium in a nucleus-nucleus collision and this time makes an intrinsic limitation to the study of fully thermalized nuclei of high T. Third, from an experimental view point, one has to consider simultaneously two initially heated nuclei (the projetile- and target-like nuclei) and in most of the cases a hot neck region. This multi-source characterization is one of the major difficulties encountered in most of the studies.

The mentioned difficulties can be overcome by using light particles as projectiles. It was one of the aims of the present experiment to investigate the amount of thermal energy that such particles are able to deposit into a target nucleus, the second aim being a detailed study of the decay properties of the thus heated nuclei. Are they explainable considering current models? Is there any need to invoke new phenomena (for instance multifragmentation) which are not observed at modest excitation energies?

The experimental set-up

The large efficiency, 4 m^3 scintillator detector ORION, was utilized in order to measure on an event-by-event basis the number of emitted neutrons which is closely related to the dissipated energy[1]. Two other types of particles were simultaneously detected: light charged particles and intermediate mass fragments by a set of ten Si telescopes located from 15 up to 150 degrees. Finally for the U target, fission was measured using two PPAC detectors mounted vis-à-vis and parallel to the beam direction. The experiment was run at the national facility SATURNE with proton beams at 475 MeV and 2 GeV and ^{3}He at 2 GeV.

Excitation energy distributions

The first question which was answered in this experiment was the extent of thermal energies reached in such collisions. This was achieved through the measurement of the neutron multiplicity distributions as shown in Fig.1. Their interpretation was done using a two-step model: an Intra Nuclear Cascade[2], followed by an evaporation process[3]. The neutron data are satisfactorily reproduced thus allowing to carry out the distribution of thermal energy at the end of the INC process. It could be shown (Fig.2) in the case of the Au target, that thermal equilibrium was achieved after 30 fm/c and that at

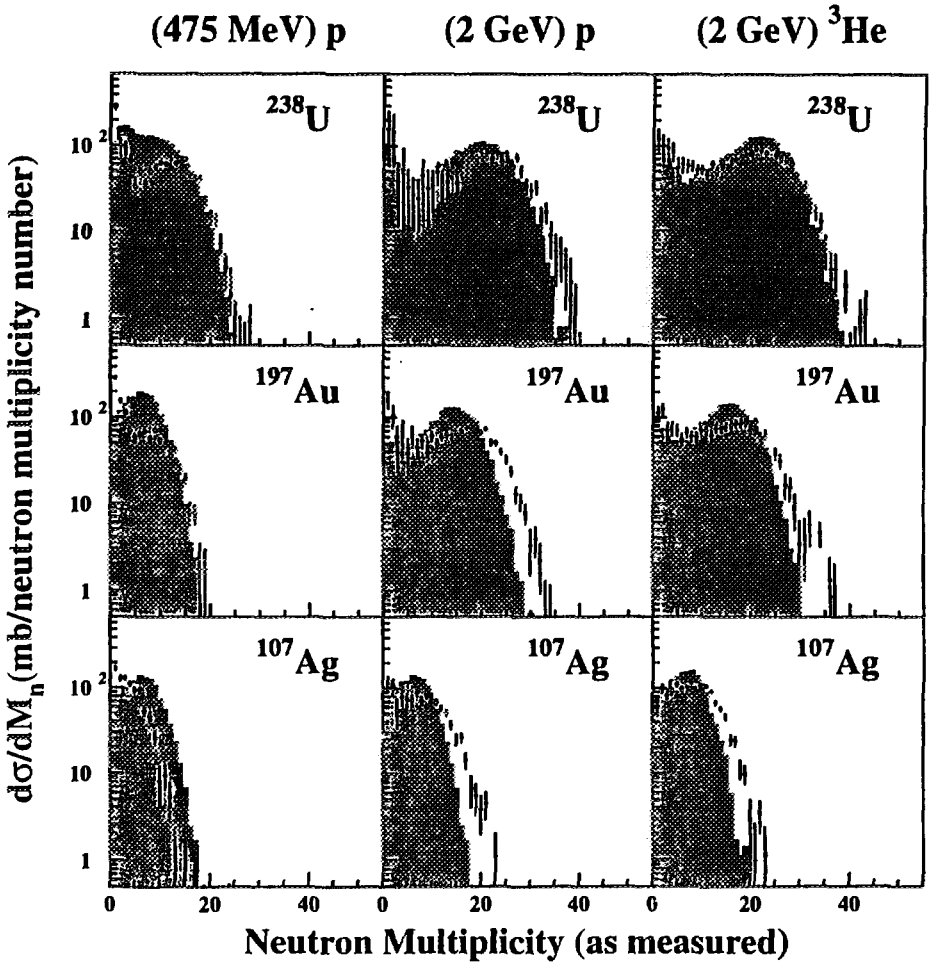

Fig.1 Neutron multiplicty distributions and comparison with a two-step model (shaded area). For details see text

least 10% of the events correspond to energy depositions larger than 500 MeV (i.e. T>5 MeV, using a level density parameter a=A/10). Such energies may appear quite modest to heavy-ion practitioners. However and in contrast with many quoted excitation energies, there is in the present approach no ambiguity on the complete thermal character of these energies. In the present case, no collective expansion can contribute to the estimated energies. The multiplicities of evaporated-like charged particles, measured backwards, are quite consistent with the neutron data, giving strong support to the deduced energies.

How does a heavy nucleus raised at more than T=5 MeV decay?

The decay channel referred to as "statistical multifragmentation" has been predicted to show up for nuclei raised at temperatures larger than 5 MeV. Even if the present experimental set-up for intermediate mass fragment (IMF) detection does not cover 4π, and thus does not permit a detailed study of possible multifragmentation, it allows to infer average multiplicities of evaporated-like IMF as a function of neutron multiplicity, i.e. thermal energy. The average measured values are essentially compatible with what is predicted by a conventional step-by-step evaporation code like GEMINI. Moreover no sudden increase of the IMF multiplicity is observed as a function of neutron multiplicity in the experimental data at variance with what is predicted by statistical multifragmentation models. When counting the IMF one should be cautious not to take into account those detected at high energy and essentially at forward angles which are of pre-equilibrium origin and which have thus nothing to do with a statistical process whatever it could be, sequential or simultaneous.

The binary fission channel for a target like U is prominent at moderate excitation energies and then falls off steadily with increasing excitation energies (even if it always

Heating nuclei with energetic antiprotons

F. Goldenbaum[1], W. Bohne[1], J. Eades[2], T.v. Egidy[3], P. Figuera[1], H. Fuchs[1], J. Galin[4], Yc. S. Golubeva[5], K. Gulda[6], M. Hassinof[7], D. Hilscher[1], A.S. Iljinov[5], U. Jahnke[1], J. Jastrzebski[6], M. Krause[3], W. Kurcewicz[6], X. Ledoux[4], B. Lott[4], M. Manrique de Lara[3], M. Morjean[4], G. Pausch[8] A. Péghaire[4], L. Pienkowski[1,6], D. Polster[1], S. Proschitzki[9], B.M. Quednau[4], H. Rossner[1], S. Schmid[3], W. Schmid[3], W. Schott[3], W.U. Schröder[10], J. Tõke[10], P. Ziem[1]

[1] *HMI Berlin, Germany*
2 CERN, Switzerland
3 TU-München, Germany
4 GANIL, France
5 INR Moscow, Russia
6 University of Warsaw, Poland
7 University of British Columbia, Canada
8 FZ-Rossendorf, Germany
9 IPN Orsay, France
10 University of Rochester, USA

Introduction

Heating up a nucleus by means of an antiproton annihilating on its surface offers [1,2] in principle several advantages over heavy-ion collisions. The pions produced in the annihilation (about 6 at $\sqrt{s}$= 2.5 GeV) propagates the released energy within the nuclear medium on a very-short time scale, in a soft, radiation-like fashion, allowing thermalization to be achieved very rapidly while both the mass loss due to preequilibrium emission and the excitation of collective degrees of freedom remain moderate. These considerations motivated a series of experiments at the Low-Energy Antiproton Ring (LEAR) at CERN where beams of 200 MeV/c, 1.2 GeV/c and 2 GeV/c antiprotons were employed. The most important issues addressed in these experiments were the assessment of the heat energy deposited into the host nucleus and the amount of mass and energy losses suffered during the thermalization stage. The former issue was investigated by measuring the multiplicities of evaporated neutrons and light charged fragments while the latter was tackled by means of inclusive $d^2\sigma/dEd\Omega$ distributions measured for various particles.

Experimental method

In the earlier run, the incoming antiprotons were tagged thanks to a scintillator system located 16 m upstream from the reaction chamber and focused onto ^{nat}Cu, ^{165}Ho, ^{197}Au and ^{238}U targets with thicknesses of 1-2 mg/cm^2. The experimental setup comprised mainly two 4π devices devoted to detecting neutrons, charged particles and fragments. The Berlin Neutron Ball (BNB) with a volume of 1.5 m^3

present at the highest energies). This decrease is qualitatively understandable since the more energy deposited, the larger the number of ejected particles in the first step of the reaction is, leading to lighter and thus less fissionable nuclei. However fission still represents about half of the decay mode at the highest registered energies. We are led to conclude that, since binary fission cannot account for the whole cross section at high temperatures and multifragmentation is negligible, the missing events must be found as

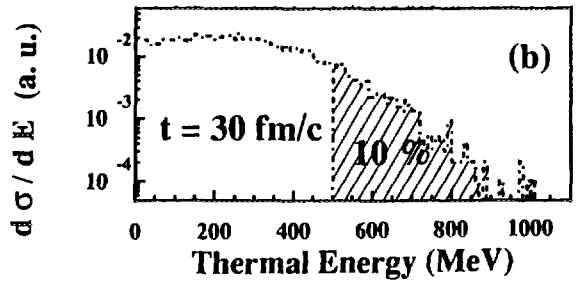

Fig.2 Thermal energy distributions as deduced from the comparison between experimental data and model calculations.

evaporation residues. This should be confirmed in further experiments performing on-line gamma-ray spectroscopy (the only way to identify the residual nuclei close to rest and thus stopped within the target) in conjonction with 4π neutron measurements.

The fate of nuclei submitted to proton bombardment is of current interest when considering high intensity spallation sources of neutrons[4].

Summary

A great deal has been learnt from the present experiments on the energy deposition when using GeV beams of light particles on heavy target nuclei. Large amounts of thermal energy (>500 MeV on a Au target) can be reached with a sizeable probability and the neutron multiplicity has been found as a good observable to study the events as a function of excitation energy. Evaporated light charge particles show average multiplicities which are compatible with the neutron ones when considering an evaporation process. IMF emission is weak and remains compatible with a step-by-step evaporation process. From the average IMF multiplicity there is no indication of a statistical multifragmentation process. The binary fission probability tends to diminish at the highest excitation energies and we are led to conclude that evaporation residues must then be more and more abundantly produced.

More exclusive data are needed to fully understand all aspects of the p-nucleus interaction and further experiments are planed on COSY (Jülich). On the theoretical side, some deficiencies of the current INC+evaporation approach have been identified (lack of production of complex particles and IMF of non-evaporative origin). In this respect the QMD or VUU approaches appear to be promising.

References

1) L.Pienkowski et al., Phys. Lett.B336 (1994) 147; an extended papr is being submitted for publication in Nucl. Phys.
2) J.Cugnon, Nucl. Phys. 462 (1987) 751
3) R.J.Charity et al.,Nucl. Phys. A483 (1988) 391)
4) D.Hilscher et al., contribution to this volume

housed the Berlin Silicon Ball (BSiB), consisting of 157 500μm-thick Si-detectors. The BNB measured the neutron multiplicity on an event-by-event basis while the BSiB provided energy and identification for stopped particles with Z< 2 as well as a rough identification for heavier fragments.

The second experiment made use of a TOF spectrometer consisting of 8 NE213 scintillation counters associated with 3 mm thick plastic scintillators allowing one to discriminate between neutral and charged particles. Spectra for neutrons and high-energy protons, α-particles, pions and kaons were obtained.

Experimental results

A partial account of the results has been given in ref. [3]. Fig. 1 top displays joint multiplicity distributions measured at 1.2 GeV for a variety of targets. The measured multiplicities increase with the target mass because of the larger number of nucleons the pions can interact with, giving rise to a larger excitation energy in the nucleus.

Another interesting finding concerns the light charged particle multiplicities observed for the Copper target, which reach values up to 14, which means that the system basically vaporizes into light fragments for some part of the events. Further analysis is underway to explore whether or not these events exhibit a critical behavior.

The patterns of the distributions of Fig. 1 top point to evaporation as the dominant emission process, since for heavy targets, light charged particle emission sets in only for events associated with a large number of neutrons. The Galilei-invariant velocity distributions (Fig. 1 bottom) of the detected light charged particles are found virtually isotropic in the laboratory frame, and therefore fortify the above conclusion that most detected particles are evaporated. This observation enables one to assess the excitation energy from the measured *total* light particle multiplicity on an event-by-event basis, the connexion between the two parameters being established by means of the statistical model. It is worth mentioning that for a given so-obtained excitation energy, the partial multiplicities for the different light particle species are found in good agreement with those predicted by the statistical model. Such a procedure yields [3] the excitation energy distributions displayed in Fig. 2, which are well reproduced by predictions of the Intra-Nuclear Cascade model (histograms). The distributions extend to energies as large as 3-4 MeV/nucleon with a sizeable cross-section, confirming the relevance of this approach to investigations devoted to hot nuclei.

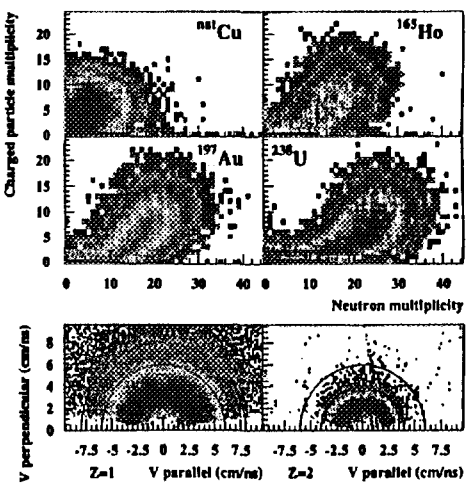

Figure 1.

The intermediate-mass fragments (IMF) observed in this experiment were found

to exhibit Poisson-like multiplicity distributions with mean values compatible with those predicted by the statistical model for a given excitation energy, at variance with what is observed in intermediate-energy heavy-ion collisions. This finding suggests that the IMF excess found in the latter collisions are mostly of dynamical origin and do not manifest the failure of the conventional statistical model at high excitation energy.

Fig. 3 displays a neutron double-differential cross section $d^2\sigma/dEd\Omega$ measured at forward angles in the interaction of a 2 GeV/c antiproton with a Uranium target. In this spectrum, two components corresponding to the evaporated neutrons and preequilibrium ones are readily distinguishable as a low-energy peak and a high-energy tail respectively.

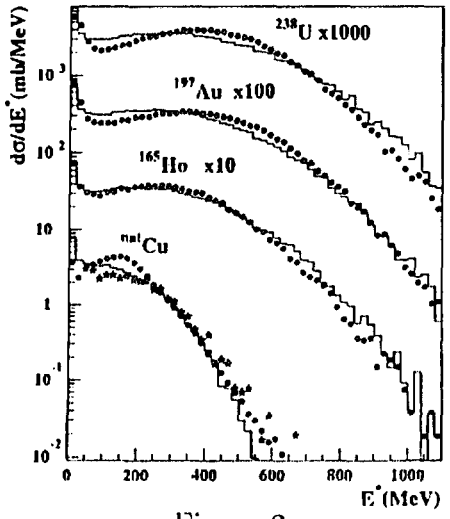

Figure 2

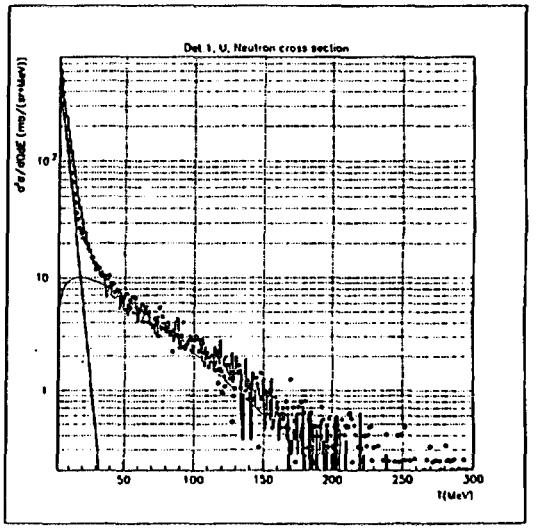

Figure 3

The curves in Fig. 3 depict maxwellian fits for the two components, with slope parameters T_1=3.4 MeV and T_2=34.0 MeV. Also included in Figure 2 are predictions [4] (histogram) of an INC model combined with a statistical model, which reproduce the data quite well.

Conclusion

The recent results obtained in the LEAR runs seem to confirm the interesting prospects put forward by earlier theoretical works. Although the total available energy in the system is tangibly lower than that involved in heavy ions collisions, this drawback is largely offset by cleaner experimental conditions making the conclusions regarding the decay of hot nuclei less ambiguous.

References

1. J. Cugnon et al., Nucl. Phys. A**484** (1988) 542.
2. Ye.S. Golubeva et al., Nucl. Phys. A**483** (1988) 539.
3. F. Goldenbaum et al., submitted for publication in Phys. Rev. Lett..
4. Ye.S. Golubeva et al., Phys. of Atom. Nucl. **57** (1994) 2007.

B3 - FLOW AND RELATED PHENOMENA

FR9700894

A NEW METHOD TO DETERMINE THE ENERGY OF VANISHING FLOW, USING PARTICLE-PARTICLE AZIMUTHAL CORRELATIONS

A. Buta[1-a)], J.C. Angélique[1)], G. Auger[2)],, G. Bizard[1)], R. Brou[1)], C. Cabot[2)], Y Cassagnou[3)], E. Crema[1-b)], D. Cussol[1)], Y. El Masri[4)], Ph. Eudes[5)], M. Gonin[6)], K. Hagel[6)], Z.Y. He[8)], A. Kerambrun[1)], C. Lebrun[5)], R. Legrain[3)], J.P. Patry[1)], A. Péghaire[2)], J. Péter[1)], R. Popescu[1-a)], R. Regimbart[1)], E. Rosato[7)], F. Saint Laurent[2)], J.C. Steckmeyer[1)], B. Tamain[1)], E. Vient[1)], R. Wada[6)]

1) LPC Caen, FRANCE, 2) GANIL, 3) DAPNIA, CEN Saclay, 4) Institut de Physique Nucléaire, LOUVAIN LA NEUVE, BELGIUM, 5) Laboratoire de Physique Nucléaire, NANTES, 6) Cyclotron Institute, Texas A&M University, USA, 7) Dipartimento di Scienze Fisiche, NAPOLI, ITALY, 8) Institute of Modern Physics, LANZHOU, CHINA, a) I.F.A., BUCHAREST, ROMANIA, b) Inst. di Fisica, Univ. de SAO PAULO, BRAZIL

Measuring the in-plane flow parameter appears to be a promising method to gain information on the equation of state of nuclear matter. The energy domain of the GANIL facility (up to 95 MeV/nucleon) is of special interest because it is in (or near) this energy range that the transition from positive to negative flow (or from attractive to repulsive interaction) is expected. This energy of vanishing flow (EVF) can be determined by well-known methods, using the reaction plane determination. However, this reaction plane determination suffers from quite large uncertainties inducing on the flow parameter large errors which are difficult to estimate and to correct. A new method, based on particle-particle azimuthal correlations is proposed. This method does not require the knowledge of the reaction plane.

Experimentally, for a given interval of rapidity, the azimuthal correlation function ($C(\Phi)$) shows maxima at $\Phi = 0°$ and $\Phi = 180°$. It is easy to understand that the ratio $\lambda_1=[C(0°)-C(180°)]/[C(0°)+C(180°)]$ increases with the magnitude of the flow parameter (whatever its sign). So, plotting R as a function of energy, the minimum of R corresponds to the EVF. An example is given in figure 1, for the Zn + Ni and Ar + Al systems and for an impact parameter around 5.5 fm. The energy locations of the minima of these curves are in good agreement with the EVF estimated by other methods.

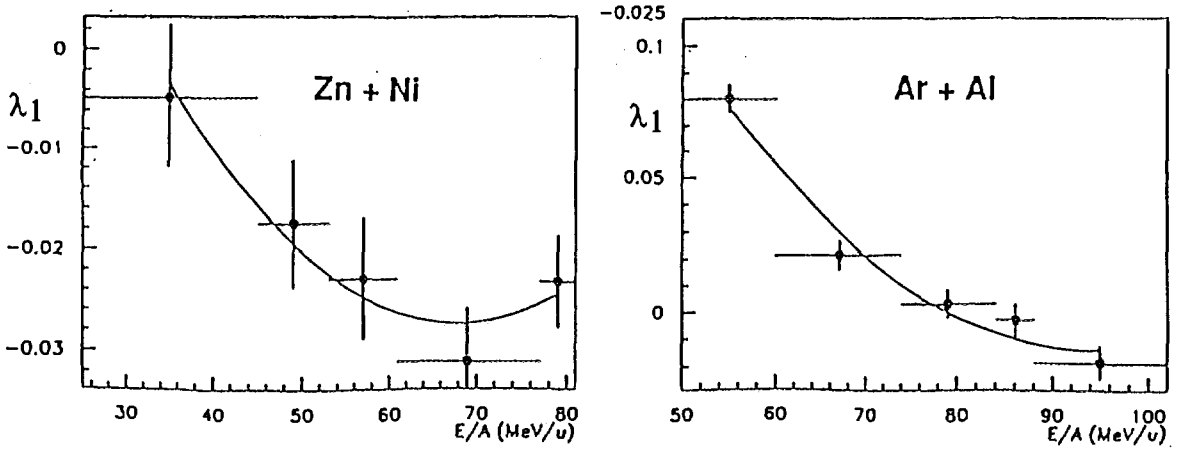

Figure 1 : λ_1 as a function of E/A

Publication : A. Buta et al., Nucl. Phys. A584 (1995) 397

DISAPPEARANCE OF FLOW AND THE IN-MEDIUM NUCLEON-NUCLEON CROSS SECTION FOR $^{64}Zn + ^{27}Al$ COLLISIONS AT INTERMEDIATE ENERGIES

Zhi-Yong He[1-2], J. Peter[1], J.C. Angelique[1], A. Auger[3], G. Bizard[1], R. Broul, A. Buta[1-a], C. Cabot[3], E. Crema[3], D. Cussol[1], Guang-Xi Dai[2], Y. El Masri[4], Ph. Eudes[5], M. Gonin[6], K. Hagel[6], Gen-Ming Jin[2], A. Kerambrun[1], C. Lebrun[5], Yu Gang Ma[7], A. Peghaire[3], R. Popescu[1-a], R. Regimbart[1], E. Rosato[8], F. Saint Laurent[3], Wen-Qing Shen[7], J.C. Steckmeyer[1], B. Tamain[1], E. Vient[1], R. Wada[6], Feng-Shou Zhang[2]

1 LPC Caen, ISMRA,IN2P3-CNRS, 14050 CAEN CEDEX, FRANCE
2 Institute of Modern Physics, Academia Sinica, 730000 LANZHOU, CHINA
3 GANIL BP 5027, 14021 CAEN CEDEX, FRANCE
4 Institut de Physique Nucléaire, UCL, 1348 LOUVAIN LA NEUVE, BELGIUM
5 SUBATECH, 44072 NANTES CEDEX, FRANCE
6 Cyclotron Institute, Texas A & M University, College Station, TX77843, USA
7 Institute of Nuclear Research, Academia Sinica, 201800 SHANGHAI, CHINA
8 Dipartimento di Scinze Fisiche, Universita di Napoli, 80125 NAPLES, ITALY
a IFA, Heavy Ion Department, BUCHAREST, ROMANIA

The experimental measurement and the theoretical comparison of collective flow can give important information about the nuclear equation of state (EOS) and the in-medium nucleon - nucleon cross section. Experimental measurements for $^{64}Zn+^{27}Al$ collision from 35 to 79 MeV/u with the 4π array MUR = TONNEAU. The results were compared to BUU calculations.

We used the sum of the parallel momentum of all detected particles ($\sum_i P_{i//}$) to determine the completeness of our events. In order to get an impact parameter sorting, several global variables related to the violence of the collisions have been tried and we used "the average parallel velocity".

The experimental determination of flow is based on the transverse momentum projected into the estimated reaction plane. Several methods of the reaction plane determination were proposed. For this reaction system and the energy ranges, the transverse momentum analysis is still the best one.

The average in-plane transverse momentum $< p^{x'}/A >$ as a function of the fractional particle rapidity (Y/Y_{proj}) exhibits the characteristic signature of directed collective motion for fragments Z=1,2,3 ; around mid-rapidity a linear increase of $p^{x'}/A$ versus the rapidity.

Fig. 1 shows the excitation functions of the measured flow for different fragments emitted at 0-2, 2-3, and 4-5 fm. It is clear that above 49 MeV/u there is a monotonous decrease of the collective flow versus the beam energy. At b=2-3 fm, the flow varies from the largest value at 49 MeV/u to around zero at 79 MeV/u and E_{bal} is around 79 MeV/u. Since the step of beam energy is 10 MeV/u and the flow obviously exist at 69 MeV/u, E_{bal} at b=2-3 fm is thought to be 79±5 MeV/u. However, at b=4-5 fm, a larger flow values are observed even at 79 MeV/u and E_{bal} is more than 79 MeV/u. In central collisions (0-2 fm), E_{bal} may be between 69 and 79 MeV/u and the flow values at 79 MeV/u are expected to be positive.

One of the current theoretical models of nuclear collisions in this energy range is the Boltzmann-Uehling-Uhlenbeck (BUU) model. Two sets of parameter were used in the calculations, one corresponds to a stiff nuclear equation of stage (EOS) with an incompressibility coefficient K=380 MeV ; the other one corresponds to a soft EOS with K=200 KeV.

Fig. 2 shows the calculated $< P^x/A >$ as a function of rapidity with a stiff EOS, and at b=2.5 fm and beam energies E/A=49, 69 and 79 MeV respectively. At the lowest energy, 49 MeV, the transverse momentum distributions are characterized by negative slopes in the midrapidity region (around $Y_{NN}=0.5\ Y_p$) for all values of the nucleon-nucleon cross sections σ_{NN}, indicating that the flow is negative and the attractive mean field is important at this energy. The flow values vary with σ_{NN} : small σ_{NN} values result in larger negative flow values. The disappeareance of flow can be seen in the calculations at E/A=69 and 79 MeV.

To study the sensitivity to the EOS, we performed the calculations with a soft EOS and stiff EOS, with σ_{NN} =35 mb and 45 mb respectively.The flow values with a soft EOS are a little smaller than those with a stiff EOS.

From these calculations, we built fig. 3 which shows the calculated flow as a function of beam energy at b=2.5 and 4.5 fm respectively. The solid squares, circles, diamonds, and triangles correspond to calculations with σ_{NN}=55, 35 and 25 mb, respectively, and with a stiff EOS (K=380 MeV). The open circles and diamonds are the calculated values with σ_{NN}=45 and 35 mb, respectively, and with a soft EOS (K=200 MeV). It is clearly seen that the calculated flow change monotonously versus the beam energy from negative values at 49 MeV to positive values at 140 MeV. The calculated flow values and E_{bal} are very sensitive to the in-medium cross section and weekly sensitive to the nuclear compressibility at b=2.5 fm. This allows us to determine σ_{NN} from the experimental data. Clearly, the value of σ_{NN} is between 35 and 45 mb, slightly varying with the nuclear compressibility.

Publication : Z.Y. He et al., Nucl. Phys. A598 (1996) 248

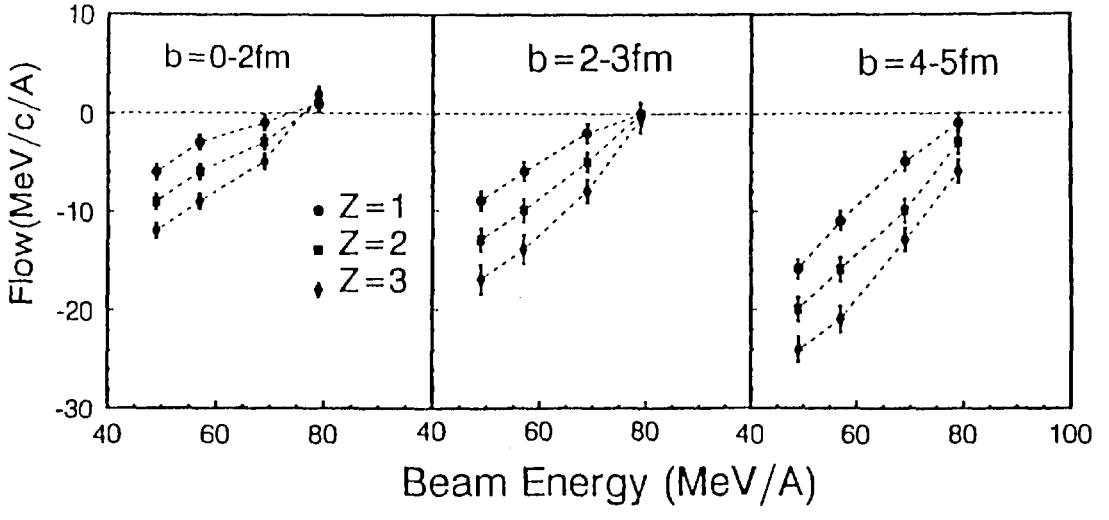

Figure 1 : Measured flow parameter as a function of beam energy for 3 impact parameter bins. The circles, squares, and diamonds indicate the flow for Z=1, 2 and 3 particles, respectively. The dashed lines are used to guide the eye.

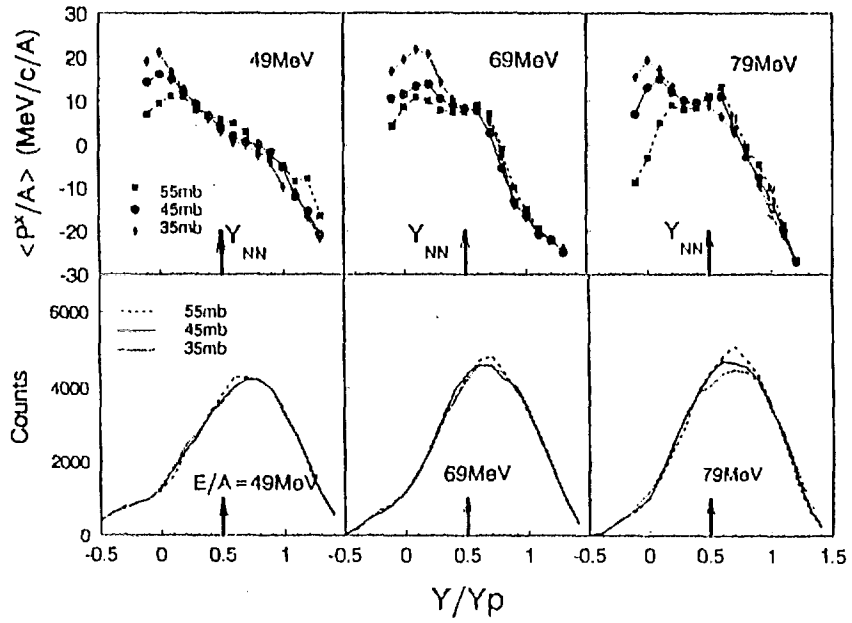

Figure 2 : Calculated average in-plane transverse momentum distribution as a function of Y/Yp for $^{54}Zn+^{27}Al$ collisions with a stiff EOS at impact parameter b=2.5 fm and three incident energies. The diamonds, circles and squares display the calculations with σ_{NN} =35, 45 and 55 bm, respectively. The rapiditiy distributions of nucleons are also shown in the bottom row with σ_{NN}=35 (dotted line), 45 (solid line) and 55 mb (dashed line), respectively.

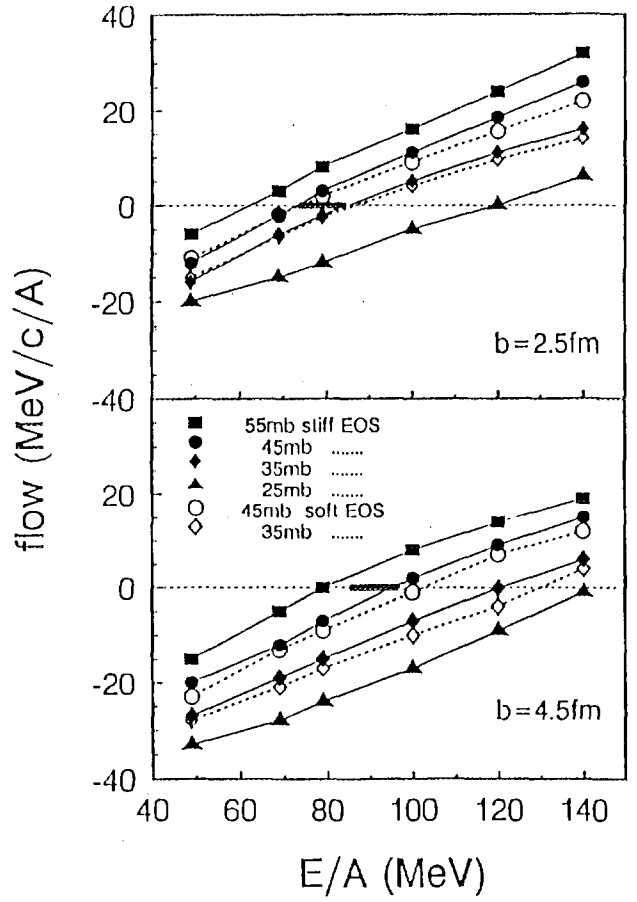

Figure 3 : Calculated flow parameter as a function of beam energy for $^{64}Zn+^{27}Al$ collisions at b=2.5 fm and 4.5 fm, respectively. The solid triangles, diamonds, circles and squares indicate the calculations with a stiff EOS and σ_{NN} = 25, 35, 45 and 55 mb, respectively. The open diamonds and circules are calculations with a soft EOS and σ_{NN}=35 and 45 mb respectively. The experimental values of Ebal are horizontal bars.

B4 MULTIFRAGMENT EMISSION

Mulitplicity distributions and multiplicity correlations in sequential, off-equilibrium fagmentation process

Robert Botet[†] and Marek Ploszajczak

[†] *Laboratoire de Physique des Solides, Bâtiment 510, Université Paris-Sud Centre d'Orsay, F-91405 Orsay, France*

GANIL, BP 5027, 14021 Caen, France

Fragmentation is a subject of intense studies in different domains of physics, including nuclear physics. This ubiquitous process is still poorly understood, mainly due to missing adequate theoretical tools, in particular, when dealing with the non-equilibrium aspects of the fragmentation. For this reason , we have proposed a new kinetic fragmentation model, the Fragmentation - Inactivation - Binary (FIB) model, where a dissipative process stops randomly the sequential, conservative and off-equilibrium fragmentation process[1, 2]. In the FIB model, one deals with fragments (e.g. clusters, partons etc.) characterized by some conservative scalar quantity (mass, energy, virtuality etc.) , that is called the *cluster mass* . The anscestor fragment of mass N is relaxing via an ordered and irreversible sequence of steps. The first step is either a binary fragmentation, $(N) \rightarrow (j) + (N-j)$, or an inactivation $(N) \rightarrow (N)^*$. Once inactive, the cluster cannot be reactivated anymore. The fragmentation leads to two fragments, with the mass partition probability $\sim F_{j,N-j}$. In the following steps, the relaxation process continues independently for each descendant fragment until either the low mass cutoff for further 'indivisible particles' is reached or all fragments are inactive. Since for any event, the fragmentation and inactivation occur with the probabilities per unit of time $\sim F_{j,k-j}$ and $\sim I_k$ respectively, therefore the knowledge of the initial state and the rate-functions $F_{j,k-j}$ and I_k , specifies the fragmenting system and its evolution.

The composed particle first moment $N_C \equiv 1 - < n_1 > /N$, where $< n_1 >$ is the average number of monomers, is an order parameter in the FIB model. If instability of smaller fragments is more important than instability of larger fragments, N_C coincides with the total mass and fragmentation is in the ∞-*cluster phase*. Conversely, when instability of larger fragments is more important than instability of smaller ones, the total mass is converted into finite-size fragments ($N_C \rightarrow 0$) and fragmentation is in the *shattered phase*. The transition line between these two phases is characterized by the fragment-size independence of both fragmentation and inactivation probabilities (the scale-invariant branching process). The transition associated with the shattering is the second order phase transition[1, 2] .

In our earlier works, we have studied the asymptotic cluster-size distribution which at the transition line is given by the power-law $n_s \sim s^{-\tau}$ with $\tau \leq 2$. In this region, FIB model describes well the fragment-size distribution and all charge-fragment correlations in the heavy-ion collisions at intermediate energies[3] . Other statistical approaches have been also tried successfully[4] . It is our experience that most of the gross measures of the cluster-mass (size) distribution do not discriminate among models unless supplemented with

more fine grained information, especially correlations of various kinds. For that reason, we have studied the multiplicity distributions and their scaling features. Various classes of the multiplicity distributions have been found for homogeneous : $F_{\lambda i,\lambda j} = \lambda^{2\alpha} F_{i,j}$ and symmetric $F_{i,j} = F_{j,i}$ fragmentation kernels[5] . For $p_F < 1/2$ (p_F is the fragmentation probability without specifying the sizes of the descendants) and for any α, the fragment multiplicity is asymptotically a constant. In this 'Cayley domain', fragmentation is analogous to the invasion percolation on the Cayley tree[6] and resembles the self-organized critical process with no characteristic time or length scales. For $p_F > 1/2$ and $\alpha > -1$, the fragment multiplicity is an algebraic function of N : $< m >_N \sim aN^{\tau-1}$ $(1 \leq \tau \leq 2)$. This is the 'Brand-Schentzle (BS) domain', where the multiplicity distribution is a special solution of the nonlinear stochastic equation with multiplicative fluctuations[7] . For $p_F > 1/2$ and $\alpha < -1$ (the 'evaporative domain') , FIB process resembles the evaporation of light fragments from one big cluster and the fragment multiplicity is approximately independent of the initial cluster mass. In the two transitional regions: (i) between Cayley and BS domains ($p_F = 1/2$, $\alpha > -1$) and (ii) between BS and evaporative domains ($\alpha = -1$, $1/2 < p_F < 1$), the fragment multiplicity is : $< m >_N \sim (\ln N)^b$. Multiplicity anomalous dimension : $\gamma(N) = d \ln < m >_N / d \ln N$, equals $\tau - 1$ $(0 < \gamma(N) < 1)$ in the BS domain, while it decreases logarithmically : $\gamma(N) \sim (\ln N)^{-1}$ with the total mass in the transitional regions and is zero elsewhere.

Interestingly, the KNO scaling[8] : $< m > P_m = f(m/ < m >)$, appears from our studies as a fundamental property of the critical FIB process, whenever the average fragment multiplicity $< m >_N$ depends on the initial system size N , i.e. in its 'low-viscosity'- ($p_F > 1/2$, $\alpha \geq -1$) or BS- phase including the transitional domain $\alpha = -1$, and is absent everywhere outside of the transition line. The appearance of the KNO scaling is hence related to the second-order phase transitions associated with breaking the initial system into a dust fragments each one having only an infinitesimal portion of the initial cluster mass. Hence, the KNO scaling is not only a property of certain relativistic field theories but more generally it appears as a property of the critical fragmentation in quantum systems as well as in the macroscopic classical objects. This new general foundation of the KNO scaling opens a possibility for its finding in many fragmentation processes in nature.

In order to analyze the higher order correlations in the multifragment (multiparticle) distributions one has to recognize that the density correlations contain usually lower order background correlations. These can be conveniently removed using the cumulant correlation functions. The statistical independence of any y_i in $K_p(y_1, \ldots, y_p)$ results in factorization of the ρ_p densities and vanishing cumulant. Hence, the cumulants K_p are key quantities to be produced by theoretical models of the fragmentation. Following the linked pair ansatz : $K_p(1, 2 \ldots p) = A_p \sum_{perm} \prod^{p-1} K_2(1, 2)$, the high order cumulants can be expressed in terms of the cumulants of order two. We have found that the critical FIB process is characterized by the appearance of the hierarchical structure of the higher order correlations. This particular structure for higher order correlations is absent in both ∞-cluster and shattering phases. Curiously, the same hierarchical correlation structures describe galaxy correlations and phase-space correlations in the multiparticle distributions in ultrarelativistic collisions.

The basic equations, relevant for a description of the FIB fragmentation of an initial fragment of a given mass (energy, virtuality etc.), such as master and cascade equations have been given before [1, 2] . Recently, we were able to demonstrate that the FIB cascade equation includes as a special case the QCD equation of gluodynamics[11] . The detailed

knowledge of the multiplicity distributions and multiplicity correlations acquired in our earlier studies,[5] , allowed to identify the QCD parton fragmentation process with a critical FIB process in the transitional region $\alpha = -1$, $p_F > 1/2$. For the first time, exact solutions of the QCD gluodynamics for the running QCD coupling constant could be obtained in this way. The extension of the FIB framework to include also quark jet fragmentation is now in progress.

References

[1] R. Botet and M. Ploszajczak, Phys. Rev. Lett. **69**, 3696 (1992).

[2] R. Botet and M. Ploszajczak, J. of Mod. Phys. **E3**, 1033 (1994).

[3] R. Botet and M. Ploszajczak, Phys. Lett. **B312**, 30 (1993).

[4] A.S. Botvina and I.N. Mishustin, Phys. Lett. **B294**, 23 (1992);
P. Kreutz et al. (ALADIN Coll.), Nucl. Phys. **A556**, 672 (1993).

[5] R. Botet and M. Ploszajczak, Preprint GANIL P 96 07.

[6] R. Botet and M. Ploszajczak, Physica **A223**, 7 (1996).

[7] A. Schenzle and H. Brand, Phys. Rev. **A20**, 1628 (1979).

[8] Z. Koba, H.B. Nielsen and P. Olesen, Nucl. Phys. **B40**, 317 (1972).

[9] R. Botet and M. Ploszajczak, in preparation.

[10] P.J.E. Peebles, *The Large Scale Structure of the Universe*, Princeton U.P., Princeton, NJ (1980).

[11] Yu.L. Dokshitzer, V.A. Khoze, A.H. Mueller and S.I. Troyan, *Basics of Perturbative QCD*, ed. Tran Thanh Van (Editions Frontieres , Gif-sur-Yvette, 1991)

Nuclear Disassembly Time Scales Using Space Time Correlations

D. Durand [a], J. Colin [a], J.F. Lecolley [a], C. Meslin [a], M. Aboufirassi [a], B. Bilwes [b], R. Bougault [a], R. Brou [a], F. Cosmo [b], J. Galin [c], A. Genoux-Lubain[a], D. Guerreau [c], D. Horn [a-e], D. Jacquet [d], J.L. Laville [a], C. Le Brun [a], O. Lopez [a], M. Louvel [a], M. Mahi [a], M. Morjean [c], A. Péghaire [c], G. Rudolf [b], F. Scheibling [b], J.C. Steckmeyer [a], L. Stuttgé [b], B. Tamain [a], S. Tomasevic [b]

a) Laboratoire de Physique Corpusculaire, ISMRa and Université de Caen
b) Centre de Recherches Nucléaires, IN2P3-CNRS, Université Louis Pasteur
c) GANIL, IN2P3-CNRS-DSM-CEA
d) Institut de Physique Nucléaire d'Orsay
e)AECL Research, Chalk River Laboratories,

The lifetime, τ, with respect to multifragmentation of highly excited nuclei is deduced from the analysis of strongly damped Pb+Au collisions at 29 MeV/u. The method is based on the study of space-time correlations induced by "proximity" effects between fragments emitted by the two primary products of the reaction and gives the time between the reseparation of the two primary products and the subsequent multifragment decay of one partner.

Recently, much attention has been paid to the measurement of time scales in nuclear fragmentation. Indeed, the knowledge of such quantities would be very helpfull to identify the instabilities responsible for the disassembly of hot nuclei.

The present experiment was performed at the Ganil facility in the Nautilus scattering chamber in which fragments (with atomic numbers larger than 8) were detected in Delf and XYZT. To measure the life time τ of a hot nucleus, we take advantage of the distortions induced by Coulomb forces between the two partners of a deep inelastic scattering. To this end, the system should be as heavy as possible and the relative velocity in the entrance channel sufficiently low so that the "proximity" effects can be enhanced due to long interaction time. In addition, the collision must remain of a two-body type (we mean by this no complete or incomplete fusion). These conditions are fullfilled in Pb+Au collisions at 29 MeV/u. Thus, we measure the kinematical characteristics of the fragments emitted by one of the excited nucleus in the Coulomb field of its partner. In the case of a very long time between separation and subsequent decay of one of the two partners, one expects that the projection of the velocities of the emitted fragments (estimated in their own center-of-mass) on the axis connecting the two primary fragments should be forward-backward symmetric. Then the distribution should be flat or it should have a minimum at 90 degrees, according to the value of the angular momentum. By contrast, for a fast disassembly process, a depletion around $\theta_{axis}=0°$ is expected due to the strong Coulomb repulsion between the fragments.

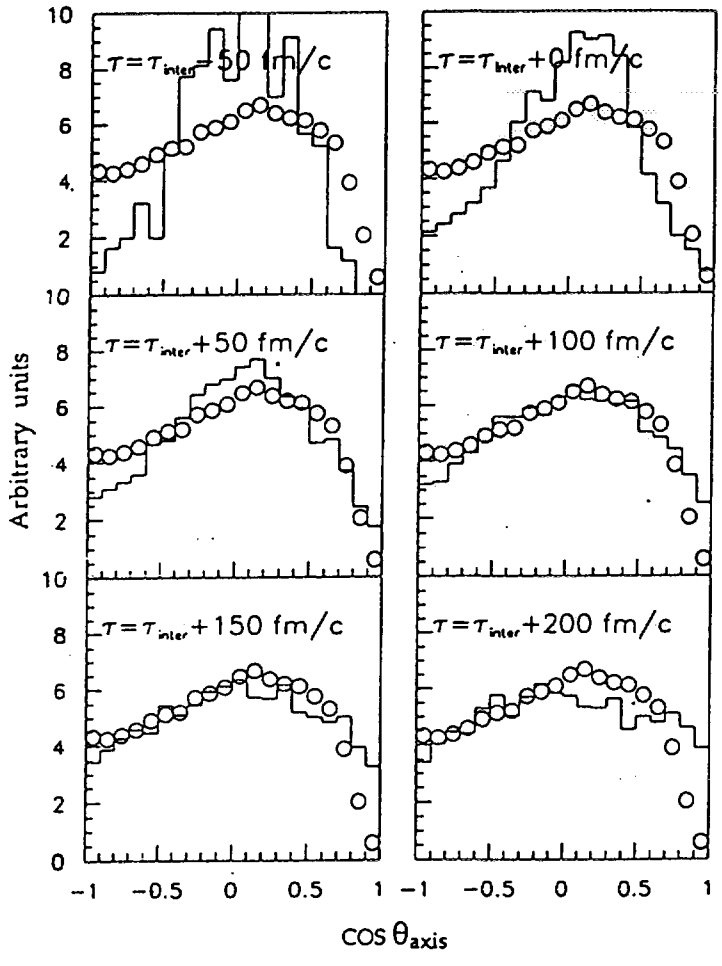

Fig. 1: Comparison between the results of the model described in the text (histograms) with the experimental data corresponding to TKEL larger than 2100 MeV. The value of τ in each panel corresponds to different time for the disassembly of one of the two partners. τ_{inter} is the time for reseparation of the two partners as given by the trajectory calculations.

To quantify such an effect, we have performed model simulations with the event generator SIMON. The deep inelastic scattering of the two incoming nuclei is described in terms of standard trajectory calculations with conventional nuclear, Coulomb and centrifugal potentials. The dissipation was taken into account with the window formula. At a given time τ (which is the main parameter of the model), the decay of one of the two partners is considered by placing a three-fragment partition in a compact configuration. The post-dynamics of the decay process is then considered by solving the equation of motion for both the three fragments and the heavy partner and by considering secondary decays.

In fig. 1, we compare the results of the model with the experimental angular distributions associated with the most central collisions for which ε^* is around 5 MeV/u. Several values of τ have been considered with respect to τ_{inter} (the interaction time). When the value of τ is increased, the agreement is better and better and the data are best fitted with values around $\tau=\tau_{inter}$+150 fm/c. This corresponds to about 300 fm/c after maximum overlap of the two nuclei. This rather large value suggests that nuclear fragmentation in this energy range could proceed through rather "gentle" shape instabilities.

D. Durand et al , Phys. Letters B345 (1995) 397

P. Chomaz, D. Durand "Perspectives scientifiques", Pour la Science (Juin 96)

Dynamical Effects and IMF Production in Peripheral and Semi-central Collisions of Xe+Sn at 50 MeV/nucleon

J. Łukasik[1a], V.Metivier[6], E. Plagnol[1], B. Tamain[3], G. Auger[2], Ch.O. Bacri[1], B. Borderie[1], J. Benlliure[2], E. Bisquer[4], R. Bougault[3], R. Brou[3], J.L. Charvet[5], A. Chbihi[2], J. Colin[3], D. Cussol[3], R. Dayras[5], E. De Filippo[5], A. Demeyer[4], D. Doré[1], D. Durand[3], P. Ecomard[2], P. Eudes[6], D. Gourio[6], F. Gulminelli[3] D. Guinet[4], R. Laforest[3], P. Lautesse[4], J.L. Laville[6], L. Lebreton[4], J.F. Lecolley[3], A. Le Fèvre[2], T. Lefort[3], R. Legrain[5], O. Lopez[3], M. Louvel[3], N. Marie[2], V. Métivier[3b], L. Nalpas[5], A. Ouatizerga[1], M. Parlog[1c], J. Péter[3], A. Rahmani[6], T. Reposeur[6], E. Rosato[3], M.F. Rivet[1], F. Saint-Laurent[2], M. Squalli[1], J.C. Steckmeyer[3], L. Tassan-Got[1], E. Vient[3], C. Volant[5], J.P. Wieleczko[2]

[1] *Institut de Physique Nucléaire, IN2P3-CNRS, 91406 Orsay Cedex, France*
[2] *GANIL, CEA, IN2P3-CNRS, B.P. 5027, 14021 Caen Cedex, France*
[3] *LPC, IN2P3-CNRS, ISMRA et Université, 14050 Caen Cedex, France*
[4] *IPN Lyon, IN2P3-CNRS et Université, 69622 Villeurbanne Cedex, France*
[5] *CEA, DAPNIA/SPhN, CEN Saclay, 91191 Gif sur Yvette Cedex, France*
[6] *SUBATECH, IN2P3-CNRS et Université, 44072 Nantes Cedex 03, France.*

1 Introduction

The understanding of the dynamical effects which lead to dissipation of energy in heavy ion collisions in the intermediate energy range (20–100 MeV/nucleon) has been a goal of many studies because they reflect intrinsic properties of nuclear matter. From recent experimental results [1, 2, 3, 4, 5] which are in agreement with theoretical calculations [6], it turns out that, for most collisions (from peripheral to almost central), the mechanisms are mainly binary. This feature can be compared with the corresponding behaviour at lower and higher bombarding energies. Below 10 MeV/nucleon binary processes, deep inelastic collisions (DIC), are indeed widely observed, mainly for heavy systems. The reaction is purely binary in the sense that it leads to two excited outgoing products which deexcite by sequential binary decays. In relativistic heavy ion collisions a third emitting source is observed, which is labeled the "participant zone". Of course one may expect a continuous evolution from a pure two source DIC picture to this three source picture, when the bombarding energy evolves in the intermediate energy range. However the nature of this transition has never been studied quantatively.

The advent of large acceptance detectors has produced a wide body of data on the deviation from the purely binary picture. Several studies [7, 8] have shown that, from 12 MeV/nucleon, fission events for a medium size system point to a very fast process where the fission products are often aligned along the deflection axis and are not isotropically distributed as they should if long fission lifetimes were assumed. For higher energies and

[a] permanent address: *Institute of Nuclear Physics, ul. Radzikowskiego 152, 31-342 Kraków, Poland*
[b] present address: *SUBATECH, IN2P3-CNRS et Université, 44072 Nantes Cedex 03, France*
[c] permanent address: *Institute of Physics and Nuclear Engineering, IFA, P.O. Box MG6, Bucharest, Romania*

various systems, a number of groups [9, 10, 11, 12, 13, 14] have shown that, for peripheral reactions, part of IMF's comes from the region in velocity space that could imply the dynamical emission of fast particles and fragments and/or the formation of a "neck".

The 4π INDRA detector has been used to perform a quantitative study of the amount of matter that can be attributed to these emissions in the case of the Xe+Sn reaction at 50 A.MeV. One of the essential qualities of a 4π detector being that it allows for the definition of an impact parameter selector, we have used the high efficiency of the detector for light particles to define this impact parameter selector as the Etrans12, ie, the transverse energy of the light particles. The events have been grouped into 8 bins, numbered 1 to 8 with increasing centrality.

This article is an extract from the contribution of J.Lukasik at the 1996 Bormio Conference[19].

2 Velocity distributions: a signature for slow and fast emissions

In order to have an overall view of the kinematical properties of emitted particles and fragments, we have plotted the invariant cross section contours $\frac{d^2\sigma}{v_\perp dv_\perp dv_\parallel}$ in a $v_\perp$ vs $v_\parallel$ plot.

In Fig. 1 such plots, in the center of mass (CM) reference frame, are shown for protons and α particles and for several Etrans12 bins. The binary source behaviour is easily recognized for bins 1–4. For more violent collisions, the separation between the two sources is not so clear and the last bin can correspond to fusion-like events. Now, an interesting observation can be drawn from the figure: when two sources are clearly resolved, all alpha particles cannot be attributed to a statistical sequential decay. Instead, a larger abundance of particles is observed in between the two sources (see also [14]). This "excess" emission can be understood in at least two ways: in the first scenario, a third zone is present, and is responsible for the so-called "neck" emission, which is reminiscent of the participant zone observed at high energies; in the second scenario, these particles are sequentially emitted from one of the outgoing partners, but on a time scale short enough to induce some memory effects in the emission. The two mechanisms probably contribute to the observed "excess" emission and there is a continuous evolution between them. In both cases, the binary system is dynamically strongly deformed, the "neck" region being either released (neck emission) or attached to one of the outgoing partners, which is hence deformed beyond a pseudo-saddle-point leading to a fast break-up. The memory of the partner direction is kept if the emission time is smaller than a few times 10^{-22} s, for an angular momentum in the range 50–100 $\hbar$. A kinematical difference between these two processes can be found in velocity distributions relatively to the main sources. In the case of a pure "neck" emission (two main sources + neck), the corresponding products are likely to be at rest in the CM frame. Such a contribution can be observed in Fig. 3 for several IMF's.

In the case of fast sequential emission, the relative kinetic energy between the detected fragment and its emission source is dominated by the corresponding Coulomb energy. Such a behaviour is observed in Fig. 2 for α particles. It has also been clearly recognized in three-body events [7, 8, 9, 10, 15].

The aim of this study is to quantify the importance of these fast emissions by measuring the charge percentage which corresponds to statistical emissions and the one which correspond to neck or fast-sequential decays.The statistical emission is estimated by "doubling"

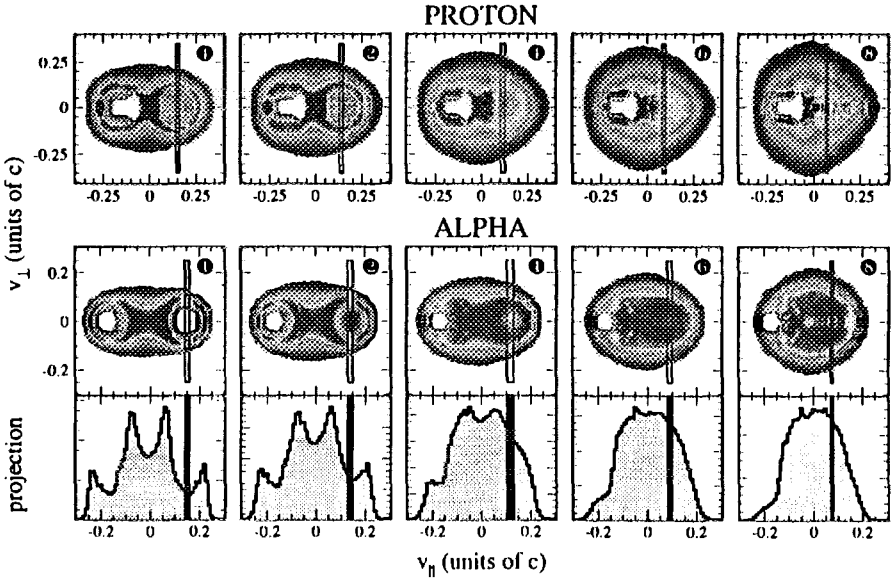

Figure 1: Invariant velocity plots for protons (upper row) and alpha particles (lower row) detected for specified Etrans12 bins. The right and left sides of the rectangles superimposed on the velocity plots correspond to the source velocities obtained with the use of method I and II, respectively (see text). The presented projections refer to alpha particle plots.

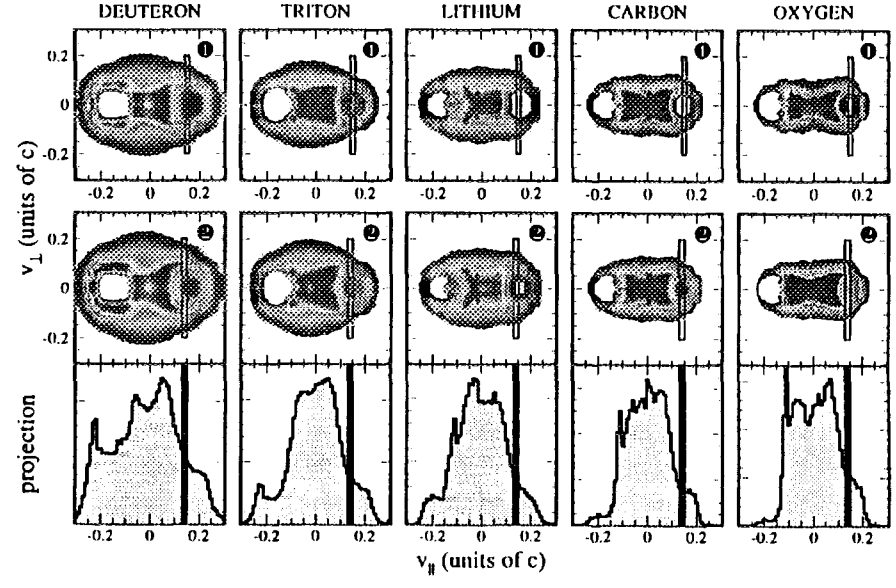

Figure 2: Invariant velocity plots in the CM frame for deuteron, triton, lithium, carbon and oxygen fragments detected in the most peripheral collisions (upper row – bin 1, and lower row – bin 2 of Etrans12). The right and left sides of the rectangles correspond to the source velocities obtained with the use of method I and II, respectively (see text). The presented projections refer to the plots for the second bin.

those products that are found forward of the velocity of the quasi-projectile. The "dynamical or neck" emission is the difference between the later and the products found forward of the total center of mass. A critical ingredient of such a method is the estimation of the mean quasi-projectile velocity for each Etrans12 bin.

We have used two methods to determine the velocity of the projectile-like source. The first one (Method I) takes, for each bin, the most probable velocity of the heaviest fragment. The second uses, event by event, the "thrust analysis" [16]. Figure 3. shows, in percent of the total charge of the quasi-projectile the amount of charge emitted dynamically (prompt and neck emissions) and the amount emitted statistically.

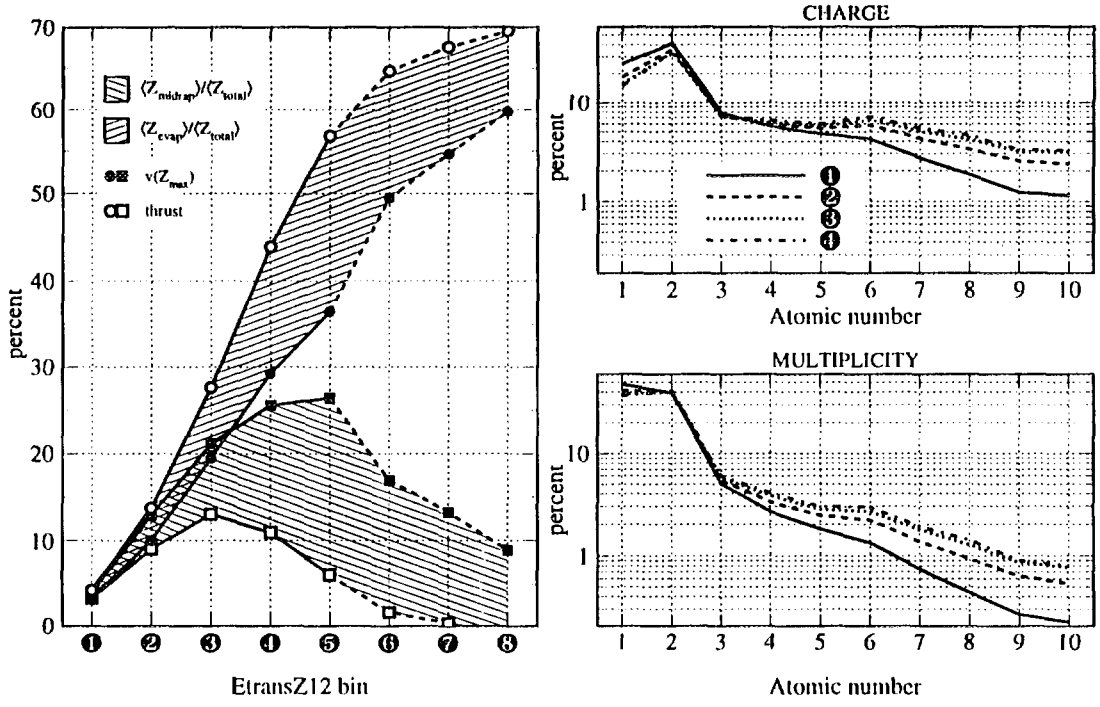

Figure 3: Left panel: the percentage of charge contained in the midrapidity (fast) component (neck + fast-sequential) – the shaded area bounded by squares; and the percentage of charge coming from statistical emission – the shaded area bounded by circles. The filled and open symbols correspond to method I and II, respectively. Upper right panel: the percentage of charge in the fast component coming from the fragments of a given Z number (Z from 1 to 10) for the Etrans12 bins 1 to 4. Lower right panel: same, but for the multiplicity.

3 Conclusions

The presented analysis (valid for about 80–90% of the total cross section) indicates that dynamical effects are quite important in peripheral and intermediate impact parameter collisions at 50 MeV/nucleon.

The nature of this non-statistical emission is probably connected with the collective behaviour, since mostly alpha particles and IMF's are involved. In that sense, it differs from

the usual prompt (preequilibrium ?) emission mechanism which reflects mainly nucleon-nucleon collisions. A better understanding will require extension of studies to other energies, to symmetric systems of different size and to asymmetric systems. The data accumulated by the INDRA collaboration will allow to do so.

Other important questions related to these observations are i) the energy (mechanical, thermal, ...) necessary for this fast emission, and the fraction it represents as compared to the excitation energy of the PLS and TLS; ii) the understanding of the nature of this emission and more precisely its connection to the size distribution of the corresponding products; and iii) the influence of the viscosity on the deformation of PLS (TLS) and on the neck formation.

The correct reproduction of all the observed features will imply strong constraints on dynamical models and the evolution of the viscosity with temperature. It may be a key requirement before applying the models to the multifragmentation data observed in more central collisions [15]. The presented experimental results offer a unique opportunity and challenge for the dynamical models, since they refer to the early phase of the reaction, and thus may not require any "afterburners". This theoretical analysis is being done in collaboration with F.Haddad, Ph.Eudes (SUBATECH, Nantes) and M.Colonna(Dapnia, Saclay) and will be published soon.

References

[1] B. Borderie *et al.*, Phys. Lett. **B205** (1988) 26,
M.F Rivet *et al.*, Proc. of Intern. Wint. Meet. on Nucl. Phys., Bormio 1993, p92.

[2] J. Péter *et al.*, Nucl. Phys. **A593** (1995) 95.

[3] J.C. Steckmeyer *et al.*, Preprint LPCC 95-13.

[4] R. Bougault *et al.*, Nucl. Phys. **A587** (1995) 499.

[5] V. Métivier *et al.*, Proc. of the ACS Nucl. Chem. Symp., Anaheim, CA, April 1995.

[6] M.F. Rivet *et al.*, Phys. Lett. **B215** (1988) 55,
M. Colonna *et al.*, Prog. Part. Nucl. Phys. **30** (1992) 17,
L. Sobotka, Phys. Rev. **C50** (1994) R1270,
M. Colonna *et al.*, Nucl. Phys. **A589** (1995) 160,
F. Haddad *et al.*, Preprint Subatech 95-14, and Z. Phys. in press.

[7] P. Glässel *et al.*, Z. Phys **A310** (1983) 185.

[8] G. Casini *et al.*, Phys. Rev. Lett. **71** (1993) 2567.

[9] L. Stuttgé *et al.*, Nucl. Phys. **A539** (1992) 511.

[10] J.F. Lecolley *et al.*, Phys. Lett. **B354** (1995) 202.

[11] C.P. Montoya *et al.*, Phys. Rev. Lett. **73** (1994) 3070.

[12] J. Töke *et al.*, Phys. Rev. Lett. **75** (1995) 2920 – Nucl. Phys. **A583** (1995) 519c.

[13] W. Lynch, Nucl. Phys. **A583** (1995) 471c.

[14] J.E. Sauvestre *et al.*, Phys. Lett. **B335** (1994) 300.

[15] V. Métivier *et al.*, to be published – V. Métivier, thesis Caen (1995),
Indra collaboration: to be published.

[16] J. Cugnon *et al.*, Nucl. Phys. **A397** (1983) 519.

[17] J. Pouthas *et al.*, Nucl. Instr. Meth. in Phys. Res. **A357** (1995) 418.

[18] C. Cavata *et al.*, Phys. Rev. **C42** (1990) 1760.

[19] J.lukasik *et al.*, Bormio Conf. (1996).

VAPORIZATION FOR THE Ar+Ni SYSTEM: THERMODYNAMICAL ASPECTS IN THE EXCITATION ENERGY RANGE 8-28 MeV

Ch.O. Bacri[1], B. Borderie[1], J.L. Charvet[5], A. Chbihi[2], D. Cussol[3], R. Dayras[5], D. Durand[3], F. Gulminelli[3] O. Lopez[3], M. Parlog[1a], A. Ouatizerga[1], M.F. Rivet[1], L. Tassan-Got[1],
G. Auger[2], J. Benlliure[2], E. Bisquer[4], R. Bougault[3], R. Brou[3], J. Colin[3], E. De Filippo[5], A. Demeyer[4], D. Doré[1], P. Ecomard[2], P. Eudes[6], D. Gourio[6], D. Guinet[4], R. Laforest[3], P. Lautesse[4], J.L. Laville[6], L. Lebreton[4], J.F. Lecolley[3], A. Le Fèvre[2], T. Lefort[3], R. Legrain[5], M. Louvel[3], J. Łukasik[1b], N. Marie[2], V. Métivier[1c], L. Nalpas[5], J. Péter[3], E. Plagnol[1], A. Rahmani[6], T. Reposeur[6], E. Rosato[3], F. Saint-Laurent[2], M. Squalli[1], J.C. Steckmeyer[3], B. Tamain[3], E. Vient[3], C. Volant[5], J.P. Wieleczko[2].

[1] *Institut de Physique Nucléaire, IN2P3-CNRS, 91406 Orsay Cedex, France*
[2] *GANIL, CEA, IN2P3-CNRS, B.P. 5027, 14021 Caen Cedex, France*
[3] *LPC, IN2P3-CNRS, ISMRA et Université, 14050 Caen Cedex, France*
[4] *IPN Lyon, IN2P3-CNRS et Université, 69622 Villeurbanne Cedex, France*
[5] *CEA, DAPNIA/SPhN, CEN Saclay, 91191 Gif sur Yvette Cedex, France*
[6] *SUBATECH, IN2P3-CNRS et Université, 44072 Nantes Cedex 03, France.*

1 MOTIVATION

To improve our knowledge of the properties of nuclear matter under peculiar conditions of temperature and pressure, it is important in studying central nucleus-nucleus collisions at intermediate energies, to determine how and at which excitation energy the highly excited nuclear system formed disassembles. At a high enough energy, the multifragmentation process is predicted to set in, from both statistical and dynamical calculations[1]; even if the mechanisms involved are not yet fully understood, experimental evidences concerning the appearance of multifragmentation are now well established[1]. A second interesting feature is expected to occur: the vaporization of the system[2, 3, 4, 5]. In the extreme only light particles ($Z \leq 2$) are produced, forming a gas phase as defined in ref[2]. However, the link between this vaporization process and the liquid-gas phase transition in infinite nuclear matter is not obvious and is much debated due to finite size effects and to the Coulomb force[6, 7]. Thus an experimental determination of the onset of vaporization and of thermodynamical properties of vaporization events should provide valuable information

[a] permanent address: *Institute of Physics and Nuclear Engineering, IFA, P.O. Box MG6, Bucharest, Romania*
[b] permanent address: *Institute of Nuclear Physics, ul. Radzikowskiego 152, 31-342 Kraków, Poland*
[c] present address: *SUBATECH, IN2P3-CNRS et Université, 44072 Nantes Cedex 03, France*

on the disassembly of hot nuclei and on the possible gas phase. The question of whether or not such very hot nuclear matter formed in violent heavy-ion collisions reaches thermodynamical equilibrium before starting to disassemble is of essential importance in validating the hypotheses assumed in statistical models[8, 9, 10].

2 CHARACTERISTICS OF VAPORIZATION EVENTS

The experimental investigation of vaporization events, which are here defined as events containing only light particles, needs devices capable of performing complete or quasi complete exclusive experiments. In an ideal experiment, an event by event detection of all the particles and fragments with their size (charge and mass), their spatial distribution and their energy should be obtained, thus permitting the exclusion of events containing fragments. Such an ideal experiment has been partially realized using the new 4π detector INDRA[11].

A $193\mu g/cm^2$ ^{58}Ni target was bombarded by different energy ^{36}Ar beams: 32, 40, 52, 63, 74, 84 and 95 AMeV.

The excitation function for vaporization, not corrected for detection efficiency, is shown in fig 2. The cross-section becomes sizeable above 52 AMeV and rises sharply to reach some 10^{-1} of the total reaction cross-section at 95 AMeV[12].

To correctly derive the properties of these events, the dynamics of the collisions must first be studied: are we dealing with the vaporization of one source, or of several sources? The answer is two sources corresponding to binary dissipatives collisions; only a small part of the events could possibly be associated with the decay of a single source and are not included in the analysis. In the following the sources will be called quasi-projectile (QP) and quasi-target (QT). A complete description of the determination of the dynamics of these collisions, and more specifically its influence on the variables described later on, will be presented in a forthcoming article [13]. The spectra of the relative velocity between the sources are broad, extending from 4. cm/ns up to 62,69,75,81 % of the beam velocity at 52,74, 84,95 AMeV respectively. This indicates:

- that the collisions leading to full vaporization of the system correspond to a broad range of impact parameters; this is in agreement with the transverse energy spectra of the vaporization events, from which the impact parameter range can be estimated between 0 and 0.4 b_{max}.
- that for the bulk of the events the relative motion is far from being fully damped, and therefore a large fraction of the available energy remains as collective translational energy.

3 THERMODYNAMICAL ASPECTS

Whatever the incident energy and the source (QP or QT) the excitation energy distributions start rising around 8 AMeV, while the maximum excitation energy reached increases

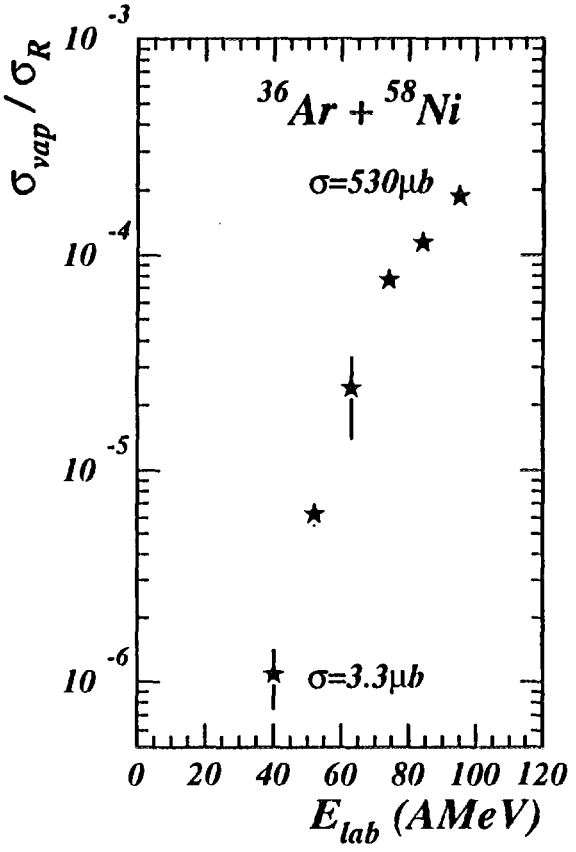

Figure 1: Excitation function for vaporization. Cross-sections are normalized to calculated reaction cross-sections.

with the incident energy, up to 28 AMeV (for the QP) at 95 AMeV. In all cases the heavy source (QT) has more excitation energy than the light one (QP), but the QP has a higher excitation energy *per nucleon* than the QT, which means that thermal equilibrium is not achieved between the two partners of the collision, due to the very short reaction time ($\leq$ 100 fm/c). The energy equilibration time was estimated to be 150-300 fm/c in ref [14]. Whether or not each sub-ensemble subsequently reaches thermal or thermodynamical (thermal and chemical) equilibrium before disintegrating can be investigated by looking at the particle energy spectra and relative abundances in each source, as a function of its excitation energy per nucleon, ϵ^*; a binning $\delta\epsilon^*$=3MeV was chosen.

We discuss first the shapes of the kinetic energy spectra which give information about thermal equilibrium for each source. They are structureless, with exponential tails whose slopes are similar within 30%. More quantitatively, for the emission from a source in thermal equilibrium, all particles should have the same average kinetic energy if we neglect in a first approximation the possible Coulomb barrier. The increase of the kinetic energy with the excitation energy is almost linear for all particles; there is a gap between the more energetic particles (d and ^3He) and the less energetic ones (p and ^4He) of 4-7

MeV or ~20%. This may appear as a significant deviation from thermal equilibrium. If we note that no extra collective expansion energy (proportional to the atomic mass) can be derived from the data, the eventual role of quantal effects and side-feeding has to be checked. In order to test this hypothesis we have modelled the emitting sources using two different approaches based on thermodynamical equilibrium [15]. In the first model, hereafter denoted EVA, we use the Weisskopf standard evaporation theory [16], by considering a series of binary break-ups into excited fragments [17]. This approach is expected to be valid only at rather low excitation energies. In the second model (CEM), which is expected to be more suited to describe the situation discussed here, the emitting source is viewed as a nuclear gas of fermions and bosons in thermal and also chemical equilibrium [18]. In this simple model for a given source density ρ and temperature T, the energy spectra of the different nuclear species (and consequently their relative yields) are uniquely determined from conservation laws and the equilibrium distributions in the grandcanonical ensemble. Corrections to the ideal gas are also included in the form of excluded volume effects [19]. In this calculation ε^* is derived, as in the experiment, from calorimetry. The experimental ε^* range is covered by varying T from 10 to 25 MeV. The freeze out density has been fixed to $\rho = \rho_0/3$, in order to reproduce the experimental ratio between the proton and alpha yields at the lowest excitation energy. EVA gives kinetic energies which are systematically too low whereas CEM reproduces rather well the measured values.

We now come to the chemical composition of the vaporized source. In Fig 2-a,-b is shown the relative particle abundance ($P_j = M_j/M_S$, where M_S is the total source multiplicity and M_j the multiplicity of particle species j in the source) versus the source excitation energy, for the QP at 95 AMeV. α-particles dominate at the lower excitation energies, while nucleons take over when the excitation energy is increased. The deuteron relative abundance is roughly constant; the isobars of mass 3 have opposite behaviours: tritons decrease and ^3He increase when raising the energy. Finally the rare ^6He behave like the α's. This evolution is not due to autocorrelations between the source composition and its excitation energy. Indeed, the mass excess part in eq. 1 accounts for $\sim$ 40% of the excitation energy around 10 AMeV, and only 20% around 22 AMeV. Therefore the increase of the source excitation energy is not only due to the increase of the nucleon abundance, but also to the increase of the kinetic energy of the particles. Note that for a given ε^* the relative yields are the same for the QP and the QT, independently of the bombarding energy. For a system without isospin like the one under consideration here, equal abundances of t and ^3He, and of p and n, are expected from chemical equilibrium, while they show slight differences in our data. Once again the significance of these differences has to be tested against models. EVA and CEM reproduce well the general evolution of the different species as a function of the excitation energy. In EVA the lack of kinetic energies has to be compensated by nucleon creation in order to conserve the energy; indeed the yield of protons is strongly overestimated while the production of Z=2 species is too low (fig. 2a). Otherwise the hierarchy of particle yields is roughly reproduced as well as the total multiplicity (fig. 2c).

Concerning the prompt scenario, for which the ratio between the proton and alpha yields was fixed at the lowest excitation energy, the yields of these two species are correctly reproduced as well as those of deuterons and ^6He. The production of isobars of mass 3 is overestimated by a factor of two (fig.2b). To further understand the significance of the observed deviations with CEM, it would be interesting to also compare the data with a more sophisticated model like the QSM of ref [10], where the contribution from higher-lying resonances is taken into account.

In conclusion, vaporization events have been studied in a broad excitation energy range from 8 to 28 AMeV. They are produced in binary collisions. After reconstruction of the two sources of emission, the yields and the energy spectra of the different species have been studied and compared with the predictions of two statistical models.The model describing the properties of a gas of fermions and bosons in thermal and chemical equilibrium reproduces rather well both the energies and the yields suggesting that thermodynamical equilibrium has been reached by each source.

References

1. L.G. Moretto and G.J. Wozniak, *Annual Rev. of Nucl. and Part. Science* **43** (1993) 379 and references therein.
2. J. Bondorf et al, *Phys. Lett.* **162B** (1985) 30.
3. D.H.E. Gross, Zhang Xiao-ze and Xu Shu-yan, *Phys. Rev. Lett.* **56** (1986) 1544.
4. E. Suraud, Symposium on Nuclear Dynamics and Nuclear Disassembly, (Dallas, USA, April 1989), ed. J. B. Natowitz, World Scientific (1989), p.464
5. M.B. Tsang et al., *Phys. Rev. Lett.* **71** (1993) 1502.
6. D.H.E. Gross, Yu-Ming Zheng and H. Massmann, *Phys. Lett.* **200B** (1988) 397.
7. H.R. Jaqaman, A.Z. Mekjian and L. Zamick, *Phys. Rev.* **C29** (1984) 2067.
8. J. Bondorf et al, *Nucl. Phys.* **A443** (1985) 321, **A444** (1985) 460, **A448** (1986) 753.
9. D.H.E. Gross, *Rep. Prog. Phys.* **53** (1990) 605. and references therein
10. H. Stocker and W. Greiner, *Phys. Rep.* **5** (1986) 277
    J. Konopka et al, *Phy. Rev.* **C50** (1994) 2085.
11. J. Pouthas et al, *Nucl. Instr. Meth. in Phys. Res.* **A357** (1995) 418, **A369** (1996) 222.
12. C.O. Bacri et al, *Phys. Lett.* **B353** (1995) 27.
13. INDRA collaboration, to be published.

14. B. Borderie et al., *Z. Phys A - Hadrons and Nuclei* **338** (1991) 369.

15. B. Borderie et al., *submitted to Phys. Lett.*

16. V.F. Weisskopf, *Phys.Rev. 52 (1937) 295*

17. D. Durand et al, code SIMON *in preparation*

18. A.Z. Mekjan, *Phys.Rev.C 17 (1978) 1051*

19. R. K. Tripathi and L.W. Townsend, *Phys.Rev.C 50 (1994) R7*

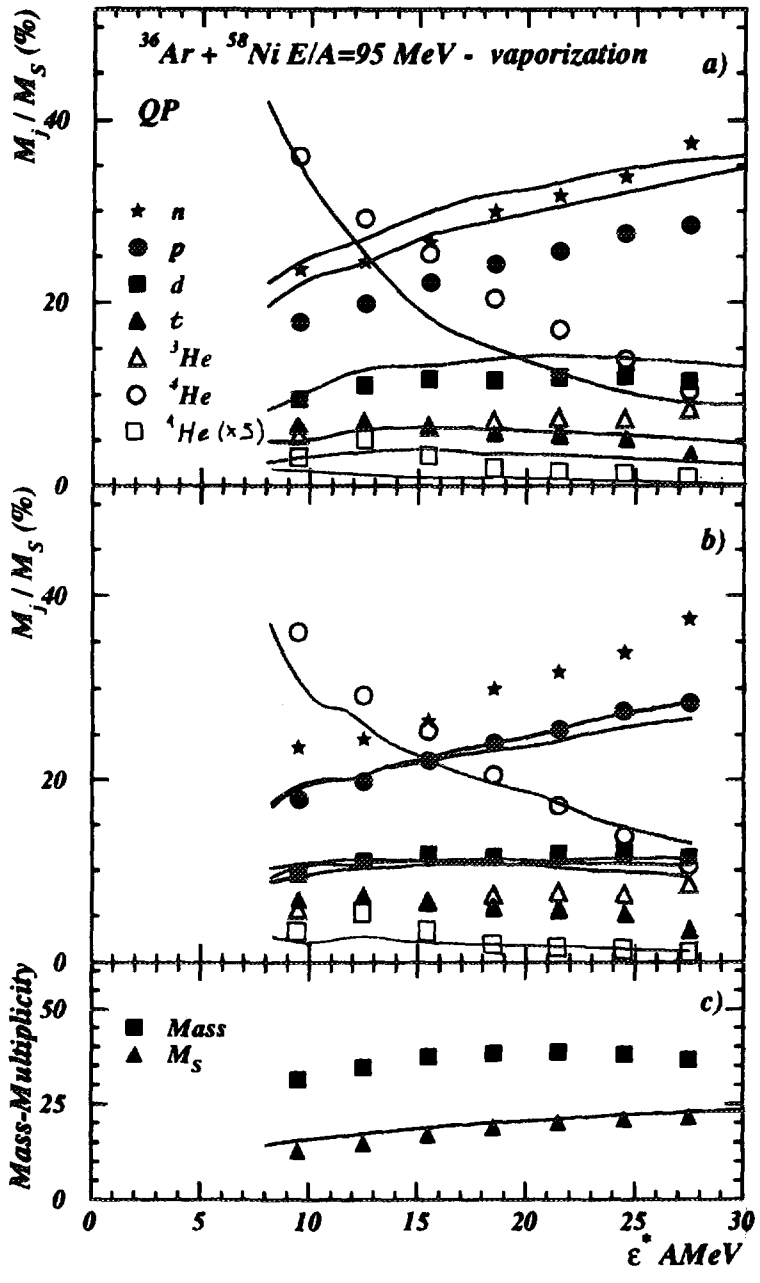

Fig. 2 : a) Composition of the QP as a function of its excitation energy. Symbols are for date while the different lines with corresponding colors are the results of the model (EVA) discussed in the text. b) Same as before but the lines are here the results of the model (CEM) discussed in the text. c) Experimental average mass and total multiplicity of the QP. The line is the result for multiplicity of the model (EVA) with a constant mass A = 36

SEARCH FOR COULOMB-INDUCED MULTIFRAGMENTATION IN THE REACTION GD+U AT 36 MEV/U

C.O. Bacri[a], M. Squalli[a], B. Borderie[a], J. Colin[b], D. Durand[b], J.D. Frankland[a], J.F. Lecolley[b], M. Parlog[a],[1], M.F. Rivet[a], L. Tassan-Got[a], G. Auger[c], J. Benlliure[c], R. Bougault[b], R. Brou[b], J.L. Charvet[d], A. Chbihi[c], D. Cussol[b], R. Dayras[d], E. De Filippo[d], A. Demeyer[e], P. Ecomard[c], P. Eudes[f], D. Gourio[f], D. Guinet[e], R. Laforest[b], P. Lautesse[e], J.L. Laville[f], L. Lebreton[e], A. Le Fèvre[c], T. Lefort[b], R. Legrain[d], O. Lopez[b], M. Louvel[b], N. Marie[c], V. Metivier[b],[2], L. Nalpas[d], A. Ouatizerga[a], J. Peter[b], E. Plagnol[a], A. Rahmani[f], T. Reposeur[f], E. Rosato[b], F. Saint-Laurent[c], J.C. Steckmeyer[b], B. Tamain[b], E. Vient[b], C. Volant[d], and J.P. Wieleczko[c].

[a] *Institut de Physique Nucléaire, CNRS-IN2P3, 91406 Orsay Cedex, France*
[b] *Laboratoire de Physique Corpusculaire, ISMRA, Bd Maréchal Juin, 14050 Caen Cedex, France.*
[c] *GANIL, CEA, IN2P3-CNRS, B.P. 5027, 14021 Caen Cedex, France*
[d] *CEA, DAPNIA, SPhN, CEN Saclay, 91191 Gif sur Yvette Cedex, France*
[e] *IPN Lyon, IN2P3-CNRS et Université, 69622 Villeurbanne Cedex, France*
[f] *SUBATECH, IN2P3-CNRS et Université, 44072 Nantes Cedex 03, France*

The knowledge of what kind of instabilities could cause a nuclear system to multifragment is important for the understanding of the dynamics of heavy ion collisions in the energy range 10-100 MeV/u [1]. For heavy systems at lower incident energies, Coulomb instabilities [2] can be responsible for the complete dissociation of the system and then, only a gentle compression phase is necessary. From a theoretical point of view, static Hartree Fock calculations have predicted that competition between surface tension and Coulomb repulsion can lead, for very heavy systems, to the formation of exotic configurations, like bubbles [3]. Borderie et al. [4] have then confirmed such conclusions by performing dynamical Landau-Vlasov calculations for the system Gd+U at 36 MeV/u.

We will present here some results obtained for Gd+U at 36 MeV/u at the GANIL facility. The experiment was performed with the 4π INDRA detector of charged products[5], which allowed the detection of quasi-complete events, for which at least 80% of the initial charge ($Z_{tot} = Z_{proj} + Z_{target} = 156$) has been measured. Such completeness is very important since we are looking for the multifragmentation of a very heavy composite system comprising almost all the nucleons ($A \approx 400$). Detection of all fragments emitted during this de-excitation stage is then crucial.

[1] *Permanent adress : Institut of physics and Nuclear Engineering,IFA, P.O. Box MG6, Bucharest, Roumania*

[2] *Present adress : SUBATECH, IN2P3-CNRS et Université, 44072 Nantes Cedex 03, France*

SELECTION OF SINGLE-SOURCE EVENTS

To classify these events, we use a combination of global variables, namely the momentum tensor analysis and the total centre of mass kinetic energy (TKEcm), in analogy with the diagram used by Wilczynski to demonstrate the presence of dissipative nuclear orbiting in collision below $10MeV/u$ [6].

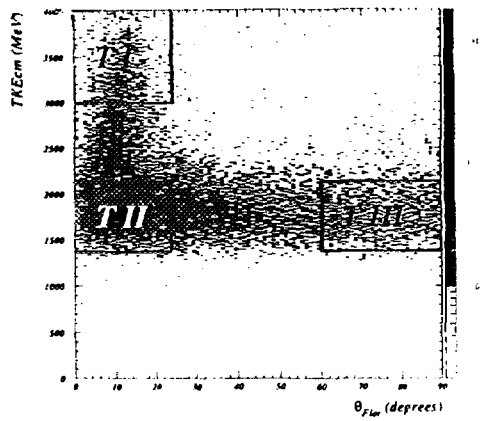

Figure 1 : *Total kinetic energy measured in the centre of mass of the reaction versus θ_{Flot}, the angle between the main axis of the energy ellipsoid and the beam direction.*

The so called "energy tensor" is defined as $Q_{ij} = \sum_\nu \frac{p_i(\nu)p_j(\nu)}{2m(\nu)}$ where the sum runs over all fragments $\nu(Z \geq 5)$. p_i and p_j denote the Cartesian momentum components of the fragment of mass $m(\nu)$ in the centre of mass (CM) frame of the system (note that the velocity of the fragment CM, averaged over all the events, is the same as the CM of the system). Diagonalization of this tensor permits the construction of an ellipsoid in energy space. Its three axes are defined by the tensor's eigenvectors $(\vec{e}_i)$, its shape by the eigenvalues $(\lambda_3 \geq \lambda_2 \geq \lambda_1$; these values are normalized to their sum). The angle between the main axis (defined by $\vec{e}_3$) and the beam direction (i.e. the direction of the velocity of the CM) will be called in the following θ_{Flot}. This angle is related to the rotation of the whole system, before it separates into two sources and/or undergoes de-excitation by evaporation or multifragmentation. In the case of a unique source of emission, the flow direction should be undefined and isotropically distributed.

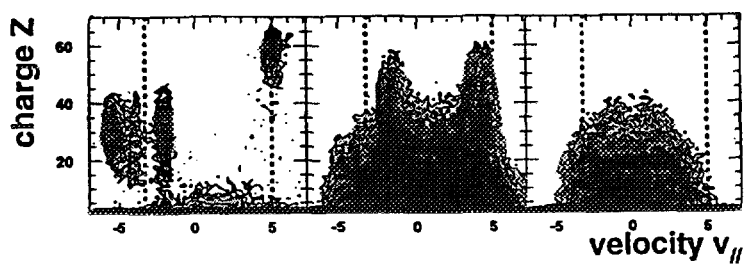

Figure 2 : *$Z - V_{\|}$ plots for the 3 regions of interest. The dashed lines indicate the target (left) and projectile (right) velocities in the centre of mass in $cm.ns^{-1}$ The different plots correspond, from left to right, to regions T1 to T3.*

Region III ($\theta_{Flot} \geq 60°$) corresponds to a flat $cos(\theta_{Flot})$ distribution and should select a unique source of emission. Indeed, the $Z - V_{\parallel}$ plot (Fig. 2) clearly shows an evolution from binary collision (T1) to a single source of emission (T3).

SHAPE OF THE MULTIFRAGMENTING SINGLE SOURCE

A shape analysis, based on the study of the eigenvalues clearly shows the unique source (T3) to be spherical, in the energy space. These events have a mean fragment multiplicity of 6.4. They correspond to a cross section of 22. mb, value to be compared with the total reaction cross-section of 8.1 b.

In order to study these events and to know if exotic shapes like bubbles have been formed, we examine the evolution of the mean kinetic energy (in MeV) of each fragment as a function of its charge. The bell shape clearly indicates that heavier fragments are emitted with lower energies as compared to lighter ones, as if heavier fragments were located closer to the centre of a nuclear system emitting isotropically (Fig. 3, solid points). Indeed, for a bubble configuration, the evacuation of the central region should lead to a lack of small CM velocities (and then energies for heavier fragments).

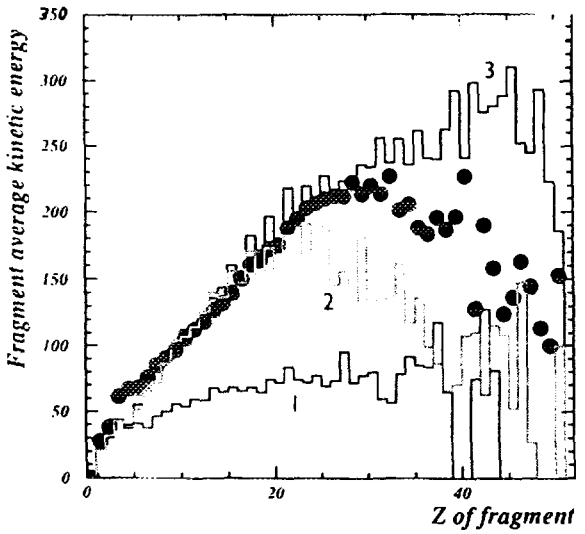

Figure 3 : *Mean kinetic energy in MeV versus Z. Solid points indicate the mean experimental values. Histograms show the result of the simulation; 1: sequential decay; 2: simultaneous de-excitation of a spherical source with 1. MeV/u expansion energy with the heavier fragment in the center. 3: simultaneous de-excitation of a spherical source with 1. MeV/u expansion energy; the sphere is then as compact as possible.*

In order to get more quantitative information, we have used the simulation code SIMON [8] with different hypotheses and we have compared its results with the experimental data. The code starts from a given excited nuclear system composed of a certain number of pre-fragments (hypothesis of freeze-out volume). Their mass and charge distributions are chosen at random. These fragments are then arranged according to a chosen shape. Coulomb trajectories are then solved, respecting conservation laws and taking into ac-

count thermal motion and a possible collective expansion (the latter being implemented by means of a self-similar motion of matter). Secondary decays (evaporation of particles and fragments, and fission) are considered, including discrete excited states for $Z < 5$. Sequential (one pre-fragment corresponding to the source) or simultaneous (more than one pre-fragment) decays can be computed. Experimental data has led us to put the following ingredients in the simulation, at least as a first step in this study : the initial nuclear system has the total charge and mass of the experimental entrance channel ($A = 393, Z = 156$) because up to now, very few pre-equilibrium effects have been found in our data; for the same reason, the initial excitation energy, E^*, is the difference between the total energy available in the centre of mass and the Q-value for the formation of the compound system — this value of $E^* = 6.7 MeV/u$ is then an upper limit; the number of pre-fragments is 5, and their masses have a minimum value of 20; as suggested by experimental data, pre-fragments are arranged in a sphere.

The results achieved are shown in Fig. 3. The sequential de-excitation (histogram 1) does not reproduce the data. In a simultaneous decay, 1.MeV/u self similar expansion is necessary to reproduce the lighter fragments ($Z \leq 30$) (histograms 2 and 3). Moreover, the shape of the calculated curve ofr heavier ones ($Z \geq 30$) is sensitive to the geometry of the source: when the heavier fragment is located in the centre of the sphere (histogram 2), it does not feel the expansion and therefore has a low energy. Conversely, when the sphere is homogeneous (histogram 3), the calculated energies are increased with the charge Z of the fragments. The experimental situation (solid points) is a mixture of these two situations. Multiplicities (total and fragment), Z and relative velocities distributions are also well reproduced, in the simultaneous scenario.

CONCLUSION

Experimental study of the Gd+U system at 36 MeV/u with the 4π INDRA detector has allowed us to evidence the multifragmentation of a single source of nearly 400 nucleons. These selected events correspond to 22. mb, as compared to 8.1 b for the total reaction cross section. A spherical shape, with the heaviest pre-fragment close to the centre, and with a self-similar expansion energy of 1. MeV/u is the only way to reproduce experimental data with the SIMON code. Such a value has to be compared with the smaller one of ≤ 0.5 MeV/u obtained when Coulomb repulsion is the only cause of expansion (this value is deduced from [4]). It seems that 36 MeV/u is too high an energy to induce a pure Coulomb multifragmentation : compression-expansion effects seem to be non-negligible at such a bombarding energy, which is in disagreement with the Landau-Vlasov model using a local force and no isospin effects [4]. A more detailed version of this text is available in [9].

References

1 L. Moretto, G. Wozniak, Ann. Rev. Nucl. Sci. **43**(1993)379.

2 S. Levit, P. Bonche, Nucl. Phys. **A437** (1985) 426.

3 P. Bonche et al., Nucl. Phys. **A436** (1985) 265.

4 B. Borderie et al., Phys. Lett. **B302** (1993)15.

5 J. Pouthas et al., NIM **A357** (1995)418.

6 J. Wilczynski et al., Phys. Lett. **B47**(1973)484.

7 D. L'Hote, J. Cugnon, Nucl. Phys. **A397** (1983)519.

8 D. Durand et al., SIMON code (in preparation).

9 C.O.Bacri et al., proceedings of XXXIV Int. Winter Meeting on Nuclear Physics, Bormio (1996).
C.O. Bacri et al., IPNO-DRE-96-93, unpublished

Abs [The multifragmentation of atomic nuclei is investigated in the framework of mean-field approximation in order to gain information on the equation of state of nuclear matter.

SPINODAL DECOMPOSITION OF ATOMIC NUCLEI

Alfio Guarnera[1,2], Maria Colonna,[1,2] and Philippe Chomaz,[1]

[1]GANIL (DSM/CEA,IN2P3/CNRS)
BP 5027, 14021 CAEN Cedex,France
[2]LNS, Viale Andrea Doria
Catania, Italy

During the multifragmentation of atomic nuclei it seems that identical (or almost identical) initial conditions are leading to very different partitions of the system in interaction. In such a case it is necessary to develop approaches that are able to describe the observed diversity of the final channels. On the other hand the multifragmentation being characterised by the formation of relatively large fragments, one may think that the mean field plays an important role to organise the system in nuclei. Indeed, the mean field (ie, the long range part of the bare nucleon-nucleon interaction) is at the origin of the cohesion of the clusters. Moreover, it has been shown that extentions of mean-field approaches including a Boltzmann-like collision term were providing excellent descriptions of many aspects of heavy ion reactions around the Fermi energy (see for example ref.[1] and references therein).

The problem with mean-field approaches is that they are unable to break spontaneously symmetries. Therefore, they cannot describe phenomena where bifurcations, instabilities or chaos occurs. However, since few years, many tests and studies have been reported showing that the stochastic extensions of mean-field approaches were good candidates for the description of such catastrophic processes. Indeed, the presence of a source of stochasticity allows to explore a large variety of evolutions. Therefore, such approaches may provide valuable descriptions of the dynamics of phase transitions (at least in the case of first-order phase transitions for which the mean-field is known to give a reasonable description of equilibrium properties).

Let us first recall that nuclei are understood as drops of a Fermi liquid [2, 3, 4] and, since we can also observe free nucleon gas, we expect the existence of at least one liquid-gas phase transition.

As matter of fact, the nuclear forces are known to have a long-range attractive tail and a short-range repulsive hard-core and so to be analogous to a Van der Waals interaction. Therefore, we expect the same phenomenology as far as phase transitions are concerned.

The phase diagram of nuclear matter is still partially unknown because it is very

difficult to extract unambiguous information from the experimental observation. Indeed, it is only possible to create in laboratory tiny short-lived fragments of excited matter. However, it is generally believed that during a nuclear collision the system may explore a large portion of the nuclear phase diagram and that the observed copious fragment production might be related to a liquid-gas phase transition.

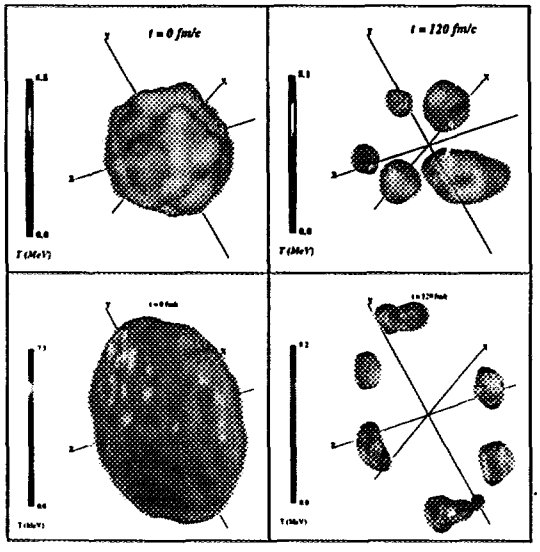

Figure 1. Stochastic mean-field evolutions of two different sources: Part a) (top) Spinodal decomposition of a spherical source; Part b) (bottom) of a disk (from ref.[13]).

In particular, it is generally believed and shown by one-body approaches that the composite system formed during a collision may enter deep in the liquid-gas coexistence region and even in the spinodal zone that is the region where the system is mechanically unstable against infinitesimal density fluctuations. Considering the involved size and time scales this is certainly a region adequate for the nuclear multifragmentation.

We can now study the fragmentation of a hot and diluted nucleus lying deep inside the spinodal zone of instabilities. We have considered masses, charges, densities, temperatures, spins, expansion,... as predicted by one-body dynamic approaches.[8] To describe the spontaneous symmetry breaking associated with the fragmentation of hot spherical sources, we have used the recently developed stochastic approaches.[9]

Figure 1.a presents one of the many predicted partitions of a large hot and diluted nucleus containing 210 nucleons that have been fragmented in 5 pieces under the influence of spinodal instabilities. This is a rather typical event (the average multiplicity computed over 400 simulation being sharply peaked on the production of 5 fragments).

This dominant multiplicity is clearly linked to the occurrence of spinodal instabilities since this is topologically the optimum way to have undulations, in a finite system, with an average distance between density lobes compatible with the most unstable wave length, $\lambda = 10fm$, of spinodal instabilities in nuclear matter.

This characteristic is better seen on the analyses presented in figures 2. On the first hand, we observe in figure 2.a radial oscillations associated with a wave length

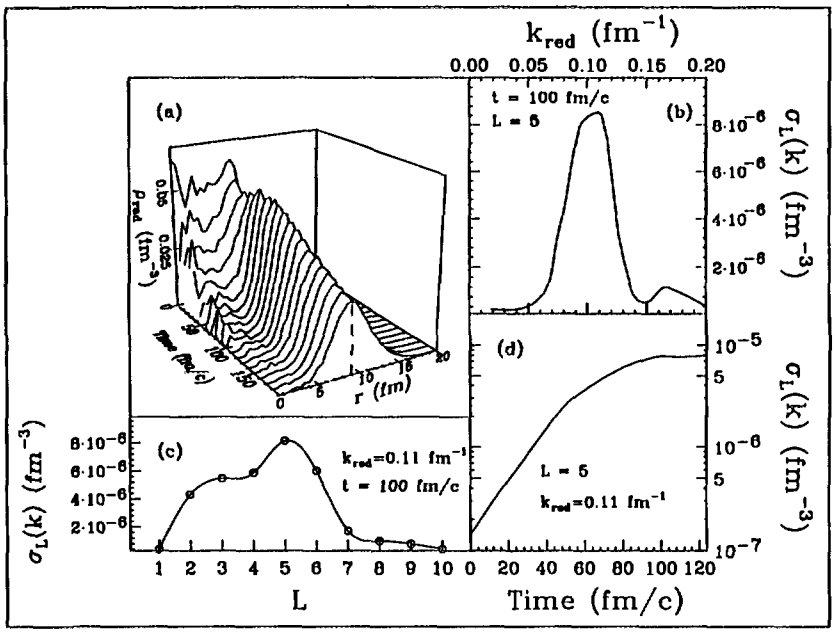

Figure 2. Analysis of the multifragmentation events analogous to the one presented in figure 1a). The part a) presents the radial projection of the density, part b) multipole expansion computed at 100 fm/c, part c) analysis in terms of Bessel functions for the multipole L=5; part d) time evolution of the L=5 fluctuations.

around 10 fm. In average the matter gets concentrated close to the surface and a hole is produced at the centre of the nucleus.

In order to get a deeper insight into the characteristic of the unstable modes in finite nuclei we have performed an analysis in terms of spherical harmonics projecting the fluctuations on the modes defined by $j_L(kr)Y_{LM}(\hat{r})$. This analysis shows that these projections are strongly peaked at wave numbers that, taking into account the L dependence of the Bessel function, correspond to a distance between two radial maxima around 10 fm. Moreover, this strong peaking of the k-dependent projection demonstrates that the actual fluctuation resembles to a Bessel function, i.e., to the multipole expansion of a plane wave with 10 fm wave length.

On the other hand, if for this k_L of maximum instability we draw the L-dependence of the measured fluctuation (figure 3.c) we can observe that the multipolarity 5 dominates the instabilities. This multipolarity L=5 corresponds to a distance of about 10 fm between two maxima of density fluctuation. As a matter of fact, this multipolarity L=5 induces the fragmentation of the system in 5 equal pieces. For this multipolarity the most unstable radial k corresponds to $k = 0.6fm^{-1}$ that is the most unstable wave number of the infinite matter system at the considered temperature and density. Finally, on figure 3.d) we can clearly see the exponential amplification of unstable modes with a characteristic growth time $\tau \approx 35fm/c$ in agreement with the nuclear matter calculation.

It might be important to study the role of the initial shape of the source on the final topology of the fragment partition. On figure 2 we show the comparison of the predicted disassembly of two different initial sources; the first one being spherical and the second one prolate with an aspect ratio 2:1. In both cases the system develops radially a spinodal instability. Making a hole at the centre is the only possible way

to develop the instabilities considering the limited size of the system. Therefore, the spinodal decomposition of both systems is generating non compact geometries with a hole in the centre. These fragmentations resemble to bubble-like or torus-like topologies but it should be notice that in the present simulations they only arise from spinodal instabilities. Such non-compact topologies might have been observed experimentally by the MSU group and the Nautilus group in GANIL.

In conclusion we have seen that a large enough finite system is developing instabilities very close to the one predicted for the equivalent infinite nuclear matter. Therefore, one may hope that studying the spinodal decomposition of finite system may directly provide information on the nuclear equation of state.

REFERENCES

1. G.F. Bertsch and S. Das Gupta, *Phys. Rep.* 160:190 (1988).
2. A. Bohr and B. Mottelson, "Nuclear Physics, " Benjamin N.Y.,(1969).
3. A. Bohr and B. Mottelson, "Nuclear Structure, " Benjamin N.Y.,(1975).
4. P. Ring and P. Shuck, "The Nuclear Many-body Problem, " Springer-Verlag N.Y.(1981).
5. A.L. Fetter and J.D. Walecka, "Quantum Theory of Many Particle Systems," Mc Graw - Hill, New York (1971).
6. C.J. Pethick and D. G. Ravenhall, Ann. Phys. (New York) 183:131 (1988).
7. X.D. Pines-Nozieres, "The Theory of Quantum Liquids," Addison-Wesley, Reading, MA, (1989).
8. M. Colonna, N. Colonna, A. Bonasera and M. Di Toro, *Nucl. Phys.* A541:295 (1992).
9. A. Guarnera, M. Colonna and Ph. Chomaz, to be published in *Phys. Lett.* (1996).
10. A. Guarnera, Ph. Chomaz and M. Colonna, to be published.

OBSERVATION OF SPINODAL DECOMPOSITION IN NUCLEI?

A. Guarnera[1,2], Ph. Chomaz[1] and M. Colonna[1,2]

[1]) *GANIL (DSM/CEA,IN2P3/CNRS), B.P. 5027, F-14021 Caen Cedex, France*

[2]) *LNS, Viale Andrea Doria, Catania, Italy*

Although the static properties of nuclear matter have been the subject of many studies [1, 2], the nuclear equation of state and the nuclear phase diagram remain open problems, because they can only be inferred from the understanding of the dynamics of nuclear reactions and of the evolution of the formed hot systems. Indeed, it is commonly believed that, during a collision, a wide zone of the nuclear matter phase diagram might be explored [3] and that the nuclear system may deeply enter in the spinodal zone, which is the region of the phase diagram where the system is mechanically unstable against infinitesimal density fluctuations.

Nowadays, the reaction mechanism responsible for the multifragment production experimentally observed in medium-energy heavy-ion reactions and its possible connection with a spinodal decomposition or a critical phenomenon are largely debated. Many models aiming to describe this multifragmentation are based on static (or equilibrium) statistical approaches and do not take into account the dynamics of the phase transition [4, 5, 6].

In the framework of mean field approaches, some studies of fragmentation induced by volume or shape instabilities have recently been published [7, 8, 9, 10]. However, as soon as instabilities are encountered in dynamical simulations, fragments are formed through the growth of fluctuations and hence a good understanding of the fluctuation sources is important to reach reliable conclusions. This is the reason why stochastic mean field approaches have been developed [11, 12].

Since this study is based on stochastic mean field approaches, let us first briefly recall their essential features. In standard mean-field approaches the system is described

Multifragmentation in heavy ion collisions is investigated in the framework of mean-field theory, in order to gain information on the equation of state of nuclear matter. Spinodal decomposition in nuclei is studied.

in terms of its one-body density $f(\mathbf{r},\mathbf{p},t)$. However, it is known that the neglected many-body correlations may become of crucial importance when instabilities or bifurcations occur, like in the multifragmentation processes we are interested in. In such a case, the mean-field trajectory is loosing its validity.

A possible way to take into account the feed-back of the unknown correlations onto the evolution of the one-body density is to add a stochastic term in the mean field equation, in analogy with the Langevin treatment of the Brownian motion. This leads to the so-called stochastic one-body theories, in which the system may experience a partly random evolution in response to the action of a source of fluctuations. Therefore, one must now follow the evolution of an ensemble of one-body densities, $\{f^{(n)}(\mathbf{r},\mathbf{p},t)\}$.

For example, the stochastic extension of the nuclear Boltzmann equation leads to the Boltzmann-Langevin (BL) approach, in which the nucleon-nucleon collisions are considered as random processes [11, 12]. The time evolution of each element $f^{(n)}(\mathbf{r},\mathbf{p},t)$ of the ensemble of one-body densities is therefore governed by the following equation:

$$\frac{\partial f^{(n)}}{\partial t} - \{h[f^{(n)}], f^{(n)}\} = K[f^{(n)}] + \delta K^{(n)}[f^{(n)}] \qquad (1)$$

where $\{.,.\}$ represents the Poisson bracket. The main ingredients that enter this equation are: i) The actual self-consistent mean field potential $U[f^{(n)}]$, introduced through the effective Hamiltonian $h[f^{(n)}] = p^2/2m + U[f^{(n)}]$; ii) The average part of the collision integral $K[f^{(n)}]$, which represents the average effect of the Pauli-blocked nucleon-nucleon collisions; iii) The Langevin term $\delta K^{(n)}[f^{(n)}]$, which accounts for the fluctuating part of the collision integral [11, 12]. Simplified methods to treat the stochasticity introduced by the term δK have been recently developed and tested, in order to be able to afford 3D calculations [13, 14, 15, 16]. In the results we show here, the stochastic mean-field method of ref. [16] has been used.

For infinite nuclear matter, the eigenmodes are plane waves and it has been shown that the most unstable wave length is close to $\lambda \approx 10$ fm in a wide part of the spinodal region [14, 17]. The growth rate of the unstable modes are intimately connected with the properties of the nuclear forces and in particular with the range of the attractive part of the potential. In fact the finite range of the interaction which can be associated with surface energy when fragments are formed, is responsible for the suppression of the small wavelength instabilities and then for the ultra-violet cut-off in the dispersion relation [1, 17] (see fig.2).

In finite systems we expect that some of these features to be preserved:the time scales, the favoured partition in equal mass fragments and even the quenching of small

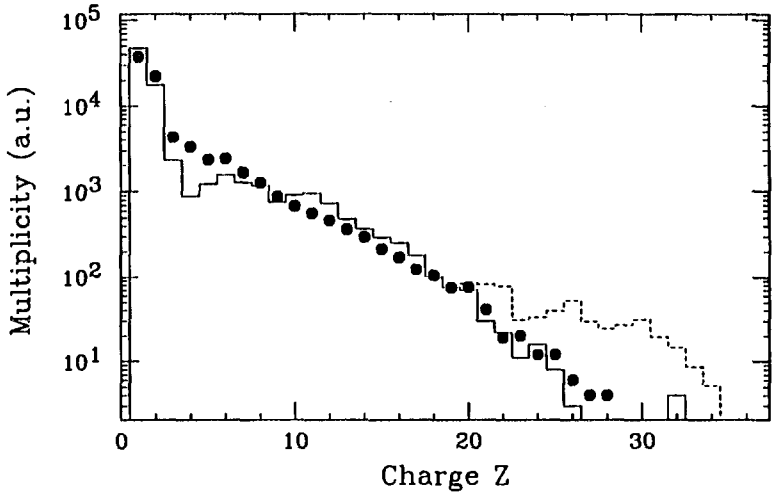

Figure 7 - Fragments charge distribution associated to the central events in the reaction $Xe + Sn$ at 50 MeV/A. The points correspond to the experimental data [19], the histograms to the results of the simulations before (dashed) and after (solid) making the same selection for the centrality as in the experimental data.

cluster production.

Some experimental data are already pleading in favour of the spinodal decomposition scenario. However, before entering this discussion, we would like to stress that it might be premature to conclude about the fact that some multifragmentation reaction might be related to a spinodal decomposition because both the experimental results might still present some ambiguities and it may be that modified versions of the actual theoretical models describing the multifragmentation might also explain the experimental data without involving spinodal instabilities. However, the fact that the composite system should enter the spinodal zone is predicted by almost all the one-body approaches and we will see that our "ab initio" stochastic mean-field simulations of subsequent spinodal decomposition are able to describe correctly various aspects of multifragmentation in central events.

The theoretical calculation have been performed as follow: i) the reaction is first treated within a regular one-body approach using the BUU code based on a lattice hamiltonien method as described in ref. [18]; This calculation is performed until the system runs across instabilities; Starting from this point, the bare mean field approach cannot be applied anymore and one should take into account correlations and fluctuations; It should be noticed that during the first stage of the reaction the inclusion of

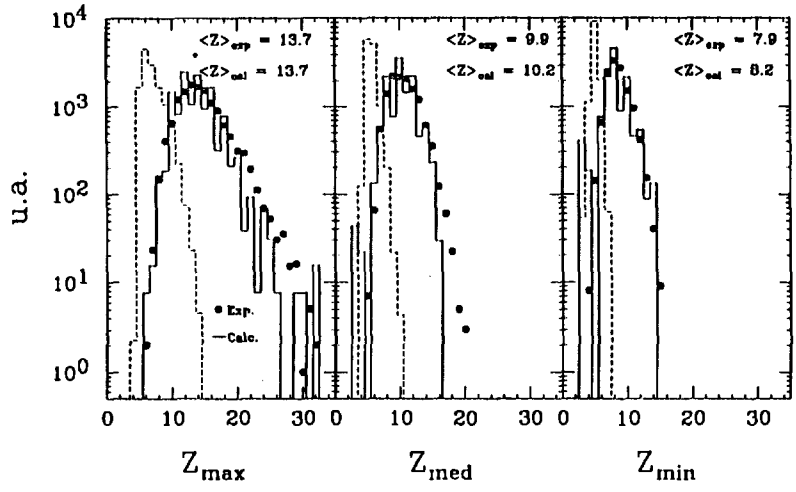

Figure 6 - Charge distributions of the three largest fragments for the reaction $Xe + Sn$ at 50 MeV/A. The points correspond to the experimental data [19] and the histogram to the simulation. Mean values are also reported.

the fluctuations was not crucial because the mean field dynamics complemented with a collision term was representing a reasonable ensemble average; ii) The unstable dynamics is simulated using a stochastic mean-field approach, as described in reference [16], which corresponds to the addition of specific noise to the BUU dynamics; This simulation is followed until fragments are formed; iii) Finally, when the fragments are formed they are still hot and their decay may take a very long time; However, this slow process is well described by statistical decay approaches; Therefore, instead of simulating this decay within the mean field approach, which is not able to predict correctly the particle and fragments emission, we prefer to use a statistical model; This part, that includes both the fragments classical trajectory and the evaporation process, is simulated using the code SIMON developed by D. Durand.

We have also performed a comparison with the recent results of the INDRA collaboration [19] concerning events with the formation of a composite source in the Xe+Sn reaction at 50 MeV per nucleon. Indeed, also in this case, our one-body approaches are predicting the formation of a composite system diving deeply in the spinodal region. Figure 7 presents the fragment charge distribution associated with these events while Figure 8 displays the individual charge distributions of the 3 largest fragments. One can see a rather good agreement between experiment and theory. In particular the tail at large Z is well reproduced by the theory. We would like to recall that this tail

is coming from both the mode beating and the final state interaction between fragments. On the other hand, the charge distributions of the 3 largest fragments are well reproduced both in centre position and in global shape (and width).

In conclusion, while more studies are certainly needed to compare detailed features of the multifragmention events with the spinodal decomposition scenario, the presented results are very encouraging. Stochastic mean-field approaches can be now applied for realistic simulation in 3D. These dynamic approaches are now able to compete with multifragmentation models and can be directly compared with experiments.

Acknowledgements

We acknowledge the Indra collaboration for the opportunity to present some of their *results prior to publication.*

This work was supported in part by the Commission of the European Community, under Contract No. ERBCHBI-CT-930619.

References

[1] H. Heiselberg, C.J. Pethick, and D.G. Ravenhall, Ann. Phys. **223** (1993) 37.

[2] M. Brack, C. Guet and H.-B. Haakansson, Phys. Rep. **123** (1985) 263.

[3] G.Bertsch and P.J. Siemens, Phys. Lett. **B126** (1983) 9.

[4] For a review see, L.G. Moretto and G.J. Wozniak, Annual Rev. of Nuclear and Particle Science, **43** (1993) 379.

[5] D.H.E.Gross, Rep. Prog. Phys. **A53** (1990) 605.

[6] X. Campi, Phys. Lett. **B208** (1988) 351.

[7] L.G. Moretto, Kin Tso, N. Colonna, and G.J.Wozniak, Phys. Rev. Lett. **69** (1992) 1884.

[8] W. Bauer, G.F. Bertsch, and H. Schulz, Phys. Rev. Lett. **69** (1992) 1888.

[9] B. Borderie, B. Remaud, M.F. Rivet, and F. Sebille, Preprint IPNO-DRE (Jul'92).

[10] H.M.Xu et al., Phys. Rev. **C48** (1993) 933.

[11] S. Ayik and C. Gregoire, Phys. Lett. **B212** (1988) 269; Nucl. Phys. **A513** (1990) 187.

[12] J. Randrup and B. Remaud, Nucl. Phys. **A514** (1990) 339.

[13] M. Colonna, G.F. Burgio, Ph. Chomaz, M. Di Toro, and J. Randrup, Phys. Rev. **C47** (1993) 1395.

[14] M. Colonna and Ph. Chomaz, Phys. Rev. **C49** (1994) 1908.

[15] Ph.Chomaz, M.Colonna, A.Guarnera and J.Randrup, Phys. Rev. Lett. **73** (1994) 3512.

[16] A.Guarnera, M.Colonna and Ph.Chomaz, to appear in Phys. Lett. B (1996).

[17] S.Ayik, M.Colonna and Ph.Chomaz, Phys.Lett. **B353** (1995) 417; B.Jacquot, M.Colonna, S.Ayik, Ph. Chomaz, in preparation.

[18] A.Guarnera, Ph.D. Thesis, 1996, GANIL

[19] N.Marie, Ph.D. Thesis, 1995, GANIL-T-95-04.

RPA Instabilities in Finite Nuclei at Low Density

B. Jacquot[1], Ph. Chomaz[1], M. Colonna[1,2,3] and S. Ayik[4,5]
[1)] GANIL, B.P. 5027, F-14021 Caen Cedex, France
[2)] CEA, DAPNIA/SPhN, CEN Saclay, 91191 Gift sur Yvette Cedex, France
[3)] Laboratorio Nazionale del Sud, Viale Andrea Doria, I-95129 Catania,Italy
[4)] Tennessee Technological University, Cookeville, Tennessee 38505, USA
[5)] Middle East Technical University, 06531 Ankara, Turkey

The experimental observation of the abundant fragment production obtained in violent heavy ion collisions has generated many theoretical efforts for understanding the mechanisms responsible for such an explosion of the nuclear systems. It has been proposed that, because of the initial collisional shock, a large part of the nuclear matter phase diagram may be explored and new states can be accessed, hence making it possible to enter the unstable region of the phase diagram [1, 2, 3]. In such a context, fragment formation may take place through a rapid amplification of dynamical instabilities in the spinodal region. In order to deal with the dynamics of these large density fluctuations, stochastic semi-classical approaches of the *Boltzmann – Langevin* type, have been developed and applied to investigate the spinodal decomposition of nuclear systems [4, 5]. As far as the early development of instabilities is concerned, useful information can be gained, more easily, in the linear response framework of such approaches [6, 7]. Also, the response of the system to small initial perturbations can be studied within the Landau theory of Fermi liquid [8, 9]. It turns out that, due to the finite range of the nucleon-nucleon attraction, the small amplitude density inhomogeneities need to have a relative large spatial extension ($\approx 5-7\ fm$) in order to grow [2, 6]. The fact that the corresponding most unstable wave numbers ($k \approx 0.8-1\ fm$) are of the same order of magnitude as the Fermi momentum of the dilute systems suggests that quantal effects may have an important influence on the spinodal decomposition process, and should be included into the treatment for a quantitative description of the growth of instabilities. In a quantal RPA framework, it has been shown in [10] that in unstable nuclear matter, the most important modes shift towards longer wave lengths ($\lambda \approx 10\ fm$) due to quantal effects.

In the calculations, we use a Skyrme-like parametrization for the effective mean-field potential and we have solved the instabilities of a dilute nucleus, linearizing the time dependent Hartree-Fock equations in the co-moving frame.

In order to solve the dispersion relation first we need to determine the single-particle representation of the constraint Hartree-Fock problem (CHF). We have also followed a more schematic approach and solve the dispersion relation by employing the harmonic oscillator wave functions and the wave functions of a Wood-Saxon-like potential, instead of the CHF wave functions. In order to obtain accurate solutions of the dispersion relation, a sufficiently large number of orbitals should be incorporated into the calculations. Here, we present calculations carried out for sources containing $A = 40$ and $A = 140$ nucleons by including 100 and 120 orbitals, respectively.

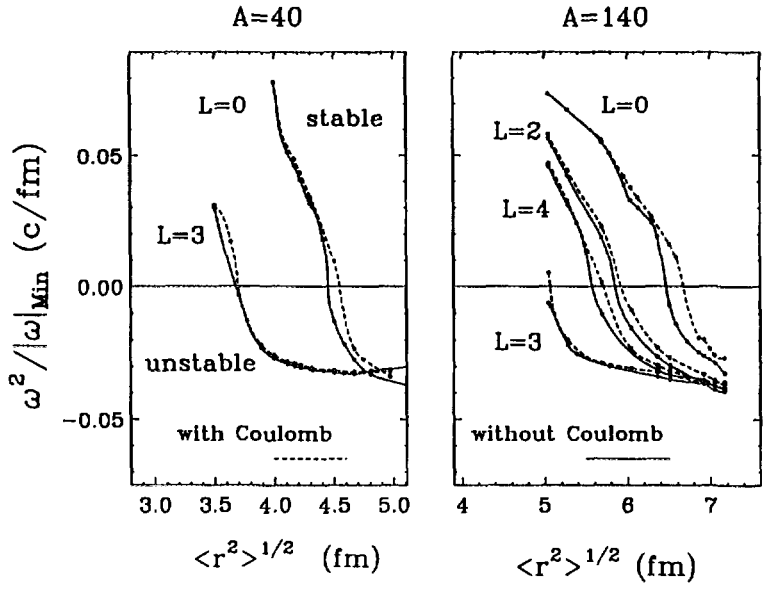

Figure 1: *Minimum values of $\omega^2/|\omega|$ for different multipole modes for $A = 40$ (left part) and $A = 140$ (right part) as a function of the root-mean-square-radius with the Coulomb force (dashed lines) and without the Coulomb force (solid lines) at zero temperature, calculated in the harmonic oscillator representation.*

In figure 1, minimum values of the quantity $\omega^2/|\omega|$ for modes with multipolarity $L = 0, 2, 3$ are plotted for two source containing $A = 40$ and 140 nucleons as a function of the root-mean-square-radius $< r^2 >^{1/2}$ of the system at zero temperature. These results are obtained by solving the dispersion relation employing the harmonic oscillator representation.

When the minimum value of the quantity $\omega^2/|\omega|$ is negative, the corresponding mode becomes unstable. In this manner the CHF calculations provide a good basis for understanding transition between the stable and the unstable regions . As seen from figure 1, for increasing root-mean-square-radius the collective modes become softer and around $< r^2 >^{1/2} \approx 3.8\ fm$ the octupole mode becomes unstable.

As seen from the figure, the Coulomb force has a minor effect in the light system, and in the case of the heavier system, the degree of the instability is slightly decreased by the Coulomb force. Here, the fluctuating part of the mean-field due to the Coulomb force is calculated according to [13].

Figure 2 shows the radial wave numbers associated with the quadrupole and octupole modes as a function of the root-mean-square-radius of the density distribution. These wave numbers correspond to the lowest mode in the stable region and the most unstable mode in the unstable region. In the figure, the crossover from stable to unstable regions is indicated by vertical lines. In the case of the quadrupole mode, the crossover occur at $< r^2 >^{1/2} \approx 4.2\ fm$, whereas the oc-

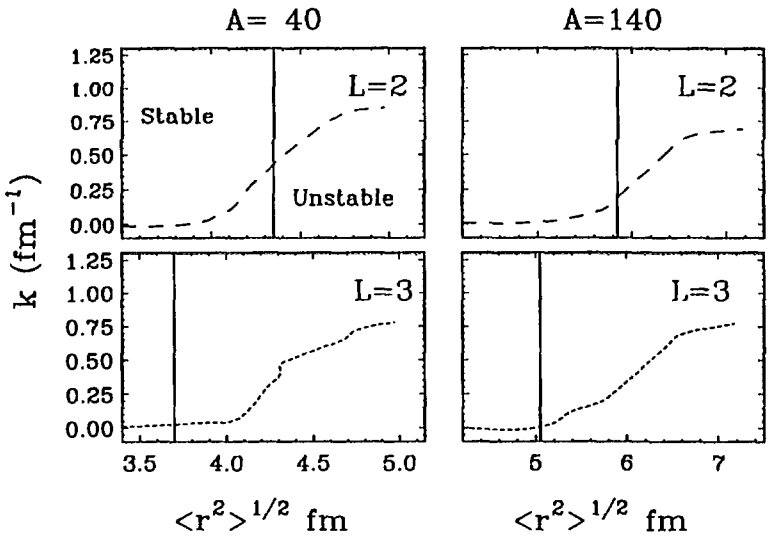

Figure 2: *The radial wave numbers associated with the quadrupole mode (top panel) and the octupole mode (bottom panel) as a function of the root-mean-square-radius at zero temperature. The vertical lines indicate the crossover from stable to unstable regions.*

tupole mode becomes unstable already at $< r^2 >^{1/2} \approx 3.7\ fm$. In both cases, modes exhibit a rather rapid transition from surface character with small values of k to volume character with large values of k at around $< r^2 >^{1/2} \approx 4.0-4.5\ fm$. It is also seen that the transitions from stable to unstable regions and from surface to volume character occur at different stages.

In figure 3, the maximum value of the frequency $|\omega_L|$ obtained in the calculations using the harmonic oscillator representation is plotted as a function of L at temperatures $T = 0, 3, 5\ MeV$. These calculations correspond to a source with the root-mean-square radius taken as $4.54 fm$ for the small system and $6.21 fm$ for the large system. It is seen that the instability in both systems decreases for increasing temperature of the source as expected, and the octupole mode appears, once again, as the most robust one. Also, in the large system, the dispersion relation has a cut at a lower multipolarity for increasing temperature.

Due to the quantal and surface effects, the multipoles with L larger than 3 for A=40 and larger than 5 for A=140 are strongly suppressed. The maximum value of the frequencies $|\omega_L(k)|$ is nearly equal for all the unstable multipoles indicating that these modes can be excited, apart from the statistical weight $2L + 1$, with nearly equal probability [14]. These results are in agreement with recent calculations based on a fluid dynamic approach to spinodal instabilities [15]. It is interesting to note that the maximum of the growth rate for a typical multipole mode in a finite source is comparable to the one obtained in nuclear matter. In fact, we perform a calculation in a periodic box by solving eq.(12) and determine the growth rates of the unstable modes as a function of the wave

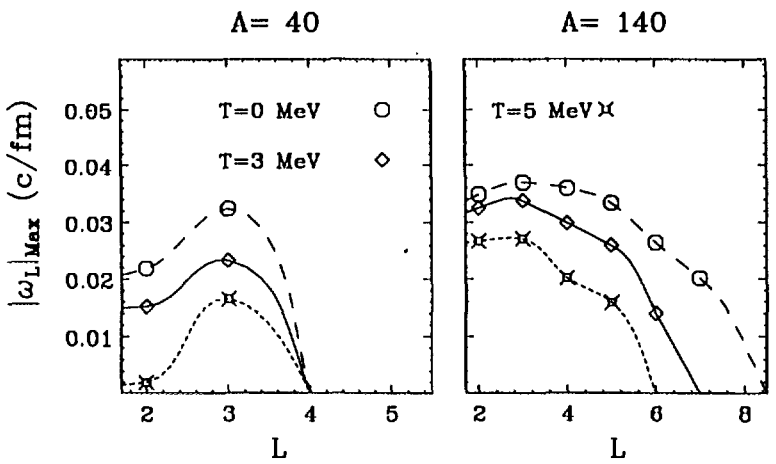

Figure 3: The maximum value of the frequency $|\omega_L|$ obtained in the harmonic oscillator representation as a function of the multipolarity L for $A = 40$ (left part) and for $A = 140$ (right part) at temperatures $T = 0, 3, 5\ MeV$.

number. We find that the maximum growth rate at a given density is close to the growth rate of a typical mode in a finite system at the same central density.

In order to investigate the early development of instabilities in a dilute nuclear source, we carry out finite temperature quantal RPA calculations for systems with $A = 40$ and $A = 140$ nucleons. A parametrization of the transition density in terms of its multipole moments leads to a simple dispersion relation for the growth rates of the unstable collective modes . We determine the growth rates as a function of the radial wave number from the dispersion relation employing a suitable single-particle representation. Under typical conditions, when the dilute system with $A = 140$ nucleons has an average density $\rho = 0.05 fm^{-3}$ and a temperature range $T = 3 - 5 MeV$ the collective modes up to $L = 5 - 6$ become unstable. Furthermore, as the source expands to lower densities, the unstable modes exhibits a transition from surface to volume character. The maximum growth rates of these unstable modes are nearly the same around 30 fm/c, indicating that the system may develop into different fragmentation channels with nearly equal probability. The results presented here are consistent with recent calculations of spinodal instabilities in finite nuclear systems based on a fluid dynamic approach.

Acknowledgements: This work is supported in part by the U.S. DOE Grant DE-FG05-89ER40530. S. A. thanks the Scientific and Technical Research Council of Turkey (TUBITAK- TOKTEN) for a partial support and the theory group at GANIL for their warm hospitality, and B. J. and Ph. C. thank the Tennessee Technological University for their warm hospitality where part of this work has been carried out.

References

[1] G. F. Bertsch and P. J. Siemens, Phys. Lett. **B126** (1983) 9

[2] H. Heiselberg, C. J. Pethick, and D. G. Ravenhall, Phys. Rev. Lett. **61** (1988) 818

[3] G. Papp and W. Nörenberg, Heavy Ion Physics **1** (1995) 241

[4] S. Ayik and C. Gregoire, Phys. Lett. **B212** (1988) 269; Nucl. Phys. **A513** (1990) 187;

[5] J. Randrup and B. Remaud, Nucl. Phys. **A514** (1990) 339

[6] M. Colonna, Ph. Chomaz, and J. Randrup, Nucl. Phys. **A567** (1994) 637; M. Colonna and Ph. Chomaz, Phys. Rev. **C49** (1994) 1908

[7] S. Ayik, Ph. Chomaz, M. Colonna and J. Randrup, preprint LBL-35987, Z. Physik **A** (1996), in press.

[8] C. J. Pethick and D. G. Ravenhall, Ann. Phys. (New York) **183** (1988) 131

[9] L. P. Csernai, J. Nemeth and G. Papp, GSI-preprint 95-45, and submitted to Heavy-Ion Physics

[10] S. Ayik, M. Colonna and Ph. Chomaz, Phys. Lett. **B353** (1995) 417

[11] D. Vautherin and M. Veneroni, proceeding of First Int. Spring Seminar on Nuclear Physics, Sorrento, Italy (1986).

[12] P. Ring and P. Shuck, The Nuclear Many-Body problem, Springer-Verlag, New York (1980)

[13] P. Bonche, S. Levit and D. Vautherin, Nucl. Phys. **A427** (1984) 278.

[14] A. Guarnera, M. Colonna and Ph. Chomaz, Phys. Lett. **B373** (1996) 267.

[15] B. Jacquot, S. Ayik, Ph. Chomaz and M. Colonna, preprint GANIL-P 96 11 and Phys. Lett. **B** (1996), in press.

A FAST VERSION OF THE FERMIONIC MOLECULAR DYNAMICS

Maria Colonna,[1,2] and Philippe Chomaz,[1]

[1]GANIL (DSM/CEA,IN2P3/CNRS)
BP 5027, 14021 CAEN Cédex,France
[2]LNS, Viale Andrea Doria
Catania, Italy

An alternative way to address the problem of the multifragmentation of Fermi liquids is to consider molecular dynamics in which the antisymmetrisation of the wave function is explicitly taken into account.[1,2,3] These approaches are based on a variational formulation of quantum mechanics complemented with the definition of an ensemble of parameterised trial wave functions. Often, these trial wave functions are nothing but Slater determinants built from gaussian wave packets. The parameters of these gaussians can be treated as classical degrees of freedom. These approaches are very appealing since they treat in an elegant way the problem of the antisymmetrisation and many applications have already been reported in the literature. However, these applications have been limited to small systems because of the numerical difficulties in the calculation of the two-body interaction.

We have developed a much faster approach based on the remark that, since the trial functions are a sub-set of the Slater determinants, i.e., of the independent-particle many-body wave function, the fermionic molecular dynamics can be seen as an approximate solution of the mean-field equations. Therefore, one can start directly with the variational formulation of the TDHF approximation using an effective force. In such a way, without any additional approximation, the numerical efforts are strongly reduced because of the introduction of the mean-field potential. In particular, the computation time just increases quadratically in the number of particles.

Figure 1 presents the first fermionic molecular dynamics simulations involving 160 particles.[4] In these simulations we have studied the evolution of a hot and diluted spherical system looking for a possible spinodal decomposition. However, we have only observed two types of behaviour i) either the global system is bound and the system will try to go back to the saturation density slowly evaporating particles; ii) either the system is unbound and it will be soon vaporised.

The key of this amazing behaviour is found in the evolution of the width of the gaussians (see fig 9) that in our calculations are considered as dynamic variables. This width appears to increase when the system gets diluted so that it introduces an addi-

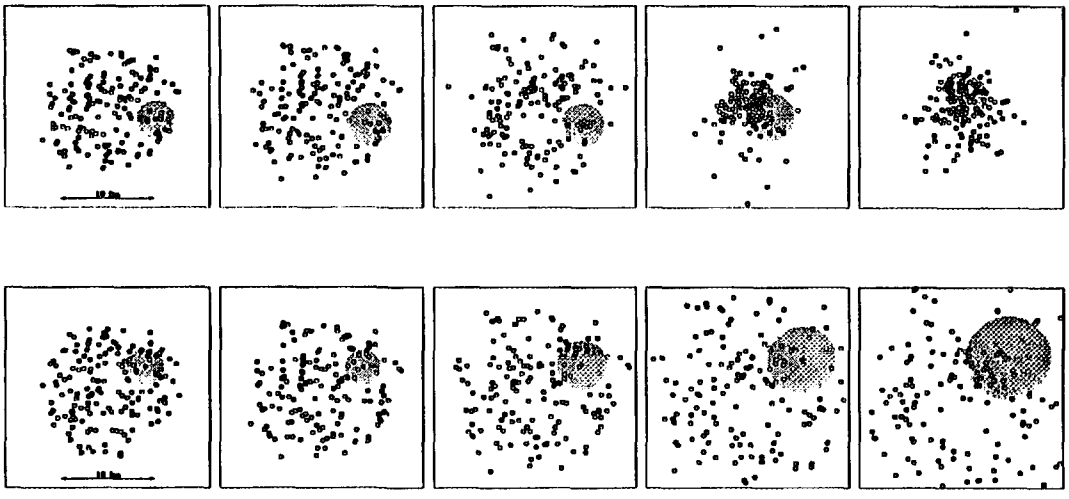

Figure 1. Fermionic molecular dynamics of large systems (A=160): Bottom part, excited at a total enegy of +2 MeV per nucleon, one can observe a total vaporisation of the system; Top part, with a total energy of -2 MeV per nucleon, in such a case a residue is formed evaporating particles. The center of each individual gaussian is represented. For one Gaussian also its width is shown. The time is evolving by steps of 25 fm/c from 0 to 100 fm/c going from the left to the right.

tional smoothing of the mean-field, washing out the spinodal instabilities and reducing the formation of fragments. In particular, the increase of the width reduces the interactions between particles and quenches the fragment formation. In the present stage of our understanding it seems that fermionic molecular dynamics without the width as a dynamic variable (i.e., with a fix width) might be a better approximation in order to treat fragments correlations. In particular, such a fix width calculation correctly converges towards classical molecular dynamics while because of the additional width parameter the full molecular dynamics seems to lead to a different phenomenology. This peculiar role of the width is now under investigation.

Acknowledgements

This work was supported in part by the Commission of the European Community, under Contract No. ERBCHBI-CT-930619.

REFERENCES

1. L.G. Yaffe, *Rev. Mod. Phys.* 54:407 (1982);
   S. Drożdż, J. Okolowicz and M. Ploszajcczak, *Phys. Lett.* 109B:145 (1982);
   E, Caurier, B. Grammaticos and T. Sami, *Phys. Lett.* 109B:150 (1982).
2. J. Aichelin and H. Stöcker, *Phys. Lett.* 176B:14 (1986);
   H. Feldmeier, *Nucl. Phys.* A515:147 (1990).
3. A. Ono et al, Phys. Rev. Lett. 68:2898 (1992).
4. M. Colonna and Ph. Chomaz, in preparation.

Regularity and chaos in Vlasov evolution of Unstable Nuclear Matter

B. Jacquot[1], A. Guarnera[1,2], Ph. Chomaz[1], M. Colonna[1,2]

[1)] GANIL, B.P. 5027, F-14021 Caen Cedex, France

[2)] Laboratorio Nazionale del Sud, Viale Andrea Doria, I-95129 Catania, Italy

Mean field equations are highly non linear, because of the presence of a self-consistent potential. Therefore the mean-field dynamics is expected to exhibit all the phenomenology of non-linear processes [1].

For example, a nucleus traveling at constant velocity can be seen as a solitary wave (or soliton) solution of the non-linear mean-field equations. The existence of large non-linearities makes the mean-field dynamics a typical candidate to exhibit a chaotic behaviour. For example, compound nuclei at finite temperature are considered as very chaotic systems. However, collective motions which correspond to regular vibrations of the compound nucleus, such as the hot giant resonances, have been observed experimentally. Therefore, the apparition and the development of chaos is actually a very delicate point because not all the degrees of freedom become chaotic at the same time.

Recently, the investigations about the collective properties of the mean-field dynamics have been extended to consider unstable situations such as the evolution of systems initialized inside the spinodal region of the nuclear matter phase diagram [2-8]. The studies of refs.[8, 9] have shown that the spinodal decomposition, simulated through full mean-field calculations, appears largely influenced by the existence of unstable collective modes, which are equivalent to zero-sound waves. On the other hand, the possibility of the occurrence of disorder and chaos during the fragmentation of the system has been discussed by many authors [10-19], in particular within the context of unstable mean-field evolution [20-23]. The occurrence of chaos would be of great importance since it may give a justification for the validity of statistical approaches in the description of multifragmentation events. Therefore a detailed analysis of when and how the chaos appears during spinodal fragmentation is called for. This is the main goal of the present article.

Abs.

In this article we perform an analysis of the onset of chaos in mean-field dynamics in presence of volume instabilities. As a main finding, ~~we~~ it is shown that the mean-field evolution presents two different regimes: a first one dominated by the almost decoupled amplification of several collective unstable modes, leading to the early condensation of the system into clusters, which is followed by a second stage dominated by a coalescence mechanism among the large-density domains. Finally we show that, even at the latest stage considered , chaos does not ap-

is performed.

pear as fully developed since a hierarchy of the different unstable modes, inherited from the initial regular amplification of instabilities, remains.

As a consequence, for fast-fragmenting systems, there is the possibility to keep the memory of the early dynamical instabilities in the final clusterization pattern in particular preserving small wave lengths to develop. Moreover, we show that these results and in particular the time and size scales involved are very sensitive to the range of the considered force.

As already discussed in the comment [22], the dynamics of an individual RPA eigenmode appears quite regular and almost insensitive to the differences in the initial density. However, in order to investigate the characteristics of the mean-field dynamics it is not sufficient to look at the propagation of normal modes, because they are very peculiar initial conditions. Therefore we have studied the dynamics of an ensemble of randomly initialized trajectories. The average initial density was chosen to be equal to 0.4 ρ_0. If one looks at the evolution of two randomly initialized systems, they appear rather different. The observed fast amplification of small initial differences might be an indication of a chaotic regime. However, this is a delicate point, since even in the regular case of independent unstable normal modes, one would observe the same features.

In order to perform a normal mode analysis, we can introduce the Fourier transform of the density fluctuations:

$$\sigma_k(t) = \left| \int dx e^{ikx} \rho(x,t) \right|^2 . \tag{1}$$

The onset of chaos can be quantitatively analyzed considering the dimensionless amplification coefficient:

$$A_k(t) = \left| \frac{\sigma_k(t)}{\sigma_k(0)} \right| \tag{2}$$

and by considering the average of $A_k(t)$ over the ensemble of N events:

$$\bar{A}_k(t) = \frac{\sum_{n=1}^{N} A_k(t)^{(n)}}{N} \tag{3}$$

and its relative fluctuation $\Delta A_k(t)$:

$$\Delta A_k(t)^2 = \frac{\sum_{n=1}^{N} (A_k(t)^{(n)} - \bar{A}_k(t))^2 / N}{\bar{A}_k(t)^2} \tag{4}$$

computed over an ensemble of events initialized using a white noise. It should be noticed that the fluctuation $\Delta A_k(t)$ is a way to measure the spreading of the two-time correlations around a straight line, i.e. the deviation from a regular correlation. When the relative width $\Delta A_k(t)$ is large compared to 1 the fluctuations are large and the correlation between initial and final time is lost. This corresponds to a chaotic regime. Conversely, if the relative width is small the system is dominated by a regular amplification dynamics. The behaviour of

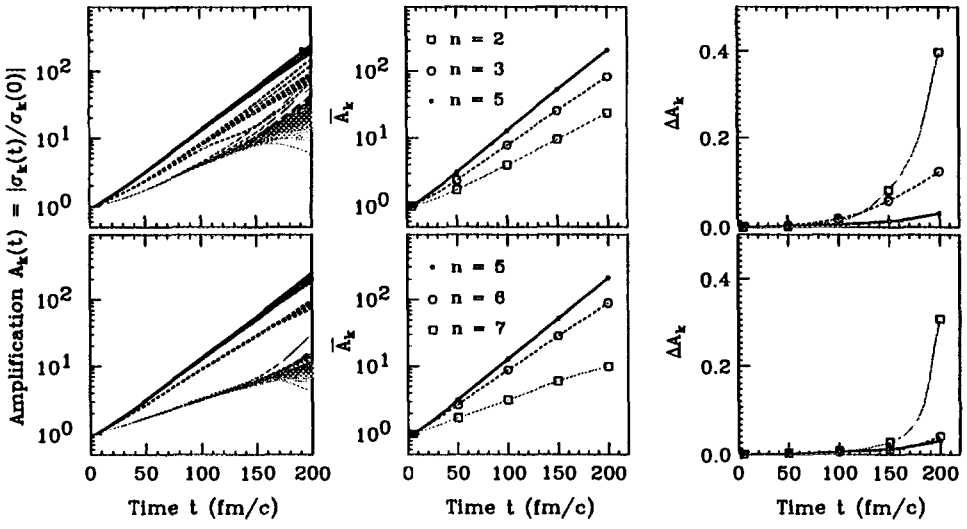

Figure 1: Study of the amplification factor as a function of time, and for various k modes around the most unstable one, labeled by their node number n. In the upper panel the thick lines correspond to n=5, the dashed lines to n=3 and the thin grey lines to n=2. In the lower panel the thick lines correspond to n=5, the dashed lines to n=6 and the thin grey lines to n=7. The left part figures present A_k computed for 100 events. The central part displays the ensemble average $\bar{A}_k$; the right part shows the fluctuation ΔA_k.

both quantities as a function of time is reported on Fig. 1 for various unstable modes. One can first see that the average amplification coefficient $\bar{A}_k(t)$ follows an exponential law during its early evolution. This is a characteristic of the linear response regime. For the different modes one observes that the fluctuation $\Delta A_k(t)$ remains small up to $5 \div 7$ instability times τ_i. Moreover, for the most unstable ones ($k = 0.6\ fm^{-1}$ for the L interaction and $k = 1.8\ fm^{-1}$ for the S interaction) at the end of our simulation, the observed relative fluctuation is found still lower than one. This demonstrates that the most unstable collective modes are robust against chaos and that their dynamics is weakly coupled to the evolution of the other degrees of freedom. This emphasizes the regularity of the first stage of spinodal decomposition.

Acknowledgements: We would like to thank M. Baldo, G. F. Burgio and A. Rapisarda for numerous and very useful discussions.

This work is supported in part by the Commission of the European Community, under Contract No. ERBCHBI-CT-930619.

References

[1] Michael Tabor, "Chaos and Integrability in Non Linear Dynamics", A Wiley-Interscience Publication, John Wiley and Sons, New York (1989); E. Ott, "Chaos in Dynamical Systems", Cambridge Univ. Press., Cambridge (1993)

[2] H. Heiselberg, C.J. Pethick, and D.G. Ravenhall, Ann. Phys. **223** (1993) 37

[3] D. Vautherin and M. Vénéroni, proceedings of the First International Spring Seminar on Nuclear Physics, (1986), Sorrento (Italy), p. 13.

[4] L.G. Moretto, Kin Tso, N. Colonna, and G.J.Wozniak, Phys. Rev. Lett. **69** (1992) 1884.

[5] W. Bauer, G.F. Bertsch, and H. Schulz, Phys. Rev. Lett. **69** (1992) 1888.

[6] B. Borderie, B. Remaud, M.F. Rivet, and F. Sebille, Preprint IPNO-DRE (Jul'92)

[7] H.M.Xu et al., Phys. Rev. **C48** (1993) 933

[8] M.Colonna, Ph.Chomaz, J.Randrup, Nucl. Phys. **A567** (1994) 637; Ph. Chomaz and M. Colonna, Phys. Rev. **C49** (1994) 1908; S.Ayik, M.Colonna, Ph.Chomaz, Phys. Lett. **B359** (1995) 268; M.Colonna, Ph.Chomaz, A.Guarnera and B.Jacquot, Phys. Rev. **C51** (1995) 2671; A.Guarnera, M.Colonna and Ph.Chomaz, Phys. Lett.**B**, in press.

[9] M. Colonna, G.F. Burgio, Ph. Chomaz, M. Di Toro, and J. Randrup, Phys. Rev. **C47** (1993) 1395; G.F.Burgio, Ph.Chomaz, M.Colonna and J.Randrup, Nucl. Phys. **A581** (1995) 356.

[10] D.H.E. Gross, Bao-An Li and A.R. De Angelis, Ann. Phys. **1** (1992) 467.

[11] G. Fai and J. Randrup, Nucl. Phys. **A404** (1983) 551;

[12] S.E. Koonin, J. Randrup, Nucl. Phys. **A471** (1987) 355c;

[13] J.B. Bondorf, Nucl. Phys. **A488** (1988) 31c; J.B. Bondorf et al., Phys. Rep. **257** (1995) 133

[14] X. Campi, Nucl. Phys. **A495** (1989) 259c.

[15] D.H.E.Gross, Rep. Prog. Phys. **A53** (1990) 605

[16] A.Bonasera, V.Latora and A.Rapisarda, Phys. Rev. Lett. **19**(1995)3434; M.Belkacem, V.Latora and A.Bonasera, Phys. Rev. **C52** (1995) 271.

[17] T.Srokowski and M.Ploszajczak, Phys. Rev. Lett. **75** (1995) 209.

[18] M.Baldo, E.G. Lanza and A.Rapisarda, Chaos **3** (1993) 691.

[19] C.H.Dasso, M.Gallardo and M.Saraceno, Nucl.Phys. **A549** (1992) 265.

[20] G.F. Burgio, M. Baldo and A. Rapisarda, Phys. Lett. **B321** (1994) 307.

[21] M. Baldo, G.F. Burgio and A. Rapisarda, Phys. Rev. **C51** (1995) 198.

[22] B.Jacquot, M.Colonna, Ph.Chomaz, A.Guarnera, Phys. Lett. **B359** (1995) 268.

[23] Ph. Chomaz, G.F. Burgio, and J. Randrup, Phys. Lett. **B254** (1991) 340; G.F. Burgio, Ph. Chomaz, and J. Randrup, Phys.Rev.Lett. **69**, 885 (1992) and Nucl. Phys. **A529** (1991) 157.

[24] Ph.Chomaz, M.Colonna, A.Guarnera and B.Jacquot, Nucl. Phys. **A583** (1995) 305; and GANIL preprint P95 12, submitted to Phys. Lett. **B**

[25] J.D. Gunton, M. San Miguel and P.S. Sahni, 1983 *Phase Transitions and Critical Phenomena* vol.8, ed. C. Domb and J.L. Lebowitz (New York: Academic) p. 267

[26] Ph. Chomaz, M. Colonna and A. Guarnera, "Fingerprints of Dynamical Instabilities", proc. of "Int. Workshop on Dynamical Features of Nuclei and Finite Fermi Systems", Sitges (Barcelona), Spain, September 13-17 1993.

B5 - MESONS AND PHOTONS

Density oscillations of nuclear matter probed via bremsstrahlung photons

F.M. Marqués, G. Martínez,
T. Matulewicz, R.W. Ostendorf and Y. Schutz

for the TAPS collaboration

GANIL Caen, GSI Darmstadt, Univ. Gießen,
KVI Groningen, NPI Řež, IFIC Valencia

From the extended experimental data on hard-photon ($E_\gamma > 80$ MeV) production at intermediate energies obtained during the last decade and from dynamic phase-space simulations of heavy-ion collisions, the dominant source of hard-photons has been attributed to the bremsstrahlung radiation emitted in first-chance proton-neutron (pn) collisions. Therefore, hard photons probe the phase-space distribution of the nucleons in the collision zone and convey information on the dynamics of the collision in its early stage.

Aside of the aforementioned dominant source which produces *direct* hard-photons, at intermediate energies BUU calculations predict the existence of a second source of pn bremsstrahlung photons occurring at a later stage of the heavy-ion collision when the system is almost fully thermalyzed, *thermal* hard-photons. A dense system is formed in the first stage of the collision, which then slowly expands until the attractive part of the nuclear force is strong enough to drive a second compression of the system. It subsequently undergoes oscillations around the saturation density. The strength of the restoring force (attractive below ρ_0 and repulsive above) depends on the incompressibility of nuclear matter K_∞: for large values the restoring force is larger than for small ones, so the second compression produces higher densities for larger K_∞.

Therefore there are two distinct hard-photon sources clearly separated in time because of the absence of photon production during the expansion phase. The second source is characterized by a softer energy spectrum, since in the later stage of the collision the energy available in the center-of-mass of pn collisions is, on average, smaller than that at the beginning of the collision. At higher bombarding energies the expansion is sufficiently violent to breakup the system into many fragments and no thermal hard-photons are produced.

Experimentally we have searched for the existence of this second photon source by analysing the energy spectra of inclusive and exclusive hard-photons and the photon-photon correlation function for three different systems.

The exclusive spectra were measured in coincidence with light-charged particles and projectile-like fragments enabling a selection on impact parameter. The slope parameters and the production rates follow the predicted behaviour: the thermal component is softer than the direct one and the production rate of thermal photons is largest for the heaviest system and the lowest bombarding energy. Because direct photons are produced in *first-chance* pn collisions their production rate does not depend on K_∞. In contrast, thermal

is searched for

photons are very sensitive to the amplitude of the density oscillation and thus to K_∞. It should be emphasized that K_∞ is deduced from the relative yield of thermal to direct hard-photons, thus making this method almost independent of the choice of the nucleon-nucleon cross-section. Comparing the measured relative rates of the hard-photon production to the ones calculated with BUU we obtain the value $K_\infty = (290 \pm 50)$. The exclusive spectra show clearly that the thermal-photon relative intensity and slope are lower for peripheral collisions, as one should expect since the compression effects are less important in these. We thus conclude that the two components observed in the experimental hard-photon spectrum confirm the predicted existence of a thermal hard-photon source in addition to the dominant hard-photon production in first-chance nucleon-nucleon collisions.

A more powerful tool to characterize the properties of the photon source is provided by the technique of Bose-Einstein correlations (or intensity interferometry) between independent hard-photons, which allow to determine directly the collision geometry. The two-photon correlation function provides a direct mapping of the Fourier transform $\varrho(q)$ of the space-time photon-source distribution $\rho(r)$:

$$C_{12}(q) = 1 + \lambda|\varrho(q)|^2 \,, \tag{1}$$

and therefore gives access to information on the medium from which they are emitted.

To study the effect of a secondary photon-source displaced in space-time by the four-vector Δr, we have assumed that both sources have the same distribution $\rho(r)$ and we have called A_D the relative intensity of direct hard-photons and $A_T = 1 - A_D$ the one of thermal hard-photons. The interference term is then modulated by a factor depending on the relative intensities of the two sources and on their space-time separation:

$$C_{12}(q) = 1 + \lambda|\varrho(q)|^2\{A_D^2 + A_T^2 + 2A_D A_T \cos(q\Delta r)\} \,. \tag{2}$$

In the case of no density oscillation, i.e. one source, as would happen at bombarding energies high enough to break the system into fragments, $A_T = 0$, and Eq. (2) reduces to Eq. (1).

This analysis has been applied to the data measured for two of the three systems studied in order to demonstrate the high sensitivity of the correlation technique to the characteristics of the photon source. The study of the projection of the experimental correlation functions onto the Lorentz-invariant relative four-momentum $Q = (\mathrm{q}^2 - q_0^2)^{1/2}$ shows that in the case of the lighter system the correlation function exhibits at small Q a clear Gaussian-like pattern, which analysed in terms of Eq. (1) corresponds to a large photon-source, while in the case of the heavier system no Gaussian-like pattern is observed. We therefore conclude that Eq. (1) that assumes one space-time source cannot represent the experimental correlation functions.

We have then analysed the correlation functions in terms of Eq. (2) and found that the assumption that hard photons are emitted from two distinct sources leads to an excellent agreement with the data. The effect of the second source is to attenuate for the light system the Gaussian pattern expected in the correlation function and to completely wash out the pattern for the heavy system where the intensities of both sources are equal. The values deduced for the source size follow the size of the compound system, demonstrating that the observed effect is related to the size of the colliding heavy-ions; the values deduced for the relative intensity of direct hard-photons are in excellent agreement with the relative intensity A_D predicted by BUU calculations.

In conclusion, we have shown that the hard-photon energy spectra and correlation functions measured for several systems different in size and bombarding energy cannot be interpreted with the assumption of a single photon-source. By introducing a second photon-source we obtain a good description of the data. This observation is in agreement with the reaction mechanism expected for heavy-ion collisions at low-intermediate bombarding energies leading to the formation of a hot nucleus oscillating in a monopole mode. It confirms also the prediction of the BUU calculation that bremsstrahlung photons are emitted during each compression phase. We have therefore at hand with hard photons a probe emitted at two very different stages of the collision, the initial one when nuclear matter is formed at high densities and the second one when nuclear matter reaches again high densities but is already thermalized. This result opens new opportunities to study the properties of hot and dense nuclear matter.

References

[1] G. Martínez *et al.*, Phys. Lett. B **349** (1995) 23.

[2] F.M. Marqués *et al.*, Phys. Lett. B **349** (1995) 30.

Importance of one- and two-body dissipation at intermediate energies studied by hard photons

J.H.G. van Pol[a], H.W. Wilschut[a], H. Löhner[a], R.H. Siemssen[a,b], P. Lautridou[b], F. Lefèvre[b], T. Matulewicz[b], M. Marqués[b,e], W. Mittig[b], R.W. Ostendorf[a,b], P. Roussel-Chomaz[b], Y. Schutz[b], S. Hlavác[c,f], R. Holzmann[c], A. Schubert[c], R.S. Simon[c], V. Wagner[c,g], M. Franke[d], W. Kühn[d], M. Notheisen[d], R. Novotny[d], F. Ballester[e], J. Díaz[e], A. Marín[e], G. Martínez[b,e], A. Kugler[g]

[a] Kernfysisch Versneller Instituut, NL-9747AA Groningen, Netherlands

[b] Grand accélérateur National d'Ions Lourds, F-14021 Caen, France

[c] Gesellschaft für Schwerionenforschung, D-64220 Darmstadt, Germany

[d] II. Physikalisches Institut, Universität Gießen, D-35392 Gießen, Germany

e Instituto de Física Corpuscular, SP-46100 Burjassot Valencia, Spain

[f] Slovak Academy of Sciences, Bratislava, Slovak Republic

[g] Nuclear Physics Institute, 25068 Řež u Prahy, Czech Republic

Abstract

Hard photons have been measured as a function of the mass of the projectile-like fragment in peripheral reactions of ^{36}Ar + ^{159}Tb at 44 MeV/nucleon. The probability for hard photon production is found to depend on the amount of mass transferred and the direction of the transfer, indicating the relative importance of one- and two-body dissipation in peripheral reactions.

The understanding of the dynamics of colliding nuclei near the Fermi-energy strongly relies on the use of transport equations of the Boltzmann type. In these the driving force in the drift term is the result of the self-consistent mean field, while the collision term describes the individual nucleon–nucleon collisions. Due to Pauli-blocking the importance of the collision term is strongly influenced by the incident energy. Experimentally, however, the partition of the dynamics into a mean-field and a collision component is much more difficult to show, since the link with experimental observables is very indirect. The strongest evidence for the importance of nucleon–nucleon collisions in the Fermi-energy domain is the observation of nuclear bremsstrahlung. The scaling of inclusive hard-photon cross sections ($E_\gamma > 30$ MeV) with projectile and target mass and its angular dependence is consistent with bremsstrahlung from energetic proton–neutron collisions occuring in the early phase of the reaction[1]. In contrast to strongly interacting particles, photons can leave the collision zone undisturbed. Therefore, they can give a direct account of the nucleon–nucleon collisions in this reaction phase.

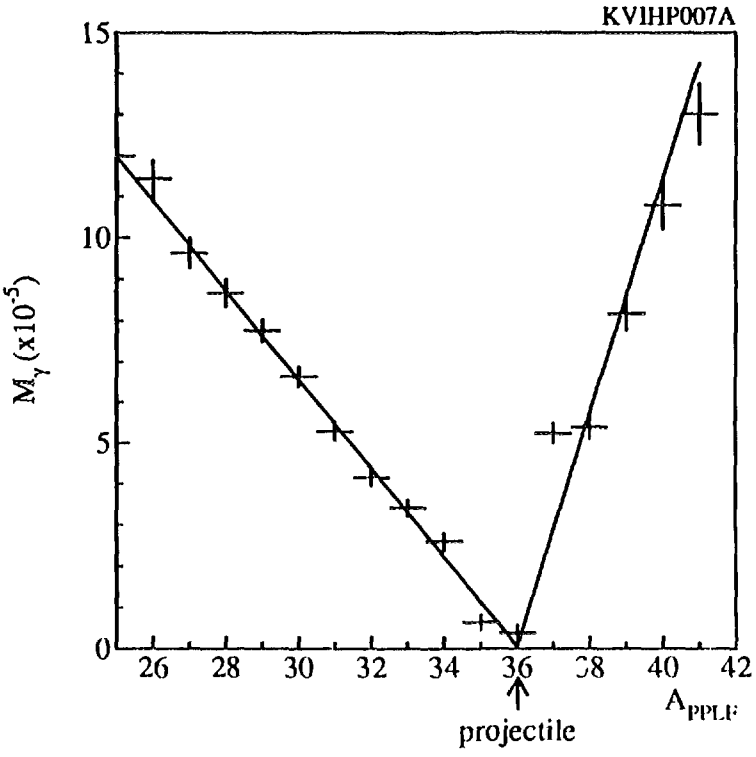

Figure 1: Photon probability as a function of the mass of the primary projectile

We have recently finalized the analysis of the reaction ^{36}Ar+^{159}Tb at 44 MeV/nucleon[2]. In this experiment, done at GANIL, projectile-like fragments were measured with the SPEG magnetic spectrograph in coincidence with bremsstrahlung photons detected with TAPS and light charged particles observed with the KVI Forward Wall. The latter detector allows to reconstruct the primary projectile-like fragments in an iterative procedure, based on the sequential charged-particle decay of the excited primary fragment. From peripheral heavy ion reactions at low energies, at which individual nucleon–nucleon collisions are relatively unimportant, one knows that for mass-asymmetric nucleus–nucleus systems the mean field drives the system towards further asymmetry, i.e. the mass drift is from the light to the heavy nucleus. Also in the present reaction such a preference is found. Even after correcting for the "trivial" effect of sequential particle emission from the excited projectile-like fragments, the largest yield is observed for fragments with nucleons removed from the light projectile.

On the other hand the occurrence of nucleon–nucleon collisions in this reaction is also clearly seen: the bremsstrahlung probability measured for the projectile-like fragments increases linearly with the removed mass (see fig. 1). Since the bremsstrahlung yield is proportional to the number of nucleon–nucleon collisions there is a linear correlation between the mass transfer and the number of nucleon–nucleon collisions. However, one can also see that for the relatively small yield of events in which the projectile-like fragment has gained mass a much more rapid increase of the bremsstrahlung yield with the transferred mass is observed. This is shown in fig. 1, in which the bremsstrahlung differential multiplicities are plotted as a function of the mass of the primary projectile-like fragment. Thus

when the projectile loses mass, which corresponds to transfer along the drift direction, less collisions are needed than when the projectile gains mass against the drift direction. The collisions are a source of fluctuations allowing reaction channels to be populated against the direction dictated by the mean field. Therefore, the observation of the asymmetry in the bremsstrahlung probability with respect to the preferred direction of mass transfer is an elegant demonstration of the simultaneous action of the nuclear mean field on the one hand and the nucleon-nucleon collisions on the other.

References

[1] H.Nifenecker and J.A.Pinston, Ann. Rev. Nucl. Part. Sci. 1990 40 113-143, (and references therein).

[2] J. van Pol et al. Phys. Rev. Lett. 76(1996)1425.

Revelations from Super-Hard Photons in HeavyIon Collisions[1] : Subthreshold Pion Dynamics.

K. K. Gudima[1], T. Matulewicz[1], H. Delagrange[1], F. M. Marqués[1], G. Martínez[1], R. W. Ostendorf[1], M. Ploszajczak[1], Y. Schutz[1],V. D. Toneev[1], P. Bożek[1], S. Hlaváč[2], R. Holzmann[2], A. Schubert[2],R.S. Simon[2], V. Wagner[2], H. Löhner[3], J. H. G. van Pol[3], R. H. Siemssen[3], H. W. Wilschut[3], J. Díaz[4], A. Marín[4]

[1] *GANIL, BP 5027, 14021 Caen Cedex, France*
[2] *Gesellschaft für Schwerionenforschung, D-64220 Darmstadt, Germany*
[3] *Kernfysich Versneller Instituut, NL-9747 AA Groningen, The Netherlands*
[4] *Instituto de Física Corpuscular, SP-46100 Burjassot Valencia, Spain*

For the systems ^{86}Kr + ^{nat}Ni at 60A MeV and ^{181}Ta+^{197}Au at 40A MeV, the experimental γ spectra extend to extremely high energies, i.e. 5 times the beam energy per nucleon. Within the framework of the Dubna cascade model, we need to implicitly consider the $(\pi N \rightarrow N\gamma)$ interaction to properly reproduce such a trend. In fact never taken into account before for the production of very hard photons in this energy range, this channel involves subthreshold pions produced in nuclear matter. Full details can be found in [2].

At intermediate bombarding energies hard photons emitted after heavy-ion collisions probe the reaction dynamics. They found their origin, mainly, from the incoherent sum of first chance (pn) bremsstrahlung processes. For a free pn bremsstrahlung process the maximum energy for γ conversion is $E_\gamma^{max}(s) \approx \frac{T_L}{2}$ where $\sqrt{s}$ is the pn center-of-mass energy and T_L, the beam energy. In heavy ion reactions, the maximum available energy s_{max} results from the coupling of the beam energy momentum per nucleon p_L with the intrinsic Fermi momentum in antiparallel configuration. It reads :

$$s_{max} = 2\frac{[E_F(m_N + E_L) + p_F p_L]^2}{m_N(m_N + E_L)},$$

where $E_F = \sqrt{m_N^2 + p_F^2}$ and $E_L = \sqrt{m_N^2 + p_L^2}$. In the case of sharp-cut off momentum distributions (p_F = 270 MeV/c), the maximum photon energy, defined as the kinematic limit, $E_\gamma^{max}(s_{max})$ reaches 167 MeV and 194 MeV, in heavy-ion induced reactions at bombarding energies of 40A MeV and 60A MeV, respectively.

The kinematic limit in an individual pn collision can be overcome only if extra energy is available. This energy gain may be found in different mechanisms, like nucleon off-shell effects, three-body collisions at high nuclear density, dynamic energy focusing fluctuations, or multistep π and Δ involvements.

For the *first time*, our results for ^{86}Kr + ^{nat}Ni at 60A MeV and ^{181}Ta + ^{197}Au at 40A MeV present γ spectra clearly indicating energies much larger than the kinematic limit. The photon spectrum end points ($\sim$ 300 MeV for Kr + Ni and $\sim$ 250 MeV for

[1] Experiment performed with TAPS

Ta + Au) correspond to the *nb* sensitivity of our experimental method (Fig. 1). Our experimental set-up consisted of the TAPS γ calorimeter complemented, at forward angles by the light-charged particle KVI hodoscope. Our trigger mode was set to emphasize central collisions. More detailed experimental information is given in [2-3].

To interpret these puzzling results, Dubna cascade model (DCM) calculations were performed. Derived from Boltzmann-Uehling-Uhlenbeck (BUU) kinetic equations, DCM incorporates a simplified mean-field evolution but including Pauli principle and nuclear binding. This model was extended to treat pion and photon yields perturbatively. First only the *pn* bremsstrahlung was invoked. In such a case the DCM calculations strongly underpredict the experimental cross-sections at high γ energies (Fig. 1) we are concentrating on. As a matter of fact genuine BUU computations exhibit the same pattern [4].

Starting from this conclusion, two more decay channels were incorporated in DCM : $\pi^o \rightarrow \gamma\gamma$ and $\Delta \rightarrow N\gamma$ after $N + N \rightarrow N + \Delta$ production. These modifications were not sufficient to improve the fit to the data. Finally at variance with standard formalisms used so far in hard photon production at intermediate energy, we added the π nucleon capture : $\pi + N \rightarrow N + \gamma$. Even if all these treatments are not sufficient to reproduce fully the experimental data, the effects are going in the right direction (Fig. 1).

What are the consequences of the πN radiative capture ? In the Kr + Ni case we have measured the π^o energy spectra. Then the influence of this latter effect could be revealed by the calculated pion yield. In DCM primordial pions are produced either directly through $N + N \rightarrow N + N + \pi$, or in two steps via Δ-resonance formation and decay, i.e. $N + N \rightarrow \Delta + N$ followed by $\Delta \rightarrow N + \pi$. As they are formed inside the nuclear medium these pions suffer from absorption and rescattering. Pions undergo absorption either directly due to the reactions $\pi + (NN)_c \rightarrow N + N$ and $\pi + N \rightarrow N + \gamma$, or in two steps $\pi + N \rightarrow \Delta$ with $\Delta + N \rightarrow N + N$.

In order to compare the experimental data with the computation results the calculated π^o energy spectra and angular distributions have been folded with the TAPS geometrical acceptance and response function. For the Kr + Ni case at $60A$ MeV the calculated spectrum reproduces nicely the experimental maximum but falls off too rapidly at higher energy (see Fig. 2). The overall calculated π^o cross section amounts to 28 μb to be compared with the experimental value of 42 ± 4 μb. This discrepancy could be linked to inaccuracies in the popular Ver West-Arndt approximation for pion production cross-section. This approximation used in DCM fails near the threshold [5].

In the γ spectra (Fig. 1) although the decay process $\pi^o \rightarrow \gamma\gamma$ exhibits a maximum at about $m_\pi/2$, it contributes quite significantly less than the *pn* bremsstrahlung. These two processes generate similar contributions at higher γ energies ($E_\gamma > 150$ MeV). In the intermediate energy regime below $100A$ MeV, emitted photons stem mainly from the reaction $\pi + N \rightarrow N + \gamma$ for the primordial pions. This emission is much more significant than those coming from bremsstrahlung and Δ-resonance decay. The πN radiative capture implies a positive correlation between the energies of the involved γ and N particles. On the contrary, they are anticorrelated in bremsstrahlung.

As already pointed out for the Kr + Ni system, the π^o spectrum predicted by

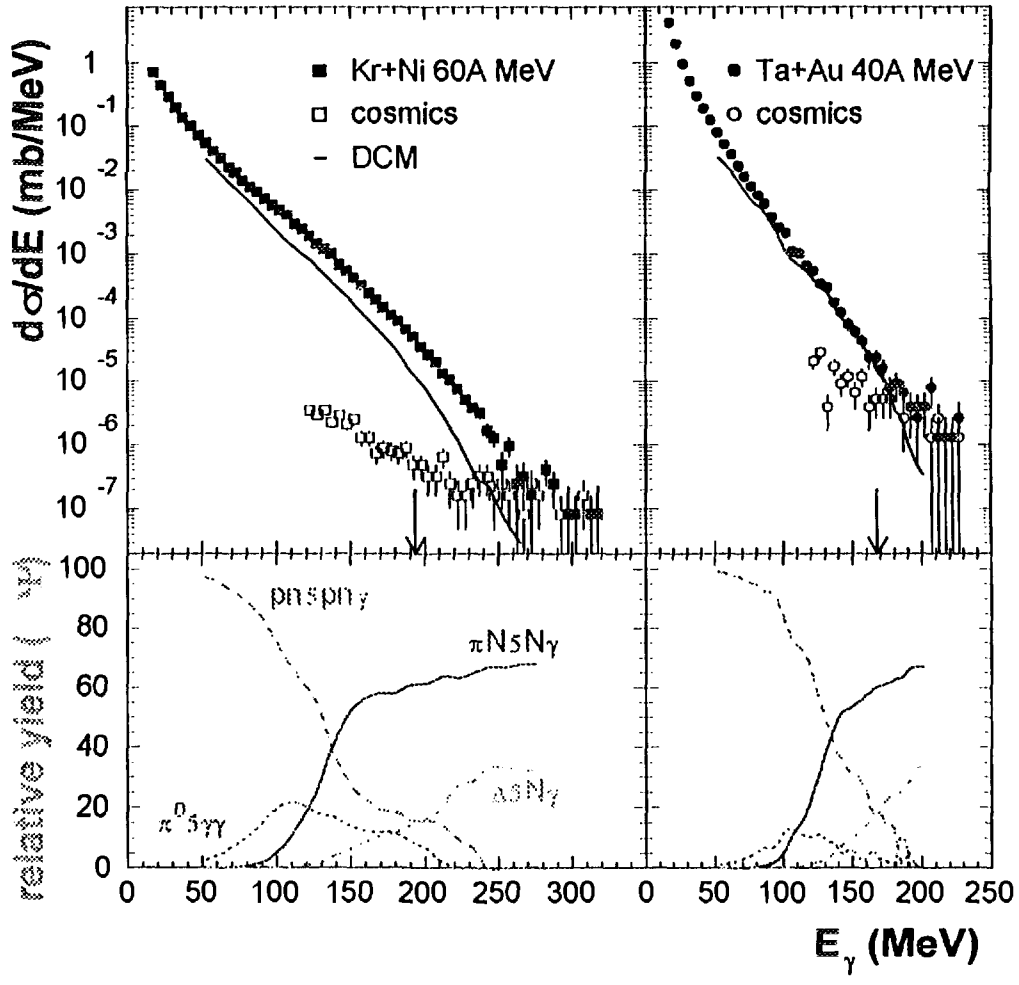

Figure 1: Measured photon spectrum (full symbols) in the reaction ^{86}Kr + ^{nat}Ni at 60A MeV (left panel) and ^{181}Ta + ^{197}Au at 40A MeV (right panel) after subtraction of the cosmic-ray contribution. The level of cosmic-ray background is shown with open symbols. The solid line represents the DCM calculations. In the lower part the calculated spectrum is decomposed into fractions corresponding to the following elementary mechanisms : $p+n \rightarrow p+n+\gamma$, $\pi+N \rightarrow N+\gamma$, $\pi^o \rightarrow \gamma\gamma$, and $\Delta \rightarrow N\gamma$. The arrows indicate the kinematic limits.

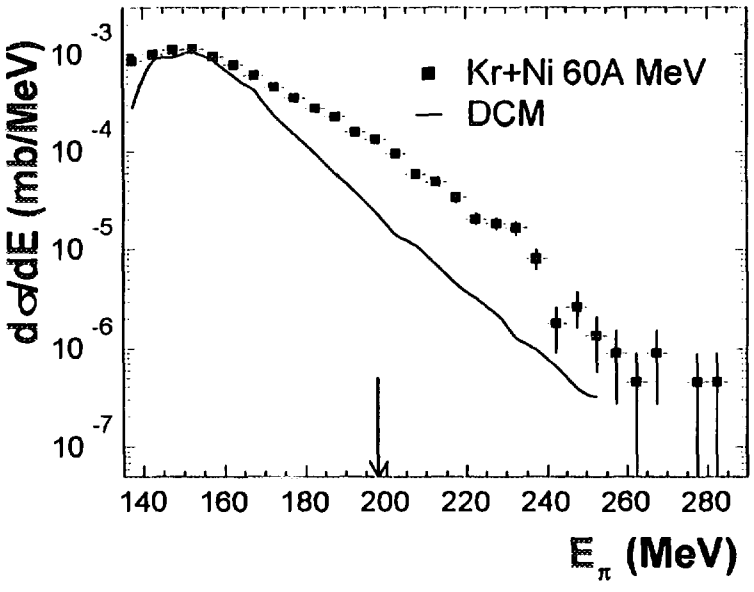

Figure 2: Energy distribution of π^o in the ^{86}Kr + ^{nat}Ni reaction at 60A MeV, compared with the DCM calculations (solid line). The arrow indicates the kinematic limit.

DCM is too soft compared the experimental data. Consequently and correlatively, above the kinematic limit the DCM γ spectrum exhibits the same trend. This deduced statement illustrates and emphasizes the major role played by the subthreshold pions in the πN radiative capture.

In summary, for Kr + Ni (60A MeV) and Ta + Au (40A MeV), the experimental γ spectra span over an extremely wide dynamical range. Such dynamical ranges have never been reported in the literature before. These spectra extend up to 5 times the beam energy per nucleon well over the kinematic limit. Based on DCM calculations, photon production originating from the incoherent sum of individual pn bremsstrahlung (the standard approach so far for such reactions) is not sufficient to reproduce the experimental data. Other(s) mechanism(s) is(are) in order. In this vein, in DCM, we have incorporate the $\pi + N \rightarrow N + \gamma$ mechanism involving the primordial pions formed in the nuclear medium. This process plays a leading role in the production of the hyper-hard photons. Nevertheless remaining discrepancies call for a better understanding of the in-medium production of subthreshold primordial pions and of its interplay with the pion propagation dynamics. It opens an unexplored exciting field of investigation.

[1] N.S. Amelin *et al.*, *The Nuclear Equation of State*, eds W. Greiner and H. Stöcker, NATO ASI Series A**216** (Plenum, New York, 1989), Part B, p 473 ; N.S. Amelin *et al.*, Sov. J. Nucl. Phys. **52** (1990) 172 ; K. K. Gudima, M. Ploszajczak and V. D. Toneev, Phys. Lett. B**328** (1994) 249.

[2] K. K. Gudima *et al.*, Phys. Rev. Lett. **76** (1996) 2412.

[3] T. Matulewicz, in *Proceedings of the XXIII Mazurian Lakes Summer School, Piaski, Poland, 1993* [Acta Phys. Pol. B **25**, 705 (1994)].

[4] G. Martínez *et al.*, Phys. Lett. B **49**, 23 (1994).

[5] B. J. Ver West and R. A. Arndt, Phys. Rev. C **25**, 1979 (1982).

NUCLEAR STOPPING IN HEAVY-ION COLLISIONS AT 100 MeV/NUCLEON FROM NEUTRAL PION MEASUREMENTS

A. Badalà, R. Barbera, A. Palmeri, G. S. Pappalardo,
F. Riggi, A. C. Russo, G. Russo, and R. Turrisi

Istituto Nazionale di Fisica Nucleare, Sez. di Catania
Dipartimento di Fisica dell'Università di Catania
Laboratorio Nazionale del Sud, Catania

I. INTRODUCTION

The production of energetic particles at energies below the free NN threshold, such as pions, has been shown to originate mainly from central collisions [1]. In that case a high amount of the available energy in the center-of-mass frame - larger than for hard photons - is required to be concentrated into a single degree of freedom, and some projectile stopping could be better evidenced. The interpretation of pion data is complicated by final state effects such as pion reabsorption and rescattering in the nuclear matter which, especially for heavy targets play a major role to determine the shape of the energy spectra and angular distribution, due to shadowing effects. This could lower the apparent source rapidity below the value of the c.m. frame. Mostly light projectiles have been used in these studies, which do not allow to reach a large overlap of nuclear matter and consequently a high degree of stopping to be evidenced. It is felt that a study of this effect as a function of the system size could be more effective to disentangle the various factors contributing to the observed yields. Moreover, a study of this effect would require exclusive measurements to characterize the centrality of the collision and to have information on the amount of transverse momentum and energy carried out by the outgoing particles.

In this report inclusive and exclusive data on π°, extracted from an experiment performed at GANIL, are discussed in terms of stopping and reabsorption. The distribution of charged baryons associated with pion emission has been also investigated.

II. EXPERIMENT AND DATA ANALYSIS

The experiment was performed at GANIL, irradiating ^{27}Al, ^{58}Ni, ^{112}Sn and ^{197}Au targets with a ^{36}Ar beam at 95 MeV/nucleon. The MEDEA array [2] was used to detect neutral pions and the associated charged particles. More details on the experimental set-up and the data analysis procedure are reported on previous publications referring to the same experimental set-up [1-8].

III. RESULTS AND DISCUSSION

A. Moving source analysis

While the production of hard photons has been generally interpreted as originating from bremmstrahlung in incoherent first-chance nucleon-nucleon collisions, the importance of secondary N-N collisions may lead to a damping of the longitudinal motion. In the limit of a complete thermalization picture, which implies more and more N-N collisions, some degree of stopping of the incoming projectile nucleons may be expected. This effect is believed to show up more dramatically the heavier is the system under study. A study of the source velocities as a function of the system size and impact parameter should help in this respect.

A dramatic reduction of the β_s value with respect to β_{NN} was observed for

all targets [8]. This effect increases with the size of the target: β_s ranges from 0.11 for the lighter system to 0.03 for the heavier one. The apparent source velocity is then even lower than the nucleus-nucleus value, which for the ^{36}Ar+^{197}Au system amounts to $\beta_{nn} = 0.07$. In case of pions however, reabsorption effects play an important role to modify the shape of the observed energy spectra and angular distributions.

A further analysis was undertaken as a function of the impact parameter b. The selection of the impact parameter in the collisions producing pions was achieved by the multiplicity of charged particles. This analysis allowed to classify the events into three classes, roughly corresponding to *central*, *midcentral* and *peripheral* collisions. Going from central to peripheral collisions β_s increases. Even for the most peripheral collisions selected in this experiment however, the apparent source velocity remains substantially lower than the β_{NN} value.

The analysis of the source velocities evidences some degree of stopping, especially for central collisions of heavy systems, whereas for light systems and most peripheral collisions, the participating nuclear matter does not have sufficient volume and density to result in a sensible nuclear stopping.

B. Distribution of pions

To further investigate the effect of the participating nuclear matter on the reaction dynamics leading to pion production, the angular distributions of pions were extracted for central, mid-central and peripheral collisions [8]. For the heavier system a backward rise of the angular distribution in the NN reference frame is observed for central collisions, whereas for peripheral collisions a nearly symmetric angular distribution is found. For the light system ^{36}Ar+^{27}Al a similar behaviour may be noted, but in this case central collisions give a backward/forward ratio smaller than for the ^{197}Au case, where reabsorption effects are more crucial. The rapidity distributions of the emitted pions in the laboratory frame of reference show the following features:

i) low energy pions (T_π=0-20 MeV) are characterized by a nearly symmetric rapidity distribution around y=0. The rapidity centroid shifts towards negative rapidities especially for the ^{36}Ar+^{197}Au data, when more central collisions are selected;

ii) energetic pions ($T_\pi > 50$ MeV) are characterized by large rapidities.

These features point out that low energy pions could be preferentially emitted by a more relaxed source as the result of successive NN collisions; this situation is better reached for the most central collisions which produce a higher energy density and overlap of nuclear matter. This component gives the bulk of the cross section. On the other hand, more energetic pions, where a total energy in excess of 200 MeV is concentrated into a single degree of freedom, are mainly originating from single NN collisions, thus retaining *memory* of the initial motion.

C. Distribution of baryon matter

If central collisions show a high degree of stopping and pions emerge from a relaxed source, this should also be reflected by the distribution of the associated baryon matter.

The rapidity distributions in the laboratory frame of all charged particles in pion events (selected by the centrality of the collision) evidence two main sources: the first source is centered around the beam rapidity, while the second at smaller rapidity. Peripheral collisions are dominated by the peak around y=0.4, while moving to more central collisions a second source shows up, reflecting a high degree of stopping. This is particularly evident for the ^{36}Ar+^{197}Au system where

the low rapidity component is dominant in central collisions.

III. CONCLUSIONS

Stopping of the projectile in nucleus-nucleus collisions indicates a substantial energy loss of the colliding nuclear matter. In high-energy heavy-ion collisions the energy lost by the colliding systems provides high energy density regions, which could be good candidates to probe the existence of a quark-gluon plasma. It is important to note that at those high bombarding energies the energy loss is usually accompanied by production of a large number of particles (mainly pions). At energies around 100 MeV/nucleon pion production corresponds to only a few hundred μb of the total reaction cross section. When central collisions are selected by the emission of a pion and an associated high multiplicity of charged baryons, some degree of stopping is however expected.

Evidence for this phenomenon was observed by several observables. First of all, both hard photons and neutral pions were shown to be associated especially for heavy systems and head-on collisions to a slowly moving sources which could stem from multiple collisions taking place. The pion reabsorption effects especially for heavy colliding systems could provide a further (apparent) reduction of the observed pion source velocity, since a substantial reduction of pion yields at forward angles is expected. Low energy pions were shown to emerge with an almost flat angular distribution, whereas energetic pions are mostly forward peaked, which could point out the importance of first chance nucleon-nucleon collisions in these cases. Moreover, additional evidence for the occurrence of stopping of baryon matter came from the investigation of the associated charged particles in pion events. By a comparison of the results obtained for several targets, it was shown that when the target nucleus is heavy enough, there is a high probability for the incident nucleus to loose a substantial fraction of its energy.

Further investigation could require a detailed knowledge of how the transverse energy is distributed among the reaction products. In conclusion, a clear evidence of the nuclear stopping was found at energies around 100 MeV/nucleon, by a systematic investigation of the energetic products of nucleus-nucleus collisions measured by a nearly 4π multidetector.

REFERENCES:

[1] A. Badalà *et al.*, Phys. Rev. C 48, 2350 (1993) and references therein.
[2] E. Migneco *et al.*, Nucl. Instr. and Meth. in Phys. Res. A **314**, 31 (1992).
[3] A. Badalà *et al.*, Nucl. Instr. and Meth. in Phys. Res. A **306**, 283 (1991).
[4] A. Badalà *et al.*, Phys. Rev. C **47**, 231 (1993).
[5] A. Badalà *et al.*, Nucl. Instr. and Meth. in Phys. Res. A **350**, 192 (1994).
[5] A. Badalà *et al.*, Nucl. Instr. and Meth. in Phys. Res. A **351**, 387 (1994).
[6] A. Badalà *et al.*, Z. Phys. A **344**, 455 (1993).
[7] A. Badalà *et al.*, Nucl. Instr. and Meth. in Phys. Res. A **357**, 443 (1995).
[8] A. Badalà *et al*, Phys. Rev. **C53**,1782 (1996).

Δ resonance absorption in intermediate-energy heavy-ion collisions

R. Holzmann[1], A. Schubert[1], S. Hlaváč[1,8], R. Kulessa[1,7], W. Niebur[1], R.S. Simon[1], V. Wagner[1,9], P. Lautridou[2], F. Lefèvre[2], M. Marqués[2,4], T. Matulewicz[1], W. Mittig[2], R.W. Ostendorf[2], P. Roussel-Chomaz[2], Y. Schutz[2], H. Löhner[3], J.H.G. van Pol[3], R.H. Siemssen[2,3], H.W. Wilschut[3], F. Ballester[4], J. Díaz[4], A. Marín[4], G. Martínez[4], W. Kühn[5], V. Metag[5], R. Novotny[5], J. Québert[6]

1. *Gesellschaft für Schwerionenforschung, D-64220 Darmstadt*
2. *Grand Accélérateur National d'Ions Lourds, F-14021 Caen*
3. *Kernfysisch Versneller Instituut, NL-9747 AA Groningen*
4. *Instituto de Física Corpuscular, SP-46100 Burjassot Valencia*
5. *II. Physikalisches Institut, Universität Gießen, D-35392 Gießen*
6. *Centre d'Etudes Nucléaires de Bordeaux-Gradignan, F-33175 Gradignan*
7. *Jagellonian University, Cracow, Poland*
8. *Slovak Academy of Sciences, Bratislava, Slovak Republic*
9. *Nuclear Physics Institute, Řež u Prahy, Czech Republic*

1 Introduction

Over the last decade it has become increasingly clear that the Δ(1232) isobar, as well as higher-lying baryon resonances, plays a major role in the dynamics of heavy-ion collisions in the few GeV/nucleon range. Calculations suggest that these resonant states serve as an intermediate energy storage and greatly enhance through multi-step processes the cross sections at threshold of high-p_t pion, as well as eta and kaon production. On the other hand, as mesons are subject to strong final-state interactions, which often involve resonance excitation, any interpretation of their propagation in the nuclear medium has to rely on an accurate knowledge of not only the resonance production, but also the destruction processes. However, elementary cross sections involving resonances in the input channel are usually unknown and have to be estimated from the inverse process, if known, by applying the principle of detailed balance [1, 2].

In case of the pion the relevant processes are largely mediated by the Δ resonance through the elementary reaction $N + N \rightarrow \Delta + N$ (resonance creation) and its inverse $\Delta + N \rightarrow N + N$ (resonance capture). Whereas the first one is accessible to direct measurement, the cross section of the latter is obtained with the aid of detailed balance [1] from the cross section $\sigma_{N+N\rightarrow\Delta+N}$. However, it has been pointed out [3] that, as these reactions involve a resonance of short lifetime, the finite width of the resonance has to be corrected for [3, 4], leading to the so-called 'extended detailed-balance principle'. The latter can be verified through an experimental determination of $\sigma_{\Delta+N\rightarrow N+N}$ and comparison with the known cross section $\sigma_{N+N\rightarrow\Delta+N}$ [5].

We present results from the 1992 campaign of TAPS at GANIL. Heavy-ion induced hard-photon and subthreshold π^0 production has been investigated in ^{36}Ar-induced reactions at 95 MeV/u, both inclusively, and in coincidence with light charged particles and projectile-like fragments. A number of novel results have been obtained and are discussed together with the experimental details in refs. [6]. Here we concentrate on neutral-pion production with particular emphasis on processes involving the Δ resonance.

is presented

2 The Δ capture cross section

From the shape of the π^0 kinetic-energy spectrum, obtained for $^{36}Ar+^{197}Au$ at 95 MeV/u, which is strongly affected by the pion final-state interactions in the nuclear medium, we have extracted a pion absorption cross section σ_{abs}. Within the standard assumptions of the Boltzmann-Uehling-Uhlenbeck (BUU) transport theory, i.e. supposing in particular that σ_{abs} encompasses both the $\pi + N \rightarrow \Delta$ and $\Delta + N \rightarrow N + N$ processes, we have obtained an experimental estimate of the elementary cross section $\sigma_{\Delta+N\rightarrow N+N}$ for center-of-mass energies $\sqrt{s} \simeq 2050 - 2250$ MeV, allowing for a test of the extensions applied to the detailed-balance principle within that framework. Here we give only a schematic outline of this analysis; more details can be found in ref. [7].

In a BUU calculation, where pion production is treated perturbatively, we find a primordial pion spectrum, i.e. the one prior to all final-state interactions, which can be well approximated by a maxwellian distribution. These calculations reproduce very well the shape of the concurrently measured *pn* bremsstrahlung spectrum, offering a direct check of their predictive power. The present BUU result suggests that, for inclusive pion events at least, the folding of the nucleon Fermi momenta with the elementary pion production cross section results in a very close to thermal phase-space occupancy. Deviations from the pure maxwellian shape are however expected and are presumed to hold information on the pion rescattering and reabsorption processes [8].

As shown in [7], the ratio of the measured and calculated π^0 kinetic-energy spectra, transformed into the NN c.m. frame, gives the pion escape factor which can be transformed into a momentum-dependent pion absorption length $\lambda_{ABS}(p)$. From this, in turn, a momentum-dependent π^0 absorption cross section σ_{abs} is obtained, which is then decomposed into an s-wave part, corresponding to the Born and rescattering terms, and a p-wave part, corresponding to the Δ resonance. Subsequently an estimate of $\sigma_{\Delta+N\rightarrow N+N}$ has been obtained in the following way: when a Δ is excited on a nucleon in the process $\pi + N \rightarrow \Delta$, it can either decay with a decay length λ_{decay} or be captured on a second nucleon with a capture length $\lambda_{capt}(s)$. We define now a Δ capture probability which, on the one hand, is related [1] to the above quantities by $P_{capt} = \lambda_{decay}/(\lambda_{decay} + \lambda_{capt})$ and, on the other hand, can be obtained experimentally from the ratio of the p-wave part of the measured π^0 absorption cross section σ^p_{abs} and the Fermi-smeared total π^0N cross section σ_{tot}, i.e. $\sigma^p_{abs} = P_{capt} \cdot \sigma_{tot}$. Next, from the experimental value of P_{capt} and the calculated λ_{decay}, the capture length λ_{capt} has been evaluated. In a last step, from λ_{capt} we have obtained the cross section for Δ capture, with $\sigma_{capt} = 1/(\lambda_{capt} \cdot \rho_0)$.

The resulting estimate of the elementary, i.e. free, capture cross section $\sigma_{\Delta+N\rightarrow N+N}$ obtained after unfolding for Fermi smearing, is finally shown in Fig. 1 as function of the c.m. energy. As we deal here with neutral pions, in first order, only processes involving the Δ^+ and Δ^0 states have to be considered. From the comparison of the data with calculations [3, 4] it clearly appears that the correction for the finite width of the Δ is required in order to reproduce the steep increase observed at low $\sqrt{s}$.

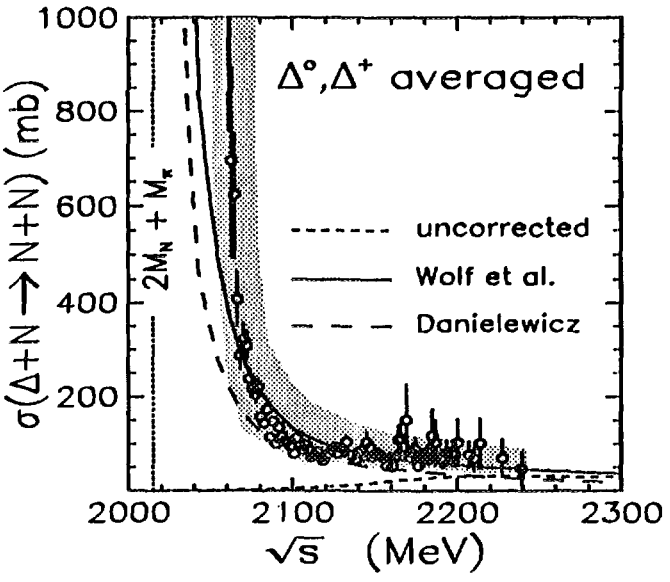

Figure 1: Elementary Δ capture cross section as function of the ΔN c.m. energy $\sqrt{s}$. The shaded band corresponds to systematic errors. Lines are detailed-balance calculations without the finite-width correction (short-dashed), and with correction according to Wolf et al. [4] (solid), and to Danielewicz and Bertsch [3] (long-dashed), respectively. The absolute threshold at $2M_N + M_\pi$ is also indicated.

3 Conclusions

In summary, we have investigated inclusive, as well as exclusive π^0 emission in heavy-ion reactions at 95 MeV/u. The behaviour of neutral-pion production displays many similarities with the emission of very hard photons, pointing to the fact that essentially the same reaction phase is probed [6]. The strong final-state interactions of pions have to be taken into account, however, and we have shown that they can even be put to good profit. We have indeed deduced an experimental estimate of the Δ capture cross section from an analysis of the pion kinetic-energy spectrum. Comparing our results with BUU calculations allows for an important consistency check of microscopic transport theories describing hadronic matter dynamics and particle production in the 50 MeV/u to few GeV/u range.

[1] Z. Fraenkel, Phys. Rev. **130**, (1963) 2407.
[2] G.F. Bertsch and S. Das Gupta, Phys. Rep. **160** (1988) 189.
[3] P. Danielewicz and G.F. Bertsch, Nucl. Phys. **A533** (1991) 712.
[4] Gy. Wolf, W. Cassing and U. Mosel, Nucl. Phys. **A545** (1992) 139c;
Nucl. Phys. **A552** (1993) 549.
[5] *B.J. VerWest and R.A. Arndt, Phys. Rev. C25 (1982) 1979.*
[6] A. Schubert et al., Phys. Rev. Lett. **72** (1994) 1608; Phys. Lett. **B328** (1994) 10;
Nucl. Phys. **A583** (1995) 385c.
[7] R. Holzmann et al., Phys. Lett. **B366** (1996) 63.
[8] R.S. Mayer et al., Phys. Rev. Lett. **70** (1993) 904.

Observation of in-medium Δ excitation via $\pi^o - p$ correlations in TAPS

T. Matulewicz[1,9], L. Aphecetche[1], Y. Charbonnier[1], H. Delagrange[1], G. Martínez[1], Y. Schutz[1], F.M. Marqués[2], M. Appenheimer[3], R. Averbeck[4], J. Díaz[5], A. Döppenschmidt[4], A. Gabler[3], M.J. van Goethem[6], S. Hlaváč[7], M. Hoefman[6], R. Holzmann[4], A. Kugler[8], F. Lefèvre[1], H. Löhner[6], A. Marín[5], V. Metag[3], W. Niebur[4], R. Novotny[3], R.W. Ostendorf[6], R.H. Siemssen[6], R.S. Simon[4], R. Stratmann[4], H. Ströher[3], P. Tlusty[8], P.H. Vogt[6], V. Wagner[8], H.W. Wilschut[6], F. Wissmann[4], M. Wolf[3].

1. *Grand Accélérateur National d'Ions Lourds, F-14021 Caen, France.*
2. *Laboratoire de Physique Corpusculaire, F-14050 Caen, France.*
3. *II Physikalisches Institut Universität Gießen, D-35392 Gießen, Germany.*
4. *Gesellschaft für Schwerionenforschung, D-64291 Darmstadt, Germany.*
5. *Instituto de Física Corpuscular, E-46100 Burjassot, Spain.*
6. *Kernfysisch Versneller Instituut, NL-9747 AA Groningen, The Netherlands.*
7. *Slovak Academy of Sciences, Bratislava, Slovakia.*
8. *Nuclear Physics Institute, 250 68 Řež, Czech Republic.*
9. *Warsaw University, PL-00-681, Warszawa, Poland.*

Baryonic resonances, like the Δ resonance, play an important role in the dynamics of heavy-ion collisions. They are excited in direct two-body nucleon-nucleon collisions and subsequently propagate through nuclear matter, collide with other nucleons or resonances, or decay through particle (mainly meson) emission. The last process is responsible for the bulk of meson production at beam energies around the nucleon-nucleon threshold. Energetic elementary collisions involving already produced resonances can subsequently excite higher lying ones, the decay of which produces more massive mesons, rarely produced if only nucleon-nucleon collisions are considered. In this way baryonic resonances act also as an intermediate energy storage, influencing the thermal equilibration of nuclear matter.

The properties of the Δ-resonance in nuclear matter have been studied in the past both theoretically and experimentally. As a matter of fact the decay

Abs.

The role of Δ particles in the dynamics of heavy ion collisions is studied, and the properties of Δ particle in nuclear matter is investigated. Correlations in the invariant mass distribution of $\pi^0 - p$ events are studied.

width of the Δ-resonance is influenced by the density of surrounding nuclear matter [1]. Experimentally the Δ-resonance in a nucleus has been studied mainly using elementary probes (photons, pions, hydrogen and helium isotopes) [2]. In heavy-ion collisions we are aware of only indirect indications of the Δ-resonance formation, with the exception of recent measurements performed at 95A MeV [3] and at 1930A MeV [4]. Heavy-ion reactions present the advantage of producing nuclear matter at higher densities where significant effects on the shape of the resonance are expected. Searching for a direct signal of the Δ-resonance excitation remains however a challenge. We have attempted to search for this signal in the reaction Ar+Ca at 180A MeV, well below the free pion production threshold. We search for a correlation in the invariant mass distribution of $\pi^0 - p$ events.

Photon pairs needed for the π^0 identification were detected in the TAPS electromagnetic calorimeter composed of 384 BaF_2 scintillation modules arranged in 6 blocks of 64 modules each. The blocks were placed in two towers positioned symmetrically with respect to the beam direction at a distance of 80 cm from the target. The position of the towers was optimized for detection of particles emitted from a mid-rapidity source. Photons detected in TAPS were identified through their time-of-flight and pulse-shape analysis of BaF_2 scintillation light by requiring adequate conditions on the correlation between these two variables [5]. Photon energy and direction were reconstructed from the electromagnetic shower using the cluster analysis described in Ref [6]. Photon pairs, needed for π^0 identification, were selected with respect to their relative timing as well. Neutral pions were identified through an invariant mass analysis of two or more photon events.

The charged-hadron events were identified with appropriate gate using the time-of-flight versus pulse-shape distribution [7]. Protons and deuterons were in that way clearly identified.

From the π^0-proton events the invariant mass was evaluated according to the formula

$$M_{p\pi}^{inv} = \sqrt{m_p^2 + m_\pi^2 + 2E_pE_\pi(1 - \beta_p\beta_\pi \cos\theta_{p\pi})} \qquad (1)$$

where m, E, β denote mass, total energy and velocity, respectively, and $\theta_{p\pi}$ the opening angle between proton and pion. In order to search for a Δ-resonance signal the precise knowledge of the shape of the background is necessary. The background spectrum was obtained by the technique of event

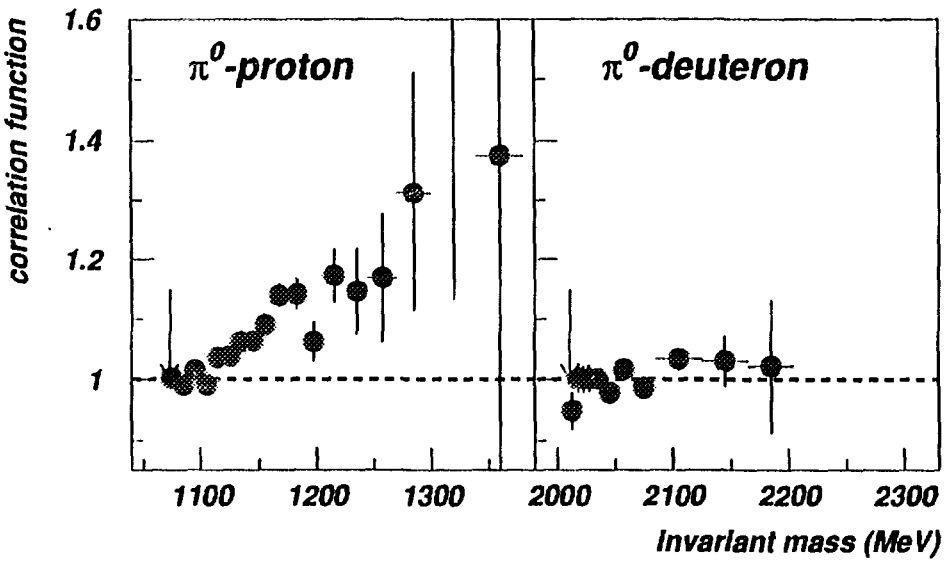

Figure 1: *Correlation function as a function of the invariant mass for the π^0-proton and the π^0-deuteron events. The arrows indicate sum of rest masses.*

mixing. Then, the correlation function $C_{p\pi}$ was constructed as the ratio of coincident $Y_{p\pi}$ to the mixed $Y_p \otimes Y_\pi$ invariant mass spectrum

$$C_{p\pi} = \frac{Y_{p\pi}}{Y_p \otimes Y_\pi} \tag{2}$$

The correlation function was normalized to unity in the region of low invariant mass, where it stays constant (Fig 1 left panel). With increasing invariant mass, approaching the Δ-resonance mass, the π°-proton correlation function systematically raises reaching values around 1.15. We interpret this correlation signal as the signature of the excitation of the Δ-resonance. To verify the validity of the correlation signal we have applied a similar analysis to a

system where no resonance is expected. We have selected the π^0-deuteron system, where no baryonic resonance exists. The whole procedure applied to protons has been repeated for deuterons and the π^0-deuteron correlation function has been obtained (Fig.1 right panel). This correlation function shows no resonance signal. This result ensures that the signal observed in π^0-proton system is really due to the Δ-resonance and not an artifact of the analysis.

[1] T. Ericson and W. Weise *Pions and Nuclei*, Clarendon, Oxford, 1988.

[2] F. Osterfeld *et al.*, Nucl. Phys. **A577** (1994) 237.

[3] A. Badalà *et al.*, in *Proceedings of XXXIII Winter Meeting on Nuclear Physics*, Bormio (1995) 431.

[4] D. Best *et al.*, in *Proceedings of XXXIII Winter Meeting on Nuclear Physics*, Bormio (1995) 505.

[5] T. Matulewicz *et al.*, in *Nouvelles du GANIL* 57 (1996) 29, and submitted to Nucl. Inst. and Meth.

[6] F.M. Marqués *et al.*, Nucl. Inst. and Meth. **A365** (1995) 392.

[7] T. Matulewicz et al., *Hydrogen isotopes identification with the electromagnetic calorimeter TAPS*, contribution to this Compilation.

FR9700912

KAON PRODUCTION IN NUCLEUS-NUCLEUS COLLISIONS AT 92 MEV PER NUCLEON

R. Legrain[a)], J.F. Lecolley[b)], F.R. Lecolley[b)], N. Alamanos[a)], L. Bianchi[c)], Y. Cassagnou[a)], H. Dabrowski[d)], B. Erazmus[d)], J. Julien[a,d)], D. Lebrun[e)], Ch. Le Brun[b)], A. Mougeot[a)], P. Hameau[a)], G. Perrin[c)], P. de Saintignon[c)], J.L. Sida[a)] and J.P. Wieleczko[c)]

a) CEA DAPNIA, CE Saclay, 91191 Gif sur Yvette Cedex, France
b) LPC, ISMRA & Université de Caen, CNRS/IN2P3, 6 Bld Maréchal Juin, 14050 Caen Cedex
c) GANIL, BP 5027, 14021 Caen Cedex, France
d) SUBATECH, 2 Rue de la Houssinière, 44072 Nantes Cedex 03, France
e) ISN Grenoble, 53 Avenue des Martyrs, 38026 Grenoble Cedex, France

In a previous experiment (1), we have demonstrated that kaons can be produced and detected in sizeable quantities in collisions of ^{36}Ar ions on a ^{48}Ti target at 92 MeV/n. The experimental procedure was based on the detection of the delayed monoenergetic muon coming from the weak decay of a stopped kaon. The main decay channel (64%) of the kaon is $K^+ \rightarrow \mu^+ + \nu$ with $T\mu$ = 152.9 MeV and a mean life of 12.4 ns. Using a range telescope technique, twelve good events were recorded leading to a total cross section σ_K=240±150 pb. Using the same technique with a new apparatus which combines low background to accept large beam intensities and segmented hodoscopes to check the muon trajectories, a new experiment has been performed. A 92 MeV/n ^{36}Ar beam was used to bombard three targets (^{12}C, ^{48}Ti, ^{181}Ta). The off-line analysis to select kaon requires :

- delayed events (> 3 ns) by respect to the beam still events
- a narrow coincidence between the various detection planes
- measured energy losses and range in agreement with 152.9 MeV muon
- trigger conditions still satisfied at the end of the analysis with only hit per detection plane.

The range and deposited energy distributions obtained in that conditions are in agreement with the distributions calculated with the GEANT simulation. The time distribution and presents a slope in agreement with the slope of the kaon decay (solid line). The total cross section is calculated for each target by extrapolating the time distribution up to t=0, by assuming isotropy and using for the detection efficiency the coefficients given by the simulation. The measured cross sections are given in the following table :

Target	E_{CM} (MeV)	σ_{tot}
^{12}C	820	82^{+49}_{-32}
^{48}Ti	1870	511^{+180}_{-140}
^{181}Ta	2744	3093^{+979}_{-928}

An analysis based on correlation decorrelation techniques gives similar results. The cross section production changes very rapidly with the target mass following a $A^{3/2}$ law(2) (full line on figure 2). The pion production near threshold follows a $A^{3/2}$ law. The variation of the observed K production near threshold as a function of the center of mass avalaible energy (fig. 3) seems to be governed by a two body phase space behaviour (full line).

Kaon production in ^{36}Ar reactions on three targets (^{12}C, ^{48}Ti, ^{181}Ta) have been investigated. Production cross sections of kaons are presented.

An analysis has been done (3) to compare the kaon production probability in nucleus-nucleus collision and nucleon-nucleus collisions. The subthreshold production in proton induced reaction is easily explained by the elementary nucleon-nucleon process taking into account a reasonable Fermi momentum distribution. The nucleus nucleus collision may be only explained by the production in a limited hot zone where the parameter which governs the reaction is the available excitation energy allowing a statistical production as soon it is energetically possible.

References :
1) J. Julien et al, Phys. Let. B264, 269, 1991
2) F.R. Lecolley et al, Nucl. Phys. A583, 1995, 379
3) R. Legrain et al, to be published in Physical Rev. C

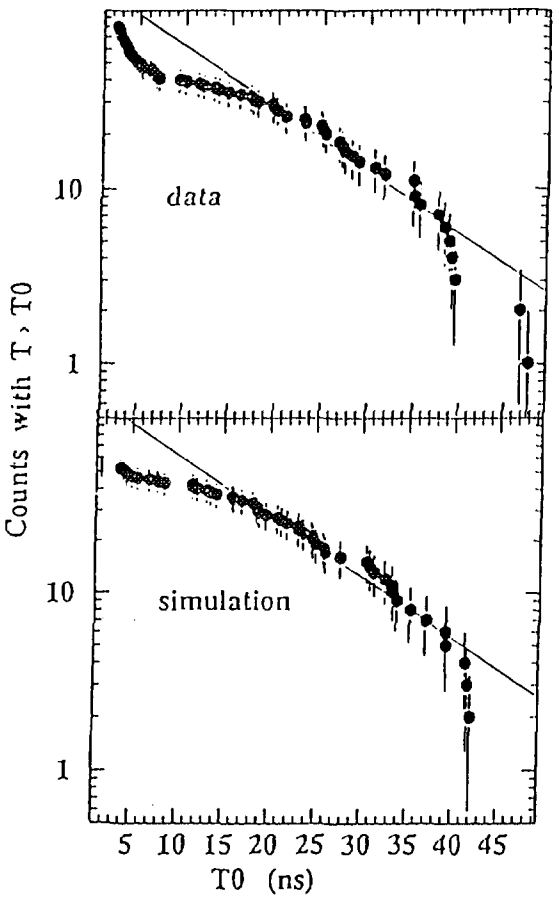

Figure 1

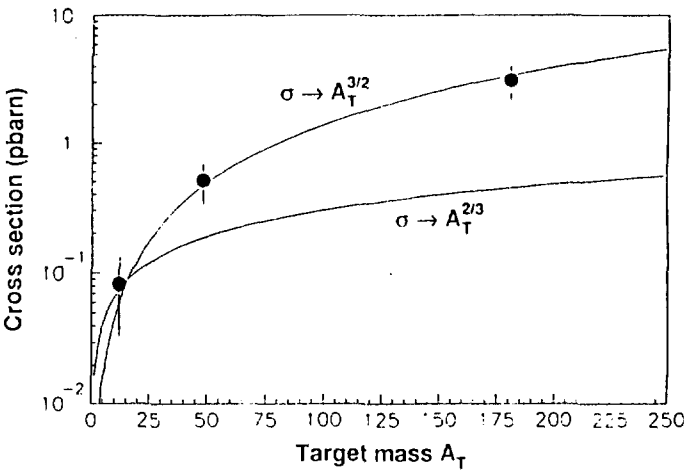

Figure 2

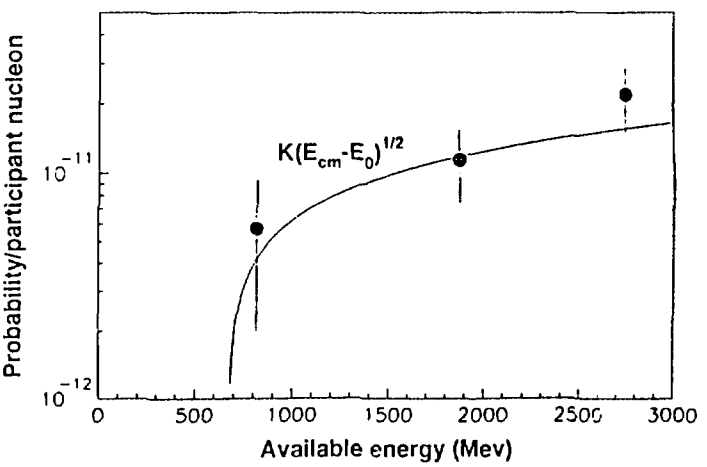

Figure 3

High transverse momentum proton emission in Ar +Ta collisions at 94 MeV/u

M.Germain,P.Eudes,F.Guilbault,P.Lautridou,J.L.Laville,C.Lebrun,M Leguay,
A.Rahmani,T.Reposeur

SUBATECH, Université, Ecoles des Mines,IN2P3-CNRS, F-44072 Nantes Cedex 03(France).
R. Bougault,F Gulminelli,O.Lopez

LPC,ISMRA,IN2P3-CNRS et Université de Caen
J Benlliure,P Gagne,JP Wieleczko

GANIL,CEA et IN2P3-CNRS,BP 5027,F14021,Caen

FR9700913

Abstract

Energy spectra of fast protons arising from collisions induced by 94 MeV/u Argon projectiles colliding with Tantalum nuclei have been measured at large angles.These data are analysed in the framework of a transport theory simulated by the BNV code.The low cross-sections observed for very energetic protons excludes a possible mechanism of kaon production via individual collisions between internal nucleons.

1 Introduction

The surprisingly high cross-sections [1, 2] measured for very subthreshold Kaon production at such a low energy than 94 MeV/u appears as a challenge in this energy domain.A possible explanation rests upon individual collisions between nucleons reaching the associate λK production threshold in their center-of-mass frame(330 MeV) [3].These collisions could be induced by dynamical fluctuations at the beginning of the reaction. We report here about a measurement of the high energy tail of protons emitted in collisions induced by 94 MeV/u Argon projectiles on tantalum nuclei.More precisely,the experiment wished to answer the following questions:
1)Do we observe a high energy tail in proton emission able to account for λK production via individual nucleon-nucleon collisions?
2) Furthermore is there some indication for any exotic process as suggested by the extension of transport theories(like fluctuations [3]).

2 Experimental details

The experiment has been done upon the GANIL facility which delivered a 94 MeV/u argon beam impinging on a 50 mg/cm**2 tantalum target.Energetic protons were detected by two telescopes consisting of three scintillators: a plastic Ne102 followed by a CsI-BGO phoswich. The performances of such a phoswich have been tested successfully prior to that experiment.They are detailed in a recent paper [4]:it is demonstrated that we got a very clear isotope separation for fast protons, deuterons and tritons.
These telescopes were set at 75 deg and 105 deg respectively. The choice of angles was led by the following requirements [5]:
1) High transverse momentum protons select central collisions and the searched emission phenomenon is assumed to occur at low impact parameter.
2) Particle emission from the participant zone is favoured at large angle where it can be easier distinguished from the projectile and target-like spectators contribution.
The energy calibration of both telescopes was achieved in special runs using secondary beams of light particles delivered by GANIL .This calibration has been done for proton energies of 150,180,200,230 and 300 MeV:it allowed to determine the proton energy with an accuracy less than 2% over the full range of interest.

3 Energy spectra and BNV analysis

The resulting energy spectra are presented on fig. 1.Only the high energy parts we are interested in are displayed at 75 and 105 degrees in the laboratory:they show an exponential fall-off with energies reaching 350 MeV;the latter value corresponds to nearly four times the beam energy per nucleon.The possible role of internal fermi momentum is illustrated by the arrow indicating the limit imposed by a sharp cut-off of the fermi motion at a value of 270 MeV/c:we see that protons are produced far away from this limit.Nevertheless we do not observe the high energy component expected from the BL code.Then,we performed a more "classical" BNV calculation which includes, together with the standard binary scattering, the possibility of ternary collisions [6].This model has already been applied with some success to subthreshold pion and photon production [9]. A ternary collision can be viewed as a cooperative process, since the extra energy of the third nucleon can be used to boost a particle far off the Fermi sea.The results are shown in fig.2, where it is seen that the standard binary processes are insufficient to account for the very energetic part of the spectra, and most energetic protons come from the ternary contribution.
However the model tends to underestimate the data, especially for the most subthreshold production at backward angles, suggesting that even more cooperative processes (higher order collisions) or off-shell contributions are needed to explain the Kaon yields.

4 conclusion and outlook

Our PHE data do not show evidence for the expected signal related to possible instabilities,as predicted by the BL code.A straightforward consequence of that result is that Kaon production does not proceed via simple NN collisions.We are probably confronted by a much more sophisticated process:a more quantitative analysis comparing the results of the BL and QMD codes is actually on progress [7].Finally,the BNV approach allows to set a link between NN process and collective effects which [8] might contribute to Kaon production.

References

[1] J. Julien et al., Phys. Lett. B264(1991)269

[2] R. Legrain et al,to be published in PRC

[3] M Belkacem et al.,PRC 47(1993)R16

[4] P Lautridou et al.,Nucl. Inst. Meth. A373(1966)135

[5] J.L. Laville et al.,Nucl. Phys. A564(1993)564

[6] A. Bonasera, F. Gulminelli, J. J. Molitoris, *Phys. Rep.* 243 (1994) 1

[7] C Hartnack et al.,to be published

[8] B Gosh, Phys. Rev. C 45(1992)R51S

[9] W. Bauer, *Phys. Rev.* 40C (1989) 715.

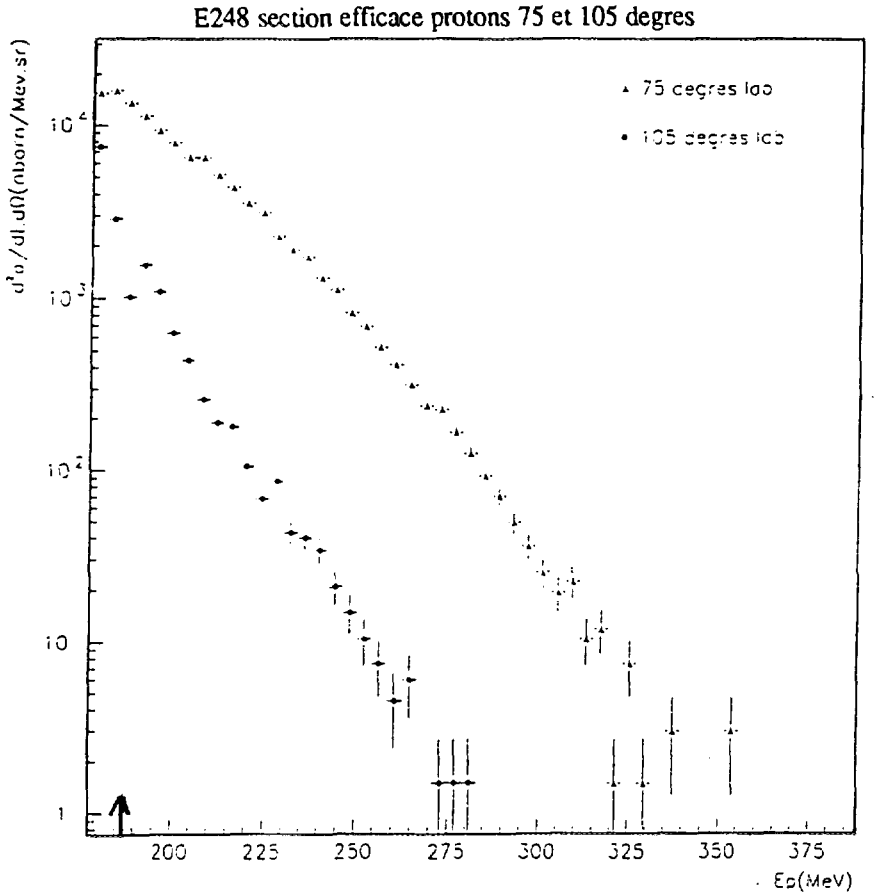

Fig. 1 : Proton energy spectra obtained from Ar + Ta interactions at 94 MeV/u at 75 and 105 deg. The arrow indicates the kinemotical limit due to Fermi momentum according to a "sharp cut-off 270 MeV/c.

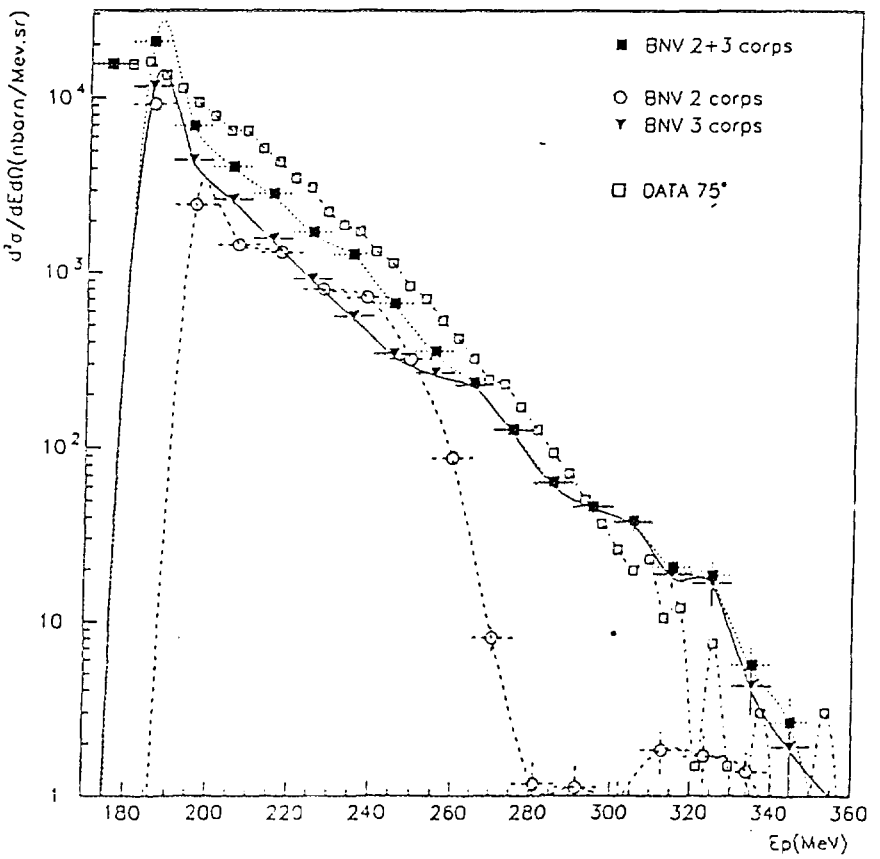

Fig. 2 : Proton energy spectrum at 75 deg. confronted with the BNV simulations (see text) : the continuous and dotted-dashed curves are drawn to guide the eye.

η's at deep subthreshold energies: Extreme behaviours of nuclear matter

G. Martínez[1], L. Aphecetche[1], Y. Charbonnier[1], H. Delagrange[1], T. Matulewicz[1,9], Y. Schutz[1], F.M. Marqués[2], M. Appenheimer[3], R. Averbeck[4], J. Díaz[5], A. Döppenschmidt[4], A. Gabler[3], M.J. van Goethem[6], S. Hlaváč[7], M. Hoefman[6], R. Holzmann[4], A. Kugler[8], F. Lefèvre[4], H. Löhner[6], A. Marín[5], V. Metag[3], W. Niebur[4], R. Novotny[3], R.W. Ostendorf[6], R.H. Siemssen[6], R.S. Simon[4], R. Stratmann[4], H. Ströher[3], P. Tlusty[8], P.H. Vogt[6], V. Wagner[8], H.W. Wilschut[6], F. Wissmann[4], M. Wolf[3].

1. *Grand Accélérateur National d'Ions Lourds, F-14021 Caen, France.*
2. *Laboratoire de Physique Corpusculaire, F-14050 Caen, France.*
3. *II Physikalisches Institut Universität Gießen, D-35392 Gießen, Germany.*
4. *Gesellschaft für Schwerionenforschung, D-64291 Darmstadt, Germany.*
5. *Instituto de Física Corpuscular, E-46100 Burjassot, Spain.*
6. *Kernfysisch Versneller Instituut, NL-9747 AA Groningen, The Netherlands.*
7. *Slovak Academy of Sciences, Bratislava, Slovakia.*
8. *Nuclear Physics Institute, 250 68 Řež, Czech Republic.*
9. *Warsaw University, PL-00-681, Warszawa, Poland.*

Abs: 228 oBal.

Subthreshold particle production has been demonstrated to be a powerful probe of heavy-ion dynamics. These particles are mainly produced in collisions between baryons during the first stage of the nuclear reaction when maximum compression and temperature are reached. Therefore particle production is a good observable for the study of nuclear matter properties. At relativistic heavy-ion collisions, the nuclear temperature is high enough so the lightest baryonic resonances are excited: $\Delta(1232)$, $N^*(1440)$, $N^*(1520)$, $N^*(1535)$, etc. In this particular case, the production of neutral mesons, π and η, is an adequate observable to study the population of these resonances. In first approximation, the population of the Δ resonance can be related to the production of π ($\Delta \rightarrow N + \pi$ with a branching ratio of 99%) and the $N^*(1535)$ resonance to the production of η mesons ($N^* \rightarrow N + \eta$ with a

branching ratio of $30 - 55\%$). At deep-subthreshold energies (less than 25% of the threshold energy for meson production in free nucleon-nucleon collisions), the energy available in one nucleon-nucleon collision is less than the difference between the N^* and the nucleon masses. The resonance cannot be excited and alternative mechanisms must be considered for the production of η mesons, like the excitation via multi-step collisions, N-body correlations or new elementary mechanisms.

Another common phenomenon, mainly observed at ultra-relativistic energies, is the scaling of meson abundances with transverse mass, known as transverse-mass scaling. The transverse mass is defined as $m_t = \sqrt{p_t^2 + m^2}$, where p_t is the transverse momentum with respect to the beam axis and m is the meson mass. This scaling has been evidenced at ultrarelativistic energies for π, η, K, and $\bar{p}$. The m_t scaling is still valid at relativistic energies, 1A GeV and 1.5A GeV, for η and π mesons. This is rather surprising since meson production proceeds through the excitation of the first baryonic resonances at variance with the mechanism involved at ultrarelativistic energies. These universal properties of the invariant transverse mass spectra of π and η have been discussed within the Quark Gluon String Model in a large range of

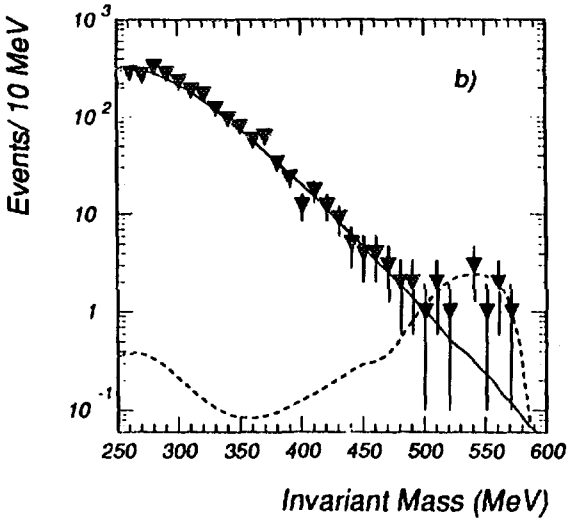

Figure 1: ***Two photon invariant mass spectrum in the η mass region measured for the system Ar+Ca at 180A MeV. The dashed line represents a simulation (with the GEANT code) of the TAPS response for the η production.***

bombarding energies [1].

The experiment was performed at GSI with the TAPS multidetector. The heavy-ion synchrotron SIS delivered an Ar beam, of 180A MeV, impinging a Ca target of 1% interaction probability. A 32 element phoswich detector, the Start Detector, placed at 10.1 cm away from the target, signed the occurrence of a nuclear reaction. Photons from meson decays were detected by the 384 hexagonal BaF_2 scintillation detectors of TAPS . The TAPS detectors were assembled in 6 square blocks of 64 detectors each, mounted in two towers positioned at 80 cm from the target. The towers were positioned at $\theta = 70°$, on each side of the target, covering the mid-rapidity region. The description of the shower reconstruction and invariant mass analysis is reported in reference [2, 3, 4].

The measured invariant mass distribution indicates a prominent peak at the neutral pion rest mass ($m_{\pi^0} = 135$ MeV). The mass resolution is 11% FWHM. Neutral pions have been identified in the invariant mass range from 80 to 150 MeV, as suggested by GEANT simulations [5]. The pion multiplicity is calculated as:

$$M_{\pi^0} = \frac{N_{\pi^0}}{N_{SD} \times \epsilon_{\pi^0}} = (3.3 \pm 0.8)\ 10^{-3} \qquad (1)$$

where N_π is the number of pions, N_{SD} the number of reaction triggers seen by the Start Detector, and ϵ_π the pion efficiency. The efficiencies for the detection of η and π^0 have been calculated from GEANT simulations including the TAPS response (*KANE* package [5]) and assuming a thermal emission in the nucleon-nucleon center of mass frame (the temperature being $T = 25$ MeV).

Between 250 and 500 MeV the experimental invariant mass (Fig. 1) coincides with the combinatorial background calculated by the event mixing technique but not at higher masses. Around the η rest mass ($m_\eta = 547$ MeV [?]) a significant excess of counts on top of the background is observed and is attributed to the η signal. The measured ratio of η to π is:

$$\frac{N_\eta}{N_{\pi^0}} = (5 \pm 2)10^{-6} \qquad (2)$$

From systematics [6], we do expect the ratio of η to the π^0 production to be $\approx 10^{-4}$. However we have found a new scaling law based on the temperature of

the pion spectra which explains satisfactorily the measured ratio of expression (2).

Unexpectecaly the m_t scaling appears to be still valid (Fig. 2). This observation is rather striking as the mechanism involved at ultrarelativistic energies are expected to be much different to those producing mesons near the absolute threshold. The distribution of the pion transverse mass has been adjusted to a thermal emission distribution, $T = (26 \pm 2)$ MeV.

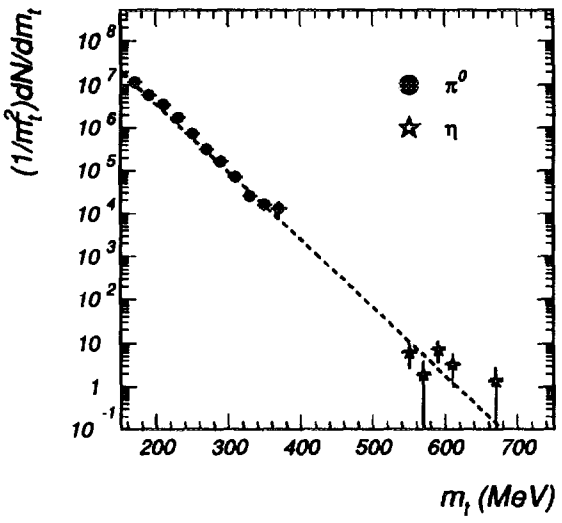

Figure 2: ***Transverse mass distribution of π° and η mesons measured for the system Ar+Ca at 180A MeV.***

In conclusion, from preliminary results on the η production at deep-subthreshold energy, the measured η probability is 20 times lower than expected from the systematics. The transverse mass scaling, established at ultrarelativistic energies well beyond the threshold in a free NN collision, is still observed at such a low energy. Therefore, the m_t scaling appears as a universal feature at all bombarding energies. An alternative scaling of the meson production multiplicities based on the temperature of the pion spectra, is proposed, which reproduces quite well the production ratio σ_η/σ_π. Theoretical approach based on a statistical model [7] reproduces satisfactorily the production ratio N_η/N_π at 180 A MeV. Moreover, calculations with the Dubna cascade model [8] will provide essential information about the mechanism involved in the production of the η meson at deep-subthreshold energies. This theoretical analysis is in progress.

References

[1] K.K. Gudima, M. Ploszajczak, V.D. Toneev, Phys. Lett **B328** (1994) 249.

[2] F.M. Marqués et al., NIM **A365** (1995) 392.

[3] T. Matulewicz et al., *Hydrogen isotopes identification with the electromagnetic calorimeter TAPS*, contribution to this Compilation.

[4] G. Martínez et al., *A new shower analysis algorithm to search for rare events detected with TAPS*, contribution to this Compilation.

[5] L. Aphecetche et al., *The TAPS software system*, contribution to this Compilation.

[6] V. Metag, Nucl. Phys. **A553** (1993) 283c.
U. Mosel and V. Metag, Nucl. Phys. News 4 (1993) 25.

[7] A. Zukov et al., Nucl. Phys. **A537** (1992) 692.

[8] K.K. Gudima et al., Phys. Rev. Lett. **76** (1996) 2412.

C - MISCELLANEOUS

TAPS Software System

L. Aphecetche[1], H. Delagrange[1], F.M. Marqués[2], G. Martínez[1], T. Matulewicz[1,3], Y. Schutz[1]

1. *Grand Accélérateur National d'Ions Lourds, F-14021 Caen, France.*
2. *Laboratoire de Physique Corpusculaire, F-14050 Caen, France.*
3. *Warsaw University, PL-00-681, Warszawa, Poland.*

In the preparation scheme of the TAPS experiments planned at AGOR (KVI, Groningen, The Netherlands), the software tools have been updated and upgraded. TAPS software system consists in three main packages :

- KANE : a simulation tool, based on GEANT3 [1], that allows to study the TAPS response ;
- FOSTER : a decoding tool, that can read, calibrate, and perform some various elementary operations on the raw data files ;
- ROSEBUD : an analysis tool box.

~~Figure 1 shows the relations between these three packages~~.

These softwares are described.

1 KANE

KANE has been designed to study the TAPS response to various kinds of particles, in various kinds of configurations (GANIL, GSI, KVI). A full description of TAPS, including additional detectors (such as the Washington University Dwarf Ball or the KVI Forward Wall) and other devices (beam tube, reaction chamber, wrapping materials) have been realized with GEANT3. An effort has been put on the ease of use as well as on the flexibility. Indeed, the user can choose between several TAPS configurations and over a wide range of event types : hard photon and neutral pion events from the systematics, white spectra (either in energy or in transverse mass) events (for all the kind of particles GEANT3 can handle), etc.... Even if a kind of event is not implemented directly in KANE, it is possible to give as an input a Ntuple to fully describe the events one wants to use. At last, KANE output files have the same structure as the ones from the experiments. In this way, they can be analysed by the very same analysis program (see section 3).

KANE has been coded in FORTRAN, and has been successfully tested on Digital Alpha machines, under VMS.

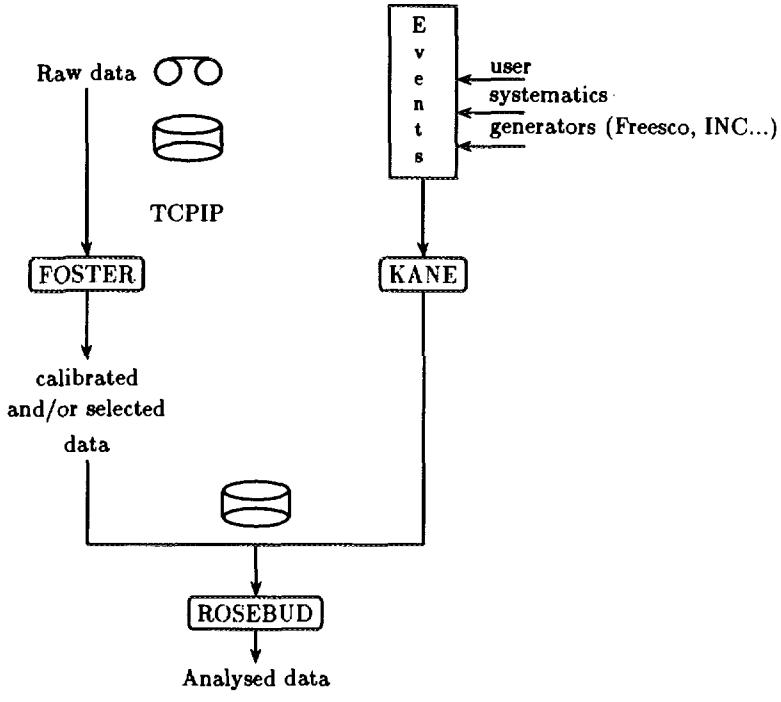

Figure 1: TAPS software relations

2 FOSTER

FOSTER is the first program that one must use, in order to decode the raw data, coming from the magnetic tapes or directly through TCPIP transfers during the acquisition. It can be used also to calibrate these raw data. A various set of additional features can be switched on and off by the user, like the Ntupling or histogramming processes, or a simplified version of the analysis, for example. When FOSTER is launched, it calls a standard PAW session. All the capabilities of PAW and KUIP are thus provided to the user.

FOSTER has been coded in C (for the parts using the CERN libraries) and in C++. It is still under development (to include other detectors as the Washington University Dwarf Ball and the KVI Forward Wall) and has been partly tested on Digital Alpha machines, under VMS.

3 ROSEBUD

ROSEBUD is the final stage software, that analyses either experimental or KANE-simulated data. Rather than a static code, it is a tool box of C++

objects that can be easily assembled to build an analysis program.

These objects are very intuitive ones : *event, block, detector, shower.* An *event* is a set of *blocks* ; a *block* is a set of *detectors* and a set of *showers*, and a *shower* is itself a set of *detectors*, plus a set of global variables that characterizes it. Some standard functions can be applied on these objects, like the clusterization of a *block* or the computation of the global variables of a *shower.*

ROSEBUD has been succesfully tested on Alpha machines, under VMS. The test was performed in two steps. First we made a comparison with an existing analysis program (written in FORTRAN) for the $180A$ MeV Ar+Ca experiment performed at GSI in 1995. Then ROSEBUD has then been extended to be able to analyse data that are expected from the KVI experiments in 1996, and has been tested with KANE-simulated data.

In the coming months, we intend to give ROSEBUD the capability to analyse data of other detectors that will be used with TAPS (Washington University Dwarf Ball and KVI Forward Wall).

References

[1] R. Brun et al. GEANT3 user's guide. Technical report, CERN/DD/EE/84, 1987.

A new shower analysis algorithm to search for rare events detected with TAPS

G. Martínez[1], L. Aphecetche[1], Y. Charbonnier[1], H. Delagrange[1], Y. Schutz[1], T. Matulewicz[1,9], F.M. Marqués[2], M. Appenheimer[3], R. Averbeck[4], J. Díaz[5], A. Döppenschmidt[4], A. Gabler[3], M.J. van Goethem[6], S. Hlaváč[7], M. Hoefman[6], R. Holzmann[4], A. Kugler[8], F. Lefèvre[4], H. Löhner[6], A. Marín[5], V. Metag[3], W. Niebur[4], R. Novotny[3], R.W. Ostendorf[6], R.H. Siemssen[6], R.S. Simon[4], R. Stratmann[4], H. Ströher[3], P. Tlusty[8], P.H. Vogt[6], V. Wagner[8], H.W. Wilschut[6], F. Wissmann[4], M. Wolf[3].

1. *Grand Accélérateur National d'Ions Lourds, F-14021 Caen, France.*
2. *Laboratoire de Physique Corpusculaire, F-14050 Caen, France.*
3. *II Physikalisches Institut Universität Gießen, D-35392 Gießen, Germany.*
4. *Gesellschaft für Schwerionenforschung, D-64291 Darmstadt, Germany.*
5. *Instituto de Física Corpuscular, E-46100 Burjassot, Spain.*
6. *Kernfysisch Versneller Instituut, NL-9747 AA Groningen, The Netherlands.*
7. *Slovak Academy of Sciences, Bratislava, Slovakia.*
8. *Nuclear Physics Institute, 250 68 Řež, Czech Republic.*
9. *Warsaw University, PL-00-681, Warszawa, Poland.*

In a recent experiment [1] performed with TAPS at GSI (Darmstadt) we aimed at measuring η-mesons produced in heavy-ion collisions at bombarding energy of $180A$ MeV, well below the free production threshold equal to 1265 MeV. The η-meson is detected in TAPS through its two-photon decay (branching ratio equal 38.9%) and identified by calculating the invariant mass of photon pairs. The standard way to identify photons among the overwhelming hadronic background exploits redundant information delivered by the TAPS modules each consisting of a BaF_2 crystal and a veto plastic scintillator. That are the time-of-flight of particles, the pulse-shape and the energy deposited in the veto [2]. This analysis requires a good calibration especially for the time-of-flight and the pulse-shape discrimination over the whole photon-energy range of interest. This is only possible if enough statistics have been accumulated during the experiment over the whole dynamical range.

The rest-mass of η-meson is 545 MeV and the average energy of the decay photons is about 300 MeV. Direct photons of that energy are rare and it becomes therefore hazardous to define strict gates on the prompt peak in the time-of-flight spectrum and on the pulse-shape spectrum which allow to distinguish photons from the abundant high energy protons. As an alternative we have developed a new algorithm [3] which only exploits the properties of electromagnetic showers inside TAPS blocks (one TAPS block consists of 64 modules). The analysis is

The detection of η mesons (with TAPS) produced in heavy ion collisions at GSI (Darmstadt) is investigated. The time-of-flight, the time dispersion, the relative time, the multiplicity and the energy dispersion of the showers are studied.

based on several global parameters characteristic of the shower. It is defined as a set of contiguous modules hit with a deposited energy of at least 3 MeV and with no energy deposited in the plastic scintillator.

- *Shower time-of-flight*
  It is defined as the average time-of-flight of the members of the shower. The resolution of the prompt peak was of the order of 1 ns reflecting mainly the time jitter of the start detector.

- *Shower time dispersion*
  It is defined for a shower as the average deviation of individual time-of-flight with respect to the shower time-of-flight. Deviations from a χ^2 distribution indicate spurious events in the shower.

- *Showers relative time*
  It is defined as the time difference between showers. The resolution of the prompt peak was 600 ps reflecting the fact that the time reference of the start detector is canceled in the time difference.

- *Shower multiplicity*
  It is defined as the number of members building up the shower. This multiplicity increases with the energy of the primary photon and is on average equal to one for protons and neutrons.

- *Energy dispersion*
  It is defined for a shower as the average difference between individual energy and the largest deposited energy . Hadrons present on average a smaller energy dispersion than photons.

For each event these global parameters are calculated and restrictive cuts were applied. These cuts were defined by analyzing in exactly the same way events generated by GEANT which included the TAPS acceptance and response function. We have tested this new algorithm on neutral pion events and compared its performances with those of the standard algorithm. We found that it allows to identify with a dramatically improved efficiency the most energetic pions, that are envolving the most energetic photons (Fig. 1). This improvement is essential for the identification in the same experiment of η-mesons.

[1] G. Martínez et al., *η's at deep subthreshold energies: Extreme behaviours of nuclear matter*, contribution to this Compilation;
G. Martínez to be published in the proceedings of *XXXIV International Winter Meeting on Nuclear Physics*, edited by I. Iori.

[2] F.M. Marqués *et al.*, Nucl. Inst. and Meth. **A365** (1995) 392.

[3] G. Martínez *et al.*, Nucl. Inst. and Meth. to be published.

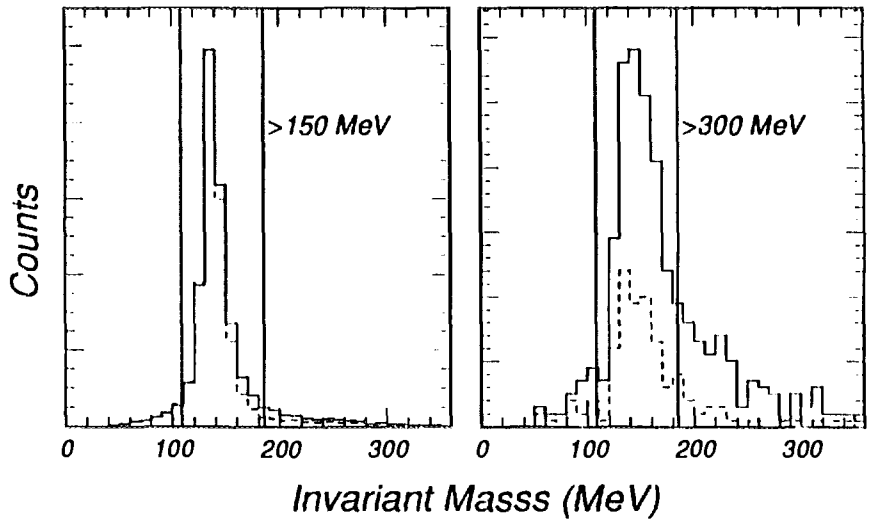

Figure 1: *Two-photon invariant-mass spectrum measured in the reaction Ar+Ca at 180A MeV plotted in the π^0 region. The dashed line represents the spectrum obtained from the standard analysis and the continuous line with the new analysis exploiting the electromagnetic shower topology.*

Hydrogen isotopes identification with the electromagnetic calorimeter TAPS

T. Matulewicz[1,9], L. Aphecetche[1], Y. Charbonnier[1], H. Delagrange[1], G. Martínez[1], Y. Schutz[1], F.M. Marqués[2], M. Appenheimer[3], R. Averbeck[4], J. Díaz[5], A. Döppenschmidt[4], A. Gabler[3], M.J. van Goethem[6], S. Hlaváč[7], M. Hoefman[6], R. Holzmann[4], A. Kugler[8], F. Lefèvre[1], H. Löhner[6], A. Marín[5], V. Metag[3], W. Niebur[4], R. Novotny[3], R.W. Ostendorf[6], R.H. Siemssen[6], R.S. Simon[4], R. Stratmann[4], H. Ströher[3], P. Tlusty[8], P.H. Vogt[6], V. Wagner[8], H.W. Wilschut[6], F. Wissmann[4], M. Wolf[3].

1. *Grand Accélérateur National d'Ions Lourds, F-14021 Caen, France.*
2. *Laboratoire de Physique Corpusculaire, F-14050 Caen, France.*
3. *II Physikalisches Institut Universität Gießen, D-35392 Gießen, Germany.*
4. *Gesellschaft für Schwerionenforschung, D-64291 Darmstadt, Germany.*
5. *Instituto de Física Corpuscular, E-46100 Burjassot, Spain.*
6. *Kernfysisch Versneller Instituut, NL-9747 AA Groningen, The Netherlands.*
7. *Slovak Academy of Sciences, Bratislava, Slovakia.*
8. *Nuclear Physics Institute, 250 68 Řež, Czech Republic.*
9. *Warsaw University, PL-00-681, Warszawa, Poland.*

The electromagnetic calorimeter TAPS has been designed to detect and identify photons and neutral mesons through their two-photon decay. However other particles emitted simultaneously with photons or mesons carry new and complementary information on the particle dynamics in nuclear matter. In particular the excitation of the baryonic resonance Δ can be detected through its deexcitation by photon or pion emission. The signal can thus be seen by measuring $\gamma - p$ or $\pi^o - p$ correlations for example [1].

We have therefore developed a new method [2] to identify protons and more generally charged massive particles, like charged pions, hydrogen isotopes and heavier particles reaching the detector. The method was tested on events from the reaction Ar+Ca at 180A MeV. TAPS was set in the tower geometry at 80 cm from the target and at $\theta = \pm 70^0$ with respect to the beam direction.

TAPS here has been developed

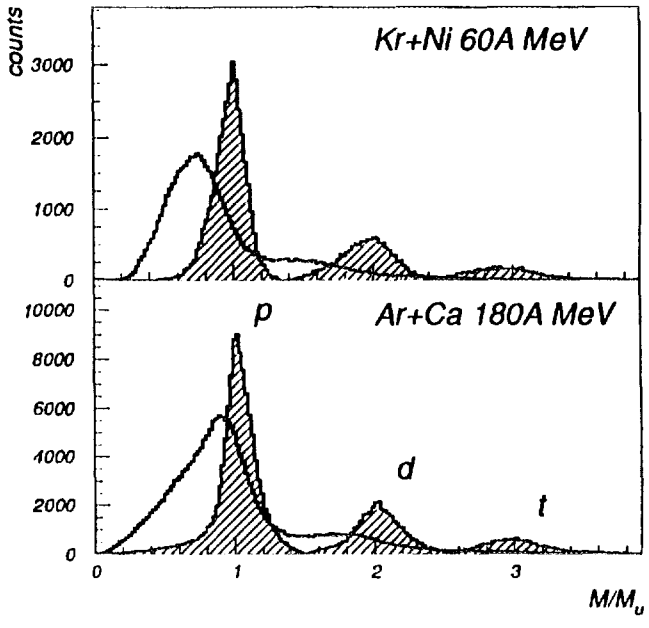

Figure 1: *Mass spectrum obtained from time-of-flight and energy deposited in TAPS without and with (shaded histogram) correction for the energy lost in materials between target and BaF_2 scintillation detectors.*

Charged-hadron events were identified with appropriate gates using the time-of-flight versus pulse-shape distribution. The mass spectrum obtained from the time-of-flight and deposited energy in TAPS scintillation modules shows a broad peak around the proton mass and a weak signal below the deuteron mass (Fig. 1, empty histograms). This poor resolution is due to the energy loss of charged particles on their way from the target to the scintillator. Apart from the target chamber and air, TAPS blocks are equipped with a system of plastic scintillators and lightguides. This complex set-up forced us to calculate the energy loss corrections individually for each module in a block. As the considered particles were already coincident with a neutral

pion, the mass resolution was further improved using as a reference a photon from neutral pion decay rather that the START detector. After correcting for energy losses, all hydrogen isotopes are very well separated (Fig. 1 shaded histograms).

[1] *Observation of in-medium* Δ *excitation via* $\pi^o - p$ *correlations measured with TAPS*, **contribution to this Compilation.**

[2] T. Matulewicz *et al.*, **submitted to Nucl. Inst. and Meth.**

[3] F.M. Marqués *et al.*, Nucl. Inst. and Meth. **A365** (1995) 392.

ORION: a multipurpose detector for neutrons
Some new developments

Y.Perier[1], E.Lienard[1], B.Lott[1], Y.El Masri[2], J.Galin[1], Th.Keutgen[2], M.Morjean[1], A.Péghaire[1], B.Quednau[1], I.Tilquin[2]

1) GANIL (IN2P3-CNRS, DSM-CEA) BP 5027, 14021 Caen-Cedex
2) Université Catholique de Louvain-la-Neuve

The 4π-neutron-detector ORION, made of liquid scintillator loaded with gadolinium, built in GANIL several years ago, has been essentially used so far as a neutron multiplicity meter: a tool giving event-wise the number of emitted neutrons in a nuclear reaction. This is of special interest to study dissipative reactions and to sort events as a function of the violence of the collision. When dealing with heavy nuclei, the neutron probe appears to be very sensitive to the temperature of the heated nuclei whatever the nature of the heater: a heavy nucleus[1] a proton[2] an antiproton[3] or a pion[4].

When using ORION as a multiplicity meter, it is the delayed response of the detector which is exploited, the one corresponding to the radiative capture by gadolinium of the neutrons after their thermalization in the scintillating medium. However as for any scintillator detector a fast reponse is also provided which can be utilized for other purposes and a detailed study has been made in order to determine the capabilities of a large area (about 2 m^2) detector used as a time-of-flight spectrometer. A sector of ORION (1.6 meter in diameter, 50 cm thick, equipped with 6 regularly spaced XP2020 phototubes from Phillips) was thus tested using tagged neutron beams at Louvain la Neuve. The tagging is made by means of neutron scattering on a hydrogen nucleus (plastic target) by detecting the recoiling proton at 45 degrees (the method of the so called "associated particle" see experimental scheme of Fig.1).

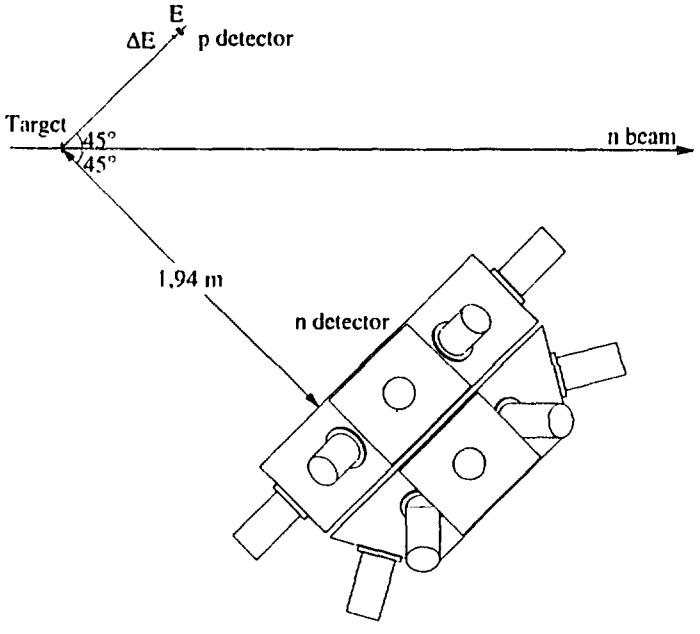

Fig.1: In the Louvain set-up two sectors of ORION were actually tested as shown in this layout but only the data obtained with the front one are considered in this contribution.

four pi neutron ORION

Different properties of the detector have been tested: its efficiency in both modes, fast and delayed, its time resolution and position sensitivity. For the later test, the impact of the neutron beam onto the detector was varied by sliding it, perpendicular to the beam direction. All the presented data are tentative with the analysis still in progress.

Efficiency of the detector

-Fast response: the results are displayed for three neutron energies (9.7, 19.2 and 34.2 MeV) in Fig.2, and different detection thresholds (due to the different amounts of background accompanying the neutron beams). The experimental data have been compared with model calculations based on the work of Cecil et al.[5] and a systematic disagreement shows up whose origin is not yet fully understood.

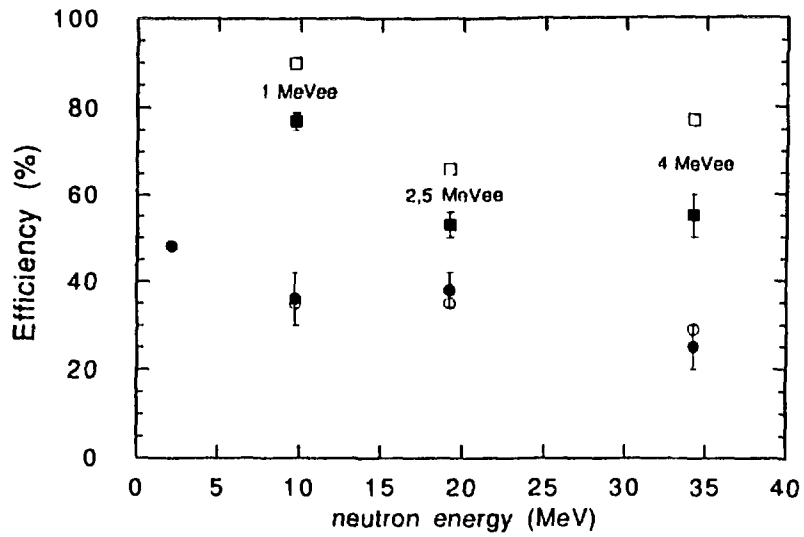

Fig.2: Measured efficiencies (black symbols) for the prompt (squares) and delayed signals (dots) compared with the simulated ones (open symbols). The detection thresholds used for the prompt signal are reported in the figure. For the delayed signal the threshold has been normalised in order to fit the Cf data (<2MeV> neutrons)

-Delayed response: for the same reasons as before the data are given for a rather high detection threshold (4.7 MeVee to be compared to 1.5-2 MeVee the usual threshold in current operation). There is a pretty good agreement between experiment and simulations by DENIS[6]

Time response

Surprisingly enough for such a large area detector ($2m^2$) and considering the pretty large uncertainty in the flight path (219cm±25cm) time resolutions of about 2.5 ns were found. Thus this detector -or at least part of it- can be considered as a genuine time of flight spectrometer of large area with decent time resolution. Note that the resolution is good enough to make a clear distinction between neutrons and gammas without any use of pulse shape discrimination (which is not achieved anyway for the Gd-loaded scintillator).

Position sensitivity

Tests of the response in position have been made and are shown in Fig.3. The light output, measured by each phototube and normalized to the total amount of light, is seen to change drastically as a function of the location of the neutron impact. The experimental data are well reproduced by a simple Monte-Carlo model which takes into account a light attenuation constant of about 2m and photons hitting the photocatode both directly and after scattering on the tank surface. The excellence of the model calculations demonstrates that the physical process responsible for the light collection is pretty well

mastered and that we are thus able to use this detector as a two-dimension position-sensitive detector.

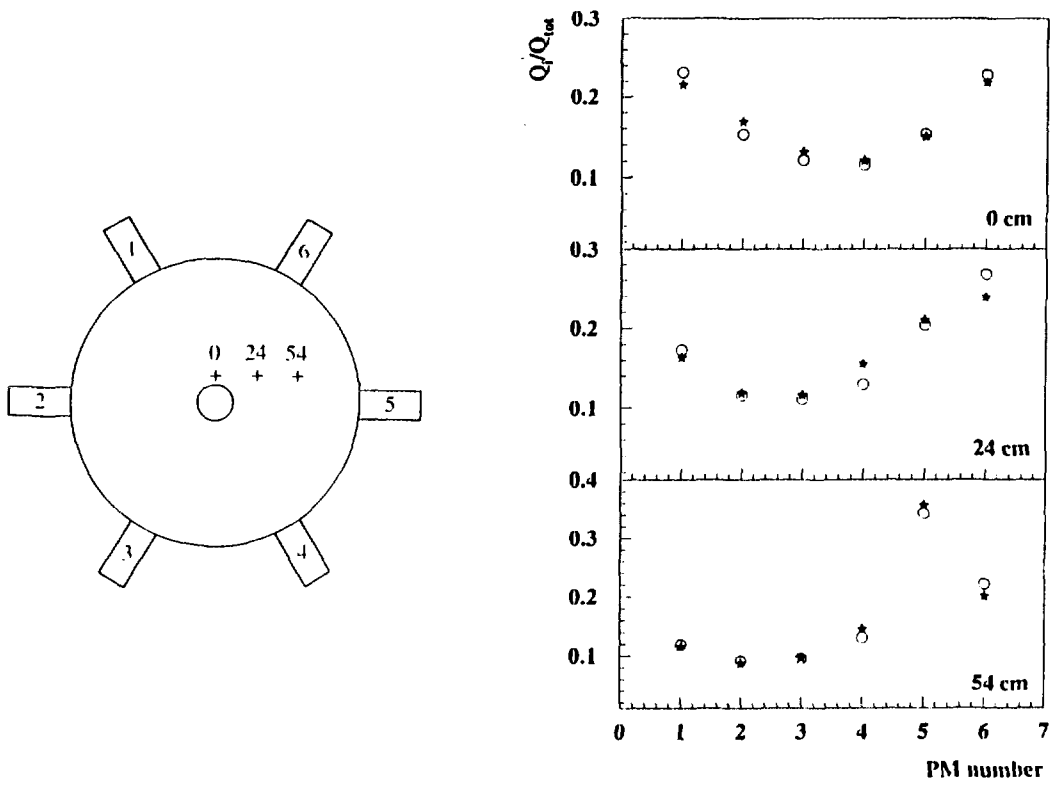

Fig.3: Ratio of the individual versus total collected light as a function of the PM number as they are referenced in the accompanying layout together with the location of the impinging neutron beam. The experimental data (open dots) are compared with simulations (stars).

Further tests are in progress using cosmic radiations in order to study the position response further. It is also planned to build a prototype detector along the same principle, with a total area of $4m^2$ (about 2.2m in diameter) and many more phototubes in order to improve the resolution in position.

Summary and propects

The ORION detector has been long used as a neutron multiplicity detector only. As a matter of fact this detector or at least part of it (the forward part) can be used as a multipurpose detector, giving in addition the velocity of the neutron and its emission angle. Such an instrument can be very valuable in some applications. It has been already utilized with success in reactions induced by 35 AMeV ^{6}He, in which the weakly bound neutrons are easily emitted and need to be characterised in order to gain some insight into the reaction mechanism (Coulomb or nuclear break up, single- or multi-neutron transfer,...)[7].

References:

1) e.g. M.Morjean et al, this volume
2) e.g. X.Ledoux et al, this volume
3) e.g. F.Goldenbaum et al, this volume
4) e.g. U.Jahnke et al, this volume
5) Cecil et al, NIM 161 (1979) 439
6) J.Poitou and C.Signarbieux, Nucl. Inst. Met. 114 (1974) 113
7) Y.Perier et al (in progress)

FR9700919

An application of high efficiency 4π-neutron detectors: Neutron multiplicity distributions for GeV proton induced spallation reactions on thin and thick targets of Pb and U

D.Hilscher, F.Goldenbaum, U.Jahnke, L.Pienkowski
Hahn Meitner Institut Berlin, Glienickerstr.100, D-14109 Berlin

J.Galin, B.Lott, B.Quednau
GANIL (IN2P3-CNRS, DSM-CEA), BP 5027, F-14021 Caen-Cedex

The aim and context of these experiments

Spallation neutron sources for various applications, be it neutron scattering, transmutation of nuclear wastes or energy amplifiers, exploit the thermal excitation of heavy nuclei with energetic protons and the subsequent decay of these nuclei by evaporation of mainly neutrons with energies of a few MeV. Energetic particles (mainly nucleons and pions) which are emitted during the initial excitation process can induce secondary reactions producing additional neutrons. Both processes are described by intra- (INC) and inter-cascade models which are widely used to design spallation neutron sources. However, the reliability of such models is questionable in particular at energies where only few data exist. In order to verify such models and possibly to identify deficiencies it is desirable not only to investigate the mean number of neutrons emitted per incident proton but rather the *whole neutron multiplicity distribution* which should be a sensitive test to any such model.

Taking advantage of the presence of the Berlin 4π-neutron detector at CERN for experiments at LEAR with antiproton beams, some exploratory measurements have been carried out on thin and thick targets of different materials with proton beams from 1.2 to 4.2 GeV, in order to investigate the efficiency of the detector when measuring neutron multiplicity distributions.

The experimental conditions[1)]

The beams:

A proton beam at 1.22 GeV was directly available from the LEAR ring when loaded with protons instead of antiprotons. At higher energy the beams were secondary beams produced from the PS proton beam at 26 GeV impinging on a thick Cu target. The secondary particles (p, π^+, K^+, e^+, and ^2H) were analysed in Bρ and time of flight and with the additional information provided by two Cerenkov detectors could be identified on an event-by-event basis. Some data will be presented thereafter for proton and pion projectiles at 2 ,3 ,4 and 5 GeV/c.

The targets:

Measurements were performed on both thin and thick targets of different materials (Ag, Ho, Au, Pb, U). The targets were cylinders aligned on the beam axis, some with a variable diameter (Φ=15 cm at most) and a variable thickness (40 cm at most) in order to investigate the influence of the geometry on the neutron production.

The 4π neutron detector:

The detector, built by U.Jahnke at HMI Berlin, is made of 1.5 m^3 of liquid scintillator, loaded with gadolinium. It is spherical (Φ=1.4m) with an inner scattering chamber of Φ=40 cm The efficiency, checked with the <2 MeV> neutrons of a Cf source, was 85%. Since most of the neutrons from a thick target are low energy neutrons (and this was checked by TOF measurements), this type of 4π detector is particularly well suited for this type of measurements. In addition and in contrast with usual TOF neutron detectors, there is no low energy threshold since the neutron must be thermalized anyway before being captured by the Gd nuclei.

The only drawback of this Berlin detector was the small size of the inner scattering chamber, limiting the target size. In this respect, the GANIL detector, ORION, would be more advantageous with an inner cylindric space with Φ=60 cm and l=150 cm for the target.

The data

The data, not yet compared with model calculations, are given in order to illustrate the influence of several parameters. The influence of the target material on the neutron production on thin targets recalls what had been measured before at SATURNE with 2 GeV protons[2]: the heavier the target nucleus, the more neutrons are produced (Fig.1). This stems from the highest stopping capability of the proton by a heavy nucleus and also from the ability of a heavy nucleus to evaporate man more neutrons than charged particles because of a strong coulomb barrier for the latter[3].

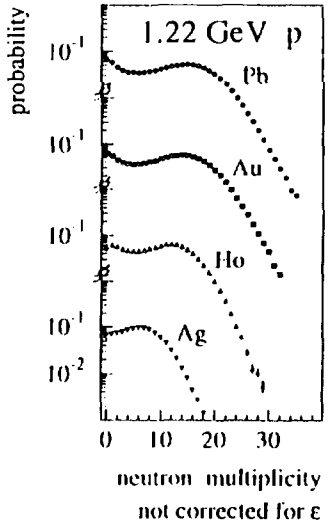

Fig.1 Neutron multiplicity distributions for 1.22 GeV proton induced reactions on thin targets[1]

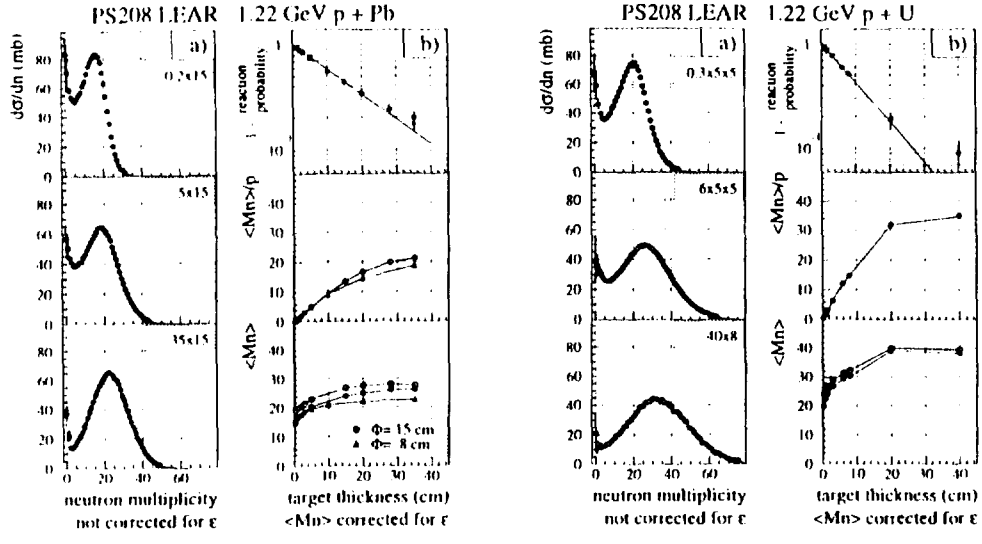

Fig.2 In a: influence of the target size (thickness versus diameter in cm) on the neutron multiplicity distribution for Pb and U. In b) are given from top to bottom, the survival probability of the proton, and the average neutron number, per incident proton (<Mn>/p) and per nuclear reaction (<Mn>), both corrected for detection efficiency[1].

The next step was dedicated to the investigation of the target size. On the left hand part of Fig.2, the whole multiplicity distributions are shown as a function of (thicknessXdiameter) for Pb and U targets. From these distributions the position of the bumps are deduced and considered thereafter to infer both the average <Mn> per event and the average <Mn> per impinging proton. In addition, the survival probability of the proton is given which is shown to fall off with increasing thickness in a well understood way, assuming interaction lengths of 18.4 and 11.6 cm for Pb and U respectively.

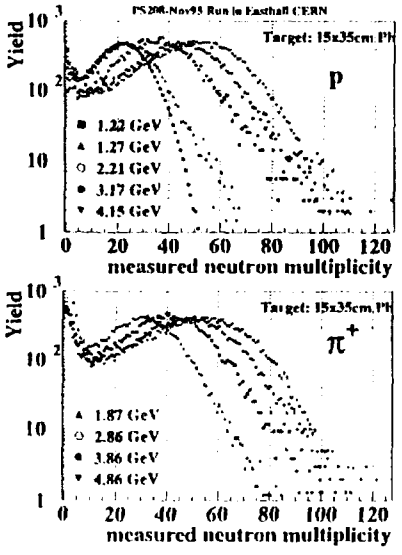

Fig.3: Measured neutron multiplicities for 2 to 5 GeV/c protons and π+ on 35 cm long Pb targets with a diameter of 15 cm.

The influence of bombarding energy on the neutron production was investigated with the biggest Pb target at our disposal for both proton and pion beams (Fig.3). The neutron production is shown to be essentially identical when considering the protons and pions at the *same* energy.

Summary and prospects

From this CERN exploratory work it was possible to demonstrate that 4π scintillator detectors loaded with Gd are best suited for efficient neutron multiplicity measurements on thick targets. Compared to a set of standard time-of-flight detector cells, they have two major advantages: a much higher efficiency (about 85%) leading to minimum biased *distributions* and not only to average values, and moreover, they present *no* low energy threshold in strong contrast with the TOF detectors.

The systematics that has been started up at CERN with a rather limited amount of beam time could be extended to other materials (the mid-mass nuclei from which windows can be made, composite materials in order to simulate the use of molten salts...). Also, it is of great interest to study the neutron production from low energy beams (from 20 up to 200 MeV) in a region where the intra nuclear cascade model is known *not* to be relevant (even if it often used as it were). Such a programme will be pursued in the coming years, at COSY (Jülich) and at GANIL (Caen) when deuton beams become available.

References:

1) D.Hilscher et al International Workshop on Nuclear Methods for Transmutation of Nuclear Waste: Problems, Perspectives, Cooperative Research (Dubna-Russia May 1996), HMI-Berlin preprint (June 1996)
2) L.Pienkowski et al Phys. Lett. B336 (1994) 147, X. Ledoux thesis (paper in preparation) and J.Galin et al, Proc. of the 8th Journées SATURNE on Accelerators applied to the nuclear waste problem, Saclay, 1994 (GANIL preprint P 94 18)
3) B.Lott et al, Z. Phys. A346 (1993) 201

A new quantum model for two-particle intensity interferometry analysis

D. Nouais, R. Lednicky*, V.L. Lyuboshitz†, B. Erazmus, L. Martin, J. Pluta
Laboratoire SUBATECH, Université de Nantes / Ecole des Mines de Nantes / IN2P3/CNRS, 4 rue A. Kastler, 44070 Nantes Cedex 03, France

Abs : p. 251

I. INTRODUCTION

The interferometry analysis in nuclear physics has been developed to measure space-time characteristics of an emitting region produced in nuclear collisions. It consists on the study of two-particle correlations induced by the quantum statistics (QS) effects for identical particles [1], and the final state (Coulomb and nuclear) interactions (FSI) [2,3] which allow to extend the technique to unlike particle pairs. The correlation function, defined as the ratio of the two-particle momentum distribution containing the QS and FSI effects, over an uncorrelated spectrum obtained by switching off all correlations, is dedicated to such analysis. Instead of the six-dimensional two-particle momentum distribution, it is suitable to project the correlation function on the relative momentum q, defined as the momentum of one particle in the rest frame of the pair.

By using a classical trajectory calculation, it has been demonstrated in references [4,5] that the two-particle correlation function is significantly influenced by the Coulomb field of the emitting residual nucleus for small relative distances between particles. Due to the validity limitation of a classical approach to describe a source with short lifetime, a model inspired by the reference [3] has been developed [6] to take into account, for the first time in a quantum approach, the influence of the emitter Coulomb field.

II. INFLUENCE OF THE EMITTING NUCLEUS COULOMB FIELD ON THE TWO-PARTICLE CORRELATION FUNCTION

If one can consider the relative motion of the two particles much slower compared to their motion with respect to the Coulomb center, the three-body problem (two particles and the nucleus) can be treated in the so-called adiabatic approximation. The wave function, solution of this problem, is then factorized as the product of three wave functions describing respectively the motion of each particle in the Coulomb field, and the relative motion of the two particles.

The analysis of the influence of the emitter Coulomb field on the two-particle correlation function, is presented in fig. 1 for the neutron-proton system (particles with unlike charge-to-mass ratio). Comparisons of two-body and full three-body calculations are shown for different lifetimes of the source. In order to obtain a realistic comparison, in the two-body calculations, the one-particle spectrum of each particle is modified to take into account the Coulomb interaction with the emitter. One can observe a strong difference between the two-body and the three-body n-p correlation functions, which increases as the source lifetime decreases. As a mater or fact, the proton is sensitive to the Coulomb field whereas the neutron is not, thus, their relative distance increases quickly, leading to an attenuation of their mutual interactions, and consequently of their correlations. However, this effect does not destroy completely the n-p correlations on contrary to the simplified calculations done by G. Bertsch [7] to explain the weak signal appearing in the experimental n-p correlation function measured by the CHIC collaboration [8] We do not expect such a strong effect of the third body on the p-p correlation function because of an equal charge-to-mass ratio of the two particles of the pair.

---

*Permanent address: Institute of Physics, Na Slovance 2, 18040 Prague 8, Czech Republic
†Permanent address: JINR Dubna, P.O.Box 79, Moscow, Russia

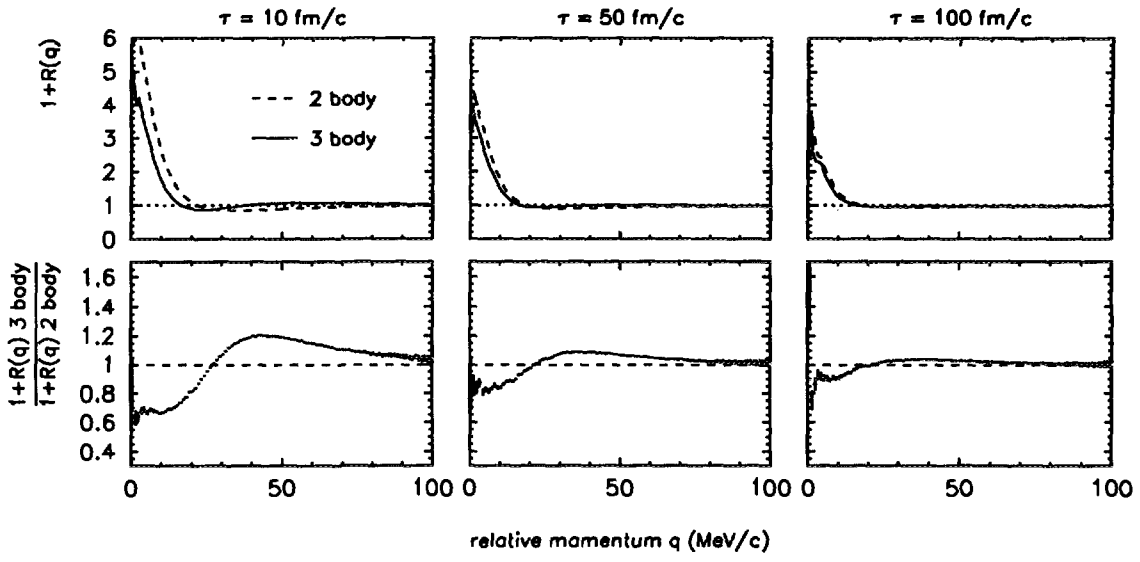

FIG. 1. Comparison of n-p correlation functions calculated with and without the influence of the emitter Coulomb field (top) and their ratios (bottom), for different values of the source lifetime

III. DIRECT MEASUREMENT OF THE DELAY IN THE EMISSION OF THE PARTICLES OF DIFFERENT TYPES

A new possibility of analysis investigated in the frame of this model, is the determination of the sequence of emission of different kinds of particles. A classical picture (fig 2) depicts qualitatively how this analysis can be performed.

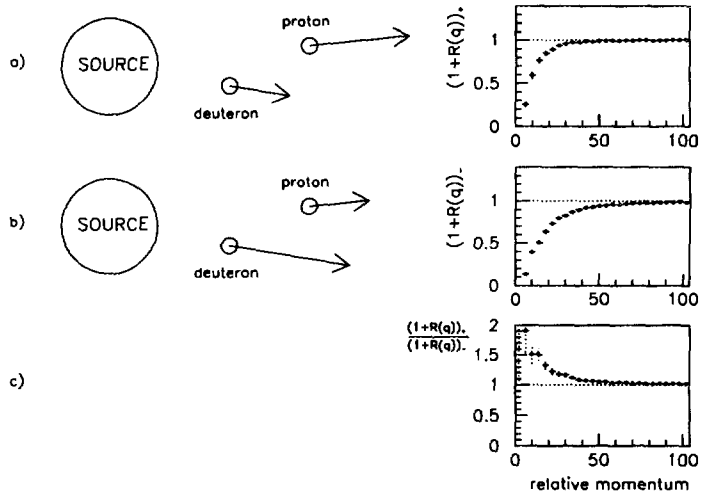

FIG. 2. Classical illustration of the sensitivity of the correlation function to the particle relative velocities in function of their emission order

Let us consider two different particle emitted by a source, for example a proton and a deuteron, and let us assume that the proton is always emitted earlier than the deuteron. When the deuteron is slower than the proton *(a)*, their relative distance increases since the deuteron is emitted, then the two particles interact weakly and the correlation function $(1 + R(q))_+$ presents only a small anti-correlation. On the

contrary, if the deuteron is faster *(b)*, it can "catch up" the proton with which it interacts a longer time, leading to a stronger effect on the correlation function $(1+R(q))_-$. Consequently, the ratio *(c)* of the two correlation functions $(1+R(q))_+/(1+R(q))_-$, is larger than unity at small relative momentum. It could be demonstrated that in the case of the deuteron emitted earlier than the proton, this ratio is lower than unity. If none of these two situations dominates, the ratio is uniformly equal to 1, but if one observes with experimental data, a structure, it means that one type of particle is preferentially emitted earlier than the other.

Such an analysis of the emission order of different types of particles is possible in the frame of the quantum model introduced in the previous section. A directional dependence of the correlation function appears in the two-particle wave function via the scalar product $\vec{q}.\vec{r}$, where r represents the distance between the two particles. Indeed, in the case of long emission time, one can do the approximation $\vec{q}.\vec{r} \approx -\vec{q}.\vec{v}.t$ where $\vec{v}$ is the pair velocity and t is the difference of the emission times of the two particles. Thus, the correlation function is sensitive not only to the absolute value of t, but also to its sign i.e. the order of emission of the two kinds of particles. Practically, to determine in modulus and sign the mean difference of emission time, one should construct the correlation functions $(1+R(q))_+$ and $(1+R(q))_-$ obtained by selecting the sign of the scalar product $\vec{q}.\vec{v}$ (accessible in the experiment), respectively positive and negative. Note that this selection is quite similar to the selection on the velocities used in the qualitative classical explanation. In fact, the two selections are identical in the case of particles of equal masses (like proton and neutron). In figure 3, we present an example of calculations for the proton-deuteron system.

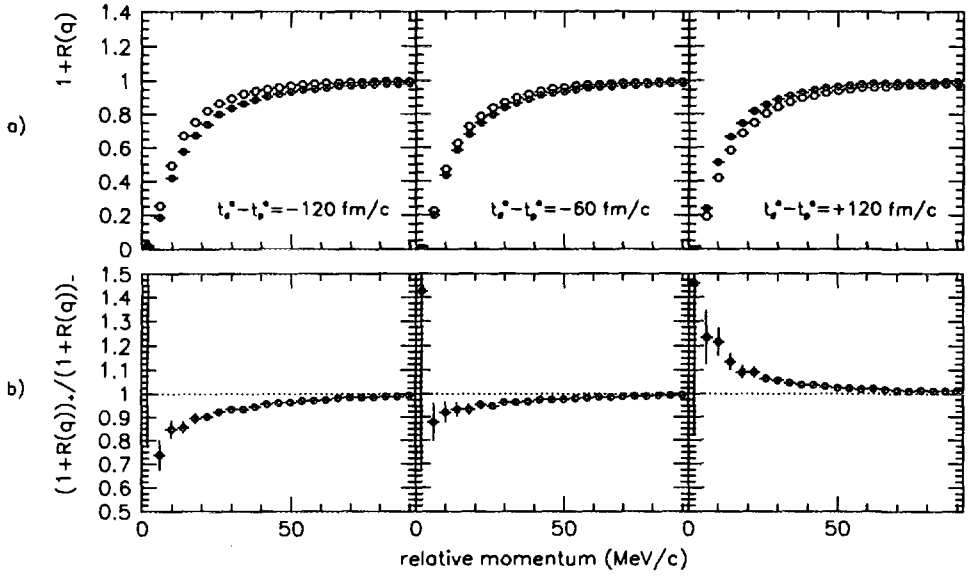

FIG. 3. a) p-d correlation functions $(1+R(q))_+$ (closee circle) and $(1+R(q))_-$ (open circle). b) the ratios $(1+R(q))_+/(1+R(q))_-$ (see text).

The particles are emitted from a source of radius r=5.9 fm/c and temperature T=4 MeV. The protons and deuterons are emitted sequentially according to exponential distributions with equal lifetime of 400 fm/c but shifted one to the other by a delay $dt^o = t_d^o - t_p^o$ equal to -120 fm/c *(a)*, -60 fm/c *(b)* (deuterons emitted earlier), and +120 fm/c *(c)* (protons emitted earlier). The two correlation functions $(1+R(q))_+$ and $(1+R(q))_-$ are represented in the upper part of the figure. The sensitivity to the delay of the emission time is reflected on the lower part of the panel by the ratios $(1+R(q))_+/(1+R(q))_-$. The calculations presented in the first and the last columns of this figure clearly demonstrate the possibility to determine the sign of the delay. We can conclude that the effect is sufficiently important to be able to observe a delay between the two distributions of the order of 10% of the source lifetime.

Abs.

~~IV. CONCLUSION~~

~~We have presented~~ Some results of a new quantum model for intensity interferometry analysis, which takes into account the influence of the Coulomb field of the emitting residual nucleus on the two-particle correlation function. This approach is particularly well suitable to compare different systems (like p-p and p-d) characterized by identical or different charge-to-mass ratios of the two particle of the pair.

Moreover, this model allows to determine not only the global space-time characteristics of the source, but also its evolution, through the determination of the sequence of emission. This model has been already used for the analysis of experimental data measured at GANIL, with two experiments using respectively the neutron calorimeter ORION [10] and the spectrometer SPEG [4].

are presented

---

[1] G.I. Kopylov, M.I. Podgoretsky, Yad. Fiz. 15 (1972) 392
(Sov. J. Nucl. Phys. 15 (1989) 219)
G.I. Kopylov, M.I. Podgoretsky, Sov. Phys. JEPT. 42 (1976) 211
Podgoretsky, Fiz. Elem. Chast. Atom. Yad. 20 (1989) 628
(Sov. J. Part. Nucl. 20 (1989) 266

[2] S.E. Koonin, Phys. Lett. B70 (1977) 43

[3] R. Lednicky, V.L. Lyuboshitz, Yad. Fiz. 35 (1982) 1316
(Sov. J. Nucl. Phys. 35 (1982) 770)
R. Lednicky, V.L. Lyuboshitz, Proc. Int. Workshop on Particle Correlations and interferometry in Nuclear Collisions, CORINNE 90, Nantes, France, 1990 (ed. D. Ardouin, World Scientific, 1990) p.42.

[4] L. Martin, Thèse de Doctorat, Université de Nantes (1993)

[5] B. Erazmus, L. Martin, Lednicky, N. Carjan, Phys. Rev. C49 (1994) 349

[6] R. Lednicky, V.L. Lyuboshitz, B. Erazmus, D.Nouais Rapport Interne SUBATECH 94-22, Submitted to Nucl. Phys. A

[7] Cronqvist *et al*, Phys. Lett. B 317 (1993) 505

[8] Ghetti *et al*, Nucl. Instr. And Meth. A 335 (1993) 156

[9] R. Lednicky, V.L. Lyuboshitz, B. Erazmus, D.Nouais. Phys. Lett. B373 (1996) 30

[10] C. Ghisalberti, Thèse de Doctorat, Université de Nantes (1994)
C. Ghisalberti *et al*, Proc. of thee XXXI International Winter Meeting on Nuclear Physics, Bormio, Italy (1993) 293

Interferometric studies close-to-0° by means of the multidetector ARGOS at GANIL

G. Lanzanò, E. De Filippo, M. Geraci, A. Pagano,
S. Aiello, A. Cunsolo, R. Fonte, A. Foti, M. L. Sperduto
Istituto Naz. Fisica Nucleare and Dipartimento di Fisica
Corso Italia 57, 95129 Catania, Italy
C. Volant, J.L. Charvet, R. Dayras, R. Legrain
DAPNIA/SPhN, CEN-Saclay, 91191 Gif-sur-Yvette Cedex, France

May 20, 1996

Abstract

The forward wall of the multidetector ARGOS has been used recently at Ganil during the E230 experiment. Its granularity and excellent timing characteristics have allowed an interferometric study of the light charged particles and light ions emitted in a restricted angular range close to 0°. ~~We report on~~ Some preliminary data relative to the reaction $^{40}Ar+^{27}Al$ at 44 MeV/n. are presented.

1 Introduction

As known, the study of two particle correlations at small relative momenta can give some insight on the spatial and temporal extension of the emitting source; further the relative populations of excited states furnishes information on the temperature of that source. This method has been succesfully used to study intermediate velocity highly excited systems produced in intermediate energy heavy ion induced reactions [1, 2]. The extension of the method to the study of highly excited projectiles or projectile-like fragments (PLF) is not straightforward, and requires the use of a suitable multidetector, because of the particle high rate and focusing in the forward direction. In the following, after a brief description of the multidetector and the experimental layout, we shall present some preliminary results on the particle-particle correlations at forward angles.

2 The multidetector Argos

Argos is a multidetector, made by 112 separate, hexagonal BaF_2 crystals modifiable into phoswichs, by means of a fast plastic scintillator foil, of suitable thickness, according to the charge and dynamical range of the ion to be detected [3, 4, 5]. Each crystal has a surface of 25 cm^2 and a thickness variable up to 10 cm, stopping protons of energy up to 200 MeV. Due to its modularity, the array can be arranged to fit different geometries. When the single detector is modified in phoswich, in addition to the light charged particles also heavy ions are detected and identified with a threshold in energy depending on the plastic thickness. Neutron detection is also allowed, with an efficiency depending mainly on the crystal thickness and on the electronic threshold. Typically, neutron efficiency values of about 8% are observed for 5cm thick crystals and 1 MeV-ee threshold. Timing characteristics of the phoswich detector are well enhanced, reaching values less than about 250 psec resolution, so that precise time-of-flight measurements are possible if suitable flight-paths and good time-resolution starts are available.

3 The E230 experimental layout

The ARGOS multidetector was placed in the Nautilus big scattering chamber, with the following geometry. A forward wall of 60 phoswichs was placed between 0.7° and 7° in shape of honeycomb at a distance of 235 cm from the target (solid angle: 0.03 sr); they detected projectile-like fragments (PLF) identified in charge and light charged particles (LCP) isotopically separated. After linearization of the total light component,

mass separation was also achieved for light ions. The angular separation between the centers of two adjacent detectors was $\approx 1.5°$.

A backward wall of 18 phoswichs was placed between 160° and 175° at a distance of 50 cm from the target (solid angle:0.2 sr), for the detection of LCP and neutrons.

A battery of about 30 phoswichs was placed in plane at a distance from the target variable from 2m to 0.5m following the expected counting rate, between 10° and 150°, detecting all the reaction products, the only limiting factor being the different thresholds.

In this experiment we used plastic scintillator thickness of 700 and 30 μm for the forward wall and the remaining detectors respectively.

Shape discrimination of the Photomultiplier signals and time-of-flight techniques [6] have been exploited for a full identification of all the charged reaction products. An example of the charge separation achieved is shown in the bidimensional plot of Fig.1a, where the fast component is reported as a function of the total one. For all detected particles the calibration was made by means of time-of-flight(TOF) measurements, gamma-rays giving a reference time for the detectors in plane and in the backward wall, the same the elastic scattering for the detectors placed in the forward wall.

In this experiment, the event was recorded every time the in-plane detectors or the backward wall triggered, a minimum multiplicity of 2 being requested.

4 Preliminary results

Due to the fine angular granularity of the multidetector and to the good spatial and temporal qualities of the beam, we made accurate measurements of the relative momenta for charged products issued from the reaction $^{40}Ar + ^{27}Al$ at 44 MeV/n, from 0.7° to 7°. TOF measurements were accomplished with a time resolution $\Delta t \approx 250$ psec over typical TOF of 25 nsec, characteristic of nuclear products emitted in the forward direction with velocity close to the one of the beam. The correlations obtained are very similar to the ones reported in [1] for different couples of LCP. An example for α-α correlations is reported in the bidimensional plot of Fig.1b, showing the α-particle velocity as a function of their relative momentum expressed in MeV/c. The ground state and the broad first excited state of ^{8}Be are clearly visible, and enhanced for α-particle velocities close to the one of the projectile (8.9 cm/ns). Fig.1c gives the relative momenta distribution for a ^{8}Be in its ground state and a third alpha-particle, showing evidence for the existence of excited ^{12}C nuclei (in this case the observed peaks correspond to the first α-particle emitting level at 7.65 MeV and a group of levels at around 10-12 MeV excitation energy) having the beam velocity.

From a preliminary analysis, more than 10% of the events involving the detection of at least one α-particle in the forward wall, are due to the break-up of a ^{8}Be.

For ion-ion coincidences and for a fixed charge of one of the two ions, the maximum of correlation is observed for velocities close to the beam velocity, and shifts towards higher relative momenta values as the charge of the coincident ion increases, as shown in Fig.1d for Z=5 ions.

5 Conclusions and perspectives

In conclusion Argos is a powerful multidetector, suitable for interferometric measurements at angles close to 0°, where the decay properties of highly excited projectiles or PLF can be studied. An improvement of the detector is now in realization, with the construction of a six fast scintillator mini-wall covering the angular range between 0.2° and 0.6°.

References

[1] J. Pochodzalla et al., *Phis. Rev.* **C35**, 1695, (1987)

[2] O. Schapiro and D.H.E. Gross, Nucl. Phys. **A573**, 143, (1994).

[3] G. Lanzanò et al., "Grandi apparati di rivelazione e prospettive della Sez. INFN di Catania", Acireale, pag. 10, 1993

[4] G. Lanzanò et al., *Nucl. Instr. and Meth.* **A323** (1992) 694

[5] E. De Filippo et al., Nuovo Cimento **107A** 775 (1994).

[6] G. Lanzanò et al., *Nucl. Instr. and Meth.* **A312** (1992) 515

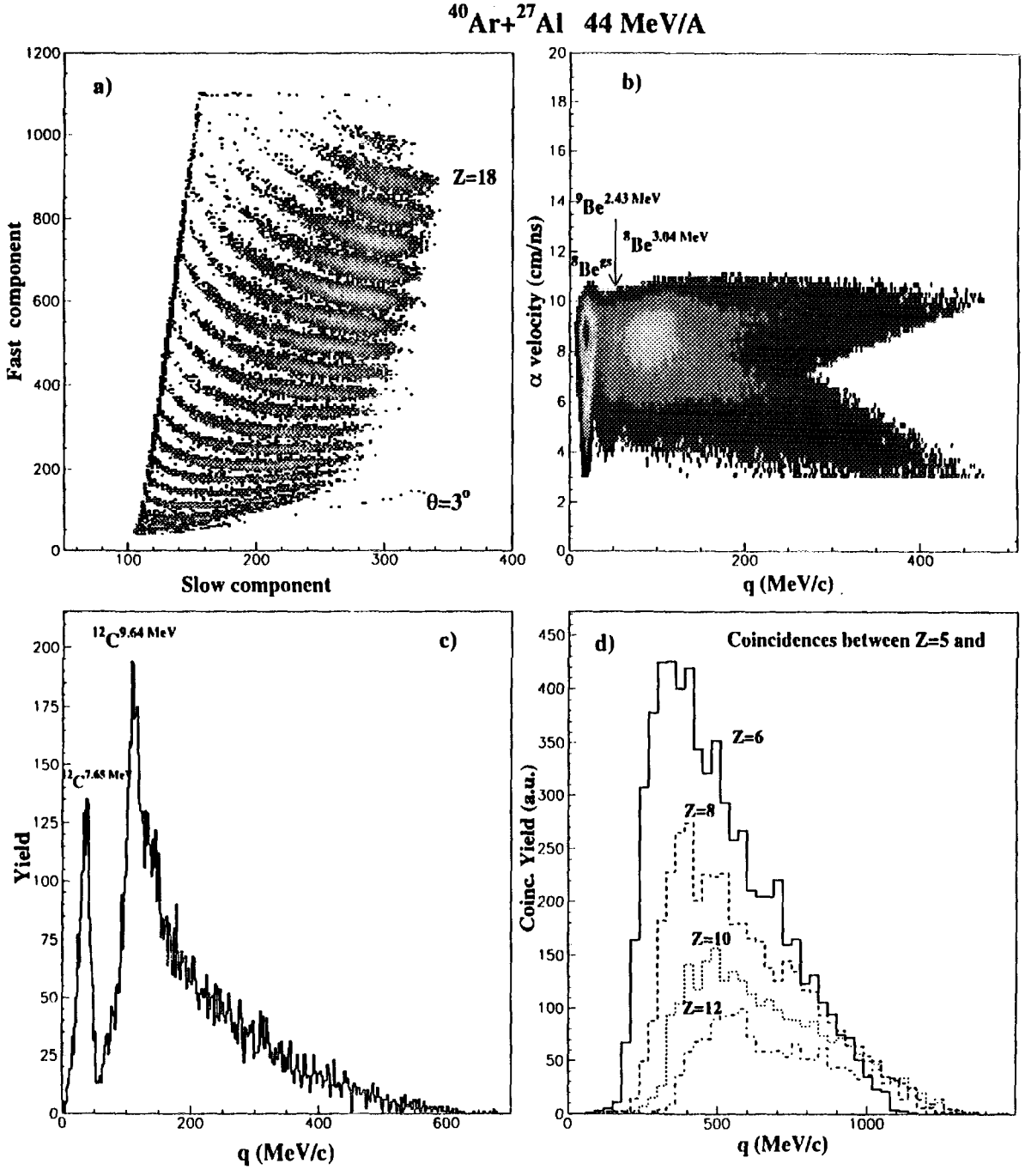

Figure 1: a) Fast component as a function of the total one; b) for $\alpha-\alpha$ correlations their velocity is reported as a function of their relative momenta q; besides the ground state and the broad first excited level in ^{8}Be, it is also visible a structure at q≈50 MeV/c, associated to the decay of the 2.43 MeV state in ^{9}Be c) relative momenta distribution for an α particle and a ^{8}Be g.s. nucleus. The two main excited levels in the primary ^{12}C nucleus are shown; d) relative momenta q distribution for Z=5 PLF in coincidence with Z=6,8,10,12 PLFs detected in the forward wall.

Detection of single high energetic heavy ions with a detector system based on Charge Coupled Devices

M.M. Meier[1], J.U. Schott[1] und K. Strauch[2]

[1] DLR, Institut für Luft- und Raumfahrtmedizin / Strahlenbiologie
[2] Medizinische Einrichtungen der RWTH Aachen, Lehrstuhl für Flugmedizin

The analysis of nuclear tracks in matter permits an estimate of energy and charge number of single projectiles. Nuclear tracks are formed by spatial distribution of secondary electrons which are liberated by ionizing collisions and mobile along a path that depends on their energy statistically. An substantial procedure of evaluating the track is to investigate the damage of non-conducting material (plastic) produced by irreversible redistribution of electrons. This necessiates a permanent damage of the detecting matter which makes a determination of the penetration time of different projectiles by employing a detector of this kind impossible. The search for a detector system which yields both spatial and temporal resolution leads to Charge Coupled Devices (CCDs), an arrangement of a few 100 000 photo-electric cells on a plane able to storage the charge carriers liberated by penetration of a particle. The storaged signals can be read out using standard TV techniques and reset for renewed detection [1].

First experiments with CCDs for spatial and temporal resolution of single heavy ions in connection with radiobiological investigations have shown that beside the projectiles δ-electrons produced in a target can be detected as well [2]. This observation led to the development of a HighEnergeticDeltaelectronYield - detector which makes an estimate of the projectile parameters energy and charge number by spatial resolved registration of the ion induced emission of δ-electrons from a target foil by CCDs possible. The employed detector system is shown in fig. 1.

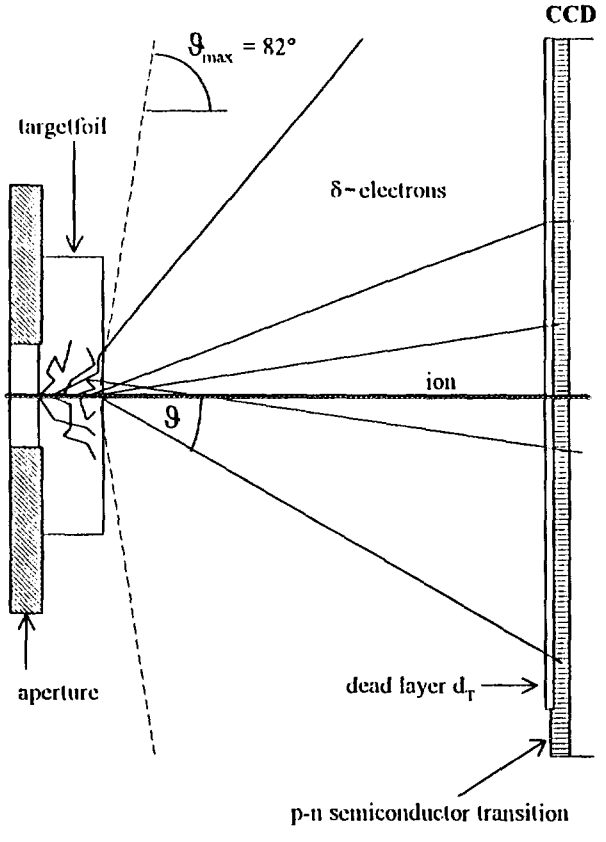

Fig. 1: Schematic drawing of the HEDY - detector.

The HEDY detector system based on Charge Coupled Devices is described. The spatial and temporal resolution of the detector is investigated.

The δ-electrons emitted at an angle ϑ during the penetration of the projectile can be registered inside the sensitive part of a pixel if they have got enough energy to pass a dead layer d_T above it which is due to the production procedure. This process is statistical and does not concern electrons with energies below 5 keV that are absorbed totally by the dead layer. The projectile itself leaves on the frame of the read out CCD a bright spot surrounded by a halo of δ-electrons which corresponds to a depiction of the high energetic electron contribution of the nuclear track caused by the projectile.
The set up for the operation of the HEDY-detector (Fig.2) consists of a beamline which includes a target selector for the use of supplementary absorbers and a beamshutter synchronized with the data acquisition system in order to reduce permanent radiation damage of the CCD.

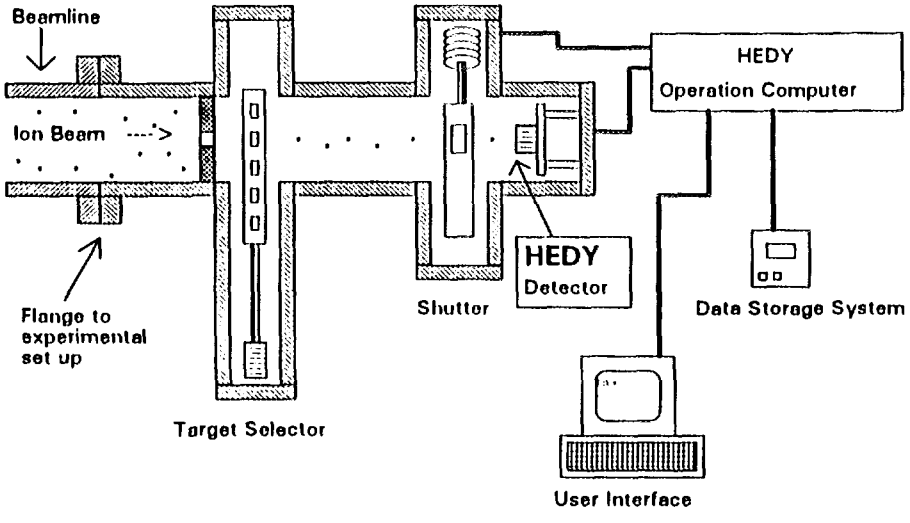

Fig.2: Experimental set up for the operation of HEDY - detector.

The operation of the experiment is run by a computer. It regulates the framegrabbing synchronized with the shutter, the digitizing of the signals and the data storage to magnetic tape. The whole course can be remote-controlled supervised by an user interface. By employing an automatical image analysis system which detects ionization effects in single pixels and ionization events of single particle traversals spectra of the angular distribution of all detected electrons generated by a single heavy ion are recorded. The frequency per interval of emission angle reveals a convergence to a characteristic distribution depending on the energy and charge number of the projectile.
The distribution of δ-electrons produced by xenon ions with energy of 44 MeV/n behind a target foil of carbon (thickness 4.2 mg/cm^2) as a result of an experiment performed at GANIL is shown in fig.3. The large errors of observation are due to the small amount of the random sample including only 17 projectiles. From the spectra the total number of the emitted electrons and the expectation value of the emission angle ϑ can be extracted as parameters for further evaluation. For these data functional correlations with projectile energy and charge number should be determined.
The solution of this problem cannot be achieved by experimental data alone due to the large scope of required beamtime and data processing. Therefore a model was evolved in addition to the experiment in order to determine the relevant angular distributions numerically. It bases on a statistical simulation of the elementary processes of δ-electron production inside the target, their propagation through the target and their detection by CCDs. This tool enables a noticeable reduction of the experiments that are still required for the check of the model.

Comparison: Experiment - Simulation HEDY

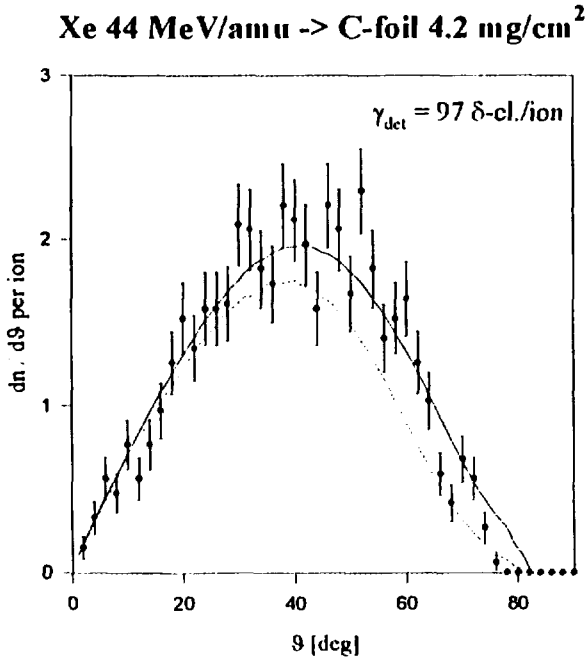

Fig.3: Angular distribution of emitted δ-electrons detected by CCDs in comparison with model calculations.

First results of the calculations using the model in comparison with the experimental data for xenon ions with energy of 44 MeV/n are shown in fig.3. The model is in a fair accord with the experiment assuming a dead layer of about 100 µg/cm^2 . The parameter d_T corresponds to the mean effective thickness of the dead layer above the p-n semiconductor transition of a pixel that must be passed by an electron to be detected. The signal amplification of the used camera module as well as the threshold of event registration are also included in d_T . Since this parameter connecting experiment and model is unknown it must be determined by fitting the calculations to the experimental data.

References

1. Schott J.U., Charge coupled devices (CCDs) - A detector system for particles with time resolution and local assignment with particle trajectories. Nucl. Tracks Radiat. Meas., 15, Nos 1-4, 81-89 (1988)

2. J.U.Schott, A.R.Kranz, K.Gartenbach, M.Zimmermann: Investigation of Single Particle Effects in Active Metabolizing Seedlings of Arabidopsis thaliana. In Nouvelles du GANIL, No.42, Oct.1992,pp.7-9

Phys.Rev.C vol53, 4(1996)1640

Subthreshold Internal Conversion to Bound States in Highly Ionized ^{125}Te

F. Karpeshin,[1,2] M.R. Harston[1], F. Attallah[1], J.F. Chemin[1], J.N. Scheurer[1]
I.M. Band[2] and M.B. Trzhaskovskaya[2]

[1] *CENBG, IN2P3-CNRS, Université de Bordeaux, 33175 Gradignan, France*

[2] *St. Petersburg Nuclear Physics Institute, Gatchina, St. Petersburg.*

Abstract

A new mode of internal conversion, in which the converted electron is excited to a bound orbital instead of a continuum orbital, is discussed. General theoritical results are presented for the relation betwen bound internal conversion and continuum internal conversion of the nucleus. It is shown that the transition rate for internal conversion decay is continuous across the energy threshold between continuum final states and bound final states. Theoritical predicitions for decay to bound states of ^{125}Te are consistent with experimental data on internal conversion in highly charged ions of this nuclide.

Dans une expérience récente faite au Ganil [1, 2], il a été mis en évidence une variation très importante de la durée de vie du 1er niveau excité à 35 keV dans le ^{125}Te. Ce niveau décroit par transition γ (M1) très convertie ($\Gamma_e/\Gamma_\gamma = 13.912$). Cet effet est attribué au *blocage de la conversion interne sur la couche électronique K de l'atome de* ^{125}Te à partir d'une charge ionique critique Q_c pour laquelle l'énergie de liaison électronique (E^Q_{BK}) devient plus grande que l'énergie de la transition nucléaire ω_γ. Cet effet se traduit par une augmentation de la vie moyenne du niveau nucléaire en raison de la réduction des modes de décroissances possibles pour le noyau. Pour un ion de ^{125}Te les modes qui subsistent sont l'émission de photons et la conversion interne sur la couche L. Les résultats expérimentaux montrent que la charge critique observée ($Q_c = 47$) pour laquelle est associée à un accroissement significatif de la période radioactive, ne correspond pas aux prévisions théoriques de l'état de charge ($Q'_c = 45$) pour lequel l'énergie de liaison devient supérieure à l'énergie de la transition. Les calculs théoriques indiquent une charge critique $Q'_c = 45$. Bien qu'il n'existe pas de mesures de la valeur *absolue* de l'énergie de liaison d'un système ionisé, l'écart entre la valeur expérimentale et la valeur prévue de la charge critique ne semble pas pouvoir s'expliquer par l'incertitude sur les valeurs théoriques, estimées pour ce système, à 50 eV.

Pour expliquer ce phénomene, nous pouvons utiliser la figure ci-dessous. Quand l'énergie disponible ($\omega_\gamma - E_{BK}$) est positive, fig.a, l'ionisation de la couche K est possible, et l'electron 1s est ejecté dans le continuum. Quand l'énergie de liaison électronique (E^Q_{BK}) devient bien plus grande que l'énergie de la transition nucléaire ω_γ, il n'est plus possible d'arracher l'electron à sa couche initiale (K), fig.c, puisque on ne peut même pas approcher le continuum. Entre ces 2 situations, se trouve le cas ou $\omega_\gamma \sim E_{BK}$, fig.b, l'ionisation de la couche K est alors impossible, et donc l'électron excité va devoir atterir sur un état liée juste en dessous du continuum, mettant a jour l'hypothèse de *l'existence* d'un processus de conversion interne vers un état lié vacant du cortège électronique qui serait à la conversion interne ce que la photoexcitation est à la photoionisation. Il est à noter que de part la largeur Γ_γ le coefficient de conversion interne (M1) présente un caractère résonant qui peut faire varier sa valeur, dans le cas d'exemple du 46^+, de 0.67 à 161.

A notre connaissance un tel processus n'a

Références :

1. Nuclear Shapes and Nuclear Structure at Low Excitation Energies International Conference, Antibes June 1994
F. Attallah & al; *Strong dependence of a nuclear lifetime on the ionic charge state.*

2. F. Attallah; *Variation des périodes radioactives en fonction de l'état de charge atomique: Cas du ^{125}Te (Nuclear Lifetime variation according to atomic charge state: case of ^{125}Te)*, thèse de Doctorat de l'Université Bordeaux I, Sep-1994, CENBG 9430, rapport interne.

3. F. Attallah et al; *Charge state dependence of internal conversion and nuclear lifetime in ^{125}Te.*, soumis à Phys.Rev. C. **4.** F. Attallah, J.F. Chemin, J.N. Scheurer; *TURTLE^{+}: Trace Unlimited Rays Through Lumped Elements*, CENBG 9428, CERN program library, non publié.

Phys.Rev.Lett Vol 75, N9(1995)1715

Charge state blocking of K-shell internal conversion in ^{125}Te

F. Attallah[1], M. Aiche[1], J.F. Chemin[1], J.N. Scheurer[1], W.E. Meyerhof[2], J.P. Grandin[3]
P. Aguer[4], G. Bogaert[4], J. Kiener[4], A. Lefebvre[4], J.P.Thibaud[4], and C. Grunberg[5]

[1] *CENBG, IN2P3-CNRS, Université de Bordeaux, 33175 Gradignan, France*
[2] *Department of Physics, Stanford University, Stanford, CA 94305, USA*
[3] *CIRIL, 14040 Caen, France*
[4] *CSNSM, IN2P3-CNRS, Université d'Orsay, 91405 Orsay, France*
[5] *GANIL, 14021 Caen, France*

Abstract

We have studied the atomic charge state dependence of the nuclear lifetime of the 35.5-keV first excited state of ^{125}Te. For the 47^+ and 48^+ ions, 300% and 640% increases, respectively, of the halflife were found with respect to the neutral-atom value (1.49 ns). These unusually large effects are due to the energetic blocking of K-shell internal conversion as the charge state increases past 47^+.

La variation du taux de décroissance de certains niveaux nucléaires avec l'état de charge atomique q est un processus connu depuis longtemps. Pour un noyau dont le mode de décroissance essentiel se fait par un couplage au champ électromagnétique, la période du niveau s'écrit en fonction des coefficients de conversion interne α_i^q sur les différentes couches i et de la largeur de décroissance par émission de photons Γ_γ:

$$T_{1/2}^q = \frac{1/\Gamma_\gamma}{1 + \sum_i \alpha_i^q} \qquad (1)$$

Les coefficients α_i^q dépendent de q de deux manières différentes. Ils varient d'une part, proportionnellement au nombre d'électrons présents sur la i^{eme} couche électronique. D'autre part ils varient selon la densité électronique au voisinage du noyau $\rho(0)$ qui dépend, du potentiel du noyau vu par chacun des électrons. Cette dépendance explique les faibles écarts enregistrés jusqu'ici entre les valeurs des périodes dans l'atome neutre et dans les ions [2].

Pour des ions très épluchés, la variation de l'énergie de liaison des électrons K avec l'état de charge peut conduire à ce que cette énergie E_B^K devienne supérieure à l'énergie de la transition E_γ à partir d'une charge critique q_c. Il y a alors blocage de la conversion interne. Le coefficient $\alpha_K^{q_c}$ devient nul bien que la couche K soit encore remplie, entrainant une variation importante de la période $T_{1/2}$ selon la relation 1.

Nous avons mis en évidence l'effet de blocage de la conversion interne [1,2] dans le transition $M1$ du premier état excité du noyau de ^{125}Te ($3/2^+$, 1.5 ns, 35.5 keV). L'expérience a été effectuée au GANIL avec un faisceau de ^{125}Te à 27 MeV/A. Pour les ions de charge q=47 et 48 la période du niveau s'accroit de 400% et 640%, pour atteindre les valeurs

$$T_{1/2}^{47} = (6 \pm 1)\ ns,\ T_{1/2}^{48} = (11 \pm 2)\ ns$$

alors que la valeur dans l'atome neutre est $T_{1/2}^{0} = (1.486 \pm 0.009)\ ns$.

Expérimentalement, la variation de la période est mesurée à partir de la modification de la trajectoire des ions dans le spectromètre SPEG lorsque la conversion interne se produit à l'intérieur des dipôles. Pour analyser les résultats nous avons utilisé le programme de simulation de trajectoires TURTLE$^+$ [4]. Les détails concernant le dispositif expérimental et l'analyse sont donnés dans la référence [2,3].

jamais été proposé. Il ne peut être important que pour une excitation vers des état formant un quasi continuum sous le seuil d'ionisation (états de Rydberg).

References

[1] F. Attallah & al; *Charge state blocking of K shell internal conversion in* ^{125}Te, Phys. Rev. Lett Vol 75, N9(1995)1715.

[2] F. Attallah et al; *Charge state dependence of internal conversion and nuclear lifetime in* ^{125}Te., soumis à Phys.Rev. C.

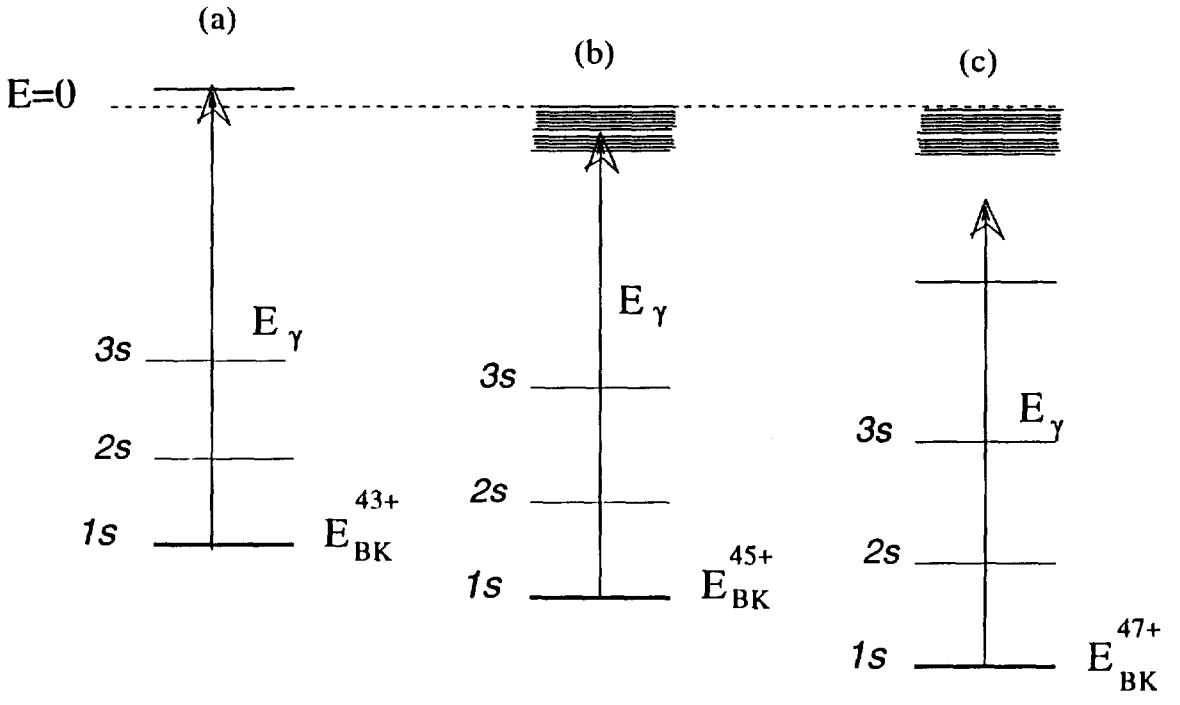

Figure 1: .

TURTLE+
Trace Unlimited Rays Through Lumped Elements

F. Attallah, J.F. Chemin, J.N. Scheurer
CENBG, IN2P3-CNRS, Université de Bordeaux I, F-33175 Gradignan

Abstract

A computer program designed to simulate charged particle beam transport systems. It allows evaluation of the effect of aberration which exist in beams with small phase-space volume. These include higher order chromatic aberrations, effects of non-linearities in magnetic fields, and higher-order geometric aberrations due to the accumulation of second-order effects. Provision has been made to include particle decay, following the parent particles and up to two kinds of daughter particles through the beam line, this allows simulation of heavy ion radioactive beams with several decay modes. ~~We can also simulat~~ Scattered beams including changes of the beam characteristics along the beam line due to scattering or collision processes.
can also be simulated

TURTLE+ [1], notre programme de simulation des systèmes de transport de faisceau d'ions, est une version du programme DECAY TURTLE du CERN [2], revue, augmentée et adaptée au cas des ions lourds. Ce programme permet d'évaluer les effets d'aberration existant pour un faisceau de faible étendue spatiale. Ceci inclu les aberrations chromatiques d'ordre élevé, les effets dus à la non-linéarité des champs magnétiques, et les aberrations géométriques d'ordre élevé.

TURTLE+ inclu aussi d'autres effets tels que: la diffusion Coulombienne par une cible, le changement d'état de charge, la dispersion en énergie, et le bruit de fond. Les possibilités de ce code ont été augmentées pour pouvoir simuler le transport des faisceaux radioactifs avec des désintégrations en vol du projectile à travers plusieurs modes de décroissances possibles, simultanées ou successives.

La sortie graphique de ce code utilise toute les possibilités de la librairie du CERN à travers HBOOK [3] et PAW [4]. Les résultats peuvent ainsi être obtenus sous forme d'histogrammes monodimensionnels ou bidimensionnels indépendants, ou sous forme d'histogrammes corrélés (NTUPLE), structurés exactement de la même façon que les données expérimentales, sur lesquels nous pouvons effectuer, en plus de la définition de contours ou fenêtres de sélection, tout genre d'opération: addition, soustraction, etc ...

Les figures ci dessous montrent la qualité de la simulation sur un exemple de spectre obtenu dans le système de détection de SPEG, après passage d'un faisceau de $^{125}Te^{38+}$ de 27 MeV/A à travers une cible de ^{232}Th de 1 mg/cm^2 [5].

Références :

1 F. Attallah et al, TURTLE+, CENBG 9428, CERN program library.
2 K. L. Brown et al, DECAY TURTLE, CERN 74-2.
3 HBOOK, Computing and Networks Division, CERN program library.
4 R. Brun et al, PAW, CERN program library.
5 F. Attallah; *Variation des périodes radioactives en fonction de l'état de charge atomique: Cas du ^{125}Te (Nuclear Lifetime variation according to atomic charge state: case of ^{125}Te)*, thèse de Doctorat de l'Université Bordeaux I, Sep-1994, CENBG 9430, rapport interne.

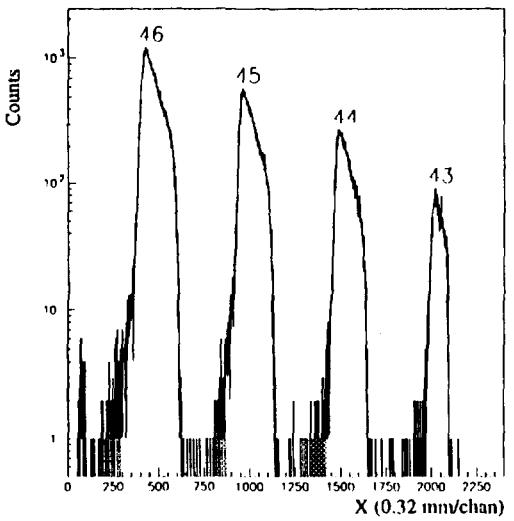

Figure 1: *The experimental horizontal distribution of the scattered ^{125}Te ions of 27 MeV/A measured in the 2nd drift chamber of the detection system of SPEG.*

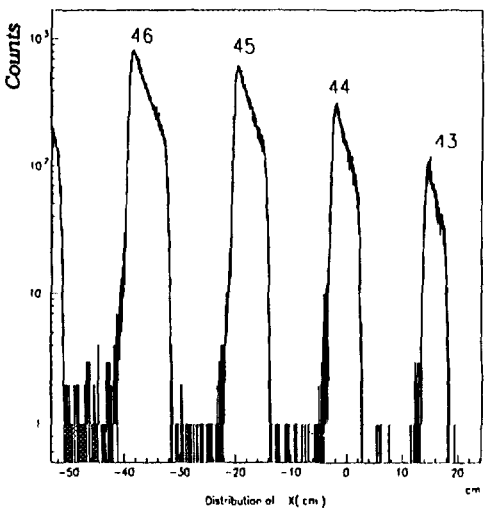

Figure 2: *The simulatted horizontal distributio of the scattered ^{125}Te ions of 27 MeV/A measured in the space region where there was the 2nd drift chamber of SPEG.*

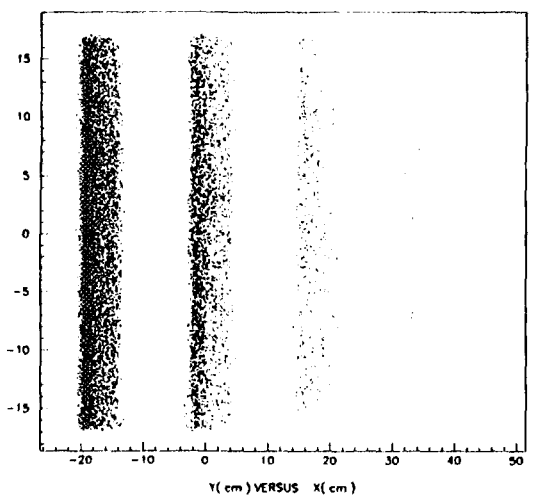

Figure 3: *The simulatted scatter plot of ^{125}Te ions measured in the 2nd drift chamber plane.*

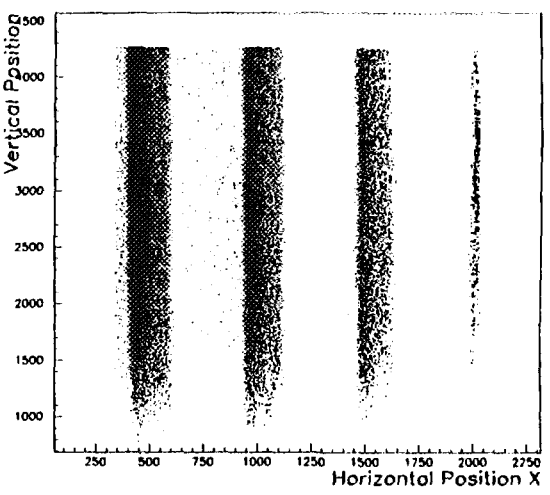

Figure 4: *The experimental scatter plot of ^{125}Te ions measured in the 2nd drift chamber plane of SPEG.*

AUTHOR INDEX

AUTHOR INDEX

II. PUBLICATION LIST

1994

EXCITATION AND FISSION DECAY OF 232 Th BY INELASTIC SCATTERING OF 17 O AT 84 MeV/u
CABOT C. ET AL.
MC GILL UNIV. - MONTREAL, DAPNIA CEN SACLAY - GIF SUR YVETTE, IPN - ORSAY, KVI - GRONINGEN
NUCL. PHYS. A568 (1994) 107.
94 15 A

MEASUREMENT OF DEVIATIONS FROM PURE MOTT-SCATTERING IN THE SYSTEM 208 Pb + 208 Pb BELOW THE COULOMB BARRIER
AUGER G. ET AL.
GANIL - CAEN, IFN - SAO PAULO, INFN - CATANIA
FRANCO-JAPANESE COLLOQUIUM ON NUCLEAR STRUCTURE AND INTERDISCIPLINARY TOPICS.6 SAINT-MALO (FR)
NUCLEAR STRUCTURE AND INTERDISCIPLINARY TOPICS
93 100 A

NEUTRON DECAY OF THE EXCITATION-ENERGY REGION UP TO 60 MeV, EXCITED BY HEAVY ION SCATTERING. (I) 208 Pb
VAN DEN BERG A.M., CHMIELEWSKA D., BORDEWIJK J.A., BRANDENBURG S., VAN DER WOUDE A., BLUMENFELD Y., FRASCARIA N., ROYNETTE J.C., SCARPACI J.A., SUOMIJARVI T., ALAMANOS N., AUGER F., GILLIBERT A., ROUSSEL-CHOMAZ P., BLOMGREN J., NILSSON L., OLSSON N., TURCOTTE R.
KVI - GRONINGEN, IPN - ORSAY, CE-SACLAY - GIF/YVETTE, DEPT. OF RADIATION SCIENCES - UPPSALA, THE SVELBERG LAB. - UPPSALA, DEPT. OF NEUTRON RESEARCH - UPPSALA, FOSTER RADIATION LAB. - MONTREAL
NUCLEAR PHYSICS A578 (1994) 238.
94 55 A

NEUTRON DECAY OF THE EXCITATION-ENERGY REGION UP TO 60 MeV, EXCITED BY HEAVY-ION SCATTERING. (II) 90 Zr AND 124 Sn
BLOMGREN J., VAN DEN BERG A.M., BORDEWIJK J.A., BRANDENBURG S., CHMIELEWSKA D., VAN DER WOUDE A., NILSSON L., OLSSON N., BLUMENFELD Y., FRASCARIA N., ROYNETTE J.C., SCARPACI J.A., SUOMIJARVI T., ALAMANOS N., AUGER F., GILLIBERT A., ROUSSEL-CHOMAZ P., TURCOTTE R.
DEPT. OF RADIATION SCIENCES - UPPSALA, KVI - GRONINGEN, THE SVEDBERG LAB. - UPPSALA, DEPT. OF NEUTRON RESEARCH - UPPSALA, IPN - ORSAY, CE-SACLAY - GIF/YVETTE, FOSTER RADIATION LAB. - MONTREAL
NUCLEAR PHYSICS A578 (1994) 267.
94 56 A

SEARCH FOR COLOR VAN DER WAALS FORCE IN 208 Pb + 208 Pb MOTT SCATTERING
VILLARI A.C.C. ET AL.
GANIL - CAEN, INSTITUTO DE FISICA - SAO PAULO, INFN - CATANIA, KVI - GRONINGEN
PHYSICAL REVIEW LETTERS 71, 16 (1993) 2551.
93 99 A

SOME RECENT RESULTS OF NEUTRON DECAY OF 208 PB EXCITED TO ENERGIES IN THE 14 TO 25 MEV RANGE
VAN DER WOUDE A. ET AL.
KVI - GRONINGEN, IPN - ORSAY, DAPNIA CEN SACLAY - GIF SUR YVETTE, DEPT. OF RADIATION SCI. - UPPSALA, THE SVEDBERG LAB. - UPPSALA, MC GILL UNIV. - MONTREAL, SOLTAN INST. NUCL. STUDIES - SWIERK
NUCL. PHYS. A569 (1994) 383c.
94 06 A

STATISTICAL SIGNATURES OF THE QUASI-PROJECTILE BREAKUP AT 70 A MeV
DORE D. ET AL.
LPN LAVAL UNIV. - SAINTE FOY, LPC/ISMRA - CAEN, DEPT. DE RADIO-ONCOLOGIE - QUEBEC
PHYS. LETT. B323 (1994) 103.
94 30 A

THE GIANT DIPOLE RESONANCE BUILT ON HIGHLY EXCITED STATES - RESULTS OF THE MEDEA EXPERIMENT
SUOMIJARVI T. ET AL.
IPN - ORSAY, INFN - CATANIA, DAPNIA CEA SACLAY - GIF SUR YVETTE, GANIL - CAEN, NBI - COPENHAGEN
NUCL. PHYS. A569 (1994) 225c.
94 05 A

TOWARDS LIMITING TEMPERATURES IN NUCLEI : THE BEHAVIOR OF COLLECTIVE MOTION
LE FAOU J.H. ET AL.
IPN - ORSAY, INFN - CATANIA, CE SACLAY - GIF-SUR-YVETTE, GANIL - CAEN, NBI - COPENHAGEN
PHYS. REV. LETT. 72, No 21 (1994) 3321.
94 33 A

DEEP INELASTIC COLLISIONS IN THE SYSTEM 40 Ar + 232 Th AT 31 MeV/NUCLEON
LIPS V. ET AL.
INST. FUR KERNPHYSIK - DARMSTADT, DAPNIA CE SACLAY - GIF SUR YVETTE
PHYS. REV. C49, 2 (1994) 1214.
94 11 B

EQUILIBRIUM VERSUS NON-EQUILIBRIUM EMISSION IN PROJECTILE FRAGMENTATION FOR THE 40 Ar + nat Ag SYSTEM AT 58.7 A MeV
SAUVESTRE J.E. ET AL.
DAPNIA CE SACLAY - GIF SUR YVETTE, INFN - CATANIA, CRN - STRASBOURG
PHYSICS LETTERS B335 (1994) 300.
94 69 B

EVIDENCE FOR STOPPING IN HEAVY-ION COLLISIONS FROM A STUDY OF HARD-PHOTON SOURCE VELOCITIES
SCHUBERT A. ET AL.
GSI - DARMSTADT, GANIL - CAEN, KVI - GRONINGEN, INST. DI FISICA CORPUSCULAR - BURJASSOT, GIESSEN UNIV. - GIESSEN, NPI - PRAHY, CENBG - GRADIGNAN
PHYS. REV. LETT. 72, 11 (1994) 1608.
94 03 B

EXCITATION ENERGY IN QUASI-ELASTIC AND TRANSFER REACTIONS IN 16 O + 197 Au AT INTERMEDIATE ENERGIES
LAFOREST R. ET AL.
LAVAL UNIV. - STE-FOY, GANIL - CAEN, AECL - CHALK RIVER
NUCL. PHYS. A568 (1994) 350.
94 12 B

ON THE ORIGIN OF FAST PROTON EMISSION IN INTERMEDIATE ENERGY HEAVY ION COLLISIONS

ALBA R., CONIGLIONE R., DEL ZOPPO A., AGODI C., BELLIA G., FINOCCHIARO P., LOUKACHINE K., MAIOLINO C., MIGNECO E., PIATTELLI P., SANTONOCITO D., SAPIENZA P., PEGHAIRE A., IORI I., MANDUCI L., MORONI A.

INFN/LNS - CATANIA, DIPART.DI FIS. DELL'UNIV. - CATANIA, GANIL - CAEN, INFN - MILANO, DIPART.DI FIS. DELL'UNIV. - MILANO

PHYSICS LETTERS B322 (1994) 38.

94 57 B

COMPARISON OF ISOTOPIC DISTRIBUTIONS FOR PROJECTILE-LIKE FRAGMENTS ISSUED FROM 40 Ar AND 40 Ca INDUCED REACTIONS ON Al TARGET AT INTERMEDIATE ENERGIES

LANZANO G. ET AL.

INFN - CATANIA, DAPNIA CE SACLAY - GIF SUR YVETTE

PHYSICS LETTERS B332 (1994) 31.

94 49 B3

A CYCLOTRON AS A HIGH RESOLUTION MASS SPECTROMETER FOR FAST SECONDARY IONS

AUGER G., MITTIG W., LEPINE-SZILY A., FIFIELD L.K., BAJARD M., BARON E., BIBET D., BRICAULT P., CASANDJIAN J.M., CHABERT M., CHARTIER M., FERME J., GAUDARD L., GILLIBERT A., LEWITOWICZ M., MOSCATELLO M.H., ORR N.A., PLAGNOL E., RICAULT C., VILLARI A.C.C., YANG YONG FENG

GANIL - CAEN, IFUSP - SAO PAULO, AUSTRALIAN NAT. UNIV. - CANBERRA, TRIUMF - VANCOUVER, CE-SACLAY - GIF/YVETTE, LPC - CAEN, IPN - ORSAY, IMP - LANZHOU

NIM A350 (1994) 235.

94 60 C

ASTROPHYSICAL RATE OF THE 11 C + p REACTION WITH COULOMB BREAK-UP OF A 12 N RADIOACTIVE BEAM

LEFEBVRE A. ET AL.

CSNSM - ORSAY, CRN - STRASBOURG, IPN - ORSAY, LPN - NANTES, GANIL - CAEN, CENBG - GRADIGNAN

INTERNATIONAL CONFERENCE ON RADIOACTIVE NUCLEAR BEAMS.3

MSU (USA)

94 24 C

CHARGE-EXCHANGE REACTIONS BETWEEN HEAVY IONS AT RELATIVISTIC ENERGIES

SUMMERER K. ET AL.

GSI - DARMSTADT, IPN - ORSAY, TECH. HOCHSCHULE - DARMSTADT, GANIL - CAEN, GIESSEN UNIV. - GIESSEN

INTERNATIONAL CONFERENCE ON RADIOACTIVE NUCLEAR BEAMS.3

MICHIGAN STATE UNIVERSITY (USA)

INTERNATIONAL CONFERENCE ON RADIOACTIVE NUCLEAR BEAMS.3

94 25 C

ELASTIC SCATTERING OF SECONDARY 8 B AND 7 Be BEAMS ON THE 12 C TARGET
LEWITOWICZ M., DLOUHY Z., CARSTOIU F., PECINA I., ANNE R., BAZIN D., BORCEA C., BORREL V., FOMICHEV A., GUILLEMAUD-MUELLER D., KELLER H., KORDYASZ A., LUKYANOV S., MUELLER A.C., NOSEK L., PENIONZHKEVICH YU., ROUSSEL-CHOMAZ P., SAINT-LAURENT M.G., SORLIN O., SKOBELEV N., TARASOV O.
GANIL - CAEN, NUCL.PHYS.INST. - REZ, INST. OF ATOMIC PHYS. - BUCHAREST, IPN - ORSAY, FLNR JINR - DUBNA, INST.OF EXP.PHYS. - WARSAW
RICERCA SCIENTIFICA ED EDUCAZIONE PERMANENTE SUPPL. No. 100 (1994) 528.
INTERNATIONAL CONFERENCE ON NUCLEAR REACTION MECHANISMS.7
VARENNA (IT)
INTERNATIONAL CONFERENCE ON NUCLEAR REACTION MECHANISMS
UNIVERSITA DEGLI STUDI DI MILANO
94 61 C

EXCLUSIVE AND RESTRICTED-INCLUSIVE REACTIONS INVOLVING THE 11 Be ONE-NEUTRON HALO
ANNE R., BIMBOT R., DOGNY S., EMLING H., GUILLEMAUD-MUELLER D., HANSEN P.G., HORNSHOJ P., HUMBERT F., JONSON B., KEIM M., LEWITOWICZ M., MOLLER P.,MUELLER A.C., NEUGART R., NILSSON T., NYMAN G., POUGHEON F., RIISAGER K., SAINT-LAURENT M.G., SCHRIEDER G., SORLIN O., TENGBLAD O., WILHELMSEN ROLANDER K.
GANIL - CAEN, IPN - ORSAY, GSI - DARMSTADT, AARHUS UNIV. - AARHUS, INST.FUR KERNPHYSIK - DARMSTADT, CHALMERS TEKNISKA HOGSKOLA - GOTEBORG, MAINZ UNIV. - MAINZ, CERN - GENEVE
NUCLEAR PHYSICS A575 (1994) 125.
94 53 C

EXPERIMENTAL RESULTS OBTAINED AT GANIL
BORREL V.
IPN - ORSAY
INTERNATIONAL CONFERENCE ON RADIOACTIVE NUCLEAR BEAMS.3
MSU (USA)
94 23 C

HARD PHOTONS AND SUBTHRESHOLD PIONS AS COMPLEMENTARY PROBES OF REACTION DYNAMICS
HOLZMANN R., SCHUBERT A., HLAVAC S., KULESSA R., SIMON R.S., WAGNER V., LAUTRIDOU P., LEFEVRE F., MARQUES M., MATULEWICZ T., MITTIG W., OSTENDORF R.W., ROUSSEL-CHOMAZ P., SCHUTZ Y., LOHNER H., VAN POL J.H.G., SIEMSSEN R.H., WILSCHUT H.W., BALLESTER F., DIAZ J., MARIN A., MARTINEZ G., METAG V., NOVOTNY R., QUEBERT J.
GSI - DARMSTADT, GANIL - CAEN, KVI - GRONINGEN, IFC - BURJASSOT, GIEBEN UNIV. - GIEBEN, CENBG - GRADIGNAN, JAGELLONIAN UNIV. - CRACOW, SLOVAK ACAD. OF SCI. - BRATISLAVA, NUCLEAR PHYSICS INST. - PRAHY
RICERCA SCIENTIFICA ED EDUCAZIONE PERMANENTE SUPPL. No. 100 (1994) 261.
INTERNATIONAL CONFERENCE ON NUCLEAR REACTION MECHANISMS.7
VARENNA (IT)
INTERNATIONAL CONFERENCE ON NUCLEAR REACTION MECHANISMS
UNIVERSITA DEGLI STUDI DI MILANO
94 62 C

IDENTIFICATION OF THE DOUBLY-MAGIC NUCLEUS 100 Sn IN THE REACTION 112 Sn + nat Ni AT 63 MeV/NUCLEON
LEWITOWICZ M. ET AL.
GANIL - CAEN, IAP - BUCHAREST-MAGURELE, IPN - ORSAY, GOTTINGEN UNIV. - GOTTINGEN, FLNR JINR - DUBNA, IFD WARSAW UNIV. - WARSAW, IKS KU - LEUVEN, GSI - DARMSTADT
PHYSICS LETTERS B332 (1994) 20.
94 35 C

LONGITUDINAL MOMENTA AND PRODUCTION CROSS-SECTIONS OF ISOTOPES FORMED BY FRAGMENTATION OF A 500 A X MeV 86 Kr BEAM
WEBER M., DONZAUD C., DUFOUR J.P., GEISSEL H., GREWE A., GUILLEMAUD-MUELLER D., KELLER H., LEWITOWICZ M., MAGEL A., MUELLER A.C., MUNZENBERG G., NICKEL F., PFUTZNER M., PIECHACZEK A., PRAVIKOFF M., ROECKL E., RYKACZEWSKI K., SAINT-LAURENT M.G., SCHALL I., STEPHAN C., SUMMERER K., TASSAN-GOT L., VIEIRA D.J., VOSS B.
GSI - DARMSTADT, IPN - ORSAY, CENBG - GRADIGNAN, INST. FUR KERNPHYSIK - DARMSTADT, GANIL - CAEN, GIEBEN UNIV. - GIEBEN, LANL - LOS ALAMOS
NUCLEAR PHYSICS A578 (1994) 659.
94 59 C

PRODUCTION OF A PURE 42 Sc m ISOMERIC BEAM
UZUREAU J.L. ET AL.
CE - BRUYERES-LE-CHATEL, GANIL - CAEN, IPN - ORSAY
PHYSICS LETTERS B331 (1994) 280.
94 48 C

PRODUCTION OF ISOMERIC 44 V AND 42 Sc IN HIGH ENERGY HEAVY ION REACTIONS
KELLER H. ET AL.
IPN - ORSAY, CRN - STRASBOURG, GANIL - CAEN, IPNL - VILLEURBANNE
Z. PHYS. A348 (1994) 67.
94 16 C

REACTION MECHANISMS IN THE DISSOCIATION OF 11 BE
WILHELMSEN K. ET AL.
CHALMERS UNIV.OF TECH. - GOTEBORG, GANIL - CAEN, INP - ORSAY, GSI - DARMSTADT, ANL - ARGONNE, AARHUS UNIV. - AARHUS, INST.FUR KERNPHYSIK - DARMSTADT, MAINZ UNIV. - MAINZ, CERN - GENEVE, SOLTAN INST.NUCL.STUDIES - OTWOCK-SWIERK
INTERNATIONAL CONFERENCE ON RADIOACTIVE NUCLEAR BEAMS.3
MSU (USA)
94 20 C

SEARCH FOR FORBIDDEN BETA-DECAYS OF THE DRIP LINE NUCLEUS 12 Be
KELLER H. ET AL.
IPN - ORSAY, GANIL - CAEN, INST.DE ESTRUCTURA DE LA MATERIA - MADRID, GSI - DARMSTADT, AARHUS UNIV. - AARHUS, INST.FUR KERNPHYSIK - DARMSTADT, CHALMERS TEKNISKA HOGSKOLA - GOTEBORG, MAINZ UNIV. - MAINZ, CERN - GENEVE
Z. PHYS. A348 (1994) 61.
94 17 C

THE BETA-DECAY OF 20 MG AND ITS IMPLICATIONS FOR THE ASTROPHYSICAL RP-PROCESS
PIECHACZEK A. ET AL.
GSI - DARMSTADT, GANIL - CAEN, IPN - ORSAY, MSU - EAST LANSING, RIKEN - WAKO, INS - TOKYO, GOTTINGEN UNIV., WASHINGTON UNIV. - SEATTLE, TOKYO UNIV., WARSAW UNIV.
INTERNATIONAL CONFERENCE ON RADIOACTIVE NUCLEAR BEAMS.3
MSU (USA)
94 19 C

VERY ENERGETIC PHOTONS FROM HEAVY-ION COLLISIONS
MATULEWICZ T.
GANIL - CAEN
ACTA PHYSICA POLONICA B25, No 3-4 (1994) 705.
94 32 C

ANGULAR AND VELOCITY ANALYSIS OF THE THREE-FOLD EVENTS IN THE Xe + Cu REACTION AT 45 MeV/u
BRUNO M. ET AL.
INFN - BOLOGNA, INFN - LEGNARO, INFN - MILANO, INFN - TRIESTE, GANIL - CAEN
NUCLEAR PHYSICS A576 (1994) 138.
94 46 D

DETERMINATION OF THERMAL EXCITATION ENERGIES PRODUCED IN HIGH-ENERGY p, 3 He, AND 84 Kr INDUCED REACTIONS VIA NEUTRON MULTIPLICITY MEASUREMENTS
QUEDNAU B.M. ET AL.
GANIL - CAEN, HMI - BERLIN, IPN - ORSAY, LNS - GIF SUR YVETTE, KVI - SAO PAULO, LIEGE UNIV. - LIEGE
WORKSHOP ON GROSS PROPERTIES OF NUCLEI AND NUCLEAR EXCITATIONS.22
HIRSCHEGG (AUSTRIA)
HIRSCHEGG '94 : MULTIFRAGMENTATION
94 26 D

EVOLUTION OF FISSION AND COMPETING DECAY MECHANISMS IN 40 Ar-INDUCED REACTIONS ON Au, Th AT 27-27 MeV/u OF INCIDENT ENERGY
SCHWINN E. ET AL.
HMI - BERLIN, CE - BRUYERES-LE-CHATEL, GANIL - CAEN, IPN - ORSAY, CRN - STRASBOURG, WARSAW UNIV. - WARSAW
NUCL. PHYS. A568 (1994) 169.
94 14 D

FROM EVAPORATION TO MULTIFRAGMENTATION OF HIGHLY EXCITED NUCLEI FORMED AT GANIL ENERGIES
ABOUFIRASSI M. ET AL.
LPC/ISMRA - CAEN, CRN - STRASBOURG, GANIL - CAEN, IPN - ORSAY, RIKKYO UNIV. - TOKYO, UCL - LOUVAIN LA NEUVE, ULB - BRUXELLES
INTERNATIONAL WORKSHOP ON GROSS PROPERTIES OF NUCLEI AND NUCLEAR EXCITATIONS.22
HIRSCHEGG (AUSTRIA)
HIRSCHEGG '94 : MULTIFRAGMENTATION
94 28 D

HOT NUCLEI IN 2 GEV P, 2 GEV 3 HE AND 150 MEV/A 84 KR INDUCED REACTIONS
GALIN J. ET AL.
GANIL - CAEN, HMI - BERLIN, IPN - ORSAY, LN SATURNE - GIF SUR YVETTE, KVI - GRONINGEN, IFUSP - SAO PAULO, LIEGE UNIV. - LIEGE
WINTER WORKSHOP ON NUCLEAR DYNAMICS.10
SNOWBIRD (US)
ADVANCES IN NUCLEAR DYNAMICS
94 67 D

HOT NUCLEI IN REACTIONS INDUCED BY 475 MeV, 2 GeV 1 H AND 2 GeV 3 He
PIENKOWSKI L., BOHLEN H.G., CUGNON J., FUCHS H., GALIN J., GATTY B., GEBAUER B., GUERREAU D., HILSCHER D., JACQUET D., JAHNKE U., JOSSET M., LEDOUX X., LERAY S., LOTT B., MORJEAN M., PEGHAIRE A., ROSCHERT G., ROSSNER H., SIEMSSEN R.H., STEPHAN C.
CE-SACLAY - GIF/YVETTE, GANIL - CAEN, HMI - BERLIN, LIEGE UNIV. - LIEGE, IPN - ORSAY
PHYSICS LETTERS B336 (1994) 147.
94 54 D

HOT-NUCLEI FORMATION AND DECAY : THE Ar + Ag SYSTEM AT 50 AND 70 MeV/u
VIENT E. ET AL.
LPC - CAEN, GANIL - CAEN, LPN - NANTES, INFN - CATANIA, NAPOLI UNIV. - NAPOLI, LPN - RABAT
NUCL.PHYS. A571 (1994) 588.
94 31 D

LIFETIMES OF WELL CHARACTERIZED HOT NUCLEI VIA SMALL-ANGLE PARTICLE-PARTICLE CORRELATIONS : 40 Ar + Ag (E/A = 7.8 AND 17 MeV)
ELMAANI A. ET AL.
STATE UNIV. OF NEW YORK - STONY BROOK, ISN - GRENOBLE, GANIL - CAEN
PHYS. REV. C49, 1 (1994) 284.
94 10 D

MULTIFRAGMENTATION IN Xe + Cu REACTION AT 45 MeV/u
BRUNO M. ET AL.
INFN - BOLOGNA, INFN - LEGNARO, INFN - MILANO, INFN - TRIESTE, GANIL - CAEN, IPN - ORSAY
INTERNATIONAL WORKSHOP ON GROSS PROPERTIES OF NUCLEI AND NUCLEAR EXCITATIONS.22 HIRSCHEGG (AT)
HIRSCHEGG'94 : MULTIFRAGMENTATION
94 36 D

RAPID DECREASE OF FRAGMENT EMISSION TIME IN THE RANGE OF 3-5 MeV/u EXCITATION ENERGY
LOUVEL M. ET AL.
LPC ISMRA - CAEN, GANIL - CAEN, FNRS IPN - LOUVAIN LA NEUVE, TSUKUBA UNIV. - TSUKUBA, TEXAS A & M UNIV. - COLLEGE STATION, FNRS ULB - BRUXELLES, IMP - LANZHOU, SHINSHU UNIV. - NAGANO-KEN, RIKKYO UNIV. - TOKYO
PHYS. LETT. B320 (1994) 221.
94 01 D

RECENT RESULTS FROM NAUTILUS AND INDRA
SAINT-LAURENT F. ET AL.
DAPNIA CEN SACLAY - GIF SUR YVETTE, 'GANIL - CAEN, IPN - ORSAY, LPC - CAEN, LPN - NANTES, IPNL - LYON
WORKSHOP ON GROSS PROPERTIES OF NUCLEI AND NUCLEAR EXCITATIONS.22 HIRSCHEGG (AUSTRIA)
HIRSCHEGG '94 : MULTIFRAGMENTATION
94 27 D

THE DECAY OF PRIMARY PRODUCTS IN BINARY HIGHLY DAMPED 208 Pb + 197 Au COLLISIONS AT 29 MeV/u
LECOLLEY J.F. ET AL.
LPC/ISMRA - CAEN, CRN - STRASBOURG, GANIL - CAEN, IPN - ORSAY
PHYS. LETT. B325 (1994) 317.
94 29 D

TOPICAL REVIEW : HOT NUCLEI AS VIEWED THROUGH 4 pi NEUTRON MULTIPLICITY FILTERS
GALIN J., JAHNKE U.
GANIL - CAEN, HMI - BERLIN
JOURNAL OF PHYSICS G20 (1994) 1105.
94 52 D

HARD PHOTON INTENSITY INTERFEROMETRY IN HEAVY ION REACTIONS
MARQUES M. ET AL.
GANIL - CAEN, CENBG - GRADIGNAN, UNIVERSIDAD DE VALENCIA - VALENCIA, GSI - DARMSTADT, KVI - GRONINGEN, GIESSEN UNIV. - GIESSEN, SOLTAN INST.NUCL.STUDIES - SWIERK
PHYSICAL REVIEW LETTERS 73, 1 (1994) 34.
94 38 E

HEAVY ION COULOMB EXCITATION AND GAMMA DECAY STUDIES OF THE ONE AND TWO PHONON GIANT DIPOLE RESONANCES IN 208 Pb AND 209 Bi
MUELLER P.E. ET AL.
ORNL - OAK RIDGE, MSU - EAST LANSING, GANIL - CAEN, KVI - GRONINGEN, IFIC - BURJASSOT
NUCL. PHYS. A569 (1994) 123c.
94 04 E

INVESTIGATING THE MULTIPARTICLE DECAY IN INTERMEDIATE ENERGY HEAVY ION COLLISIONS
DEL ZOPPO A., ALBA R., CONIGLIONE R., AGODI C., BELLIA G., FINOCCHIARO P., LOUKACHINE K., MAIOLINO C., MIGNECO E., PEGHAIRE A., PIATTELLI P., SANTONOCITO D., SAPIENZA P.
INFN/LNS - CATANIA, DIPART.DIFIS. DELL'UNIV. - CATANIA, GANIL - CAEN
PHYSICAL REVIEW C49, 6 (1994) 3334.
94 58 E

G - ARTICLES GENERAUX

GANIL INDRA ET LES NOYAUX CHAUDS
GANIL - CAEN
COURRIER CERN, JANVIER/FEVRIER 1994
94 07 G

LE PROJET SPIRAL - UNE INSTALLATION DE FAISCEAUX RADIOACTIFS AU GANIL
HARAR S.
GANIL - CAEN
BULLETIN DE LA SOCIETE FRANCAISE DE PHYSIQUE No. 97 (1994)
94 63 G

LES NOYAUX A HALOS
GUILLEMAUD-MUELLER D.
IPN - ORSAY
IMAGES DE LA PHYSIQUE (1994)
94 66 G

LES NOYAUX CHAUDS
GUERREAU D., TAMAIN B.
GANIL - CAEN, LPC - CAEN
IMAGES DE LA PHYSIQUE (1994)
94 65 G

LES NOYAUX EXOTIQUES
GUILLEMAUD-MUELLER D.
IPN - ORSAY
LA RECHERCHE 25, No.263 (1994) 286
94 13 G

NOYAUX MAGIQUES ETAIN-100 ETINCELANT
GANIL - CAEN
COURRIER CERN, JUILLET/AOUT 1994
94 47 G

H - ACCELERATEUR

THE GANIL PLUS PROGRAM FOR A RBN FACILITY AT GANIL
ANNE R. ET AL.
GANIL - CAEN, IPN - ORSAY, CSNSM - ORSAY, LPC/ISMRA - CAEN
INTERNATIONAL CONFERENCE ON RADIOACTIVE NUCLEAR BEAMS.3
MSU (USA)
94 21 H

THE NEW ACCELERATOR CONTROL SYSTEM OF GANIL
LUONG T.T. ET AL.
GANIL - CAEN
NIM A352 (1994) 96.
94 64 H

I - INSTRUMENTATION

DECELERATION OF A SECONDARY BEAM PRODUCED BY FRAGMENTATION DOWN TO THE COULOMB BARRIER
YONG FENG Y.
GANIL - CAEN, DAPNIA CEN SACLAY - GIF SUR YVETTE, IPN - ORSAY, INFN - CATANIA
INTERNATIONAL CONFERENCE ON RADIOACTIVE NUCLEAR BEAMS.3
MSU (USA)
94 22 I

LISE3 : TESTS AND RESULTS
ANNE R., MUELLER A.C.
GANIL - CAEN, IPN - ORSAY
INTERNATIONAL CONFERENCE ON EXOTIC NUCLEI
FOROS (CRIMEA)
EXOTIC NUCLEI
94 02 D

N - PHYSIQUE DES IONS RAPIDES

A STUDY ON RADIATION GRAFTING OF STYRENE INDUCED BY SWIFT HEAVY-IONS IN POLY(VINYLIDENE FLUORIDE)
BETZ N. ET AL.
CE SACLAY - GIF SUR YVETTE, CIRIL - CAEN
NIM B91 (1994) 151.
94 44 N

DAMAGE AND CONDUCTIVITY OF YTTRIUM IRON GARNET IRRADIATED WITH GeV-HEAVY IONS
COSTANTINI J.M. ET AL.
CEA - BRUYERES-LE-CHATEL, CIRIL - CAEN, CRISMAT ISMRA - CAEN
NIM B91 (1994) 288.
94 41 N

DAMAGE INDUCED IN LiNbO 3 SINGLE CRYSTALS BY GeV GADOLINIUM IONS
CANUT B. ET AL.
UNIV. CLAUDE BERNARD LYON I - VILLEURBANNE, CIRIL - CAEN
NIM B91 (1994) 312.
94 40 N

DEFECT CREATION IN ALKALI-HALIDES UNDER DENSE ELECTRONIC EXCITATIONS : EXPERIMENTAL RESULTS ON NaCl AND KBr
BALANZAT E. ET AL.
CIRIL - CAEN, ISMRA - CAEN
NIM B91 (1994) 134.
94 37 N

ELECTRONIC CAPTURE AND EXCITATION OF HIGHLY CHARGED CHANNELED IONS
ANDRIAMONJE S. ET AL.
CENBG - GRADIGNAN, IPNL - VILLEURBANNE, GROUPE DE PHYSIQUE DES SOLIDES - PARIS, CIRIL - CAEN, ECOLE POLYTECHNIQUE - PALAISEAU, UNIV. OF SCI. AND TECH. - HONG KONG
NIM B87 (1994) 116.
94 34 N

EVIDENCE OF A BOSE-GLASS TRANSITION IN SUPERCONDUCTING YBa2Cu3O7 SINGLE CRYSTALS WITH COLUMNAR DEFECTS
JIANG W. ET AL.
CALIFORNIA INST.OF TECH. - PASADENA, ECOLE POLYTECHNIQUE - PALAISEAU, THOMAS J. WATSON RESEARCH CENTER - YORKTOWN HEIGHTS
PHYS. REV. LETT. 72, 4 (1994) 550.
94 09 N

MOSSBAUER STUDY OF SAPPHIRE IRRADIATED WITH HIGH ENERGY HEAVY IONS
MARTY J.M. ET AL.
IPNL - VILLEURBANNE, CIRIL - CAEN, ISMRA - CAEN, CLAUDE BERNARD UNIV. - VILLEURBANNE
NIM B91 (1994) 274.
94 42 N

OBSERVATIONS BY X-RAY DIFFRACTION OF STRUCTURAL CHANGES IN MICA IRRADIATED BY SWIFT HEAVY IONS
CHAILLEY V. ET AL.
CIRIL - CAEN, LERMAT ISMRA - CAEN
NIM B91 (1994) 162.
94 43 N

PHYSICO-CHEMICAL MODIFICATIONS INDUCED IN POLYMERS BY SWIFT HEAVY IONS
BALANZAT E. ET AL.
CIRIL - CAEN, CEA - GIF SUR YVETTE
NIM B91 (1994) 140.
94 45 N

SHIFT HEAVY IONS IN INSULATING AND CONDUCTING OXIDES : TRACKS AND PHYSICAL PROPERTIES
TOULEMONDE M. ET AL.
CIRIL - CAEN, CRISMAT - CAEN
NIM B91 (1994) 108.
94 39 N

T - THEORIE

BROWNIAN ONE-BODY DYNAMICS IN NUCLEI
CHOMAZ PH. ET AL.
GANIL - CAEN, LNS - CATANIA, LBL - BERKELEY
PHYSICAL REVIEW LETTERS 73, No. 26 (1994) 3512.
94 68 T

FINGERPRINTS OF DYNAMICAL INSTABILITIES
CHOMAZ PH. ET AL.
GANIL - CAEN, LNS - CATANIA
INTERNATIONAL WORKSHOP ON DYNAMICAL FEATURES OF NUCLEI AND FINITE FERMI SYSTEMS SITGES (SP)
DYNAMICAL FEATURES OF NUCLEI AND FINITE FERMI SYSTEMS
94 79 T

LINEAR RESPONSE IN STOCHASTIC MEAN-FIELD THEORIES AND THE ONSET OF INSTABILITIES
COLONNA M. ET AL.
GANIL - CAEN, LNS - CATANIA, LBL - BERKELEY
NUCL. PHYS. A567 (1994) 637.
94 08 T

ON TRANSIENT EFFECTS IN VIOLENT NUCLEAR COLLISIONS
SURAUD E., AYIK S., BELKACEM M., ZHANG F.S.
PAUL SABATIER UNIV. - TOULOUSE, TENNESSEE TECH. UNIV. - COOKEVILLE, GANIL - CAEN, IMP - LANZHOU
NUCLEAR PHYSICS A580 (1994) 323.
94 51 T

QUANTUM TUNNELING IN THE DRIVEN LIPKIN N-BODY PROBLEM
KAMINSKI P. ET AL.
GANIL - CAEN, INP - KRAKOW, ISN - GRENOBLE
NUCLEAR PHYSICS A579 (1994) 144.
94 81 T

SIMULATION OF TRANSPORT EQUATIONS FOR UNSTABLE SYSTEMS : COMPARISON BETWEEN LATTICE AND TEST-PARTICLE METHODS
BURGIO G.F. ET AL.
CATANIA UNIV. AND INFN - CATANIA, GANIL - CAEN, LNS - CATANIA, LBL - BERKELEY
NUCLEAR PHYSICS A581 (1995) 356.
95 01 T

UNIVERSAL PROPERTIES OF PI AND ETA SPECTRA IN NUCLEAR COLLISIONS
KUDIMA K.K. ET AL.
GANIL - CAEN, MOLDOVA ACAD. OF SCIENCES - KISHINEU, JINR - DUBNA
PHYSICS LETTERS B328 (1994) 249.
94 80 T

1995

ASTROPHYSICAL RATE OF THE 11 C+p REACTION FROM THE COULOMB BREAK-UP OF A 12 N RADIOACTIVE BEAM
LEFEBVRE A. ET AL.
CSNSM - ORSAY, CRN - STRASBOURG, IPN - ORSAY, LPN - NANTES, GANIL - CAEN, CENBG - GRADIGNAN
NUCLEAR PHYSICS A592 (1995) 69.
95 95 A

ELASTIC SCATTERING, INELASTIC SCATTERING AND CHARGE EXCHANGE REACTION STUDIES WITH 6 He, 10,11 Be SECONDARY BEAMS
CORTINA-GIL M.D. ET AL.
GANIL - CAEN, DAPNIA CE SACLAY - GIF SUR YVETTE, Mc GILL UNIV. - MONTREAL, IPN - ORSAY, IFUSP - SAO PAULO, LPC/ISMRA - CAEN
NUCLEAR PHYSICS A583 (1995) 787.
INTERNATIONAL CONFERENCE ON NUCLEUS-NUCLEUS COLLISIONS.5
TAORMINA (IT)
95 03 A

INVESTIGATION OF GIANT RESONANCES VIA PHOTON DECAY
VARNER R.L., MUELLER P.E., BEENE J.R.
ORNL - OAK RIDGE
PROCEEDINGS OF II TAPS WORKSHOP
GUARDAMAR (SP)
GAMMMA RAY AND PARTICLE PRODUCTION IN HEAVY ION REACTIONS
95 98 A

MULTIPHONON STATES IN NUCLEI
FRASCARIA N.
IPN - ORSAY
NUCLEAR PHYSICS NEWS 5, 2 (1995) 23.
95 57 A

SEARCH FOR THE SIGNATURE OF A HALO STRUCTURE IN THE p(6 He, 6 Li)n REACTION
CORTINA-GIL M.D. ET AL.
GANIL - CAEN, CEA SACLAY - GIF-SUR-YVETTE, McGILL UNIV. - MONTREAL, IPN - ORSAY, IFUSP DFN - SAO PAULO, LPC ISMRA - CAEN
PHYS. LETT. B371 (1996) 14.
96 09 A

THE GIANT DIPOLE RESONANCE AT VERY HIGH TEMPERATURES
SUOMIJARVI T. ET AL.
IPN - ORSAY, INFN/LNS - CATANIA, DAPNIA CE SACLAY - GIF SUR YVETTE, GANIL - CAEN, NBI - COPENHAGEN
NUCLEAR PHYSICS A583 (1995) 105.
INTERNATIONAL CONFERENCE ON NUCLEUS-NUCLEUS COLLISIONS.5
TAORMINA (IT)
95 08 A

THE HIGH PRECISION MEASUREMENT OF 208 Pb + 208 Pb MOTT SCATTERING AT ENERGIES UNDER THE COULOMB BARRIER : THE OBSERVATION OF NEW ATOMIC EFFECTS
LEPINE-SZILY A. ET AL.
GANIL - CAEN, IFUSP - SAO PAULO, UNAM - MEXICO, DIPART. DI FISICA/INFN - CATANIA, LPC/ISMRA - CAEN, IPN - ORSAY, KVI - GRONINGEN
NUCLEAR PHYSICS A583 (1995) 263.
INTERNATIONAL CONFERENCE ON NUCLEUS-NUCLEUS COLLISIONS.5
TAORMINA (IT)
95 07 A

MODEL-UNRESTRICTED NUCLEUS-NUCLEUS SCATTERING POTENTIALS FROM MEASUREMENT AND ANALYSIS OF 16 O + 16 O SCATTERING
BARTNITZKY G. ET AL.
PHYSIKALISCHES INST. UNIV. TBINGEN - TBINGEN, HMI - BERLIN, GANIL - CAEN, CE SACLAY - GIF-SUR-YVETTE
NIM B365 (1996) 23.
96 01 A1

ANGULAR MOMENTUM TRANSFER IN PERIPHERAL COLLISIONS AT GANIL
COLIN J. ET AL.
LPC/ISMRA - CAEN, CRN - STRASBOURG
NUCLEAR PHYSICS A583 (1995) 449.
INTERNATIONAL CONFERENCE ON NUCLEUS-NUCLEUS COLLISIONS.5
TAORMINA (IT)
95 16 B

ANGULAR MOMENTUM TRANSFER IN PERIPHERAL REACTIONS AT GANIL
BIZARD G. ET AL.
LPC ISMRA - CAEN
SECOND EUROPEAN BIENNIAL WORKSHOP ON NUCLEAR PHYSICS
MEGEVE (FR)
SECOND EUROPEAN BIENNIAL WORKSHOP ON NUCLEAR PHYSICS
95 72 B

ANGULAR MOMENTUM TRANSFER IN PERIPHERAL REACTIONS AT INTERTMEDIATE ENERGIES
COLIN J. ET AL.
LPC ISMRA - CAEN, CRN - STRASBOURG
NUCLEAR PHYSICS A593 (1995) 48.
95 102 B

AZIMUTHAL CORRELATIONS FUNCTIONS AND THE ENERGY OF VANISHING FLOW IN NUCLEUS-NUCLEUS COLLISIONS
BUTA A. ET AL.
LPC/ISMRA - CAEN, INST.FIZI.INGI.NUCL. - BUCARESTI, GANIL - CAEN, CE SACLAY - GIF SUR YVETTE, SAO PAULO UNIV. - SAO PAULO, IPN/UCL - LOUVAIN-LA-NEUVE, LPN - NANTES, TEXAS A&M UNIV. - COLLEGE STATION, DIPART.SCI.FIS. - NAPOLI, IMP - LANZHOU
NUCLEAR PHYSICS A584 (1995) 397.
95 02 B

AZIMUTHAL DEPENDENCE OF THE DIRECTED FLOW IN COLLISIONS UP TO 95 MeV/u : FROM IN-PLANE TO OUT-OF-PLANE ENHANCEMENT
ANGELIQUE J.C. ET AL.
LPC/ISMRA - CAEN, GANIL - CAEN, TEXAS A & M UNIV. - COLLEGE STATION, SUBATECH - NANTES, FNRS/IPN - LOUVAIN-LA-NEUVE, DIPART. DI SCI. FISICHE/INFN - NAPOLI, IMA - LANZHOU, IPNE - BUCHAREST, IPN - ORSAY, SAO PAULO UNIV. - SAO PAULO
NUCLEAR PHYSICS A583 (1995) 543.
INTERNATIONAL CONFERENCE ON NUCLEUS-NUCLEUS COLLISIONS.5
TAORMINA (IT)
95 05 B

DISSIPATIVE ASPECTS IN 200 MeV/u Kr-INDUCED REACTIONS
DONZAUD C.
IPN - ORSAY, CENNB - GRADIGNAN, GANIL - CAEN, CRN - STRASBOURG, CE SACLAY - GIF-SUR-YVETTE
NUCLEAR PHYSICS A593 (1995) 503.
95 97 B

DISSIPATIVE ASPECTS IN PROJECTILE FRAGMENTATION AT 200 MEV/U
TASSAN-GOT L. ET AL.
IPN - ORSAY, GANIL - CAEN, CRN - STRASBOURG
NUCLEAR PHYSICS A583 (1995) 453.
INTERNATIONAL CONFERENCE ON NUCLEUS-NUCLEUS COLLISIONS.5
TAORMINA (IT)
95 17 B

EQUILIBRIUM VERSUS NON-EQUILIBRIUM EMISSION IN PROJECTILE FRAGMENTATION FOR THE 40 Ar + nat Ag SYSTEM AT 58.7 A MeV
SAUVESTRE J.E. ET AL.
DAPNIA CE SACLAY - GIF SUR YVETTE, INFN - CATANIA, CRN - STRASBOURG
PHYSICS LETTERS B335 (1994) 300.
94 69 B

FRAGMENT CORRELATIONS FROM NAUTILUS MULTIDETECTORS
BIZARD G.
LPC - CAEN
INTERNATIONAL WORKSHOP ON MULTIPARTICLE CORRELATIONS AND NUCLEAR REACTIONS
NANTES (FR)
CORINNE II : MULTIPARTICLE CORRELATIONS AND NUCLEAR REACTIONS
95 80 B

NECK FORMATION AND DECAY IN Pb + Au COLLISIONS AT 29 MeV/u
LECOLLEY J.F. ET AL.
LPC ISMRA - CAEN, CRN - STRASBOURG, GANIL - CAEN, IPN - ORSAY, AECL - CHALK RIVER
PHYSICS LETTERS B354 (1995) 202.
95 51 B

STUDY OF THE 12 C (alpha,gamma) 16 O REACTION BY BREAKUP OF A 16 O -BEAM AT 100 MeV/A
TATISCHEFF V. ET AL.
CSNSM - ORSAY, IPN - ORSAY, CRN - STRASBOURG, GANIL - CAEN, RIKKYO UNIV. - TOKYO, RIKEN - SAITAMA
TOURS SYMPOSIUM ON NUCLEAR PHYSICS.2
TOURS (FR)
TOURS SYMPOSIUM ON NUCLEAR PHYSICS.2
95 64 B

TWO-PROTON CORRELATION FUNCTION MEASURED AT VERY SMALL RELATIVE MOMENTA
MARTIN L. ET AL.
SUBATECH - NANTES, GANIL - CAEN, CENBG - GRADIGNAN, CSNSM - ORSAY, WARSAW UNIV. - WARSAW, INP - KRAKOW
NUCLEAR PHYSICS A583 (1995) 407.
INTERNATIONAL CONFERENCE ON NUCLEUS-NUCLEUS COLLISIONS.5
TAORMINA (IT)
95 06 B

FROM IN-PLANE TO OUT-OF-PLANE ENHANCEMENT OF THE DIRECTED FLOW IN 64 Zn ON 58 Ni COLLISIONS BETWEEN 35 AND 79 MeV/u
POPESCU R. ET AL.
LPC - CAEN, GANIL - CAEN, TEXAS A&M UNIV. - COLLEGE STATION, LPN - NANTES, FNRS/IPN - LOUVAIN-LA-NEUVE, DIPART.DE SCI. FISICHE/INFN - NAPOLI
PHYSICS LETTERS B331 (1994) 285.
94 50 B1

ROLE OF THE BREAKUP PROCESS IN THE 48 Ca(20 Ne, 19 Ne n) REACTION AT 48A MeV
LAURENT H. ET AL.
IPN - ORSAY, SPhN DAPNIA CE SACLAY - GIF-SUR-YVETTE, GANIL - CAEN, KVI - GRONINGEN
PHYSICAL REVIEW C52, 6 (1995) 3066.
95 110 B1

STUDY OF THE NUCLEAR MULTIFRAGMENTATION : RECENT RESULTS OBTAINED WITH THE INDRA DETECTOR IN THE INTERMEDIATE ENERGY DOMAIN
SAINT-LAURENT F.
GANIL - CAEN
NUCLEAR PHYSICS A583 (1995) 481.
INTERNATIONAL CONFERENCE ON NUCLEUS-NUCLEUS COLLISIONS.5
TAORMINA (IT)
95 19 B1

BETA-DECAY STUDIES OF FAR FROM STABILITY NUCLEI NEAR N = 28
SORLIN O. ET AL.
IPN - ORSAY, GANIL - CAEN, MAINZ UNIV. - MAINZ, JINR - DUBNA
NUCLEAR PHYSICS A583 (1995) 763.
INTERNATIONAL CONFERENCE ON NUCLEUS-NUCLEUS COLLISIONS.5
TAORMINA (IT)
95 04 C

BETA-DECAY STUDIES OF NUCLEI FAR FROM STABILITY NEAR N = 28
SORLIN O. ET AL.
IPN - ORSAY, GANIL - CAEN, MAINZ UNIV. - MAINZ, JINR - DUBNA
INTERNATIONAL CONFERENCE ON NUCLEAR SHAPES AND NUCLEAR STRUCTURE AT LOW EXCITATION ENERGIES
ANTIBES (FR)
NUCLEAR SHAPES AND NUCLEAR STRUCTURE AT LOW EXCITATION ENERGIES
95 33 C

BETA-DELAYED PROTON EMISSION FROM THE PROTON-RICH ISOTOPES 67 Se, 71 Kr, AND 75 Sr
BLANK B. ET AL.
CENBG - GRADIGNAN, GSI - DARMSTADT, INST.FUR KERNPHYSIK - DARMSTADT, WARSAW UNIV. - WARSAW, GANIL - CAEN, CE BRUYERES-LE-CHATEL
PHYSICS LETTERS B364 (1995) 8.
95 109 C

CHARGE-EXCHANGE REACTIONS BETWEEN HEAVY IONS AT RELATIVISTIC ENERGIES
SUMMERER K. ET AL.
GSI - DARMSTADT, IPN - ORSAY, TECH. HOCHSCHULE - DARMSTADT, GANIL - CAEN, GIESSEN UNIV. - GIESSEN
INTERNATIONAL CONFERENCE ON RADIOACTIVE NUCLEAR BEAMS.3
MICHIGAN STATE UNIVERSITY (USA)
INTERNATIONAL CONFERENCE ON RADIOACTIVE NUCLEAR BEAMS.3
94 25 C

COMPARISON OF RADIOACTIVE ION-BEAM INTENSITIES PRODUCED BY MEANS OF THICK TARGETS BOMBARDED WITH NEUTRONS, PROTONS AND HEAVY IONS
RAVN H.L. ET AL.
CERN - GENEVE, GANIL - CAEN, INFN/LNS - CATANIA, SERC DARESBURY LAB. - WARRINGTON, THE STUDSVIK NEUTRON RES.LAB. - NYKOPING, KJEMISK INST. OSLO UNIV. - OSLO, IKS/KU - LEUVEN, GSI - DARMSTADT, IPN - ORSAY, ISN - GRENOBLE
NIL B88 (1994) 441.
94 88 C

FUSION STUDIES WITH LIGHT NEUTRON-RICH NUCLEI AT SUB-COULOMB ENERGIES
FEKOU-YOUMBI ET AL.
DAPNIA CE SACLAY - GIF SUR YVETTE, GANIL - CAEN, INST. FOR PHYS. AND NUCL. ENGINERING - BUCHAREST, IPN - ORSAY, DIPART. DI FISICA AND INFN - CATANIA, IFU - SAO PAULO, IMP - LANZHOU
HEAVY-ION FUSION : EXPLORING THE VARIETY OF NUCLEAR PROPERTIES
PADOVA (IT)
HEAVY-ION FUSION : EXPLORING THE VARIETY OF NUCLEAR PROPERTIES
94 70 C

IDENTIFICATION OF 100 Sn AND OTHERS PROTON DRIP-LINE NUCLEI IN THE REACTION 112 Sn(63 MeV/nucl.) + nat Ni
LEWITOWICZ M. ET AL.
GANUL - CAEN, IFD WARSAW UNIV. - WARSAW, IAP - BUCHAREST-MAGURELE, IPN - ORSAY, GOTTINGEN UNIV. - GOTTINGEN, FLNR/JINR - DUBNA, IDS KU - LEUVEN, GSI - DARMSTADT
NUCLEAR PHYSICS A588 (1995) 197c.
95 37 C

IDENTIFICATION OF NEW NUCLEI AT AND BEYOND THE PROTON DRIP LINE NEAR THE DOUBLY MAGIC NUCLEUS 100 Sn
RYKACZEWSKI K. ET AL.
WARSAW UNIV. - WARSAW, GANIL - CAEN, INST. APPLIED PHYS. - BUCAREST-MAGURELE, IPN - ORSAY, GOTTINGEN UNIV. - GOTTINGEN, FLNR JINR - DUBNA, LEUVEN UNIV. - LEUVEN, GSI - DARMSTADT
PHYSICAL REVIEW C52, 5 (1995) R2310.
95 107 C

IDENTIFICATION OF THE DOUBLY MAGIC NUCLEUS 100 Sn AT GANIL
SAINT-LAURENT M.G. ET AL.
GANIL - CAEN, IAP - BUCHAREST-MAGURELE, IPN - ORSAY, GOTTINGEN UNIV. - GOTTINGEN, FLNR JINR - DUBNA, IFD WARSAW UNIV. - WARSAW, IKS KU - LEUVEN, GSI - DARMSTADT
TOURS SYMPOSIUM ON NUCLEAR PHYSICS.2
TOURS (FR)
TOURS SYMPOSIUM ON NUCLEAR PHYSICS.2
95 61 C

IDENTIFICATION OF İS-ISOMERS PRODUCED IN THE FRAGMENTATION OF A 112 Sn BEAM
CRZYWACZ R. ET AL.
IFD WARSAW UNIV. - WARSAW, GANIL - CAEN, IAP - BUCHAREST-MAGURELE, IPN - ORSAY, GOTTINGEN UNIV. - GOTTINGEN, FLNR JINR - DUBNA, IKS KU - LEUVEN, GSI - DARMSTADT
PHYSICS LETTERS B355 (1995) 439.
95 65 C

NEUTRON HALOS IN O ISOTOPES
REN Z. ET AL.
GANIL - CAEN, NANJING UNIV. - NANJING, CHINA INST. OF AT. PHYS. - BEIJING
PHYSICAL REVIEW C52, 1 (1995) R20.
95 54 C

NEUTRON MOMENTUM DISTRIBUTIONS FROM "CORE BREAK-UP" REACTIONS OF HALO NUCLEI
NILSSON T. ET AL.
FYS.INST.-GOTEBORG,INST.KERNCHEM.-MAINZ,IEM-MADRID,RSC-MOSCOW,
INST.KERNPHY.-FRANKFURT,GSI-DARMSTADT,IPN-ORSAY,IFA-AARHUS,INST.KERNPHY.-DARMSTADT,
MAINZ UNIV.-MAINZ,RUHR UNIV.-BOCHUM,JAGEL.UNIV.-KRAKOW,GANIL-CAEN,MSU-EAST-LANSING,
CERN-GENEVE
EUROPHYSICS LETTERS 30, 1 (1995) 19.
95 93 C

NEW ISOMER 32 Al m
ROBINSON M. ET AL.
GANIL - CAEN, IAP - BUCHAREST, JINR - DUBNA, LPC ISMRA - CAEN
PHYS. REV. C53 (1996) 1465.
96 37 C

NEW ISOTOPES FROM 78 Kr FRAGMENTATION AND THE ENDING POINT OF THE ASTROPHYSICAL RAPID-PROTON-CAPTURE PROCESS
BLANK B. ET AL.
CENBG - GRADIGNAN, INST.EXP.PHYS. - WARSAW, INST.KERNPHYS. - DARSMTADT, GANIL - CAEN,
CE - BRUYERES-LE-CHATEL, GSI - DARMSTADT
PHYSICAL REVIEW LETTERS 74, No.23 (1995) 4611.
95 38 C

NEW ISOTOPES, SECONDARY REACTIONS AND SPECTROSCOPY FOR MEDIUM-MASS NUCLEI AT THE PROTON DRIP LINE
BLANK B. ET AL.
CENBG - GRADIGNAN, GSI - DARMSTADT, INST. FUR KERNPHYSIK - DARMSTADT,
WARSAW UNIV. - WARSAW, GANIL - CAEN, CE BRUYERES-LE-CHATEL
NUCLEAR PHYSICS A588 (1988) 171c.
95 36 C

OBSERVATION OF 100 Sn
LEWITOWICZ M. ET AL.
GANIL - CAEN, INST. OF ATOMIC PHYS. - BUCHAREST, GOTTINGEN UNIV. - GOTTINGEN,
WARSAW UNIV. - WARSAW, IPN - ORSAY, INST. VOOR KERN EN STRALINGSFYSIKA - LEUVEN,
GSI - DARMSTADT, JINR - DUBNA
NUCLEAR PHYSICS A583 (1995) 857.
INTERNATIONAL CONFERENCE ON NUCLEUS-NUCLEUS COLLISIONS.5
TAORMINA (IT)
95 22 C

PHYSICS WITH EXOTIC NUCLEI
GUERREAU D.
GANIL - CAEN
TOURS SYMPOSIUM ON NUCLEAR PHYSICS.2
TOURS (FR)
TOURS SYMPOSIUM ON NUCLEAR PHYSICS.2
95 62 C

PRODUCTION OF MULTICHARGED METALLIC IONS BY THE ASSOCIATION OF AN EXCIMER LASER AND AN ECR ION SOURCE
BEX L. ET AL.
GANIL - CAEN, CRISMAT ISMRA - CAEN
NIM A365 (1995) 564.
95 103 C

PROJECTILE COULOMB EXCITATION WITH FAST RADIOACTIVE BEAMS
ANNE R. ET AL.
GANIL - CAEN, CHALMERS TEK. HOGSKOLA - GOTEBORG, IPN - ORSAY, GSI - DARMSTADT, AARHUS UNIV. - AARHUS, MAINZ UNIV. - MAINZ, INST. KERNPHYSIK - HOCHSCHULE, CERN - GENEVE
ZEITSCHRIFT FUR PHYSIK A352 (1995) 397.
95 94 C

QUASIELASTIC SCATTERING OF 8 B AND 7 Be ON 12 C AT 40 MeV/NUCLEON
PECINA I. ET AL.
GANIL - CAEN, NPI - REZ, IAP - BUCHAREST-MAGURELE, IPN - ORSAY, JINR - DUBNA, IEP WARSAW UNIV. - WARSAW
PHYSICAL REVIEW C52, 1 (1995) 191.
95 55 C

"FUN" DURCH SUPERNOVAEXPLOSIONEN UND KERNPHYSIK MIT LISE
KRATZ K.L. ET AL.
INST. FUR KERNCHEMIE MAINZ UNIV. - MAINZ
PHYS. Bl. 51 (1995) Nr.3, p. 183.
95 23 C

BINARY DISSIPATIVE PROCESSES AND FORMATION OF HOT NUCLEI IN 36 Ar + 27 Al REACTIONS FROM 55 TO 95 MeV/u
PETER J. ET AL.
LPC - CAEN, GANIL - CAEN, IPN - LOUVAIN LA NEUVE, SUBATECH- NANTES, DSF INFN - CATANIA, IMP - LANZHOU, SOONGSIL UNIV. - SEOUL, DAPNIA CE SACLAY - GIF SUR YVETTE
NUCLEAR PHYSICS A593 (1995) 95
95 101 D

BREAKUP OF INTERMEDIATE-MASS FRAGMENTS, 8 Be AND 6 Li, FORMED IN THE REACTION 40 Ar + Ag AT 7.8 A AND 17 A MeV
ELMAANI A. ET AL.
STATE UNIV. OF NEW YORK - STONY BROOK, ISN - GRENOBLE, GANIL - CAEN
PHYSICAL REVIEW C48, 6 (1994) 2864.
94 84 D

BUILDING A TOOL FOR HEAVY ION COLLISION STUDIES : THE EVENT GENERATOR GENEVE
WIELECZKO J.P. ET AL.
GANIL - CAEN
PROCEEDINGS OF II TAPS WORKSHOP
GUARDAMAR (SP)
GAMMA RAY AND PARTICLE PRODUCTION IN HEAVY ION REACTIONS
95 100 D

CALIBRATION OF FORWARD WALL AND FIRST RESULTS
VAN POL J.H.G.
KVI - GRONINGEN
PROCEEDINGS OF II TAPS WORKSHOP
GUARDAMAR (SP)
GAMMA RAY AND PARTICLE PRODUCTION IN HEAVY ION REACTIONS
95 99 D

CHARGE-EXCHANGE REACTIONS BETWEEN HEAVY IONS AT RELATIVISTIC ENERGIES
SUMMERER K. ET AL.
GSI - DARMSTADT, INP - ORSAY, TECHNISCHE HOCHSCHULE - DARMSTADT, GANIL - CAEN, GIESSEN UNIV. - GIESSEN
THIRD INTERNATIONAL CONFERENCE ON RADIOACTIVE NUCLEAR BEAMS
MICHIGAN STATE UNIVERSITY
THIRD INTERNATIONAL CONFERENCE ON RADIOACTIVE NUCLEAR BEAMS
94 18 D

COMPLETE ENERGY DAMPING IN 29 MeV/NUCLEON Pb + Au TWO-BODY FINAL-STATE REACTIONS
BOUGAULT R. ET AL.
LPC - CAEN, CRN - STRASBOURG, GANIL - CAEN, IPN - ORSAY
NUCLEAR PHYSICS A587 (1995) 499.
95 30 D

DISAPPEARANCE OF FLOW AND THE IN-MEDIUM NUCLEON-NUCLEON CROSS SECTION FOR 64 Zn + 27 Al COLLISIONS AT INTERMEDIATE ENERGIES
ZHI YONG HE ET AL.
LPC ISMRA - CAEN, IMP - LANZHOU, GANIL - CAEN, IPN - LOUVAIN-LA-NEUVE, SUBATECH - NANTES, TEXAS A&M UNIV. - COLLEGE STATION, INST.NUCL.RES. - SHANGHAI, VAPOLI UNIV. - NAPLES
NUCL. PHYS. A598 (1996) 248.
96 05 D

DYNAMICAL ANALYSIS OF DISSIPATIVE COLLISIONS BETWEEN Ar AND Ag NUCLEI IN THE FERMI ENERGY DOMAIN
HADDAD F. ET AL.
SUBATECH - NANTES, TEXAS A&M UNIV. - COLLEGE STATION, IPN - ORSAY
Z. PHYS. A354 (1996) 321.
96 10 D

EVOLUTION OF THE MULTIFRAGMENT EMISSION REGIME BETWEEN 3 AND 5.5 MeV/u EXCITATION ENERGY
LOUVEL M. ET AL.
LPC ISMRA - CAEN
SECOND EUROPEAN BIENNIAL WORKSHOP ON NUCLEAR PHYSICS
MEGEVE (FR)
SECOND EUROPEAN BIENNIAL WORKSHOP ON NUCLEAR PHYSICS
95 74 D

HIGHLY EXCITED NUCLEI FORMED IN p - AND 3He - INDUCED REACTIONS AT 2 GEV
MORJEAN M. ET AL.
GANIL - CAEN, HMI - BERLIN, LIEGE UNIV. - LIEGE, IPN - ORSAY, LNS SACLAY - GIF SUR YVETTE, WARSAW UNIV. - WARSAW, KVI - GRONINGEN
TOURS SYMPOSIUM ON NUCLEAR PHYSICS.2
TOURS (FR)
TOURS SYMPOSIUM ON NUCLEAR PHYSICS.2
95 59 D

HOT NUCLEI AND FRAGMENTATION
GUERREAU D.
GANIL - CAEN
NUCLEAR PHYSICS A574 (1994) 111c.
94 92 D

HOT NUCLEI IN 2 GEV P, 2 GEV 3 HE AND 150 MEV/A 84 KR INDUCED REACTIONS
GALIN J. ET AL.
GANIL - CAEN, HMI - BERLIN, IPN - ORSAY, LN SATURNE - GIF SUR YVETTE, KVI - GRONINGEN, IFUSP - SAO PAULO, LIEGE UNIV. - LIEGE
WINTER WORKSHOP ON NUCLEAR DYNAMICS.10
SNOWBIRD (US)
ADVANCES IN NUCLEAR DYNAMICS
94 67 D

MAXIMUM EXCITATION ENERGY IN FUSION-EVAPORATION REACTIONS FROM LIGHT PARTICLE MULTIPLICITY MEASUREMENTS IN 32 S + 58 Ni AT 25 MeV/A
FIGUERA P. ET AL.
HMI - BERLIN, GANIL - CAEN, WARSAW UNIV. - WARSAW
ZEITSCHRIFT FUR PHYSIK A352 (1995) 315.
95 66 D

MULTIFRAGMENTATION IN CENTRAL KR+AU COLLISIONS AT 60 MeV/u
LOPEZ O. ET AL.
LPC - CAEN, CRN - STRASBOURG, GANIL - CAEN, AECL - CHALK RIVER, INFN - CATANIA, CAEN UNIV. - CAEN
SECOND EUROPEAN BIENNIAL WORKSHOP ON NUCLEAR PHYSICS
MEGEVE (FR)
SECOND EUROPEAN BIENNIAL WORKSHOP ON NUCLEAR PHYSICS
95 73 D

MULTIFRAGMENTATION STUDIED WITH INDRA
BACRI CH.O. ET AL.
IPN - ORSAY, CE SACLAY - GIF SUR YVETTE, LPC - CAEN, GANIL - CAEN, LPN - NANTES, IPN LYON - VILLEURBANNE
TOURS SYMPOSIUM ON NUCLEAR PHYSICS.2
TOURS (FR)
TOURS SYMPOSIUM ON NUCLEAR PHYSICS.2
95 60 D

NEW EMULSION RESULTS ON MULTIFRAGMENTATION AND FLOW FROM : 1. PARTICIPANTS IN LOW ENERGY HEAVY ION REACTIONS AND 2. SPECTATORS IN HIGH ENERGY HEAVY ION REACTIONS
JAKOBSSON B.
COSMIC AND SUBATOMIC PHYS. LUND UNIV. - LUND
INTERNATIONAL WORKSHOP ON MULTIPARTICLE CORRELATIONS AND NUCLEAR REACTIONS
NANTES (FR)
CORINNE II : MULTIPARTICLE CORRELATIONS AND NUCLEAR REACTIONS
95 83 D

NUCLEAR DISASSEMBLY TIME SCALES USING SPACE-TIME CORRELATIONS
DURAND D. ET AL.
LPC - CAEN, CRN - STRASBOURG, GANIL - CAEN, IPN - ORSAY, AECL - CHALK RIVER
PHYSICS LETTERS B345 (1995) 397.
95 26 D

ONSET OF VAPORIZATION FOR THE Ar + Ni SYSTEM
BACRI CH.O. ET AL.
IPN ORSAY, CE SACLAY - GIF-SUR-YVETTE, LPC ISMRA - CAEN, GANIL - CAEN, IPN LYON - VILLEURBANNE, SUBATECH - NANTES
PHYSICS LETTERS B353 (1995) 27.
95 50 D

PRODUCTION OF HEAVY FRAGMENTS IN THE REACTION 40 Ar + 232 Th
POLLACCO E.C. ET AL.
DAPNIA CE SACLAY - GIF SUR YVETTE, INFN - CATANIA, GSI - DARMSTADT,
INFN/LAB. NAZ. DEL SUD - CATANIA, GANIL - CAEN, INST. FUR KERNPHYSIK - DARMSTADT,
IOWA UNIV. - IOWA, LPC/ISMRA - CAEN
NUCLEAR PHYSICS A583 (1995) 441.
INTERNATIONAL CONFERENCE ON NUCLEUS-NUCLEUS COLLISIONS.5
TAORMINA (IT)
95 15 D

REACTION MECHANISMS IN 24.3 MeV/NUCLEON 238 U INDUCED REACTIONS THROUGH A COMPREHENSIVE STUDY OF FISSION
PIASECKI E. ET AL.
IEP WARSAW UNIV. - WARSAW, GANIL - CAEN, SAO PAULO UNIV. - SAO PAULO, SINS - SWIERK,
IPN - ORSAY, HIL WARSAW UNIV. - WARSAW, HMI - BERLIN,
WARSAW UNIV. OF AGRICULTURE - WARSAW
PHYSICS LETTERS B351 (1995) 412.
95 41 D

REACTION PLANE DETERMINATION FOR 64 Zn + 27 Al COLLISIONS AT INTERMEDIATE ENERGY
ZHI-YONG He ET AL.
IMP - LANZHOU, LPC - CAEN, GANIL - CAEN, TEXAS A&M UNIV. - COLLEGE STATION,
LPN - NANTES, NAPOLI UNIV. - NAPLES, UCL - LOUVAIN-LA-NEUVE, IFA - BUCHAREST
CHINESE JOURNAL OF NUCLEAR PHYSICS, VOL. 16, No. 3 (1994) 207.
94 73 D

STUDY OF INPLANE FLOW AND AZIMUTHAL DISTRIBUTION WITH 4pi DETECTORS
ANGELIQUE J.C. ET AL.
LPC - CAEN, GANIL - CAEN, CE SACLAY - GIF SUR YVETTE, LPN - NANTES, UNIV. DI NAPOLI,
SUNY - STONY BROOK, IMP - LANZHOU, TSUKUBA UNIV.- TSUKUBA,
JAPAN INST.OF TECH.- TOKYO, RIKKYO - TOKYO, FNRS & IPN - LOUVAIN-LA-NEUVE
TOURS SYMPOSIUM ON NUCLEAR PHYSICS.2
TOURS (FR)
TOURS SYMPOSIUM ON NUCLEAR PHYSICS.2
95 63 D

TEMPERATURE AND EXCITATION ENERGY DETERMINATION IN 208 Pb + 197 Au REACTIONS AT 29 MeV/u
MORJEAN M. ET AL.
GANIL - CAEN, SUBATECH - NANTES, IPN - ORSAY, CENBG - GRADIGNAN, KVI - GRONINGEN
NUCLEAR PHYSICS A591 (1995) 371.
95 69 D

VAPORIZATION OF THE Ar + Ni SYSTEM STUDIED WITH THE 4pi MULTIDETECTOR INDRA
BACRI CH.O. ET AL.
DAPNIA CE SACLAY - GIF SUR YVETTE, GANIL - CAEN, IPN - ORSAY, LPC ISMRA - CAEN,
IPN LYON - VILLEURBANNE, SUBATECH - NANTES
INTERNATIONAL WORKSHOP ON MULTIPARTICLE CORRELATIONS AND NUCLEAR REACTIONS
NANTES (FR)
CORINNE II : MULTIPARTICLE CORRELATIONS AND NUCLEAR REACTIONS
95 81 D

VIOLENT COLLISIONS BETWEEN Ar AND Ag IN THE ENERGY RANGE 30-60 MeV PER NUCLEON : PERSISTENCE OF DEEPLY INELASTIC COLLISIONS AND TEMPERATURE LIMITS

BOX P. ET AL.

IPN - ORSAY, IPN UCL - LOUVAIN-LA-NEUVE, FNRS & ULB - BRUSSELS, LPN - NANTES, KONAN UNIV. - KOBE

SECOND EUROPEAN BIENNIAL WORKSHOP ON NUCLEAR PHYSICS

MEGEVE (FR)

SECOND EUROPEAN BIENNIAL WORKSHOP ON NUCLEAR PHYSICS

95 78 D

TIME SCALE AND FREEZE-OUT VOLUME IN THE Xe + Cu REACTION AT 45 MeV/u

D'AGOSTINO M. ET AL.

INFN - BOLOGNA, INFN - LEGNARO, INFN - MILANO, GANIL - CAEN, INFN - TRIESTE

Z. PHYS. A353 (1995) 191.

95 105 D1

SUB-COULOMB FUSION WITH HALO NUCLEI

FEKOU-YOUMBI V. ET AL.

DAPNIA CE SACLAY - GIF SUR YVETTE, GANIL - CAEN, INST. FOR PHYS. AND NUCL. ENG. - BUCHAREST, IPN - ORSAY, INFN - CATANIA, IFU - SAO PAULO, IMP - LANZHOU

NUCLEAR PHYSICS A583 (1995) 811.

INTERNATIONAL CONFERENCE ON NUCLEUS-NUCLEUS COLLISIONS.5

TAORMINA (IT)

95 21 D3

LIGHT PARTICLE-EVAPORATION RESIDUE COINCIDENCES FOR THE 79 Br + 27 Al SYSTEM AT 11.8 MeV/NUCLEON

GOMEZ DEL CAMPO J. ET AL.

ORNL - OAK RIDGE, GANIL - CAEN, UNIV.NACIONAL AUTONOMA DE MEXICO - MEXICO, DAPNIA CE SACLAY - GIF-SUR-YVETTE

PHYSICAL REVIEW C53, 1 (1996) 222.

96 04 D4

BREMSSTRAHLUNG PHOTONS AS A PROBE OF HOT NUCLEI

MARTINEZ G. ET AL.

IFC - BURJASSOT, GANIL - CAEN, GSI - DARMSTADT, GIESSEN UNIV. - GIESSEN, KVI - GRONINGEN, CENBG - GRADIGNAN, SINS - SWIERK, NPI - REZ

PHYSICS LETTERS B349 (1995) 23.

95 27 E

COHERENT AND INCOHERENT PROCESSES PROBED THROUGH gamma gamma CORRELATIONS

QUEBERT J.

CENBG - GRADIGNAN

PROCEEDINGS OF II TAPS WORKSHOP

GUARDAMAR (SP)

GAMMA RAY AND PARTICLE PRODUCTION IN HEAVY ION REACTIONS

95 84 E

DENSITY OSCILLATIONS IN SYSTEMS OF COLLIDING HEAVY IONS OBSERVED VIA HARD-PHOTON INTERFEROMETRY MEASUREMENTS
MARQUES F.M. ET AL.
GANIL - CAEN, IFC - BURJASSOT, GIESSEN UNIV. - GIESSEN, GSI - DARMSTADT, KVI - GRONINGEN, CENBG - GRADIGNAN, SINS - SWIERK, NPI - REZ
PHYSICS LETTERS B349 (1995) 30.
95 28 E

DYNAMICAL PROPERTIES OF HEAVY-ION COLLISIONS FROM PHOTON INTENSITY INTERFEROMETRY
RAZUMOV L.V., WEINER R.M.
MARBURG UNIV. - MARBURG
PROCEEDINGS OF II TAPS WORKSHOP
GUARDAMAR (SP)
GAMMA RAY AND PARTICLE PRODUCTION IN HEAVY ION REACTIONS
95 86 E

EVIDENCE FOR AN ANTICORRELATION EFFECT IN THE PRODUCTION OF HARD PHOTONS AND PREEQUILIBRIUM PROTONS IN HEAVY ION COLLISIONS
SAPIENZA P. ET AL.
INFN/LNS - CATANIA, DIPART.DI FIS. DELL'UNIV. - CATANIA, GANIL - CAEN
PHYSICAL REVIEW LETTERS 73, 13 (1994) 1769.
94 91 E

IMPACT PARAMETER DEPENDENCE OF HARD PHOTON PRODUCTION IN INTERMEDIATE ENERGY HEAVY-ION COLLISIONS
MARTINEZ G. ET AL.
IFC - BURJASSOT, GIESSEN UNIV. - GIESSEN, GSI - DARMSTADT, GANIL - CAEN, KVI - GRONINGEN, CENBG - GRADIGNAN, SINS - SWIERK, NPI - REZ
PHYSICS LETTERS B334 (1994) 23.
94 87 E

IMPACT PARAMETER DEPENDENCE OF HARD-PHOTON PRODUCTION IN HEAVY-ION COLLISIONS
MARTINEZ G.
IFIC - VALENCIA
PROCEEDINGS OF II TAPS WORKSHOP
GUARDAMAR (SP)
GAMMA RAY AND PARTICLE PRODUCTION IN HEAVY ION REACTIONS
95 87 E

INTERFEROMETRY MEASUREMENTS SELECTED BY NEUTRON CALORIMETRY
GHISALBERTI C. ET AL.
LPN - NANTES, GANIL - CAEN, INP - CRACOW, ACAD. OF SCI. - PRAGUE, WARSAW TECH. UNIV. - WARSAW, CENBG - GRADIGNAN, KVI - GRONINGEN
NUCLEAR PHYSICS A583 (1995) 401.
INTERNATIONAL CONFERENCE ON NUCLEUS-NUCLEUS COLLISIONS.5
TAORMINA (IT)
95 14 E

INVESTIGATION OF POLAR AND AZIMUTHAL DISTRIBUTIONS OF SUBTHRESHOLD PIONS AT INTERMEDIATE ENERGIES
SCHUBERT A. ET AL.
GSI - DARMSTADT, GANIL - CAEN, KVI - GRONINGEN, IFC - BURJASSOT, GIESSEN UNIV. - GIESSEN, NPI - PRAHY, CENBG - GRADIGNAN
PHYSICS LETTERS B328 (1994) 10.
94 86 E

INVESTIGATION OF REABSORPTION EFFECTS IN SUBTHRESHOLD pi O PRODUCTION
HOLZMANN R.
GSI - DARMSTADT
SECOND EUROPEAN BIENNIAL WORKSHOP ON NUCLEAR PHYSICS
MEGEVE (FR)
SECOND EUROPEAN BIENNIAL WORKSHOP ON NUCLEAR PHYSICS
95 75 E

LIGHT CHARGED PARTICLE AND INTERMEDIATE MASS FRAGMENT EMISSION IN THE REACTION 640 MeV 86 Kr + 63 Cu
BOGER J. ET AL.
STATE UNIV. OF NEW YORK - STONY BROOK, CARNEGIE MELLON UNIV. - PITTSBURGH, LBL - BERKELEY, HOPE COLLEGE - HOLLAND, RICHMOND UNIV. - RICHMOND
PHYSICAL REVIEW C49, 3 (1994) 1576.
94 83 E

PROBING THE NUCLEUS-NUCLEUS COLLISIONS AT THE PREEQUILIBRIUM STAGE
DEL ZOPPO A. ET AL.
INFN/LNS - CATANIA, DIPART. DI FISICA DELL'UNIV. - CATANIA, GANIL - CAEN
NUCLEAR PHYSICS A583 (1995) 363.
INTERNATIONAL CONFERENCE ON NUCLEUS-NUCLEUS COLLISIONS.5
TAORMINA (IT)
95 09 E

TWO-PHOTON INTERFEROMETRY : THE EXPERIMENT
MARQUES M.
GANIL - CAEN
PROCEEDINGS OF II TAPS WORKSHOP
GUARDAMAR (SP)
GAMMA RAY AND PARTICLE PRODUCTION IN HEAVY ION REACTIONS
95 85 E

A SYSTEMATIC STUDY OF NEUTRAL PION SQUEEZE-OUT AT INTERMEDIATE ENERGIES
SCHUBERT A. ET AL.
GSI - DARMSTADT, GANIL - CAEN, KVI - GRONINGEN, IFC - BURJASSOT, GIEBEN UNIV. - GIEBEN, CENBG - GRADIGNAN, JAGELLONIAN UNIV. - CRACOW, SLOVAK ACAD. OF SCI. - BRATISLAVA, NPI - REZ
NUCLEAR PHYSICS A583 (1995) 385.
INTERNATIONAL CONFERENCE ON NUCLEUS-NUCLEUS COLLISIONS.5
TAORMINA (IT)
95 11 F

EXCLUSIVE MEASUREMENTS OF NEUTRAL PION PRODUCTION AT INTERMEDIATE ENERGIES
BADALA A. ET AL.
INFN - CATANIA, DIPART. DI FISICA - CATANIA, INFN LNS - CATANIA, GANIL - CAEN
SECOND EUROPEAN BIENNIAL WORKSHOP ON NUCLEAR PHYSICS
MEGEVE (FR)
SECOND EUROPEAN BIENNIAL WORKSHOP ON NUCLEAR PHYSICS
95 76 F

HARD PHOTONS AS A PROBE TO STUDY DISSIPATION MECHANISMS
VAN POL J.H.G. ET AL.
KVI - GRONINGEN, GSI - DARMSTADT, GANIL - CAEN, GIEBEN UNIV. - GIEBEN,
IFC - BURJASSOT, SLOVAK ACAD. OF SCI. - BRATISLAVA, NPI - REZ
NUCLEAR PHYSICS A583 (1995) 373.
INTERNATIONAL CONFERENCE ON NUCLEUS-NUCLEUS COLLISIONS.5
TAORMINA (IT)
95 13 F

IMPORTANCE OF ONE- AND TWO-BODY DISSIPATION AT INTERMEDIATE ENERGIES STUDIED BY HARD PHOTONS
VAN POL J.H.G. ET AL.
KVI - GRONINGEN, GANIL - CAEN, GSI - DARMSTADT, GIESSEN UNIV. - GIESSEN,
IFC - BURJASSOT, SLOVAK ACAD.SCI. - BRATISLAVA, NPI - PRAHY
PHYS. REV. LETT. 76 (1996) 1425.
96 08 F

KAON PRODUCTION IN NUCLEUS-NUCLEUS COLLISIONS AT 92 MeV PER NUCLEON
LECOLLEY F.R. ET AL.
LPC/ISMRA - CAEN, DAPNIA CE SACLAY - GIF SUR YVETTE, GANIL - CAEN,
LPN - NANTES? ISN - GRENOBLE
NUCLEAR PHYSICS A583 (1995) 379.
INTERNATIONAL CONFERENCE ON NUCLEUS-NUCLEUS COLLISIONS.5
TAORMINA (IT)
95 12 F

NEUTRAL MESON PRODUCTION IN RELATIVISTIC HEAVY ION COLLISIONS
KUHN W. (TAPS COLLABORATION & HADES COLLABORATION)
TAPS COLLABORATION
INTERNATIONAL WORKSHOP ON MULTIPARTICLE CORRELATIONS AND NUCLEAR REACTIONS
NANTES (FR)
CORINNE II : MULTIPARTICLE CORRELATIONS AND NUCLEAR REACTIONS
95 82 F

PION REABSORPTION IN HEAVY-ION COLLISIONS INTERPRETED IN TERMS OF THE DELTA CAPTURE PROCESS
HOLZMANN R. ET AL.
GSI - DARMSTADT, GANIL - CAEN, KVI - GRONINGEN, IFC - BURJASSOT,
GIESSEN UNIV. - GIESSEN, NPI - PRAHY, CENBG - GRADIGNAN
PHYSICS LETTERS B366 (1996) 63.
96 02 F

POLAR AND AZIMUTHAL DISTRIBUTIONS OF SUBTHRESHOLD pi O's: A PROBE OF REACTION DYNAMICS AND PION FINAL-STATE INTERACTIONS
SCHUBERT A., HOLZMANN R.
GSI - DARMSTADT
PROCEEDINGS OF II TAPS WORKSHOP
GUARDAMAR (SP)
GAMMA RAY AND PARTICLE PRODUCTION IN HEAVY ION REACTIONS
95 88 F

SUBTHRESHOLD PION DYNAMICS AS A SOURCE FOR HARD PHOTONS BEYOND PROTON-NEUTRON BREMSSTRAHLUNG IN HEAVY-ION COLLISIONS
GUDIMA K.K. ET AL.
GANIL - CAEN, GSI - DARMSTADT, KVI - GRONINGEN, IFC - BURJASSOT
PHYS. REV. LETT. 76 (1996) 2412.
96 06 F

G - ARTICLES GENERAUX

100 Sn IDENTIFIED AT GANIL
RYKACZEWSKI K.
WARSAW UNIV. - WARSAW
NUCLEAR PHYSICS VIEWS VOL. 4, No. 4, 1995
94 71 G

BROKEN HALO REVEALS ALL
GELLETLY W.
SURREY UNIV. - GUILDFORD
NATURE 376 (1995) 119.
95 70 G

LE PROJET SPIRAL - UNE INSTALLATION DE FAISCEAUX RADIOACTIFS AU GANIL
HARAR S.
GANIL - CAEN
BULLETIN DE LA SOCIETE FRANCAISE DE PHYSIQUE No. 97 (1994)
94 63 G

LES NOYAUX A HALOS
GUILLEMAUD-MUELLER D.
IPN - ORSAY
IMAGES DE LA PHYSIQUE (1994)
94 66 G

LES NOYAUX CHAUDS
GUERREAU D., TAMAIN B.
GANIL - CAEN, LPC - CAEN
IMAGES DE LA PHYSIQUE (1994)
94 65 G

NUCLEAR PHYSICS AT GANIL - TRENDS
HARAR S.
GANIL - CAEN
INTERNATIONAL SCHOOL OF HEAVY ION PHYSICS - 3rd COURSE : PROBING THE NUCLEAR PARADIGM WITH HEAVY ION REACTIONS
ERICE (IT)
INTERNATIONAL SCHOOL OF HEAVY ION PHYSICS - 3rd COURSE : PROBING THE NUCLEAR PARADIGM WITH HEAVY ION REACTIONS
95 58 G

NUCLEAR VAPORIZATION : 4 PI EXPERIMENTS WITH INDRA
BORDERIE B. AND THE INDRA COLLABORATION
IPN - ORSAY
NUCLEAR PHYSICS NEWS, VOL. 4, No. 4 (1994)
94 72 G

UN HALO POUR LE CARBONE 19
BAZIN D. ET AL.
GANIL - CAEN
LA RECHERCHE 279, No.26 (1995) 851.
95 79 G

H - ACCELERATEUR

ABSOLUTE MEASUREMENT OF THE GANIL BEAM ENERGY
CASANDJIAN J.M. ET AL.
GANIL - CAEN, IFUSP - SAO PAULO, DIPART.DI FIS. AND INFN - CATANIA, KVI - GRONINGEN
NIM A334 (1993) 301.
94 96 H

PRINCIPLE OF A NEW KIND OF LARGE ACCEPTANCE MASS SEPARATOR
CHABERT A. ET AL.
GANIL - CAEN
NIM A351 (1994) 371.
94 94 H

RECENT PROGRESS IN MAKING HIGHLY CHARGED ION BEAMS
SORTAIS P.
GANIL - CAEN
NIM B98 (1995) 508.
95 39 H

THE HIGH POWER TARGET SYSTEM FOR SISSI, AN INTENSE SOURCE OF SECONDARY IONS
BARON E. ET AL.
GANIL - CAEN
NIM A362 (1995) 90.
95 68 H

THE NEW ACCELERATOR CONTROL SYSTEM OF GANIL
LUONG T.T. ET AL.
GANIL - CAEN
NIM A352 (1994) 96.
94 64 H

I - INSTRUMENTATION

4pi PHYSICS WITH THE NEW MULTIDETECTOR INDRA AT GANIL
LAVILLE J.L.ET AL.
CE SACLAY - GIF SUR YVETTE, GANIL - CAEN, IPN - ORSAY, LPC - CAEN
SECOND EUROPEAN BIENNIAL WORKSHOP ON NUCLEAR PHYSICS
MEGEVE (FR)
SECOND EUROPEAN BIENNIAL WORKSHOP ON NUCLEAR PHYSICS
95 77 I

A CONTEXTUAL IMAGE SEGMENTATION SYSTEM USING A PRIORI INFORMATION FOR AUTOMATIC DATA CLASSIFICATION IN NUCLEAR PHYSICS
BENKIRANE A. ET AL.
GANIL - CAEN, ISMRA - CAEN, IPN - ORSAY
NIM A355 (1995) 559.
95 45 I

A TIME PROJECTION CHAMBER WITH MICROSTRIP READ-OUT
BOOTSMA T.M.V. ET AL.
UTRECHT UNIV./NIKHEF - UTRECHT, GANIL - CAEN
NIM A349 (1994) 204
94 89 I

COSMIC RAYS IN TAPS
MATULEWICZ T. ET AL.
GANIL - CAEN, TAPS COLLABORATION
PROCEEDINGS OF II TAPS WORKSHOP
GUARDAMAR (SP)
GAMMA RAY AND PARTICLE PRODUCTION, IN HEAVY ION REACTIONS
95 91 I

INDRA, A 4 PI CHARGED PRODUCT DETECTION ARRAY AT GANIL
POUTHAS J. ET AL.
GANIL - CAEN, IPN - ORSAY, CE SACLAY - GIF-SUR-YVETTE, LPC - CAEN, LAL - ORSAY
NIM A357 (1995) 418.
95 24 I

PERFORMANCE OF THE HUYGENS DETECTORS AT INTERMEDIATE ENERGIES
SNELLINGS R.J.M. ET AL.
NIKHEF - UTRECHT, GANIL - CAEN
NUCLEAR PHYSICS A583 (1995) 457.
INTERNATIONAL CONFERENCE ON NUCLEUS-NUCLEUS COLLISIONS.5
TAORMINA (IT)
95 18 I

SHIMMING OF HIGH RESOLUTION MAGNETIC SPECTROGRAPHS : A NEW ANALYTICAL AND NUMERICAL METHOD
MITTIG W. ET AL.
GANIL - CAEN, DAPNIA CE SACLAY - GIF SUR YVETTE
NIM A334 (1994) 557.
94 97 I

SPECTROMETRES MAGNETIQUES ET ELECTRIQUES COMME DETECTEURS DE HAUTE RESOLUTION ET COMME FILTRES SELECTIFS
MITTIG W.
GANIL - CAEN
ECOLE INTERNATIONALE JOLIOT-CURIE DE PHYSIQUE NUCLEAIRE
MAUBUISSON (FR)
PHYSIQUE NUCLEAIRE INSTRUMENTALE : DES ELEMENTS POUR UN BON CHOIX
94 74 I

THE ELECTRONICS OF THE INDRA 4pi DETECTION ARRAY
POUTHAS J. ET AL.
GANIL - CAEN, IPN - ORSAY, DAPNIA CE SACLAY - GIF-SUR-YVETTE, LPC - CAEN, LAL - ORSAY
NIM A369 (196) 222.
96 03 I

THE PHOSWICH DETECTOR ARRAY OF THE FORWARD RING OF INDRA
STECKMEYER J.C. ET AL.
LPC ISMRA & CAEN UNIV. - CAEN
NIM A361 (1995) 472.
95 53 I

THE RESPONSE OF A LARGE CsI (TI) DETECTOR TO LIGHT PARTICLES AND HEAVY IONS IN THE INTERMEDIATE ENERGY RANGE
FOMICHEV A.S. ET AL.
FLNR JINR - DUBNA, RCR - DRESDEN, GANIL - CAEN, NPI - REZ, LAP - BUCHAREST
NIM A344 (1994) 378.
94 95 I

J - APPLICATIONS

INDUSTRIAL APPLICATIONS OF ION BEAMS : GANIL APPROACH AND PROSPECTS
DELAGRANGE H.
GANIL - CAEN
NIM B105 (1995) 345.
95 116 J

N - PHYSIQUE DES IONS RAPIDES

120-keV Kr 8 + - Li COLLISIONS STUDIED BY NEAR UV AND VISIBLE PHOTON SPECTROSCOPY
JACQUET E. ET AL.
ISMRA - CAEN, UFR CAEN UNIV. - CAEN, SAINT-ETIENNE UNIV. - SAINT-ETIENNE, MISSOURI-ROLLA UNIV. - MISSOURI, CE SACLAY - GIF SUR YVETTE, ROYAL HOLLOWAY UNIV. OF LONDON - EGHAM
PHYSICA SCRIPTA VOL. 49 (1994) 154.
94 75 N

ACTIVATION OF THICK TARGETS BY ENERGETIC HEAVY IONS AND THE RESULTANT RADIATION LEVELS
CLAPIER F. ET AL.
IPN - ORSAY, GANIL - CAEN
RADIAT. ENVIRON. BIOPHYS. 34 (1995) 213.
95 117 N

AMORPHIZATION KINETICS OF POLY(VINYLIDENE FLUORIDE) ON HIGH-ENERGY ION IRRADIATION
CHAILLEY V. ET AL.
CIRIL - CAEN
NIM B105 (1995) 110.
95 112 N

AMORPHIZATION OF MICA THROUGH THE FORMATION OF GeV HEAVY ION TRACKS
CHAILLEY V. ET AL.
CIRIL - CAEN, LERMAT ISMRA - CAEN
NIM B107 (1996) 199.
PROCEEDINGS OF THE THIRD INTERNATIONAL CONFERENCE ON SWIFT HEAVY IONS IN MATTER CAEN (FR)
BEAM INTERACTIONS WITH MATERIALS AND ATOMS
96 27 N

ATOMIC MIXING INDUCED IN METALLIC BILAYERS BY HIGH ELECTRONIC EXCITATIONS
LEGUAY R. ET AL.
LSI CEA/ECOLE POLYTECHNIQUE - PALAISEAU, CEA SACLAY - GIF-SUR-YVETTE, INST. D'OPTIQUE UNIV. D'ORSAY - ORSAY, UNIVERSITY OF AARHUS - AARHUS, LPS UNIV.D'ORSAY - ORSAY, LAB. LEON BRILLOUIN CEA SACLAY - GIF-SUR-YVETTE, CEA - GRENOBLE
NIM B106 (1995) 28.
95 106 N

AUGER ELECTRON EMISSION FOLLOWING DOUBLE ELECTRON CAPTURE IN 150-keV Ne 10+ + He COLLISIONS
FREMONT F. ET AL.
ISMRA - CAEN, HMI - BERLIN
PHYSICAL REVIEW A50, 4 (1994) 3117.
94 78 N

BASIC PHENOMENA INDUCED BY SWIFT HEAVY IONS IN POLYMERS
BOUFFARD S. ET AL.
CIRIL - CAEN
NIM B105 (1995) 1.
95 115 N

CARBON ION INDUCED MODIFICATIONS OF THE CURIE TRANSITION IN FERROELECTRIC POLYMERS
SCHLBER D. ET AL.
CE SACLAY - GIF-SUR-YVETTE, CIRIL - CAEN
NIM B105 (1995) 278.
95 114 N

CHANGES IN MAGNETIC PROPERTIES OF MAGNETITE Fe 3 O 4 CERAMICS INDUCED BY HIGH ENERGY HEAVY ION IRRADIATION
MEILLON S. ET AL.
LSI ECOLE POLYTECHNIQUE - PALAISEAU, CRISMAT ISMRA - CAEN
NIM B107 (1996) 363.
PROCEEDINGS OF THE THIRD INTERNATIONAL CONFERENCE ON SWIFT HEAVY IONS IN MATTER CAEN (FR)
BEAM INTERACTIONS WITH MATERIALS ANS ATOMS
96 17 N

CHARGE STATE BLOCKING OF K-SHELL INTERNAL CONVERSION IN 125 Te
ATTALLAH F. ET AL.
CENBG - GRADIGNAN, STANDORD UNIV. - STANFORD, CIRIL - CAEN, CSNSM - ORSAY, GANIL - CAEN
PHYSICAL REVIEW LETTERS 75, 9 (1995) 1715.
95 67 N

DAMAGE OF M-TYPE BARYUM HEXAFERRITES INDUCED BY GeV-HEAVY ION IRRADIATIONS
COSTANTINI J.M. ET AL.
CEA - BRUYERES-LE-CHATEL, CIRIL - CAEN, CRISMAT ISMRA - CAEN
NIM B106 1995) 567.
95 108 N

DEPTH PROFILES OF INTERSTITIAL HALOGEN DEFECTS IN HIGH ENERGY ION BOMBARDED ALKALI IODIDES BY MICRO-RAMAN SPECTROSCOPY
PARISELLE M.A. ET AL.
LABOR. DE PHYSIQUE CRISTALLINE IMN - NANTES, ECOLE NAVALE - BREST, WITWARTERSRAND UNIV. - WITS, CIRIL - CAEN
NIM B107 (1996) 250.
PROCEEDINGS OF THE THIRD INTERNATIONAL CONFERENCE ON SWIFT HEAVY IONS IN MATTER CAEN (FR)
BEAM INTERACTIONS WITH MATERIALS AND ATOMS
96 21 N

DYNAMICS OF Xe 44 + (6.7 MeV/A) + Ar AND He COLLISIONS
JARDIN P. ET AL.
CIRIL - CAEN, LSA ISMRA - CAEN
NIM B107 (1996) 41.
PROCEEDINGS OF THE THIRD INTERNATIONAL CONFERENCE ON SWIFT HEAVY IONS IN MATTER CAEN (FR)
BEAM INTERACTIONS WITH MATERIALS AND ATOMS
96 34 N

EFFECT OF RADIAL ENERGY DISTRIBUTION ON ION TRACK ETCHING IN AMORPHOUS METALLIC Fe 81 B 13.5 Si 3.5 C 2
TRAUTMANN C. ET AL.
GSI - DARMSTADT, CIRIL - CAEN, LERMAT ISMRA - CAEN
NIM B108 (1996) 94.
96 07 N

ELECTRONIC STOPPING POWER THRESHOLD OF SPUTTERING IN YTTRIUM IRON GARNET
MEFTAH A. ET AL.
USTHB INSTITUT DE PHYSIQUE - ALGER, CRN GROUPE PHASE - STRASBOURG, CRISMAT CAEN UNIV. - CAEN, CIRIL - CAEN
NIM B107 (1996) 242.
PROCEEDINGS OF THE INTERNATIONAL CONFERENCE ON SWIFT HEAVY IONS IN MATTER CAEN (FR)
BEAM INTERACTIONS WITH MATERIALS AND ATOMS
96 23 N

ETACHA : A PROGRAM FOR CALCULATING CHARGE STATES AT GANIL ENERGIES
ROZET J.P. ET AL.
GPS UNIV. PARIS 7 ET 6 - PARIS, IPN - ORSAY
NIM B107 (1996) 67.
PROCEEDINGS OF THE THIRD INTERNATIONAL CONFERENCE ON SWIFT HEAVY IONS IN MATTER CAEN (FR)
BEAM INTERACTIONS WITH MATERIALS AND ATOMS
96 33 N

EUROPIUM DIFFUSION ENHANCEMENT IN LiNbO 3 IRRADIATED WITH gEV NICKEL IONS : INFLUENCE OF THE DAMAGE MORPHOLOGY
RAMOS S.M.M. ET AL.
DPM UNIV. CLAUDE BERNARD - VILLEURBANNE, CIRIL - CAEN
NIM B107 (1996) 254.
PROCEEDINGS OF THE THIRD INTERNATIONAL CONFERENCE ON SWIFT HEAVY IONS IN MATTER CAEN (FR)
BEAM INTERACTIONS WITH MATERIALS AND ATOMS
96 20 N

EXCITATION IN SWIFT HEAVY ION-ATOM COLLISIONS
VERNHET D. ET AL.
GPS UNIV. PARIS 7 ET 6 - PARIS, IPN - ORSAY, CIRIL - CAEN
NIM B107 (1996) 71.
PROCEEDINGS OF THE THIRD INTERNATIONAL CONFERENCE ON SWIFT HEAVY IONS IN MATTER CAEN (FR)
BEAM INTERACTIONS WITH MATERIALS AND ATOMS
96 32 N

EXPERIMENTAL STUDY BY "IN SITU" RESISTIVITY MEASUREMENTS OF SWIFT HEAVY ION INDUCED DEFECTS IN GaAs CRYSTALS
MIKOU M. ET AL.
LERMAT ISMRA - CAEN
NIM B107(1996) 246.
PROCEEDINGS OF THE THIRD INTERNATIONAL CONFERENCE ON SWIFT HEAVY IONS IN MATTER CAEN (FR)
BEAM INTERACTIONS WITH MATERIALS AND ATOMS
96 22 N

FIELD DEPENDENCE STUDY OF THE REVERSIBLE MAGNETIZATION IN HEAVY IONS IRRADIATED THALLIUM BASED SINGLE CRYSTALS

WAHL A. ET AL.

CRISMAT ISMRA - CAEN, DRFMC CEN - GRENOBLE

NIM B107 (1996) 403.

PROCEEDINGS OF THE THIRD INTERNATIONAL CONFERENCE ON SWIFT HEAVY IONS IN MATTER CAEN (FR)

BEAM INTERACTIONS WITH MATERIALS AND ATOMS

96 13 N

FLUENCE DEPENDENT ELECTRON EMISSION AS A MEASURE OF SURFACE MODIFICATION INDUCED BY SWIFT HEAVY IONS

ROTHARD H. ET AL.

CIRIL - CAEN, IPN LYON - VILLEURBANNE, INST.F.KERNPHYSIK GOETHE UNIV. - FRANKFURT

NIM B107 (1996) 108.

PROCEEDINGS OF THE THIRD INTERNATIONAL CONFERENCE ON SWIFT HEAVY IONS IN MATTER CAEN (FR)

BEAM INTERACTIONS WITH MATERIALS AND ATOMS

96 30 N

INFLUENCE OF INTRASHELL EXCITATION (n = 2) ON THE POPULATION OF MESTASTABLES STATES OF H- AND He-LIKE KRYPTON IONS IN CHANNELING CONDITIONS

ANDRIAMONJE S. ET AL.

CENBG - GRADIGNAN, IPNL - VILLEURBANNE, GPS UNIV. PARIS 7 ET 6 - PARIS, THE HONG KONG UNIV.OF SCI.& TECH. - HONG KONG, CIRIL - CAEN, LSI ECOLE POLYTECHNIQUE - PALAISEAU

NIM B107 (1996) 1.

PROCEEDINGS OF THE THIRD INTERNATIONAL CONFERENCE ON SWIFT HEAVY IONS IN MATTER CAEN (FR)

BEAM INTERACTIONS WITH MATERIALS AND ATOMS

96 36 N

MODIFICATION BY HIGH ENERGY ION IRRADIATION OF IRON-ALUMINA NANO-COMPOSITES

LAURENT CH. ET AL.

LCMI PAUL SABATIER UNIV. - TOULOUSE, CIRIL - CAEN, LERMAT ISMRA - CAEN

NIM B107 (1996) 232.

PROCEEDINGS OF THE THIRD INTERNATIONAL CONFERENCE ON SWIFT HEAVY IONS IN MATTER CAEN (FR)

BEAM INTERACTIONS WITH MATERIALS AND ATOMS

96 25 N

NEW INVESTIGATIONS OF NEAR UV AND VISIBLE PHOTON EMISSION RESULTING FROM 60-keV C 4+ -Li COLLISIONS

JACQUET E. ET AL.

ISMRA - CAEN, UFR/CAEN UNIV. - CAEN, SAINT-ETIENNE UNIV. - SAINT-ETIENNE, ROYAL HOLLOWAY UNIV. OF LONDON - EGHAM

PHYSICA SCRIPTA 51 (1995) 64.

95 25 N

OPTICAL AND ELECTRICAL PROPERTIES OF 6H ALPHA-SIC IRRADIATED BY SWIFT XENON IONS
LAVALOIS M. ET AL.
LERMAT ISMRA - CAEN, CIRIL - CAEN
NIM B107 (1995) 239.
PROCEEDINGS OF THE THIRD INTERNATIONAL CONFERENCE ON SWIFT HEAVY IONS IN MATTER CAEN (FR)
BEAM INTERACTIONS WITH MATERIALS AND ATOMS
96 24 N

RELATION BETWEEN THE BASIC PHENOMENA AND THE OBSERVED DAMAGE
BOUFFARD S.
CIRIL - CAEN
NIM B107 (1996) 91.
PROCEEDINGS OF THE THIRD INTERNATIONAL CONFERENCE ON SWIFT HEAVY IONS IN MATTER CAEN (FR)
BEAM INTERACTIONS WITH MATERIALS AND ATOMS
96 31 N

SENSITIVITY OF METALLIC MATERIALS UNDER IRRADIATION WITH SWIFT HEAVY IONS
DUFOUR CH. ET AL.
LERMAT ISMRA - CAEN, CIRIL - CAEN
NIM B107 (1996) 218.
PROCEEDINGS OF THE THIRD INTERNATIONAL CONFERENCE ON SWIFT HEAVY IONS IN MATTER CAEN (FR)
BEAM INTERACTIONS WITH MATERIALS AND ATOMS
96 26 N

STOPPING POWERS OF GASES FOR VERY HEAVY IONS
BIMBOT R. ET AL.
IPN - ORSAY, NICE UNIV. LAB RADIOCHIMIE - NICE, GANIL - CAEN
NIM B107 (1996) 9.
PROCEEDINGS OF THE THIRD INTERNATIONAL CONFERENCE ON SWIFT HEAVY IONS IN MATTER CAEN (FR)
BEAM INTERACTIONS WITH MATERIALS AND ATOMS
96 35 N

STRONG DEPENDENCE OF A NUCLEAR LIFETIME ON THE IONIC CHARGE STATE
ATTALLAH F.
CENBG - GRADIGNAN, CSNSM - ORSAY, CIRIL - CAEN, GANIL - CAEN, STANFORD UNIV. - STANFORD
INTERNATIONAL CONFERENCE ON NUCLEAR SHAPES AND NUCLEAR STRUCTURE AT LOW EXCITATION ENERGIES
ANTIBES (FR)
NUCLEAR SHAPES AND NUCLEAR STRUCTURE AT LOW EXCITATION ENERGIES
95 42 N

STRUCTURAL ANALYSIS OF FERROMAGNETIC LATENT TRACKS IN RCo2 THIN FILMS (R = Y, Tm,Ce) BY MEANS OF X-RAY DIFFRACTION
GHIDINI M. ET AL.
LABOR. LOUIS NEEL - GRENOBLE, CIRIL - CAEN
NIM B107 (1996) 344.
PROCEEDINGS OF THE THIRD INTERNATIONAL CONFERENCE ON SWIFT HEAVY IONS IN MATTER CAEN (FR)
BEAM INTERACTIONS WITH MATERIALS AND ATOMS
96 18 N

STRUCTURAL STUDY OF POLYSTYRENE GRAFTED IN IRRADIATED POLYVINYLIDENE FLUORIDE THIN FILMS
GEBEL G. ET AL.
CEA DRFMC - GRENOBLE, CEA CE SACLAY - GIF-SUR-YVETTE
NIM B105 (1995) 145.
95 113 N

STUDY OF PHOTON SPECTRA EMITTED DURING N 5 + -Li COLLISIONS
RIEGER G. ET AL.
ISMRA - CAEN, UFR CAEN UNIV. - CAEN, ROYAL HOLLOWAY UNIV. - EGHAM
PHYSICA SCRIPTA VOL. 50 (1994) 493.
94 77 N

SURFACE MODIFICATIONS OF LiNbO 3 SINGLE CRYSTALS INDUCED BY SWIFT HEAVY IONS
CANUT B. ET AL.
LYON DPM UNIV. CLAUDE BERNARD - VILLEURBANNE, ECOLE CENTRALE DE LYON - ECULLY, CIRIL - CAEN
NIM B107 (1996) 194.
PROCEEDINGS OF THE THIRD INTERNATIONAL CONFERENCE ON SWIFT HEAVY IONS IN MATTER CAEN (FR)
BEAM INTERACTIONS WITH MATERIALS AND ATOMS
96 28 N

SWIFT HEAVY ION MODIFICATION OF POLYMERS
BALANZAT E. ET AL.
CIRIL - CAEN, CEA DSM - GIF-SUR-YVETTE
NIM B105 (1995) 46.
95 111 N

TRACK ETCHING IN AMORPHOUS METALLIC Fe 81 B 13.5 Si 3.5 C2
TRAUTMANN C. ET AL.
GSI - DARMSTADT, CIRIL - CAEN, LERMAT ISMRA - CAEN
NIM B107 (1996) 397.
PROCEEDINGS OF THE THIRD INTERNATIONAL CONFERENCE ON SWIFT HEAVY IONS IN MATTER CAEN (FR)
BEAM INTERACTIONS WITH MATERIALS AND ATOMS
96 14 N

Tb/Fe AMORPHOUS MULTILAYERS : TRANSFORMATIONS UNDER IONS IRRADIATION
RICHOMME F. ET AL.
LMA FACULTE DES SCIENCES DE ROUEN - MONT-SAINT-AIGNAN, CIRIL - CAEN
NIM B107 (1996) 374.
PROCEEDINGS OF THE THIRD INTERNATIONAL CONFERENCE ON SWIFT HEAVY IONS IN MATTER CAEN (FR)
BEAM INTERACTIONS WITH MATERIALS AND ATOMS
96 16 N

VELOCITY EFFECT ON THE DAMAGE CREATION IN METALS IN THE ELECTRONIC STOPPING POWER REGIME
WANG Z.G. ET AL.
CIRIL - CAEN, LERMAT ISMRA - CAEN, LYON DPM UNIV. CLAUDE BERNARD - VILLEURBANNE
NIM B107 (1996) 175.
PROCEEDINGS OF THE THIRD INTERNATIONAL CONFERENCE ON SWIFT HEAVY IONS IN MATTER CAEN (FR)
BEAM INTERACTIONS WITH MATERIALS AND ATOMS
96 29 N

VISIBLE AND NEAR UV PHOTON SPECTROSCOPY OF CHARGE-EXCHANGE COLLISIONS BETWEEN Ar 7 + AND Li AT 105 keV
JACQUET E. ET AL.
ISMRA - CAEN, UFR CAEN UNIV. - CAEN, SAINT-ETIENNE UNIV. - SAINT-ETIENNE, ROYAL HOLLOWAY UNIV. OF LONDON - EGHAM
PHYSICA SCRIPTA VOL. 49 (1994) 423.
94 76 N

VORTEX PINNING AND COLUMNAR DEFECTS IN SUPERCONDUCTING OXIDES
SIMON CH. ET AL.
CRISMAT ISMRA - CAEN
NIM B107 (1996) 384.
PROCEEDINGS OF THE THIRD INTERNATIONAL CONFERENCE ON SWIFT HEAVY IONS IN MATTER CAEN (FR)
BEAM INTERACTIONS WITH MATERIALS AND ATOMS
96 15 N

S - SPIRAL

RADIOACTIVE ION BEAMS AT SPIRAL
VILLARI A.C.C. ET AL.
GANIL - CAEN, LPC/ISMRA - CAEN, CENBG - GRADIGNAN, IPN - ORSAY, IFUSP - SAO PAULO, CSNSM - ORSAY
NUCLEAR PHYSICS A588 (1995) 267c.
95 35 S

T - THEORIE

ALGEBRAIC MODELS OF NUCLEAR STRUCTURE
VAN ISACKER P.
GANIL - CAEN
INTERNATIONAL CONFERENCE ON NUCLEAR SHAPES AND NUCLEAR STRUCTURE AT LOW EXCITATION ENERGIES
ANTIBES (FR)
NUCLEAR SHAPES AND NUCLEAR STRUCTURE AT LOW EXCITATION ENERGIES
95 43 T

ANHARMONICITIES AND NON-LINEARITIES IN THE EXCITATION OF DOUBLE GIANT RESONANCES
VOLPE C. ET AL.
GANIL - CAEN, DFAMN SEVILLA UNIV. - SEVILLA, DIPART. DI FIS. & INFN - CATANIA
NUCLEAR PHYSICS A589 (1995) 521.
95 52 T

ANOMALOUS DIFFUSION IN CHAOTIC SCATTERING
SROKOWSKI T., PLOSZAJCZAK M.
GANIL - CAEN
PHYSICAL REVIEW LETTERS 75, 2 (1995) 209.
95 56 T

BROWNIAN ONE-BODY DYNAMICS IN NUCLEI
CHOMAZ PH. ET AL.
GANIL - CAEN, LNS - CATANIA, LBL - BERKELEY
PHYSICAL REVIEW LETTERS 73, No. 26 (1994) 3512.
94 68 T

COMMENT ON THE PRESENCE OF CHAOS IN MEAN FIELD DYNAMICS INSIDE THE SPINODAL REGION
JACQUOT B. ET AL.
GANIL - CAEN, LNS - CATANIA
PHYSICS LETTERS B359 (1995) 268.
95 96 T

DOES THE GROUND-STATE RESONANCE OF 10 Li OVERLAP NEUTRON THRESHOLD ?
McVOY K.W., VAN ISACKER P.
GANIL - CAEN, WISCONSIN UNIV. - MADISON
NUCLEAR PHYSICS A576 (1994) 157.
94 93 T

FINGERPRINTS OF DYNAMICAL INSTABILITIES
CHOMAZ PH. ET AL.
GANIL - CAEN, LNS - CATANIA
INTERNATIONAL WORKSHOP ON DYNAMICAL FEATURES OF NUCLEI AND FINITE FERMI SYSTEMS
SITGES (SP)
DYNAMICAL FEATURES OF NUCLEI AND FINITE FERMI SYSTEMS
94 79 T

FLUCTUATION IN NUCLEAR DYNAMICS AND MULTIFRAGMENTATION
CHOMAZ PH. ET AL.
GANIL - CAEN, LNS - CATANIA, LBL - BERKELEY, GSI - DARMSTADT
SECOND EUROPEAN BIENNIAL WORKSHOP ON NUCLEAR PHYSICS
MEGEVE (FR)
SECOND EUROPEAN BIENNIAL WORKSHOP ON NUCLEAR PHYSICS
95 71 T

FLUCTUATIONS AND INSTABILITIES IN MULTIFRAGMENTATION
CHOMAZ PH. ET AL.
GANIL - CAEN, LNS - CATANIA
NUCLEAR PHYSICS A583 (1995) 305.
INTERNATIONAL CONFERENCE ON NUCLEUS-NUCLEUS COLLISIONS.5
TAORMINA (IT)
95 10 T

FLUCTUATIONS IN THE MULTIPARTICLE DYNAMICS
BOZEK P., PLASZAJCZAK M.
INP - KRAKOW, GANIL - CAEN
PROCEEDINGS OF II TAPS WORKSHOP
GUARDAMAR (SP)
GAMMA RAY AND PARTICLE PRODUCTION IN HEAVY ION REACTIONS
95 90 T

ISOSPIN INVARIANT BOSON MODELS FOR fp-SHELL NUCLEI
VAN ISACKER P.
GANIL - CAEN
PHYSICA SCRIPTA T56 (1995) 103.
95 49 T

ISOSPIN MIXING IN PROTON-RICH N = Z NUCLEI
COLO G. ET AL.
IPN - ORSAY, DIPART.DI FISICA AND INFN - MILANO, INFN - LEGNARO, GANIL - CAEN, DIPART.DI FISICA AND INFN - PADOVA
PHYSICAL REVIEW C52, 3 (1995) R1175.
95 104 T

MEAN FIELD INSTABILITIES IN DISSIPATIVE HEAVY ION COLLISIONS
COLONNA M. ET AL.
GANIL - CAEN, LNS/INFN AND UNIV. DI CATANIA
NUCLEAR PHYSICS A589 (1995) 160.
95 47 T

MULTIPLE PHONON EXCITATION IN NUCLEI : EXPERIMENTAL RESULTS AND THEORETICAL DESCRIPTIONS
CHOMAZ PH. ET AL.
GANIL - CAEN, IPN - ORSAY
PHYSICS REPORTS 252 (1995) 275.
95 40 T

MULTI-PARTICLE MULTI-HOLE EXCITATIONS AND NEW SYMMETRIES NEAR CLOSED SHELLS
HEYDE K. ET AL.
INST. FOR THEOR. PHYSICS - GENT, GANIL - CAEN, UNIV. DI FRIBOURG - FRIBOURG, GEORGIA INST. OF TECH. - ATLANTA
PHYSICA SCRIPTA T56 (1995) 133.
95 48 T

NECK INSTABILITIES IN DEEP INELASTIC COLLISIONS AT MEDIUM ENERGIES
COLONNA M. ET AL.
GANIL - CAEN, LNS/INFN - CATANIA, IMP - LANZHOU
NUCLEAR PHYSICS A583 (1995) 525.
INTERNATIONAL CONFERENCE ON NUCLEUS-NUCLEUS COLLISIONS.5
TAORMINA (IT)
95 20 T

QUANTAL EFFECTS ON GROWTH OF INSTABILITIES IN NUCLEAR MATTER
AYIK S. ET AL.
TENNESSEE TECH. UNIV. - COOKEVILLE, GANIL - CAEN, LNS - CATANIA
PHYSICS LETTERS B353 (1995) 417.
95 46 T

QUANTUM TUNNELING IN THE DRIVEN LIPKIN N-BODY PROBLEM
KAMINSKI P. ET AL.
GANIL - CAEN, INP - KRAKOW, ISN - GRENOBLE
NUCLEAR PHYSICS A579 (1994) 144.
94 81 T

SIMULATION OF TRANSPORT EQUATIONS FOR UNSTABLE SYSTEMS : COMPARISON BETWEEN LATTICE AND TEST-PARTICLE METHODS
BURGIO G.F. ET AL.
CATANIA UNIV. AND INFN - CATANIA, GANIL - CAEN, LNS - CATANIA, LBL - BERKELEY
NUCLEAR PHYSICS A581 (1995) 356.
95 01 T

SPINODAL INSTABILITIES IN EXPANDING FERMI LIQUIDS
COLONNA M. ET AL.
GANIL - CAEN, LNS - CATANIA
PHYSICAL REVIEW C51, No.5 (1995) 2671.
95 29 T

SYMMETRIES IN ODD-MASS NUCLEI AND THEIR APPLICATIONS
VAN ISACKER P.
GANIL - CAEN
PERSPECTIVES FOR THE INTERACTING BOSON MODEL
PADOVA (IT)
94 90 T

TEST OF WIGNER'S SPIN-ISOSPIN SYMMETRY FROM DOUBLE BINDING ENERGY DIFFERENCES
VAN ISACKER P. ET AL.
GANIL - CAEN, DARESBURY LABORATORY - WARRINGTON, CLARK UNIV. - WORCESTER
PHYSICAL REVIEW LETTERS 74, No.23 (1995) 4607.
95 34 T

TUNNELING CONTROL IN THE DRIVEN SU(2) N-BODY SYSTEM
KAMINSKI P. ET AL.
GANIL - CAEN, INP - KRAKOW, ISN - GRENOBLE
EUROPHYSICS LETTERS 26, 1 (1994) 1.
94 85 G

TWO AND MANY PARTICLE CORRELATIONS IN NUCLEAR AND HIGH ENERGY PHYSICS
BOZEK P. ET AL.
INP - CRACOW, GANIL - CAEN, LPS UNIV. PARIS-SUD - ORSAY
PHYSICS REPORTS 252 (1995) 101.
95 44 T

UNIVERSAL PROPERTIES OF PI AND ETA SPECTRA IN NUCLEAR COLLISIONS
KUDIMA K.K. ET AL.
GANIL - CAEN, MOLDOVA ACAD. OF SCIENCES - KISHINEU, JINR - DUBNA
PHYSICS LETTERS B328 (1994) 249.
94 80 T

UNSTABLE INFINITE NUCLEAR MATTER IN STOCHASTIC MEAN FIELD APPROACH
COLONNA M., CHOMAZ PH.
GANIL - CAEN, LNS - CATANIA
PHYSICAL REVIEW C49 (1994) 1908.
94 82 T

V - APPLICATIONS INDUSTRIELLES

INDUSTRIAL APPLICATIONS AT GANIL
DELAGRANGE H.
GANIL - CAEN
PROCEEDINGS OF II TAPS WORKSHOP
GUARDAMAR (SP)
GAMMA RAY AND PARTICLE PRODUCTION IN HEAVY ION REACTIONS
95 89 V

Imprimerie ALFA B Caen
- Octobre 1996 -